

Topics in Current Chemistry 341

Volker Schurig *Editor*

Differentiation of Enantiomers II

 Springer

341

Topics in Current Chemistry

Editorial Board:

K.N. Houk, Los Angeles, CA, USA

C.A. Hunter, Sheffield, UK

M.J. Krische, Austin, TX, USA

J.-M. Lehn, Strasbourg, France

S.V. Ley, Cambridge, UK

M. Olivucci, Siena, Italy

J. Thiem, Hamburg, Germany

M. Venturi, Bologna, Italy

C.-H. Wong, Taipei, Taiwan

H.N.C. Wong, Shatin, Hong Kong

For further volumes:

<http://www.springer.com/series/128>

Aims and Scope

The series *Topics in Current Chemistry* presents critical reviews of the present and future trends in modern chemical research. The scope of coverage includes all areas of chemical science including the interfaces with related disciplines such as biology, medicine and materials science.

The goal of each thematic volume is to give the non-specialist reader, whether at the university or in industry, a comprehensive overview of an area where new insights are emerging that are of interest to larger scientific audience.

Thus each review within the volume critically surveys one aspect of that topic and places it within the context of the volume as a whole. The most significant developments of the last 5 to 10 years should be presented. A description of the laboratory procedures involved is often useful to the reader. The coverage should not be exhaustive in data, but should rather be conceptual, concentrating on the methodological thinking that will allow the non-specialist reader to understand the information presented.

Discussion of possible future research directions in the area is welcome.

Review articles for the individual volumes are invited by the volume editors.

Readership: research chemists at universities or in industry, graduate students.

Volker Schurig
Editor

Differentiation of Enantiomers II

With contributions by

F. Balzano · T. Brotin · J.H. Bredehöft · J.-P. Dutasta ·
A.C. Evans · C. Giri · L. Guy · S.V. Hoffmann · N.C. Jones ·
K. Manoli · M. Magliulo · A. Martinez · C. Meinert ·
U.J. Meierhenrich · A.E. Sorochinsky · V.A. Soloshonok ·
L. Torsi · O. Trapp · G. Uccello-Barretta · T.J. Wenzel

 Springer

Editor
Volker Schurig
Institute of Organic Chemistry
University of Tübingen
Tübingen
Germany

ISSN 0340-1022 ISSN 1436-5049 (electronic)
ISBN 978-3-319-03715-8 ISBN 978-3-319-03716-5 (eBook)
DOI 10.1007/978-3-319-03716-5
Springer Cham Heidelberg New York Dordrecht London

Library of Congress Control Number: 2013956811

© Springer International Publishing Switzerland 2013

This work is subject to copyright. All rights are reserved by the Publisher, whether the whole or part of the material is concerned, specifically the rights of translation, reprinting, reuse of illustrations, recitation, broadcasting, reproduction on microfilms or in any other physical way, and transmission or information storage and retrieval, electronic adaptation, computer software, or by similar or dissimilar methodology now known or hereafter developed. Exempted from this legal reservation are brief excerpts in connection with reviews or scholarly analysis or material supplied specifically for the purpose of being entered and executed on a computer system, for exclusive use by the purchaser of the work. Duplication of this publication or parts thereof is permitted only under the provisions of the Copyright Law of the Publisher's location, in its current version, and permission for use must always be obtained from Springer. Permissions for use may be obtained through RightsLink at the Copyright Clearance Center. Violations are liable to prosecution under the respective Copyright Law.

The use of general descriptive names, registered names, trademarks, service marks, etc. in this publication does not imply, even in the absence of a specific statement, that such names are exempt from the relevant protective laws and regulations and therefore free for general use.

While the advice and information in this book are believed to be true and accurate at the date of publication, neither the authors nor the editors nor the publisher can accept any legal responsibility for any errors or omissions that may be made. The publisher makes no warranty, express or implied, with respect to the material contained herein.

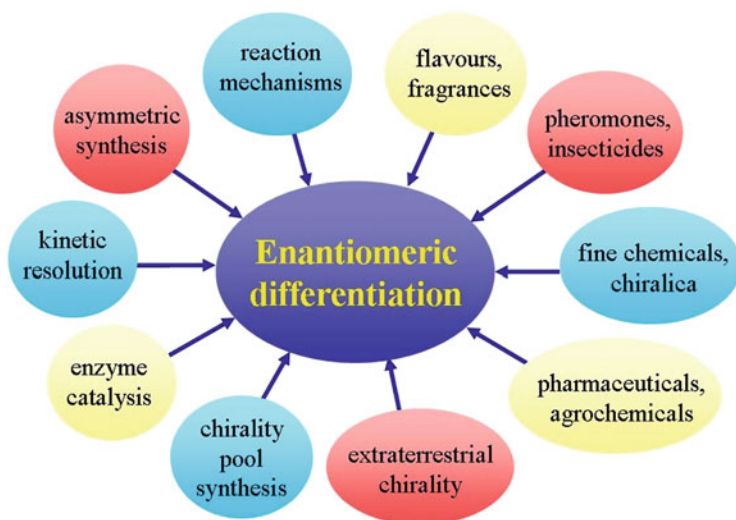
Printed on acid-free paper

Springer is part of Springer Science+Business Media (www.springer.com)

Preface

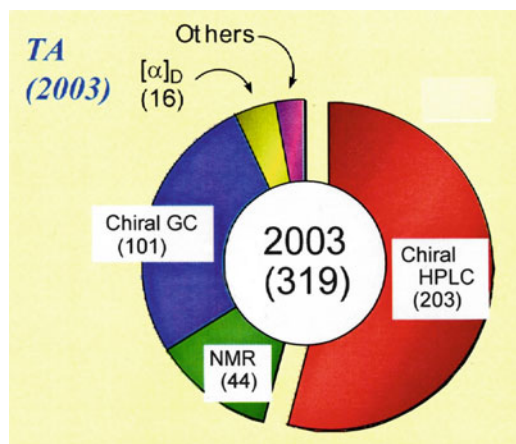
In the wake of enantioselective syntheses and chiral technologies, efficient analytical methods for the differentiation of enantiomers have become essential.

Earlier compendia in this area [1–5] need updating due to important recent advances made in the realm of enantiomeric differentiation. Precise analytical tools for the determination of enantiomeric proportions are important in many contemporary fields associated with various aspects of chirality.



The distribution of enantioselective methods for the determination of enantiomeric proportions utilized in 319 published articles of *Tetrahedron Asymmetry* 2003, i.e., polarimetry [α], gas chromatography (GC), high performance liquid

chromatography (HPLC), and nuclear magnetic resonance spectroscopy (NMR), has been compiled previously [6].



These two volumes of Topics in Current Chemistry review various modern methods and techniques of enantiomeric differentiation. Individual chapters have been written by pioneers in the field and emerge from renowned laboratories which have contributed significantly to recent research. In each chapter emphasis has been given to an extended reference format including the titles of related original work which will enable readers to appreciate and consult the important secondary literature.

The first volume begins with an introduction to historic and fundamental aspects of chirality followed by recommendations on how to quantify mixtures of stereoisomers. Enantiomeric differentiation by chiral liquid chromatography utilizing supramolecular chiral recognition systems and various chiroptic approaches is described. Enantiomeric differentiation by gas chromatography and capillary electrophoresis concludes the first volume. The second volume begins with enantiomeric differentiation by NMR spectroscopy and sensor devices followed by chiral recognition phenomena in supramolecular chemistry, chromatographic studies of stereolabile interconverting enantiomers, and anisotropy spectroscopy as a novel extension of circular dichroism. The second volume is concluded with the self-disproportionation of enantiomers due to nonlinear effects.

We hope that these volumes on the differentiation of enantiomers will provide inspiration and impetus to further advances in the ever-growing area of stereochemistry. The editor is grateful to all the colleagues who have helped to create this survey on modern tools for the differentiation of enantiomers.

References

1. Raban M, Mislow K (1967) Modern methods for the determination of optical purity. *Top Stereochem* 2:199–230
2. Morrison JD (ed) (1983) *Asymmetric synthesis*, vol 1: analytical methods. Academic Press, Inc., New York
3. Schurig V (1985/1986) Current methods for the determination of enantiomeric compositions. Part 1: definitions, polarimetry. Part 2: NMR spectroscopy with chiral lanthanide shift reagents. Part 3: gas chromatography on chiral stationary phases. *Kontakte Merck (Darmstadt)* 1985 (1):54–60; 1985(2):22–40; 1986(1):3–22
4. Schurig V, Lindner W (1995) Determination of enantiomeric purity. In: Helmchen G, Hoffmann RW, Mulzer J, Schaumann E (eds) *Stereoselective synthesis, methods of organic chemistry (Houben-Weyl)*, vol E 21a. Thieme, Stuttgart, New York, pp 147–192; 193–252
5. Schreier P, Bernreuther A, Huffer M (1995) *Analysis of chiral organic molecules, methodology and applications*. Walter de Gruyter, Berlin, New York
6. Chen X, Yamamoto C, Okamoto Y (2007) Polysaccharide derivatives as useful chiral stationary phases in high-performance liquid chromatography. *Pure Appl Chem* 79(9):1561–1573

Contents

Chiral Derivatizing Agents, Macrocycles, Metal Complexes, and Liquid Crystals for Enantiomer Differentiation in NMR Spectroscopy	1
Thomas J. Wenzel	
Chiral NMR Solvating Additives for Differentiation of Enantiomers	69
Gloria Uccello-Barretta and Federica Balzano	
Chiral Sensor Devices for Differentiation of Enantiomers	133
Kyriaki Manoli, Maria Magliulo, and Luisa Torsi	
Enantiopure Supramolecular Cages: Synthesis and Chiral Recognition Properties	177
Thierry Brotin, Laure Guy, Alexandre Martinez, and Jean-Pierre Dutasta	
Interconversion of Stereochemically Labile Enantiomers (Enantiomerization)	231
Oliver Trapp	
Anisotropy Spectra for Enantiomeric Differentiation of Biomolecular Building Blocks	271
A.C. Evans, C. Meinert, J.H. Bredehöft, C. Giri, N.C. Jones, S.V. Hoffmann, and U.J. Meierhenrich	
Self-disproportionation of Enantiomers of Enantiomerically Enriched Compounds	301
Alexander E. Sorochinsky and Vadim A. Soloshonok	
Index	341

Chiral Derivatizing Agents, Macrocycles, Metal Complexes, and Liquid Crystals for Enantiomer Differentiation in NMR Spectroscopy

Thomas J. Wenzel

Abstract Enantiomerically pure chiral auxiliary agents are often used in NMR spectroscopy to facilitate the differentiation of enantiomers. Chiral derivatizing agents are covalently bound to the substrate and differences in chemical shifts of the resulting diastereomeric complexes are used in the analysis. Macrocycles such as cyclodextrins, crown ethers, and calix[4]resorcinarenes are chiral solvating agents that associate with the substrate through non-covalent interactions. Enantiomeric differentiation occurs in the NMR spectrum because of the diastereomeric nature of the associated complexes and/or because of the differences in association constants between the two enantiomers and the chiral reagent. Metal complexes are Lewis acids that bind to suitable Lewis base donor compounds. Exchange of substrate can be slow or fast depending on the particular metal ion, mimicking the behavior of a chiral derivatizing or solvating agent, respectively. Chiral liquid crystals undergo a partial alignment in an applied magnetic field and enantiomers dissolved in the liquid crystal undergo a partial alignment as well. If the alignment of the two enantiomers is different, enantiomeric differentiation can potentially be observed by differences in chemical shifts, differences in dipolar coupling constants, and different magnitudes of splitting of quadrupolar nuclei such as deuterium. The chiral reagents described herein can be used to determine enantiomeric composition and sometimes to assign absolute configuration. Significant discoveries as well as recent findings with each of these types of systems are described.

T.J. Wenzel (✉)

Department of Chemistry, Bates College, Lewiston, ME 04240, USA
e-mail: twenzel@bates.edu

Keywords Absolute configuration · Chiral derivatizing agents · Chiral liquid crystals · Chiral solvating agents · Enantiomeric differentiation · NMR shift reagents

Contents

1	Introduction	2
2	Chiral Derivatizing Agents	4
2.1	Carboxylic Acids	4
2.2	Anhydrides	15
2.3	Alcohols	15
2.4	Amines	16
2.5	Miscellaneous Reagents	17
2.6	Phosphorus-Containing Reagents	20
2.7	Boron-Containing Reagents	22
2.8	Selenium-Containing Reagents	23
3	Macrocycles	24
3.1	Cyclodextrins	24
3.2	Crown Ethers	28
3.3	Calix[4]Resorcinarenes	32
4	Metal Complexes	36
4.1	Lanthanide Complexes	37
4.2	Rhodium Complexes	42
4.3	Palladium Complexes	45
4.4	Platinum Complexes	46
4.5	Silver Complexes	47
5	Liquid Crystals	47
	References	55

1 Introduction

The use of NMR spectroscopy for the determination of enantiomeric composition of a compound was first reported in 1965 [1]. In this pioneering work, Raban and Mislow recognized that the derivatization of a pair of enantiomers with an enantiomerically pure reagent would result in diastereomers that could have different chemical shifts in the NMR spectrum. The area of the peaks was used to determine the enantiomeric composition of the mixture. The analysis of 1-(*o*-fluorophenyl) ethanol with 2-phenylpropionic acid in this first report demonstrated the viability of NMR spectroscopy for the determination of enantiomeric composition. Since this report there have been numerous other examples of chiral NMR derivatizing agents that form a covalently coupled derivative with the chiral compound under study.

In 1966 Pirkle showed that the strategy described by Raban and Mislow for determining enantiomeric composition could also be exploited through the use of an enantiomerically pure chiral NMR solvating agent [2]. Instead of forming covalently coupled diastereomeric complexes, a chiral solvating agent associates with the compound under study through non-covalent interactions. Differentiation

of the enantiomers is possible because the associated complexes are diastereomeric and/or because the enantiomers often have different association constants with the chiral solvating agent. Except for a description of certain cyclodextrin, crown ether, and calix[4]resorcinarene cavity compounds, this chapter will not discuss the application of chiral NMR solvating agents. Chiral solvating agents are discussed in a separate chapter of this volume.

In 1970, Whitesides and Lewis described the first application of a chiral lanthanide complex for determining enantiomeric composition in NMR spectroscopy [3]. Many other chiral lanthanide complexes have since been examined in NMR applications. A variety of transition metal complexes have been evaluated as well. The metal in these complexes is a Lewis acid that forms donor-acceptor complexes with Lewis bases. The exchange of donor molecules may be fast or slow on the NMR time scale depending on the particular metal complex. Under fast exchange, chiral metal complexes are more similar in function to chiral NMR solvating agents. Under slow exchange, chiral metal complexes are more similar to chiral NMR derivatizing agents.

The first application of a chiral liquid crystal for the differentiation of enantiomers was reported in 1968 [4]. Unlike the rapid development and exploitation that occurred with chiral derivatizing agents, chiral solvating agents, and chiral metal complexes in NMR spectroscopy, the use of chiral liquid crystals in NMR spectroscopy experienced little exploration until the mid-1990s. Over the past decade there has been an extensive amount of work on the development and use of chiral liquid crystals as NMR differentiating agents.

This chapter will describe the use of chiral derivatizing agents, metal complexes, and liquid crystals for NMR analysis. The studies described herein involve the use of an auxiliary reagent that brings about the differentiation of the enantiomers under study. Applications aimed at the determination of enantiomeric composition or the assignment of absolute configuration will be discussed. The major emphasis of this chapter is on work that has been published since 2007. Any work on systems described that occurred prior to 2007 is included because of its particular significance within the area of chiral NMR differentiation.

There have been a number of important recent reviews of the use of NMR spectroscopy for chiral discrimination. A book published in 2007 provides an exhaustive review of the entire field prior to that time [5]. More recent journal articles and book chapters have focused on the use of NMR reagents for chiral differentiation [6, 7] and for the assignment of absolute configuration [8]. Comprehensive reviews of NMR methods for assigning the absolute configuration of 1- and 2-hydroxy and 1- and 2-aminophosphonates [9] and of the use of chiral NMR reagents for the analysis of ethers and epoxides have been published [10]. Recent review articles specific to systems discussed herein are cited in the appropriate section of this chapter.

2 Chiral Derivatizing Agents

There are several criteria that must be met when using a chiral derivatizing agent for the analysis of enantiomeric composition. One is that the chiral derivatizing agent must be enantiomerically pure. Another is that there can be no loss of configuration of the reactants during the derivatizing procedure. Finally, it is essential that there be no kinetic resolution in the derivatization reaction. Kinetic resolution occurs if one enantiomer reacts faster than the other and the reaction has not been run long enough to insure that both enantiomers have reacted fully with the chiral derivatizing agent. There are examples of chiral derivatizing agents where the reaction occurs rapidly enough to carry out directly in an NMR tube.

A more common use of chiral NMR derivatizing agents today is in the assignment of absolute configuration. Many of these systems involve formation of a derivative that adopts a specific conformation, such that resonances in the derivative exhibit predictable perturbations in their chemical shifts that can be used to assign the absolute configuration.

2.1 Carboxylic Acids

The first report in which chiral derivatizing agents were used in the assignment of absolute configuration was by Dale and Mosher in 1973 [11]. In this landmark study, α -methoxy- α -trifluoromethylphenylacetic acid (**1** – MTPA) was used as a chiral derivatizing agent for the assignment of the absolute configuration of secondary alcohols. The derivatization produces an ester and two key features allow the assignment of absolute configuration. One is that the ester derivative adopts a preferred conformation. The other is that the phenyl ring of the MTPA shields the substrate and allows differentiation of the two substituent groups of the secondary alcohol. The protocol is to prepare derivatives of the compound under study with (*R*)- and (*S*)-MTPA. The chemical shifts are measured in each of the derivatives and subtracted from each other. If the value in the (*S*)-derivative is subtracted from that in the (*R*)-derivative, a series of $\Delta\delta^{RS}$ values are obtained.

Figure 1 illustrates the use of MTPA in assigning the absolute configuration of secondary alcohols. There is rotation about the bond connecting the MTPA to the secondary alcohol; however, the derivative has a preference for the *syn-periplanar* (*sp*) conformation in which the H–C–O–C(O)–C atoms are in the same plane. A detailed computational investigation of MTPA esters of secondary alcohols indicates that stabilization of the *sp* conformation is attributable to hyperconjugative interactions [12]. Of special significance is shielding by the phenyl ring of the substituent groups of the alcohol. As illustrated in Fig. 1, in the (*R*)-MTPA derivative, the phenyl ring shields the L₁ substituent. In the (*S*)-MTPA derivative the phenyl ring shields the L₂ substituent. Therefore, $\Delta\delta^{RS}$ values will be negative for L₁ and positive for L₂.

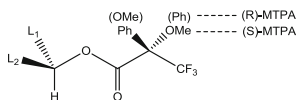
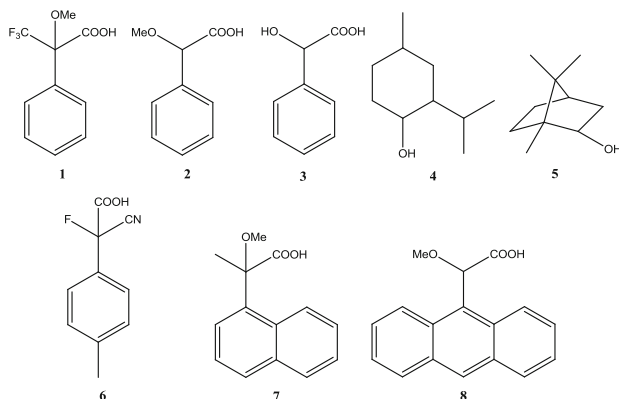


Fig. 1 Conformational model for the (*R*)- and (*S*)-MTPA derivatives of a secondary alcohol

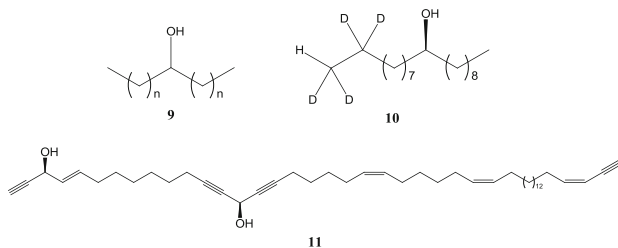
The general features observed with MTPA – adoption of a preferred conformation and aromatic ring for shielding – have been exploited in numerous other chiral NMR derivatizing agents. In fact, in their first report, Dale and Mosher examined α -methoxyphenylacetic acid (**2** – MPA) and mandelic acid (**3**) as chiral derivatizing agents and observed that the $\Delta\delta^{RS}$ values with both were larger than those with MTPA [11, 13]. A problem with MPA in early studies was excessive racemization of the reagent. The use of MPA as a chiral derivatizing agent became more practical in 1986 when a derivatization procedure that minimized racemization of the reagent was developed [14]. Another advantage of MTPA over MPA and mandelic acid early on was the use of systematic trends in the ^{19}F signal of the trifluoromethyl group in assigning absolute configuration. Since most investigators only had access to low-field NMR spectrometers, typically 60–90 MHz, inadequate resolution of resonances in the ^1H NMR spectrum compromised the ability to assign reliably the absolute configuration of many compounds. Today, the “modified Mosher method” combines the use of high field instruments with 2D NMR methods to determine the chemical shifts of overlapped resonances in ^1H NMR spectra [15]. It is possible to use ^{13}C resonances as well, which can be especially helpful if one or more of the substituent groups of the compound under study has no hydrogen atoms [16].

In complicated ^1H NMR spectra with overlapping resonances it is possible to record a selectively excited one-dimensional NMR spectrum as a way of simplifying the spectrum. This procedure was demonstrated on the MPA derivatives of menthol (**4**), borneol (**5**), and several natural products. Selective excitation of the α -proton on MPA enables the observation of nearby protons in the same coupling network. Signals from other impurities are no longer in the spectrum. Using a derivatization mixture consisting of two parts (*R*)-MPA and one part (*S*)-MPA, it is possible to analyze both derivatives simultaneously in the same NMR tube and eliminate the need for two separate derivatization reactions [17].

Even though MTPA has been used to assign the configuration of hundreds of compounds, and a detailed protocol for its use as a chiral differentiating agent has recently been published [18], there are several reagents that routinely produce larger $\Delta\delta^{RS}$ values than MTPA and therefore more reliable assignments of absolute configuration. The magnitude of the $\Delta\delta^{RS}$ values is influenced by the degree to which the derivative adopts the preferred conformation, whether the aryl ring in the preferred conformation is positioned in a manner that causes shielding of resonances, and the size of the aryl ring. Everything else being equal, the larger the aryl ring the larger the shielding such that the magnitude of the $\Delta\delta^{RS}$ values varies in the order anthryl > naphthyl > phenyl. Reagents that are noteworthy for the analysis of alcohols include MPA, α -cyano- α -fluoro-*p*-tolylacetic acid (**6** – CFTA), 2-methoxy-2-(1-naphthyl) propionic acid (**7** – M α NP), and α -(9-anthryl)- α -methoxyacetic acid (**8** – 9-AMA).



A recent study compared the magnitude of the $\Delta\delta^{RS}$ values produced in the ^1H NMR spectrum of **4** after derivatization with α -methoxy aryl-containing carboxylic acids with phenyl, 1- and 2-naphthyl, 2- and 9-anthryl, and 9-phenanthryl substituent groups. Derivatives with the naphthyl and anthryl rings produced much greater $\Delta\delta^{RS}$ values than those with the phenyl rings. The 1-naphthyl and 9-anthryl reagents were especially effective. In a study of symmetrical secondary alcohols, which have prochiral methylene and terminal methyl groups (**9**), the 1-naphthyl reagent was the best at producing long-range differentiation and caused differentiation of the terminal methyl groups when they were up to 15 carbon atoms away from the carbinol site. An interesting observation is that the signs of the $\Delta\delta^{RS}$ values cross over from positive to negative in the region from six to eight carbon atoms removed from the carbinol site. This was unequivocally demonstrated by an analysis of (*S*)-nonadecanol-1,1,2,2-*d*₄ (**10**), which is chiral by virtue of the location of the deuterium atoms [19]. The compound (*S,S*)-petrocortyne (**11**) has rather similar substituent groups about the secondary carbinol at C14 and is symmetrical about this site from C8 to C20. Instead of using $\Delta\delta^{RS}$ values of the MTPA derivatives of **11** in assigning the absolute configuration, it is possible to subtract the chemical shifts of symmetrically-related pairs of methylene groups. These sets exhibit positive and negative values that correlate with the absolute configuration [20].



MPA [21] and CFTA [22] esters of secondary alcohols produce larger $\Delta\delta^{RS}$ values than MTPA because of a greater preference for the preferred conformation that leads to larger shielding by the aryl rings. M α NP and 9-AMA are more effective than MTPA because the larger aryl rings cause more shielding. Another potential advantage of CFTA and M α NP over MPA and 9-AMA is that the stereogenic center on the chiral reagent is a quaternary carbon and is less prone to racemization.

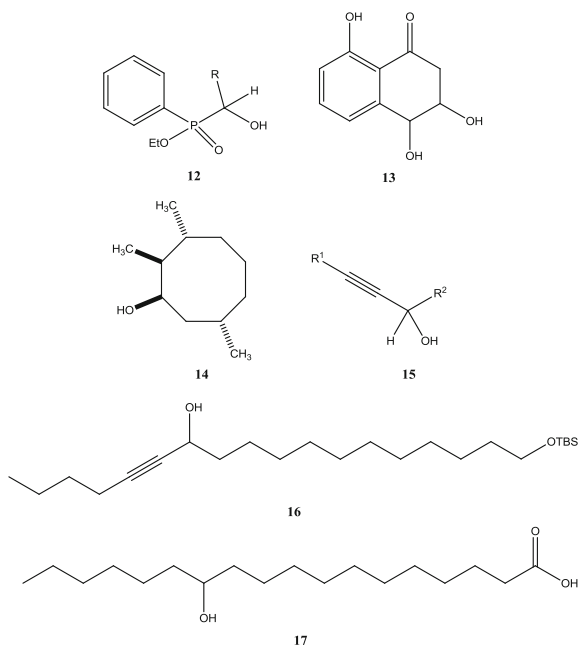
α -Hydroxyphosphinates such as **12** have two stereogenic centers, one about the carbon atom and the other about the phosphorus atom. The absolute configuration of the α -carbon atom in **12** was assigned on the basis of $\Delta\delta^{RS}$ values in the MTPA derivative. Once the configuration of the α -carbon was known, NMR data obtained using quinine as a chiral NMR solvating agent enabled a tentative assignment of the configuration about the phosphorus atom. Theoretical studies were then used to confirm these assignments [23].

The methods described so far for assigning the absolute configuration all involve the use of the (*R*) and (*S*) form of the chiral reagent. Sometimes it is possible to prepare a derivative of the chiral compound under study with only one enantiomer of the chiral derivatizing agent, record changes in the chemical shifts that occur on lowering the NMR probe temperature, and correlate the $\Delta\delta^{T1T2}$ values with absolute configuration [24, 25]. The absolute configuration of (+)-*cis*-4-hydroxy-6-deoxyscytalone (**13**), a metabolite isolated from *Colletotrichum acutatum*, was found to be (3*R*,3*S*) by preparing a single diastereomeric MPA derivative and comparing the NMR spectrum at 25°C and -70°C. The hydroxyl group at the 3-position was selectively acylated so that the MPA derivative at the 4-hydroxy group could be examined in making the assignment [26].

Several recent reports, including a comprehensive review [27], have examined the utilization of M α NP for assigning the absolute configuration of secondary alcohols [28–33]. Derivatives of secondary alcohols with M α NP adopt a *syn-syn* conformation, which was confirmed by the X-ray crystal structures of the esters of 22 different substrates [28]. The *syn-syn* conformation is stabilized by an intramolecular hydrogen bond. A protic solvent such as methanol-*d*₄ is especially useful at stabilizing the M α NP esters of secondary alcohols, leading to significant enhancements in the $\Delta\delta^{RS}$ values. While suitable $\Delta\delta^{RS}$ values of M α NP esters are often obtained in chloroform-*d*, if the $\Delta\delta^{RS}$ values are small and the assignment of absolute configuration is compromised, recording the spectrum in methanol-*d*₄ is recommended [29].

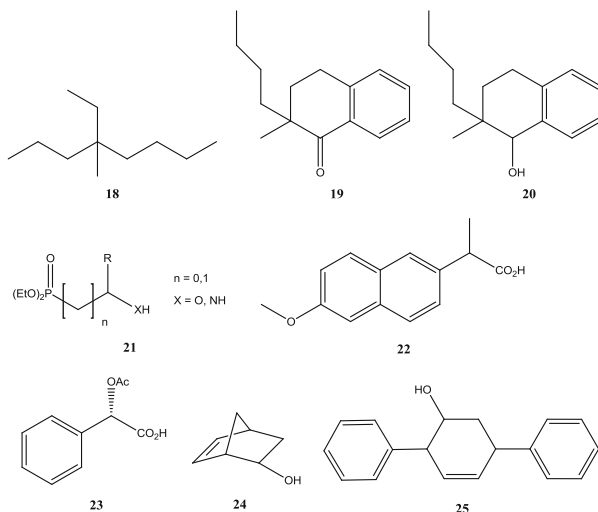
A combination of 2D NMR methods and $\Delta\delta^{RS}$ values of M α NP esters of (1*R*,2*S*,3*R*,7*S*)-2,3,7-trimethylcyclooctanol (**14**), which was prepared from the corresponding cyclooctanone, was used to assign both the relative and absolute configurations of the methyl-substituted sites [30]. M α NP derivatives of a range of aliphatic acetylenic alcohols (**15**) [31] and 18-(*tert*-butyldimethylsilyloxy)-5-octadecayne-7-ol (**16**) [32] were used to assign absolute configurations. In both cases the compounds were not enantiomerically pure and the diastereomeric

M α NP derivatives were separated. A crystal structure of the M α NP derivative of one of the aliphatic acetylenic alcohols was obtained to confirm the NMR configurational assignment [31]. The absolute configuration of 12-hydroxystearic acid (**17**) can be assigned using the M α NP ester. NMR data obtained on the M α NP ester were used to confirm the absolute stereochemistry of **17** isolated as a natural product [32].



4-Ethyl-4-methyloctane (C*MeEtPrBu) (**18**) is the simplest chiral saturated hydrocarbon with a quaternary stereogenic center. The synthesis of **18** can be performed using ketone precursor **19**. Conversion of the ketone group in **19** to a hydroxyl group (**20**) results in (+/-)-*cis*- and (+/-)-*trans*-alcohols. The *cis*-alcohol was converted to its M α NP ester, the two diastereomers were separated and the absolute configuration assigned on the basis of $\Delta\delta^{RS}$ values. This information facilitated assignment of the absolute configuration of **18**, which was confirmed by vibrational circular dichroism of **18** and X-ray crystallography of the M α NP ester of **20** [33].

An issue with these chiral derivatizing agents is whether the derivative actually adopts the expected conformation. The infrared spectrum of CFTA esters of 12 secondary alcohols exhibits distinct bands for the carbonyl stretch of the *sp* (1,770 cm⁻¹) and *ap* (1,750 cm⁻¹) conformers. The infrared spectrum can be used to confirm that the CFTA derivatives adopt the desired conformation [34].



A variety of other aryl-containing carboxylic acids have been used as chiral NMR derivatizing agents in recent studies. The absolute configurations of 1- and 2-hydroxyphosphonates (**21**, X = O) and 1- and 2-aminophosphonates (**21**, X = N) can be assigned using derivatives with (*R*)- and (*S*)-naproxen (**22**). Both sets of derivatives have a preference for the *ap* conformer and $\Delta\delta^{RS}$ values in the ^1H and ^{31}P NMR spectra are used to assign the stereochemistry [35]. Esters with mandelic acid (**3**) [36] and (*S*)-*O*-acetyl mandelic acid (**23**) [37] have been used to assign the absolute configuration of secondary alcohols such as *endo/exo*-norborn-5-en-2-ol (**24**) and *endo/exo*-monocyclic cyclohexenols such as **25** [36, 37]. (*R*)- and (*S*)-2-Methoxy-2-phenylpent-3-ynoic acid (**26**) have been evaluated as chiral NMR derivatizing agents for secondary alcohols and primary amines. An advantage of **26** is that it has no racemizeable α -carbon. Ester derivatives with **26** preferentially adopt an *sp* conformation and $\Delta\delta^{RS}$ values are better than those with MTPA and similar to those with MPA and CFTA [38].

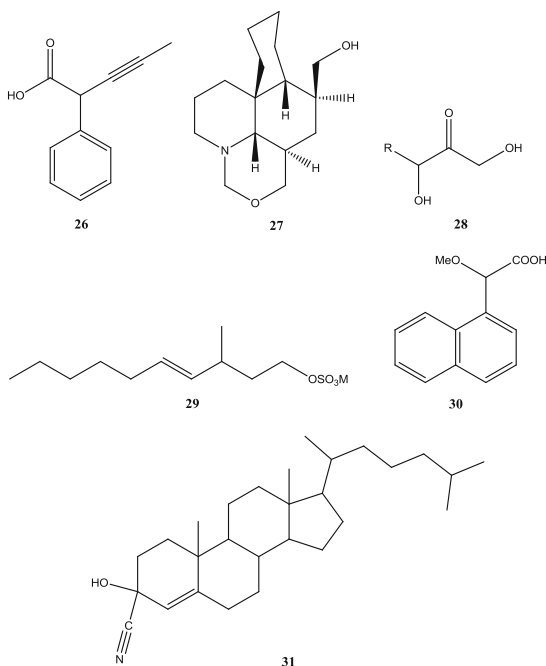
There are a few reports in which aryl-containing carboxylic acids have been used to assign the absolute configuration of primary [39–41] and tertiary [42, 43] alcohols. 9-AMA is especially effective for assigning the absolute configuration of C2 chiral primary alcohols. Greater shielding from the anthryl ring combined with a conformational preference that leads to more shielding from the anthryl ring accounts for its enhanced effectiveness over MTPA or MPA [41].

The absolute configuration of β -chiral primary alcohols in which one of the substituents has no observable hydrogen resonances can be assigned using $\Delta\delta^{RS}$ values of 9-AMA derivatives provided the substituent group without any hydrogen atoms has a heteroatom and is polar. The $\Delta\delta^{RS}$ values for the hydrogen-containing substituent and the C β -hydrogen are used in assigning the absolute configuration. Lowering the probe temperature to 213 K results in considerably larger $\Delta\delta^{RS}$ values and improves the reliability of the assignment [44]. Myrioneurinol (**27**) contains a

β -chiral primary alcohol and its absolute configuration has been assigned based on $\Delta\delta^{RS}$ values of the 9-AMA esters [45].

MTPA derivatives have been used to determine the enantiomeric composition and assign the absolute configuration of products of a transketolase reaction of structure **28**. The derivatization reaction produces almost exclusively the mono-MTPA derivative at the primary hydroxyl group. The signs of the $\Delta\delta^{RS}$ values are used in assigning the absolute configuration [46]. The stereochemistry at C3 in 3-methyl-4*E*-decenyl sulfate (**29**) was assigned using $\Delta\delta^{RS}$ values with α -methoxy-(1-naphthyl)acetic acid (**30** – 1-NMA). The alkene was hydrogenated to produce an alkane, after which the sulfate group was converted to a hydroxyl group. Derivatization with (*R*)- and (*S*)-1-NMA allowed assignment of the stereochemistry of the γ -chiral primary alcohol [47].

The absolute configurations of ketone cyanohydrins with a polar substituent group, one example of which is **31**, have been assigned on the basis of the (*R*)- and (*S*)-MPA derivatives. The ester derivatives have two main *sp* conformers that lead to the different signs of the $\Delta\delta^{RS}$ values for the L_1 and L_2 substituent groups. A wide range of ketone cyanohydrins were examined to confirm the use of $\Delta\delta^{RS}$ values with MPA esters in assigning the absolute configuration [48].



Aryl-containing carboxylic acids can be used to assign the absolute configuration of secondary thiols. The effectiveness of MPA, MTPA, *N*-Boc phenylglycine (**32** – BPG), 9-AMA, 2-*tert*-butoxy-2-phenylacetic acid, 2-*tert*-butoxy-2-(2-naphthyl)acetic acid (**33**), and 2-(9-anthryl)-2-*tert*-butoxyacetic acid has been

compared. The largest $\Delta\delta^{RS}$ values are obtained with **33**, and the thioester derivative has a preference for an *ap* conformation. MPA produces the next largest $\Delta\delta^{RS}$ values, which are still sufficient in magnitude to enable reliable assignment of absolute configuration. Also, addition of barium(II) to the MPA derivatives alters the conformational preference toward the *sp* conformer, thereby causing specific changes in the $\Delta\delta^{RS}$ values that provide additional confirmation of the configurational assignment [49]. The absolute configuration of the thiol site in 4-mercapto-2-alkenones (**34**) can be assigned on the basis of M α NP derivatives. Alterations in the spectrum of the M α NP thioester are sufficiently large that assignment can be reliably performed using only a single M α NP derivative [50].

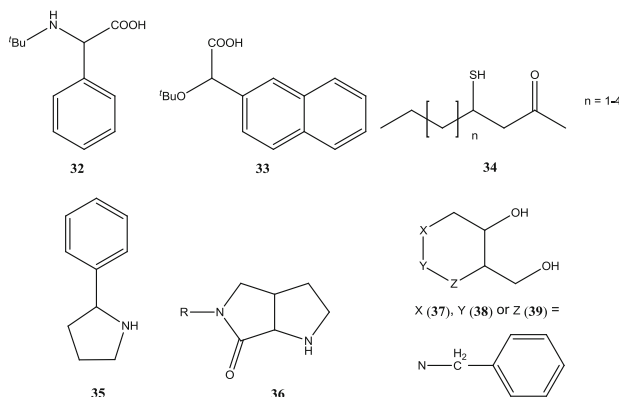
Aryl-containing carboxylic acids can also be used to assign the absolute configuration of amines. The amide derivative adopts a preferred conformation, and shielding by the aryl ring causes different signs of the $\Delta\delta^{RS}$ values for the substituent groups of the amine. A potential complication that must be considered with amide derivatives is their ability to adopt *syn*- and *anti*-rotamers that undergo slow exchange and produce two sets of peaks in the ^1H NMR spectrum. One rotamer is usually predominant and used for the analysis. The conformational preference within the predominant rotamer must be examined. Reports that describe the use of these reagents for assigning absolute configuration address the topic of rotamer and conformer preference. Among the various aryl-containing carboxylic acids, BPG is particularly suitable for the analysis of primary amines. In a comparison of MPA, MTPA, and BPG, $\Delta\delta^{RS}$ values in the amide derivatives with BPG were typically two to three times larger than those with MTPA and MPA [51]. $\Delta\delta^{RS}$ values with MTPA are usually larger than those with MPA because of a greater preference for the *sp* conformer in the MTPA amides [52]. Amide derivatives with BPG have a preference for the *ap* conformer [51].

For secondary amines, amide derivatives with MTPA exhibit exceptionally large $\Delta\delta^{RS}$ values. A set of conformational rules have been established that take into account the presence of the two rotamers. With some secondary amines, differentiation is so large that only a single MTPA derivative is necessary [53, 54]. Recent work describes the utility of MTPA for assigning the absolute configuration of 2-arylpiperidines, one example of which is **35**. An interesting observation is that the preferred conformation of the piperidine ring is different in the (*R*)- and (*S*)-MTPA derivatives. Coupling of the H2 resonance is especially sensitive to the conformational difference and the shape of the multiplet can be used to assign the absolute configuration [55].

MPA has been used to assign the absolute configuration of hindered cyclic secondary amines such as **36**. *Syn*- and *anti*-rotamers are observed in the ^1H NMR spectrum and the *syn* rotamer is predominant. The H α resonance of the MPA moiety exhibits changes in its chemical shifts that correlate with the absolute configuration of the amine. Steric crowding inhibits the reaction of MTPA with the amine, recommending the use of MPA for these substrates [56].

CFTA is an effective chiral derivatizing agent for hindered α -chiral primary amines. CFTA was found to be about 500 times more reactive with amines than

MTPA. The *ap* conformer of the amide is more stable and $\Delta\delta^{RS}$ values in the ^1H and ^{19}F NMR spectra can be used to assign the absolute configuration [57].



Aryl-containing carboxylic acids can be used to assign the absolute configurations of diols, polyols, and amino alcohols. If the two functionalities are far enough apart from each other, the stereochemistry about each site can be analyzed independent of the other. In recent work, the configurations of both stereogenic centers of three different *trans*-*N*-benzylhydroxypiperidinemethanols (**37–39**) were assigned using bis-MTPA ester derivatives. The assignment was confirmed by X-ray crystallography [58]. If the sites are close together, the aryl rings of the two covalently coupled chiral reagents may both influence the chemical shifts of nearby nuclei and complicate the normal rules for determining absolute configuration.

In recent years, Riguera and coworkers have published a series of articles in which they have systematically and thoroughly explored the assignment of absolute configuration of diols, triols, and amino alcohols using systems such as MPA or 9-AMA. These include secondary,secondary-1,*n*-diols ($n = 2-5$), primary,secondary-1,2-diols, secondary,secondary-1,2-amino alcohols, secondary,primary- and primary,secondary-1,2-amino alcohols, and primary,secondary,secondary-1,2,3-triols. In each case they have been able to identify one or more ^1H signals of either the substrate or derivatizing agent that show a consistent trend in behavior that correlates with the relative and absolute configurations of the system. In many cases it is possible to compare the spectra at ambient and lower probe temperatures and observe specific changes that correlate with and provide additional confirmation of the absolute configuration. Instead of describing the studies on each individual system herein, a recent review article provides a comprehensive overview of the use of MPA, 9-AMA, and MTPA for assigning the absolute configuration of diols, triols, and amino alcohols [59].

A derivatization procedure referred to as the “mix-and-shake” method that employs polystyrene-bound chiral derivatizing agents such as MTPA, MPA, 9-AMA, BPG, and 2-NTBA has been developed. The resin, which is either in a single enantiomeric form or contains a combination of the (*R*)- and (*S*)-enantiomers at

unequal but known ratios, is mixed with the compound to be derivatized in an NMR tube and a solvent such as chloroform-*d*, acetonitrile-*d*₃, or carbon disulfide/methylene chloride-*d*₂. The report provides the exact conditions to use for each derivatization reaction. The mixture is shaken for several minutes to complete the reaction. The resin floats on the solvent so the NMR spectrum can be recorded without having to filter the sample. The efficacy of the procedure was demonstrated on chiral substrates with alcohol, amine, and thiol functionalities [60].

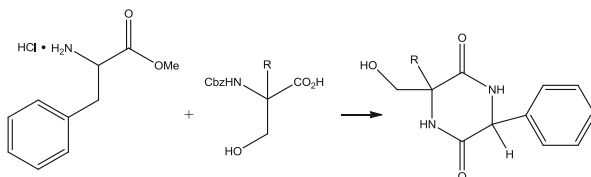
2-(Anthracene-2,3-dicarboximido)cyclohexane carboxylic acid (**40**) is noteworthy for its use in the analysis of primary and secondary alcohols with stereogenic centers that are remotely disposed from the carbinol site. The configuration of **40** places the aliphatic chain of the alcohol over the anthryl ring such that shielding of resonances occurs over a considerable number of carbon atoms of the aliphatic chain. For primary alcohols, non-equivalence in the NMR spectrum is observed as far away as the C9 group [61, 62]. For secondary alcohols, differentiation of a secondary alcohol with a chiral carbon at C16 and in which the two substituents differ by only one carbon is possible [63, 64]. Furthermore, the $\Delta\delta^{RS}$ values show trends that correlate with the absolute configuration for both primary [61] and secondary [65] alcohols. A recent application of **40** involves assigning the stereochemistry at C4 in 4,8-dimethylnonylsulfate (**41**). The sulfate group in **41** was converted to a hydroxyl group before analysis with **40** [47].

Several recent studies have used carboxylic acid-containing reagents for chiral NMR differentiation. *N*-(2-Nitrophenyl)proline (**42**) reacts with α -chiral primary amines. Two intramolecular hydrogen bonds lead to a stable *anti* conformation in the derivatives. One hydrogen bond is between the amide hydrogen and proline nitrogen. The other is a hydrogen bond between the 2-nitro and amide group. The preferred conformation positions the phenyl ring to cause predictable shielding. $\Delta\delta^{RS}$ values for a variety of amines containing different substituent groups are much larger than those with MTPA or MPA. Much smaller $\Delta\delta^{RS}$ values in the 4-nitrophenylproline derivatives, which cannot form the second hydrogen bond between the nitro and amide group, indicate the importance of this hydrogen bond in the effectiveness of the 2-nitrophenyl derivative. The intramolecular hydrogen bond and *anti* conformation are retained in solvents such as pyridine-*d*₅, acetone-*d*₆, methanol-*d*₄, acetonitrile-*d*₃, and dimethylsulfoxide-*d*₆ [66, 67].

The enantiomeric composition of a palladium dimer containing an α -ferrocenylethylphosphine unit (**43**) was determined by reaction with (*S*)-prolinate. Complexation of the prolinate with the dimer creates a monomeric species and the ³¹P NMR spectrum exhibits four singlets corresponding to differentiation of the planar chirality and stereogenic carbon center [68].

3-Arylcarbonyl-2,2-dimethylloxazolidine-4-carboxylic acids derived from serine (**44**) are effective chiral derivatizing agents for the analysis of chiral secondary alcohols. The amide functionality with benzoyl, 1-naphthoyl, and 2-naphthoyl groups in these pseudoproline reagents adopts a *cis* conformation. Reaction of **44** with secondary alcohols produces esters in which $\Delta\delta^{RS}$ values can be used to assign absolute configurations. The values are largest with the 2-naphthyl reagent

Fig. 2 Reaction of the methyl ester of phenyl alanine with Cbz derivatives of serine to form a diketopiperazine

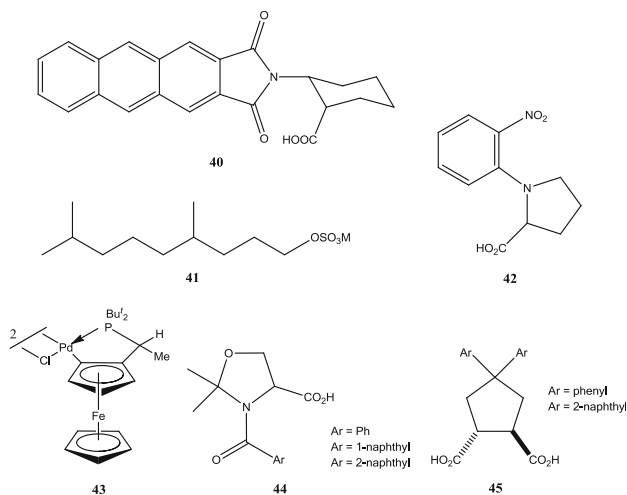


and the system is effective in acetone- d_6 , acetonitrile- d_3 , dimethylsulfoxide- d_6 , chloroform- d , toluene- d_8 , and methanol- d_4 [69].

The methyl ester of L- and D-phenyl alanine reacts with Cbz derivatives of α -substituted serines in a three-step process to form diastereomeric diketopiperazines as shown in Fig. 2. Shielding by the phenyl ring of the alanine causes very large $\Delta\delta^{RS}$ values for certain hydrogen atoms in the diketopiperazine, which facilitates assigning the absolute configuration of the original serine [70].

2,2-Diphenyl-[1, 3]-dioxolane-4,5-dicarboxylic acid and its corresponding 2-naphthyl derivative (**45**), which are cyclic ketals of tartaric acid, have been employed as chiral derivatizing agents for α -chiral primary amines. Two amines are coupled to **45** in the derivatization reaction. An intramolecular hydrogen bond stabilizes the conformation of the derivative. $\Delta\delta^{RS}$ values with the 2-naphthyl reagent are much larger than those observed with MTPA and MPA and can be used to assign the absolute configuration of the amine [71].

Tetrahydro-1,4-epoxynaphthalene-1-carboxylic acid (**46**) has been explored as a chiral derivatizing agent for chiral secondary alcohols. The derivative adopts an *sp* conformation. $\Delta\delta^{RS}$ values can be used to assign the absolute configuration. Eleven alcohols were tested, but the $\Delta\delta^{RS}$ values were generally smaller than those with MPA [72].



2.2 Anhydrides

(1-Naphthyl)(trifluoromethyl) *O*-carboxy anhydride (**47**) is an effective chiral derivatizing agent for α -chiral primary amines. The resulting α -hydroxyamide has an eclipsed conformation that is held in place through an intramolecular hydrogen bond. The corresponding compound with a methoxy group in place of the hydroxyl group has a staggered conformation and is not nearly as useful for chiral analysis. $\Delta\delta^{RS}$ values are larger than those obtained with MTPA, MPA, and NPP [73].

The stereochemistry of glucose and galactose formed by hydrolyzed products of polysaccharides produced by *Streptococcus thermophilus* were assigned using ^1H NMR of the per-*O*-(*S*)-2-methyl butyrate derivatives. The derivatives were prepared using (*S*)-2-methylbutyric anhydride and compared to monosaccharides of known configuration. A combination of ^1H , ^{13}C , and 2D NMR methods were used in analyzing the mixtures and assigning the stereochemistry [74].

2.3 Alcohols

Enantiomerically pure alcohols have the potential to be used as chiral derivatizing agents for chiral carboxylic acids. Among those that have been used for this purpose, ethyl-2-(9-anthryl)-2-hydroxyacetate (**48**) is especially useful for the analysis of α -chiral carboxylic acids. The derivatives adopt an *ap* conformation. The effectiveness of 9-AHA was compared to several other aryl alkyl alcohols and, except for *trans*-2-phenyl-1-cyclohexanol, 9-AHA caused the largest $\Delta\delta^{RS}$ values [75].

2,2,2-Trifluoro-1-(9-anthryl)ethanol (**49**), commonly known as Pirkle's alcohol, is often used as a chiral NMR solvating agent. It is also possible to derivatize carboxylic acids with **49** and use the $\Delta\delta^{RS}$ values of the corresponding esters to assign absolute configuration. Such a procedure was used to determine the stereochemistry in *trans* α -benzyl paraconic acid (**50**). The procedure was unsuccessful with the corresponding *cis*-isomer as there was no reaction with either enantiomer of **49** [76].

A strategy for assigning the stereochemistry of glycosides is to hydrolyze them to the corresponding monosaccharides and derivatize them with (*R*)- or (*S*)-2-butanol. Characteristic trends in the chemical shifts in the ^1H and ^{13}C NMR spectra are used in making the assignment. A protocol for rapid and automatic analysis and assignment of the data of the 2-butanol derivatives of monosaccharides using software called CASPAR has been described. Either 2-butanol enantiomer can be used and ^1H , ^{13}C , and/or ^1H - ^{13}C -HSQC data are needed. The software reports back structures and ranks them according to how well they fit the data. No prior assignment of the NMR data is needed [77].

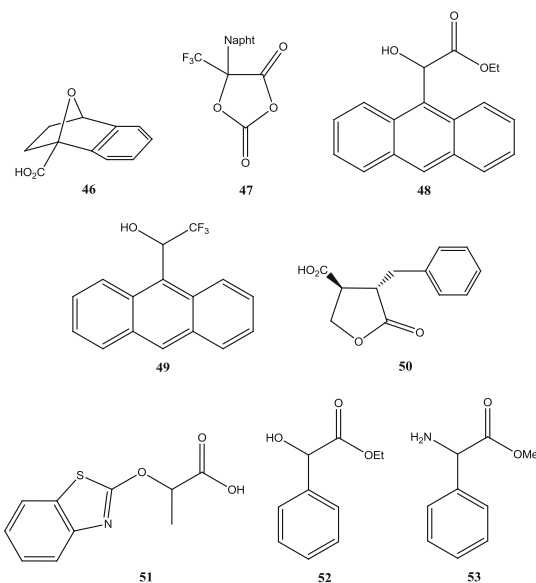
2-Octanol derivatives of β -glycopyranosides and α -arabinopyranosides produce specific trends in ^1H data that correlate with absolute configuration. If the absolute configuration of the attached monosaccharide is known, the ^1H NMR of the alicyclic peracetylated glycoside can also be used to assign the configuration at

the aglycone moiety. The method was applied to marine steroid glycosides and acetates that contained glycosylated side chains as alicyclic fragments [78].

A series of α -substituted chiral carboxylic acids that are derivatives of clofibric acid, one example of which is **51**, were examined as esters of ethylmandelate (**52**). The derivatives adopt a conformational preference that is supported by density functional theory calculations. $\Delta\delta^{RS}$ values of the ethylmandelate derivatives could be used to assign the absolute configurations of the carboxylic acids [79].

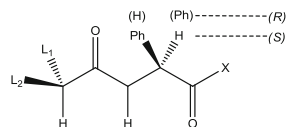
2.4 Amines

Several chiral amines have been used successfully for the assignment of absolute configuration of chiral carboxylic acids. Most notable among the many amines that have been studied is phenylglycine methyl ester (**53** – PGME) [80]. X-Ray and NOE data confirm that amide derivatives of PGME adopt the conformation shown in Fig. 3, which then leads to predictable signs for the $\Delta\delta^{RS}$ values of the two substituent groups [81]. The use of PGME for assigning the absolute configuration of carboxylic acids has been reviewed [5, 82].

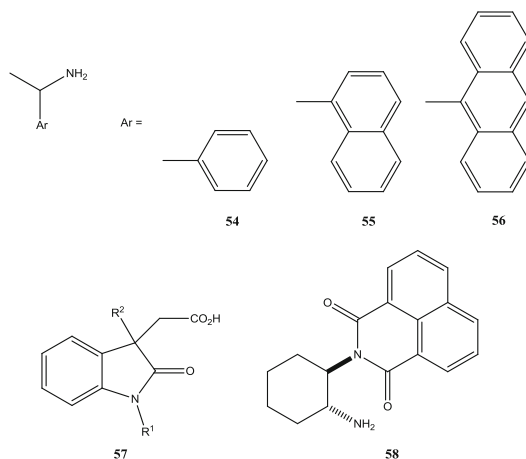


Amides of three related compounds, 1-phenylethylamine (**54** – PEA), 1-(1-naphthyl)ethylamine (**55** – NEA), and 1-(9-anthryl)ethylamine (**56** – AEA), have also been used quite frequently for assigning the absolute configuration of α -chiral carboxylic acids. Amides of PEA, NEA, and AEA have major and minor rotamers that must be considered in the analysis of the spectra. The $\Delta\delta^{RS}$ values usually vary in the order AEA > NEA > PEA [83]. AEA is not commercially available, and PEA and

Fig. 3 Conformational preference of PGME amide derivatives of α -chiral carboxylic acids



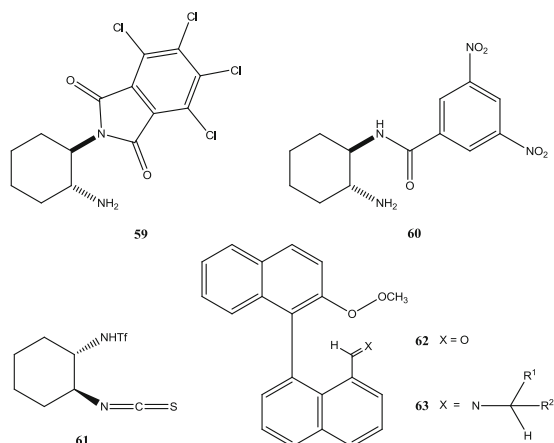
NEA have been used more frequently for enantiomeric analysis. They have also been used in the analysis of β -chiral carboxylic acids [84, 85]. In recent studies, PEA amides have been used to assign the absolute configuration at the C3 stereogenic center of 3-(2-oxo-3-indolyl)acetic acids (**57**). The derivatives have a preference for *ap* (C=O)–(N–H)–(C–H) arrays. The N1-methyl, C3-methyl, and H8A signals are particularly diagnostic in making the assignment. X-Ray structural data confirmed the reliability of the NMR method [85].



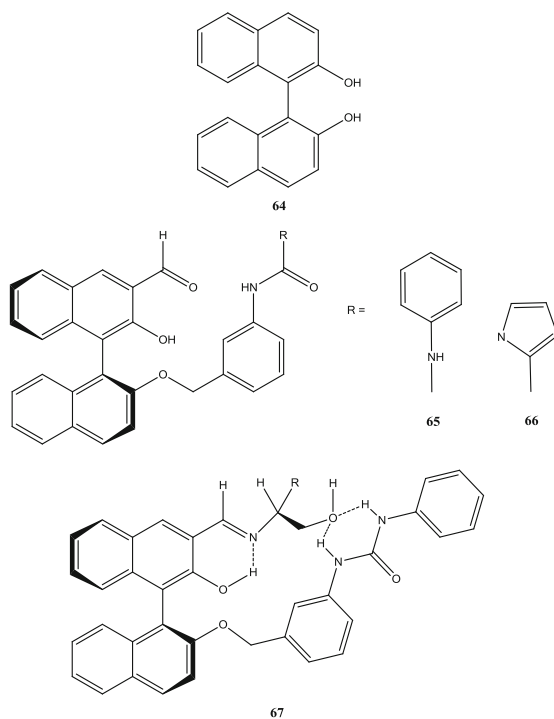
58, **59**, and **60**, which are prepared from either (*R,R*)- or (*S,S*)-*trans*-1,2-diaminocyclohexane, react with the carboxylic acid moiety of *N*-Boc α -amino acids. The resulting amide derivatives have a preferred conformation in which the CH–NH–C(O)–CH unit has an *anti*-orientation. $\Delta\delta^{RS}$ values for the *tert*-butyl resonance and R group of the amino acid can be used to assign the absolute configuration. The largest $\Delta\delta^{RS}$ values are observed with **58**. Reaction of **58–60** with triphosgene converts the amine to an isocyanate group. The isocyanates of **59** and **60** react with the amine functionality of α -amino acid esters and $\Delta\delta^{RS}$ values of the corresponding urea derivatives can be used to assign the absolute configuration [86].

2.5 Miscellaneous Reagents

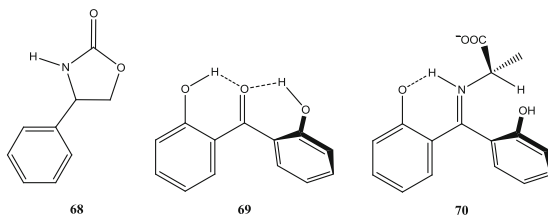
(1*S*,2*S*)-*N*-[(2-Isothiocyanto)cyclohexyl] trifluoromethanesulfonamide (**61**) has been used as a chiral derivatizing agent for determining the enantiomeric composition of α -chiral primary and secondary amines. The ^{19}F NMR spectrum of the thiourea derivatives is conveniently monitored [87].



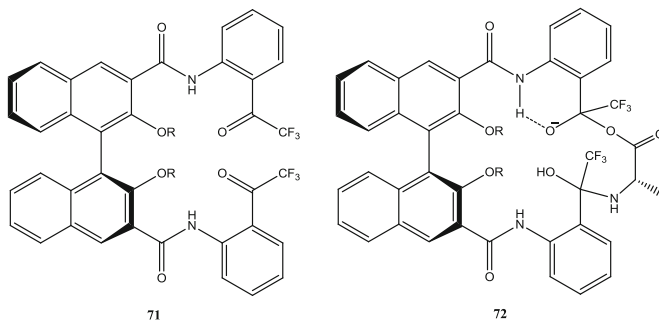
Reaction of 2'-methoxy-1,1'-binaphthalene-8-carbaldehyde (**62**) with amines produces the corresponding imine (**63**). Shielding from the second naphthalene ring causes $\Delta\delta^{RS}$ values that can be used to assign the absolute configuration of the amine. The method was demonstrated on several substrates including amino acids and cyclic chiral amines [88]. 2,2'-Dihydroxy-1,1'-binaphthalene (**64** – BINOL) based receptors **65** [89] and **66** [90] have aldehyde groups that can form imine derivatives with 1,2-amino alcohols. **67** shows the resulting product of the reaction of **65** with a 1,2-amino alcohol. Intramolecular hydrogen bonding in **67** constrains the motion of the derivative and results in enantioselective recognition of the substrates.



A procedure for assigning the absolute configuration of 2-oxo-3-indolylicetic acids (**57**) using (*R*)- or (*S*)-2-phenyl-2-oxazolidinone (**68**) as a chiral derivatizing agent has been reported. The carboxylic acid reacts at the NH group of the oxazolidinone to produce an amide. Shielding by the phenyl ring of the oxazolidinone moiety causes predictable $\Delta\delta^{RS}$ values that correlate with the absolute configuration. X-Ray structures of some of the derivatives confirm the NMR results and efficacy of the procedure [91].

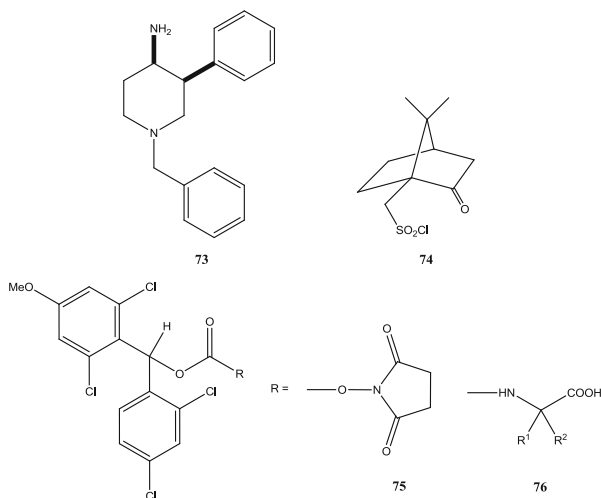


Tetramethylammonium salts of α -amino acids such as alanine react with helically chiral 2,2'-dihydroxybenzophenone (**69**) to form the corresponding imine (**70**). The conformation of the derivative is constrained by intramolecular hydrogen bonding and splitting of signals is observed in a protic solvent like methanol-*d*₄ [92].



Compound **71** is a C_2 -symmetric homoditopic receptor that forms adducts (**72**) with α -amino acids through the formation of reversible covalent bonds. Only one adduct forms in the reaction, and splitting of signals in the ^1H and ^{19}F NMR can be used to differentiate the enantiomers. The differentiation in the ^{19}F signals correlates with absolute configuration [93].

Reaction of *cis*-4-amino-1-benzyl-3-phenylpiperidine (**73**) with camphor sulfonyl chloride (**74**) produces the corresponding camphor sulfonamide. The two methyl singlets of the camphor moiety split in the sulfonamide derivatives, enabling the determination of the enantiomeric composition of the amine [94].



A carbonate of (2,6-dichloro-4-methoxyphenyl)(2,4-dichlorophenyl)methanol (**75**) undergoes reactions with free amino acids to produce the corresponding carbamate derivative (**76**). A 3:1 mixture of (*S*)-(**75**) and (*R*)-(**75**) is used in the procedure. Over 50 substrates including α -amino acids, α,α -disubstituted amino acids, one β -amino acid, and amino alcohols were examined and all showed a consistent trend in the NH resonance that correlates with absolute configuration [95].

2.6 Phosphorus-Containing Reagents

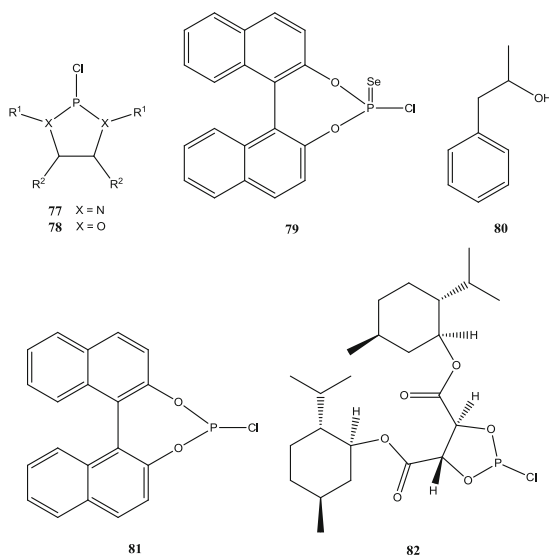
Many phosphorus-containing reagents have been explored for applicability as chiral NMR derivatizing agents. The majority of these are used for the determination of enantiomeric composition. Usually the ^{31}P NMR spectrum consists of a single resonance that splits into two when diastereomers form in the derivatization reaction. Most of the reagents have a chiral moiety attached to the phosphorus atom and a P–Cl group that reacts rapidly with alcohols and amines, such that most derivatization reactions can be performed directly in the NMR tube. The reagents can be used in either the P(III) or P(V) form. The P(III) species usually has larger differentiation between the ^{31}P signals of the two diastereomers, but the P(V) species are usually more stable in solution. When integrating the phosphorus signals to determine enantiomeric composition, it is important to recognize that the relaxation times may be different for the two diastereomers and appropriate delay times need to be employed [96]. The use of phosphorus-containing chiral derivatizing agents has been comprehensively reviewed [5, 97].

Two common families of phosphorus-containing reagents involve complexes with chiral diamine (**77**) or diol (**78**) moieties. These reagents are usually prepared by reaction of the diamine or diol with phosphorus trichloride. Many examples of

these that have been examined and their effectiveness are discussed in recent review articles [5–7]. Only the most recent work in this area will be included herein.

A recent study used a phosphoroselenenyl reagent with BINOL (**79**) to determine the enantiomeric composition of alcohols and amines. Either the ^{31}P or ^{77}Se NMR spectrum can be used for the analysis [98]. Derivatization of 1-aryl-2-propanols (**80**) with **79** produces trends in the ^1H , ^{13}C , ^{31}P , and ^{77}Se NMR spectra that correlate with absolute configuration [99]. (*S*)-(1,1'-Binaphthalen-2,2-dioxy)chlorophosphine (**81**), a reagent identical to **79** without the selenium, is effective for determining the enantiomeric composition of alcohols, amines, and *N*-Boc amino acids. Enantiomeric differentiation in the ^{31}P NMR spectrum was largest for alcohols and smallest for carboxylic acids. **81** can also be used to analyze the enantiomeric composition of ketones. In one procedure a transfer hydrogenation is used to convert the ketone to an alcohol, which is then reacted with the phosphorus reagent. In another procedure the ketone is subjected to an asymmetric hydrosilylation before reaction with the phosphorus reagent [100].

2-Chloro-(4*R*,5*R*)-bis[(1*S*,2*S*,5*R*)-menth-1-yloxy]carbonyl]-1,3,2-dioxaphospholane (**82**), which is prepared by reacting PCl_3 with bis[(1*R*,2*S*,5*R*)-menth-1-yl]tartrate, is effective for determining the enantiomeric composition of chiral primary, secondary, and tertiary alcohols using the ^{31}P NMR spectrum. The reaction is run directly in an NMR tube in chloroform-*d*/THF and only requires a few minutes. The complex is largely inert toward moisture and is stored in anhydrous THF after preparation [101]. In more recent work, the effectiveness of bornenyl and fenchyl tartrates similar in structure to **82** were prepared and compared to **82**. The menthyl reagent was judged the most versatile and could be stored in contact with air for 24 h without much degradation [102].



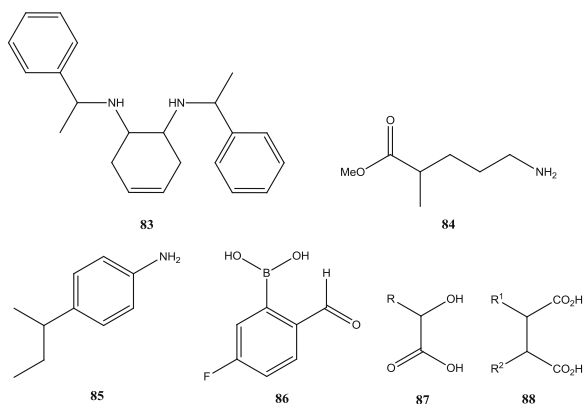
A phosphorus reagent of structure **77** prepared using (1*R*,2*R*)- and (1*S*,2*S*)-*trans*-*N,N'*-bis[(*S*)- α -phenylethyl]cyclohexane-1,2-diamine and the corresponding

4-cyclohexene derivative (**83**) has been used to determine the enantiomeric composition of α - and β -chiral carboxylic acids. The diamine and PCl_3 are mixed together in an NMR tube after which the carboxylic acid is added. The ^{31}P NMR spectrum can be recorded on the P(III) species or elemental sulfur can be added to generate the P(V) species. Enantiomeric differentiation is greatest for the P(III) species of the (*S,R,R,S*)-cyclohexene moiety, although the P(V) species is more stable [103].

2.7 Boron-Containing Reagents

A variety of boron-containing reagents have been employed as chiral NMR differentiating agents and the use of these is covered in recent reviews [5–7]. Many of these reagents are mostly suitable for the analysis of either diols or primary amines.

2-Formylphenylboronic acid, a diol, and an amine react as shown in Fig. 4. If an enantiomerically pure alcohol such as (*R*)- or (*S*)-BINOL is used, then the enantiomeric composition of the amine can be determined [104, 105]. This system has been used to assign the configuration of β -chiral primary amines as well as **84** and **85**, both of which have stereogenic centers at remote positions relative to the amine group [106]. Alternatively, an enantiomerically pure amine such as PEA can be used and the enantiomeric composition of the diol can be determined [107]. Detailed protocols for using this system have been reported [104, 107]. Using 4-fluoro-2-formylphenylboronic acid (**86**) in the procedure allows the use of the ^{19}F signals for determining the enantiomeric composition [108].



The combination of 2-formylphenylboronic acid with (*R*)-PEA has been used to determine the enantiomeric composition of chiral α -hydroxy acids (**87**). Alternatively, the use of (*S*)-mandelic acid (**3**) allows the enantiomeric composition of chiral primary amines to be determined with this system [109]. The same procedure with 2-formylphenylboronic acid with enantiomerically pure PEA can be used to determine the enantiomeric composition of chiral acyclic (**88**) and cyclic (**89**) diacids [110]. The enantiomeric composition of amines can be determined if

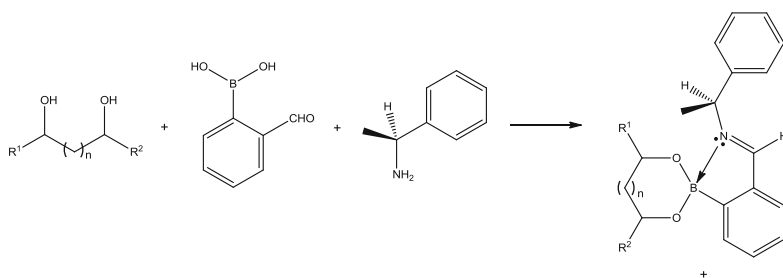


Fig. 4 Borate–imine complex formed by the reaction of a diol, 2-formylphenylboronic acid, and 1-phenylethylamine

enantiomerically pure *trans*-1,2-cyclohexane dicarboxylic acid (**90**) is employed in the boron reagent [110].

2-Formylphenylboronic acid has also been used in a procedure to analyze the enantiomeric composition of 1,2-amino alcohols. Enantiopure (*syn*)-methyl-2,3-dihydroxy-3-phenylpropionate (**91**) is used as the diol in creating the chiral reagent. The hydroxyl group of the amino alcohol is silylated with *tert*-butyldimethylsilyl chloride and an imine derivative is formed by reaction of the amine functionality with the aldehyde on the 2-formyl phenyl ring [111].

A procedure for assigning the absolute configuration of α - (**87**) and β -hydroxyacids using a boron reagent has been developed. One equivalent of $\text{B}(\text{OMe})_3$, the hydroxy acid, and (*R*)- or (*S*)-BINOL are mixed with 3 equiv. of triethylamine and reacted directly in an NMR tube. Molecular sieves are added to remove water. The naphthyl rings on the BINOL give predictable $\Delta\delta^{RS}$ values for the H_α and H_β methine protons on the α - or β -hydroxyacid, respectively [112].

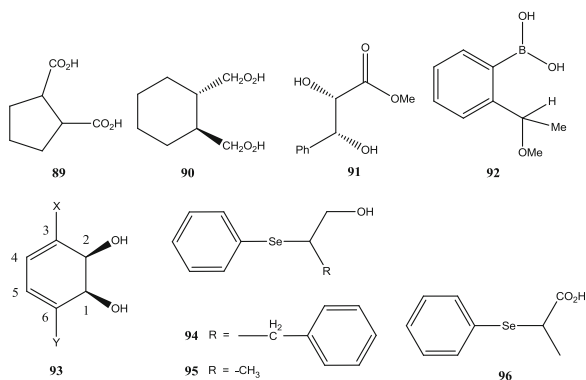
Boronate esters of (*R*)- or (*S*)-2-(1-methoxyethyl)phenylboronic acid (**92**) have been used to determine the enantiomeric composition of chiral *cis*-1,2-diols (**93**) with substituent groups at the 4,6- and 3,4-positions [113] and the 3,6-position [114]. In some cases, attempts at using di-MTPA esters are ineffective either because the products do not form or are unstable [114].

Data from three boronic acids used in combination with three pH indicators were incorporated into a sensor array for 1,2-secondary, secondary diols. The array consists of a series of patterns for different diols. The data set is recorded for a diol with an unknown configuration and pattern recognition techniques identify the best match. It is especially effective for *threo* diols and allows for the simultaneous determination of their identity, enantiomeric composition, and concentration [115].

2.8 Selenium-Containing Reagents

Recent studies have used selenium-containing reagents for determining enantiomeric composition. One employed (*S*)-3-phenyl-2-(selenophenyl)propan-1-ol (**94**) as a chiral derivatizing agent for carboxylic acids. The reaction is run directly in the

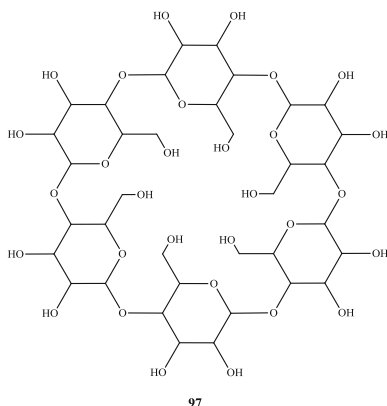
NMR tube. Differentiation in the ^{77}Se NMR spectrum is larger than that observed with the analogous (*S*)-2-(selenophenyl)propan-1-ol (**95**) [116].



(*R*)-2-Phenylselenopropanoic acid (**96**) has been used as a chiral derivatizing agent for chiral alcohols and amines. Derivatization is performed in chloroform-*d* in an NMR tube. Solid byproducts float on the solvent and do not interfere with the spectrum. Enantiomeric differentiation in the ^{77}Se NMR spectrum is monitored [117].

3 Macrocycles

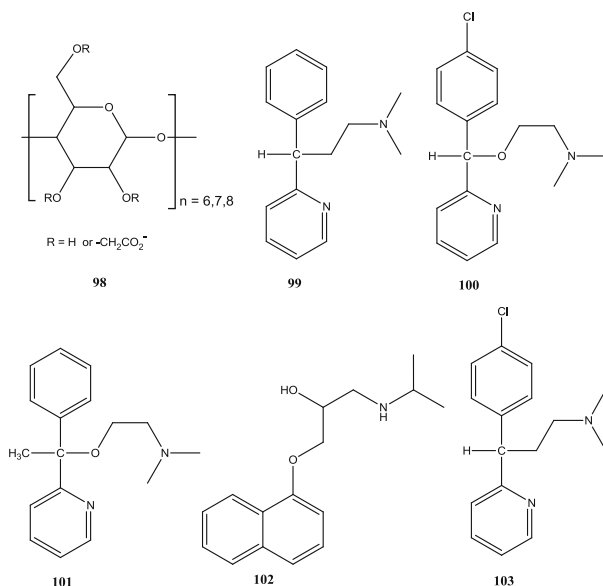
3.1 Cyclodextrins



Cyclodextrins are cavity compounds comprised of six (α) (**97**), seven (β), or eight (γ) glucose units. Secondary hydroxyl groups at the 2- and 3-positions are at

the wider opening of the cavity, whereas primary hydroxyl groups at the 6-position are at the smaller opening to the cavity. Underivatized native α - and γ -cyclodextrin are highly water-soluble. β -Cyclodextrin is soluble to a lesser degree in water (approximately 20 mM), but is soluble enough for NMR studies. The different sizes of the α -, β -, and γ -cyclodextrin cavity allows for the study of a diverse variety of substrates. Differentiation of chiral substrates that insert into the cavity usually occurs through different interactions of the enantiomers with the secondary hydroxyl groups. Alkylations and/or acylations of the hydroxyl groups have been used to prepare a wide variety of cyclodextrin derivatives, many of which have been examined as chiral NMR differentiating agents [5].

Several studies have shown that anionic cyclodextrin derivatives are more effective at causing enantiomeric differentiation in the NMR spectra of cationic substrates than native cyclodextrins [5]. An early study examined commercially available sulfated and carboxymethylated (**98**) β -cyclodextrin derivatives. The sulfate derivative had a high degree of substitution of sulfate groups (nine in β -cyclodextrin), whereas the degree of substitution of the carboxymethyl groups was lower (3.5 in β -cyclodextrin). These anionic reagents produce greater enantiomeric differentiation in the ^1H NMR spectra of the ammonium salts of pheniramine (**99**), carbinoxamine (**100**), doxylamine (**101**), and propranolol (**102**) than native cyclodextrins. The H3 and H5 hydrogen atoms are inside the cyclodextrin cavity and perturbations in the chemical shifts of these resonances indicate that **99–102** insert into the cavity. Ion pairing between the cationic substrate and anionic groups on the cyclodextrin likely accounts for the improved enantiomeric differentiation compared to native cyclodextrins [118].



In subsequent work, synthetic procedures to incorporate carboxymethyl groups selectively at the 6-position, 2-position, and indiscriminately at the 2-, 3-, and 6-positions of α -, β -, and γ -cyclodextrin were described [119]. Comparative studies of these water-soluble systems on a wide range of cationic substrates show that the indiscriminately-substituted derivatives, which have the highest degree of substitution of carboxymethyl groups, always produce the largest enantiomeric differentiation in the ^1H NMR spectrum [119–121]. Substrates include hydrochloride salts of aryl-containing amines (**104**), aryl-containing amino alcohols (**105**) [120], and aromatic amino acids [121]. Figure 5 shows a portion of the ^1H NMR spectrum of chlorpheniramine (**103**) in the presence of neutral α -cyclodextrin (Fig. 5b) and an indiscriminately-substituted carboxymethylated α -cyclodextrin (Fig. 5c). Large enantiodifferentiation of the H3' and H4' resonances of the pyridyl ring of **103** is observed in the presence of the carboxymethylated α -cyclodextrin. The neutral α -cyclodextrin causes no enantiodifferentiation of the resonances of any hydrogen atoms of **103**.

Other studies have examined the coupling of paramagnetic lanthanide ions to cyclodextrins to enhance enantiomeric differentiation in the ^1H NMR spectra of substrates. A synthetic scheme in which diethylenediaminepentaacetic acid (DTPA) is bound to the primary (6-position) and secondary (2-position) side of cyclodextrin through an ethylenediamine (EN) [122] (Fig. 6) or amine (NH) [123] linker has been described. When dysprosium(III) nitrate is added to the DTPA derivatives of the cyclodextrin, it binds to the DTPA moiety and causes significant perturbations and substantial enhancements in enantiomeric differentiation in the NMR spectrum of the substrate. For the EN derivative, incorporation of the Dy(III)-DTPA at the 2-position is much more effective than the derivative with Dy(III)-DTPA at the 6-position [122]. Presumably the closer proximity of the Dy(III) to the chiral recognition sites in the secondary derivative accounts for this observation. In some cases, broadening from the paramagnetic dysprosium(III) is significant but recording spectra at 50°C causes substantial reduction of the broadening without eliminating enantiomeric differentiation.

The primary NH-linked Dy(III)-DTPA derivative causes larger lanthanide-induced shifts and enhances the enantiomeric differentiation compared to the primary EN-linked Dy(III)-DTPA derivative. The closer distance of the dysprosium(III) to the cavity in the primary NH derivative likely accounts for this observation. The NH derivative with Dy-DTPA at the 2-position is less effective than the corresponding EN derivative. The Dy(III)-DTPA is closer to the opening of the cavity in the NH derivative and appears to block access of the substrate to the cavity [123].

Lanthanide ions also associate with the anionic groups of sulfated and carboxymethylated cyclodextrins. The addition of dysprosium(III) nitrate or ytterbium(III) nitrate to commercially available sulfated and carboxymethylated cyclodextrins causes enhancements in the enantiomeric differentiation in the ^1H NMR spectra of cationic substrates [118, 124]. For indiscriminately-substituted

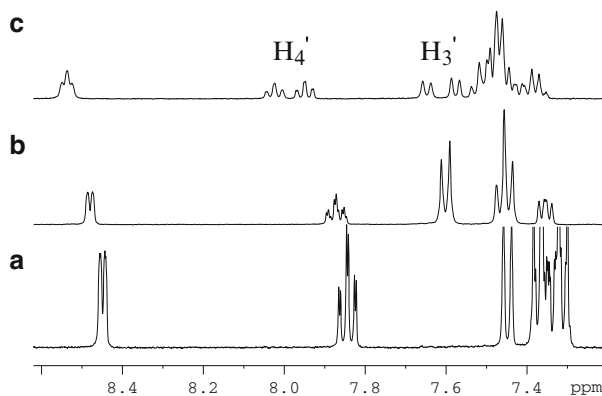


Fig. 5 ^1H NMR spectrum (400 MHz, D_2O , 23°C) of the aromatic region of (a) 10 mM chlorpheniramine (**103** – racemic mixture) with (b) 10 mM α -cyclodextrin and (c) 10 mM carboxymethylated α -cyclodextrin

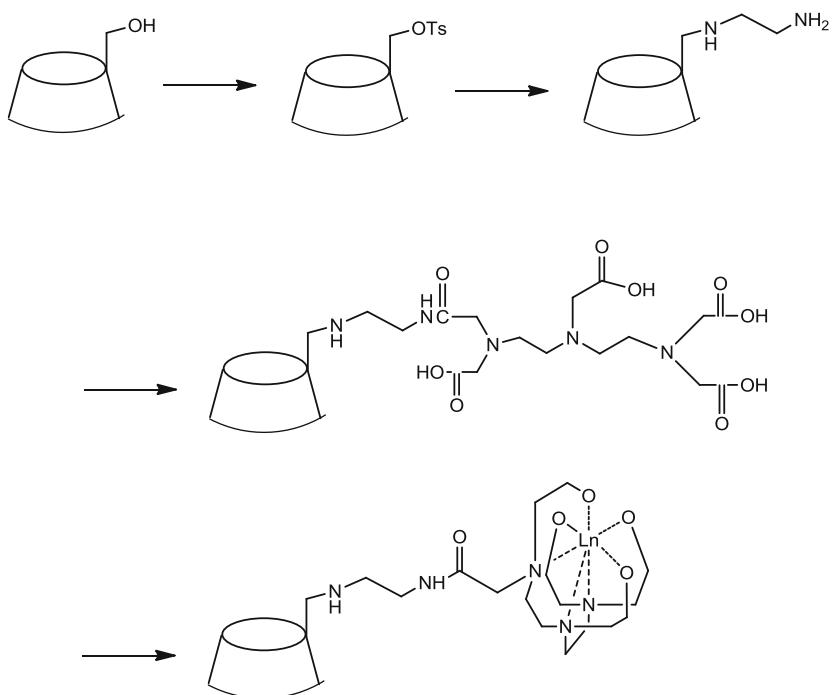
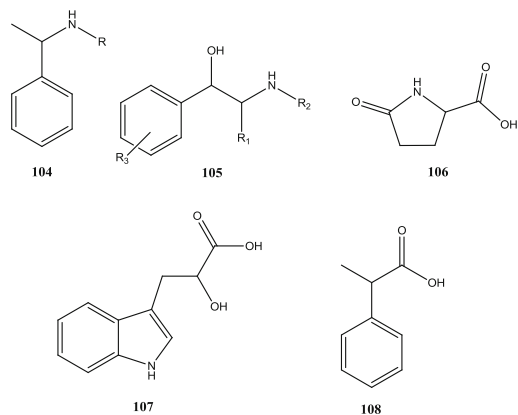


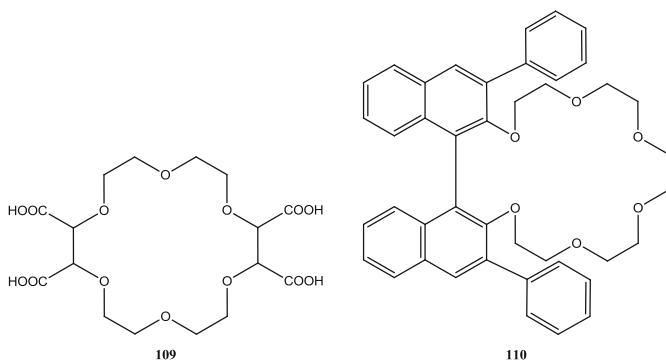
Fig. 6 Scheme used to couple lanthanide ions to cyclodextrins through a DTPA amide unit

carboxymethylated cyclodextrins with high degrees of substitution, the addition of praseodymium(III) nitrate or ytterbium(III) nitrate causes pronounced improvements in enantiomeric differentiation in the ^1H NMR spectra of a wide range of cationic substrates [120, 121].



It has also been shown that water-soluble cationic cyclodextrins are more effective for anionic substrates than native cyclodextrins. Cationic cyclodextrins were prepared by reacting glycidyl trimethylammonium chloride with α -, β -, and γ -cyclodextrin as shown in Fig. 7. An advantage of the system in Fig. 7 is that the quaternary amine retains a positive charge irrespective of the pH. Degrees of substitution ranging from one to three per glucose ring are achieved by varying the reaction conditions. Derivatives with degrees of substitution of 1–1.5 are most effective at causing enantiomeric differentiation in the ^1H NMR spectra of anionic substrates. A wide range of substrates such as sodium salts of aryl-containing amino acids, pyroglutamic acid (**106**), 3-indolelactic acid (**107**), 2-phenylpropanoic acid (**108**), and others have been examined [125].

3.2 Crown Ethers



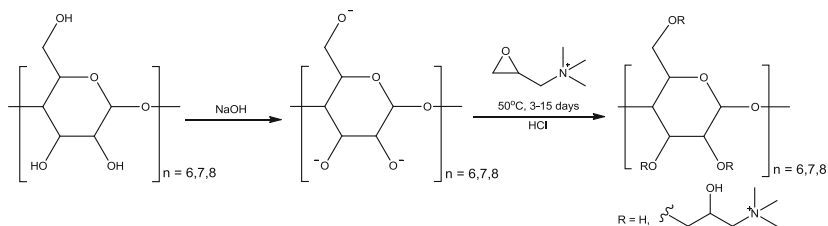
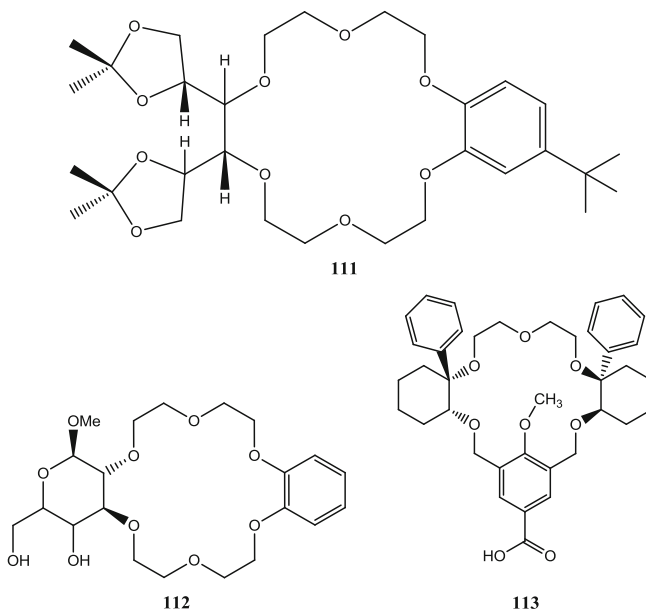


Fig. 7 Preparation of cationic cyclodextrins

A wide variety of crown ethers have been evaluated as chiral NMR differentiating agents for primary amines [5]. Protonated primary amines form three hydrogen bonds to oxygen atoms of 18-crown-6 ethers as shown in Fig. 8. Most notable of the crown ethers that have been examined in NMR applications is (18-crown-6)-2,3,11,12-tetracarboxylic acid (**109**), both isomers of which are commercially available. In comparative studies the enantiomeric differentiation in the ^1H NMR spectra of substrates with **109** is larger than observed with other notable crown ethers (**110–113**) that have been studied in NMR applications [126–130].



109 is effective for α -amino acids [130–132], aryl-containing primary amines, amino alcohols, 1-cyclohexylethylamine (**114**) [130], and α -methylamino acids [131]. The largest enantiomeric differentiation is usually observed in methanol- d_4 . The amine substrate can be used in its protonated (e.g., hydrochloride salt of the amine) or neutral form. When a neutral amine is mixed with **109**, a neutralization

Fig. 8 Interaction of a protonated primary amine with an 18-crown-6 ether

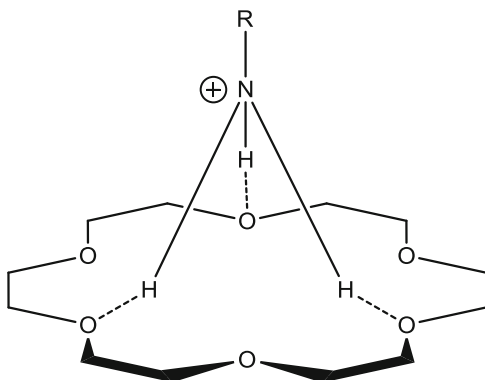
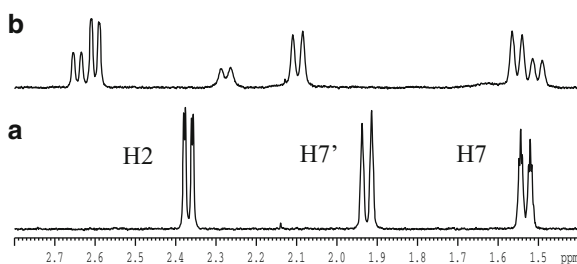


Fig. 9 ^1H NMR spectrum (400 MHz, methanol- d_4 , 23°C) of (1) the aliphatic region of **117** [10 mM – enriched in (1*R*,2*R*,3*S*,4*S*)] with **109** at 5 mM

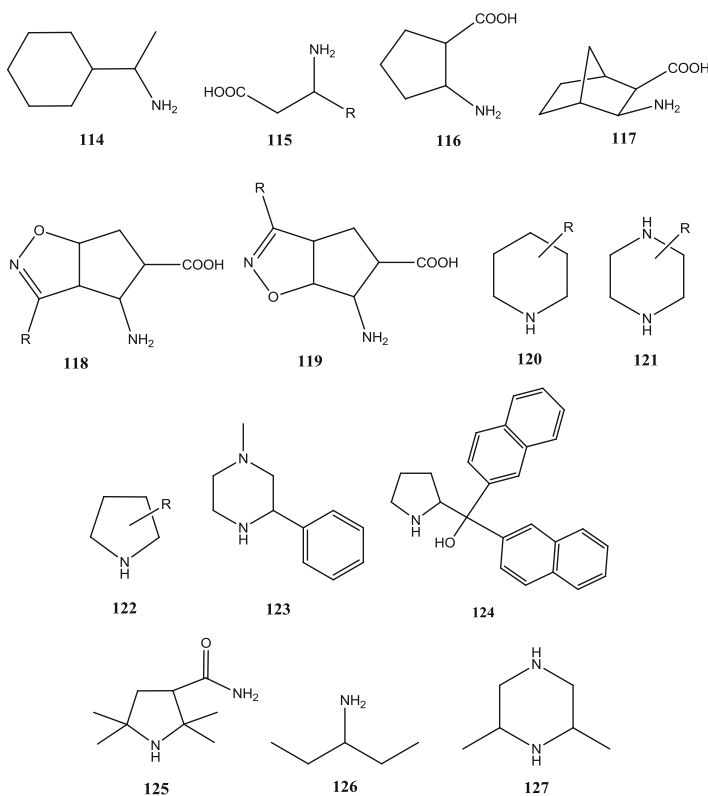


reaction between a carboxylic acid group of **109** and the amine occurs to produce the protonated amine needed for favorable association with the crown ether [130]. The addition of paramagnetic ytterbium(III) to mixtures of protonated primary amines and neutral **109** in methanol- d_4 causes enhancements in enantiomeric differentiation. The ytterbium(III) binds to the carboxylic acid moieties of **109** and causes perturbations in the NMR spectra of the bound substrate.

Recent work has demonstrated the effectiveness of **109** for the analysis of β -amino acids (**115**) that have a variety of aliphatic or aromatic substituent groups. Substantial enantiomeric differentiation of the methylene and methine resonances of the β -amino acid is observed. Furthermore, the methylene and methine resonances show specific trends that correlate with absolute configuration [133]. **109** is also an effective chiral NMR differentiating agent for cyclic β -amino acids with cyclopentane (**116**), cyclopentene, cyclohexane, cyclohexene, bicyclo[2.2.1]heptane, and bicyclo[2.2.1]heptene rings (**117**). Figure 9b shows a portion of the ^1H NMR spectrum of **117** in the presence of **109**. Enantiomeric differentiation of the H2, H7, and H7' resonances is apparent and is especially large for H7'. The neutral β -amino acid is mixed with **109** in methanol- d_4 . Resonances of the hydrogen atoms α to the amine and carboxylic acid groups exhibit enantiomeric differentiation in every substrate, and some show trends that correlate with absolute configuration [134]. **109** is also effective for isoxazoline-fused β -amino acids (**118**,**119**). Protonated salts of **118** and **119** are mixed with **109** in methanol- d_4 . Enantiomeric differentiation of two or more resonances is observed in the ^1H NMR spectrum of each substrate [135].

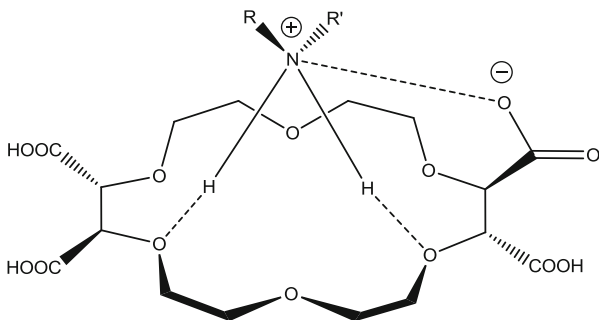
Chiral 18-crown-6 ethers are usually ineffective at binding to and causing enantiomeric differentiation in the NMR spectra of secondary amines. Secondary amines exhibit weaker binding to 18-crown-6 ethers because they can only form two hydrogen bonds. Steric hindrance from the second substituent group on the amine also reduces the binding of secondary amines to 18-crown-8 ethers relative to primary amines. However, **109** exhibits strong binding to secondary amines provided it is mixed with a neutral amine.

Mixing **109** with a neutral secondary amine leads to a neutralization reaction that produces a carboxylate of **109** and a cationic protonated amine. Interaction of **109** and the protonated secondary amine involves two hydrogen bonds and an ion pair as shown in Fig. 10. **109** is an exceptionally effective chiral NMR differentiating agent for secondary amines [136–139]. This includes aryl- and alkyl-containing secondary amines [136, 139], piperidines (**120**), piperazines (**121**) [137], and pyrrolidines (**122**) [138]. Enantiomeric differentiation is even observed in piperazines (**123**) and pyrrolidines (**124**, **125**) that have high degrees of steric hindrance.



109 also causes enantiomeric differentiation in the ^1H NMR spectra of prochiral amines such as 2-aminopentane (**126**) and 2,5-dimethylpiperidine (**127**) in the ^1H and ^{13}C NMR spectra of tertiary amines. Enantiomeric differentiation in the NMR spectra

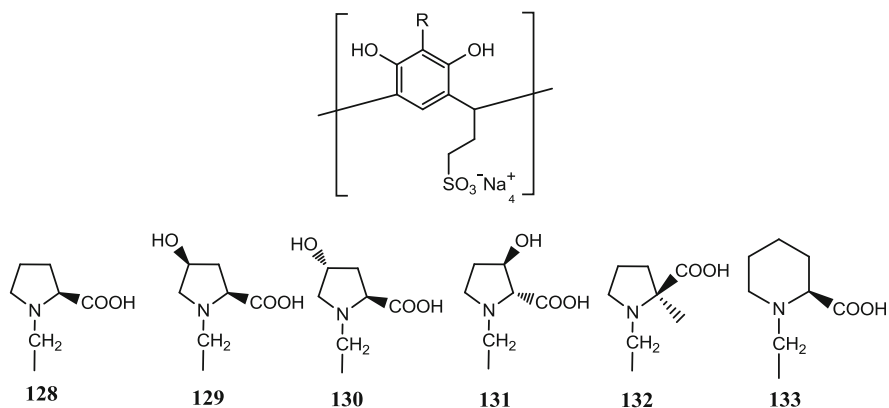
Fig. 10 Interaction of a protonated secondary amine with the carboxylate ion of **109**



of tertiary amines with **109** is much less than in primary and secondary amines, but is still sufficient for determining enantiomeric composition. ^{13}C NMR spectra are best for examining enantiomeric differentiation of tertiary amines with **109** [139].

3.3 Calix[4]Resorcinarenes

Calix[4]resorcinarenes are cavity compounds formed by the reaction of resorcinol with an aldehyde as shown in Fig. 11. Varying the R group on the aldehyde facilitates the solubilization of calix[4]resorcinarenes in a wide range of solvents. Reaction of the calix[4]resorcinarene with a secondary amine and formaldehyde adds an amine substituent to the resorcinol ring as shown in Fig. 12. Calix[4]resorcinarenes have several possible conformations caused by flipping of the aryl rings. If all the rings have the same orientation, a cone-shaped cavity compound results. Water-soluble derivatives prepared using a sulfonated aldehyde and L-proline (**128**) [140–142], hydroxyl-L-proline (**129–131**) [143–146], α -methylproline (**132**) [147, 148], and L-pipecolic acid (**133**) [149, 150] groups have been evaluated as chiral NMR differentiating agents.



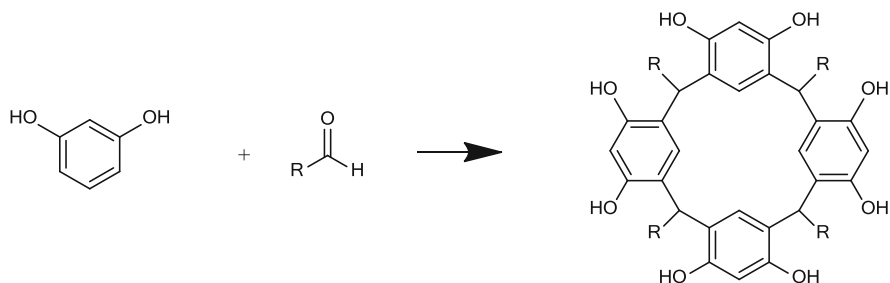


Fig. 11 Reaction of resorcinol with an aldehyde to form a calix[4]resorcinarene

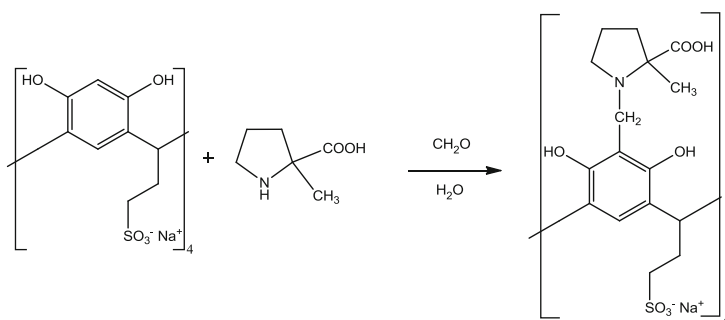
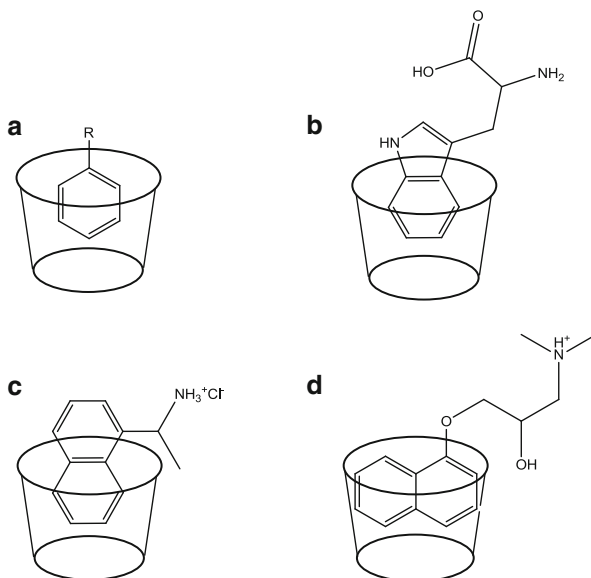


Fig. 12 Coupling of a secondary amine (proline) to a calix[4]resorcinarene

128–133 adopt a cone conformation and are especially effective chiral NMR differentiating agents for water-soluble substrates that have an aromatic ring free of steric hindrance. The ring of the substrate inserts into the cavity as evidenced by large shielding of the aryl resonances of the substrate by the resorcinol rings. Water-soluble substrates with mono- or *ortho*-substituted phenyl, 2,3- and 1,8-disubstituted naphthyl, *ortho*-substituted pyridyl, indole (**134**), dihydroindole (**135**), and indane (**136**) rings associate favorably with **128–133** [145]. Substrates with naphthyl rings have higher association constants than those with phenyl rings, presumably because of the higher hydrophobicity of the naphthyl ring [141, 142].

The magnitude of the shielding of the aryl resonances of the substrate is indicative of the geometry of association of substrates in the cavity of **128–133**. Mono-substituted aryl rings insert as shown in Fig. 13a. The indole ring of tryptophan inserts as shown in Fig. 13b. The shielding of the aryl resonances of NEA and propranolol provide an interesting contrast. For NEA, the H6 and H7 resonances exhibit the largest shielding in the presence of **128–133**, indicating the association geometry shown in Fig. 13c. For propranolol, H4 and H5 exhibit the largest shielding in the presence of **128–133**, indicating the association geometry shown in Fig. 13d. Interactions between the aliphatic groups of NEA and propranolol with the proline moieties of **128–133** must account for the difference in geometries [141, 142].

Fig. 13 Geometry of association of (a) mono-substituted phenyl rings, (b) tryptophan, (c) 1-(1-naphthyl)ethylamine, and (d) propranolol with calix [4]resorcinarenes **127–132**



99 and **101** have phenyl and pyridyl rings that are free of steric hindrance and the perturbations in chemical shifts in the presence of **128–133** indicate that both rings associate to some degree in the cavity. The phenyl ring in **100**, **103**, and brompheniramine (**137**) is sterically hindered by the halide and the perturbations in chemical shifts indicate that association of these substrates with **128–133** only involves insertion of the pyridyl ring [141].

128–133 are effective chiral NMR differentiating agents for a broad range of neutral, cationic, and anionic aryl-containing substrates. The general effectiveness is in the order *L*-pipecolinic acid (**133**) > α -methyl-*L*-proline (**132**) > hydroxyl-*L*-prolines (**129–131**) > *L*-proline (**128**) [141–150]. The enhanced effectiveness of **129–131** compared to **128** likely occurs because the hydroxyl group in **129–131** provides an additional site for hydrogen bonding with the substrate. The effectiveness of **133** and **132** is likely due to the increased steric hindrance at the opening of the cavity caused by the methyl group in **132** and the larger six-membered ring in **133**.

Figure 14 shows the enantiodifferentiation caused by **133** in the three aromatic resonances of phenylalanine methyl ester hydrochloride. The substantial shielding of the resonances caused by insertion of the phenyl ring of the substrate into the cavity of **133** is apparent in the spectrum. Figure 15 shows the progression of the methyl doublet of 2-phenylpropanoic acid (**108**) as increasing concentrations of **133** are added. The spectra in Figs. 14 and 15 are representative of the enantiomeric differentiation of aryl and alkyl hydrogen resonances that are obtained for water-soluble substrates in the presence of **133**.

Fig. 14 ^1H NMR spectrum (400 MHz, D_2O , 23°C) of the aromatic region of (a) phenylalanine methyl ester hydrochloride (2/3 D, 1/3 L) with (b) **133** at 20 mM

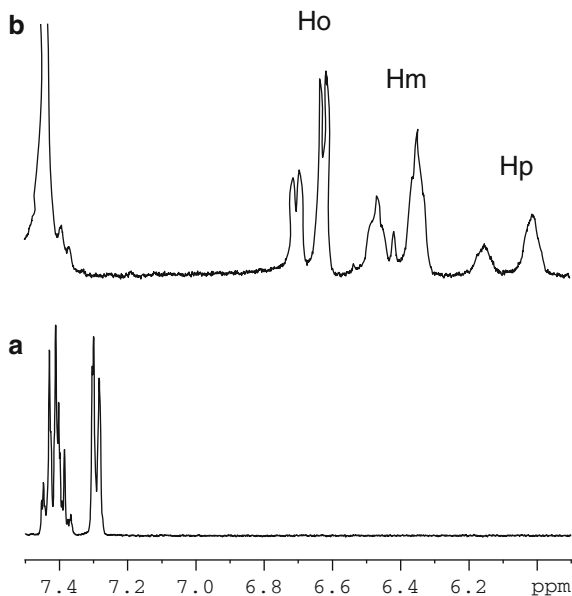
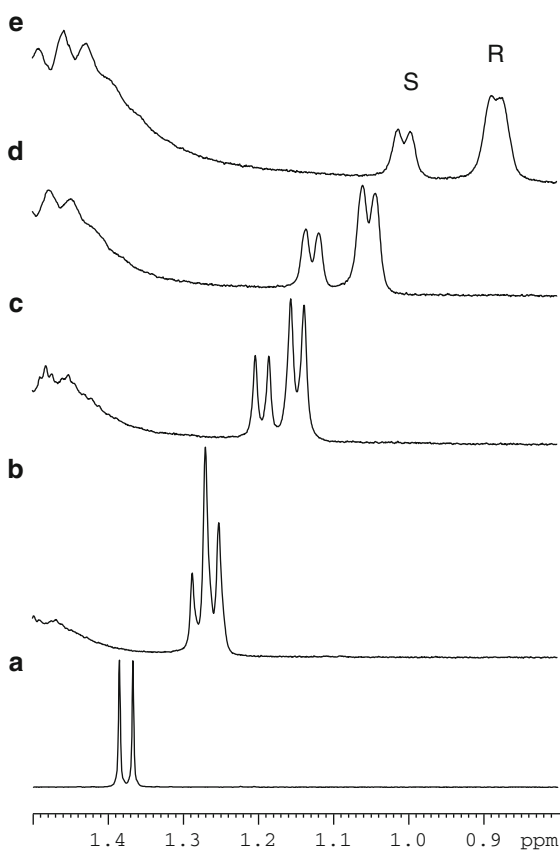
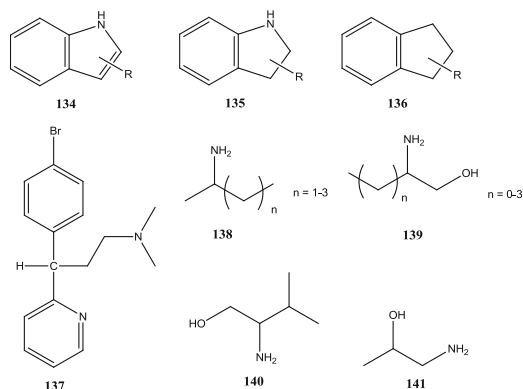
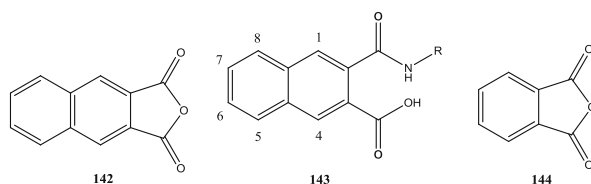


Fig. 15 ^1H NMR spectrum (400 MHz, D_2O , 23°C) of the methyl doublet of (a) 2-phenylpropanoic acid (**108**) (2/3 R, 1/3 S) with (b) **133** at 6 mM, (c) 10 mM, (d) 15 mM, and (e) 25 mM





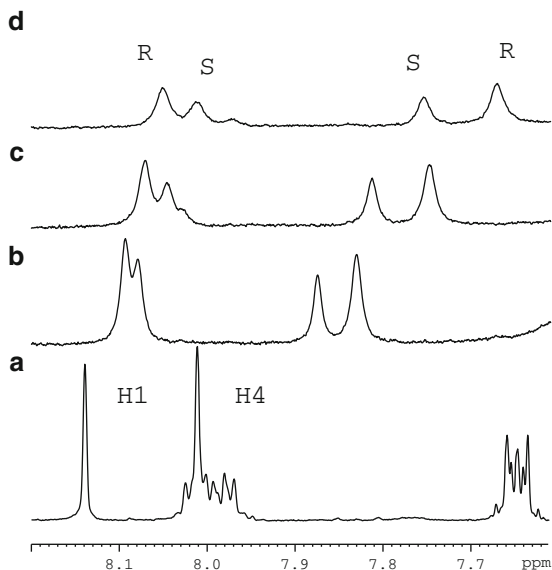
128, **132**, and **133** have been used in a scheme to analyze aliphatic amines (**138**) and amino alcohols (**139–141**). The amines are reacted with achiral naphtho[2,3-*c*]furan-1,3-dione (**142**) to prepare the corresponding amide (**143**). Some of the naphthyl amide derivatives are water-soluble. If not, the carboxylic acid group of **143** is converted to a water-soluble sodium salt by the addition of 1 equiv. of sodium bicarbonate. Mixing **143** with **128**, **132**, or **133** leads to substantial perturbation and enantiomeric differentiation of the naphthyl resonances. The corresponding amides prepared from isobenzofuran-1,3-dione (**144**) exhibit rather small perturbations in chemical shifts, indicating that the carboxylic acid and amide groups *ortho* on the phenyl ring inhibit association with **128**, **132**, and **133**. The H1 and H4 singlets of **143** are especially useful for monitoring enantiomeric differentiation. Figure 16 shows the enantiomeric differentiation of the H1 and H4 resonances of the naphthyl amide derivative of 2-amino-1-butanol with **128**. An interesting observation is the reversal in shift order for the (*R*)- and (*S*)-resonances of H1 and H4 in the presence of **128**. This reversal was consistent with all substrates and the order of the H1 and H4 resonances in the (*R*)- and (*S*)-enantiomers in the presence of **128**, **132**, and **133** correlate with the absolute configuration of the amines and amino alcohols [151].



4 Metal Complexes

A variety of metal complexes have been used as chiral NMR differentiating agents. The metal ions are Lewis acids and form donor-acceptor complexes with Lewis bases. In some cases the donor substrate undergoes rapid exchange between its

Fig. 16 ^1H NMR spectrum (400 MHz, D_2O , 23°C) of the aromatic region of (a) the naphthyl amide derivative of 2-amino-1-butanol ((*S*)-isomer, 3 mM; (*R*)-isomer, 7 mM) with (b) **128** at 6 mM, (c) 10 mM, and (d) 15 mM



bound and unbound form and the NMR spectrum is a time average of the two species. In other cases the exchange of the donor substrate is slow. With slow exchange it is desirable to have only bound substrate since the presence of unbound substrate combined with enantiomeric differentiation of bound substrate can lead to three signals in the spectrum and complicate the analysis. Of special importance is the use of lanthanide, rhodium, platinum, palladium, and silver complexes. Lanthanide complexes are primarily used with hard Lewis bases and rhodium, platinum, and palladium complexes are primarily used with soft Lewis bases.

4.1 Lanthanide Complexes

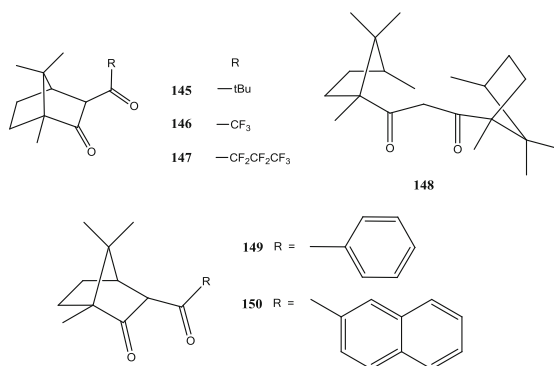
Chiral lanthanide tris β -diketonate complexes are among the earliest group of chiral NMR differentiating agents ever developed. Whitesides and Lewis first described the use of organic-soluble lanthanide complexes of 3-(*tert*-butylhydroxymethylene)-(1*R*)-camphor (**145**) as chiral NMR shift reagents in 1970 [3]. Soon after, lanthanide complexes with 3-trifluoroacetyl-(1*R*)-camphor (**146** – *tfc*) [152], 3-heptafluorobutyryl-(1*R*)-camphor (**147** – *hfc*) [153], and (1*R*), (1*R*)-dicampholylmethane (**148** – *dcm*) [154] were developed and found to be superior to the complexes with **145**. While chelates with *tfc* and *hfc* have been most frequently used because of their widespread commercial availability, comparative studies show that lanthanide chelates with *dcm* usually produce superior chiral differentiation [5, 154]. It has been proposed that lanthanide complexes of *dcm* are more sterically crowded, which enhances the enantiomeric differentiation of bound donor substrate molecules when compared to complexes with *tfc* and *hfc* [154].

Since lanthanide tris β -diketonates can bind to almost any compound with an oxygen or nitrogen atom, they are incredibly versatile reagents with exceptionally wide applicability. Comprehensive reviews describe the impressive range of compounds for which chiral lanthanide tris β -diketonates have been used to determine enantiomeric composition [5, 155, 156]. Lanthanide tris β -diketonate complexes are fluxional in nature making it impossible to predict absolute stereochemistry of bound substrates based on precise geometrical considerations. However, there are many classes of compounds where empirical patterns in the chemical shifts for similar structures show trends that correlate with absolute configuration. These have been discussed in reviews of this field [5, 155, 156].

In the 1970s and early 1980s, when most investigators only had access to relatively low field NMR spectrometers, the paramagnetism of many of the lanthanide ions, and especially europium(III), praseodymium(III), and ytterbium(III), facilitated the analysis of chiral complexes. The magnetic field of a paramagnetic lanthanide ion produces a through-space, dipolar shift of the resonances of the substrate. The perturbations in chemical shifts and degree of enantiomeric differentiation caused by paramagnetic lanthanide complexes is quite large, while the line broadening that is caused by paramagnetic substances is reasonably small on instruments operating at frequencies of 200 MHz or lower. In most cases, coupling information is still retained in the resonances at these field strengths. Unfortunately, the combination of paramagnetic line broadening with exchange broadening under conditions of intermediate exchange is more significant at higher field strengths. Therefore, paramagnetic lanthanide complexes are used much less frequently today in NMR applications than they were 3–4 decades ago.

There are several strategies that have been used to reduce line broadening with paramagnetic lanthanide complexes. One is to use more polar solvents such as acetonitrile- d_3 that compete with the donor substrate for the lanthanide ion. The reduction in the binding constant of the donor reduces the broadening, but in some cases sufficient binding still occurs to observe enantiomeric differentiation in the NMR spectrum [157, 158]. Another strategy is to warm the sample to speed up the exchange rate and reduce the contribution of exchange broadening. On some occasions this reduces broadening to acceptable levels while still maintaining enantiomeric differentiation in the NMR spectrum [122, 159]. Among the paramagnetic lanthanide ions, Sm(III) generally causes relatively small perturbations in chemical shifts and produces a commensurate reduction in the level of broadening. Esters of amino acids were successfully analyzed using Sm(tfc) $_3$ at 400 MHz without complications from paramagnetic line broadening [160].

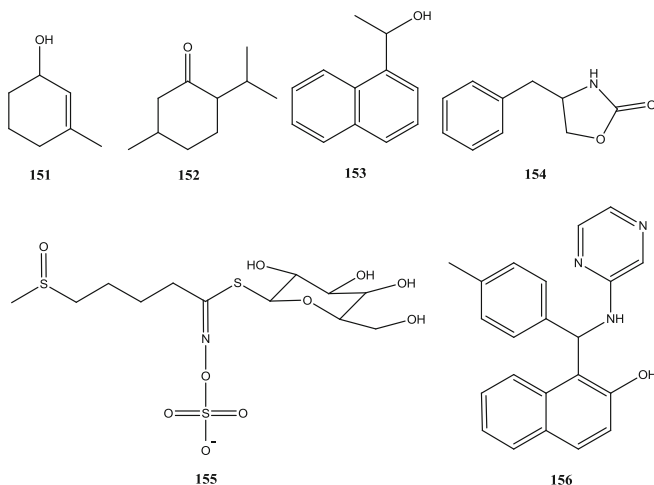
Diamagnetic lanthanum(III) and lutetium(III) tris β -diketonates of tfc, hfc, and dcm have been examined as organic-soluble chiral NMR shift reagents. Enantiomeric differentiation is observed in the 400-MHz ^1H NMR spectra of substrates with alcohol, amine, epoxide, sulfoxide, and oxazolidine groups. Perturbations in the ^1H NMR spectrum result from complexation of the hard Lewis base substrate with the lanthanide ion. No single combination of diamagnetic metal or ligand is consistently most effective at causing enantiomeric differentiation. Better results are obtained in benzene- d_6 or cyclohexane- d_{12} than in chloroform- d [161].



Very recent work has found that lanthanum and lutetium complexes of 3-(benzoyl)-(1*R*)-camphor (**149** – bc) and 3-(2-naphthoyl)-(1*R*)-camphor (**150** – 2np) are more effective chiral NMR shift reagents than those of tfc, hfc, and dcm. The diamagnetic lanthanide complexes of **149** and **150** cause enantiomeric differentiation in the 400-MHz ^1H NMR spectra of a considerably wider range of substrates. Significant shielding of substrate resonances by the aryl groups of complexes with **149** or **150** accounts for much of their effectiveness. In several cases, diamagnetic lanthanide chelates of **149** or **150** cause enantiomeric differentiation of resonances remote from the stereogenic center. This includes the methyl group at the 4-position of 2-butanol, which exhibits larger enantiomeric differentiation with La(2np) $_3$ than the methyl group at the 1-position. The methyl group at the 8-position of 2-aminoctane exhibits a small degree of enantiomeric differentiation in the presence of La(bc) $_3$ and La(2np) $_3$. Resonances of the methyl groups in menthol (**4**), 3-methylcyclohex-2-en-1-ol (**151**), menthone (**152**), and aryl hydrogen atoms in **153** and **154** are fairly distant from the stereogenic center, but are significantly shielded and exhibit enantiomeric differentiation in the presence of the diamagnetic lanthanide chelates of **149** and **150**. Similar to the lanthanum(III) and lutetium(III) complexes with tfc, hfc, and dcm, better enantiomeric differentiation is usually observed in benzene- d_6 or cyclohexane- d_{12} than in chloroform- d . The remarkable versatility of paramagnetic lanthanide complexes at lower field strengths is realized by the use of lanthanum(III) or lutetium(III) complexes of **149** and **150** on spectrometers operating at frequencies of 400 MHz or higher [162].

Recording ^{13}C NMR spectra is another way to analyze chiral compounds with paramagnetic lanthanide tris β -diketonates and keep broadening to acceptable levels. The effect of the exchange broadening on the ^{13}C nucleus is reduced relative to that on the ^1H nucleus at comparable field strengths. Also, if broadband proton decoupling is employed, line broadening will have less of an impact on observing enantiomer differentiation of sharp ^{13}C singlets. A strategy for assigning the absolute configuration of secondary and tertiary alcohols using ^{13}C NMR spectra recorded in the presence of (*R*)- and (*S*)-Pr(hfc) $_3$ has been described. The carbon atoms adjacent to the carbinol site show specific trends in their $\Delta\delta^{RS}$ values that correlate with absolute configuration [163].

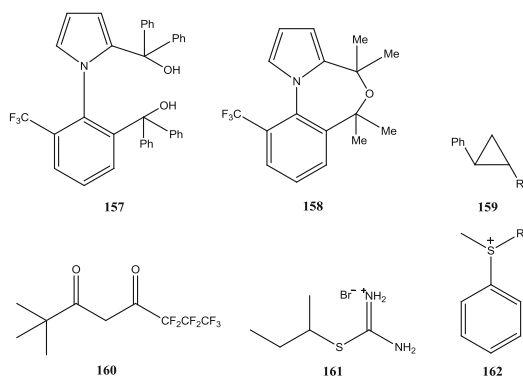
Even though broadening is often a problem with paramagnetic lanthanide tris β -diketonates, there are recent examples of their use to determine enantiomeric composition. Splitting of the methyl signal of 4-methylsulfinylbutylglucosinolate (**155**) isolated from broccoli and *Arabidopsis thaliana* is observed in the 400-MHz ^1H NMR spectrum in the presence of $\text{Eu}(\text{hfc})_3$. The use of a polar solvent mixture (9:1 ratio of acetonitrile- d_3 and methanol- d_4) and a probe temperature of 50°C kept broadening to acceptable levels [164].



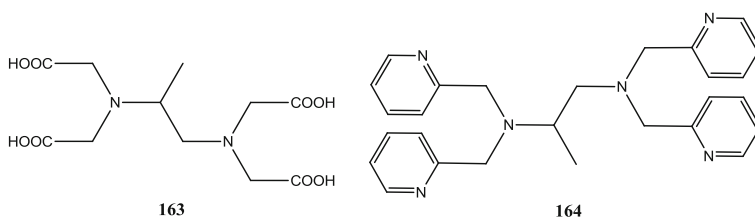
The methyl singlet of **156** splits in the presence of $\text{Eu}(\text{hfc})_3$ in chloroform- d at 500 MHz [165]. The enantiomeric purities of 1-substituted phenyl pyrrole atropisomers **157** and **158** have been determined using $\text{Yb}(\text{tfc})_3$. Enantiomeric differentiation is observed in the ^{19}F NMR spectrum at 470 MHz in benzene- d_6 . Certain resonances of the ^1H NMR spectrum of **158** also show enantiomeric differentiation [166]. *trans*-2-Phenylcyclopropane derivatives (**159**) with a range of functional groups have been examined with $\text{Eu}(\text{tfc})_3$ in chloroform- d at 200 MHz. Specific patterns occur for resonances of the (*R*)- and (*S*)-isomers that correlate with absolute configuration [167].

The combination of a lanthanide(III) tris β -diketonate [$\text{Ln}(\beta\text{-dik})_3$] with a silver(I) β -diketonate [$\text{Ag}(\beta\text{-dik})$] in a solvent such as chloroform- d forms a lanthanide tetrakis chelate anion that ion pairs with silver [$\text{Ln}(\beta\text{-dik})_4^-\text{Ag}^+$]. The silver ion in the bimetallic reagent binds to soft Lewis bases such as alkenes, aromatics, halogenated compounds, and phosphines. The lanthanide ion causes perturbations in the chemical shifts of the donor compound [168]. Chiral analogues are formed using lanthanide chelates of *tfc* or *hfc* [169, 170]. A variety of achiral or chiral silver β -diketonates can be employed, although the silver chelate with 6,6,7,7,8,8,8-heptafluoro-2,2-dimethyl-3,5-octanedione (**160**) is commercially available. Recent reviews describe uses of the bimetallic reagents for enantiomeric analysis [5, 6]. In some cases the bimetallic reagent is better for differentiating substrates with both hard and soft Lewis base functionalities than lanthanide tris β -diketonates [171–174]. This may be because the

greater distance between the lanthanide ion and the substrate in the bimetallic reagent, as compared to the lanthanide tris β -diketonate, reduces broadening in the spectrum.



Bimetallic lanthanide-silver reagents can also be used to analyze organic cations. A mixture of the bimetallic reagent with an organo halide salt forms a precipitate of silver chloride and an ion pair between the organic cation and the lanthanide tetrakis chelate anion [175, 176]. Enantiomeric differentiation of chiral isothiuronium (**161**) [176] and sulfonium salts (**162**) [177] has been described.



Water-soluble lanthanide complexes have also been developed for NMR applications. Thorough discussions of the use of chiral water-soluble lanthanide complexes are provided in recent reviews [5, 6]. The most widely used water-soluble reagents employ the anionic ligand propylenediaminetetraacetic acid (**163** – pdta) or the neutral ligand *N,N,N',N'*-tetrakis(pyridylmethyl)propylene diamine (**164** – TPPN). Lanthanide reagents with **163** and **164** are suitable for the analysis of carboxylic acids and amino acids. Eu(pdta) causes trends in the H_{α} resonance of α -amino acids [178] and α -methyl signals of α -methyl amino acids [179] that correlate with absolute configuration. Similarly, perturbations of the α - and β -proton resonances of β -amino acids in the presence of Eu(pdta) correlate with absolute configuration [180].

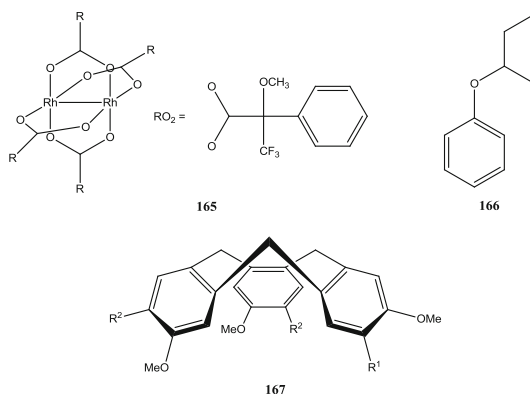
As with the organic-soluble paramagnetic lanthanide reagents, broadening with water-soluble europium(III) complexes may be too severe at high field strengths. The use of Ce(III) [181] or Sm(III) [182] complexes of pdta reduces the broadening to acceptable levels and facilitate the analysis of the 1H and ^{13}C NMR spectra of α -amino acids. The ^{13}C NMR spectra of α -amino acids show enantiomeric differentiation with

Pr(dtpa) without significant line broadening [183]. An improved synthesis of (*S*)-pdta that starts from *L*-alanine involves five steps and occurs in just over 50% yield has been described [184]. Sm(pdta)-*d*₈ has been employed in the analysis of amino acids from peptide hydrolysates. By using Sm(III) complexes with (*R*)- and (*S*)-pdta, $\Delta\delta^{RS}$ values for the H α resonances are obtained that allow the assignment of absolute configuration. Mixtures with up to ten amino acids can be analyzed [185].

When using complexes with pdta, the pH is usually basic, which deprotonates the amino acid and facilitates binding to the lanthanide ion. Lanthanide complexes with TPPN can be used with amino acids at neutral pH. Broadening with TPPN complexes can be reduced through the use of Ce(III) [186] or La(III) [187]. Perturbations in the spectra of α -amino acids with lanthanide complexes of TPPN show trends that correlate with absolute configuration [186, 187].

4.2 Rhodium Complexes

Most notable among the rhodium complexes that have been studied as chiral NMR differentiating agents is a rhodium dimer of MTPA (**165** – Rh₂(MTPA)₄). Rh₂(MTPA)₄ exhibits strong binding to soft Lewis bases including alkenes and compounds with phosphorus, sulfur, and iodine atoms. Substrates can form 1:1 or 2:1 complexes with Rh₂(MTPA)₄ as shown in Fig. 17. Exchange of the substrate may be fast or slow depending on the nature of the substrate. Most reports using this reagent provide the optimal concentration ratio for the analysis. In recent work, the use of Rh₂(MTPA)₄ has been extended to systems with hard Lewis base nitrogen and oxygen atoms. Comprehensive reviews that discuss the utility of Rh₂(MTPA)₄ for chiral NMR differentiation have been published [5, 188].



In recent work, 2-butylphenyl ethers such as **166** bind to Rh₂(MTPA)₄ and enantiomeric differentiation is observed in the ¹³C NMR spectrum [189, 190]. The methoxy groups of cycloveratrylenes **167** and cryptophanes **168** bind to Rh₂(MTPA)₄ and enantiomeric differentiation is observed in the ¹H and ¹³C NMR spectra. Binding

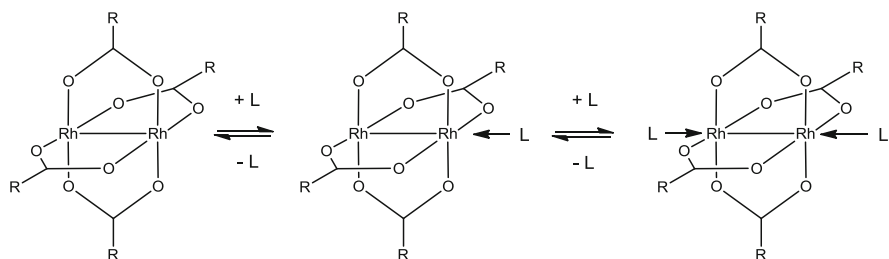
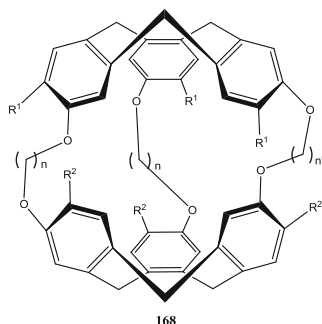


Fig. 17 Binding of substrate ligands to $\text{Rh}_2(\text{MTPA})_4$

of ethers to rhodium primarily involves an electrostatic interaction [191]. This contrasts with the analogous thioethers of **167** and **168** that bind more strongly to $\text{Rh}_2(\text{MTPA})_4$. Interaction between the sulfur HOMO and rhodium LUMO accounts for the more favorable association of sulfur compared to oxygen with rhodium [190, 191].



Schiff base substrates of general structure **169**, which are derivatives of *ortho*-hydroxyaldehydes, bind to $\text{Rh}_2(\text{MTPA})_4$ preferentially at the oxygen atom of the hydroxyl group. Evidence for 2:1 and 1:1 adducts was observed and a 2:1 substrate/ $\text{Rh}_2(\text{MTPA})_4$ dimer ratio is recommended. Enantiomeric differentiation is noted in the ^1H and ^{15}N NMR spectra. The spectra of some substrates are severely broadened [192, 193].

3-Aryl-2-oxo-4-oxazolidinones (**170**) [194] and bicyclic lactams (**171**) [195] bind to $\text{Rh}_2(\text{MTPA})_4$ and exhibit enantiomeric differentiation in their ^1H and ^{13}C NMR spectra. The corresponding thiocarbonyl analogues of **170** and **171** bind much more strongly to the rhodium and show a much greater enantiomeric differentiation in their NMR spectra.

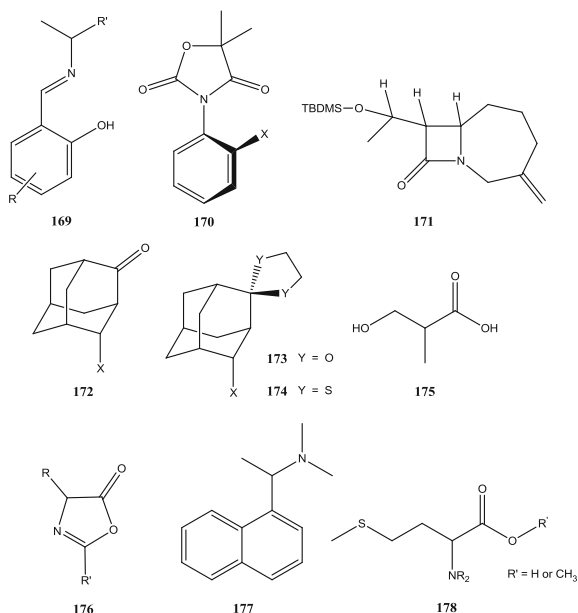
The NMR spectra of adamantanones (**172**), dioxolanoadamantanes (**173**), and dithiolano adamantanes (**174**) have been examined with $\text{Rh}_2(\text{MTPA})_4$. All were examined as 1:1 mixtures in chloroform-*d*. Binding of **172** to $\text{Rh}_2(\text{MTPA})_4$ occurs through the carbonyl group. When X in **172** was an iodine or bromine, substrate binding involved the halogen atom. The dithio adamantanes bind through the sulfur atom and exhibit the largest enantiomeric differentiation of the various adamantanes

studied. The perturbations in chemical shifts of the dithio adamantanes correlate with absolute configuration [196].

The relative binding of oxygen-containing substrates to $\text{Rh}_2(\text{MTPA})_4$ was investigated with 38 derivatives of 3-hydroxy-2-methylpropanoic acid (**175**). Each compound has two possible binding sites, facilitating a determination of which one preferentially binds. Enantiomeric differentiation is observed in the ^1H NMR spectrum of equimolar substrate- $\text{Rh}_2(\text{MTPA})_4$ mixtures of most of the compounds. The relative binding order is epoxides > primary alcohols > ethers > esters > amides > carbonates > tertiary alcohols [197].

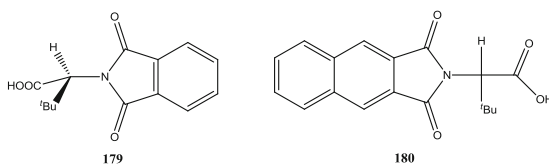
A procedure in which $\text{Rh}_2(\text{MTPA})_4$ is used to assign the absolute configuration of amino acids has been developed. The amino acid is converted to a 4-substituted 2-aryl or 2-alkyl-5(4*H*)oxazolone (**176**). ^1H NMR spectra recorded in chloroform-*d* with equimolar concentrations of substrate and $\text{Rh}_2(\text{MTPA})_4$ show trends for certain resonances that correlate with absolute configuration. Binding occurs through the *N*-atom except when cysteine is the amino acid. For cysteine, binding occurs through the sulfur atom of the substituent group. A partial racemization of the amino acid occurs in the reaction to produce the oxazolone, so care must be taken if using this method [198].

$\text{Rh}_2(\text{MTPA})_4$ has been used to study diastereomerization rates of nitrogen inversion in substrates such as (*S*)-*N,N*-dimethyl-1-phenylethylamine (**177**) and other *N*-substituted 1-phenylethylamine derivatives. A twofold molar excess of the (*R*)-MTPA or (*S*)-MTPA dimer is used. Splitting in the ^1H and ^{13}C NMR spectra indicates that both the C_5N_R and C_5N_S forms of the complexed substrates are observed. Vicinal NH coupling constants and NOE experiments are used to assign the configuration at the nitrogen atom [199].



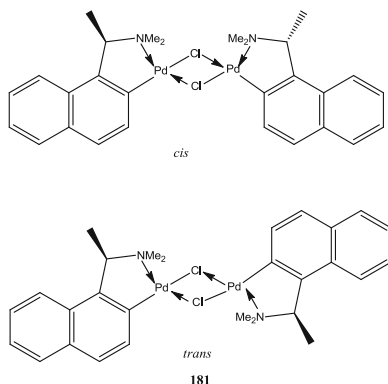
$\text{Rh}_2(\text{MTPA})_4$ has been used for enantiomeric differentiation of methionine (**178**) derivatives. ^1H and ^{13}C NMR spectra were recorded in chloroform-*d*. Binding of the substrate occurs at the sulfur atom. Both 1:1 and 1:2 adducts form, which can complicate the NMR spectra. Enantiomeric differentiation is most apparent in the SCH_3 and OCH_3 ^1H NMR resonances of 2:1 substrate- $\text{Rh}_2(\text{MTPA})_4$ mixtures [200].

Recent studies have explored the use of rhodium dimers with ligands other than MTPA. One study compared the effectiveness of rhodium dimers with MTPA, $\text{M}\alpha\text{NP}$, and (*S*)-*N*-phthaloyl-(*S*)-*tert*-leucine (**179**). Substrates that spanned a range of binding groups were examined. The complex with **179** is especially effective at causing enantiomeric differentiation. It was proposed that the phthaloyl group extended out away from the rhodium core toward the substrate to cause substantial shielding of substrate resonances [201].



More recently the NMR spectra of five substrates with varying binding properties ranging from soft to hard Lewis bases were recorded in the presence of 13 different rhodium dimers including **179**. The best results were obtained using the complex with (*S*)-*N*-2,3-naphthalenedicarboxyl-*tert*-leucinate groups (**180**). A combination of ring shielding effects from the large naphthyl ring with conformational flexibility that allows binding of the substrate are responsible for the enhanced effectiveness of **180** compared to the other ligands [202].

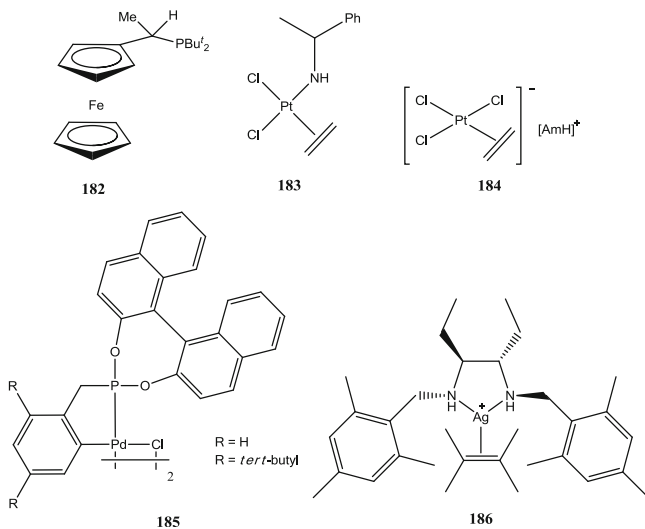
4.3 Palladium Complexes



Several palladium complexes have been used as chiral NMR reagents to determine the enantiomeric composition of soft Lewis bases. Most notable among them are dimeric complexes with *N,N*-dimethyl-(1-phenyl)ethylamine or *N,N*-dimethyl-1-(1-naphthyl)ethylamine (**181**) ligands. The ligands are commercially available and synthesis of the complexes is straightforward. The palladium dimers consist of *cis* and *trans* isomers. However, reaction with mono- and diphosphines, arsines, bidentate aminophosphines, α - and β -amino acids, and diamines lead to monomeric species so the initial *cis* or *trans* form of the palladium complex does not matter. Both ^1H and ^{31}P NMR can be used for monitoring enantiomer differentiation. Many of the complexes undergo slow exchange so resonances on the metal complex or substrate can be employed in the NMR analysis. The fixed geometry of the complexes sometimes allows NOESY or ROESY data to be used in assigning absolute configuration. The naphthyl derivative is usually more effective than the phenyl derivative at causing enantiomeric differentiation. The geometry of the *C*-methyl group of the five-membered metallocycle is constrained by the H8 atom of the naphthyl ring, explaining the effective enantiomeric differentiation. Recently, the phenyl reagent analogous to **181** was used to determine the enantiomeric composition of an α -ferrocenylethylphosphine (**182**). The ^{31}P NMR spectrum had two well resolved signals [68]. The use of these [203] and other palladium reagents has been thoroughly discussed in review articles [5].

4.4 *Platinum Complexes*

The most notable platinum reagents employed for chiral NMR differentiation consist of an amine species either covalently attached to platinum (**183**) or ion paired to an anionic platinum species (**184**). These reagents are effective for determining the enantiomeric composition of alkenes and allenes. The ethylene group of the platinum complex is displaced by the substrate. Usually the ^{195}Pt NMR is examined for enantiomeric differentiation. A potential complication with these reagents is that alkenes and allenes have prochiral faces. Some enantiomeric substrates bind at both faces which, if enantiomeric differentiation is present in the spectrum, results in four signals in the ^{195}Pt spectrum. Others bind at only two faces, causing only two ^{195}Pt signals in the spectrum. A variety of chiral amines have been examined to explore which give the best enantiomeric differentiation. An advantage of **184** over **183** is that sterically crowded amines can be used in the ionic reagent, which often leads to greater enantiomeric differentiation. A comprehensive review article summarizes the work that has been done with these systems and recommends options among the covalent and ionic metal complexes for different categories of substrates [204].



In recent work, platinum dimers containing BINOL groups (**185**) were evaluated as chiral shift reagents with racemic PEA. Reaction of the dimer with 2 equiv. of PEA in methylene chloride- d_2 causes the formation of a monomeric species. Splitting of the ^{31}P signal is monitored for determining enantiomeric composition [205].

4.5 Silver Complexes

The enantiomeric composition of alkenes can be determined using a silver complex of *N,N'*-bis(mesitylmethyl)-1,2-diphenyl-1,2-ethanediamine (**186**) and the corresponding cyclohexyl-1,2-diamine derivative. The reagent is prepared directly in an NMR tube by mixing silver triflate, the amine ligand and the alkene. The aryl rings of the reagent cause shielding in the substrate that enable the enantiomeric differentiation of alkenes with a stereogenic center α to the double bond [206].

5 Liquid Crystals

The utilization of liquid crystals for differentiation of enantiomers by NMR spectroscopy has advanced considerably over the past 2 decades. Liquid crystals are unique among chiral differentiating agents in that there is no need for a directed interaction between the compound under study and the liquid crystal. The chiral liquid crystal is dissolved in an achiral co-solvent and partially aligns in the NMR probe. Molecules dissolved in the liquid crystal/co-solvent mixture partially align

as well. A pair of enantiomers will often have different alignments, meaning they are oriented differently relative to the applied magnetic field. NMR spectra of enantiomers dissolved in a chiral liquid crystal may show differentiation in NMR spectra in three different ways.

The first and usually least useful is that the enantiomers may have different chemical shifts, which is what occurs with the other systems discussed in this chapter. Because there are usually no directed forces between the substrate and the liquid crystals, the differences in chemical shifts between the enantiomers are often quite small and not that useful for chiral differentiation.

The second involves differences in dipolar ^1H - ^1H and ^1H - ^{13}C coupling constants in the two enantiomers. The magnitude of dipolar coupling constants depends on the orientation of the molecule relative to the applied magnetic field. In solution, molecules tumble and the coupling constant between a pair of nuclei is a single value that represents a time average of all of the contributing orientations. If, in the chiral liquid crystal, a comparable pair of coupled nuclei in two enantiomers have different alignments relative to the applied magnetic field, then the coupling constant between them will be different and two multiplets will appear in the spectrum for each nucleus. The relative area of each multiplet corresponds to the proportion of each enantiomer in the mixture. The doubling of all multiplets combined with the uncertainty of the magnitude of the coupling constants creates complex ^1H and ^{13}C spectra.

Because of the desirability of using ^1H NMR spectra for enantiomeric analysis in liquid crystals, investigators have developed a variety of methodologies to simplify the spectra. A comprehensive review article published in 2007 describes the various procedures developed until that time for simplification and analysis of ^1H and ^{13}C NMR spectra [207]. These include homonuclear and heteronuclear selective refocusing sequences. Many more sequences and strategies have been described in the past few years. The general strategy is to excite selectively a single resonance and measure information about other hydrogen atoms it is coupled to. Techniques include one- and two-dimensional NMR spectra as well as single and multiple quantum methods. A discussion of the details of the extensive number of methods described in the literature in just the past 5 years is beyond the scope of this chapter. Comprehensive review articles published in 2009 [208] and 2010 [209] describe the various methods that have been developed until that point in time for recording more useful ^1H NMR spectra in chiral liquid crystals. These articles discuss the advantages and limitations of each method.

More recent developments include procedures for selective refocusing experiments that allow assignment of all the dipolar couplings of each enantiomer in racemic mixtures. This method makes it possible to observe the signals of one enantiomer even if it overlaps with another [210]. Another procedure uses a selective refocusing that facilitates the determination of all the coupling experienced by a given proton in a single two-dimensional spectrum [211]. Still another refocusing technique allows the measurement of short- and long-range ^1H - ^1H as well as one-bond ^1H - ^{13}C coupling [212]. The development of these techniques has enhanced the ability to use information in ^1H NMR spectra in chiral liquid crystals.

The third way in which enantiomeric differentiation can be observed in liquid crystals is in the NMR spectra of quadrupolar nuclei such as deuterium. When molecules rapidly tumble, deuterium nuclei exhibit no quadrupolar splitting. When the molecule is partially aligned relative to the applied magnetic field, deuterium nuclei experience a quadrupolar interaction and appear as doublets. As with the dipolar coupling described earlier, the magnitude of the quadrupolar splitting depends on the orientation of the nucleus to the applied magnetic field. If two enantiomers have different alignments, each deuterium nucleus will appear in the spectrum as two doublets with a different degree of splitting. The areas of the two doublets are proportional to the concentration of the two enantiomers.

Natural abundance ^2H NMR spectra in liquid crystals are compromised by several factors. One is low sensitivity because of the limited isotopic abundance of the ^2H nucleus. Another is that the spectra are complicated because each signal is now two doublets and because the magnitude of the quadrupolar splittings is quite large and often greater than the chemical shift differences between nuclei.

Many studies with chiral compounds in liquid crystals have involved species that are enriched in deuterium. In some cases this involves a derivatization reaction that adds a ^2H enriched substituent group to the compound. Since the purpose of the derivatization is only to add a substituent group with an intense ^2H signal, these reactions involve achiral moieties and kinetic resolution is not a concern.

Because it is not always practical to enrich compounds with deuterium, a variety of NMR methods have been developed to simplify natural abundance ^2H NMR spectra to improve sensitivity and to ease interpretation. An overview of these methods has been published [213]. Recent advances in obtaining natural abundance ^2H NMR spectra include the development of a three-dimensional double quantum sequence. This report also notes the advantage of using a cryogenically cooled probe to increase sensitivity [214]. More recently a procedure for recording natural abundance ^2H NMR spectra involving non-uniform sampling and a covariance transform was described. This procedure improves spectral resolution while reducing measurement times by a factor of 2–4 [215].

^2H spectra can be complicated in some cases even when the molecule is isotopically enriched. An example is **187**, which has two stereocenters. Since the stereocenters can have the same or different configurations, there is the possibility of getting two chiral (*RR* and *SS*) and one achiral (*RS*) *meso* species. When ordered in a liquid crystal, four quadrupolar doublets are observed. Two are from differentiation of the enantiomeric *SS* and *RR* isomers. The other two are from differentiation of the enantiotopic deuterons associated with the *meso* isomer. Homo- and heteronuclear 2D NMR strategies to facilitate assignment of the signals in the ^2H NMR spectrum are described in this report [216].

Poly- γ -benzyl-L-glutamate (PBLG) is the most common liquid crystal that has been used for chiral differentiation studies. Poly- γ -ethyl-L-glutamate (PELG) and poly- ϵ -carbobenzyloxy-L-lysine (PCBLL) are other chiral liquid crystals that have been used in NMR studies. The co-solvent used with these materials needs to be chosen to ensure adequate solubility of the compound being studied. Methylene chloride, chloroform, and *N,N*-dimethylformamide are common co-solvents.

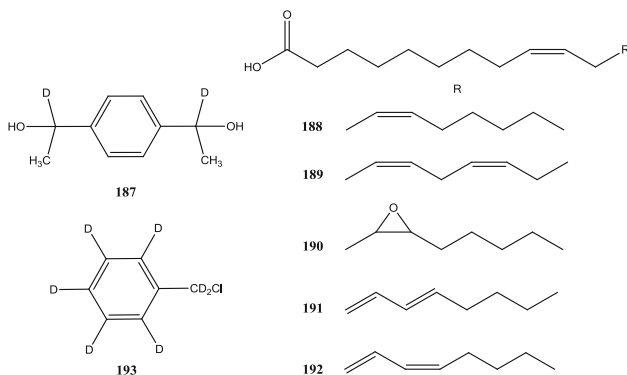
Some recent studies have focused on developing other chiral liquid crystal systems for use in NMR applications. Mixed polypeptide systems comprised of PBLG and PCBLL in chloroform often provide more differentiation between the ordering of enantiomeric compounds or differentiation of enantiotopic directions in prochiral compounds than either of the pure liquid crystals. The enantiodifferentiation, resolution and sensitivity in the ^2H NMR spectrum can be simultaneously optimized by altering the proportion of the two polypeptides [217].

Gelatin materials comprised of polysaccharides or carrageenans have been examined as well. Differentiation of the prochiral hydrogen atoms in glycine and dimethylsulfoxide- d_6 (DMSO) is observed with these gels. Enantiomeric differentiation in the ^1H , ^{13}C , and ^2H NMR spectra of alanine is also observed. The gel can be stretched to alter the alignment of molecules for more favorable enantiomeric differentiation [218].

Irradiation by accelerated electrons produces a covalently cross-linked gelatin that is effective for differentiating the prochiral groups in DMSO- d_6 and L- and D-alanine. This system has a significant temperature effect. The spectrum of D- and L-alanine shows enantiomeric differentiation at 55°C but not at 37°C . Differentiation of the prochiral CD_3 groups of DMSO- d_6 occurs at temperatures greater than 60°C . It is possible to use water as the co-solvent with these gels [219]. An overview of the use of these biodegradable gelatin polymers as the basis of chiral liquid crystals has been published [220]. The ability to use water as the co-solvent and stretch the gels to alter their properties are two attributes of these systems.

Fragmented DNA strands consisting of 100–500 base pairs have also been examined as chiral liquid crystals [221, 222]. Enantiomeric differentiation of alanine was observed in the ^1H NMR spectrum [221]. ^2H NMR could be used to differentiate the enantiomers of deuterated amino acids and the prochiral hydrogen atoms in deuterated glycine and DMSO- d_6 [222]. An advantage of these DNA phases is that water can be used as the solvent. One report noted that orientation of the fragmented DNA in the magnetic field can take up to 3–4 h [221].

A few studies have used chiral liquid crystals to examine the $^2\text{H}/^1\text{H}$ ratios in the methylene groups of fatty acids [223–225]. Enzymatic synthesis of fatty acids often leads to different distributions of ^2H atoms into the methylene groups. The *pro-R* and *pro-S* positions are distinguishable in compounds such as methyl linoleate (**188**), methyl linolenate (**189**), and methyl vernoleate (**190**) using natural abundance ^2H NMR with the chiral liquid crystal PBLG. Using a 50/50 mixture of PBLG and poly- γ -benzyl-D-glutamate (PBDG) it is possible to assign the chain positions. In PBLG alone there is a duplication of signals because of the quadrupolar splitting. It is possible to assign almost all the *pro-R* and *pro-S* positions in a C18 fatty acid [223].



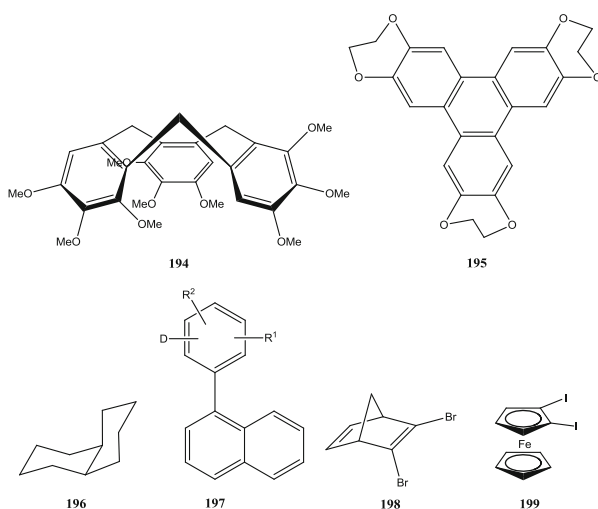
Subsequent work extended this method to α -eleostearic acid (**191**) and punicic acid (**192**). The influence of co-solvents was explored in this study and pyridine is particularly effective at facilitating enantiodifferentiation of larger numbers of prochiral methylene groups and enhancing the degree of enantiomeric differentiation. The procedure facilitated assignment of the *pro-R* and *pro-S* sites without requiring cleavage of the fatty acid to smaller units [224]. This method has been used to explore the distribution of ^2H that occurs in the epoxidation of linoleate (**188**) to vernoleate (**190**) with two different plant enzymes [225].

An advantage of chiral liquid crystals in NMR applications is that they may enantiodifferentiate any compound because no specific interaction has to occur. Many studies published to date have focused on expanding the range of compounds that can be successfully analyzed with chiral liquid crystals. This even includes aliphatic hydrocarbons. Recent reviews discuss the range of compounds that can be analyzed using chiral liquid crystals [5–7].

Recent studies continue to expand the range of compounds that can be differentiated with chiral liquid crystals. The analysis of primary and secondary amines using chiral liquid crystals such as PBLG is enhanced if *N,N*-dimethylformamide is used as the co-solvent. Chloroform and methylene chloride are usually not suitable for use with amines because of solubility issues. Perdeuterobenzyl chloride (**193**) is an excellent achiral derivatizing agent for amines, providing intense ^2H signals for the aromatic and methylene hydrogen atoms to analyze for differentiation. Derivatization of primary amines leads to a dibenzyl species but the ^2H NMR spectrum is a time average of the two and only one set of signals is observed [226].

Several recent studies demonstrate the utility of chiral liquid crystals in exploring the chirality of conformationally flexible species. ^{13}C and ^2H NMR was used to differentiate the crown and saddle isomers of nonamethoxy-cyclotrimeratrylene in PBLG (**194** – M-enantiomer depicted for crown isomer). ^{13}C spectra were recorded in natural abundance and for a compound enriched in the ring methylene and one methoxy group. Chemical shift anisotropy was observed in the ^{13}C NMR spectrum. ^2H spectra were on a sample enriched at methylene and aromatic sites [227].

Tridioxyethylenetriphenylene (**195**) has a fast chair-chair flip of the side chains and is axially symmetric with pairs of enantiotopic ethylene groups. Using a compound in which the side chains were partially deuterated, large differentiation of these enantiotopic groups was observed in the ^2H NMR in PBLG [228]. *cis*-Decalin (**196**) is enantiomeric under conditions of slow exchange. Its methylene groups are enantiotopic under conditions of fast exchange. ^2H and ^{13}C NMR were used to examine both of these processes in PBLG/chloroform [229].



Liquid crystals are also useful for studying atropisomeric di-aryls. Deuterated di-aryls of general structure **197** were examined by ^2H NMR in PBLG/chloroform or methylene chloride. Observation of the enantiomeric forms of these compounds is dependent on temperature. Using variable temperature measurements, both enantiomeric differentiation and the differentiation of enantiotopic directions in prochiral substrates is observed [230]. Similarly, PBLG/chloroform enables the differentiation of enantiotopic directions in **198** and **199**, both of which are prochiral compounds [231]. The enantiomeric composition of cationic planar chiral (η^6 -arene) $\text{Mn}(\text{CO})_3^+$ complexes (**200**) has been determined using proton decoupled ^2H NMR of a monodeuterated species in PBLG/chloroform [232].

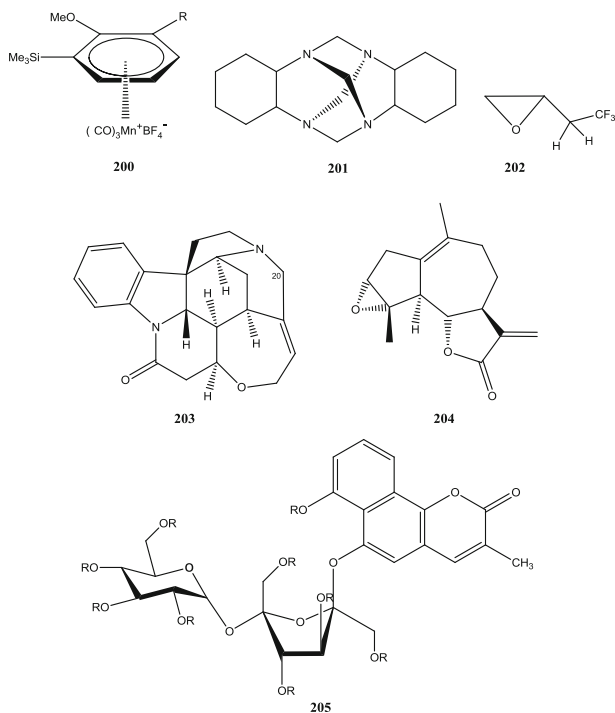
Compound **201** is a prochiral rigid molecule with S_4 symmetry. The derivative with deuterium at the four core methylene groups was studied by ^2H NMR in PBLG/pyridine and differentiation of the enantiotopic groups was observed. With this achievement, chiral liquid crystals have now been shown to bring about enantiotopic differentiation in all possible symmetry groups containing enantiotopic groups [233].

Chiral liquid crystals have been used mostly for determination of enantiomeric composition. The use of liquid crystals for assignment of absolute configuration has been limited. In one study it was shown that a series of isostructural rigid epoxides of known configuration, one example of which is **202**, had similar ordering in

PBLG/chloroform and other liquid crystal/co-solvent combinations such that the empirical trends could likely be used to assign the absolute configuration to an unknown compound of a similar structure [234].

A more intriguing prospect is the potential to use residual dipolar couplings (RDCs) in chiral liquid crystals to assign absolute configuration. RDCs can be measured for molecules that are aligned in a magnetic field. A pair of (*R*)- and (*S*)-enantiomers will have different RDCs in a chiral liquid crystal. Since the magnitude of the RDCs depends on the ordering parameters, if the ordering parameters are known for a compound, RDCs can be related back to its absolute configuration.

RDCs measured in PBLG/chloroform have been used to assign the diastereotopic methylene atoms at C20 in strychnine (**203**) [235]. Subsequently it was discovered that PELG provided a more favorable alignment and all of the diastereotopic protons in **203** could be assigned [236]. Similarly, the diastereotopic protons at the C2, C8, and C9 positions of ludartin (**204**) were assigned using natural abundance ^1H - ^{13}C RDCs. The RDCs were measured in a stretched poly(methyl methacrylate) gel (PMMA) with chloroform as the co-solvent [237].

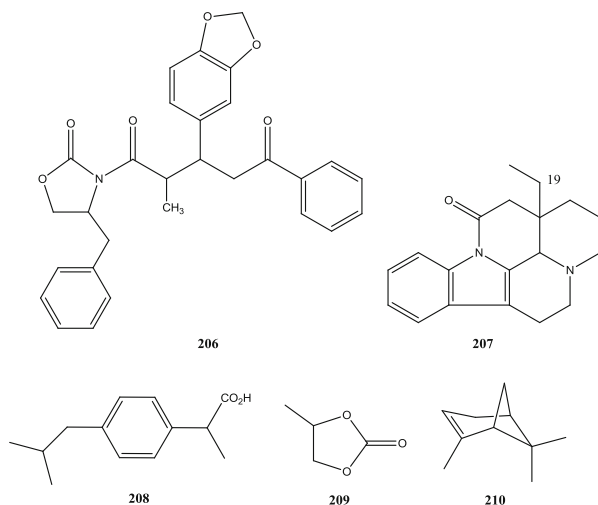


The RDCs for the two enantiomers of tryptophan methyl ester hydrochloride were measured in a high molecular weight PBLG. The co-solvent was a 2:1 ratio of chloroform and DMSO, where the DMSO was needed to solubilize the tryptophan salt [238]. In recent work, RDCs from t_2 -coupled ^1H and ^{13}C HSQC spectra were used

to assign the stereochemistry about some of the sites in sucro-neolambertellin (**205**). Spectra of the peracetate species were recorded in three aligning polymers. Only the *RSSR* isomer was judged clearly consistent with the RDCs and other NOE data for the compound [239].

206, which is the result of a Michael addition, has three stereogenic centers in the flexible chain. RDCs measured in polyacrylamide and poly(acrylonitrile) gels reduced the number of possible conformations and configurations for the compound. DFT was then used to predict optical rotation dispersion spectra. The results were compared to experimental data and enabled an assignment of the absolute stereochemistry [240].

The stereochemistry of eburnamonine (**207**) and its 19-hydroxy derivative was investigated in part through the use of RDCs obtained in liquid crystals. RDCs were measured in a PMMA gel swollen in chloroform. The configuration at C21 was fixed and all possible configurations at C19 and C20 were generated. Computed RDCs were compared to measured RDCs for the best match. Finally, these results were correlated with CD data and DT-DFT computed circular dichroism spectra to arrive at an absolute configuration [241].



The reports described above involve the assignment of stereochemistry either in compounds where some stereochemical information is already known or in combination with other analysis methods such as NOE data, circular dichroism spectra, or DFT calculations. Two reports used only RDCs measured in liquid crystals to assign absolute stereochemistry. One involved assigning the absolute stereochemistry of ibuprofen (**208**) through RDCs measured in PBLG/chloroform [242]. The other involved assigning the absolute configuration of 3-methyl-1,3-dioxolan-2-one (**209**) through RDCs measured in PBLG/chloroform [243]. Recently a paper coauthored by many of the leading investigators in the field called into question

the conclusions in these two earlier reports [244]. The fundamental problems with using RDCs measured in chiral liquid crystals to assign absolute stereochemistry is that there is no means of predicting the alignment tensors from first principles or predicting the ensembles of conformers for the enantiomers. To demonstrate this problem further, the authors show the unreliability in being able to predict alignment tensors for a rigid compound such as α -pinene (**210**). Flexible compounds will present even more difficulties [244].

Other work has shown that it would be possible to assign absolute configurations of compounds in chiral liquid crystals if one could predict the sign of the rotation of the principal axis system of the Saupe matrix in molecules when going from a racemic (50:50 PBLG/PBDG) to an enantiomerically pure (PBLG) liquid crystal [245]. Unfortunately, at this time the predictive theory and computational tools do not yet exist to complete this task.

Two recent reviews describe the use of chiral liquid crystals for enantiomeric differentiation. One emphasizes the use of RDCs for configurational and conformational analysis [246]. The other gives a thorough overview of the NMR methods that can be used in chiral liquid crystals to differentiate enantiomers [247]. A third review has a briefer coverage of chiral liquid crystals and a more extensive discussion of recent work in which solid-state NMR spectra is used to examine chiral compounds. The use of one-dimensional exchange spectroscopy by sideband alteration (ODESSA) for analysis of solids is discussed. The method can be used to determine enantiomeric composition, but relies on using nuclei other than ^1H such as ^{31}P , ^{19}F , ^2H , ^{13}C , or ^{15}N [248].

References

1. Raban M, Mislow K (1965) The determination of optical purity by nuclear magnetic resonance spectroscopy. *Tetrahedron Lett* 6:4249–4253
2. Pirkle WH (1966) The nonequivalence of physical properties of enantiomers in optically active solvents. Differences in nuclear magnetic resonance spectra. I. *J Am Chem Soc* 88:1837
3. Whitesides GM, Lewis DW (1970) Tris[3-(*tert*-butylhydroxymethylene)-d-camphorato]europium(III). A reagent for determining enantiomeric purity. *J Am Chem Soc* 92:6979–6980
4. Sackmann E, Meiboom S, Snyder LC (1968) The nuclear magnetic resonance spectra of enantiomers in optically active liquid crystals. *J Am Chem Soc* 90:2183–2184
5. Wenzel TJ (2007) *Discrimination of chiral compounds using NMR spectroscopy*. Wiley, Hoboken
6. Wenzel TJ, Chisholm CD (2011) Using NMR spectroscopic methods to determine enantiomeric purity and assign absolute stereochemistry. *Prog NMR Spectrosc* 59:1–63
7. Wenzel TJ (2012) Spectroscopic analysis: NMR and shift reagents. *Compr Chirality* 8:545–570
8. Wenzel TJ, Chisholm CD (2011) Assignment of absolute configuration using chiral reagents and NMR spectroscopy. *Chirality* 23:190–214
9. Blazewska KM, Gajda T (2009) Assignment of the absolute configuration of hydroxy- and aminophosphonates by NMR spectroscopy. *Tetrahedron Asymmetry* 20:1337–1361

10. Duddeck H, Gomez ED (2009) Chiral recognition of ethers by NMR spectroscopy. *Chirality* 21:51–68
11. Dale JA, Mosher HS (1973) Nuclear magnetic resonance enantiomer reagents. Configurational correlations via nuclear magnetic resonance chemical shifts of diastereomeric mandelate, *O*-methylmandelate, and α -methoxy- α -trifluoromethylphenylacetate (MTPA) esters. *J Am Chem Soc* 95:512–519
12. Brand DJ, Steenkamp JA, Brandt EV, Takeuchi Y (2007) Conformational studies of (–)-epicatechin-Mosher ester. *Tetrahedron Lett* 48:2769–2773
13. Dale JA, Mosher HS (1968) Nuclear magnetic resonance nonequivalence of diastereomeric esters of α -substituted phenylacetic acids for the determination of stereochemical purity. *J Am Chem Soc* 90:3732–3738
14. Trost BM, Belletire JL, Godleski S, McDougal PG, Balkovec JM (1986) On the use of the *O*-methylmandelate ester for establishment of absolute configuration of secondary alcohols. *J Org Chem* 51:2370–2374
15. Kusumi T, Ohtani I (1999) Determination of the absolute configuration of biologically active compounds by the modified Mosher's method. In: Cooper R, Snyder JK (eds) *Biology-chemistry interface*. Marcel Dekker, New York, pp 103–137
16. Louzao I, Seco JM, Quinoa E, Riguera R (2010) ^{13}C NMR as a general tool for the assignment of absolute configuration. *Chem Commun* 46:7903–7905
17. Ghiviriga I (2012) Selective excitation 1D-NMR experiments for the assignment of the absolute configuration of secondary alcohols. *J Org Chem* 77:3978–3985
18. Hoye TR, Jeffrey CS, Shao F (2007) Mosher ester analysis for the determination of absolute configuration of stereogenic (chiral) carbinol carbons. *Nat Protoc* 2:2451–2458
19. Hoye TR, Erickson SE, Erickson-Birkedahl SL, Hale CRH, Izgu EC, Mayer MJ, Notz PK, Renner MK (2010) Long-range shielding effects in the ^1H NMR spectra of Mosher-like ester derivatives. *Org Lett* 12:1768–1771
20. Curran DP, Sui B (2009) A “shortcut” Mosher ester method to assign configurations of stereocenters in nearly symmetric environments. Fluorous mixture synthesis and structure assignment of petrocortyne A. *J Am Chem Soc* 131:5411–5413
21. Latypov SK, Galiullina NF, Aganov AV, Kataev VE, Riguera R (2001) Determination of the absolute stereochemistry of alcohols and amines by NMR of the group directly linked to the chiral derivatizing reagent. *Tetrahedron* 57:2231–2236
22. Takeuchi Y, Itoh N, Satoh T, Koizumi T, Yamaguchi K (1993) Chemistry of novel compounds with multifunctional carbon structure. 9. Molecular design, synthetic studies, and NMR investigation of several efficient chiral derivatizing reagents which give very large ^{19}F NMR $\Delta\delta$ values in enantiomeric excess determination. *J Org Chem* 58:1812–1820
23. Majewska P, Doscoczek M, Lejczak B, Kafarski P (2009) Enzymatic resolution of α -hydroxyphosphinates with two stereogenic centres and determination of absolute configuration of stereoisomers obtained. *Tetrahedron Asymmetry* 20:1568–1574
24. Seco JM, Latypov S, Quinoa E, Riguera R (1995) Determination of the absolute configuration of alcohols by low temperature ^1H NMR of aryl(methoxy)acetates. *Tetrahedron Asymmetry* 6:107–110
25. Seco JM, Quinoa E, Riguera R (2004) The assignment of absolute configuration by NMR. *Chem Rev* 104:17–117
26. Jimenez-Teja D, Daoubi M, Collado IG, Hernandez-Galan H (2009) Lipase-catalyzed resolution of 5-acetoxy-1,2-dihydroxy-1,2,3,4-tetrahydronaphthalene. Application to the synthesis of (+)-(3*R*,4*S*)-*cis*-4-hydroxy-6-deoxyscytalone, a metabolite isolated from *Colletotrichum acutatum*. *Tetrahedron* 65:3392–3396
27. Harada N (2008) Determination of absolute configurations by X-ray crystallography and ^1H NMR anisotropy. *Chirality* 20:691–723
28. Kuwahara S, Naito J, Yamamoto Y, Kasai Y, Fujita T, Noro K, Shimanuki K, Akagi M, Watanabe M, Matsumoto T, Watanabe M, Ichikawa A, Harada N (2007) Crystalline-state

- conformational analysis of $M\alpha$ NP esters, powerful resolution and chiral ^1H NMR anisotropy tools. *Eur J Org Chem* 2007:1827–1840
29. Kasai Y, Sugio A, Sekiguchi S, Kuwahara S, Matsumoto T, Watanabe M, Ichikawa A, Harada N (2007) Conformational analysis of $M\alpha$ NP esters, powerful chiral resolution and ^1H NMR anisotropy tools – aromatic geometry and solvent effects on $\Delta\delta$ values. *Eur J Org Chem* 2007:1811–1826
 30. Naito J, Kuwahara S, Watanabe M, Decatur J, Bos PH, Van Summeren RP, Horst BT, Feringa BL, Minnaard AJ, Harada N (2008) Stereoselective synthesis of 2,3,7-trimethylcyclooctanone and related compounds and determination of their relative and absolute configurations by the $M\alpha$ NP acid method. *Chirality* 20:1053–1065
 31. Sekiguchi S, Akagi M, Naito J, Yamamoto Y, Taji H, Kuwahara S, Watanabe M, Ozawa Y, Toriumi K, Harada N (2008) Synthesis and enantionpure aliphatic acetylene alcohols and determination of their absolute configurations by ^1H NMR and/or X-ray crystallography. *Eur J Org Chem* 2008:2313–2324
 32. Murakami S, Satou K, Kijima T, Watanabe M, Izumi T (2011) Determination of optical purity and absolute configuration of natural 12-hydroxystearic acid by the ^1H NMR anisotropy method. *Eur J Lipid Sci Technol* 113:450–458
 33. Fujita T, Obata K, Kuwahara S, Miura N, Nakahashi A, Monde K, Decatur J, Harada N (2007) (*R*)-(+)-[VCD(+)]945]-4-ethyl-4-methyloctane, the simplest chiral saturated hydrocarbon with a quaternary stereogenic center. *Tetrahedron Lett* 48:4219–4222
 34. Omata K, Kotani K, Kabuto K, Fujiwara T, Takeuchi Y (2010) Confirmation by IR of the preferred conformations of CFTA esters in solution: a highly reliable criterion for the stereochemistry assignment of chiral alcohols. *Chem Commun* 46:3610–3612
 35. Blezewska K, Paneth P, Gajda T (2007) The assignment of the absolute configuration of diethyl hydroxyl- and aminophosphonates by ^1H and ^{31}P NMR using naproxen as a reliable chiral derivatizing agent. *J Org Chem* 72:878–887
 36. Sarotti AM, Pisano PL, Pellegrinet SC (2011) Evaluation of the use of mandelate derivatives to determine the enantiomeric purity and the absolute configuration of secondary cyclohexenols. *Arkivoc* 7:343–357
 37. Pisano PL, Sarotti AM, Pellegrinet SC (2009) An experimental/theoretical approach to determine the optical purity and the absolute configuration of *endo*- and *exo*-norborn-5-*en*-2-ol using mandelate derivatives. *Tetrahedron Lett* 50:6121–6125
 38. Perez-Estrada S, Joseph-Nathan P, Jimenez-Vazquez HA, Medina-Lopez ME, Ayala-Mata F, Zepeda LG (2012) Diastereoselective preparation of (*R*)- and (*S*)-2-methoxy-2-phenylpent-3-ynoic acids and their use as reliable chiral derivatizing agents. *J Org Chem* 77:1640–1652
 39. Tsuda M, Toriyabe Y, Endo T, Kobayashi J (2003) Application of modified Mosher's method for primary alcohols with a methyl group at C2 position. *Chem Pharm Bull* 51:448–451
 40. Yasuhara F, Yamaguchi S, Kasai R, Tanaka O (1986) Assignment of absolute configuration of 2-substituted-1-propanols by ^1H NMR spectroscopy. *Tetrahedron Lett* 27:4033–4034
 41. Latypov SK, Ferreiro MJ, Quinoa E, Riguera R (1998) Assignment of the absolute configuration of β -chiral primary alcohols by NMR: scope and limitations. *J Am Chem Soc* 120:4741–4751
 42. Izumi S, Moriyoshi H, Hirata T (1994) Identification of absolute configuration of tertiary alcohols by combination of Mosher's method and conformational analysis. *Bull Chem Soc Jpn* 67:2600–2602
 43. Takahashi H, Kato N, Iwashima M, Iguchi K (1999) Determination of absolute configurations of tertiary alcohols by NMR spectroscopy. *Chem Lett* 1181–1182
 44. Freire F, Seco JM, Quinoa E, Riguera R (2007) Challenging the absence of observable hydrogens in the assignment of absolute configurations by NMR: application to chiral primary alcohols. *Chem Commun* 43:1456–1458
 45. Pham VC, Jossang A, Sevenet T, Nguyen VH, Bodo B (2007) Myrioneurinol: a novel alkaloid skeleton from *Myrioneuton nutans*. *Tetrahedron* 63:11244–11249

46. Galman JL, Hailes HC (2009) Application of a modified Mosher's method for the determination of enantiomeric ratio and absolute configuration at C-3 of chiral 1,3-dihydroxy ketones. *Tetrahedron Asymmetry* 20:1828–1831
47. Yasumoto K, Nishigami A, Aoi H, Tsuchihashi C, Kasai F, Kusumi T, Ooi T (2008) Isolation and absolute configuration determination of aliphatic sulfates as the *Daphnia* Kairomones inducing morphological defense of a phytoplankton – Part 2. *Chem Pharm Bull* 56:129–132
48. Louzao I, Garcia R, Seco JM, Quinoa E, Riguera R (2009) Absolute configuration of ketone cyanohydrins by ^1H NMR: the special case of polar substituted tertiary alcohols. *Org Lett* 11:53–56
49. Porto S, Seco JM, Ortiz A, Quinoa E, Riguera R (2007) Chiral thiols: the assignment of their absolute configuration by ^1H NMR. *Org Lett* 9:5015–5018
50. Wakabayashi M, Wakabayashi H, Eisenreich W, Morimitsu Y, Kubota K, Engel KH (2011) Determination of the absolute configurations of 4-mercapto-2-alkanones using the ^1H NMR anisotropy method and enzyme catalyzed kinetic resolution of the corresponding 4-acetylthio-2-alkanones. *Eur Food Res Technol* 232:753–760
51. Seco JM, Quinoa E, Riguera R (1999) Boc-phenylglycine: the reagent of choice for the assignment of the absolute configuration of α -chiral primary amines by ^1H NMR spectroscopy. *J Org Chem* 64:4669–4675
52. Latypov SK, Seco JM, Quinoa E, Riguera R (1995) Determination of the absolute stereochemistry of chiral amines by ^1H NMR of arylmethoxyacetic acid amides: the conformational model. *J Org Chem* 60:1538–1545
53. Hoye TR, Renner MK (1996) MTPA (Mosher) amides of cyclic secondary amines: conformational aspects and a useful method for assignment of amine configuration. *J Org Chem* 61:2056–2064
54. Hoye TR, Renner MK (1996) Applications of MTPA (Mosher) amides of secondary amines: assignment of absolute configuration in chiral cyclic amines. *J Org Chem* 61:8489–8495
55. Vidal P, Pedregal C, Diaz N, Broughton H, Acena JL, Jimenez A, Espinosa JF (2007) Assignment of absolute configuration on the basis of the conformational effects induced by chiral derivatizing agents: the 2-arylpiperidine case. *Org Lett* 9:4123–4126
56. Gao J, Haas H, Wang KY, Chen Z, Breitenstein W, Rajan S (2008) The use of MPA amide for the assignment of absolute configuration of a sterically hindered cyclic secondary amine by “mix and shake” NMR method. *Magn Reson Chem* 46:17–22
57. Fujiwara T, Segawa M, Fujisawa H, Murai T, Takahashi T, Omata K, Kabuto K, Ludwig SN, Unkefer CJ, Takeuchi Y (2008) Reliable assignment of absolute configuration of chiral amines based on the analysis of ^1H NMR spectra of their CFTA amide diastereomers. *Tetrahedron Asymmetry* 19:847–856
58. Clerc C, Matarazzo I, Ruedi P (2009) The absolute configuration of the (+)- and (–)-*cis*- and (+)- and (–)-*trans*-1-benzyl-4-hydroxypiperidine-3-methanols: an unusual application of the ^1H -NMR Mosher method. *Helv Chim Acta* 92:14–28
59. Seco JM, Quinoa E, Riguera R (2012) Assignment of the absolute configuration of polyfunctional compounds by NMR using chiral derivatizing agents. *Chem Rev* 112:4603–4641
60. Porto S, Seco JM, Espinosa JF, Quinoa E, Riguera R (2008) Resin-bound chiral derivatizing agents for assignment of configuration by NMR spectroscopy. *J Org Chem* 73:5714–5722
61. Ohru H, Terashima H, Imaizumi K, Akasaka K (2002) A solution of the “intrinsic problem” of diastereomer method in chiral discrimination. Development of a method for highly efficient and sensitive discrimination of chiral alcohols. *Proc Jpn Acad Ser B Phys Biol Sci* 78:69–72
62. Imaizumi K, Terasima H, Akasaka K, Ohru H (2003) Highly potent chiral labeling reagents for the discrimination of chiral alcohols. *Anal Sci* 19:1243–1249
63. Nishida Y, Itoh E, Abe M, Ohru H, Meguro H (1995) Synthesis of a series of fluorescent carboxylic acids with a 1,3-benzodioxole skeleton and their evaluation as chiral derivatizing reagents. *Anal Sci* 11:213–220

64. Akasaka K, Imaizumi K, Sakakibara R, Terashima H, Ohru H (2000) Chiral discrimination of branched alkyl chain by labeling with chiral derivatization reagents. *Tennen Yuki Kagobutsu Toronkai Koen Yoshishu* 42:565–570
65. Ohtaki T, Akasaka K, Kabuto C, Ohru H (2005) Chiral discrimination of secondary alcohols by both $^1\text{H-NMR}$ and HPLC after labeling with a chiral derivatization reagent, 2-(2,3-anthracenedicarboximide)cyclohexane carboxylic acid. *Chirality* 17:S171–S176
66. Ahn HC, Choi K (2007) *N*-(2-Nitrophenyl)proline: an intramolecular hydrogen bond forming reagent for the determination of the absolute configuration of primary amines. *Org Lett* 9:3853–3855
67. Ahn HC, Choi K (2007) Determination of the absolute configuration of primary amines in polar NMR solvents. *Chem Lett* 36:1330–1331
68. Gorunova ON, Livantsov MV, Grishin YK, Kataeva NA, Kochetkov KA, Churakov AV, Kuz'mina LG, Dunina VV (2012) Asymmetric synthesis and absolute configuration of a planar chiral phosphapalladacycle with a ferrocenyl framework. *Polyhedron* 31:37–43
69. Han SY, Choi K (2011) *N*-Arylcarbonylpseudoprolines as tunable chiral derivatizing agents for the determination of the absolute configuration of secondary alcohols. *Eur J Org Chem* 2011:2920–2923
70. Sano S, Nakao M, Takeyasu M, Kitaike S, Yoshioka Y, Nagao Y (2009) Use of diketopiperazines for determining absolute configurations of α -substituted serines by ^1H NMR spectroscopy. *Heterocycles* 79:781–789
71. Shim YJ, Choi K (2010) Cyclic ketals of tartaric acid: simple and tunable reagents for the determination of the absolute configuration of primary amines. *Org Lett* 12:880–882
72. Sungsuwan S, Ruangsupapichart N, Prabpai S, Kongsaree P, Thongpanchang T (2010) Tetrahydro-1,4-epoxynaphthalene-1-carboxylic acid: a chiral derivatizing agent for the determination of the absolute configuration of secondary alcohols. *Tetrahedron Lett* 51:4965–4967
73. du Boullay OT, Alba A, Oukhatar F, Martin-Vaca B, Bourissou D (2008) (1-Naphthyl) (trifluoromethyl) *O*-carboxy anhydride as a chiral derivatizing agent: eclipsed conformation enforced by hydrogen bonding. *Org Lett* 10:4669–4672
74. Sawen E, Huttunen E, Zhang X, Yang Z, Widmalm G (2010) Structural analysis of the exopolysaccharide produced by *Streptococcus thermophilus* ST1 solely by NMR spectroscopy. *J Biomol NMR* 47:125–134
75. Ferreiro MJ, Latypov SK, Quinoa E, Riguera R (2000) Assignment of the absolute configuration of α -chiral carboxylic acids by ^1H NMR spectroscopy. *J Org Chem* 65:2658–2666
76. Berti F, Forzato C, Furlan G, Nitti P, Pitacco G, Valentin E, Zangrando E (2009) Synthesis of optically active α -benzyl paraconic acids and their esters and assignment of their absolute configuration. *Tetrahedron Asymmetry* 20:313–321
77. Lundborg M, Fontana C, Widmalm G (2011) Automatic structure determination of regular polysaccharides based solely on NMR spectroscopy. *Biomacromolecules* 12:3851–3855
78. Makarieva TN, Shubina LK, Guzii AG, Ivanchina NV, Denisenko VA, Afiyatullof SS, Dmitrenok PS, Kalinovsky AI, Stonik VA (2011) Determination of absolute stereochemistry of natural alicyclic glycosides by ^1H NMR spectroscopy without application of chiral reagents – an indication. *Nat Prod Commun* 6:673–676
79. Ammazalorso A, Bettoni G, De Filippis B, Fantacuzzi M, Giampietro L, Giancristofaro A, Maccallini C, Re N, Amoroso R, Coletti C (2008) Synthesis of 2-aryloxypropanoic acids analogues of clofibric acid and assignment of the absolute configuration by ^1H NMR spectroscopy and DFT calculations. *Tetrahedron Asymmetry* 19:989–997
80. Yabuuchi T, Kusumi T (2000) Phenylglycine methyl ester, a useful tool for absolute configuration determination of various chiral carboxylic acids. *J Org Chem* 65:397–404
81. Nagai Y, Kusumi T (1995) New chiral anisotropic reagents for determining the absolute configuration of carboxylic acids. *Tetrahedron Lett* 36:1853–1856
82. Kusumi T, Ohtani II (1999) Determination of the absolute configuration of biologically active compounds by the modified Mosher's method. *Biol-Chem Interface* 103–137

83. Hoye TR, Koltun DO (1998) An NMR strategy for determination of configuration of remote stereogenic centers: 3-methylcarboxylic acids. *J Am Chem Soc* 120:4638–4643
84. Hoye TR, Hamad AS, Koltun DO, Tennakoon MA (1998) An NMR method for determination of configuration of β -substituted carboxylic acids. *Tetrahedron Lett* 41:2289–2293
85. Suarez-Castillo OR, Melendez-Rodriguez M, Castelan-Duarte LE, Sanchez-Zavala M, Rivera-Becerril E, Morales-Rios MS, Joseph-Nathan P (2009) Absolute configuration determination of 2-(2-oxo-3-indolyl)acetamide derivatives. *Tetrahedron Asymmetry* 20:2374–2389
86. Kaik M, Gajewy J, Grajewski J, Gawronski J (2008) Discrimination of enantiomers of α -amino acids by chiral derivatizing reagents from *trans*-1,2-diaminocyclohexane. *Chirality* 20:301–306
87. Sabot C, Mosser M, Antheaume C, Mioskowski C, Baati R, Wagner A (2009) Novel chiral derivatizing isothiocyanate-based agent for the enantiomeric excess determination of amines. *Chem Commun* 45:3410–3412
88. Fukui H, Fukushi Y (2010) NMR determinations of the absolute configuration of α -chiral primary amines. *Org Lett* 12:2856–2859
89. Nandhakumar R, Ryu J, Park H, Tang L, Choi S, Kim KM (2008) Effects of ring substituents on enantioselective recognition of amino alcohols and acids in uryl-based binol receptors. *Tetrahedron* 64:7704–7708
90. Nandhakumar R, Soo AY, Hong J, Ham S, Kim KM (2009) Enantioselective recognition of 1,2-amino alcohols by the binol receptor dangled with pyrrole-2-carboxamide and its analogues. *Tetrahedron* 65:666–671
91. Suarez-Castillo OR, Melendez-Rodriguez M, Castelan-Duarte LE, Zuniga-Estrada EA, Cruz-Borbolla J, Morales-Rios MS, Joseph-Nathan P (2011) Absolute configuration assignment of 3-oxoindolylacetyl-4-phenyloxazolidinone derivatives. *Tetrahedron Asymmetry* 22:2085–2098
92. Kim H, So SM, Yen CPH, Vinhato E, Lough AJ, Hong JI, Kim HJ, Chin J (2008) Highly stereospecific generation of helical chirality by imprinting with amino acids: a universal sensor for amino acid enantiopurity. *Angew Chem Int Ed* 47:8657–8660
93. Sambasivan S, Kim D, Ahn KH (2010) Chiral discrimination of α -amino acids with a C_2 -symmetric homoditopic receptor. *Chem Commun* 46:541–543
94. Schramm H, Christoffers J (2009) Synthesis, resolution and absolute configuration of 4-amino-3-phenylpiperidine. *Tetrahedron Asymmetry* 20:2724–2727
95. Kurosu M, Li K (2009) New chiral derivatizing agents: convenient determination of absolute configurations of free amino acids by ^1H NMR. *Org Lett* 11:911–914
96. Davies SR, Mitchell MC, Cain CP, Devitt PG, Taylor RJ, Kee TP (1998) Phospho-transfer catalysis. On the asymmetric hydrophosphonylation of aldehydes. *J Organomet Chem* 550:29–57
97. Hulst R, Kellogg RM, Feringa BL (1995) New methodologies for enantiomeric excess (ee) determination based on phosphorus NMR. *Recl Trav Chim Pays-Bas* 114:115–138
98. Murai T (2008) Phosphoroselenoic acid derivatives bearing a binaphthyl group as a chiral molecular tool. *Phosphorus Sulfur Silicon* 189:889–896
99. Murai T, Tsuji H, Imaizumi S, Maruyama T (2010) Assignment of the absolute configurations of 1-aryl-2-propanols with the use of phosphoroselenoyl chlorides as chiral derivatizing agents. *Chem Lett* 39:524–526
100. Reiner T, Naraschewski FN, Eppinger J (2009) ^{31}P NMR assays for rapid determination of enantiomeric excess in catalytic hydrosilylations and transfer hydrogenations. *Tetrahedron Asymmetry* 20:362–367
101. Amberg M, Bergstrasser U, Stapf G, Hartung J (2008) 2-Chloro-(4*R*,5*R*)-bis[(1*R*,2*S*,5*R*)-menth-1-yloxy-carbonyl]-1,3,2-dioxaphospholane: a practical chiral pool-derived reagent for determining enantiomeric purity of alcohols. *J Org Chem* 73:3907–3910
102. Amberg M, Kempter I, Bergstrasser U, Stapf G, Hartung J (2011) Derivatizing agents from phosphorus trichloride and terpenyl tartrates for determining enantiomeric purity of alcohols. *Tetrahedron Asymmetry* 22:752–760

103. Mastranzo VM, Quintero L, De Parrodi CA (2007) Determination of the enantiomeric excess of chiral carboxylic acids by ^{31}P NMR with phosphorylated derivatizing agents from C_2 -symmetrical diamines containing the (*S*)- α -phenylethyl group. *Chirality* 19:503–507
104. Perez-Fuertes Y, Kelly AM, Fossey JS, Powell ME, Bull SD, James TD (2008) Simple protocols for NMR analysis of the enantiomeric purity of chiral primary amines. *Nat Protoc* 3:210–214
105. Kelly AM, Bull SD, James TD (2008) Simple chiral derivatisation protocols for NMR analysis of the enantiopurity of 1,2-diphenylethane-1,2-diamine and *N*-Boc-cyclohexane-1,2-diamine. *Tetrahedron Asymmetry* 19:489–494
106. Perez-Fuertes Y, Kelly AM, Johnson AL, Arimori S, Bull SD, James TD (2006) Simple protocol for NMR analysis of the enantiomeric purity of primary amines. *Org Lett* 8:609–612
107. Kelly AM, Perez-Fuertes Y, Fossey JS, Yeste SL, Bull SD, James TD (2008) Simple protocols for NMR analysis of the enantiomeric purity of chiral diols. *Nat Protoc* 3:215–219
108. Yeste SL, Powell ME, Bull SD, James TD (2009) Simple chiral derivatization protocols for ^1H NMR and ^{19}F NMR spectroscopic analysis of the enantiopurity of chiral diols. *J Org Chem* 74:427–430
109. Chaudhari SR, Suryaprakash N (2012) Three-component chiral derivatizing protocols for NMR spectroscopic enantiodiscrimination of hydroxyl acids and primary amines. *J Org Chem* 77:648–651
110. Chaudhari SR, Suryaprakash N (2012) Simple and efficient methods for discrimination of chiral diacids and chiral alpha-methyl amines. *Org Biomol Chem* 10:6410–6419
111. Powell ME, Kelly AM, Bull SD, James TD (2009) A simple chiral derivatisation protocol for ^1H NMR spectroscopic analysis of the enantiopurity of *O*-silyl-1,2-amino alcohols. *Tetrahedron Lett* 50:876–879
112. Freire F, Quinoa E, Riguera R (2008) In tube determination of the absolute configuration of α - and β -hydroxy acids by NMR via chiral BINOL borates. *Chem Commun* 44:4147–4149
113. Kwit M, Sharma ND, Boyd DR, Gawronski J (2008) Determination of absolute configuration of conformationally flexible *cis*-dihydrodiol metabolites: effect of diene substitution pattern on the circular dichroism spectra and optical rotations. *Chirality* 20:609–620
114. Boyd DR, Sharma ND, Coen GP, Gray PJ, Malone JF, Gawronski J (2007) Enzyme-catalysed synthesis and absolute configuration assignments of *cis*-dihydrodiol metabolites from 1,4-disubstituted benzenes. *Chem Eur J* 13:5804–5811
115. Shabbir SH, Joyce LA, da Cruz GM, Lynch VM, Sorey S, Anslyn EV (2009) Pattern-based recognition for the rapid determination of identity, concentration, and enantiomeric excess of subtly different threo diols. *J Am Chem Soc* 131:13125–13131
116. Ferreira JG, Goncalves SMC (2010) Enantiomeric excess detection with (*S*)-3-phenyl-2-(selenophenyl)propan-1-ol derivatizing agent via mix and shake ^{77}Se NMR. *J Braz Chem Soc* 21:2023–2026
117. Orlov NV, Ananikov VP (2010) First principles design of derivatizing agent for direct determination of enantiomeric purity of chiral alcohols and amines by NMR spectroscopy. *Chem Commun* 46:3212–3214
118. Wenzel TJ, Amoono EP, Shariff SS, Aniagyei SE (2003) Sulfated and carboxymethylated cyclodextrins and their lanthanide complexes as chiral NMR differentiating agents. *Tetrahedron Asymmetry* 14:3099–3104
119. Dignam CF, Randall LA, Blacken RD, Cunningham PR, Lester SG, Brown MJ, French SC, Aniagyei SE, Wenzel TJ (2006) Carboxymethylated cyclodextrin derivatives as chiral NMR differentiating agents. *Tetrahedron Asymmetry* 17:1199–1208
120. Provencher KA, Wenzel TJ (2008) Carboxymethylated cyclodextrins and their paramagnetic lanthanide complexes as water-soluble chiral NMR solvating agents. *Tetrahedron Asymmetry* 19:1797–1803
121. Provencher KA, Weber MA, Randall LA, Cunningham PR, Dignam CF, Wenzel TJ (2010) Carboxymethylated cyclodextrins and their complexes with Pr(III) and Yb(III) as water-soluble chiral NMR solvating agents for cationic compounds. *Chirality* 22:336–346

122. Wenzel TJ, Bogyo MS, Lebeau EL (1994) Lanthanide-cyclodextrin complexes as probes for elucidating optical purity by NMR spectroscopy. *J Am Chem Soc* 116:4858–4865
123. Wenzel TJ, Miles RD, Zomlefer K, Frederique DE, Roan MA, Troughton JS, Pond BV, Colby AL (2000) Dysprosium(III)-diethylenetriaminepentaacetate complexes of aminocyclodextrins as chiral NMR shift reagents. *Chirality* 12:30–37
124. Smith KJ, Wilcox JD, Mirick GE, Wacker LS, Ryan NS, Vensel DA, Readling R, Domush HL, Amonoo EP, Shariff SS, Wenzel TJ (2003) Calix[4]arene, calix[4]resorcarene, and cyclodextrin derivatives and their lanthanide complexes as chiral NMR shift reagents. *Chirality* 15:S150–S158
125. Chisholm CD, Wenzel TJ (2011) Enantiomeric discrimination of aromatic-containing anionic substrates using cationic cyclodextrins. *Tetrahedron Asymmetry* 22:62–68
126. Lingenfelter DS, Helgeson RC, Cram DJ (1981) Host-guest complexation. 23. High chiral recognition of amino acid and ester guests by hosts containing one chiral element. *J Org Chem* 46:393–406
127. Weinstein SE, Vining MS, Wenzel TJ (1997) Lanthanide-crown ether mixtures as chiral NMR shift reagents for amino acid esters, amines and amino alcohols. *Magn Reson Chem* 35:273–280
128. Wenzel TJ, Thurston JE, Sek DC, Joly J (2001) Utility of crown ethers derived from methyl β -D-galactopyranoside and their lanthanide couples as chiral NMR discriminating agents. *Tetrahedron Asymmetry* 12:1125–1130
129. Wenzel TJ, Freeman BE, Sek DC, Zopf JJ, Nakamura T, Yongzhu J, Hirose K, Tobe Y (2004) Chiral recognition in NMR spectroscopy using crown ethers and their ytterbium(III) complexes. *Anal Bioanal Chem* 378:1536–1547
130. Wenzel TJ, Thurston JE (2000) (+)-(18-Crown-6)-2,3,11,12-tetracarboxylic acid and its ytterbium(III) complex as chiral NMR discriminating agents. *J Org Chem* 65:1243–1248
131. Wenzel TJ, Thurston JE (2000) Enantiomeric discrimination in the NMR spectra of underivatized amino acids and α -methyl amino acids using (+)-(18-crown-6)-2,3,11,12-tetracarboxylic acid. *Tetrahedron Lett* 41:3769–3772
132. Machida Y, Kagawa M, Nishi H (2003) Nuclear magnetic resonance studies for the chiral recognition of (+)-(*R*)-18-crown-6-tetracarboxylic acid to amino compounds. *J Pharm Biomed Anal* 30:1929–1942
133. Wenzel TJ, Bourne CE, Clark RL (2009) (18-Crown-6)-2,3,11,12-tetracarboxylic acid as a chiral NMR solvating agent for determining the enantiomeric purity and absolute configuration of β -amino acids. *Tetrahedron Asymmetry* 20:2052–2060
134. Chisholm CD, Fulop F, Forro E, Wenzel TJ (2010) Enantiomeric discrimination of cyclic β -amino acids using (18-crown-6)-2,3,11,12-tetracarboxylic acid as a chiral NMR solvating agent. *Tetrahedron Asymmetry* 21:2289–2294
135. Howard JA, Fulop F, Nonn M, Wenzel TJ (2013) Enantiomeric discrimination of isoxazoline fused β -amino acid derivatives using (18-crown-6)-2,3,11,12-tetracarboxylic acid as a chiral NMR solvating agent. *Chirality* 25:48–53
136. Lovely AE, Wenzel TJ (2006) Chiral NMR discrimination of secondary amines using (18-crown-6)-2,3,11,12-tetracarboxylic acid. *Org Lett* 8:2823–2826
137. Lovely AE, Wenzel TJ (2006) Chiral NMR discrimination of piperidines and piperazines using (18-crown-6)-2,3,11,12-tetracarboxylic acid. *J Org Chem* 71:9178–9182
138. Lovely AE, Wenzel TJ (2006) Chiral NMR discrimination of pyrrolidines using (18-crown-6)-2,3,11,12-tetracarboxylic acid. *Tetrahedron Asymmetry* 17:2642–2648
139. Lovely AE, Wenzel TJ (2008) Chiral NMR discrimination of amines: analysis of secondary, tertiary and prochiral amines using (18-crown-6)-2,3,11,12-tetracarboxylic acid. *Chirality* 20:370–378
140. Yanagihara R, Tominaga M, Aoyama Y (1994) Chiral host-guest interaction. A water-soluble calix[4]resorcarene having L-proline moieties as a non-lanthanide chiral NMR shift reagent for chiral aromatic guests in water. *J Org Chem* 59:6865–6867

141. Dignam CF, Richards CJ, Zopf JJ, Wacker LS, Wenzel TJ (2005) An enantioselective NMR shift reagent for cationic aromatics. *Org Lett* 7:1773–1776
142. Dignam CF, Zopf JJ, Richards CJ, Wenzel TJ (2005) Water-soluble calix[4]resorcinarenes as enantioselective NMR shift reagents for aromatic compounds. *J Org Chem* 70:8071–8078
143. O'Farrell CM, Hagan KA, Wenzel TJ (2009) Water-soluble calix[4]resorcinarenes as chiral NMR solvating agents for bicyclic aromatic compounds. *Chirality* 21:911–921
144. Hagan KA, O'Farrell CM, Wenzel TJ (2009) Water-soluble calix[4]resorcinarenes with hydroxyproline groups as chiral NMR solvating agents for phenyl- and pyridyl-containing compounds. *Eur J Org Chem* 2009:4825–4832
145. O'Farrell CM, Wenzel TJ (2008) Water-soluble calix[4]resorcinarenes as chiral NMR solvating agents for phenyl-containing compounds. *Tetrahedron Asymmetry* 19:1790–1796
146. O'Farrell CM, Chudomel JM, Collins JM, Dignam CF, Wenzel TJ (2008) Water-soluble calix[4]resorcinarenes with hydroxyproline groups as chiral NMR solvating agents. *J Org Chem* 73:2843–2851
147. Pham NH, Wenzel TJ (2011) A water-soluble calix[4]resorcinarene with α -methyl-L-prolinylmethyl groups as a chiral NMR solvating agent. *J Org Chem* 76:986–989
148. Pham NH, Wenzel TJ (2011) A sulfonated calix[4]resorcinarene with α -methyl-L-prolinylmethyl groups as a water-soluble chiral NMR solvating agent. *Tetrahedron Asymmetry* 22:641–647
149. Pham NH, Wenzel TJ (2011) A sulfonated calix[4]resorcinarene with L-pipecolinic acid groups as a water-soluble chiral NMR solvating agent. *Tetrahedron Asymmetry* 22:1574–1580
150. Pham NH, Wenzel TJ (2012) A water-soluble calix[4]resorcinarene with L-pipecolinic acid groups as a chiral NMR solvating agent. *Chirality* 24:193–200
151. Wenzel TJ, Rollo RD, Clark RL (2012) Chiral discrimination of aliphatic amines and amino alcohols using NMR spectroscopy. *Magn Reson Chem* 50:261–265
152. Goering HL, Eikenberry JN, Koerner GS (1971) Tris[3-(trifluoromethylhydroxymethylene)-d-camphorato]europium(III). A chiral shift reagent for direct determination of enantiomeric compositions. *J Am Chem Soc* 93:5913–5914
153. Fraser RR, Petit MA, Saunders JK (1971) Determination of enantiomeric purity by an optically active nuclear magnetic resonance shift reagent of wide applicability. *Chem Commun* 1450–1451
154. McCreary MD, Lewis DW, Wernick DL, Whitesides GM (1974) The determination of enantiomeric purity using chiral lanthanide shift reagents. *J Am Chem Soc* 96:1038–1054
155. Wenzel TJ (1978) NMR shift reagents. CRC, Boca Raton
156. Wenzel TJ, Provencher KA (2009) Lanthanide enolates as nuclear magnetic resonance shift reagents. In: Abicky J (ed) *The chemistry of metal enolates*. Wiley, West Sussex, p 788–822
157. Sweeting LM, Crans DC, Whitesides GM (1987) Determination of enantiomeric purity of polar substrates with chiral lanthanide NMR shift reagents in polar solvents. *J Org Chem* 52:2273–2276
158. DeArment M, Eastabrooks M, Venkatasubban KS, Benschafut R, Rothchild R, Wyss H (1994) NMR studies of drugs. Application of a chiral lanthanide shift reagent to methoxamine in chloroform-*d* or acetonitrile-*d*₃. *Spectrosc Lett* 27:533–555
159. Polivka Z, Budesinsky M, Holubek J, Schneider B, Sedivy Z, Svatek E, Matousova O, Metys J, Valchar M, Soucek R, Protiva M (1989) 4H-Benzo[4,5]cyclohepta[1,2-b]thiophenes and 9,10-dihydro derivatives – sulfonium analogues of pizotifen and ketotifen; chirality of ketotifen; synthesis of the 2-bromo derivative of ketotifen. *Collect Czech Chem Commun* 54:2443–2469
160. Omata K, Aoyagi S, Kabuto K (2004) Observing the enantiomeric ¹H chemical shift non-equivalence of several α -amino ester signals using tris[3-(trifluoromethylhydroxy-methylene)-(+)-camphorato]samarium(III): a chiral lanthanide shift reagent that causes minimal line bordering. *Tetrahedron Asymmetry* 15:2351–2356
161. Wenzel TJ, Wenzel BT (2009) Diamagnetic lanthanide tris β -diketonates as organic-soluble chiral NMR shift reagents. *Chirality* 21:6–10

162. Clark RL, Wenzel BT, Wenzel TJ (2013) Diamagnetic lanthanide tris β -diketonate complexes with aryl-containing ligands as chiral NMR discriminating agents. *Tetrahedron Asymmetry* 24:297–304
163. Ghosh I, Zeng H, Kishi Y (2004) Application of chiral lanthanide shift reagents for assignment of absolute configuration of alcohols. *Org Lett* 6:4715–4718
164. Vergara F, Wenzler M, Hansen BG, Kleibenstein DJ, Halkier BA, Gershenzon J, Schneider B (2008) Determination of the absolute configuration of the glucosinolate methyl sulfoxide group reveals a stereospecific biosynthesis of the side chain. *Photochem* 69:2737–2742
165. Ghandi M, Olyaei A, Raoufmoghaddam S (2008) One-pot, three-component uncatalyzed quantitative synthesis of new aminonaphthols (Betti bases) in water. *Synth Commun* 38:4125–4138
166. Faigl F, Tarkanyi G, Fogassy K, Tepfenhardt D, Thurner A (2008) Synthesis and stereochemical stability of new atropisomeric 1-(substituted phenyl)pyrrole derivatives. *Tetrahedron* 64:1371–1377
167. Cho NS, Kim HS, Song MS (2011) NMR-based enantiodifferentiation of chiral *trans*-2-phenylcyclopropane derivatives using a chiral lanthanide shift reagent. *Bull Korean Chem Soc* 32:2076–2078
168. Wenzel TJ, Bettles TC, Sadlowski JE, Sievers RE (1980) New binuclear lanthanide NMR shift reagents effective for aromatic compounds. *J Am Chem Soc* 102:5903–5904
169. Wenzel TJ, Sievers RE (1982) Nuclear magnetic resonance studies of terpenes with chiral and achiral lanthanide(III)-silver(I) binuclear shift reagents. *J Am Chem Soc* 104:382–388
170. Offermann W, Mannschreck A (1981) Chiral recognition of alkene and arene hydrocarbons by ^1H and ^{13}C NMR. Determination of enantiomeric purity. *Tetrahedron Lett* 22:3227–3230
171. Nijhuis WHN, Verboom W, El-Fadl AA, van Hummel GJ, Reinhoudt DN (1989) Stereochemical aspects of the “tert-amino effect”. 2. Enantio- and diastereoselectivity in the synthesis of quinolines, pyrrolo[1,2-*a*]quinolines, and [1,4]oxazino [4,3-*a*]quinolines. *J Org Chem* 54:209–216
172. Wang Q, Fan SY, Wong HNC, Li Z, Fung BM, Twieg RJ, Nguyen HT (1993) Enantioselective synthesis of chiral liquid crystalline compounds from monoterpenes. *Tetrahedron* 49:619–638
173. Carreira EM, Hastings CA, Shepard MS, Yerkey LA, Millward DB (1994) Asymmetric induction in intramolecular [2 + 2]- photocycloadditions of 1,3-disubstituted allenes with enones and enoates. *J Am Chem Soc* 116:6622–6630
174. Thompson A, Dolphin D (2000) Nuclear magnetic resonance studies of helical dipyrromethene-zinc complexes. *Org Lett* 2:1315–1318
175. Wenzel TJ, Zaia J (1985) Lanthanide tetrakis (β -diketonates) as effective NMR shift reagents for organic salts. *J Org Chem* 50:1322–1324
176. Wenzel TJ, Zaia J (1987) Organic-soluble lanthanide nuclear magnetic resonance shift reagents for sulfonium and isothiuronium salts. *Anal Chem* 59:562–567
177. Green TK, Whetstone JR, Son E (1997) Enantiomeric purity of alkylmethylphenylsulfonium ions with chiral NMR shift reagents: racemization by pyramidal inversion as observed by ^1H NMR spectroscopy. *Tetrahedron Asymmetry* 8:3175–3181
178. Kabuto K, Sasaki Y (1987) Highly consistent correlation between absolute configuration of α -amino acids and their shift induced by the NMR. Chiral shift reagent propylenediaminetetraacetatoeuropium(III) in aqueous solution. *Chem Commun* 23:670–671
179. Kabuto K, Sasaki Y (1990) A facile NMR method for assigning absolute configuration of underivatized α -methyl- α -amino acids using a chiral lanthanoid shift reagent for aqueous solution. *Tetrahedron Lett* 31:1031–1034
180. Sasaki M, Omata K, Kabuto K, Sasaki Y (2003) Enantiomer signal separation of β -amino acids induced by Eu(III)-pdt; relation between the absolute configurations and relative shifts of enantiomer signals. *Kidorui* 42:198–199

181. Ogasawara K, Omata K, Kabuto K, Jin H, Sasaki Y (1999) Optically active Ce(III) – propylenediaminetetraacetate complex: a chiral shift reagent for aqueous solution causing less signal broadening. *Kidorui* 34:152–153
182. Inamoto A, Ogasawara K, Omata K, Kabuto K, Sasaki Y (2000) Samarium(III)–propylenediaminetetraacetate complex: a water-soluble chiral shift reagent for use in high-field NMR. *Org Lett* 2:3543–3545
183. Arnaud GF, Florini N, Caglioti L, Zucchi C, Palyi G (2009) Fast enantioselective amino acid quantitative ^{13}C NMR determination by a praseodymium chiral shift reagent. *Tetrahedron Asymmetry* 20:1633–1636
184. Florini N, Arnaud GF, Konya B, Zucchi C, Palyi G (2009) Synthesis of a water-soluble chiral NMR shift reagent: (*S*)-PDTA. *Tetrahedron Asymmetry* 20:1036–1039
185. Omata K, Fujioka M, Kabuto K, Sasaki Y (2008) Use of Sm(III)-{1,2-propanediamine-*N,N,N',N'*-tetra(α,α -dideuterioacetate)} complex for NMR determination of absolute configuration of each α -amino acid in peptide hydrolysate mixtures. *Comm Commun* 4903–4905
186. Sato J, Omata K, Kabuto K, Jin H, Umakoshi K, Sasaki Y (1998) Properties of chiral Ce(III)-tppn complex as a chiral shift reagent in aqueous solution. *Kidorui* 32:58–59
187. Sato J, Jin H, Omata K, Kabuto K, Sasaki Y (1999) Resolution of enantiomer signals by diamagnetic lanthanum(III)-*N, N, N', N'*-tetrakis(2-pyridinylmethyl)-(*R*)-propylenediamine complex in ^1H NMR. *Enantiomer* 4:147–150
188. Duddeck H (2005) $\text{Rh}_2[\text{MTPA}]_4$, a dirhodium complex as NMR auxiliary for chiral recognition. *Chem Rec* 5:1–14
189. Gomez ED, Duddeck H (2008) Origin of ^{13}C complexation shifts in the adduct formation of 2-butyl phenyl ethers with a dirhodium tetracarboxylate complex. *Magn Reson Chem* 46:23–29
190. Mattiza JT, Meyer VJ, Duddeck H (2010) Experimental verification of diverging mechanisms in the binding of ether, thioether, and sulfone ligands to a dirhodium tetracarboxylate. *Magn Reson Chem* 48:192–197
191. Gomez ED, Brotin T, Duddeck H (2007) Enantiodifferentiation of polyethers by the dirhodium method. Part 2: cyclotrimeratrylenes and cryptophanes. *Tetrahedron Asymmetry* 18:2155–2164
192. Rozwadowski Z (2007) Chiral recognition of the Schiff bases by NMR spectroscopy in the presence of a chiral dirhodium complex. Deuterium isotope effect on ^{13}C chemical shift of the optically active Schiff bases and their dirhodium adducts. *Magn Reson Chem* 45:605–610
193. Rozwadowski Z, Nowak-Wydra B (2008) Chiral recognition of Schiff bases by ^{15}N NMR spectroscopy in the presence of a dirhodium complex. Deuterium isotope effect on ^{15}N chemical shift of the optically active Schiff bases and their dirhodium tetracarboxylate adducts. *Magn Reson Chem* 46:974–978
194. Gomez ED, Dogan I, Yilmaz M, Demir-Ordu O, Albert D, Duddeck H (2008) Atropisomeric 3-aryl-2-oxo-4-oxazolidinones and some thione analogues – enantiodifferentiation and ligand competition in applying the dirhodium method. *Chirality* 20:344–350
195. Gomez ED, Frelek J, Woznica M, Kowalska P, Jazwinski J, Duddeck H (2007) Chalcogen atom competition in the coordination of bicyclic β -lactam derivatives to a dirhodium tetracarboxylate complex. *Heterocycles* 74:357–367
196. Duddeck H, Toth G, Simon A, Gomez ED, Mattiza JT (2011) Adamantanes as spherical nanosondes in adducts with a chiral dirhodium complex – discriminating enantiomers and probing spatial proximities. *Magn Reson Chem* 49:326–342
197. Mattiza JT, Meyer V, Ozuduru G, Heine T, Fohrer J, Duddeck H (2012) Competition of ester, amide, ether, carbonate, alcohol and epoxide ligands in the dirhodium experiment (chiral discrimination by NMR spectroscopy). *Nat Prod Commun* 7:359–362
198. Gomez ED, Duddeck H (2009) A new method proposed for the determination of absolute configurations of α -amino acids. *Magn Reson Chem* 47:222–227

199. Jazwinski J, Sadlej A (2009) Studies on the configuration of nitrogenous stereogenic centres in adducts of rhodium(II) tetraacylates with chiral amines: the application of ^1H and ^{13}C NMR spectroscopy. *Tetrahedron Asymmetry* 20:2331–2343
200. Glaszczka R, Jazwinski J, Kamiński B, Kamińska M (2010) Adducts of rhodium(II) tetraacylates with methionine and its derivatives: ^1H and ^{13}C nuclear magnetic resonance spectroscopy and chiral recognition. *Tetrahedron Asymmetry* 21:2346–2355
201. Mattiza JT, Harada N, Kuwahara S, Hassan Z, Duddeck H (2009) Comparing various chiral dirhodium tetracarboxylates in the dirhodium method. *Chirality* 21:843–849
202. Mattiza JT, Fohrer JGG, Duddeck H, Gardiner MG, Ghanem A (2011) Optimizing dirhodium(II) tetrakis-carboxylates as chiral NMR auxiliaries. *Org Biomol Chem* 9:6542–6550
203. Wild SB (1997) Resolutions of tertiary phosphines and arsines with orthometallated palladium(II)-amine complexes. *Coord Chem Rev* 166:291–311
204. Uccello-Barretta G, Bernardini R, Balzano F, Salvadori P (2002) Overall view of the use of chiral platinum(II) complexes as chiral derivatizing agents (CDAs) for the enantiodiscrimination of unsaturated compounds by ^{195}Pt NMR. *Chirality* 14:484–489
205. Li J, Siegler MA, Lutz M, Spek AL, Gebbink RJMK, van Koten G (2009) Chiral *ortho*-palladated and –platinated arylphosphite complexes. *Organomet* 28:5323–5332
206. Cucciolo ME, Flores G, Vitagliano A (2004) Chiral recognition in silver(I) olefin complexes with chiral diamines. Resolution of racemic alkenes and NMR discrimination of enantiomers. *Organometallics* 23:15–17
207. Farjon J, Ziani L, Beguin L, Merlet D, Courtieu J (2007) Selective NMR excitations in chiral analysis. *Annual Rep NMR Spectrosc* 61:283–293
208. Baishya B, Prabhu UR, Suryaprakash N (2009) Analyses of proton NMR spectra of strongly and weakly dipolar coupled spins: special emphasis on spectral simplification, chiral discrimination, and discerning of degenerate transitions. *Annual Rep NMR Spectrosc* 67:331–423
209. Nath N, Hebbar S, Prabhu UR, Suryaprakash N (2010) One and two dimensional single quantum and multiple quantum NMR methodologies: tools for chiral analyses. *J Indian Inst Sci* 90:1–36
210. Farjon J, Merlet D (2011) SERF-filtered experiments: new enantio-selective tools for deciphering complex spectra of racemic mixtures dissolved in chiral oriented media. *J Magn Reson* 210:24–30
211. Merlet D, Beguin L, Courtieu J, Giraud N (2011) Spin-spin coupling edition in chiral liquid crystal NMR solvent. *J Magn Reson* 209:315–322
212. Nath N, Suryaprakash N (2011) Quantification of enantiomeric excess by ^1H -detected heteronuclear refocusing and homonuclear multiple quantum NMR experiments. *Chem Phys Lett* 502:136–143
213. Lesot P, Courtieu J (2009) Natural abundance deuterium NMR spectroscopy: developments and analytical applications in liquids, liquid crystals and solid phases. *Prog NMR Spectrosc* 55:128–159
214. Lesot P, Lafon O (2008) Enantiomeric analysis using natural abundance deuterium 3D NMR spectroscopy in polypeptide chiral oriented media. *Chem Phys Lett* 458:219–222
215. Lafon O, Hu B, Amoureux JP, Lesot P (2011) Fast and high-resolution stereochemical analysis by nonuniform sampling and covariance processing of anisotropic natural abundance 2D ^2H NMR datasets. *Chem Eur J* 17:6716–6724
216. Ali KB, Lafon O, Zimmermann H, Guittet E, Lesot P (2007) Homo- and heteronuclear 2D NMR approaches to analyse a mixture of deuterated unlike/like stereoisomers using weakly ordering chiral liquid crystals. *J Magn Reson* 187:205–215
217. Lesot P, Lafon O, Aroulanda C, Dong RY (2008) ^2H NMR studies on two-homopolypeptide lyotropic enantiodiscriminating mesophases: experimental quantification of solute-fiber affinities. *Chem Eur J* 14:4082–4092
218. Naumann C, Kuchel PW (2009) NMR (pro)chiral discrimination using polysaccharide gels. *Chem Eur J* 15:12189–12191

219. Kummerlowe G, Kiran MU, Luy B (2009) Covalently cross-linked gelatin allows chiral differentiation at elevated temperatures and in DMSO. *Chem Eur J* 15:12192–12195
220. Buchler SSD, Kummerlowe G, Luy B (2011) Naturally occurring biodegradable polymers as the basis of chiral gels for the differentiation of enantiomers by partially oriented NMR spectroscopy. *Int J Artif Organs* 34:134–138
221. Sau SP, Ramanathan KV (2009) Visualization of enantiomers in liquid-crystalline phase of a fragmented DNA solution. *J Phys Chem B* 113:1530–1532
222. Lesot P, Reddy UV, Suryaprakash N (2011) Exploring the spectral enantiodiscrimination potential of a DNA-based orienting medium using deuterium NMR spectroscopy. *Chem Commun* 47:11736–11738
223. Lesot P, Baillif V, Billault I (2008) Combined analysis of C-18 unsaturated fatty acids using natural abundance deuterium 2D NMR spectroscopy in chiral oriented solvents. *Anal Chem* 80:2963–2972
224. Lesot P, Serhan Z, Billault I (2011) Recent advances in the analysis of the site-specific isotopic fractionation of metabolites such as fatty acids using anisotropic natural-abundance ^2H NMR spectroscopy: application to conjugated linolenic methyl esters. *Anal Bioanal Chem* 399:1187–1200
225. Billault I, Le Du A, Ouethrani M, Serhan Z, Lesot P, Robins RJ (2012) Probing substrate-product relationships by natural abundance deuterium 2D NMR spectroscopy in liquid-crystalline solvents: epoxidation of linoleate to vernoleate by two different plant enzymes. *Anal Bioanal Chem* 402:2985–2998
226. Solgadi A, Jean L, Lasne MC, Rouden J, Courtieu J, Meddour A (2007) NMR in chiral polypeptide liquid crystals: the problem of amines. *Tetrahedron Asymmetry* 18:1511–1516
227. Lafon O, Lesot P, Zimmermann H, Poupko R, Luz Z (2007) Chiral discrimination in the ^{13}C and ^2H NMR of the crown and saddle isomers of nonamethoxy-cyclotrimeratrylene in chiral liquid-crystalline solutions. *J Phys Chem B* 111:9453–9467
228. Lesot P, Lafon O, Zimmermann H, Luz Z (2008) Enantiodiscrimination in deuterium NMR spectra of flexible chiral molecules with average axial symmetry dissolved in chiral liquid crystals: the case of tridioxymethylenetriphenylene. *J Am Chem Soc* 130:8754–8761
229. Aroulanda C, Lafon O, Lesot P (2009) Enantiodiscrimination in flexible cyclic solutes using NMR spectroscopy in polypeptide chiral mesophases: investigation of *cis*-decalin and THF. *J Phys Chem B* 113:10628–10640
230. Lafon O, Lesot P, Fan CA, Kagan HB (2007) Analysis of intramolecular dynamic processes in enantiomeric diaryl atropisomers and related derivatives by ^2H NMR spectroscopy in polypeptide liquid crystals. *Chem Eur J* 13:3772–3786
231. Fan CA, Ferber B, Kagan HB, Lafon O, Lesot P (2008) Two aspects of the desymmetrization of selected prochiral aromatic or vinylic dihalides: enantioselective halogen-lithium exchange and prochiral recognition in chiral liquid crystals. *Tetrahedron Asymmetry* 19:2666–2677
232. Eloi A, Rose-Munch F, Rose E, Pille A, Lesot P, Herson P (2010) Cationic planar chiral $(\eta^6\text{-arene})\text{Mn}(\text{CO})_3^+$ complexes: resolution, NMR study in chiral-oriented solvents, and applications to the enantioselective synthesis of 4-substituted cyclohexenones and $(\eta^6\text{-phosphinoarene})\text{Mn}(\text{CO})_3^+$ complexes. *Organomet* 29:3876–3886
233. Aroulanda C, Zimmermann H, Luz Z, Lesot P (2011) Enantiotopic discrimination in the deuterium NMR spectrum of solutes with S_4 symmetry in chiral liquid crystals. *J Chem Phys* 134:134502–134508
234. Ziani L, Lesot P, Meddour A, Courtieu J (2007) Empirical determination of the absolute configuration of small chiral molecules using natural abundance ^2H NMR in chiral liquid crystals. *Chem Commun* 43:4737–4739
235. Thiele CM, Berger S (2003) Probing the diastereotopicity of methylene protons in strychnine using residual dipolar couplings. *Org Lett* 5:705–708
236. Thiele CM (2004) Simultaneous assignment of all diastereotopic protons in strychnine using RDCs: PELG as alignment medium for organic molecules. *J Org Chem* 69:7403–7413

237. Gil RR, Gayathri C, Tsarevsky NV, Matyjaszewski K (2008) Stretched poly(methyl methacrylate) gel aligns small organic molecules in chloroform. Stereochemical analysis and diastereotopic proton NMR assignment in ludartin using residual dipolar couplings and 3J coupling constant analysis. *J Org Chem* 73:840–848
238. Marx A, Bottcher B, Thiele CM (2010) Enhancing the orienting properties of poly(γ -benzyl-L-glutamate) by means of additives. *Chem Eur J* 16:1656–1663
239. Schuetz A, Murakami T, Takada N, Junker J, Hashimoto M, Griesinger C (2008) RDC-enhanced NMR spectroscopy in structure elucidation of sucro-neolambertellin. *Angew Chem Int Ed* 47:2032–2034
240. Sun H, d’Auvergne EJ, Reinscheid UM, Dias LC, Andrade CKZ, Rocha RO, Griesinger C (2011) Bijvoet in solution reveals unexpected stereoselectivity in a Michael addition. *Chem Eur J* 17:1811–1817
241. Trigo-Mourino P, Sifuentes R, Navarro-Vazquez A, Gayathri C, Maruenda H, Gil RR (2012) Determination of the absolute configuration of 19-OH-(–)-eburnamonine using a combination of residual dipolar couplings, DFT chemical shift predications and chiroptics. *Nat Prod Commun* 7:735–738
242. Marathias VM, Tawa GJ, Goijer I, Bach AC (2007) Stereochemical identification of (*R*)- and (*S*)-ibuprofen using residual dipolar couplings, NMR, and modeling. *Chirality* 19:741–750
243. Nath N, Suryaprakash N (2011) Spin-selective correlation experiment for measurement of long-range *J* couplings and for assignment of (*R/S*) enantiomers from residual dipolar couplings and DFT. *J Phys Chem B* 115:6868–6875
244. Berger R, Courtieu J, Gil RR, Griesinger C, Kock M, Lesot P, Luy B, Merlet D, Navarro-Vazquez A, Reggelin M, Reinscheid UM, Thiele C, Zweckstetter M (2012) Is enantiomer assignment possible in NMR spectroscopy using residual dipolar couplings from chiral nonracemic alignment media? – A critical assessment. *Angew Chem Int Ed* 51:8388–8391
245. Courtieu J, Aroulanda C, Lesot P, Meddour A, Merlet D (2010) Evolution of the Sauepe order parameters of enantiomers from a racemic to a non-racemic liquid crystal solvent: an original light on the absolute configuration determination problem. *Liq Cryst* 37:903–912
246. Kummerlowe G, Luy B (2009) Residual dipolar couplings for the configurational and conformational analysis of organic molecules. *Annu Rep NMR Spectrosc* 68:193–230
247. Luy B (2010) Differentiation of enantiomers by NMR spectroscopy using chiral orienting media. *J Indian Inst Sci* 90:119–132
248. Potrzebowski MJ, Jeziorna A, Kazmierski S (2008) NMR studies of chiral organic compounds in non-isotropic phases. *Concepts Magn Reson Part A* 32A:201–218

Chiral NMR Solvating Additives for Differentiation of Enantiomers

Gloria Uccello-Barretta and Federica Balzano

Abstract This chapter will describe the general features and main categories of chiral solvating agents (CSAs) for NMR spectroscopy, spanning from low-medium sized CSAs to macrocyclic ones. CSAs based on chiral ionic liquids (CILs) will be introduced in view of their increasing popularity, and, finally, a short paragraph will be dedicated to special applications of CSAs in particular experimental conditions. Several valuable works, which are mainly devoted to investigate enantiodifferentiation mechanisms by NMR, will not be discussed. The main objective is to identify the current trend in the research areas dedicated to the development of new CSAs for NMR spectroscopy.

Keywords Chiral discrimination · Chiral solvating agents · Enantiomeric excess · Nuclear magnetic resonance

Contents

1	Introduction	70
2	Small to Medium Sized CSAs	74
3	Molecular Tweezers	84
4	Natural Products	87
5	Cyclodextrins	90
6	Synthetic Macrocycles	96
7	Ionic Liquids	109
8	Special Applications	113
8.1	Pattern Recognition Approach and 2D F1 Decoupled COSY Experiments	113
8.2	Coupling of CSAs and Achiral Lanthanide Shift Reagents	114

8.3 Chiral Sensing	114
8.4 Chiral Metabolites and Drug Formulations	115
9 Conclusions	117
References	117

1 Introduction

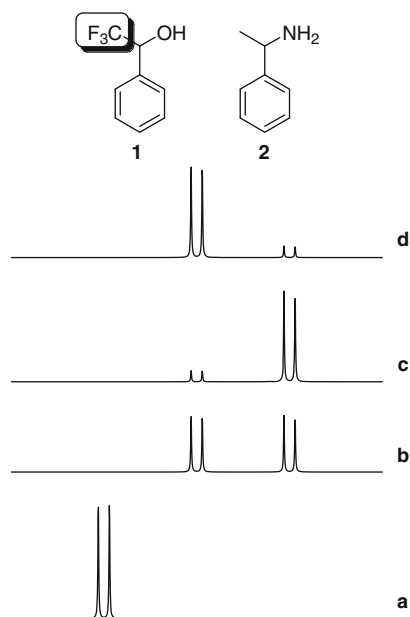
The quantification and identification of chiral compounds constitutes a fundamental issue for both the pharmaceutical industry and the regulatory authorities, which involves the continuous growth of the research areas devoted to the development of direct methods for the differentiation of enantiomers. NMR spectroscopy has enormous potential in the field of structural determinations, but corresponding nuclei of enantiomers cannot be distinguished since they reside in the same chemical environment and, hence, are isochronous. The problem of the intrinsic equivalence of enantiotopic nuclei can be overcome by putting them in a diastereoisomeric environment, which renders them diastereotopic and, hence, distinguishable by NMR [1–22]. The diastereoisomeric environment may originate from the reaction of the two enantiomers with an enantiopure chiral auxiliary (chiral derivatizing agents, CDAs) in order to obtain pairs of diastereoisomers in which the substrate and the chiral auxiliary are covalently assembled. Alternatively, non-covalent interactions between the two enantiomers and the chiral auxiliary can be exploited in diastereoisomeric solvates or adducts, which are formed simply by mixing the enantiomeric mixture and the complexing agent. In this last case, the chiral complexing agent may be diamagnetic (chiral solvating agents, CSAs) or paramagnetic (chiral lanthanide shift reagents, CLSRs).

Once the signals of the enantiomers have been differentiated, the determination of the enantiomeric excess simply requires the identification of the corresponding resonances of the two enantiomers and their integration under conditions of quantitative analysis. In principle any NMR active nucleus of the chiral substrate can be detected, which may also belong to the chiral auxiliary in the cases of CDAs, and the choice should be subject to the following general considerations: the detected nucleus should have high isotopic abundance, high gyromagnetic ratio, and, if possible, it should be dipolar [23]. The enantiomeric excess determinations should be performed on the basis of the integration of well separated signals with simple structures (singlets or doublets). Therefore, nuclei such as ^1H , ^{31}P , ^{19}F , with natural abundance of about 100% and spin $I = 1/2$, are preferred, whereas low abundant nuclei, such as ^{13}C (natural abundance 1.1%), although dipolar, should be avoided.

The effectiveness of the chiral auxiliary is evaluated on the basis of the magnitude of the nonequivalence ($\Delta\delta = |\delta_R - \delta_S|$, the absolute value of the difference of the chemical shifts of the two enantiomers in the chiral environment), and the relative positions of the enantiomers signals (the so-called “sense of nonequivalence”) are correlated to their respective absolute configurations.

The roots for the development of CSAs are found in some earlier experiments carried out by using CDAs, during which the remarkable effect of the solvent

Fig. 1 Simulation of the ^{19}F NMR spectra of (a) (*R,S*)-2,2,2-trifluoro-1-phenylethanol (**1**), (b) (*R,S*)-1/(*S*)- α -phenylethylamine (**2**), (c) enantiomerically enriched 1/(*R*)-**2**, and (d) enantiomerically enriched 1/(*S*)-**2**



employed for the NMR measurements on the magnitude of nonequivalence was evidenced [3, 4]. The direct consequence of these preliminary observations was the hypothesis, first formulated by Raban and Mislow in 1965 [1], that the solvent, if optically active, could itself generate the chiral environment needed for inducing nonequivalence in the enantiotopic nuclei of two enantiomeric solutes. The first experimental evidence of the above-mentioned hypothesis was given by Pirkle in 1966 [2] with an experiment which will be described in detail since it embodies all the main features of the CSAs and represents a milestone in the field of the development and optimization of this class of chiral auxiliaries for NMR spectroscopy.

In CCl_4 , the fluorine resonance of racemic 2,2,2-trifluoro-1-phenylethanol (**1**) appeared as a doublet ($J_{\text{HF}} = 6.7$ Hz) at 4,445 Hz from internal CFCl_3 (Fig. 1a).

In optically active α -phenylethylamine (**2**), the ^{19}F spectrum showed the appearance of two doublets with equal integrated areas, which are centered at +4,374 and +4,376 Hz (Fig. 1b). A sample of the partially resolved fluorinated alcohol in optically active amine again showed two doublets, but with different intensities (Fig. 1c, d). When the opposite enantiomer of the amine was employed as solvent, the two resonances were inverted (Fig. 1c, d). In both cases the relative intensities of the two signals accurately corresponded to the enantiomeric excess of the alcohol. The dissolution of the fluorinated alcohol into racemic amine caused the coalescence of the signals of the enantiomers and, hence, the exchange of the two enantiomers of the solvent on the solvated fluorinated alcohol is fast. In view of the fact that the observed differentiation of the fluorine signals should be attributed to

the formation of diastereoisomeric solvates, the chiral solvent, α -phenylethylamine, was denoted as "CSA."

Obviously the use of the chiral auxiliary as solvent is not acceptable from economic and practical points of view. The resonances of the CSA could hamper the observation of ^1H nuclei of the two enantiomers and its very high concentration could become detrimental in terms of spectral resolution. Luckily, analogous differentiation of the corresponding resonances of the two enantiomers is observed in achiral solvents in the presence of few equivalents of the CSA, taking care to avoid the use of solvents which could compete with the CSA in the interaction with the chiral substrate.

The first experiments carried out by Pirkle highlighted some fundamental peculiarities of the CSAs: (1) the absolute configuration of the CSA affects exclusively the sense of nonequivalence (i.e., the relative positions of the resonances of the two enantiomers) and (2) the enantiomeric purity of the CSA affects only the magnitude of the nonequivalence: the higher the enantiomeric purity of the CSA, the greater the observed separations between corresponding signals of the two enantiomers of the solute. This last property of the CSA represents an intrinsic advantage with respect to CDAs, which are required to be enantiomerically pure in order to obtain reliable enantiomeric excess (ee) determinations. However, even if it is not essential to employ enantiopure CSAs it is strongly advisable, especially considering that the magnitudes of nonequivalences which are produced by CSAs are frequently not as high as in the case of paramagnetic CLSRs. Finally, only one set of resonances is detected for the CSA in the two diastereoisomeric solvates and, hence, the probe nucleus for the enantiomeric purity determination must belong to the chiral substrate and cannot be predetermined on the basis of the structural features of the CSA, as in the case of CDAs.

All the features of the CSAs can be easily understood when one considers that the differentiation of the NMR signals of the two enantiomers in the presence of the CSA relies on the formation of the diastereoisomeric solvates, rapidly equilibrating with the unbound species.

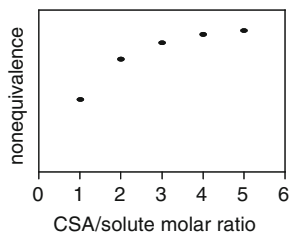
In the fast exchange conditions, only one set of signals is observed in the NMR spectrum for the free and bound species, and the measured chemical shifts (δ_{obs}) of each enantiomer are the weighted average of the corresponding chemical shifts in the free (δ_{f}) and bound (δ_{b}) states:

$$\delta_{\text{obs}} = x_{\text{f}}\delta_{\text{f}} + x_{\text{b}}\delta_{\text{b}}, \quad (1)$$

where x_{f} and x_{b} are the molar fractions of the solute in the free and bound states.

Therefore, the differentiation of the chemical shifts of the two enantiomers has two possible sources: differences in the x_{b} values of the two enantiomers and differences in their δ_{b} values. Different values of x_{b} are the result of differences in the association constants of the two diastereoisomeric solvates; differences in the δ_{b} values reflect their different stereochemical arrangements. This aspect could be envisaged as the main distinctive feature of enantiodiscrimination by NMR methods in comparison to chiral chromatography, which relies only on an energy

Fig. 2 Dependence of nonequivalence on CSA/solute molar ratio



difference existing between the diastereoisomeric complexes formed from the analyte enantiomers and the chiral selector of the stationary phase. In principle, very large differentiation of the NMR signals could also be observed when very labile diastereoisomeric solvates are formed in solution on condition that the CSA contains groups which produce strong anisotropic effects, enhancing the chemical shift dispersion of the solvated enantiomers.

The choice of solvent is critical for the success of enantiomeric excess determinations and it is subject to the knowledge of the interactions which contribute to the formation of the diastereoisomeric solvates. When the CSA and the enantiomers of the solute are likely held together by means of attractive interactions between polar groups, such as hydrogen bond interactions, rather apolar solvents (CDCl_3 , CCl_4 , CD_2Cl_2 , C_6D_6) represent the best choice, since a polar solvent (CD_3OD , DMSO , acetone) could effectively solvate the enantiomeric solutes in place of the CSA, and then the two enantiomers are no longer affected by the chiral environment and their nuclei become isochronous. On the other hand, when there are indications that attractive hydrophobic interactions between apolar groups of the CSA and the solute are involved, then a polar solvent might be preferred. Furthermore, it is not uncommon to perform low-temperature measurements in order to optimize the nonequivalences and, in these cases, a solvent having a low freezing point is required.

Lowering the temperature gives rise to an increase of the nonequivalence in two ways: as a consequence of the corresponding increase of the stability constants of the diastereoisomeric solvates and by a greater restriction of the conformational freedom of the CSA and of the solute. A similar increase of the differentiation of the enantiomers could be attained by increasing the total concentration of the mixture. In both cases great care must be taken to the concomitant loss of spectral resolution which is always detrimental for quantitative analysis.

The effect of the CSA to solute molar ratio on the nonequivalence is illustrated in Fig. 2: in general, higher nonequivalences correspond to a higher CSA/solute molar ratio, up to a saturation point, which occurs generally in the presence of an excess of CSA, beyond which any further significant increase of the separation between the signals of the two enantiomers is not observed [7].

The application of sub-stoichiometric amounts of the chiral auxiliary would be desirable: commercially available CSAs are often expensive, the synthesis of several of them is time consuming, and, at low CSA/substrate molar ratios, there is less spectral interference from the signals of the CSA and spectral resolution is

often better. Therefore the application of sub-stoichiometric amounts of CSA in NMR enantiodiscrimination experiments should be attempted. Recently Klika [24] carefully analyzed this topic, highlighting the limits and advantages of the use of sub-stoichiometric amounts of CSA. A problem can potentially arise in such experimental conditions, when the NMR signal of the less-stable diastereoisomeric complex is positioned further from the corresponding free enantiomer signal than for the more-stable diastereoisomeric complex. Depending on the relative values of the association constants of the two diastereoisomeric complexes, the sense of nonequivalence may reverse during the progressive additions of CSA. Furthermore, the optimization of experimental conditions cannot rely on a single measurement on the racemic mixture and then applying this condition to the analytical sample, as the chemical shift order is also dependent on the enantiomeric ratio. Thus a sample which may appear to be enantiopure can instead be just exhibiting a lack of enantiodifferentiation.

2 Small to Medium Sized CSAs

The majority of CSAs developed in the past have some common features: the presence of hydrogen bond acceptor and donor groups, which are necessary for the stabilization of attractive interactions in the diastereoisomeric adducts, and the presence of aromatic substituents for the efficient differentiation of the chemical shift of the enantiomers by virtue of strong anisotropy effects. Such CSAs are aromatic fluorinated alcohols **1**, **3** (Figs. 1 and 3), wherein fluorine enhances the hydrogen bond donor propensity of the OH group, or aromatic amines **2**, **4a** (Figs. 1 and 3) [7]. Among them, 2,2,2-trifluoro-1-(9-anthryl)ethanol (Pirkle's alcohol) (**3b**) (Fig. 3) is very effective in the enantiodifferentiation of several classes of polar compounds [25, 26].

Pirkle's alcohol still remains one of the most popular and widely employed CSA. Some recent applications include the differentiation of the stereoisomeric forms of mono-, di-, and trispirocyclic phosphazenes (Fig. 4) [27–29]. Dispirocyclic phosphazenes have 2 equiv. stereogenic P atoms and are expected to exist as *cis* and *trans* geometric isomers, which constitute *meso* and *rac* forms, respectively. The trispirocyclic derivatives have three stereogenic P atoms. The *trans* and *cis* stereoisomers are directly differentiated in the ^{31}P NMR spectra and, upon addition of the CSA at a mole ratio of CSA/compound of 10:1, there is no splitting of signals for the *cis* isomer, as was expected for a *meso* compound, but the signals of the *trans* isomer split into two peaks of equal intensities corresponding to the two enantiomers.

The stereochemical analysis of biosynthetic fatty acyl sulfoxides has also been reported [30–32], where ^{19}F nuclei of the fluorine-tagged sulfoxide enantiomers (Fig. 5) are distinguished at the trace (nanomole) level in the presence of Pirkle's alcohol [32].

The enantiodiscriminating efficiency and versatility of Pirkle's alcohol is witnessed by the flourishing literature which is devoted to the development of CSAs structurally related to **3b**: its anthracene derivatives contains bulky substituents

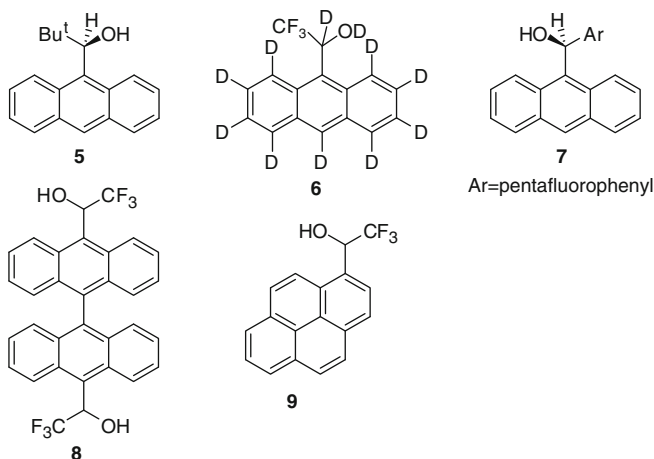


Fig. 6 CSAs structurally related to Pirkle's alcohol **3b**

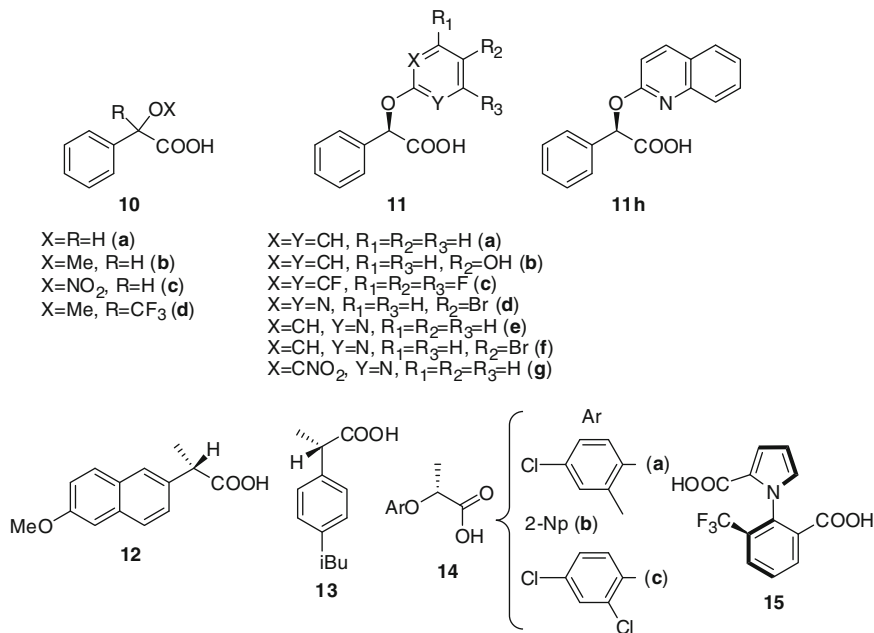


Fig. 7 CSAs based on carboxylic acids

classes of chiral compounds, with **10a**, **10c**, and **10d** mainly suitable for the analyses of amines or diamines [38, 40]; its derivative **10b** has a general applicability to the stereochemical analysis of chiral sulfoxides [39]. In recent years, several *O*-aryl and *O*-heteroaryl mandelic acids **11** (Fig. 7) have been proposed for the optimization of

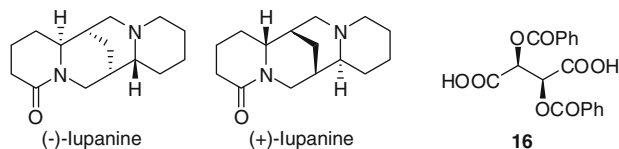


Fig. 8 Lupanine enantiomers and the CSA **16** employed for their differentiation

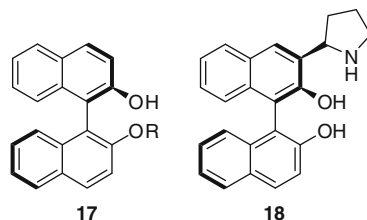


Fig. 9 Binaphthyl CSAs

NMR nonequivalences in mixtures containing several clinically and pharmacologically relevant amines [41].

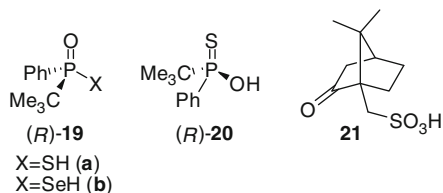
Anti-inflammatory drugs (*S*)-naproxen (**12**) and (*S*)-ibuprofen (**13**) (Fig. 7) are an interesting alternative to mandelates for sulfoxide derivatives [42]; CSA **12** shows good enantiodifferentiating efficiency also towards mono-phosphine oxides and bis-phosphine dioxides [43]. Simple derivatives **14** (Fig. 7) of very cheap lactic acid afford efficient CSAs for amines or amino alcohols [44]. The atropisomeric dicarboxylic acid 1-[2-carboxy-6-(trifluoromethyl)phenyl]pyrrole-2-carboxylic acid (**15**) (Fig. 7) is an enantiodifferentiating agent for different chiral oxiranes, oxetanes, and *cis*-but-2-ene-1,4-diol derivatives with a tertiary amino group [45].

In selected cases, when the chiral auxiliary is employed as resolving agent on a preparative scale it can also be employed as CSA for testing the enantiomeric excesses by NMR. The preparative and analytical resolution of lupinus alkaloids (Fig. 8) using dibenzoyltartaric acid (**16**) (Fig. 8) as resolving agent constitutes an example [46].

Due to their anisotropy features and ability to form host–guest diastereoisomeric pairs, 1,1'-binaphthyl-2,2'-diol and its derivatives **17** (Fig. 9) have attracted great attention as CSAs for amines, amides, amino alcohols, sulfoxides, and sulfinimines [47–54]. 1,1'-Binaphthyl-2,2'-diol has been employed for the NMR enantiodifferentiation of omeprazole [51] and other important drugs [50], as well as for the enantioanalysis of phytoalexin spiobrassinin derivatives [52].

A new binaphthol derivative containing a pyrrolidinyl substituent **18** (Fig. 9) has been very recently proposed [55] for the enantiodifferentiation of carboxylic acids; extraordinarily high nonequivalences are obtained at room temperature in mixtures CSA/acid at 2:1 molar ratio and moderately low concentration of the acid. The resonances of the enantiomers are differentiated by 0.2–0.3 ppm in fast exchange

Fig. 10 Phosphorus and sulfur CSAs



conditions. Interestingly, the efficient enantiodifferentiation of a carboxylic acid devoid of aromatic substituent is also reported.

(-)-(*S*)- or (+)-(*R*)-*t*-Butylphenylphosphinothioic acid (**19a**) (Fig. 10) has been known for a long time and has also been applied to the determination of the enantiomeric purities of poly-functional compounds [56]. Some interesting applications of the above CSA can be found in the literature, such as the analysis of substrates with sulfur or phosphorus atoms [57, 58]. More recently the use of **20** (Fig. 10) has been reported for enantiomeric excess determinations of chiral bis-imidazole *N*-oxides [59]. The analysis of the pharmacologically active crispine alkaloid [60–62] is also reported. In this last case the phosphinoselenic congener **19b** (Fig. 10) can be used as CSA with comparable results [62].

Equilibrating atropisomeric compounds have been discriminated by using (*R*)-camphorsulfonic acid (**21**) (Fig. 10) [63] as chiral auxiliary.

Among amines-based CSAs, an interesting example is constituted by the Tröger's base (**22a**) (Fig. 11), which is not itself very effective as an enantiodifferentiation agent for chiral carboxylic acids, but its enantiodifferentiating efficiency has been improved by putting a greater electron donating substituent on the aromatic ring (**22b**, Fig. 11) [64].

Amides are very attractive CSAs due to their ability to give cooperative hydrogen bond donor and acceptor interactions. Amides (*S*)-**23a** and (*S*)-**23b** (Fig. 11), first used by Kagan and coworkers [65] for the analysis of chiral sulfoxides, have been extended to the ^1H and ^{31}P NMR analysis of chiral phospholenes [66]. For the analysis of chiral amines, Kemp's acid diamide CSA **24** [67, 68] (Fig. 11) constitutes a useful alternative to the use of chiral acids, thus avoiding the formation of diastereoisomeric salts. The chiral lactam **25** (Fig. 11) is an effective enantiodifferentiating reagent for chiral lactams, quinolones, and oxazolidinones [69].

By reacting (*1R,2R*)-1,2-diaminocyclohexane with the appropriate 1,8-naphthalic anhydride, the CSAs **26a–c** (Fig. 11) are obtained with excellent enantioselective recognition ability for some chiral carboxylic acids [70]. Enantioselective differentiation could be achieved only in the less polar solvents and only for lipophilic guests. The use of chiral amino alcohol instead of diaminocyclohexane leads to the amphiphilic CSAs **27a** and **27b** (Fig. 11), which are effective CSAs. In particular, **27a** can be used to enantiodifferentiate not only lipophilic guests but also some hydrophilic guests such as tartaric acid and lactic acid or hydroxylated acids in protic polar solvents [71]. They could be used in many solvents, such as deuterated methanol, ethanol, acetonitrile, acetone, chloroform, and ethyl acetate [71].

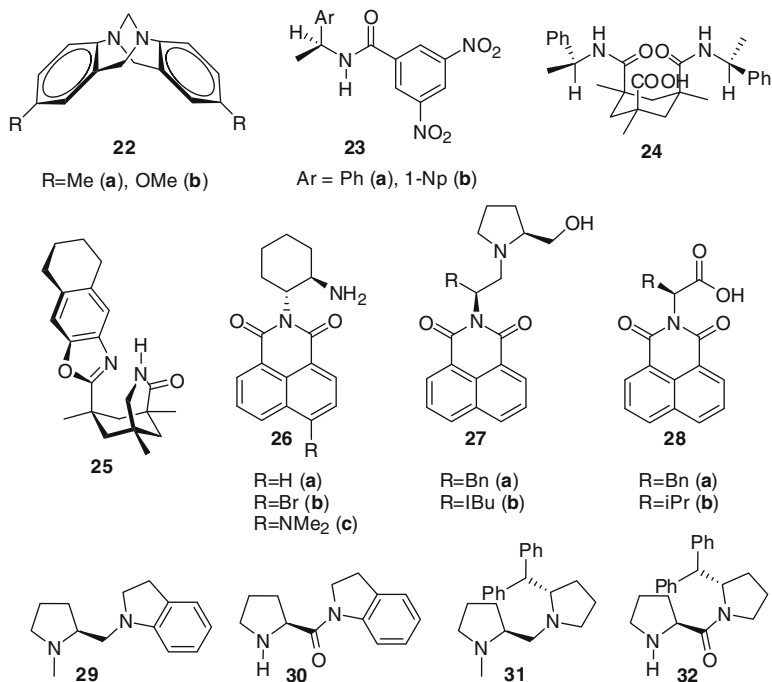


Fig. 11 Amine and amide CSAs

Benzo[*de*]isoquinoline 1,3-dione amino acids **28** (Fig. 11) are CSAs for the ¹H NMR enantiodifferentiation of α-arylalkylamines [72].

Enantiodifferentiation of carboxylic acids is also achieved by using proline-based chiral receptors **29–32** (Fig. 11) as CSAs, among which **30** and **32** have better enantioselective recognition abilities toward carboxylic acids [73].

Rigidly connected amide moieties as in (*S*)-1-benzyl-6-methylpiperazine-2,5-dione (**33a**) (Fig. 12) allow complementary hydrogen bond interactions with analogous racemic compounds, which give detectable NMR nonequivalences [74, 75]. The effect of substituents on analogous 1,6-dialkylpiperazine-2,5-diones (**33b–g**) (Fig. 12) has also been evaluated [76] by using methyl (*RS*)-*N*-benzoylleucinate as the model analyte. Several enantiomer signals were resolved by 0.1–0.2 ppm in spite of the fact that the association constants of the diastereoisomeric pairs were not high or remarkably differentiated.

A good cooperativity between hydrogen bond donor–acceptor groups and aromatic moieties is obtained by means of the bisimidazoline-based CSA **34** (Fig. 13) for the enantiomeric differentiation of chiral carboxylic acids [77]. The chiral auxiliary has a highly symmetric structure with very simple NMR signals, reducing the probability of accidental overlap with resonances of the substrate. The signals of the enantiomers are resolved in the presence of 1 equiv. of the CSA in diluted solutions [77].

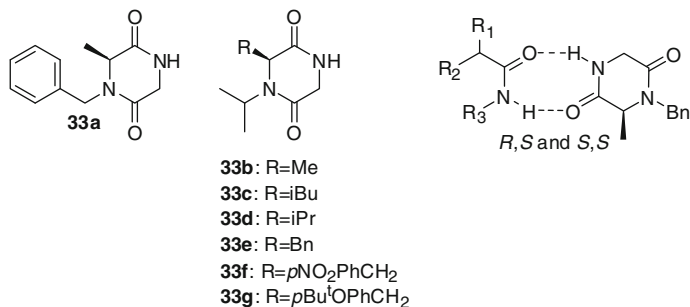


Fig. 12 Amide CSAs and complementary hydrogen bond interactions with amide counterparts

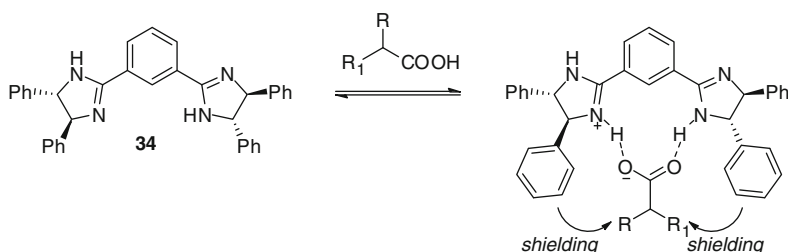


Fig. 13 Bisimidazole-based CSA and its interaction mechanisms

For the enantiodifferentiation of α -chiral carboxylic acids (2-chloropropionic acid, α -hydroxyisovaleric acid, ibuprofen, mandelic acid, and 2-chloromandelic acid), chiral receptors **35–38** (Fig. 14), bearing both an amino group and a hydroxyl group, give good nonequivalences, which are suitable for enantiomeric excess determinations within $\pm 1\%$ of the predetermined enantiopurity of the samples [78]. In spite of the occurrence of salification processes, fast exchange conditions are guaranteed, probably due to a co-operation between the polar groups of the CSAs and their aromatic moieties and, hence, a good balance of hydrophilic and hydrophobic interactions with the enantiomeric substrates [78].

Attempts to modify the structure of α -phenylethylamine by the incorporation of two anisotropic groups (naphthyl and phenyl) and increasing the number of stereogenic centers led to the diamine CSAs **39** and **40** (Fig. 14) with improved efficiency in the enantiodifferentiation of carboxylic acids [79, 80]. Analogs of **40** are discussed in the section devoted to macrocyclic CSAs. Zhang's contributions to the development of efficient CSAs for the NMR differentiation of enantiomers of the same class of chiral compounds include the amino alcohols-based CSAs **41–43** (Fig. 14), in which strong anisotropic groups and further hydrogen bond acceptor interaction sites are present [81].

Derivatives of amino acids are attractive CSAs since several of them are commercially available and inexpensive. As an example, *N*-Fmoc-*N'*-Boc-L-tryptophan reveals good enantiodifferentiating efficiency towards stereogenic phosphorus centers in phosphine oxides, phosphinates, phosphonates, phosphates, and phosphonamides.

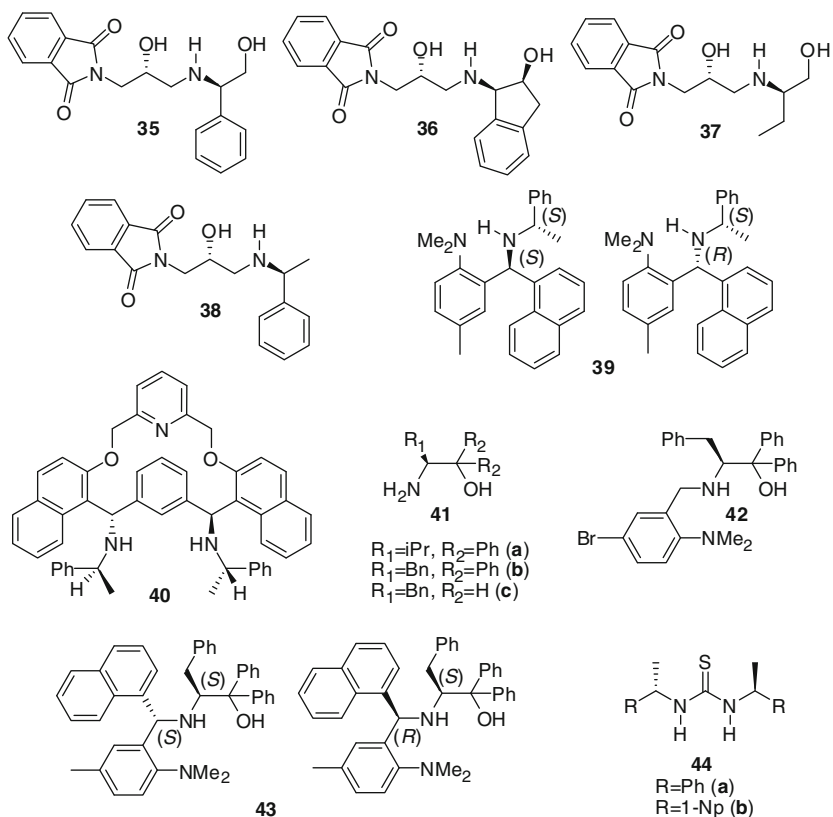


Fig. 14 Amino alcohol, diamine, and thiourea CSAs

Enantiomeric excess determinations can be performed by detecting ^{31}P , ^{13}C , and 1H NMR nuclei and substantial separations of the enantiomer resonances is obtained in ^{31}P NMR spectra, with the sole exception of chiral phosphates and phosphine oxides, for which the separation of the signals is relatively small [82].

The synthesis of C_2 -symmetrical chiral thioureas (*S,S*)-**44** (Fig. 14) is very simple and involves inexpensive reagents. The thiourea chiral auxiliaries have the capacity to act as receptors for anionic species via hydrogen bonding and produce high separations of the NMR signals of chiral α -hydroxy and α -amino carboxylic acids. The methine C–H signal of racemic phenylglycine was doubled by 0.05 ppm in the presence of thiourea CSAs, and a reliable correlation between the relative positions of the signals of the two enantiomers and their absolute configuration was found [83].

Diamagnetic chiral hexacoordinate phosphate anions BINPHAT (**45**) and TRISPHAT (**46**) (Fig. 15) associate efficiently with chiral organic or organometallic cations endowed with different types of chirality and give rise to good non-equivalences [84–90].

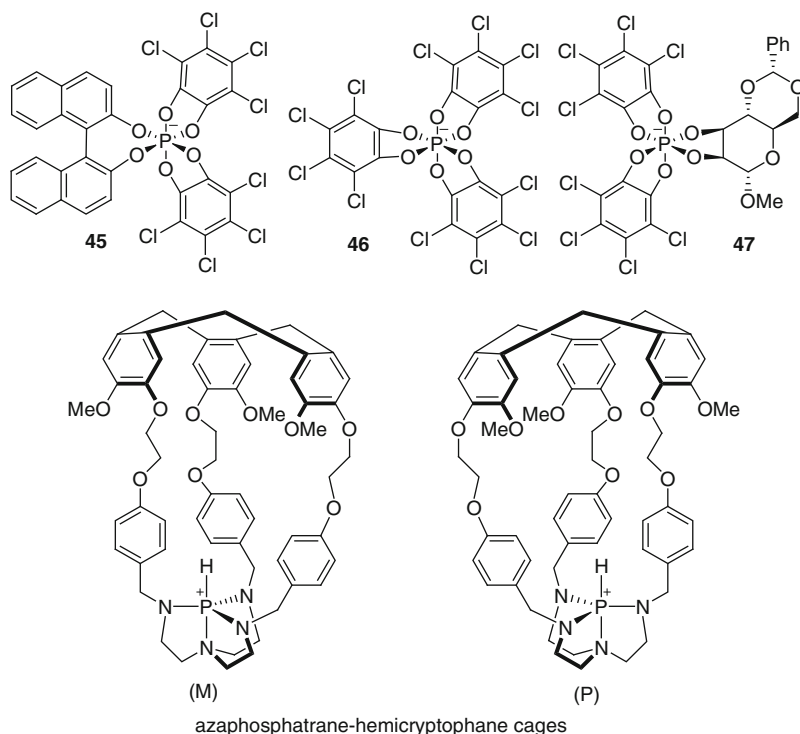


Fig. 15 Phosphate anion CSAs and selected examples of enantiodifferentiated substrates

By using ionic CSAs, efficient NMR enantiodifferentiation is regularly achieved in low polarity halogenated solvents: in polar solvents, cations and anions (small organic ones in particular) tend to behave as dissociated ion pairs as a result of weaker electrostatic interactions, and hence a sharp decrease in the NMR enantiodifferentiation is found [3]. Surprisingly, BINPHAT anion is an efficient CSA for quaternary ammonium cations derived from Tröger's base leading to large separations of the proton signals of the enantiomers even in polar solvent such as CD_3CN , where nonequivalences up to 0.12 ppm are measured [86].

Interesting applications of the above-mentioned CSAs are the differentiation of Δ and Λ forms of organometallic Ru(II) complexes [87] and (*M*)- and (*P*)-enantiomers of the azaphosphatrane-hemicryptophane cages [88] (Fig. 15), for which both ^1H and ^{31}P resonances are differentiated, and very efficient differentiation of octanuclear metalla-cages were achieved in spite of the use of polar solvents [89].

The analogous mannose-derived hexacoordinated phosphate **47** (Fig. 15) is a chiral anionic auxiliary with broad efficiency for the enantiodifferentiation both of organic cations and organometallic species [90].

Among CSAs based on chiral anions, bis[*(R)*-1,1'-bi-2-naphtholato]borate (**48**) (Fig. 16) should also be mentioned. It was reported in 2003 [91] as a ^1H NMR shift reagent for cationic copper(I) complexes. Its diborate analog **49** (Fig. 16) has found more recent [92] applications in the differentiation of enantiomeric

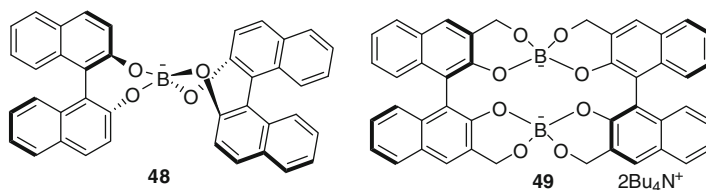


Fig. 16 Borate CSAs

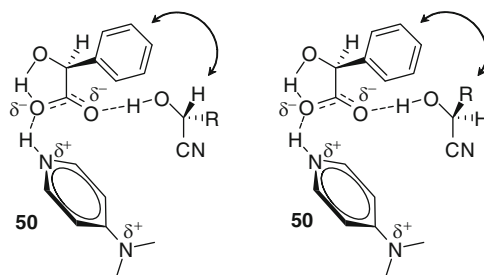


Fig. 17 Mandelic acid-dimethylaminopyridine ion pair CSA and its ternary complex with cyanohydrins

triphenylphosphonium salts. In particular, the differentiation of the ^1H NMR signals of triphenyl(1-phenylethyl)phosphonium bromide is obtained by addition of only 0.25 equiv. of the diborate CSA. Analogously responsive are the ^{31}P resonances. More additive leads to higher complexation-induced shifts, but the separation is already complete after the addition of 0.25 equiv. of diborate.

The ion pair formed by optically active mandelic acid and dimethylaminopyridine **50** (Fig. 17) constitutes an excellent chiral shift reagent (CSR) for the determination of enantiomeric excess and absolute configuration of cyanohydrins, for which the use of CSAs is quite unusual [93, 94]. Two diastereoisomeric ternary complexes were formed in solution with 1:1 association of the ion pair and the cyanohydrin enantiomer (Fig. 17). The association constants of the two ternary complexes are well differentiated.

Another important class of CSAs has a completely different origin: the considerable demand for new chiral stationary phases (CSPs) for the direct control of the enantiomeric excess of chiral substrates, mainly chiral drugs, by high performance liquid chromatography (HPLC), prompted researchers to investigate the enantiodifferentiating mechanism operating in chromatographic separations [95–97]. To this end, reliable NMR investigations were carried out in solution on the mixtures formed by the enantiomers of the substrates well separated on the CSPs and a suitable soluble model of the CSP. In most cases these NMR investigations showed that the soluble model of the CSP was able to induce nonequivalences in the enantiotopic nuclei of the enantiomeric substrates and, hence, acted as CSA for them. Some CSAs, soluble models of CSPs, were the following (Fig. 18): *N*-3,5-dinitrobenzoyl derivatives of amino acid methyl esters **51a, b** [98], quinine **52** [99–104], *N*-(*n*-butylamide) of

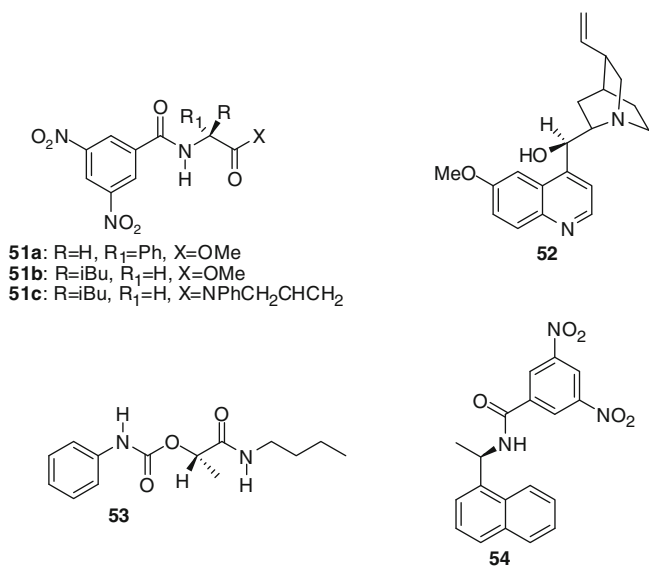


Fig. 18 Soluble models of chiral stationary phases used in liquid chromatography

(*S*)-2-(phenylcarbamoyloxy)propionic acid **53** [97, 105], and others. Common applications of these selectors involve the observation of ¹H nuclei of the enantiomeric substrates, although selected examples of observation of ¹⁵N (as for CSA **53**) and ¹³C (as for CSA **51c**) nuclei are reported for enantiomeric excess determinations of amino acid derivatives. In recent work [106], which describes the use as CSA of the Pirkle's selector **51c** (Fig. 18), the issue of comparison of the accuracy of chromatographic and NMR methods has been addressed.

The Whelk-*O* chiral selector [107, 108] was originally developed for HPLC. Numerous studies demonstrated its cleft-like structure into which only one enantiomer of a chiral compound can be included, thus originating impressive chromatographic separations. Unfortunately its synthesis is quite difficult, thus limiting its availability as CSA for NMR spectroscopy. By contrast, the analogous 3,5-dinitrobenzoyl-derived 1-naphthylethyl amide **54** (Fig. 18) can be prepared in a single step by the condensation of 1-(1-naphthyl)ethylamine [109]. This chiral auxiliary differentiated very efficiently pivaloyl derivatives of chiral amines. NMR differentiation of the enantiomeric substrates was also detected in the presence of sub-stoichiometric amounts of this CSA.

3 Molecular Tweezers

Chiral noncyclic compounds with two aromatic groups separated by a semi-rigid spacer, in which U-shaped cavities are generated, are called molecular tweezers or clips. Their flexibly sized cavities are potentially able to fit several kinds of chiral substrates. The muconate of α,α' -(bis-trifluoromethyl)-9,10-anthracenedimethanol

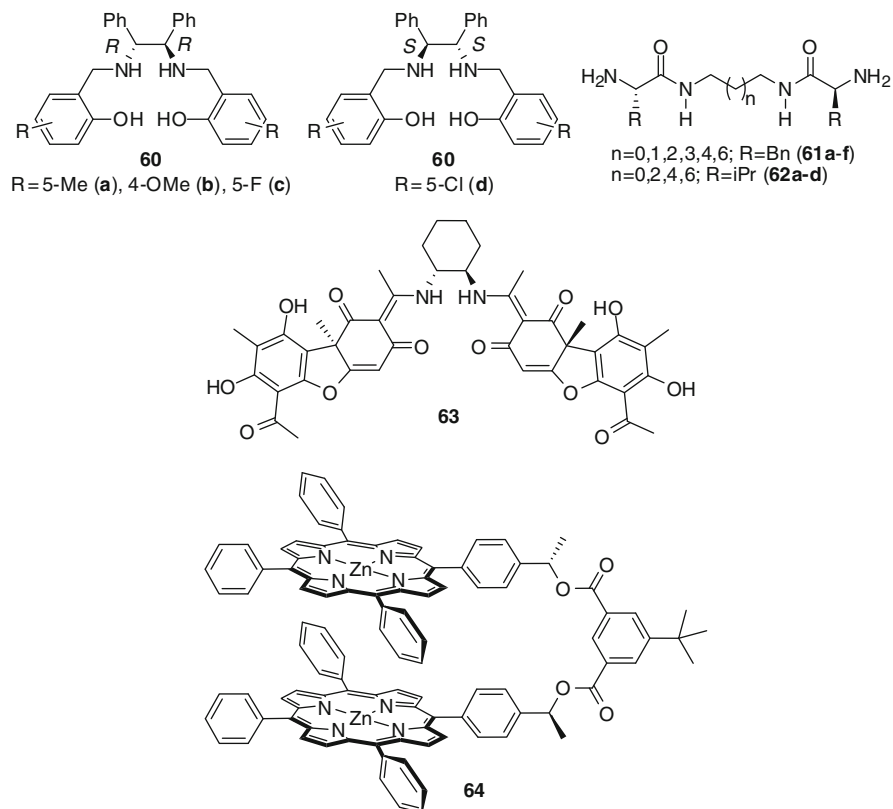


Fig. 21 Pincer-like CSAs

receptor **58** shows a very good peak resolution for lactic acid, but it causes a concomitant line broadening, which suggests the co-presence of different conformations as a consequence of the lesser rigidity of the cavity of **58** due to the change of carbonyl by methylenic units and to the presence of two possible basic protonation sites. The elimination of one half of the pincer biting cavity drastically reduces the splitting for most of the acids, which demonstrates the strong cooperative effect of the two side arms.

Salen ligand-based aminophenol compounds **60a–d** (Fig. 21) are very attractive CSAs for chiral carboxylic acids. Only a few ^1H NMR signals are due to the CSAs, so that the resonances of the enantiomeric compounds can be detected very easily and also accurately integrated. Very good differentiation of the enantiomeric signals is obtained at the 3:1 CSA/substrate molar ratio, corresponding to the complexation stoichiometry [114].

The co-presence of the amide and amino groups in open chain peptide-mimetics bis(amino amide) ligands **61** and **62** (Fig. 21) derived from natural amino acids also allows the enantioselective interaction with carboxylic acids: the maximum

enantiodifferentiating efficiency is found by using the CSAs with aliphatic spacers containing 3 to 5 carbon atoms, whereas low enantiomeric differentiation is detected for the shortest and the longest aliphatic spacers [115]. The presence of an aromatic moiety in the side chain favors the differentiation of the enantiomeric substrates [115].

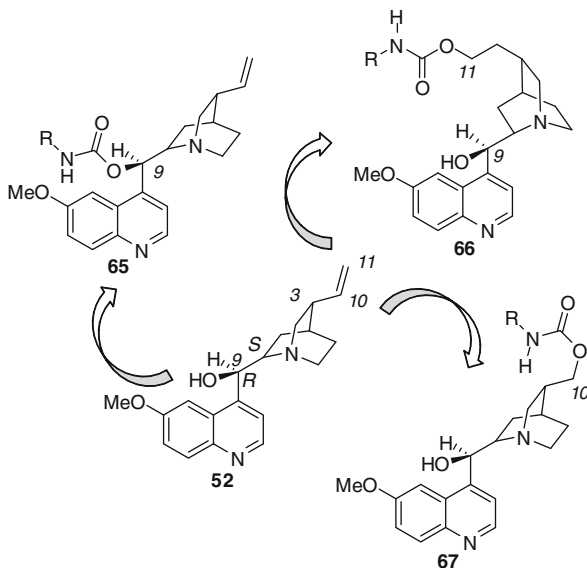
trans-1,2-Diaminocyclohexane can be employed as spacer for the preparation of pincers CSAs, as in the case of the compound **63** (Fig. 21), with usnic acid units, which doubles the resonances of various chiral esters containing an electron-poor aromatic moiety [116].

Dimeric metalloporphyrins (**64** in Fig. 21) are well suited to enforce strong cooperative interactions during the encapsulation of multifunctional molecules. Upon binding to the diporphyrin, all the signals of the chiral compounds are greatly upfield-shifted due to the ring-current effect of the porphyrin rings, which strongly supports their encapsulation between the two porphyrins. Very high enantiomeric differentiations are detected, which demonstrate the usefulness of the porphyrin-based tweezers as a highly sensitive CSR for the determination of the enantiomeric purity of chiral diamines, aziridine, and isoxazoline at the microgram level [117].

4 Natural Products

Chiral auxiliaries derived from inexpensive, chiral natural sources are remarkably very attractive. Among them, quinine (**52** in Fig. 18) has many favorable features: it is commercially available in pure stereoisomeric form, it is very cheap, well soluble in CDCl_3 , the complex chemical structure (a secondary alcoholic group, two basic nitrogen atoms, a heteroaromatic system) renders this molecule capable of interacting with the enantiomers of many organic compounds and, hence, of being of potential use as a CSA. In fact in 1969 Uskokovic recognized its ability to generate chemical shift nonequivalence in the proton NMR spectra [118]. The first work, specifically dedicated to the use of quinine as CSA for NMR spectroscopy, was published in 1988 by Salvadori's research group [99] and represented the starting point of intense research activity [19] that extends to the present time and which is aimed at the exploitation of the modulability of the quinine selector: its reactive groups can, in fact, be easily modified to make it suitable for interaction with and enantiodifferentiation of a wide range of organic compounds. First, the derivatization of the hydroxyl group of quinine was attempted, which led to C_9 carbamates **65** (Fig. 22) [119] with complementary enantiodifferentiating properties with respect to non-derivatized alkaloids. Subsequently, C_{11} carbamates **66** (Fig. 22) were proposed [104, 120], in which the alkaloid double bond was derivatized, thus preserving the hydroxyl function at the C_9 site. The carbamate function and the quinuclidine moiety of this last kind of derivative were separated by two methylene groups, which gave a high degree of mobility to the newly introduced carbamate function. C_{11} carbamates showed enhanced versatility and combined the enantiodifferentiating properties of C_9 carbamates and non-derivatized quinine. With the aim of ascertaining the role of the spacer located

Fig. 22 CSAs based on C₉, C₁₀, and C₁₁ carbamates derivatives of quinine



at C₃ of the quinuclidine ring (Fig. 22), both on the enantiodifferentiating efficiency and on the versatility of carbamoyl derivatives of quinine, a different kind of quinine double bond derivatization was used by designing the C₁₀ carbamate **67** (Fig. 22) [121]. The ability of 10-(pentafluorophenylcarbamoyloxy)-6'-methoxy-11-norcinchonan-9-ol to induce NMR anisochrony of selected enantiomeric substrates was analyzed in comparison with both the corresponding C₉ carbamate 9-*O*-(pentafluorophenylcarbamoyl)quinine and quinine [121]. The pentafluorophenyl group was selected in order to have an aromatic moiety potentially able to develop π -stacking interaction, but without any spectral interference in the ¹H NMR analyses.

C₁₀ carbamate does not allow cooperation between the carbamate function and the other functional groups (quinoline ring or quinuclidine nitrogen), which is the prerequisite for efficient enantiodifferentiation. Probably, joining the quinuclidine moiety and the carbamate function by means of a short spacer does not allow cooperation between the different functional groups which are present in the chiral auxiliary [121].

In the majority of applications of quinine-derived CSAs the enantiomeric pairs were detected by ¹H NMR spectroscopy. Suitably fluorinated chiral compounds can be alternatively detected by ¹⁹F NMR spectroscopy, minimizing the spectral interference caused by the complex spectral pattern of the chiral auxiliary [122].

Alternatively, enantiomeric mixtures of 1-hydroxy and 1,2-dihydroxyalkane-phosphonates and 1-*N*-benzyloxycarbonylaminoalkane-phosphonic and phosphinic acids can be differentiated in the ³¹P NMR spectra [102, 123, 124]. The opportunity of differentiating chiral compounds with phosphorus centers encouraged the combination of quinine with a phosphate moiety in the phosphorylated quinines **68a, b**

Fig. 23 Phosphorus derivatives of quinine **68**, quinidine, and selected enantiodiscriminated substrate

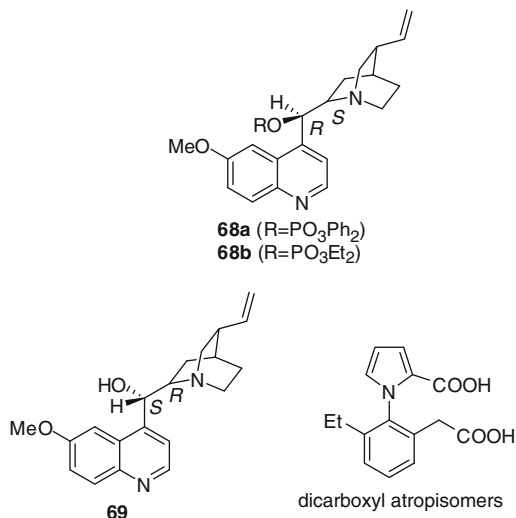


(Fig. 23) that show good complexing properties towards different kinds of ligands [125]. 3,5-Dinitrobenzoyl amino acids with free carboxylic groups are differentiated efficiently in the ¹H NMR spectra. The salification of the chiral auxiliary causes a significant loss of enantiodifferentiating efficiency, revealing the role of the quinuclidine nitrogen in the diastereoisomeric ion pair stabilization. In order to detect the diastereoisomeric interactions in the ³¹P NMR spectra, low-exchange conditions must be forced by means of low-temperature experiments.

Interestingly, quinidine (**69**) (Fig. 23) has been reported for enantiomeric excess determinations of dicarboxylic atropisomers (Fig. 23) with rotational barriers (30–40 kcal/mol or higher) high enough to separate and keep the enantiomers of the target molecules for a long time without spontaneous enantiomerization at room temperature. The alkaloid seems to be much better chiral auxiliary than chiral lanthanides as it produces narrow resonances [126].

In the field of CSAs from natural sources, an isolate application of octasaccharide subunits of succinoglycan **70** (Fig. 24), which consist of one galactose and seven glucose residues joined by β-glycosidic linkages, has been reported for the ¹³C NMR differentiation of catechin enantiomers, following their use as chiral additives in capillary electrophoresis (CE) [127].

Several other kinds of natural products are potentially useful for applications of CSAs, such as glycopeptides, which are very popular in enantioselective chromatography [128]. Unfortunately, even if potentially highly effective in the stabilization of diastereoisomeric solvates, they produce complex spectral patterns which generate extended overlap with the signals of the enantiomeric substrates and, hence, are not suited for the NMR evaluation of the stereoisomeric purities.

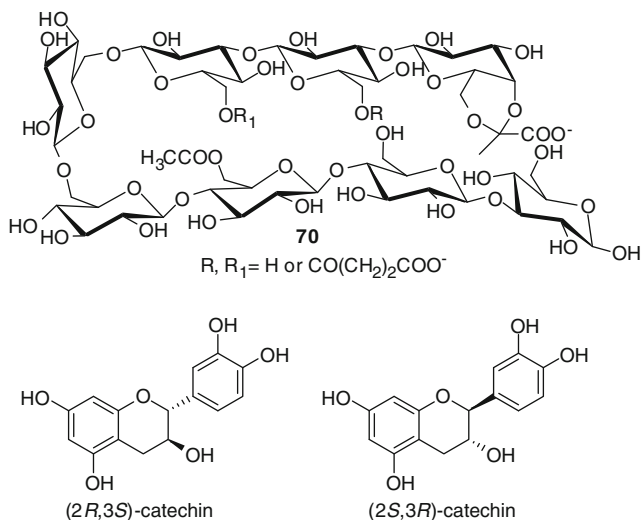


Fig. 24 Succinoglycan monomers **70** and catechin

5 Cyclodextrins

Similar to what occurred for a large number of chiral selectors for NMR spectroscopy, chiral chromatography has given a strong impulse to the development of cyclodextrins (CDs) as CSAs for NMR enantiodiscrimination [129], as extensively highlighted by Chankvetadze's in several valuable publications [130–134].

Cyclodextrins **71** have found enormous technological applications [135–141] by virtue of their unique structural features (Fig. 25). They are truncated cone shaped cyclic oligosaccharides endowed with an apolar cavity in which apolar molecules or apolar molecular fragments may be included, whereas their external surface is hydrophilic due to the presence of the hydroxyl groups bound to the secondary and primary sites on the wide and narrow rims. A good fit between the size of the cyclodextrin cavity and that of the substrate to be included may be achieved by selecting one of the three α -, β -, γ -cyclodextrins congeners **71a–c** (Fig. 25). Cyclodextrins are largely employed as solubility promoters and for the transport and controlled release of drugs in the pharmaceutical industry [141]. The chirality of the glucopyranose units renders cyclodextrins well suited to host enantiomeric compounds and, hence, to form diastereoisomeric inclusion solvates with them, which, in principle, could be differentiated by NMR. In virtue of their C_n -symmetry properties, cyclodextrins are very attractive as CSAs due to the fact that their NMR spectra are constituted by only a few signals, leaving available extended spectral regions for the NMR analyses.

It should be noted that the introduction of cyclodextrins as CSAs for NMR spectroscopy has filled a serious gap from the analytical point of view, regarding the analysis of chiral compounds in aqueous medium, in contrast with the majority of

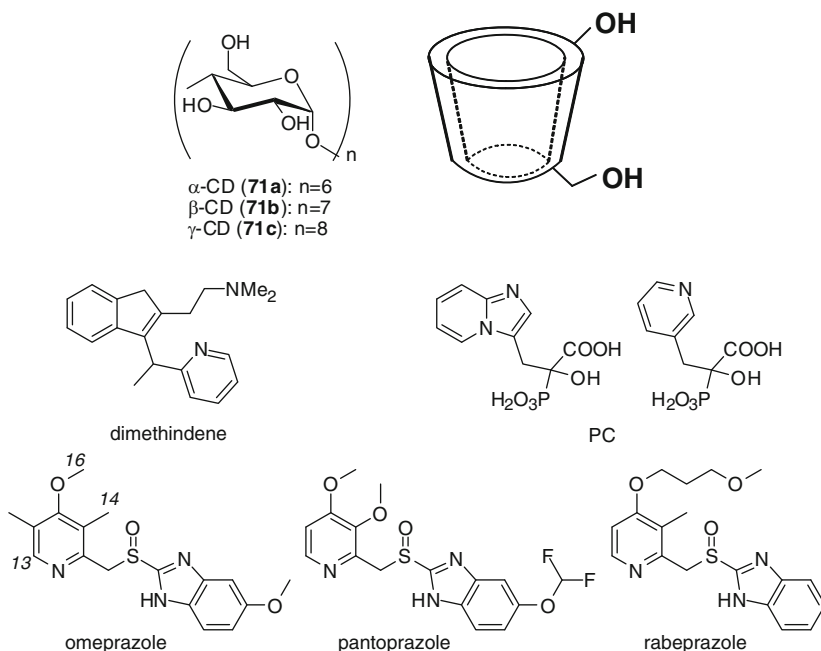


Fig. 25 Native cyclodextrins and selected examples of chiral substrates enantiodiscriminated in D_2O

the CSAs with low-medium molecular weight, which are suitable for enantiomeric excess determinations in organic solvents.

Importantly, a thin and delicate balance between hydrophilic interactions involving the polar groups on the narrow and wide edges and hydrophobic interactions with the internal cavity makes cyclodextrin suitable for analyses in aqueous medium of both hydrophilic and lipophilic substrates, with huge implications in the field of direct analysis of chiral metabolites in biological fluids [142].

Cyclodextrins have three different kinds of hydroxyl groups – two secondary groups and a primary one on each unit, the acidity and reactivity of which are quite different. Thus, these cyclic oligosaccharides can be derivatized selectively or exhaustively in order to introduce different kinds of derivatizing groups, which change their solubility properties and may cooperate with the cavity in the stabilization of diastereoisomeric solvates or, alternatively, may direct the interaction towards the external surface of the cyclodextrin rather than inside the cavity [17–19, 22, 129, 139, 143–145]. In any case, in the design of new CSAs based on cyclodextrin derivatives, the spectral pattern of their derivatives should always be considered with great care: the selective derivatization of individual units would be attractive in some cases, but it causes loss of symmetry. Consequently, the proton nuclei of the different glucopyranose units are no longer isochronous and the cyclodextrin derivative is less suited for use as a CSA. The exhaustive derivatization of the glucopyranose rings

causes a great increase of the molecular weight, but does not perturb the system symmetry, at least in the majority of cases [146–148].

Cyclodextrins have, in fact, been used in native form for the NMR enantio-differentiation of apolar and polar compounds in aqueous medium, but, when suitably derivatized, they can be used as CSAs in the majority of organic solvents [13, 14, 16–22]. As a consequence of their high level of modulability, we could assess that an alternative category of macrocycle chiral auxiliaries with equal versatility cannot be found.

The literature on the use of native cyclodextrins CSAs for enantiomeric excess determinations [13, 14, 16–22, 129] in aqueous environment is also huge by virtue of the close connection with activities aimed to promote their use as solubility enhancers. Casy and Greatbanks devoted some of the earliest papers to this topic, in which the ability of native cyclodextrins to induce NMR nonequivalence in the NMR spectra of chiral antihistamines and other kinds of drugs was demonstrated [149, 150]; as an example, in the case of (*R,S*)-dimethindene maleate (Fig. 25) the pyridyl signals are duplicated in D₂O in the presence of β-CD (71b) due to the formation of 1:1 diastereoisomeric inclusion complexes. Among the recent flourishing literature devoted to the same subject, the ³¹P NMR analysis of phosphonocarboxylate (PC) analogues of bisphosphonates (Fig. 25) [151] could be considered. However, more and more investigations on the use of cyclodextrins CSAs are coupled to accurate parallel investigations on enantiomeric differentiation mechanisms and are addressed to the development of reliable protocols for the accurate quantitative analyses of the enantiomers, which could complement the chromatographic methods. Redondo et al. [152] have exploited the considerable potential of NMR spectroscopy in the optimization of analytical protocols and simultaneous analysis of chiral recognition processes of sodium salts of the proton-pump inhibitors omeprazole, pantoprazole, and rabeprazole (Fig. 25) by using the three cyclodextrin congeners α-CD, β-CD, and γ-CD as chiral complexing agents in D₂O. The basic structure of the three guests consists of a benzimidazole group linked to a pyridine ring through a sulfoxide group, with the sulfur atom constituting a center of chirality. For the optimal observation of selected ¹H NMR signals of the three substrates, which resonate approximately at the same frequency of the intense HDO signal, and in order to gain more signal-to-noise for the resonances of interest, diffusion-filtered ¹H NMR spectra [153] with substantially attenuated HDO signal are recorded instead of using conventional signal suppression techniques. The induced magnetic nonequivalence of the guest protons at room temperature by 1 equiv. of any of the three CDs is important in most cases and its magnitude depends on the cavity sizes, according to the formation of diastereoisomeric inclusion complexes. The pyridine proton signal H-13 of omeprazole (Fig. 25) is split by 0.043 ppm in the presence of α-CD. The larger congener β-CD induces important nonequivalence on 14-Me and 16-OMe, whereas γ-CD gives significantly lower enantiodifferentiation. Pantoprazole behaves similarly, but rabeprazole is the less enantiodifferentiated one. Interestingly, the two enantiomers of pantoprazole are also efficiently differentiated in the ¹⁹F NMR spectra with doublings to 0.085 ppm. Enantiomeric purities to 98% are accurately

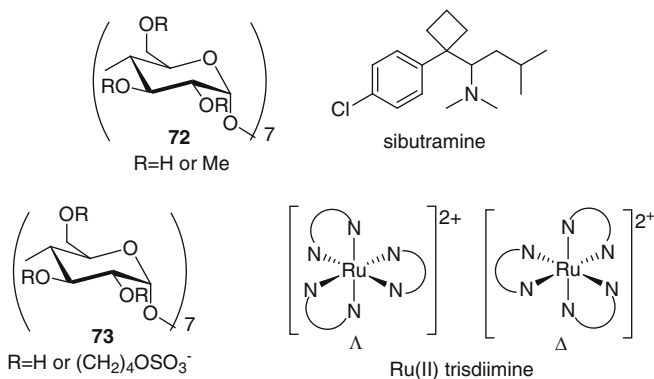


Fig. 26 CSAs based on water soluble cyclodextrins and selected examples of substrates enantiodifferentiated by NMR in D_2O

determined. The results of ROESY analyses suggested a preferential binding of the benzimidazole moiety of the guest molecules within the macrocyclic cavity of α -CD, whereas the higher dimensions of β -CD and γ -CD also permitted the inclusion of the highly substituted pyridine moieties.

β -CD, which is the less expensive of the three native cyclodextrins, has poor solubility in aqueous medium. Therefore the optimization of the nonequivalences by increasing the total concentration or the molar ratio of the mixtures CSA/substrate cannot be exploited. Several alternative well soluble β -CD derivatives are produced on large scale and commercially available. As an example, accurate enantiomeric excess determinations of sibutramine (Fig. 26), a serotonin and noradrenaline re-uptake inhibitor, have been performed by using methyl- β -cyclodextrin (72) (Fig. 26) as CSA [154], in comparison with capillary electrophoretic measurements. *N*-Methyl resonances giving well resolved resonances were selected for the enantiomers quantification. Once again, the authors proposed a correlation between CE and NMR resolution factors. Compounds with stereogenic phosphorus centers are also differentiated by ^{31}P NMR in the presence of neutral and anionic CDs [155].

Ionic derivatives of cyclodextrins [156–164] are water soluble and are effective CSAs for ionic chiral compounds, also including organometallic ionic complexes, as for the analysis of Λ and Δ enantiomers of Ru(II) trisdiimine complexes [164] by using anionic CDs (like 73 in Fig. 26).

Several factors contribute to enhance chiral differentiation by ionic CDs: ion-pairing interactions upon complex formation, the extension of the cyclodextrin cavity, and the enhancement of the hydrophilicity of the external surface. Relevant contributions in this field come from Wenzel's group [156–161] and will be extensively discussed by the same author in this volume.

The introduction of lipophilic groups on the CDs rims breaks the ordered network of hydrogen bonds between the secondary hydroxyl groups of adjacent rings of underivatized cyclodextrins, which is responsible for their global truncated

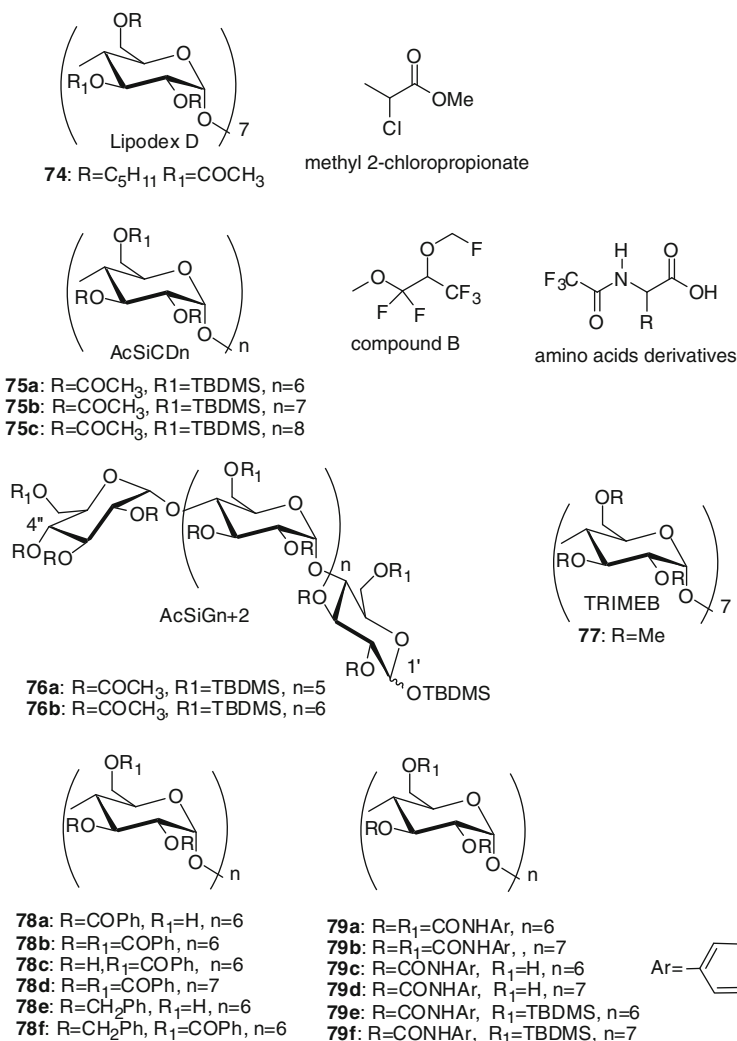
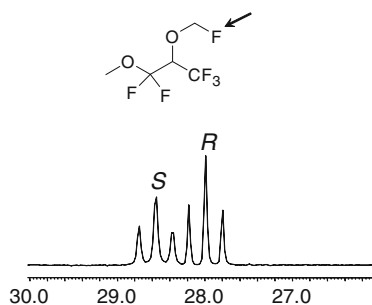


Fig. 27 Cyclodextrin derivatives and compounds enantiodifferentiated in organic solvents by NMR (TBDMS = *tert*-butyldimethylsilyl)

cone shapes. More flexible structures are obtained with remarkably different solubility, complexing, and enantiodifferentiating properties. The development of lipophilic CDs as CSAs for enantiomeric excess determinations in organic solvents has received a strong impulse from the brilliant results attained in the field of chiral gas chromatography (GC). Enantioselective inclusive processes by cyclodextrin derivatives were reported in 1992 by König and coworkers [165], who described the interaction of methyl (*R,S*)-2-chloropropionate with heptakis(3-*O*-acetyl-2,6-di-*O*-pentyl)- β -cyclodextrin (**74**, Lipodex D) (Fig. 27). NMR spectra recorded in

Fig. 28 ^{19}F NMR (282 MHz, C_6D_{12} , 25°C) spectral region corresponding to the fluorine nuclei of the CH_2F -group of compound B (60 mM) in the presence of 1 equiv. of AcSiCD7 (**75b**)



cyclohexane- d_{12} showed very high differentiation of methine protons of methyl 2-chloropropionate enantiomers, which were also significantly differentiated in line-width.

Schurig and his coworkers' elaborate activities [135–138] in the enantioselective gas chromatographic area not only had a scientific and technological impact, but have also urged and promoted parallel spectroscopic activities suggesting the use of the same CDs as CSAs for NMR spectroscopy. This is the case for heptakis(2,3-di-*O*-acetyl-6-*O*-*tert*-butyldimethylsilyl)- β -cyclodextrin (AcSiCD7) (**75b**, Fig. 27), which exhibits a surprisingly high gas chromatographic enantioseparation factor α of 4.1 for 1,1,1,3,3-pentafluoro-2-(fluoromethoxy)-3-methoxypropane (compound B) (Fig. 27), a chiral degradation product of the inhalation anesthetic sevoflurane [166]. The separation factor drops to 2.70 for the γ -CD analogue AcSiCD8 (**75c**) (Fig. 27) and no enantioseparation at all is obtained for the α -CD analogue AcSiCD6 (**75a**) (Fig. 27) [167]. Surprisingly, the separation of compound B also occurs on the corresponding open chain selectors AcSiG7 (**76a**) (Fig. 27) and AcSiG8 (**76b**) (Fig. 27) [167].

NMR investigations [168] demonstrated that in apolar solvents, which better mimic gas chromatographic conditions, AcSiCD7 leads to very high NMR anisochrony of the two enantiomers of compound B (Fig. 28).

ROESY experiments revealed that both enantiomers are not deeply inserted into the cyclodextrin cavity in a such a way as to make possible the Si–F attractive interaction between the silyl groups on the primary sites, which are bent at the external surface of the cyclodextrin, and the fluorinated head of the enantiomers protruding from the wide rim of the cyclodextrin cavity. The Si–F attractive interaction is favored by the increased cyclodextrin flexibility, which allows the rotation of the glucopyranose rings around the glycosidic linkages. The relevance of superficial fluorine–silicon interactions is confirmed by the ability of analogous acyclic oligosaccharides, for which inclusion is not possible, to enantiodifferentiate compound B by gas chromatography [167], although with minor enantio-differentiating efficiency.

The silylated–acetylated β -cyclodextrin **75b** (Fig. 27) was also proposed as an efficient CSA for direct determinations of enantiomeric purities of fluorinated α -amino acid derivatives [169]. Interestingly, in this last case a regular correlation exists between the relative positions of enantiomer amide resonances and amino acids absolute configuration [169]. The acyclic linear heptasaccharide AcSiG7

(Fig. 27) is also able to bring about NMR enantiodifferentiation, but to a smaller extent than CSA **75b**.

Several other kinds of CSAs based on exhaustively derivatized cyclodextrins have been proposed. Permethylylated- β -cyclodextrin (**77**, TRIMEB) (Fig. 27), which did not show any propensity to include chiral apolar substrates in CD₃OD solution, constitutes a very efficient CSA for trisubstituted allenes [170, 171] or aromatic hydrocarbons [172] in the same solvent, in spite of the fact that the association constants of the diastereoisomeric complexes are very low and almost equal. The above result confirmed that subtle time-averaged stereochemical differentiation of the two diastereoisomeric solvates contribute to differentiate them, even though the interactions involved in the stabilization of the diastereoisomeric complexes are not able to give rise to detectable thermodynamic differentiation. The use of permethylated cyclodextrin as CSA also afforded a reliable empirical tool for the assignment of the absolute configurations inside the same classes of chiral compounds [170]. It is noteworthy that none of the traditional low molecular weight CSAs could have been successfully applied for apolar compounds like allenes and aromatic hydrocarbons. Benzylated and/or benzoylated CDs **78** (Fig. 27) [173, 174] or carbamoylated CDs **79** (Fig. 27) [175–178] are chiral auxiliaries that are very soluble in CDCl₃, being applicable to the analyses of polar substrates, derivatized or underivatized, insoluble in D₂O. In these last cases the formation of the diastereoisomeric solvates, which are responsible for NMR nonequivalences, relies on superficial interactions with the derivatizing groups located on the primary and/or secondary sites. Bulky benzoyl derivatizing groups on the secondary sites of α -CD led to a symmetry change from C₆ to C₃ which was clearly detected in the ¹H NMR spectra recorded in CDCl₃: two sets of resonances were observed corresponding to two different kinds of glucopyranose rings [174, 179].

6 Synthetic Macrocycles

One goal of molecular recognition is selective binding of stereoisomers by synthetic host structures, where the target molecule is completely surrounded by a receptor that provides a complementary, congruent surface. Encapsulation meets some of these desired characteristics and, for this reason, synthetic macrocycle chiral auxiliaries for NMR spectroscopy have long attracted great attention [180, 181]. Their complexing properties, solubility characteristics, and enantiodifferentiating capabilities can be predetermined in a truly and distinctly targeted rational approach. Supramolecular interactions can take place effectively, such as the ion–dipole interactions in crown ethers, the CH/ π and π – π interactions in calixarenes, hydrogen bonding and salt formation in macrocyclic amides and amines, and π – π stacking and metal coordination in porphyrins. Additional functional groups on the periphery of the macrocyclic structures offer additional opportunities as the interaction sites and the high level of structural preorganization may generate a high degree of chiral recognition, which could be exploited for the efficient NMR separation of enantiomeric compounds. In particular, major effort is being addressed to the assembling of complex structures

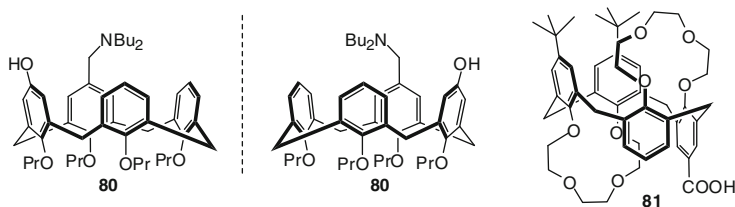


Fig. 29 CSAs based on inherently chiral calixarenes

in which hydrogen bonding interactions target the chiral guests into hydrophobic cavity inside which steric or π - π interactions cooperate for chiral discrimination: the NMR nonequivalence has its roots in the different stereochemical arrangements and thermodynamic stabilities of the two diastereoisomeric solvates. Anisotropic effects generated by aromatic moieties may also give the major contribution to NMR enantiodifferentiation when very weak diastereoisomeric adducts are formed in solution.

In recent years we are witnessing a fervent activity in the field of the development of new calix[*n*]arenes and resorc[4]arenes. These host molecules are relatively easy to synthesize in a wide range of molecular sizes and functional groups and behave as receptors for a variety of guest molecules. Some of them are chiral by virtue of derivatization. Alternatively, enantiomeric differentiation effects can be obtained by exploiting inherently chiral macrocycles.

The inherently chiral calix[4]arene **80** (Fig. 29) [182, 183], which possesses both amino and hydroxyl groups at proximal positions on the wide rim, provides a rigid chiral environment and differentiates efficiently the enantiomers of mandelic acid in CDCl_3 . Even in the presence of a less than stoichiometric amount of host, different chemical shifts of the benzylic proton of (*R*)- and (*S*)-mandelic acid are observed and the nonequivalence does not depend on the molar ratio of CSA/mandelic acid. The addition of more than an equimolar amount of host shows no further change in the chemical shifts of the mandelic acid, thus suggesting the formation of a 1:1 complex.

Inherently chiral calix[4]crown carboxylic acid **81** (Fig. 29) in the 1,2-alternate conformation is able to interact enantioselectively with 2-phenylglycinol and, hence, its use as CSA for NMR spectroscopy is suggested [184].

It is easier to generate chirality by appropriate substitution on the calixarene aromatic rings with suitable chiral pendants as in the case of bis(ethyl lactate) derivative of *p*-*tert*-butylcalix[4]arene (**82**) (Fig. 30), which brings about efficient enantiodifferentiation of simple amino acid derivatives [185].

Enantiodifferentiation mainly depends on the stabilization of its rigid cone conformation, by virtue of the efficient hydrogen-bond network between the lactate moieties and the residual phenolic hydroxyls. The importance of inclusion phenomena is confirmed by the fact that none of the acyclic models **83** or **84** (Fig. 30) are able to produce efficient enantiodifferentiation. The proximity of the lactate stereogenic center to the calixarene rim is important as confirmed by the low

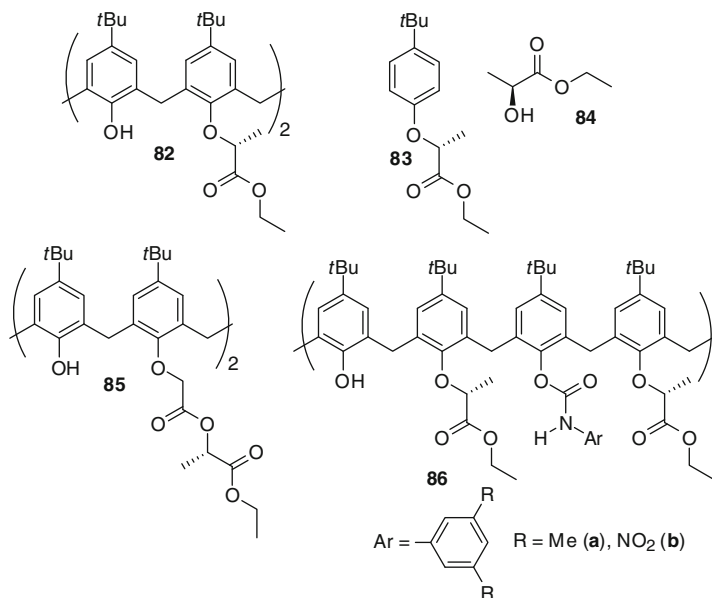


Fig. 30 Lactate derivatives of calix[4]arenes

efficiency of **85** (Fig. 30) with the lactate moiety further away from the calixarene lower rim. It probably does not permit the cooperative processes involved in enantiodifferentiation by **82**. Such a kind of cooperation is not allowed for carbamate derivatives **86a, b** (Fig. 30), in which the interaction with the enantiomeric substrates are addressed at the external surface instead of at the internal cavity, in spite of the fact that the calixarene cone conformation is not perturbed.

Chiral underivatized acids are differentiated by calix[4]arene derivatives **87** (Fig. 31) with appended chiral aminonaphthol moieties at the lower rim [186].

Compared with calixarene grafted with amino acid units **88** (Fig. 31) [187, 188], thiacalix[4]arene **89** (Fig. 31) gives the highest enantioselectivity, probably due to the fact that the cavity of thiacalix[4]arene is larger than it is in classical calix[4]arene, and thiacalixarene derivatives also display remarkably high flexibility in solution [189, 190].

In the field of calix[4]resorcinarene-based CSAs, Wenzel's contribution is noticeable and has led to the development of several efficient water soluble CSAs for the enantiodiscrimination of phenyl-containing chiral compounds. The calix[4]resorcinarene hosts have *L*-proline, hydroxy-*L*-proline, α -methyl-*L*-prolinylmethyl, and *L*-pipercolinic pendants attached on the lower rim and produce baseline separations of the enantiomeric resonances (refer to Wenzel's [191] for a more in-depth description of the enantiodifferentiating properties of above-mentioned macrocycles CSAs) [192–199]. The NMR enantiodifferentiation of aliphatic amines can be enhanced by reacting them with isobenzofuran-1,3-dione, which is commercially available, and naphtho[2,3-*c*]furan-1,3-dione [200].

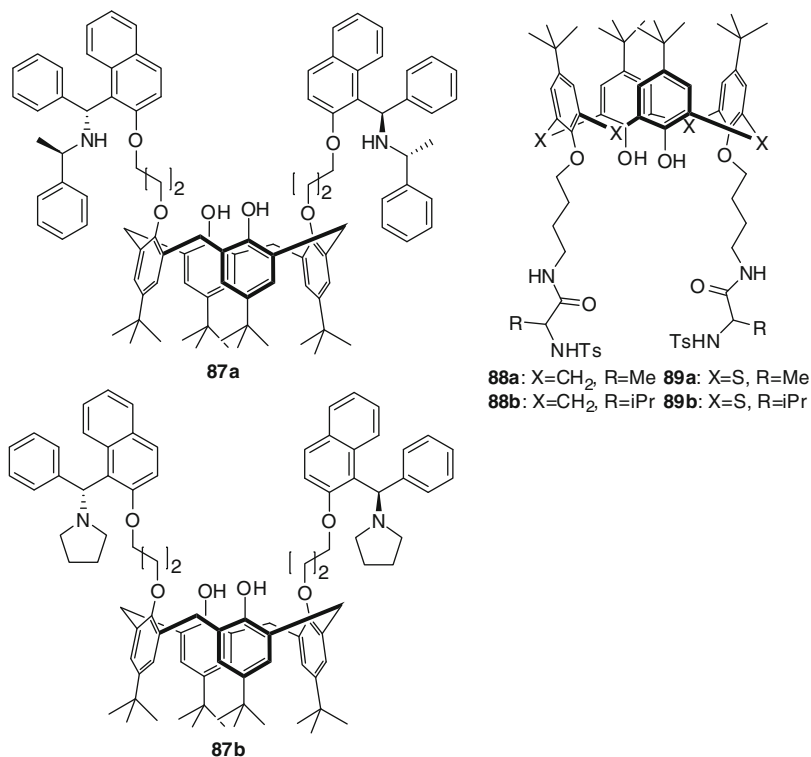


Fig. 31 Calix[4]arenes and thiacalix[4]arenes based CSAs

An effective approach is to introduce chiral pendant groups on the upper rim of the resorc[4]arene by generating new resorcinarene-based cavitands. The elongated cavitand design has potential advantages: amino acids can be bonded to the resorc[4]arene and, as a result, the acidity of the host can be suitably modulated and non-covalent hydrogen bonding and electrostatic interactions with guests maybe suitably addressed.

Modification of the lower rim with long alkyl chains can be additionally exploited, making it possible to absorb the compounds onto a hydrophobic surface for applications in preparative separations or for controlling host solubility. Harrison and coworkers [201] described a detailed structural study of new alanine-containing cavitands **90** (Fig. 32), which were constituted by two major components, the resorc[4]arene scaffold and the quinoxaline panels. The alanine moiety, with the underivatized carboxylic group, is bound to the resorc[4]arene upper rim by exploiting the quinoxaline panel, thus providing stereogenic centers for chiral discrimination and binding sites for chiral primary, secondary, and tertiary amines (Fig. 32). However, different amino acids can be bound to the resorc[4]arene and, as a result, the acidity of the host and design of the stereogenic

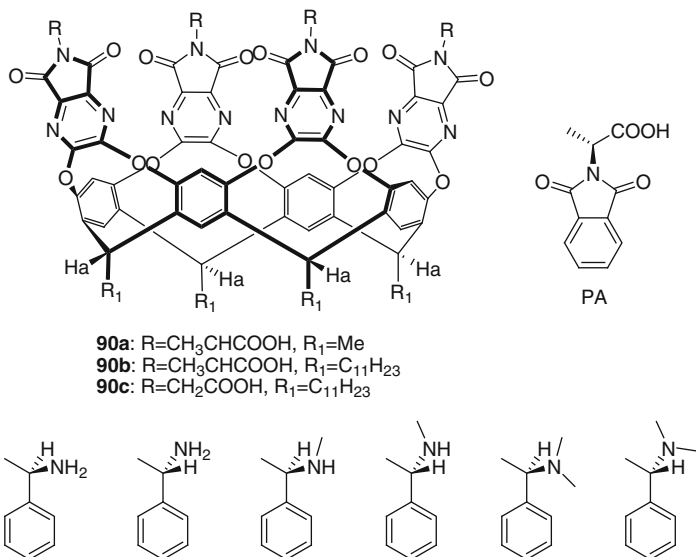


Fig. 32 Resorc[4]arene-based cavitands, model CSA PA and enantiodifferentiated amines

center can be modified depending on the enantiomeric compounds features. The *n*-undecyl chains are incorporated into some of the molecules to increase solubility in non-polar solvents. The conformational preference, which is fundamental for the enantiodifferentiation processes, can be very easily predicted on the basis of the chemical shift of the methine proton (H_a, Fig. 32) on the lower rim bridge. The simultaneous presence of polar and non-polar ends might promote micellar structures. The enantiodifferentiation ability of the chiral cavitands was compared to phthalaldehyde (PA) (Fig. 32), an analog of the cavitand side panel, in NMR titration experiments where the chemical shifts changes of enantiomeric amines are monitored on chiral auxiliaries additions. Cavitands bind amine guests more strongly compared to the monoacid analog PA, and the chemical shift changes also depend on the nature of the apolar head on the lower rim. The titration curves demonstrate that the alanine cavitand with methyl groups at the lower rim (**90a**, Fig. 32) does not differentiate (*R*)- and (*S*)-methyl benzyl amine and binds both enantiomers similarly to achiral glycine derivative **90c** (Fig. 32). Primary and tertiary amines are not enantiodifferentiated by the alanine derivative with *n*-undecyl chains at the lower rim (**90b**, Fig. 32), whereas differentiation of secondary amines is obtained after addition about of 2 equiv. of amine, i.e., in the region of weaker guest binding.

The chiral pocket of the cavitand can also be generated by exploiting the salen framework, which can coordinate to the uranyl dication in uranyl–cavitand–salen systems (**91**, Fig. 33) through the imine nitrogen and the phenolic oxygen atoms. In this way both a Lewis acid uranyl center, which can bind the counter-anion of an ion pair, and the electron-rich cavity able to recognize the corresponding counter-cation,

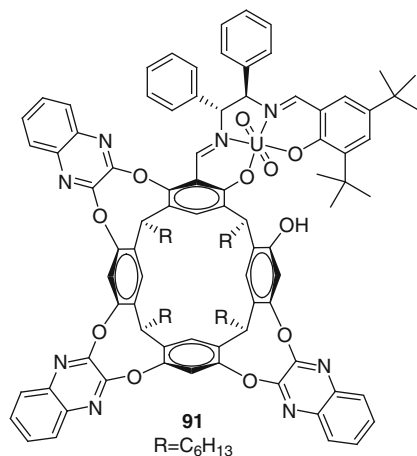


Fig. 33 Uranyl–cavitand–salen CSA

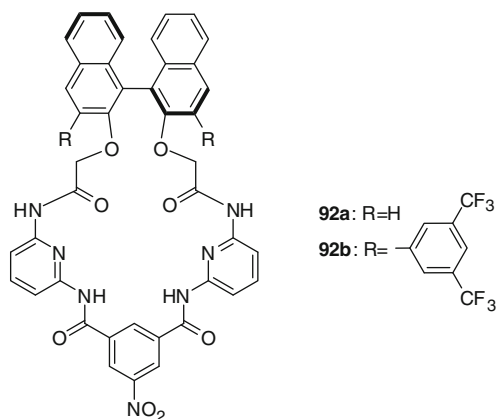


Fig. 34 Selected CSAs

are present [202]. The host has a potential enantiodiscriminating capability towards chiral tetramethylammonium iodides, amino acid methyl esters with the amino group transformed into a tetraalkylammonium iodide, and amino acid derivatives as tetraalkylammonium carboxylates.

Ema et al. developed the bifunctional macrocycle **92a** (Fig. 34), which is effective in the enantiodifferentiation of a variety of chiral compounds with carboxyl, oxazolidinone, lactone, alcohol, sulfoxide, sulfoximine, isocyanate, and epoxide functional groups. *N,N'*-Bis(6-acylamino-2-pyridinyl)isophthalamide was selected as a binding unit, which has both hydrogen-bond donor and acceptor sites [203]. A nitro group was introduced to strengthen the hydrogen bond donor ability of the nearest amide groups and 1,1'-bi(2-naphthol) was selected to generate the macrocyclic cavity as it is an inexpensive chiral unit having a strong anisotropic

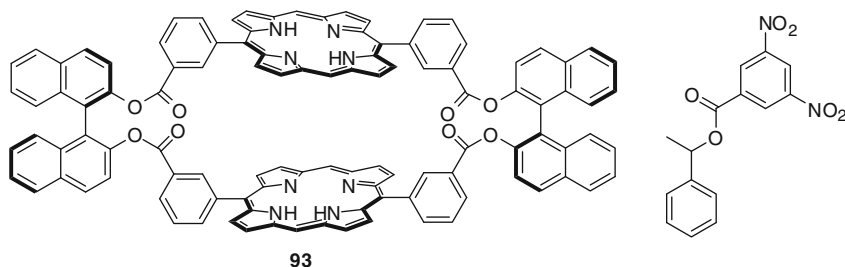


Fig. 35 Diporphyrin receptor **93** and a chiral substrate

ring-current. Relatively large association constants were measured for several enantiomeric guests, hence a very good fit is realized inside the cavity. Sulfoxides are enantiodifferentiated very efficiently with nonequivalence to 0.55 ppm. In one case, the addition of only 5 mol% (69 μg , 0.15 mM) of **92a** resolved the enantiomeric resonances [203, 204]. The principal binding site of **92a** is the hydrogen-bond amide group between the isophthalic moiety and the pyridine moiety, where lactones and sulfoxides are fixed by double hydrogen bonds. The third interaction takes place at the pyridyl nitrogen for carboxylic acids and oxazolidinones. The V-shaped arrangement of the two 2,6-diacylaminopyridine moieties is fundamental for the effective guests binding. The presence of the 3,5-bis(trifluoromethyl)phenyl group as in the host **92b** (Fig. 34) improved enantioselectivity for small molecules such as 2-chloropropionic acid and methyl lactate as evaluated by the binding constants [205]. It is noteworthy that macrocycle **92a** can also be used as a chiral selector in enantioselective HPLC by immobilization to silica gel [206].

Ema et al. designed and synthesized a chiral diporphyrin receptor **93** (Fig. 35) where two porphyrins are connected by means of two binaphthol moieties which position them at a distance suitable for sandwiching aromatic molecules (about 7 Å) [207]. Excellent enantiomeric differentiation of π -acidic chiral compounds is achieved despite the use of only stacking as the driving force of complexation. The association constant values are very small [for examples 4.2 and 1.2 M^{-1} for (*R*)- and (*S*)-enantiomers of the substrate reported in Fig. 35] and hence the percentages of the host–guest complex are less than 10% for both enantiomers at the concentration employed [207].

trans-1,2-Diaminocyclohexane and (1*R*,2*R*)- or (1*S*,2*S*)-1,2-diphenylethylenediamine are the precursors of several macrocyclic chiral auxiliaries, which have found interesting applications as CSAs for NMR.

Chiral A2B2 tetraamidic cyclic receptors have been developed by Gasparri et al. for the preparation of CSPs with efficient performances in the enantio-separation of chiral compounds having a π -acidic moiety [208] and subsequently proposed as efficient CSAs [209] for the enantiodifferentiation of the same classes of compounds. By virtue of their C_2 -symmetry, CSAs **94** and **95** (Fig. 36) have very favorable spectroscopic properties: the sharp few proton resonances of the two chiral auxiliaries leave free wide spectral regions, where the signals of the chiral

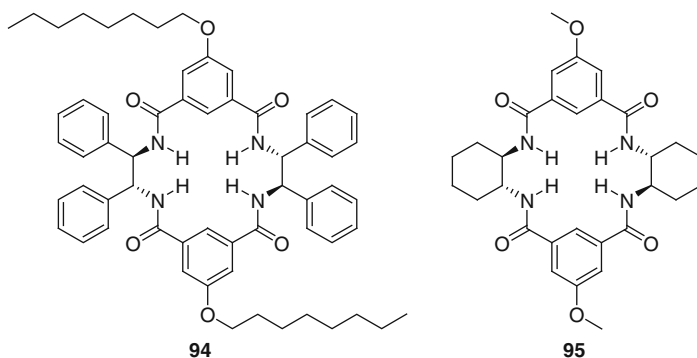


Fig. 36 Tetraamidic cyclic CSAs

compounds to be analyzed can be detected without significant interference. The nonequivalences are also high at very low concentrations (3.6 mM), reducing the amount of the chiral auxiliary needed. The origin of enantiomeric differentiation has been ascertained [210] by a combined computational-spectroscopic approach: the high efficiency of the macrocyclic tetraamidic chiral selector both in solution and chromatographic environments is probably determined by a concomitance of favorable structural features: (1) the presence in **94** of adjacent cooperative π -donor aromatic groups able to sandwich π -acidic moieties of the enantiomeric compounds and (2) the location of groups able to originate attractive intermolecular interactions in the inner part of the molecule, which are at the same time adjacent to the stereogenic centers and hindered by the flanking aryl groups. Thus, the enantiomeric pairs able to establish attractive interactions in this crowded region are strongly differentiated as a consequence of steric repulsive interactions. The extended network of NH and CO groups of the receptors allows substrates endowed with two amide functions to act as bidentate ligands and hence to be efficiently stabilized.

(*R,R*)-1,2-Cyclohexanediamine is the precursor of several chiral macrocyclic amines, such as **96** [211] or **97** and **98** (Fig. 37) [212]. CSAs **96a, b** are useful for the determination of enantiomeric excess and the absolute configuration of a wide range of carboxylic acid and amino acid derivatives. For all the carboxylic acids (Fig. 37) tested, the signals for the protons attached to the stereogenic center were split and baseline separation was enough for accurate integration, with very high nonequivalences (in the range 0.052–0.150 ppm) (Fig. 37) in spite of the use of 0.25 equiv. of CSAs [211].

The chiral peraza-macrocyclic selector **97d** gives good results as CSA for carboxylic acids [213]. The enantiodifferentiation experiments were performed by adding increasing amounts of racemic α -chiral carboxylic acids (PhCHRCOOH) to a solution of **97d** (10 mM in CDCl₃) directly into the NMR tube. The most stable complex of mandelic acid with **97d** involves the interaction of two units of acid and one unit of the macrocycle, even if multiple equilibria coexist in solution. The optimal ratio between **97d** and the racemic acid for a baseline separation

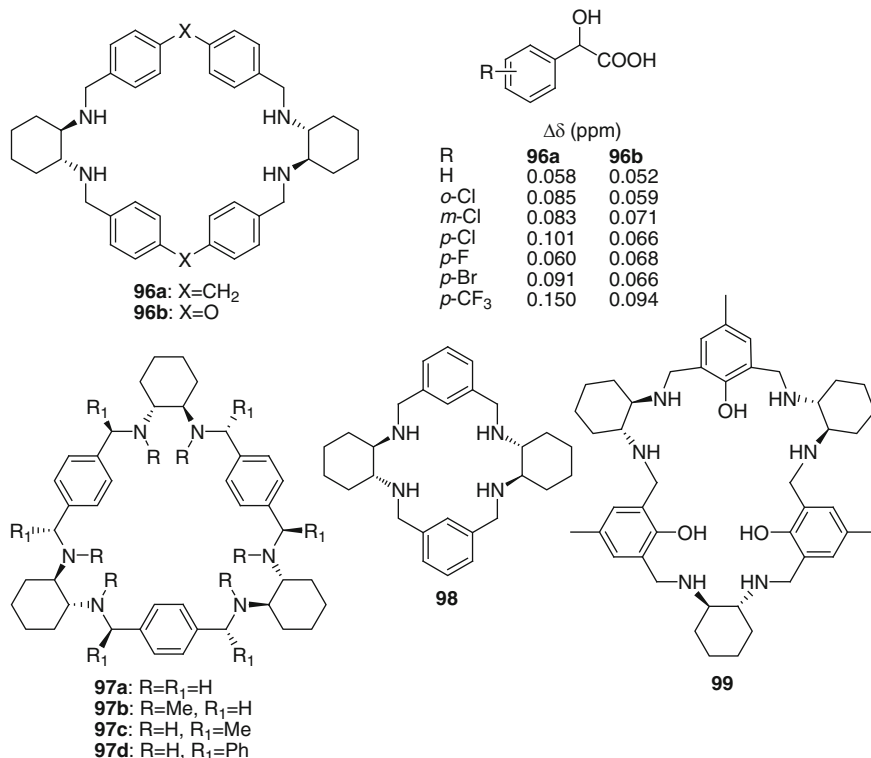


Fig. 37 Macrocyclic amine CSAs and substrates enantiodiscriminated

of the enantiomers signals depends on the type of acid, in particular on its degree of acidity: the stronger the acid, the lower the ratios required; the weaker the acid, the higher the ratios needed. A correlation between the NMR enantiodifferentiation and the host/guest ratio was obtained considering the acidity of the carboxylic acid, as suggested by Zhang et al. [79, 214, 215]. Lower host/guest ratios are required when the strength of the acid increases in order to achieve the optimal separation of corresponding signals of the enantiomers of the acid. Weaker acids (e.g., 2-phenylpropionic acid, R = Me) give partial proton transfer with **97d**, whereas stronger acids (e.g., mandelic acid, R = H) gave complete proton transfer in a non-polar solvent. When further amounts of a strong acid are added to **97d**, multiprotonated species are quantitatively formed and no residual free acid remains in solution, and thus the nonequivalence increases [213]. On increasing the amount of a weak acid with respect to **97d**, the amount of free acid increases, and thus the nonequivalence decreases. Interestingly, the analyte and the CSA are separated and recovered by a simple acid–base extraction and reused without any purification [213].

Tanaka et al. reported that the analogous CSA **97a** devoid of a phenyl group is useful as CSA for secondary alcohols, cyanohydrins, and propargylic alcohols, but

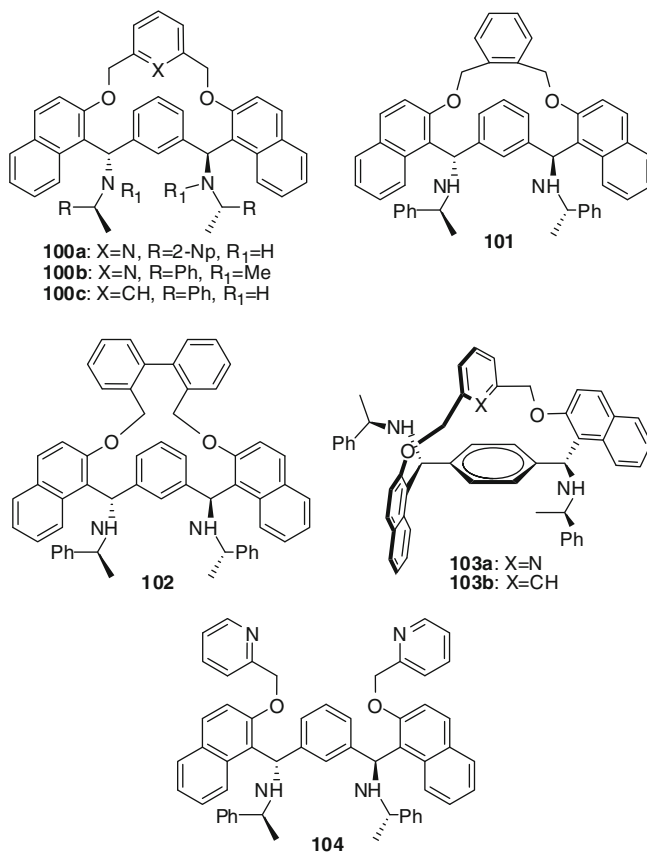


Fig. 38 Selected CSAs

unsuccessful results are obtained with the same receptor in the case of carboxylic acids at 1:1 or 2:1 CSA/substrate ratio [216]. In a recent study, Periasamy et al. has demonstrated that the derivatives **97a, b** and **98** (Fig. 37) are able to act as CSAs for carboxylic acids, but when used in small amounts. Indeed, in consideration of their polytopic nature, such a kind of receptors binds up to three molecules of guest, so that good separation of the resonances are obtained in the presence of 0.17–0.33 equiv. of CSA [212]. Better results for the determination of the enantiomeric purity of carboxylic acids can be obtained by using small amounts (0.25–0.50 equiv.) of the host **99** (Fig. 37) [217], with phenolic hydrogen bond donors groups.

Zhang et al. has designed several macrocyclic hosts **100–104** (Fig. 38) with excellent enantiodifferentiating capabilities towards carboxylic acids, phosphinic, phosphonic, and phosphoric acids [79, 214, 215]. Nonequivalences up to 0.80 ppm are measured in ¹H NMR and/or ³¹P NMR. The author also reports a detailed

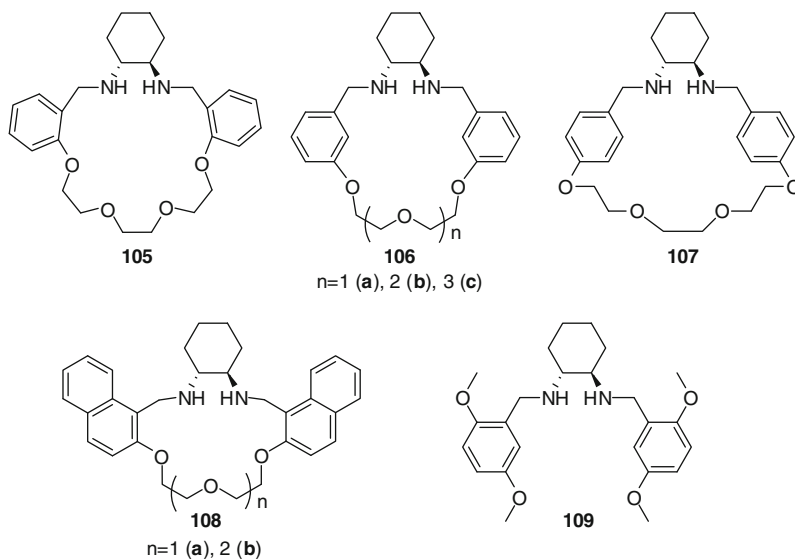


Fig. 39 Aza-crown macrocyclic CSAs and non-macrocyclic control compound **109**

analysis of the factors affecting the NMR enantiodifferentiations: solvent, concentration, CSA to acid molar ratio, temperature.

Folmer-Andersen et al. reported new aza-crown macrocycles **105–109** (Fig. 39), which are effective CSAs for mandelic acid. Each receptor contains a *trans*-1,2-diaminocyclohexane moiety that is joined through *N*-benzyl linkages to a flexible oligoethylene glycol bridge [218]. The 1,2-diaminocyclohexane subunits impart chirality and C_2 symmetry onto the structures. (*R,R*)-**109** (Fig. 39) serves as a non-macrocyclic control compound. Multiple stoichiometry complexes are formed at different CSA/mandelic acid molar ratios, with the 2:1 acid/receptor complex responsible for NMR chiral discrimination. As expected, the stabilization of the diastereoisomeric solvates is mainly due to interactions between the carboxylic acid and amine groups of the substrates and macrocycles, respectively. The abilities of the macrocycles to differentiate the ^1H NMR spectra of the enantiomers of mandelic acid by binding in CDCl_3 was markedly dependent on the nature of the arene group, the arene linkage geometry, and the length of the ethereal bridge.

The *cis*-2-alkyl-3-oxy-tetrahydropyran unit is the basis of macrocyclic chiral auxiliaries **110** (Fig. 40) with C_2 -symmetry, which display high association constants with ammonium salts of α -amino acid methyl esters and very high enantioselectivities [219]. The enantiomeric differentiation is conserved in different solvents or in the presence of different anions. Particularly high enantioselectivity is shown for amino acids that bear aromatic side chains. Tryptophan displays the best chiral discrimination with K_D/K_L up to 30. Interestingly, authors demonstrated that a single $\text{CH}\cdots\pi$ interaction causes 70% of the enantioselectivity

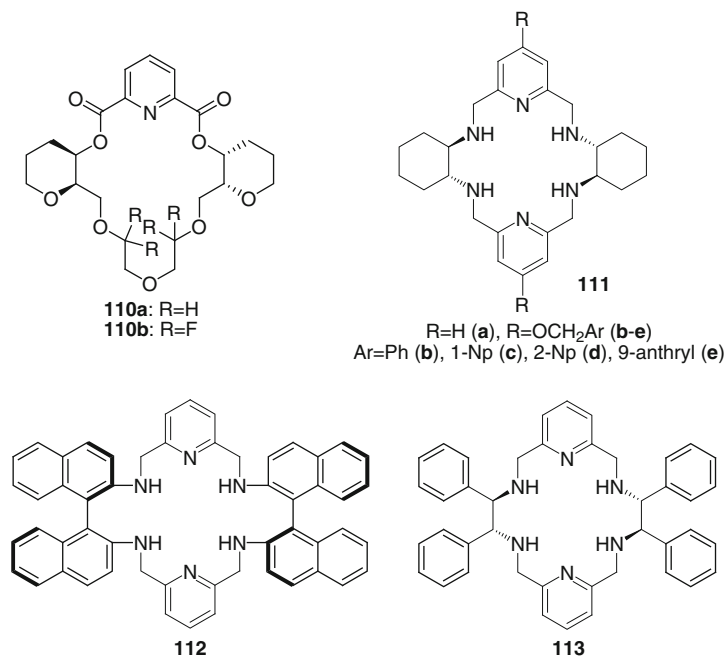


Fig. 40 Selected CSAs

and, hence, weak non-covalent interactions may govern the whole process of enantiodifferentiation.

The condensation of pyridine-based dialdehydes with (1*R*,2*R*)-(–)-1,2-diaminocyclohexane by using the metal template technique gave a family of enantiopure hexaazapyridinophanes **111** (Fig. 40), some of which are substituted at the periphery [220, 221]. The presence of four protonable amino groups would lead to the formation of the corresponding diastereoisomeric salts with chiral carboxylic acids. Besides, the two pyridine moieties could display additional interactions (H-bonding, solvophobic or π - π interactions) and highly anisotropic environments due to the electronic π -cloud of the aromatic rings. Different acid to receptor molar ratios were analyzed. Good splitting of the carboxylic acids NMR signals (up to $\Delta\delta = 0.20$ ppm) were observed using sub-stoichiometric amounts of the receptor (1:4). According to the occurrence of a tetra-protonation process, the 1:4 receptor/acid stoichiometry for both enantiomers of the acid was found.

In the attempt to enhance enantiodifferentiation of bound guest molecules by exerting additional ring current effects, new chiral polyazamacrocyclic hosts **112** and **113** (Fig. 40) containing binaphthyl and phenyl moieties have very recently been proposed [222], the enantiodifferentiating efficiency of which has been probed. However, the enantiodifferentiation is not improved compared to the macrocycles **111** derived from the chiral aliphatic diamine. The likely explanation for this is the reduced basicity of **112** and **113** and the fact that the aromatic

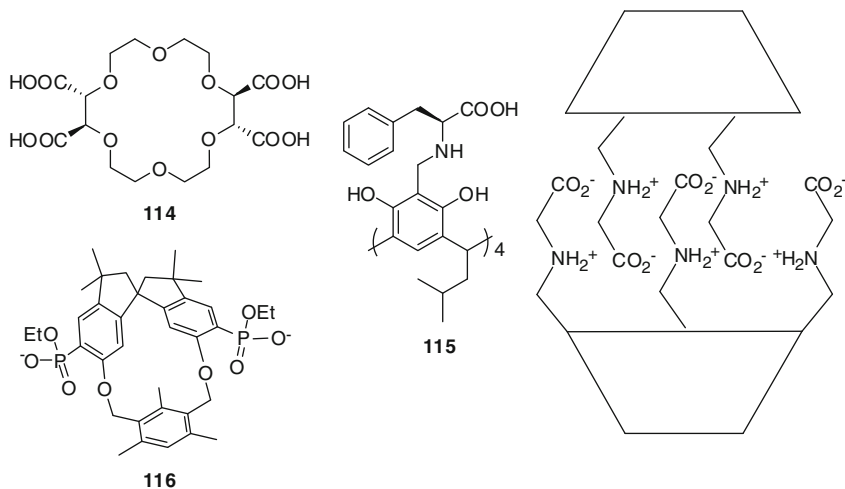


Fig. 41 Selected CSAs

substituents make the formation of protonated cationic forms of these macrocycles less favorable.

Chiral crown ethers are a class of cyclic compounds that are complementary to cyclodextrins, possessing a polar cavity able to include positively charged polar groups, such as ammonium cations. Among them, (+)-(*R*)-18-crown-6-tetracarboxylic acid (**114**) (Fig. 41) represents the most popular CSR for the enantiodifferentiation of amino acids, amines, and amino alcohols [223–234].

Because chiral crown ethers are expensive, the use of achiral crown ether/cyclodextrin mixtures has been proposed as the way of improving the enantio-differentiating ability of the cyclic oligosaccharides towards amines [229]. This last application, primarily applied to capillary electrophoresis uses, has also been investigated by ^1H NMR spectroscopy (see Wenzel's [191]).

Some chiral macrocycles are very interesting from the technological point of view, but they have only limited applications as chiral auxiliaries for NMR, mainly in cases where inclusion processes of the guests involve slow exchange conditions, which are not suited for analytical application. This is the case for chiral capsules, which sequester molecules with suited sizes. As an example the amino acid substituted resorc[4]arene **115** (Fig. 41) quantitatively self-assembles into a dimer, which can be considered as a molecular inverted micelle because it has charged groups inside and hydrophobic groups outside the shell [235]. The capsule easily includes alcohols, carboxylic acids, *N*-protected amino acids, and even inorganic salts of carboxylic acids. Encapsulation in solution requires long equilibration times. Chiral discrimination occurs, but the NMR spectra reveal the co-presence of several slow exchanging species.

Macrocyclic hosts with negative charges arising from phosphonate moieties (such as **116** in Fig. 41) and hydrophobic binding sites in a cyclophane structure

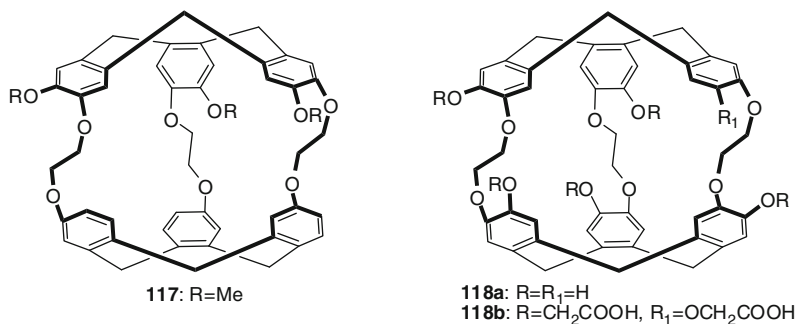


Fig. 42 Cryptophane derivatives CSAs

appear to be very promising for constructing effective artificial receptors for amino alcohols and di-cationic amino acids molecules [236, 237].

Cryptophane derivatives are rigid, hollow organic host compounds which can be designed and synthesized with interior cavities large enough to include organic guest compounds [238]. They have attracted a lot of attention since the beginning of the 1980s and are still of high interest to bind small neutral atoms or molecules. The differentiation of the enantiomers of CHFCIBr and CHFCII molecules by chiral cryptophane-C (**117**) (Fig. 42) [239] and a thiomethylated cryptophane [240] are examples of enantioselective encapsulation processes reported in the past.

The pentahydroxyl cryptophane-A (**118a**) (Fig. 42) is a water soluble cryptophane-A congener which is able to differentiate between the two enantiomers of propylene oxide under basic conditions [241]. The enantiodifferentiation is easily detected in the ¹H NMR spectra as the six protons of the bound oxide are located at negative chemical shift values due to the strong shielding effect of the six aromatic rings surrounding the guest molecule.

The analogous enantiopure hexacarboxylic acid cryptophane-A (**118b**) (Fig. 42) interacts enantioselectively with propylene oxide, epichlorohydrin, and 1,2-epoxybutane, but not 2,3-epoxybutane [242]. In this case, binding of the guests to the cryptophane causes remarkable low-frequencies shifts.

7 Ionic Liquids

“Ionic liquid” (IL) is the commonly accepted term for low-melting salts (mp < 100°C) formed by the combination of organic cations and a variety of anions. Ionic liquids are attracting considerable attention for several technological applications [243]. Their properties are strongly dependent on their physicochemical properties which, in turn, depend on the interaction established between the cation and the anion: ions interact via hydrogen bonding, π - π , dispersive, dipolar, electrostatic, and hydrophobic forces; diffusion-ordered NMR spectroscopy (DOSY-NMR) constitutes the method of choice for investigating their pairing [244].

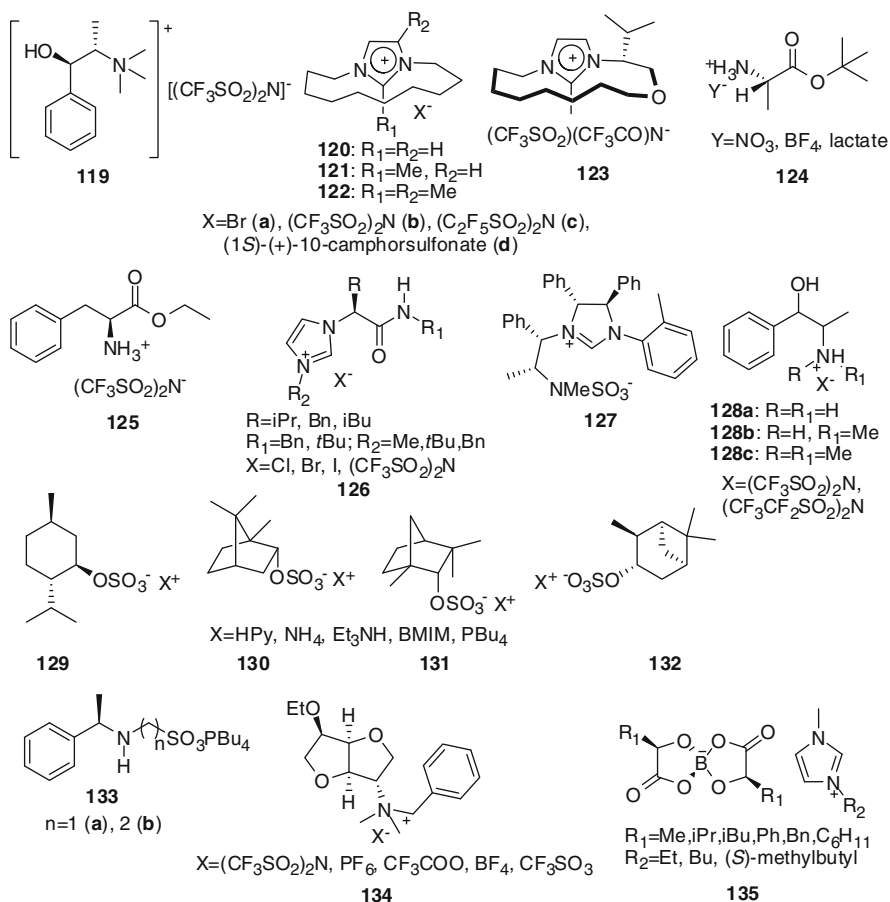


Fig. 43 CILs chiral solvating agents (BMIM = 1-butyl-3-methylimidazolium)

The structural tuneability of ILs is ideal for the design of new chiral auxiliaries for enantioselective applications [245, 246]. Either the cation or the anion, or both, can be chiral and the chirality may be either central, axial, or planar. Chiral ionic liquids (CILs) have recently gained popularity based on their potential applications as CSPs in gas chromatography [247] and as additives for enantiomeric separations in micellar electrokinetic electrochromatography [248] or HPLC [249].

CIL directly derived from the “chirality pool” were reported in 2002 by Wasserscheid et al. [250]. The easy preparation, thermal and chemical stability, and low viscosity were the criteria for the design of CILs and, among them, IL **119** (Fig. 43), which is readily obtained from the alkaloid ephedrine in a three step synthesis, was able to split the ^{19}F NMR signal of the CF_3 -group of racemic Mosher’s acid sodium salt [250]. The magnitude of nonequivalence was affected not only by the total concentration and substrate/CSA molar ratio, but also,

interestingly, by the amount of water added to the solvent (CD_2Cl_2). In the same year, imidazolium salts with cyclophane-type planar chirality **120–122** (Fig. 43) were proposed by Saigo and coworkers [251]. The ability of the cyclophane-type ionic liquids to participate in chiral recognition processes was demonstrated by ^1H NMR analysis of the diastereoisomeric adduct formed by the racemic cation and (1*S*)-(+)-10-camphorsulfonate anion, which caused doubling of selected resonances of the CIL cation [251]. The single stereoisomers of the chiral cationic CIL **123** (Fig. 43) enabled the differentiation of racemic or enantiomerically enriched potassium salt of racemic α -methoxy- α -(trifluoromethyl)phenylacetic acid in the presence of 18-crown-6 in CDCl_3 and also recognized the P-chirality of *O*-ethyl phenylphosphonothioate anion by ^{31}P NMR spectroscopy [252].

The development of CILs based on biocompatible and non-toxic materials, such as amino acids, is strongly encouraged. Differentiation of fluorine signals of Mosher's salt was obtained by using CILs derived from L- and D-alanine *tert*-butyl ester chloride with a variety of counterions such as lithium bis(trifluoromethane) sulfonimide, silver nitrate, silver lactate, and silver tetrafluoroborate (**124**, Fig. 43) [253].

A new fluorescent CIL, L-phenylalanine ethyl ester bis(trifluoromethane) sulfonimide **125** (Fig. 43), capable of serving simultaneously as solvent, chiral selector, and fluorescent reporter in chiral analytical measurements, was proposed by Warner and coworkers [254]. In the presence of 10 equiv. of **125** the ^{19}F resonances of the enantiomers of Mosher's sodium salt are doubled by 0.04 ppm in a solvent mixture of CD_2Cl_2 and DMSO, suggesting that **125** has good potentialities as a CSA for NMR spectroscopy.

Amino acids can be used as starting materials for introducing chirality in imidazolium CILs [255, 256]. The enantiodifferentiating ability of **126** (Fig. 43) was evaluated and compared by using racemic triethylamine mandelate salt as probe compound [255]. One to two equivalents of CIL are needed to detect NMR differentiation (about 0.02 ppm) for the methyl protons of mandelate. CILs derived from L-phenylalanine, L-valine, and L-leucine with benzyl amide groups constitute the best CSAs; when aromatic moieties are not present in the amide functionality of the chiral auxiliaries, any NMR nonequivalence cannot be detected [255].

N-Heterocyclic-based zwitterions incorporating imidazolium and alkyl-sulfonate or sulfamate groups (such as **127** in Fig. 43) proved to be versatile CSAs for Mosher's acid, alcohols, cyanohydrins, amino alcohols, nitro alcohols, thiols, and carboxylic acids with very high shifts in the ^1H and ^{19}F NMR [257].

A series of novel structurally related protic CILs derived from enantiopure norephedrine, ephedrine, and methylephedrine with protonated primary, secondary, and tertiary amines (**128**, Fig. 43) have been obtained and evaluated as CSAs for the ^{19}F NMR enantiomer differentiation of potassium Mosher's salt in comparison to the precursors of CILs [258]. The solubility of potassium Mosher's salt in CDCl_3 is enhanced by forming a complex between potassium cation and a crown ether. Both the precursors and their CILs derivatives are able to differentiate the fluorine resonances of Mosher's salt, with a threefold increase of the nonequivalence in the presence of the ionic liquid. However, the magnitudes of nonequivalences are

small (less than 0.05 ppm) in spite of the high mixture concentration and the presence of a relevant excess of the CILs. The primary amine shows the best enantiodifferentiating efficiency.

Sulfate and sulfonate CILs were prepared from alcohols (**129–132**, Fig. 43) and (*R*)-phenylethylamine (**133**, Fig. 43), respectively, and used as CSRs for 2,2,2-trifluoro-1-phenylethanol and Mosher's carboxylic acid [259]. The choice of the solvent is critical for the success of the enantiodifferentiation experiments: CILs show the best solubility in CDCl_3 , but toluene, where the chiral auxiliaries have poor solubilities, interferes to a less extent in the interaction with the enantiomeric compounds, giving nonequivalences to about 0.02 and 0.11 ppm for 2,2,2-trifluoro-1-phenylethanol and Mosher's carboxylic acid, respectively.

Carbohydrate-based chiral ammonium ionic liquids (**134**, Fig. 43) were obtained by using isomannide as a bio-renewable substrate. The diastereoisomeric interactions of these chiral ammonium ionic liquids with racemic Mosher's acid were studied using NMR and suggested their potential applications in enantiomeric differentiation [260]. Mosher's carboxylate is the counterion of the ionic liquid, but the presence of achiral anion is advantageous for enhancing NMR nonequivalences.

Structurally novel CILs which have either chiral cation, chiral anion, or both have been proposed [261]. Cations are an imidazolium group, while anions are based on the borate ion and chiral substituents (**135**, Fig. 43). The synthesis in enantiomerically pure form of the stereoisomers involves a simple one-step process from commercially available reagents. The CILs in this series are liquid at room temperature and have relatively high thermal stability. NMR experiments demonstrated that CILs exhibit intramolecular as well as intermolecular enantiomeric recognition. For a CIL composing with a chiral anion and a racemic cation, enantiomeric recognition of the chiral anion toward both enantiomers of the cation leads to differentiation of the NMR resonances of the cation enantiomers, which strongly depends on solvent dielectric constant, concentration, and structure of the ILs. Enhancing the steric hindrance, high concentrations of CIL, and solvents with low dielectric constants all are factors favoring enantiodifferentiation.

Combinatorial chemistry permits systematic exploration of the influence of structural variations in candidates by accelerating the rates at which they are created and evaluated. Using a combinatorial approach, a library of 27 novel CIL-modified silanes were synthesized [262]. Three chiral tertiary amines, Pro, Eph, and Peu (Fig. 44) were used as building blocks to synthesize chiral cations by use of quaternization reactions. These three chiral tertiary amines consist of different functional groups including hydroxyl, phenyl, pyridyl, urea, and ester groups, which are conducive to multiple-site interactions essential for chiral recognition of analytes. ^{19}F NMR was used as a high-throughput screening tool to identify quickly and conveniently the best chiral selectors from a group of CIL-modified silanes which were synthesized using a combinatorial approach. Three major parameters (type of chiral cations, anions, and linker chain lengths) were included and investigated during the synthesis and screening. As expected, the structure of the chiral cation was found to play an important role in determining enantiodifferentiation abilities. In addition, several types of intermolecular interactions

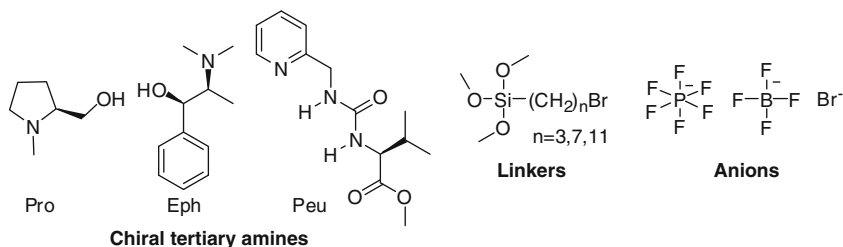


Fig. 44 CILs: combinatorial approach

including ion-pair, hydrogen bonding, π - π stacking, dipole stacking, and steric interactions were found to impact enantiodifferentiation.

8 Special Applications

8.1 Pattern Recognition Approach and 2D F1 Decoupled COSY Experiments

To minimize the amount of chiral auxiliary to be used in the determination of the enantiomeric excesses is a current focus: the measurements are more convenient from the economic point of view and NMR signals of the CSA generate less interference with the signals of the enantiomeric compounds. Unfortunately, unlike what is observed with paramagnetic chiral auxiliaries, the magnitude of NMR differentiation produced by diamagnetic CSAs may be quite small. This makes it necessary to operate in concentrated solutions and, in the majority of cases, in the presence at least of 1 equiv. of CSA. The pattern recognition approach is a good alternative of undoubted interest, particularly in view of eventual applications in the area of the analysis of chiral metabolites. It was first proposed by Anslyn and coworkers [263] and then extended to the NMR analysis of biologically relevant chiral compounds [264] just applied to the enantiodifferentiation of Boc-protected alanine. Spectra of mixtures containing a catalytic amount of quinine (**52**, Fig. 18) (16:84, quinine to chiral substrate) and the amino acid derivative with different enantiomeric excesses were recorded. Under this condition a true chemical shift differentiation of the NMR signals of the two enantiomers cannot be detected, but the signals of selected spectral regions are a fingerprint of the enantiomeric excesses. A reliable analytical protocol can be obtained by using principal component analysis (PCA). The influence of the presence of impurities on the method reliability was also investigated.

Multiplets belonging to (*R*)- and (*S*)-enantiomers, which overlap severely at low solute/chiral auxiliary concentrations, can be resolved by eliminating ^1H - ^1H coupling interactions in the indirect dimension of a decoupled ^1H - ^1H COSY experiment. In this way, multiplets collapse into singlets in the incremented dimension of a 2D spectrum

and quantitative determinations can be performed by determining the contour volumes of the peaks. The decoupled ^1H - ^1H COSY experiment was firstly reported for enantiomeric purities determinations of enantiomers aligned in organic chiral liquid crystal [265] and more recently the method has been applied to CLSRs and CSAs [266].

8.2 *Coupling of CSAs and Achiral Lanthanide Shift Reagents*

Much literature has been addressed to the attractive strategy of enhancing the NMR enantioresolution power of CSAs by combining them with achiral lanthanides, as first suggested by Pirkle and Sikkenga [267] and extensively developed by Wenzel [17, 18, 22]: provided the CSA shows different association constants with the two enantiomers and the lanthanide preferentially binds the substrate but not the CSA, the enantiomer which is less strongly bound to the CSA and, hence, is the one in excess in solution as a free species, will be bound preferentially to the lanthanide and will show enhanced shift.

8.3 *Chiral Sensing*

An intriguing and challenging issue is the analysis of the enantiomeric excesses by using non-CSAs. Such an approach requires non-chiral receptors, such as porphyrins, which are responsive to the enantiomeric excess of the chiral substrates to be analyzed [268, 269]. Chiral sensing is due to the fast exchange of analyte molecules at a protonated *meso*-substituted porphyrin di-cation rather than to the formation of diastereoisomeric complexes with a chiral solvating reagent. In CDCl_3 solutions of tetraphenylporphine (**136a**) (Fig. 45) with (*R*)-2-phenoxypropionic acid at -32.5°C the resonances of the *ortho*-phenyl protons and pyrrole protons are split into two sets of symmetrical signals [269]. The separation of the respective signals depends on the enantiomeric excess of the chiral carboxylic acid with high values (about 0.2 ppm) in the presence of the pure enantiomer. The magnitude of the signals separation is linearly correlated to the enantiomeric excesses of the chiral substrate. A linear relationship between the signals splittings and ee has also been found in solutions of ibuprofen and *meso*-tetra(*tert*-butyl)porphine (**136b**) (Fig. 45), which has increased basicity over **136a**. The main inconveniences of non-chiral-chiral sensing systems are that a calibration curve must be built and low-temperature measurements are required. The advantages overcome these problems due to the fact that porphine macrocycles are available in large quantities and the accuracy of ee determinations increases approaching the enantiopure state, in contrast to the accuracy trend of traditional CSAs [269].

Some higher fullerenes, having dissymmetrically curved π -electronic surfaces, are chiral. However, sensing of the dissymmetric structures of these carbon clusters

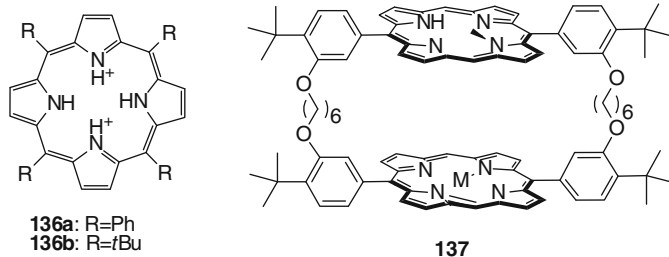


Fig. 45 Chiral sensing receptors

is a challenging issue in chiral chemistry, because they do not possess suitable functionalities needed for the interaction with common CSAs. Cyclic host molecules, having a chiral *N*-methylporphyrin unit (**137**, Fig. 45), include C₇₆ in their asymmetrically distorted π -electronic cavity and differentiate the enantiomers of C₇₆ as shown by ¹H NMR [270, 271]. Encapsulation of fullerene into the porphyrin cavity brings about a strong conformational prevalence of the host and the enantiomers of the cyclic host can be used for the accurate determination of the enantiodifferentiation of C₇₆ as the splitting of the NH signals of the porphyrin is entirely dependent on the enantiomeric purities of guest C₇₆ [270, 271].

8.4 Chiral Metabolites and Drug Formulations

Among the chiral auxiliaries for NMR spectroscopy, CSAs have gained increasing popularity over time, especially for the analysis of compounds of biological and pharmaceutical relevance. They do not suffer kinetic resolution problems, as with CDAs, which may adversely affect the quantitative analysis. No discrepancies between diastereoisomeric and enantiomeric ratios exist. All these issues are critical when the demanding requirements of the regulatory agencies have to be met, as clearly addressed by several authors [272–274].

The CLSRs do not suffer from the same drawbacks, but the considerable shift induced by them in the resonances of enantiomers render them not always reproducible and even difficult for identification of the corresponding resonances of the two enantiomers, especially in complex matrices like pharmaceutical formulations or biological fluids. In addition, the line broadening caused by the paramagnetic metal center could lead to less accurate quantitative determinations.

As an example, in a recent paper, (*R*)-(–)- α -methoxyphenylacetic acid, (*S*)-(–)-1,1'-(2-naphthol), and (*R*)-(+)- α -methoxy- α -trifluoromethylphenylacetic acid have been evaluated as CSRs for ¹H NMR spectroscopic differentiation of the (*R*)- and (*S*)-enantiomers of 2-(diphenylmethanesulfinyl)acetamide (modafinil, MDL) in bulk drugs and formulations in CDCl₃ solutions [275]. MDL is a drug potentially useful to treat narcolepsy, obstructive sleep apnea/hypopnea syndrome, and shift work sleep disorders. The methine signal of the MDL appears as sharp singlet and

did not overlap with CSAs or excipients resonances. The quantitative analysis was validated with respect to specificity, linearity, recovery, limit of detectability, and limit of quantification and then extended to the direct analysis of tablets, without any prior separation of the excipients which remained mainly undissolved in CDCl_3 .

An even more challenging target, which has been pursued in recent years, is to perform the direct analysis of chiral metabolites which are present in intact biological fluids with non-invasive techniques. The determination of chiral metabolites produced in the post-administration stages of drugs or due to the occurrence of external stimuli has become a subject of considerable impact and growing interest both for diagnosis of specific pathologies and for the optimization of therapeutic approaches. NMR spectroscopy is the technique of choice in this area, as the analysis of samples does not require any pre-treatment, apart from the addition of a small aliquot of deuterated water for locking and shimming which, however, may be avoided by using a coaxial tube containing such a component, and the presence of an appropriate chiral auxiliary is needed, which must be well soluble in the aqueous medium characteristic of the system under consideration. The direct use of chiral auxiliaries within biological fluids is limited, unfortunately, by the remarkable spectral complexity of the samples and by the need to guarantee good reproducibility of the data. The different metabolic profile may, in fact, generate different responses to the addition of the chiral auxiliaries. It may be difficult to control the molar ratio between the chiral metabolites and the chiral auxiliary, since the amount of metabolite cannot be exactly predetermined. In addition, competition with other metabolites for the interaction with the chiral auxiliary may occur and, therefore, the extent of differentiation of the enantiomeric components may also be different depending on the sample under investigation. All these issues have been carefully taken into consideration in a recently published work [142] dealing with the direct ^1H NMR enantiodifferentiation in urine of ibuprofen, and one of its major metabolites, the glucuronidated carboxylate derivative (2-[4-(2-carboxy-2-methylpropyl)phenyl]propionic acid), after the direct addition of the CSA. β -Cyclodextrin was selected as water soluble CSA and its enantio-recognition ability of ibuprofen enantiomers has been already demonstrated [276]. A standardization procedure is reported, where racemic ibuprofen was titrated with β -CD in D_2O . Nonequivalence was achieved for several ibuprofen protons with maximum values in the presence of 10 equiv. of the β -cyclodextrin. Each set of resonances was assigned to the corresponding ibuprofen enantiomer by spiking the mixture with pure (*S*)-ibuprofen. In order to establish the effect of the multicomponent matrix of the urine samples on the enantiodifferentiating ability of the CSA, racemic ibuprofen was added to urine samples and, by choosing ibuprofen concentration in the same order of magnitude as endogenous metabolites, the effect of β -CD addition was then assessed. Only slight differences were found regarding the nonequivalence values and the relative positions of the enantiomeric resonances remained unchanged. Then urine samples were collected from human volunteers after the intake of racemic ibuprofen. No ibuprofen was detected, whereas its glucuronidated metabolites were identified.

9 Conclusions

The enormous perspectives of CSAs as effective tools for the direct, accurate, and reliable determinations of enantiomeric purities are fully confirmed by the fervent activities which are specifically dedicated to this research area. The development of low-medium molecular weight CSAs seems to be oriented to the enhancement of the enantiodifferentiating versatility and efficiency of already existing CSAs by means of suitable structural modifications, whereas macrocyclic CSAs seem to have better enantioselectivity, rendering them more suited for biological applications. Cyclodextrins and macrocyclic chiral selectors which are soluble in the aqueous medium deserve special comment in view of their enormous potentialities in the field of the analysis of chiral metabolites directly into the biological fluids, in such a way as to avoid more invasive analytical methods.

References

1. Raban M, Mislow K (1965) Determination of optical purity by nuclear magnetic resonance spectroscopy. *Tetrahedron Lett* 6:4249–4253
2. Pirkle WH (1966) The nonequivalence of physical properties of enantiomers in optically active solvents. Differences in nuclear magnetic resonance spectra. I. *J Am Chem Soc* 88:1837
3. Raban M, Mislow K (1967) Modern methods for the determination of optical purity. *Top Stereochem* 2:199–230
4. Dale JA, Mosher HS (1968) Nuclear magnetic resonance nonequivalence of diastereoisomeric esters of α -substituted phenylacetic acids for the determination of stereochemical purity. *J Am Chem Soc* 90:3732–3738
5. Campbell J (1972) Determination of optical and enantiomeric purity by nuclear magnetic resonance spectroscopy (NMR). *Aldrichimica Acta* 5:29–32
6. Sullivan GR (1978) Chiral lanthanide shift reagents. *Top Stereochem* 10:287–329
7. Pirkle WH, Hoover DJ (1982) NMR chiral solvating agents. *Top Stereochem* 13:263–331
8. Yamaguchi S (1983) Nuclear magnetic resonance analysis using chiral derivatives. In: Morrison JD (ed) *Asymmetric synthesis*, vol 1. Academic, New York, pp 125–152
9. Fraser RR (1983) Nuclear magnetic resonance analysis using chiral shift reagents. In: Morrison JD (ed) *Asymmetric synthesis*, vol 1. Academic, New York, pp 173–196
10. Weisman GR (1983) Nuclear magnetic resonance analysis using chiral solvating agents. In: Morrison JD (ed) *Asymmetric synthesis*, vol 1. Academic, New York, pp 153–171
11. Schurig V (1985) Current methods for determination of enantiomeric compositions. Part 2. NMR spectroscopy with chiral lanthanide shift reagents. *Kontakte (Darmstadt)* 22–36
12. Aboul-Enein HY (1988) NMR methods for optical purity determination of pharmaceuticals. *Anal Lett* 21:2155–2163
13. Parker D (1991) NMR determination of enantiomeric purity. *Chem Rev* 91:1441–1457
14. Casy AF (1983) Chiral discrimination by NMR spectroscopy. *Trends Anal Chem* 12:185–189
15. Hulst R, Kellogg RM, Feringa BL (1995) New methodologies for enantiomeric excess (ee) determination based on phosphorus NMR. *Rec Trav Chim Pays Bas* 114:115–138
16. Rothchild R (2000) NMR methods for determination of enantiomeric excess. *Enantiomer* 5:457–471
17. Wenzel TJ (2007) *Discrimination of chiral compounds using NMR spectroscopy*. Wiley, New York

18. Wenzel TJ, Wilcox JD (2003) Chiral reagents for the determination of enantiomeric excess and absolute configuration using NMR spectroscopy. *Chirality* 15:256–270
19. Uccello-Barretta G, Balzano F, Salvadori P (2006) Enantiodiscrimination by NMR spectroscopy. *Curr Pharm Des* 12:4023–4045
20. Kumar AP, Jin D, Lee Y-I (2009) Recent development on spectroscopic methods for chiral analysis of enantiomeric compounds. *Appl Spectrosc Rev* 44:267–316
21. Yip Y, Wong S, Choi S (2011) Assessment of the chemical and enantiomeric purity of organic reference materials. *Trends Anal Chem* 30:628–640
22. Wenzel TJ, Chisholm CD (2011) Using NMR spectroscopic methods to determine enantiomeric purity and assign absolute stereochemistry. *Prog Nucl Magn Reson Spectrosc* 59:1–63
23. Brevard C (1983) *The multinuclear approach to NMR spectroscopy*. Reidel Publishing Company, Boston, pp 1–27
24. Klika KD (2009) Use of sub-stoichiometric amounts of chiral auxiliaries for enantiodifferentiation by NMR; caveats and potential utility. *Tetrahedron Asymmetry* 20:1099–1102
25. Pirkle WH, Sikkenga DL (1977) The use of chiral solvating agent for nuclear magnetic resonance determination of enantiomeric purity and absolute configuration of lactones. Consequences of three-point interactions. *J Org Chem* 42:1370–1374
26. Pirkle WH, Rinaldi PL (1977) Nuclear magnetic resonance determination of enantiomeric compositions of oxaziridines using chiral solvating agents. *J Org Chem* 42:3217–3219
27. Isiklan M, Asmafiliz N, Ozalp EE, Iler EE, Kilic Z, Cosut B, Yesilot S, Kilic A, Ozturk A, Hokelek T, Koc Bilir LY, Acik L, Akyuz E (2010) Phosphorus–nitrogen compounds. 21. Syntheses, structural investigations, biological activities, and DNA interactions of new N/O spirocyclic phosphazene derivatives. The NMR behaviors of chiral phosphazenes with stereogenic centers upon the addition of chiral solvating agents. *Inorg Chem* 49:7057–7071
28. Cosut B, Ibisoglu H, Kilic A, Yesilot S (2009) Synthesis and enantiomeric analysis of cyclotriphosphazene derivatives with one center of chirality. *Inorg Chim Acta* 362:4931–4936
29. Coles SJ, Davies DB, Eaton RJ, Hursthouse MB, Kilic A, Shaw RA, Uslu A (2006) The structural and stereogenic properties of pentaerythritoxy-bridged cyclotriphosphazene derivatives: spiro–spiro, spiro–ansa and ansa–ansa isomers. *Dalton Trans* 1302–1312
30. Lao KYY, Hodgson DJ, Dawson B, Buist PH (2005) A micromethod for the stereochemical analysis of fatty acid desaturase-mediated sulfoxidation reactions. *Bioorg Med Chem Lett* 15:2799–2802
31. Tremblay AE, Tan N, Whittle E, Hodgson DJ, Dawson B, Buist PH, Shanklin J (2010) Stereochemistry of 10-sulfoxidation catalyzed by a soluble Δ^9 desaturase. *Org Biomol Chem* 8:1322–1328
32. Tremblay AE, Lao KYY, Hodgson DJ, Dawson B, Buist PH (2009) Synthesis of chiral fluorine-tagged reference standards for the ^{19}F NMR-based stereochemical analysis of sulfoxides at trace analytical levels. *Bioorg Med Chem Lett* 19:5146–5150
33. De Moragas M, Cervello E, Port A, Jaime C, Virgili A, Ancian B (1998) Behavior of the 9-anthryl-*tert*-butylcarbinol as a chiral solvating agent. Study of diastereochemical association by intermolecular NOE and molecular dynamics calculations. *J Org Chem* 63:8689–8695
34. Gil J, Virgili A (1999) The first chiral solvating agent (CSA) without ^1H NMR signals: the perdeuterio-2,2,2-trifluoro-1-(9-anthryl)ethanol. Preparation and chiral induction on protonated Pirkle alcohol. *J Org Chem* 64:7274–7276
35. Perez-Trujillo M, Virgili A, Molins E (2004) Preparation, conformational analysis and behavior as chiral solvating agents of 9-anthrylpentafluorophenylmethanol enantiomers: study of the diastereomeric association. *Tetrahedron Asymmetry* 15:1615–1621
36. Sanchez-Aris M, Estivill C, Virgili A (2003) Synthesis and structural study of the enantiomers of α , α' -bis(trifluoromethyl)-10,10'-(9,9'-bianthryl)dimethanol as a chiral solvating agent. *Tetrahedron Asymmetry* 14:3129–3135

37. Munoz A, Virgili A (2002) Preparation and behavior of (*R*)- and (*S*)-2,2,2-trifluoro-1-(1-pyrenyl)ethanol as chiral solvating agents: study of the diastereomeric association by Job's plots, intermolecular NOE and binding constants. *Tetrahedron Asymmetry* 13: 1529–1534
38. Benson SC, Cai P, Colon M, Haiza MA, Tokles M, Snyder JK (1988) Use of carboxylic acids as chiral solvating agents for the determination of optical purity of chiral amines by NMR spectroscopy. *J Org Chem* 53:5335–5341
39. Buist PH, Marecak D (1995) (*S*)- α -Methoxyphenyl acetic acid: a new NMR chiral shift reagent for the stereochemical analysis of sulfoxides. *Tetrahedron Asymmetry* 6:7–10
40. Haiza MA, Sanyal A, Snyder JK (1997) *O*-Nitromandelic acid: a chiral solvating agent for the NMR determination of chiral diamine enantiomeric purity. *Chirality* 9:556–562
41. Cavalluzzi MM, Bruno C, Lentini G, Lovece A, Catalano A, Carocci A, Franchini C (2009) One-step synthesis of homochiral *O*-aryl and *O*-heteroaryl mandelic acids and their use as efficient ^1H NMR chiral solvating agents. *Tetrahedron Asymmetry* 20:1984–1991
42. Fauconnot L, Nugier-Chauvin C, Noiret N, Patin H (1997) Enantiomeric excess determination of some chiral sulfoxides by NMR: use of (*S*)-ibuprofen and (*S*)-naproxen as shift reagents. *Tetrahedron Lett* 38:7875–7878
43. Demchuk OM, Swierczynska W, Michal Pietrusiewicz K, Woznica M, Wojcik D, Frelek J (2008) A convenient application of the NMR and CD methodologies for the determination of enantiomeric ratio and absolute configuration of chiral atropisomeric phosphine oxides. *Tetrahedron Asymmetry* 19:2339–2345
44. Chinchilla R, Foubelo F, Najera C, Yus M (1995) (*R*)-*O*-Aryllactic acids: convenient chiral solvating agents for direct ^1H NMR determination of the enantiomeric composition of amines and aminoalcohols. *Tetrahedron Asymmetry* 6:1877–1880
45. Faigl F, Thurner A, Tarkanyi G, Kovari J, Mordini A (2002) Resolution and enantioselective rearrangements of amino group-containing oxiranyl ethers. *Tetrahedron Asymmetry* 13: 59–68
46. Przybyl AK, Kubicki M (2011) Simple and highly efficient preparation and characterization of (–)-lupanine and (+)-sparteine. *Tetrahedron* 67:7787–7793
47. Michalik M, Doebler C (1990) Determination of the chiral purity of amino alcohols by proton NMR spectroscopy. *Tetrahedron* 46:7739–7744
48. Iuliano A, Bartalucci D, Uccello-Barretta G, Balzano F, Salvadori P (2001) 3,5-Dinitrobenzoylphenylglycine analogues bearing the 1,1'-binaphthalene moiety – synthesis, conformational study, and application as chiral solvating agents. *Eur J Org Chem* 2177–2184
49. Ardej-Jakubisiak M, Kawecki R (2008) NMR method for determination of enantiomeric purity of sulfonimines. *Tetrahedron Asymmetry* 19:2645–2647
50. Salsbury JS, Isbester PK (2005) Quantitative ^1H NMR method for the routine spectroscopic determination of enantiomeric purity of active pharmaceutical ingredients fenfluramine, sertraline, and paroxetine. *Magn Reson Chem* 43:910–917
51. Redondo J, Capdevila A, Latorre I (2010) Use of (*S*)-BINOL as NMR chiral solvating agent for the enantiodiscrimination of omeprazole and its analogs. *Chirality* 22:472–478
52. Klika KD, Budovska M, Kutschy P (2010) Enantiodifferentiation of phytoalexin spiobrossinin derivatives using the chiral solvating agent (*R*)-(+)-1,1'-bi-2-naphthol in conjunction with molecular modeling. *Tetrahedron Asymmetry* 21:647–658
53. Toda F, Mori K, Okada J, Node M, Itoh A, Oomine K, Fuji K (1988) New chiral shift reagents, optically active 2,2'-dihydroxy-1,1'-binaphthyl and 1,6-bis(*o*-chlorophenyl)-1,6-diphenyl-2,4-hexadiyne-1,6-diol. *Chem Lett* 131–134
54. Drabowicz J, Duddeck H (1989) Proton NMR spectral nonequivalence of sulfoxide enantiomers in the presence of 2,2'-dihydroxy-1,1'-binaphthyl. *Sulfur Lett* 10:37–40
55. Ma Q, Ma M, Tian H, Ye X, Xiao H, Chen L, Lei X (2012) A novel amine receptor based on the binol scaffold functions as a highly effective chiral shift reagent for carboxylic acids. *Org Lett* 14:5813–5815

56. Omelanczuk J, Mikolajczyk M (1996) Chiral *t*-butylphenylphosphinothioic acid: a useful chiral solvating agent for direct determination of enantiomeric purity of alcohols, thiols, amines, diols, amino alcohols, and related compounds. *Tetrahedron Asymmetry* 7: 2687–2694
57. Drabowicz J, Budzinski B, Mikolajczyk M (1992) Chiral *tert*-butylphenylphosphinothioic acid: a new NMR solvating agent for determination of enantiomeric excesses of sulfoxides. *Tetrahedron Asymmetry* 3:1231–1234
58. Gulea M, Kwiatkowska M, Lyzwa P, Legay R, Gaumont A-C, Kielbasinski P (2009) Michael addition to a chiral non-racemic 2-phosphono-2,3-didehydrothiolane *S*-oxide. *Tetrahedron Asymmetry* 20:293–297
59. Mucha P, Mloston G, Jasinski M, Linden A, Heimgartner H (2008) A new approach to enantiomerically pure bis-imidazoles derived from *trans*-1,2-diaminocyclohexane. *Tetrahedron Asymmetry* 19:1600–1607
60. Szawkalo J, Zawadzka A, Wojtasiewicz K, Leniewski A, Drabowicz J, Czarnocki Z (2005) First enantioselective synthesis of the antitumour alkaloid (+)-crispine A and determination of its enantiomeric purity by ¹H NMR. *Tetrahedron Asymmetry* 16:3619–3621
61. Louafi F, Moreau J, Shahane S, Golhen S, Roisnel T, Sinbandhit S, Hurvois J-P (2011) Electrochemical synthesis and chemistry of chiral 1-cyanotetrahydroisoquinolines. An approach to the asymmetric syntheses of the alkaloid (–)-crispine A and its natural (+)-antipode. *J Org Chem* 76:9720–9732
62. Czarnocki SJ, Wojtasiewicz K, Jozwiak AP, Maurin JK, Czarnocki Z, Drabowicz J (2008) Enantioselective synthesis of (+)-tryptargine and (+)-crispine E. *Tetrahedron* 64:3176–3182
63. Maier NM, Zoltewicz JA (1997) Dynamic equilibration of diastereomeric salts of atropisomers. Proton NMR spectra of 1,8-di(3'-pyridyl)naphthalene in the presence of *R*-camphorsulfonic acid. *Tetrahedron* 53:465–468
64. Satishkumar S, Periasamy M (2009) Chiral recognition of carboxylic acids by Troeger's base derivatives. *Tetrahedron Asymmetry* 20:2257–2262
65. Deshmukh M, Dunach E, Juge S, Kagan HB (1984) A convenient family of chiral shift reagents for measurement of enantiomeric excesses of sulfoxides. *Tetrahedron Lett* 25: 3467–3470
66. Pakulski Z, Demchuk OM, Kwiatosz R, Osinski PW, Swierczynska W, Pietrusiewicz KM (2003) The classical Kagan's amides are still practical NMR chiral shift reagents: determination of enantiomeric purity of P-chirogenic phospholene oxides. *Tetrahedron Asymmetry* 14: 1459–1462
67. Hirose T, Naito K, Shitara H, Nohira H, Baldwin BW (2001) ¹H NMR study of chiral recognition of amines by chiral Kemp's acid diamide. *Tetrahedron Asymmetry* 12:375–380
68. Hirose T, Naito K, Nakahara M, Shitara H, Aoki Y, Nohira H, Baldwin BW (2002) New chiral Kemp's acid diamides for chiral amine recognition by ¹H NMR. *J Incl Phenom Macrocycl Chem* 43:87–93
69. Bergmann H, Grosch B, Sitterberg S, Bach T (2004) An enantiomerically pure 1,5,7-trimethyl-3-azabicyclo[3.3.1]nonan-2-one as ¹H NMR shift reagent for the ee determination of chiral lactams, quinolones, and oxazolidinones. *J Org Chem* 69:970–973
70. Yang X, Wang G, Zhong C, Wu X, Fu E (2006) Novel NMR chiral solvating agents derived from (1*R*,2*R*)-diaminocyclohexane: synthesis and enantiodiscrimination for chiral carboxylic acids. *Tetrahedron Asymmetry* 17:916–921
71. Luo Z, Zhong C, Wu X, Fu E (2008) Amphiphilic chiral receptor as efficient chiral solvating agent for both lipophilic and hydrophilic carboxylic acids. *Tetrahedron Lett* 49:3385–3390
72. Luo Z, Li B, Fang X, Hu K, Wu X, Fu E (2007) Novel chiral solvating agents derived from natural amino acid: enantiodiscrimination for chiral α -arylalkylamines. *Tetrahedron Lett* 48: 1753–1756
73. Naziroglu HN, Durmaz M, Bozkurt S, Sirit A (2011) Application of L-proline derivatives as chiral shift reagents for enantiomeric recognition of carboxylic acids. *Chirality* 23:463–471

74. Wagger J, Grdadolnik SG, Groselj U, Meden A, Stanovnik B, Svete J (2007) Chiral solvating properties of (*S*)-1-benzyl-6-methylpiperazine-2,5-dione. *Tetrahedron Asymmetry* 18: 464–475
75. Malavasic C, Wagger J, Stanovnik B, Svete J (2008) (*S*)-*N*-Benzyl-3(6)-methylpiperazine-2,5-diones as chiral solvating agents for *N*-acylamino acid esters. *Tetrahedron Asymmetry* 19:1557–1567
76. Malavasic C, Stanovnik B, Wagger J, Svete J (2011) The effect of substituents on the chiral solvating properties of (*S*)-1,6-dialkylpiperazine-2,5-diones. *Tetrahedron Asymmetry* 22:1364–1371
77. Kim S, Choi K (2011) A practical solvating agent for the chiral NMR discrimination of carboxylic acids. *Eur J Org Chem* 4747–4750
78. Bozkurt S, Durmaz M, Naziroglu HN, Yilmaz M, Sirit A (2011) Amino alcohol based chiral solvating agents: synthesis and applications in the NMR enantiodiscrimination of carboxylic acids. *Tetrahedron Asymmetry* 22:541–549
79. Ma F, Ai L, Shen X, Zhang C (2007) New macrocyclic compound as chiral shift reagent for carboxylic acids. *Org Lett* 9:125–127
80. Wang W, Ma F, Shen X, Zhang C (2007) New chiral auxiliaries derived from (*S*)- α -phenylethylamine as chiral solvating agents for carboxylic acids. *Tetrahedron Asymmetry* 18:832–837
81. Wang W, Shen X, Ma F, Li Z, Zhang C (2008) Chiral amino alcohols derived from natural amino acids as chiral solvating agents for carboxylic acids. *Tetrahedron Asymmetry* 19:1193–1199
82. Li Y, Raushel FM (2007) Differentiation of chiral phosphorus enantiomers by ^{31}P and ^1H NMR spectroscopy using amino acid derivatives as chemical solvating agents. *Tetrahedron Asymmetry* 18:1391–1397
83. Hernandez-Rodriguez M, Juaristi E (2007) Structurally simple chiral thioureas as chiral solvating agents in the enantiodiscrimination of α -hydroxy and α -amino carboxylic acids. *Tetrahedron* 63:7673–7678
84. Lacour J (2010) Chiral hexacoordinated phosphates: from pioneering studies to modern uses in stereochemistry. *C R Chim* 13:985–997
85. Bergman SD, Frantz R, Gut D, Kol M, Lacour J (2006) Effective chiral recognition among ions in polar media. *Chem Commun* 850–852
86. Michon C, Goncalves-Farbos M-H, Lacour J (2009) NMR enantiodifferentiation of quaternary ammonium salts of Troeger base. *Chirality* 21:809–817
87. Lacour J, Goujon-Ginglinger C, Troche-Haldimann S, Jordry JJ (2000) Efficient enantioselective extraction of tris(diimine)ruthenium(II) complexes by chiral, lipophilic TRISPHAT anions. *Angew Chem Int Ed* 39:3695–3697
88. Payet E, Dimitrov-Raytchev P, Chatelet B, Guy L, Grass S, Lacour J, Dutasta J-P, Martinez A (2012) Absolute configuration and enantiodifferentiation of a hemicyclopentane incorporating an azaphosphatane moiety. *Chirality* 24:1077–1081
89. Barry NPE, Austeri M, Lacour J, Therrien B (2009) Highly efficient NMR enantiodiscrimination of chiral octanuclear metalla-boxes in polar solvent. *Organometallics* 28: 4894–4897
90. Perollier C, Bernardinelli G, Lacour J (2008) Sugar derived hexacoordinated phosphates: chiral anionic auxiliaries with general asymmetric efficiency. *Chirality* 20:313–324
91. Llewellyn DB, Arndtsen BA (2003) The use of a chiral borate counteranion as a ^1H NMR shift reagent for cationic copper(I) complexes. *Can J Chem* 81:1280–1284
92. Loewer Y, Weiss C, Biju AT, Froehlich R, Glorius F (2011) Synthesis and application of a chiral diborate. *J Org Chem* 76:2324–2327
93. Moon LS, Jolly RS, Kasetti Y, Bharatam PV (2009) A new chiral shift reagent for the determination of enantiomeric excess and absolute configuration in cyanohydrins. *Chem Commun* 1067–1069

94. Moon LS, Pal M, Kasetti Y, Bharatam PV, Jolly RS (2010) Chiral solvating agents for cyanohydrins and carboxylic acids. *J Org Chem* 75:5487–5498
95. Pirkle WH, Pochapsky TC (1987) Chiral molecular recognition in small bimolecular systems: a spectroscopic investigation into the nature of diastereomeric complexes. *J Am Chem Soc* 109:5975–5982
96. Salvadori P, Rosini C, Pini D, Bertucci C, Altemura P, Uccello-Barretta G, Raffaelli A (1987) A novel application of Cinchona alkaloids as chiral auxiliaries: preparation and use of a new family of chiral stationary phases for the chromatographic resolution of racemates. *Tetrahedron* 43:4969–4978
97. Uccello-Barretta G, Rosini C, Pini D, Salvadori P (1990) A spectroscopic study of the interaction of (D)- and (L)-*N*-(3,5-dinitrobenzoyl)valine methyl ester with *n*-butylamide of (S)-2-[(phenylcarbamoyl)oxy]propionic acid: direct evidence for a chromatographic chiral recognition rationale. *J Am Chem Soc* 112:2707–2710
98. Pirkle WH, Tspouras A (1985) 3,5-Dinitrobenzoyl amino acid esters. Broadly applicable chiral solvating agents for NMR determination of enantiomeric purity. *Tetrahedron Lett* 26:2989–2992
99. Rosini C, Uccello-Barretta G, Pini D, Abete C, Salvadori P (1988) Quinine: an inexpensive chiral solvating agent for the determination of enantiomeric composition of binaphthyl derivatives and alkylarylcarbinols by NMR spectroscopy. *J Org Chem* 53:4579–4581
100. Salvadori P, Pini D, Rosini C, Bertucci C, Uccello-Barretta G (1992) Chiral discriminations with Cinchona alkaloids. *Chirality* 4:43–49
101. Uccello-Barretta G, Pini D, Mastantuono A, Salvadori P (1995) Direct NMR assay of enantiomeric purity of chiral β -hydroxy esters by using quinine as chiral solvating agent. *Tetrahedron Asymmetry* 6:1965–1972
102. Maly A, Lejczak B, Kafarski P (2003) Quinine as chiral discriminator for determination of enantiomeric excess of diethyl 1,2-dihydroxyalkanephosphonates. *Tetrahedron Asymmetry* 14:1019–1024
103. Uccello-Barretta G, Bardoni S, Balzano F, Salvadori P (2001) Versatile chiral auxiliaries for NMR spectroscopy based on carbamoyl derivatives of dihydroquinine. *Tetrahedron Asymmetry* 12:2019–2023
104. Uccello-Barretta G, Mirabella F, Balzano F, Salvadori P (2003) C11 versus C9 carbamoylation of quinine: a new class of versatile polyfunctional chiral solvating agents. *Tetrahedron Asymmetry* 14:1511–1516
105. Pini D, Uccello-Barretta G, Rosini C, Salvadori P (1991) *N*-(*n*-Butylamide) of (S)-2-(phenylcarbamoyloxy)propionic acid: a new chiral solvating agent, derived from L-lactic acid, for the enantiomeric purity determination of derivatized amino acids. *Chirality* 3:174–176
106. Heo KS, Hyun MH, Cho YJ, Ryoo JJ (2011) Determination of optical purity of 3,5-dimethoxybenzoyl-leucine diethylamide by chiral chromatography and ^1H and ^{13}C NMR spectroscopy. *Chirality* 23:281–286
107. Pirkle WH, Welch CJ, Lamm B (1992) Design, synthesis, and evaluation of an improved enantioselective naproxen selector. *J Org Chem* 57:3854–3860
108. Pirkle WH, Welch CJ (1992) An improved chiral stationary phase for the chromatographic separation of underivatized naproxen enantiomers. *J Liq Chromatogr* 15:1947–1955
109. Iwaniuk DP, Wolf C (2010) A versatile and practical solvating agent for enantioselective recognition and NMR analysis of protected amines. *J Org Chem* 75:6724–6727
110. Palomino-Schaetzlein M, Virgili A, Gil S, Jaime C (2006) Di-(*R,R*)-1-[10-(1-hydroxy-2,2,2-trifluoroethyl)-9-anthryl]-2,2,2-trifluoroethyl muconate: a highly chiral cavity for enantiodiscrimination by NMR. *J Org Chem* 71:8114–8120
111. Gil S, Palomino-Schaetzlein M, Burusco KK, Jaime C, Virgili A (2010) Molecular tweezers for enantiodiscrimination in NMR: di-(*R,R*)-1-[10-(1-hydroxy-2,2,2-trifluoroethyl)-9-anthryl]-2,2,2-trifluoroethyl benzenedicarboxylates. *Chirality* 22:548–556

112. Pena C, Gonzalez-Sabin J, Alfonso I, Rebolledo F, Gotor V (2007) New pincer-like receptor derived from *trans*-cyclopentane-1,2-diamine as a chiral shift reagent for carboxylic acids. *Tetrahedron Asymmetry* 18:1981–1985
113. Pena C, Gonzalez-Sabin J, Alfonso I, Rebolledo F, Gotor V (2008) Cycloalkane-1,2-diamine derivatives as chiral solvating agents. Study of the structural variables controlling the NMR enantiodiscrimination of chiral carboxylic acids. *Tetrahedron* 64:7709–7717
114. Liu L, Ye M, Hu X, Yu X, Zhang L, Lei X (2011) Chiral solvating agents for carboxylic acids based on the salen moiety. *Tetrahedron Asymmetry* 22:1667–1671
115. Altava B, Burguete MI, Carbo N, Escorihuela J, Luis SV (2010) Chiral bis(amino amides) as chiral solvating agents for enantiomeric excess determination of α -hydroxy and arylpropionic acids. *Tetrahedron Asymmetry* 21:982–989
116. Legouin B, Gayral M, Uriac P, Tomasi S, van de Weghe P (2010) Recognition of enantiomers with chiral molecular tweezers derived from (+)- or (–)-usnic acid. *Tetrahedron Asymmetry* 21:1307–1310
117. Ema T, Ouchi N, Doi T, Korenaga T, Sakai T (2005) Highly sensitive chiral shift reagent bearing two zinc porphyrins. *Org Lett* 7:3985–3988
118. Williams T, Pitcher RG, Bommer P, Gutzwiller J, Uskokovic M (1969) Diastereomeric solute–solute interactions of enantiomers in achiral solvents. Nonequivalence of the nuclear magnetic resonance spectra of racemic and optically active dihydroquinine. *J Am Chem Soc* 91:1871–1872
119. Uccello-Barretta G, Vanni L, Balzano F (2009) NMR enantiodiscrimination phenomena by quinine C9-carbamates. *Eur J Org Chem* 860–869
120. Uccello-Barretta G, Balzano F, Salvadori P (2005) Rationalization of the multireceptorial character of chiral solvating agents based on quinine and its derivatives: overview of selected NMR investigations. *Chirality* 17:S243–S248
121. Uccello-Barretta G, Vanni L, Berni MG, Balzano F (2011) NMR enantiodiscrimination by pentafluorophenylcarbamoyl derivatives of quinine: C10 versus C9 derivatization. *Chirality* 23:417–423
122. Abid M, Toeroek B (2005) Cinchona alkaloid induced chiral discrimination for the determination of the enantiomeric composition of α -trifluoromethylated-hydroxyl compounds by ^{19}F NMR spectroscopy. *Tetrahedron Asymmetry* 16:1547–1555
123. Zymanczyk-Duda E, Skwarczynski M, Lejczak B, Kafarski P (1996) Accurate assay of enantiopurity of 1-hydroxy- and 2-hydroxyalkylphosphonate esters. *Tetrahedron Asymmetry* 7:1277–1280
124. Rudzinska E, Berlicki L, Kafarski P, Lammerhofer M, Mucha A (2009) Cinchona alkaloids as privileged chiral solvating agents for the enantiodiscrimination of *N*-protected amino-alkanephosphonates – a comparative NMR study. *Tetrahedron Asymmetry* 20:2709–2714
125. Gorecki L, Berlicki L, Mucha A, Kafarski P, Slepokura K, Rudzinska-Szostak E (2012) Phosphorylation as a method of tuning the enantiodiscrimination potency of quinine – an NMR study. *Chirality* 24:318–328
126. Faigl F, Vas-Feldhoffer B, Kubinyi M, Pal K, Tarkanyi G, Czugler M (2009) Efficient synthesis of optically active 1-(2-carboxymethyl-6-ethylphenyl)-1H-pyrrole-2-carboxylic acid: a novel atropisomeric 1-arylpyrrole derivative. *Tetrahedron Asymmetry* 20:98–103
127. Kwon C, Yoo KM, Jung S (2009) Chiral separation and discrimination of catechin by sinorhizobial octasaccharides in capillary electrophoresis and ^{13}C NMR spectroscopy. *Carbohydr Res* 344:1347–1351
128. D'Acquarica I, Gasparini F, Misiti D, Pierini M, Villani C (2008) HPLC chiral stationary phases containing macrocyclic antibiotics: practical aspects and recognition mechanism. *Adv Chromatogr* 46:109–173
129. Uccello-Barretta G, Vanni L, Balzano F (2010) Nuclear magnetic resonance approaches to the rationalization of chromatographic enantio-recognition processes. *J Chromatogr A* 1217: 928–940

130. Chankvetadze B, Blaschke G (1999) Selector-selectand interactions in chiral capillary electrophoresis. *Electrophoresis* 20:2592–2604
131. Chankvetadze B, Burjanadze N, Maynard DM, Bergander K, Bergenthal D, Blaschke G (2002) Comparative enantioseparations with native β -cyclodextrin and heptakis-(2-*O*-methyl-3,6-di-*O*-sulfo)- β -cyclodextrin in capillary electrophoresis. *Electrophoresis* 23:3027–3034
132. Chankvetadze B (2004) Combined approach using capillary electrophoresis and NMR spectroscopy for an understanding of enantioselective recognition mechanisms by cyclodextrins. *Chem Soc Rev* 33:337–347
133. Vega ED, Lomsadze K, Chankvetadze L, Salgado A, Scriba GKE, Calvo E, Lopez JA, Crego AL, Marina ML, Chankvetadze B (2011) Separation of enantiomers of ephedrine by capillary electrophoresis using cyclodextrins as chiral selectors: comparative CE, NMR and high resolution MS studies. *Electrophoresis* 32:2640–2647
134. Lomsadze K, Vega ED, Salgado A, Crego AL, Scriba GKE, Marina ML, Chankvetadze B (2012) Separation of enantiomers of norephedrine by capillary electrophoresis using cyclodextrins as chiral selectors: comparative CE and NMR studies. *Electrophoresis* 33:1637–1647
135. Schurig V (2012) Separation of enantiomers. In: Poole CF (ed) *Gas chromatography*. Elsevier, Oxford, pp 495–517
136. Schurig V (2011) Gas chromatographic enantioseparation of derivatized α -amino acids on chiral stationary phases – past and present. *J Chromatogr B* 879:3122–3140
137. Schurig V (2010) Use of derivatized cyclodextrins as chiral selectors for the separation of enantiomers by gas chromatography. *Ann Pharm Fr* 68:82–98
138. Wistuba D, Schurig V (2009) The separation of enantiomers on modified cyclodextrins by capillary electrochromatography (CEC). *LC-GC Eur* 22:60, 62–64, 66–69
139. Szejtli J (2004) Past, present, and future of cyclodextrin research. *Pure Appl Chem* 76:1825–1845
140. Dodziuk H (ed) (2008) *Cyclodextrins and their complexes*. Wiley-VCH, Weinheim
141. Loftsson T, Brewster ME (2012) Cyclodextrins as functional excipients: methods to enhance complexation efficiency. *J Pharm Sci* 101:3019–3032
142. Perez-Trujillo M, Lindon JC, Parella T, Keun HC, Nicholson JK, Athersuch TJ (2012) Chiral metabonomics: ^1H NMR-based enantiospecific differentiation of metabolites in human urine via direct cosolvation with β -cyclodextrin. *Anal Chem* 84:2868–2874
143. Dodziuk H, Kozminski W, Ejchart A (2004) NMR studies of chiral recognition by cyclodextrins. *Chirality* 16:90–105
144. Schneider H-J, Hacket F, Ruediger V, Ikeda H (1998) NMR studies of cyclodextrins and cyclodextrin complexes. *Chem Rev* 98:1755–1785
145. Szejtli J (1998) Introduction and general overview of cyclodextrin chemistry. *Chem Rev* 98:1743–1753
146. Uccello-Barretta G, Balzano F, Cuzzola A, Menicagli R, Salvadori P (2000) NMR detection of the conformational distortion induced in cyclodextrins by introduction of alkyl or aromatic substituents. *Eur J Org Chem* 449–453
147. Uccello-Barretta G, Sicoli G, Balzano F, Salvadori P (2003) A conformational model of per-*O*-acetyl-cyclomaltoheptaose ($-\beta$ -cyclodextrin) in solution: detection of partial inversion of glucopyranose units by NMR spectroscopy. *Carbohydr Res* 338:1103–1107
148. Uccello-Barretta G, Sicoli G, Balzano F, Salvadori P (2005) NMR spectroscopy: a powerful tool for detecting the conformational features of symmetrical per-substituted mixed cyclomaltoheptaoses (β -cyclodextrins). *Carbohydr Res* 340:271–281
149. Casy AF, Mercer AD (1988) Application of cyclodextrins to chiral analysis by proton NMR spectroscopy. *Magn Reson Chem* 26:765–774
150. Greatbanks D, Pickford R (1987) Cyclodextrins as chiral complexing agents in water, and their application to optical purity measurements. *Magn Reson Chem* 25:208–215

151. Blazewska KM, Ni F, Haiges R, Kashemirov BA, Coxon FP, Stewart CA, Baron R, Rogers MJ, Seabra MC, Ebetino FH, McKenna CE (2011) Synthesis, stereochemistry and SAR of a series of minodronate analogues as RGGT inhibitors. *Eur J Med Chem* 46: 4820–4826
152. Redondo J, Capdevila A, Latorre I, Bertran J (2012) Host–guest complexation of omeprazole, pantoprazole and rabeprazole sodium salts with cyclodextrins: an NMR study on solution structures and enantiodiscrimination power. *J Incl Phenom Macrocycl Chem* 73:225–236
153. Esturau N, Espinosa JF (2006) Optimization of diffusion-filtered NMR experiments for selective suppression of residual nondeuterated solvent and water signals from ^1H NMR spectra of organic compounds. *J Org Chem* 71:4103–4110
154. Lee Y-J, Choi S, Lee J, Nguyen NVT, Lee K, Kang JS, Mar W, Kim KH (2012) Chiral discrimination of sibutramine enantiomers by capillary electrophoresis and proton nuclear magnetic resonance spectroscopy. *Arch Pharm Res* 35:671–681
155. Molaabasi F, Talebpour Z (2011) Enantiomeric discrimination and quantification of the chiral organophosphorus pesticide fenamiphos in aqueous samples by a novel and selective ^{31}P nuclear magnetic resonance spectroscopic method using cyclodextrins as chiral selector. *J Agric Food Chem* 59:803–808
156. Smith KJ, Wilcox JD, Mirick GE, Wacker LS, Ryan NS, Vensel DA, Reading R, Domush HL, Amonoo EP, Shariff SS, Wenzel TJ (2003) Calix[4]arene, calix[4]resorcarene, and cyclodextrin derivatives and their lanthanide complexes as chiral NMR shift reagents. *Chirality* 15:S150–S158
157. Wenzel TJ, Amonoo EP, Shariff SS, Aniagyei SE (2003) Sulfated and carboxymethylated cyclodextrins and their lanthanide complexes as chiral NMR discriminating agents. *Tetrahedron Asymmetry* 14:3099–3104
158. Dignam CF, Randall LA, Blacken RD, Cunningham PR, Lester S-KG, Brown MJ, French SC, Aniagyei SE, Wenzel TJ (2006) Carboxymethylated cyclodextrin derivatives as chiral NMR discriminating agents. *Tetrahedron Asymmetry* 17:1199–1208
159. Provencher KA, Weber MA, Randall LA, Cunningham PR, Dignam CF, Wenzel TJ (2010) Carboxymethylated cyclodextrins and their complexes with Pr(III) and Yb(III) as water-soluble chiral NMR solvating agents for cationic compounds. *Chirality* 22:336–346
160. Provencher KA, Wenzel TJ (2008) Carboxymethylated cyclodextrins and their paramagnetic lanthanide complexes as water-soluble chiral NMR solvating agents. *Tetrahedron Asymmetry* 19:1797–1803
161. Chisholm CD, Wenzel TJ (2011) Enantiomeric discrimination of aromatic-containing anionic substrates using cationic cyclodextrins. *Tetrahedron Asymmetry* 22:62–68
162. Rekharsky M, Yamamura H, Kawai M, Inoue Y (2001) Critical difference in chiral recognition of *N*-Cbz-*D/L*-aspartic and -*L*-glutamic acids by mono- and bis(trimethylammonio)- β -cyclodextrins. *J Am Chem Soc* 123:5360–5361
163. Park KK, Lim HS, Park JW (1999) Chiral discrimination of phenylacetic acid derivatives by xylylenediamine-modified β -cyclodextrins. *Bull Korean Chem Soc* 20:211–213
164. Sun P, MacDonnell FM, Armstrong DW (2009) Enantioselective host–guest complexation of Ru(II) trisdiimine complexes using neutral and anionic derivatized cyclodextrins. *Inorg Chim Acta* 362:3073–3078
165. Koehler JEH, Hohla M, Richters M, König WA (1992) Cyclodextrin derivatives as chiral selectors. Investigation of interaction with (*R,S*)-methyl 2-chloropropionate by enantioselective gas chromatography, NMR spectroscopy and molecular dynamics simulation. *Angew Chem Int Ed Engl* 31:319–320
166. Schmidt R, Roeder M, Oeckler O, Simon A, Schurig V (2000) Separation and absolute configuration of the enantiomers of a degradation product of the new inhalation anesthetic sevoflurane. *Chirality* 12:751–755
167. Sicoli G, Jiang Z, Jicsinsky L, Schurig V (2005) Modified linear dextrans (“acyclodextrins”) as new chiral selectors for the gas-chromatographic separation of enantiomers. *Angew Chem Int Ed* 44:4092–4095

168. Uccello-Barretta G, Sicoli G, Balzano F, Schurig V, Salvadori P (2006) Highly efficient NMR enantio-discrimination of 1,1,1,3,3-pentafluoro-2-(fluoromethoxy)-3-methoxypropane, a chiral degradation product of sevoflurane, by heptakis(2,3-di-*O*-acetyl-6-*O*-*tert*-butyldimethylsilyl)- β -cyclodextrin. *Tetrahedron Asymmetry* 17:2504–2510
169. Uccello-Barretta G, Balzano F, Pertici F, Jicsinszky L, Sicoli G, Schurig V (2008) External vs. internal interactions in the enantio-discrimination of fluorinated α -amino acid derivatives by heptakis[2,3-di-*O*-acetyl-6-*O*-(*tert*-butyldimethylsilyl)]- β -cyclodextrin, a powerful chiral solvating agent for NMR spectroscopy. *Eur J Org Chem* 1855–1863
170. Uccello-Barretta G, Balzano F, Caporusso AM, Iodice A, Salvadori P (1995) Permethylyated β -cyclodextrin as chiral solvating agent for the NMR assignment of the absolute configuration of chiral trisubstituted allenes. *J Org Chem* 60:2227–2231
171. Uccello-Barretta G, Balzano F, Caporusso AM, Salvadori P (1994) Direct determination of the enantiomeric purity of chiral trisubstituted allenes by using permethylated cyclodextrin as a chiral solvating agent. *J Org Chem* 59:836–839
172. Uccello-Barretta G, Balzano F, Menicagli R, Salvadori P (1996) NMR chiral analysis of aromatic hydrocarbons by using permethylated β -cyclodextrin as chiral solvating agent. *J Org Chem* 61:363–365
173. Uccello-Barretta G, Cuzzola A, Balzano F, Menicagli R, Salvadori P (1998) Benzoylated and benzylated cyclodextrins. A new class of chiral solvating agents for chiral recognition of 3,5-dinitrophenyl derivatives by ^1H -NMR spectroscopy. *Eur J Org Chem* 2009–2012
174. Uccello-Barretta G, Cuzzola A, Balzano F, Menicagli R, Iuliano A, Salvadori P (1997) A new stereochemical model from NMR for benzoylated cyclodextrins, promising new chiral solvating agents for the chiral analysis of 3,5-dinitrophenyl derivatives. *J Org Chem* 62: 827–835
175. Uccello-Barretta G, Ferri L, Balzano F, Salvadori P (2003) Partially versus exhaustively carbamoylated cyclodextrins: NMR investigation on enantiodiscriminating capabilities in solution. *Eur J Org Chem* 1741–1748
176. Yashima E, Yamada M, Yamamoto C, Nakashima M, Okamoto Y (1997) Chromatographic enantio-separation and chiral discrimination in NMR by trisphenylcarbamate derivatives of cellulose, amylose, oligosaccharides, and cyclodextrins. *Enantiomer* 2:225–240
177. Kubota T, Yamamoto C, Okamoto Y (2002) Chromatographic enantioseparation by cycloalkylcarbamate derivatives of cellulose and amylose. *Chirality* 14:372–376
178. Uccello-Barretta G, Balzano F, Sicoli G, Scarselli A, Salvadori P (2005) NMR enantio-discrimination of polar and apolar substrates by multifunctional cyclodextrins. *Eur J Org Chem* 5349–5355
179. Boger J, Corcoran RJ, Lehn JM (1978) Cyclodextrin chemistry. Selective modification of all primary hydroxyl groups of α - and β -cyclodextrins. *Helv Chim Acta* 61:2190–2218
180. Ema T, Ura N, Eguchi K, Ise Y, Sakai T (2011) Chiral porphyrin dimer with a macrocyclic cavity for intercalation of aromatic guests. *Chem Commun* 47:6090–6092
181. Ema T (2012) Synthetic macrocyclic receptors in chiral analysis and separation. *J Incl Phenom Macrocycl Chem* 74:41–55
182. Shirakawa S, Moriyama A, Shimizu S (2007) Design of a novel inherently chiral calix[4] arene for chiral molecular recognition. *Org Lett* 9:3117–3119
183. Shirakawa S, Moriyama A, Shimizu S (2008) Synthesis, optical resolution and enantiomeric recognition ability of novel, inherently chiral calix[4]arenes: trial application to asymmetric reactions as organocatalysts. *Eur J Org Chem* 5957–5964
184. Xia Y-X, Zhou H-H, Shi J, Li S-Z, Zhang M, Luo J, Xiang G-Y (2012) An inherently chiral calix[4]crown carboxylic acid in the 1,2-alternate conformation. *J Incl Phenom Macrocycl Chem* 74:277–284
185. Uccello-Barretta G, Berni M-G, Balzano F (2007) Enantiodiscrimination by inclusion phenomena inside a bis(ethyl lactate) *p*-*tert*-butylcalix[4]arene derivative. *Tetrahedron Asymmetry* 18:2565–2572

186. Durmaz M, Yilmaz M, Sirit A (2011) Synthesis of chiral calix[4]arenes bearing aminonaphthol moieties and their use in the enantiomeric recognition of carboxylic acids. *Org Biomol Chem* 9:571–580
187. Ben Sdira S, Felix CP, Giudicelli M-BA, Seigle-Ferrand PF, Perrin M, Lamartine RJ (2003) Synthesis and structure of lower rim C-linked *N*-tosyl peptidocalix[4]arenes. *J Org Chem* 68:6632–6638
188. Ben Sdira S, Baudry R, Felix CP, Giudicelli M-BA, Lamartine RJ (2004) Synthesis and structure of lower rim C-linked tetra-*N*-tosyl peptidocalix[4]arenes. *Tetrahedron Lett* 45:7801–7804
189. Bois J, Bonnamour I, Duchamp C, Parrot-Lopez H, Darbost U, Felix C (2009) Enantioselective recognition of amino acids by chiral peptido-calix[4]arenes and thiocalix[4]arenes. *New J Chem* 33:2128–2135
190. Lhotak P (2004) Chemistry of thiocalixarenes. *Eur J Org Chem* 1675–1692
191. Wenzel TJ (2013) Chiral derivatizing agents, macrocycles, metal complexes, and liquid crystals for enantiomer differentiation in NMR spectroscopy. *Top Curr Chem*. doi:10.1007/128_2013_433
192. Pham NH, Wenzel TJ (2012) A water-soluble calix[4]resorcinarene with L-pipecolinic acid groups as a chiral NMR solvating agent. *Chirality* 24:193–200
193. Pham NH, Wenzel TJ (2011) A water-soluble calix[4]resorcinarene with α -methyl-L-prolinylmethyl groups as a chiral NMR solvating agent. *J Org Chem* 76:986–989
194. O'Farrell CM, Chudomel JM, Collins JM, Dignam CF, Wenzel TJ (2008) Water-soluble calix[4]resorcinarenes with hydroxyproline groups as chiral NMR solvating agents. *J Org Chem* 73:2843–2851
195. O'Farrell CM, Hagan KA, Wenzel TJ (2009) Water-soluble calix[4]resorcinarenes as chiral NMR solvating agents for bicyclic aromatic compounds. *Chirality* 21:911–921
196. Pham NH, Wenzel TJ (2011) A sulfonated calix[4]resorcinarene with α -methyl-L-prolinylmethyl groups as a water-soluble chiral NMR solvating agent. *Tetrahedron Asymmetry* 22:641–647
197. Pham NH, Wenzel TJ (2011) A sulfonated calix[4]resorcinarene with L-pipecolinic acid groups as a water-soluble chiral NMR solvating agent. *Tetrahedron Asymmetry* 22:1574–1580
198. Hagan KA, O'Farrell CM, Wenzel TJ (2009) Water-soluble calix[4]resorcinarenes with hydroxyproline groups as chiral NMR solvating agents for phenyl- and pyridyl-containing compounds. *Eur J Org Chem* 4825–4832
199. O'Farrell CM, Wenzel TJ (2008) Water-soluble calix[4]resorcinarenes as chiral NMR solvating agents for phenyl-containing compounds. *Tetrahedron Asymmetry* 19:1790–1796
200. Wenzel TJ, Rollo RD, Clark RL (2012) Chiral discrimination of aliphatic amines and amino alcohols using NMR spectroscopy. *Magn Reson Chem* 50:261–265
201. Li N, Yang F, Stock HA, Dearden DV, Lamb JD, Harrison RG (2012) Resorcinarene-based cavitands with chiral amino acid substituents for chiral amine recognition. *Org Biomol Chem* 10:7392–7401
202. Amato ME, Ballistreri FP, D'Agata S, Pappalardo A, Tomaselli GA, Toscano RM, Sfrassetto GT (2011) Enantioselective molecular recognition of chiral organic ammonium ions and amino acids using cavitand-salen-based receptors. *Eur J Org Chem* 5674–5680
203. Ema T, Tanida D, Sakai T (2006) Versatile and practical chiral shift reagent with hydrogen-bond donor/acceptor sites in a macrocyclic cavity. *Org Lett* 8:3773–3775
204. Ema T, Tanida D, Sakai T (2007) Versatile and practical macrocyclic reagent with multiple hydrogen-bonding sites for chiral discrimination in NMR. *J Am Chem Soc* 129:10591–10596
205. Ema T, Tanida D, Hamada K, Sakai T (2008) Tuning the chiral cavity of macrocyclic receptor for chiral recognition and discrimination. *J Org Chem* 73:9129–9132
206. Ema T, Tanida D, Sugita K, Sakai T, Miyazawa K, Ohnishi A (2008) Chiral selector with multiple hydrogen-bonding sites in a macrocyclic cavity. *Org Lett* 10:2365–2368

207. Ema T, Ura N, Eguchi K, Sakai T (2012) Molecular recognition of chiral diporphyrin receptor with a macrocyclic cavity for intercalation of aromatic compounds. *Bull Chem Soc Jpn* 85:101–109
208. Gasparrini F, Misiti D, Pierini M, Villani C (2002) A chiral A2B2 macrocyclic minireceptor with extreme enantioselectivity. *Org Lett* 4:3993–3996
209. Uccello-Barretta G, Balzano F, Martinelli J, Berni M-G, Villani C, Gasparrini F (2005) NMR enantiodiscrimination by cyclic tetraamidic chiral solvating agents. *Tetrahedron Asymmetry* 16:3746–3751
210. Uccello-Barretta G, Balzano F, Martinelli J, Gasparrini F, Pierini M, Villani C (2011) NMR and computational investigations of the chiral discrimination processes involving a cyclic tetraamidic chiral selector. *Eur J Org Chem* 3738–3747
211. Tanaka K, Nakai Y, Takahashi H (2011) Efficient NMR chiral discrimination of carboxylic acids using rhombamine macrocycles as chiral shift reagent. *Tetrahedron Asymmetry* 22: 178–184
212. Periasamy M, Dalai M, Padmaja M (2010) Chiral *trans*-1,2-diaminocyclohexane derivatives as chiral solvating agents for carboxylic acids. *J Chem Sci* 122:561–569
213. Gualandi A, Grilli S, Savoia D, Kwit M, Gawronski J (2011) C-Hexaphenyl-substituted triethylamine as a chiral solvating agent for carboxylic acids. *Org Biomol Chem* 9:4234–4241
214. Ma F, Shen X, Ming X, Wang J, Ou-Yang J, Zhang C (2008) The novel macrocyclic compounds as chiral solvating agents for determination of enantiomeric excess of carboxylic acids. *Tetrahedron Asymmetry* 19:1576–1586
215. Ma F, Shen X, Ou-Yang J, Deng Z, Zhang C (2008) Macrocyclic compounds as chiral solvating agents for phosphinic, phosphonic, and phosphoric acids. *Tetrahedron Asymmetry* 19:31–37
216. Tanaka K, Fukuda N, Fujiwara T (2007) Triethylamine as a new chiral shift reagent for secondary alcohols. *Tetrahedron Asymmetry* 18:2657–2661
217. Tanaka K, Fukuda N (2009) “Calixarene-like” chiral amine macrocycles as novel chiral shift reagents for carboxylic acids. *Tetrahedron Asymmetry* 20:111–114
218. Quinn TP, Atwood PD, Tanski JM, Moore TF, Folmer-Andersen JF (2011) Aza-crown macrocycles as chiral solvating agents for mandelic acid derivatives. *J Org Chem* 76: 10020–10030
219. Carrillo R, Lopez-Rodriguez M, Martin VS, Martin T (2009) Quantification of a CH- π interaction responsible for chiral discrimination and evaluation of its contribution to enantioselectivity. *Angew Chem Int Ed* 48:7803–7808
220. Busto E, Gonzalez-Alvarez A, Gotor-Fernandez V, Alfonso I, Gotor V (2010) Optically active macrocyclic hexaazapyridinophanes decorated at the periphery: synthesis and applications in the NMR enantiodiscrimination of carboxylic acids. *Tetrahedron* 66: 6070–6077
221. Gonzalez-Alvarez A, Alfonso I, Gotor V (2006) An azamacrocyclic receptor as efficient polytopic chiral solvating agent for carboxylic acids. *Tetrahedron Lett* 47:6397–6400
222. Gospodarowicz K, Holynska M, Paluch M, Lisowski J (2012) Novel chiral hexaazamacrocycles for the enantiodiscrimination of carboxylic acids. *Tetrahedron* 68:9930–9935
223. Wenzel TJ, Thurston JE (2000) Enantiomeric discrimination in the NMR spectra of underivatized amino acids and α -methyl amino acids using (+)-(18-crown-6)-2,3,11,12-tetracarboxylic acid. *Tetrahedron Lett* 41:3769–3772
224. Wenzel TJ, Thurston JE (2000) (+)-(18-Crown-6)-2,3,11,12-tetracarboxylic acid and its ytterbium(III) complex as chiral NMR discriminating agents. *J Org Chem* 65:1243–1248
225. Machida Y, Kagawa M, Nishi H (2003) Nuclear magnetic resonance studies for the chiral recognition of (+)-(*R*)-18-crown-6-tetracarboxylic acid to amino compounds. *J Pharm Biomed Anal* 30:1929–1942
226. Lee W, Bang E, Baek C-S, Lee W (2004) Chiral discrimination studies of (+)-(18-crown-6)-2,3,11,12-tetracarboxylic acid by high-performance liquid chromatography and NMR spectroscopy. *Magn Reson Chem* 42:389–395

227. Lovely AE, Wenzel TJ (2006) Chiral NMR discrimination of secondary amines using (18-crown-6)-2,3,11,12-tetracarboxylic acid. *Org Lett* 8:2823–2826
228. Chisholm CD, Fueloep F, Forro E, Wenzel TJ (2010) Enantiomeric discrimination of cyclic β -amino acids using (18-crown-6)-2,3,11,12-tetracarboxylic acid as a chiral NMR solvating agent. *Tetrahedron Asymmetry* 21:2289–2294
229. Lovely AE, Wenzel TJ (2008) Chiral NMR discrimination of amines: analysis of secondary, tertiary, and prochiral amines using (18-crown-6)-2,3,11,12-tetracarboxylic acid. *Chirality* 20:370–378
230. Koide T, Ueno K (2001) Mechanistic study of enantiomeric recognition of primary amino compounds using an achiral crown ether with cyclodextrin by capillary electrophoresis and nuclear magnetic resonance. *J Chromatogr A* 923:229–239
231. Wenzel TJ, Boume CE, Clark RL (2009) (18-Crown-6)-2,3,11,12-tetracarboxylic acid as a chiral NMR solvating agent for determining the enantiomeric purity and absolute configuration of β -amino acids. *Tetrahedron Asymmetry* 20:2052–2060
232. Lovely AE, Wenzel TJ (2006) Chiral NMR discrimination of piperidines and piperazines using (18-crown-6)-2,3,11,12-tetracarboxylic acid. *J Org Chem* 71:9178–9182
233. Howard JA, Nonn M, Fulop F, Wenzel TJ (2013) Enantiomeric discrimination of isoxazoline fused β -amino acid derivatives using (18-crown-6)-2,3,11,12-tetracarboxylic acid as a chiral NMR solvating agent. *Chirality* 25:48–53
234. Bang E, Jin JY, Hong JH, Kang JS, Lee W, Lee W (2012) Comparative studies on enantiomer resolution of α -amino acids and their esters using (18-crown-6)-tetracarboxylic acid as a chiral crown ether selector by NMR spectroscopy and high-performance liquid chromatography. *Bull Korean Chem Soc* 33:3481–3484
235. Szumna A (2009) Chiral encapsulation by directional interactions. *Chem Eur J* 15: 12381–12388
236. Wehner M, Schrader T, Finocchiaro P, Failla S, Consiglio G (2000) A chiral sensor for arginine and lysine. *Org Lett* 2:605–608
237. Consiglio GA, Failla S, Finocchiaro P (2008) New cleft-like molecules and macrocycles from phosphonate substituted spirobisindanol. *Molecules* 13:678–700
238. Holman KT (2004) Cryptophanes: molecular containers. In: Atwood JL, Steed JW (eds) *Encyclopedia of supramolecular chemistry*. CRC, New York, pp 340–348
239. Canceill J, Lacombe L, Collet A (1985) Analytical optical resolution of bromochlorofluoromethane by enantioselective inclusion into a tailor-made cryptophane and determination of its maximum rotation. *J Am Chem Soc* 107:6993–6996
240. Soulard P, Asselin P, Cuisset A, Aviles Moreno JR, Huet TR, Petitprez D, Demaison J, Freedman TB, Cao X, Nafie LA, Crassous J (2006) Chlorofluoroiodomethane as a potential candidate for parity violation measurements. *Phys Chem Chem Phys* 8:79–92
241. Bouchet A, Brotin T, Linares M, Aagren H, Cavagnat D, Buffeteau T (2011) Enantioselective complexation of chiral propylene oxide by an enantiopure water-soluble cryptophane. *J Org Chem* 76:4178–4181
242. Bouchet A, Brotin T, Linares M, Cavagnat D, Buffeteau T (2011) Influence of the chemical structure of water-soluble cryptophanes on their overall chiroptical and binding properties. *J Org Chem* 76:7816–7825
243. Petkovic M, Seddon KR, Rebelo LPN, Pereira CS (2011) Ionic liquids: a pathway to environmental acceptability. *Chem Soc Rev* 40:1383–1403
244. Sachnov SJ, Schneiders K, Schulz PS, Wasserscheid P (2010) Chirality transfer in mandelate ionic liquids through ion pairing effects. *Tetrahedron Asymmetry* 21:1821–1824
245. Bica K, Gaertner P (2008) Applications of chiral ionic liquids. *Eur J Org Chem* 3235–3250
246. Payagala T, Armstrong DW (2012) Chiral ionic liquids: a compendium of syntheses and applications (2005–2012). *Chirality* 24:17–53
247. Ding J, Welton T, Armstrong DW (2004) Chiral ionic liquids as stationary phases in gas chromatography. *Anal Chem* 76:6819–6822

248. Rizvi SAA, Shamsi SA (2006) Synthesis, characterization, and application of chiral ionic liquids and their polymers in micellar electrokinetic chromatography. *Anal Chem* 78: 7061–7069
249. Yuan LM, Han Y, Zhou Y, Meng X, Li ZY, Zi M, Chang YX (2006) (*R*)-*N,N,N*-Trimethyl-2-aminobutanol-bis(trifluoromethane-sulfon)imidate chiral ionic liquid used as chiral selector in HPCE, HPLC, and CGC. *Anal Lett* 39:1439–1449
250. Wasserscheid P, Boesmann A, Bolm C (2002) Synthesis and properties of ionic liquids derived from the “chiral pool”. *Chem Commun* 200–201
251. Ishida Y, Miyauchi H, Saigo K (2002) Design and synthesis of a novel imidazolium-based ionic liquid with planar chirality. *Chem Commun* 2240–2241
252. Ishida Y, Sasaki D, Miyauchi H, Saigo K (2006) Synthesis and properties of a diastereopure ionic liquid with planar chirality. *Tetrahedron Lett* 47:7973–7976
253. Bwambok DK, Marwani HM, Fernand VE, Fakayode SO, Lowry M, Negulescu I, Strongin RM, Warner IM (2008) Synthesis and characterization of novel chiral ionic liquids and investigation of their enantiomeric recognition properties. *Chirality* 20:151–158
254. Bwambok DK, Challa SK, Lowry M, Warner IM (2010) Amino acid-based fluorescent chiral ionic liquid for enantiomeric recognition. *Anal Chem* 82:5028–5037
255. Gonzalez L, Altava B, Bolte M, Burguete MI, Garcia-Verdugo E, Luis SV (2012) Synthesis of chiral room temperature ionic liquids from amino acids – application in chiral molecular recognition. *Eur J Org Chem* 4996–5009
256. Altava B, Barbosa DS, Isabel Burguete M, Escorihuela J, Luis SV (2009) Synthesis of new chiral imidazolium salts derived from amino acids: their evaluation in chiral molecular recognition. *Tetrahedron Asymmetry* 20:999–1003
257. Tabassum S, Gilani MA, Wilhelm R (2011) Imidazolium sulfonate and sulfamate zwitterions as chiral solvating agents for enantiomeric excess calculations. *Tetrahedron Asymmetry* 22:1632–1639
258. De Rooy SL, Li M, Bwambok DK, El-Zahab B, Challa S, Warner IM (2011) Ephedrinium-based protic chiral ionic liquids for enantiomeric recognition. *Chirality* 23:54–62
259. Winkel A, Wilhelm R (2010) New chiral ionic liquids based on enantiopure sulfate and sulfonate anions for chiral recognition. *Eur J Org Chem* 5817–5824
260. Kumar V, Pei C, Olsen CE, Schaeffer SJC, Parmar VS, Malhotra SV (2008) Novel carbohydrate-based chiral ammonium ionic liquids derived from isomannide. *Tetrahedron Asymmetry* 19:664–671
261. Yu S, Lindeman S, Tran CD (2008) Chiral ionic liquids: synthesis, properties, and enantiomeric recognition. *J Org Chem* 73:2576–2591
262. Li M, Gardella J, Bwambok DK, El-Zahab B, de Rooy S, Cole M, Lowry M, Warner IM (2009) Combinatorial approach to enantiomeric discrimination: synthesis and ¹⁹F NMR screening of a chiral ionic liquid-modified silane library. *J Comb Chem* 11:1105–1114
263. Folmer-Andersen JF, Kitamura M, Anslyn EV (2006) Pattern-based discrimination of enantiomeric and structurally similar amino acids: an optical mimic of the mammalian taste response. *J Am Chem Soc* 128:5652–5653
264. Zhu X, Jiang J, Lei X, Chen X (2012) Rapid determination of enantiomeric excess of protected amino acids by catalytic amounts of chiral reagent. *Anal Methods* 4:1920–1923
265. Prabhu UR, Suryaprakash N (2010) Selective homonuclear decoupling in ¹H NMR: application to visualization of enantiomers in chiral aligning medium and simplified analyses of spectra in isotropic solutions. *J Phys Chem A* 114:5551–5557
266. Nath N, Kumari D, Suryaprakash N (2011) Application of selective F1 decoupled ¹H NMR for enantiomer resolution and accurate measurement of enantiomeric excess at low chiral substrate/auxiliary concentration. *Chem Phys Lett* 508:149–154
267. Pirkle WH, Sikkenga DL (1975) Use of achiral shift reagents to indicate relative stabilities of diastereomeric solvates. *J Org Chem* 40:3430–3434

268. Shundo A, Labuta J, Hill JP, Ishihara S, Ariga K (2009) Nuclear magnetic resonance signaling of molecular chiral information using an achiral reagent. *J Am Chem Soc* 131: 9494–9495
269. Labuta J, Ishihara S, Shundo A, Arai S, Takeoka S, Ariga K, Hill JP (2011) Chirality sensing by nonchiral porphines. *Chem Eur J* 17:3558–3561
270. Shoji Y, Tashiro K, Aida T (2006) Sensing of chiral fullerenes by a cyclic host with an asymmetrically distorted π -electronic component. *J Am Chem Soc* 128:10690–10691
271. Shoji Y, Tashiro K, Aida T (2008) Chirality sensing of fullerenes using cyclic hosts having a chiral *N*-substituted porphyrin: a remote substituent effect. *Chirality* 20:420–424
272. Hanna GM (2006) NMR regulatory analysis: enantiomeric purity determination for (*R*)-(-)-desoxyephedrine and antipode methamphetamine. *Pharmazie* 61:188–193
273. Casy AF (1967) Applications of nuclear magnetic resonance spectroscopy in medicinal and pharmaceutical chemistry. *J Pharm Sci* 56:1049–1063
274. Holzgrabe U (2010) Quantitative NMR spectroscopy in pharmaceutical applications. *Prog Nucl Magn Reson Spectrosc* 57:229–240
275. Rao RN, Ramachandra B, Santhakumar K (2012) Evaluation of (*R*)-(-)- α -methoxyphenylacetic acid as a chiral shift reagent for resolution and determination of *R* and *S* enantiomers of modafinil in bulk drugs and formulations by ^1H NMR spectroscopy. *Chirality* 24:339–344
276. Nunez-Agüero C-J, Escobar-Llanos C-M, Diaz D, Jaime C, Garduno-Juarez R (2006) Chiral discrimination of ibuprofen isomers in β -cyclodextrin inclusion complexes: experimental (NMR) and theoretical (MD, MM/GBSA) studies. *Tetrahedron* 62:4162–4172

Chiral Sensor Devices for Differentiation of Enantiomers

Kyriaki Manoli, Maria Magliulo, and Luisa Torsi

Abstract Differentiation of enantiomers remains one of the most attractive and important research areas in analytical chemistry due to its impact on pharmaceutical, chemical, biotechnology, and food industries. For a long time chiral separation techniques, such as high performance liquid chromatography (HPLC), gas chromatography (GC), and capillary electrophoresis (CE), have represented the gold standard for the separation and determination of enantiomers. These techniques, besides being time consuming and expensive, are also not suitable for real time analysis. Therefore, the development of fast and reliable chiral sensors remains a challenge to achieve on-line analysis of enantiomers in both gas and liquid samples. The scope of this chapter is to provide an overview on the basic functioning principles, as well as on the performance level, of solid-state sensing devices for enantiomers differentiation. Particular attention is paid to work providing a set of analytical figures of merit (sensitivity, repeatability, reproducibility, limit-of-detection, etc.) as well as to studies involving miniaturized (or miniaturizable) analytical devices that can deliver real-time, on-line, and label-free information on chiral compounds.

Keywords Chiral sensors · Enantiomeric differentiation · Molecular recognition · OFET sensors · Real-time monitoring

Contents

1	Introduction	135
2	Electrochemical Sensors	136
2.1	Potentiometric Sensors	137
2.2	Voltammetric Sensors	143

3	Gravimetric-Mass Sensors-Resonators	149
3.1	QCM Devices Based on Cyclodextrins	150
3.2	QCM Devices Based on Molecular Imprinted Polymers	153
3.3	QCM Devices Based on Biological Recognition Elements	155
3.4	Other Approaches Used for QCM Sensors Development	157
4	Electrical Sensors	158
4.1	Chemiresistors	158
4.2	Organic Field Effect Transistors	159
4.3	Chemocapacitors	161
5	Optical Sensors	165
5.1	Surface Plasmon Resonance (SPR) Sensors	165
5.2	Reflectometric Interference Spectroscopy-Based Sensors	168
6	Summary, Conclusions, and Outlook	170
	References	170

Abbreviations

AFM	Atomic force microscopy
Ala	Alanine
Apt	Aptamer
APTES	3-Aminopropyltriethoxysilane
Asp	Aspartic acid
CD	Cyclodextrins
CLEP	Chiral ligand exchange potentiometry
CSA	Camphor sulfonic acid
CV	Cyclic voltammetry
Cy	Cysteine
DOPA	Dopamine
DPV	Differential pulse voltammetry
EIS	Electrochemical impedance spectroscopy
GC	Gas chromatography
Glu	Glutamic acid
GSA	Goat serum albumin
Hcy	Homocysteine
His	Histidine
HSA	Human serum albumin
ISE	Ion-selective electrode
ISFET	Ion-selective field effect transistor
ITO	Indium tin oxide
MA	Mandelic acid
MIP	Molecular imprinted polymer
MPTMS	(3-Mercaptopropyl)trimethoxysilane
OCD	Optical circular dichroism
OFET	Organic film effect transistor
OTS	Octadecyltrichlorosilane
PDMS	Polydimethylsiloxane

PET	Polyethyleneterephthalate
PPE	Poly(phenylenethynylene)
PPy	Poly(pyrrole)
PVC	Polyvinylchloride
QCM	Quartz crystal microbalance
RbSA	Rabbit serum albumin
SAM	Self-assembled monolayer
Try	Tryptophan
TSMR	Thickness shear mode resonator
Tym	Tyrosinamide
Tyr	Tyrosine

1 Introduction

The majority of metabolic and regulatory processes conducted by biological systems are closely related to stereochemistry. Therefore chiral molecules are involved in numerous enzymatic reactions, guest-host interactions, and several other biological phenomena [1]. Moreover, living organisms behave mostly in an enantioselective manner. For this reason, the human organism can differentiate the different enantiomers of a racemic drug, and, while one enantiomer may produce the desired therapeutic activities, the other may be inactive or could cause even undesired effects [2]. Thus the ability to differentiate the two enantiomers of a chiral molecule and to determine its enantiomeric purity is rather important in drug development. Enantiomeric purity is also relevant to the agrochemical industries since several chiral pesticides appear to have different impacts on the environment [3, 4]. Organoleptic characteristics of edibles are related to stereochemistry as well since olfactory and taste receptors are chiral. For instance, the enantiomers of carvone are the primary odor constituents of caraway and spearmint. Most of the natural amino acids have a bitter taste, while their enantiomers are sweet [5]. In this respect, it is essential to develop the technology for analysis and separation of racemic mixtures. Moreover, research on enantiomeric differentiation can lead to a better understanding of the mechanisms of chiral recognition of biological systems and to further development of useful molecular devices for biomedical and environmental applications.

Enantiomers can be differentiated only in a chiral environment. Chiral recognition is based on enantiospecific interactions between a chiral selector and the enantiomers resulting in transient diastereomeric complexes. The equilibrium constant for the formation or dissolution of the complex has to be different for two enantiomers in order to be differentiated [6]. The formation of the complexes is related to intermolecular non-covalent interactions such as ionic, ion-dipole or dipole-dipole, hydrogen bonding, van der Waals, and π - π interactions. Due to the structural variety of chiral selectors, steric interactions contribute to the chiral recognition processes as well. The “three points binding” model [7] and the

“lock-key” rule [8] are simplified tools proposed so far for the interpretation of the formation of diastereomeric complexes and the resulting enantioselectivity [9].

There is a multitude of compounds available that can be used as chiral selectors of natural or synthetic origin [10]. Receptors like polysaccharide derivatives [9, 11, 12], cyclodextrins (CD) [13], proteins and antibodies [9], aptamers [14, 15], molecular imprinted polymers (MIPs) [9, 16], helical [17, 18] and conducting polymers [19], crown ethers [20], calixarenes [21, 22], and resorcinarenes [23] are some of the most frequently used chiral selectors in conventional separation techniques as mobile/or stationary phase and background electrolytes or as recognition elements in transducer-based sensors.

Enantiomeric differentiation by using sensors is an alternative method that allows real time analysis, low cost instrumentation, and almost zero waste of expensive reagents. Chiral sensors based on different transduction principles have been utilized [24]. Such devices could allow, for instance, the direct monitoring of the enantiomeric purity in asymmetric synthesis, rendering this approach appealing for industrial scale production of an enantiopure molecule [25]. Besides, a sensor can also act as a fast, low cost method of screening stationary phases used in chromatographic columns for the separation of enantiomers [26]. Enantioselective chemical microsensors have also been proposed for investigating extraterrestrial homochirality in space [27].

A crucial parameter for the development of a reliable sensing system is the selection and functionalization of the chiral recognition element on the transducer. Moreover, binding dynamics and kinetics of complex molecules on complex surfaces are not easily quantitatively understood in terms of interactions, adsorption sites, electron charge transfer, etc.; thus chiral sensing is a difficult task and still under development.

The purpose of this chapter is to provide an overview of the basic functioning principles, as well as of the performance level, of solid-state sensing devices for differentiation of enantiomers in both liquid or gas phase. The focus is to outline the chiral selectors used for enantioselective sensors development as well as to describe the specific features and the analytical performance of sensors based on different transduction principles such as electrochemical, piezoelectric, electronic, and label-free optical devices. A critical examination of such technologies will be provided too.

2 Electrochemical Sensors

Electrochemical sensors are considered as the most reliable alternative of conventional high resolution chromatographic techniques to be used for enantiomeric differentiation and detection. The main advantage of these transducers is that they can provide simple means for interfacing, at a molecular level, the recognition element with the signal transduction element. The high sensitivity, coupled with their inherent miniaturization, small volume consumption, low power requirements,

and independence of sample purity, renders electrochemical sensors excellent candidates for molecular recognition sensing. However, short life time and the need for a reference electrode have so far impaired their full integration into a CMOS system.

Basically the structure of an electrochemical sensor resembles an electrochemical cell which employs a two- or three-electrode arrangement. According to the measured electrical parameter, e.g., potential difference, current, they are categorized into two types. If the difference of two potentials is measured one refers to potentiometric sensors. Voltammetric and amperometric sensors involve measuring current.

The use of electrochemical sensors for chiral differential detection has been reviewed up to 2008 [6, 28, 29]; therefore only more recent contributions will be discussed, providing an overall evaluation of this class of device performance.

2.1 Potentiometric Sensors

A potentiometric sensor reads an electrochemical potential against a reference electrode at equilibrium. According to the Nernst equation, the sensor's potential is related to the ion activity normalized to that of a standard solution. The voltage is proportional to the logarithm of the ionic activity. A potentiometric sensor constitutes a quite simple structure and can be easily miniaturized by thick-film screen printing technologies. It is especially suitable due to its simplicity, low cost, high reproducibility, and efficiency in large-scale production. Examples of potentiometric sensors are reported below.

2.1.1 Ion Selective Electrodes

An ion-selective electrode (ISE) is a potentiometric sensor that converts the activity of a specific ion dissolved in a solution into an electrical potential. It consists of two parts, an ion-sensitive membrane along with a reference electrode.

The enantioselectivity of the response of an ISE electrochemical sensor is achieved by the addition of a chiral selector interfaced with the electrode on which the interaction of the selector with the analyte is detected. The immobilization techniques include physical sorption, covalent binding, and the formation of self-assembled monolayers (SAMs). Plasticized polyvinyl chloride (PVC), glassy carbon paste, as well as conductive polymers are the most widespread types of membranes explored for the fabrication of ISEs for enantiomeric differentiation.

Maltodextrins with different dextrose equivalent (DE) have been integrated in carbon paste electrodes as chiral selectors for enantiomeric differentiation of several drugs. The different DE values result in maltodextrins of varying physico-chemical properties. A recent review on this topic has been reported by Stefan-van Staden et al. [12]. Enantioselective membrane carbon paste electrodes based on

maltodextrins have been proposed for detection of L-pipecolic acid (PA) [30], (S)-(+)-ibuprofen [31], (S)-(+)-flurbiprofen [32], L-proline [33], (S)-captopril [34], and (S)-perindopril [35]. Moreover, α -, β - and γ -cyclodextrins (CDs) as well as 2-hydroxy-3-trimethylaminopropyl- β -CD for enantiomeric analysis of (S)-flurbiprofen [36] and several angiotensin-converting enzyme inhibitors (e.g., (S)-captopril, (S)-pentopril, (S)-ramipril) have been reported during the last decade by Stefan-van Staden et al. [37, 38] and Aboul-Enein et al. [39]. In all cases, enantioselective coefficients $K_{S,R}^{\text{pot}}$ of 10^{-4} magnitude order were obtained.

The same constructions of a graphite paste sensor incorporated with macrocyclic antibiotics (i.e., vancomycin and teicoplanin) have been reported as enantioselective potentiometric sensors for the differentiation of pipecolic acid and carnitine enantiomers by Ratko et al. Carbon paste electrodes incorporated with vancomycin were shown to have Nernstian response with linearity from 1 nM to 1 mM of D-PA and neither linear nor Nernstian was the response for L-PA ($\log K_{L,D}^{\text{pot}} = 3.52$) [40]. With the use of teicoplanin, L-carnitine was differentiated with enantioselectivity coefficient $\log K_{L,D}^{\text{pot}} = 2.38$ [41]. The same macrocyclic antibiotics have been used for enantiomeric differentiation of L,D-methotrexate (Mtx) [42]. Vancomycin was employed as chiral selector for the L-enantiomer and teicoplanin for the D-enantiomer. A third electrode with modified teicoplanin with acetonitrile was also fabricated. The electrodes proposed proved to be successful for determination of enantiopurity of Mtx as a raw material in pharmaceutical tablets and injections. The potentiometric enantioselectivity coefficients were $K_{L,D}^{\text{pot}} = 5.4 \times 10^{-3}$ for the vancomycin-based sensor and $K_{D,L}^{\text{pot}} = 6.2 \times 10^{-3}$ for the modified teicoplanin sensor.

In addition, different potentiometric and amperometric microsensors based on porphyrins and polymer surfactants have been proposed by Stefan-van Staden et al. for differentiating the enantiomers of PA in biological samples [43]. The amperometric sensors served as quality detectors and the potentiometric sensors were used for the quantitative enantiomeric analysis. Carbon and diamond paste electrodes modified with Zn-5,10,15,20-tetra(4-sulfophenyl)porphyrin (ZnTSPP) and 5,10,15,20-tetra(4-sulfophenyl)porphyrin (TSPP) and polysodium *N*-undecanoyl-L-vanilate (SUV) and polysodium *N*-undecanoyl-L-leucylvanilate (SULV) were tested as enantioselective membrane electrodes. The sensors exhibited a linear response with concentrations in a range from 1 nM to 1 mM for the L-PA and 10 pM to 0.1 mM for the D-PA. The best potentiometric enantioselective coefficients K^{pot} obtained from the ZnTSPP and SUV carbon paste sensors were 3.5×10^{-3} for the D-PA and 3.8×10^{-3} for the L-PA, respectively.

The enantioselectivity of different types of ion selective membranes containing different chiral ionophores was investigated recently by Kaniewska et al. [44]. More specifically, PVC membranes with modified β -CDs selectors by using different plasticizers were prepared so as to study the effect of the plasticizer's nature in the performance of the sensor. The sensors were tested upon different concentrations of 1,4-nitrophenylethylamine enantiomers. From the results

obtained it was shown that the nature of plasticizer affects the selectivity of the sensor and thus can improve the figures of merit of the device. In addition, a comparison between PVC and carbon paste membrane was made, using the same chiral selector (teicoplanin) suitable for binding carnitine. It was shown that a carbon paste-based electrode had the ability to discriminate the enantiomers tested, exhibiting enantioselectivity coefficient ($\log K_{L,D}^{\text{pot}} = 0.42$) similar to the plasticized PVC membrane ($\log K_{L,D}^{\text{pot}} = 0.38$). However, the latter exhibited longer life time and good reproducibility.

The use of molecular imprinted polymers (MIPs) as sensitive membranes has become rather popular since selective, reversible, long-term stable, and low cost electrodes can be fabricated. Such artificial receptors have attracted much attention since they are considered as good substitutes for natural selectors. MIPs have been used as chiral coatings in different types of transducers [16]. They are polymeric films prepared in the presence of a template-target analyte molecule. Briefly, the MIP synthesis consists of two steps. First the template molecules are mixed with the monomer, and after the polymerization they are removed, leaving binding sites of specific shape and size capable of rebinding the template molecule. Two different imprinting strategies are used: (1) covalent [45] and (2) non-covalent [46] template polymerization.

A recent example is a potentiometric sensor for the discrimination of phenylalanine (Phe) enantiomers [47]. Poly[2-(*N*-carbazolyl)ethyl methacrylate-*co*-methacrylic acid]s (PCEMMAs) were formatted on indium tin oxide (ITO) glass by electropolymerization. In this MIP sensing film, the recognition sites, the insulating polymethacrylic acid (PMAA), were covalently bonded to the conducting polycarbazole which is used as signal transfer interface between recognition layer and electrode. Although both enantiomers were used as template molecules for the preparation of MIPs, only the *L*-Phe imprinted sensor exhibited good selectivity for the respective enantiomer with an enantioselectivity coefficient $K_{L,D}^{\text{pot}} = 5.75 \times 10^{-4}$ and 1.37 μM limit of detection (LOD).

In addition, numerous studies are found in the literature regarding chiral sensing using chiral ligand exchange potentiometry (CLEP) [48, 49]. Ligand exchange involves the reversible formation of diastereomeric complexes of transition metal ions (i.e., Cu, Zn) with chiral ligands (e.g., amino acids and derivatives) [50]. When mixing an enantiomer with a metal ion, an enantiomeric complex is formed in solution. In the presence of another competitive chiral substance (e.g., a chiral receptor) the former complex reaction equilibrium is affected by the formation of diastereomeric complexes. Due to conformational flexibility of the molecules and/or steric interactions, desirable stereoselectivity can occur. This technique is successfully used in HPLC and CE for enantiomeric separation [51, 52]. Impressive stereoselectivity has been achieved with potentiometric sensors as well. Therefore some recent representative examples will be discussed in the following paragraphs.

A novel potentiometric sensor exhibiting high enantioselectivity and recognition ability to discriminate between enantiomers of the same amino acid (aspartic) but also different amino acids was reported by Zhou et al. [53]. An octadecyltrichlorosilane

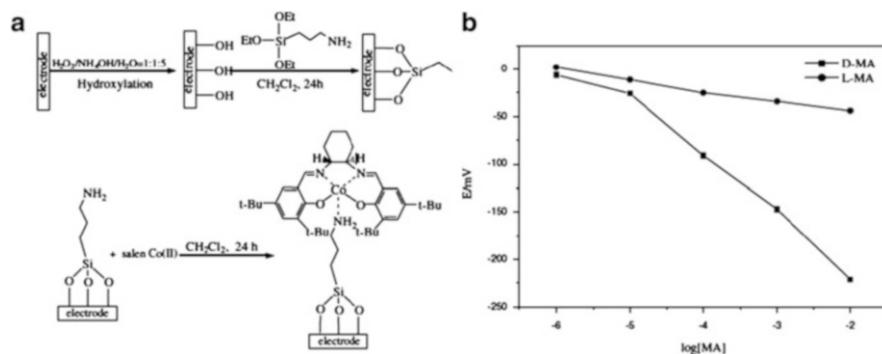


Fig. 1 (a) Basic steps for the immobilization of chiral salen Co(II) complex onto a conductive surface of ITO electrode. (b) Calibration curves of salen Co(II)-modified ITO electrode for D-MA and L-MA at various concentrations. Reprinted with permission from [54], © 2010 The Chemical Society of Japan

layer (OTS) was covalently bound on an ITO electrode in the presence of a chiral ligand, *N*-carbobenzyloxy-*L/D*-aspartic acid (*N*-CBZ-*L/D*-Asp). The recognition mechanism relies on the chiral ligand exchange reaction at the *N*-CBZ-*L/D*-Asp modified ITO-coated electrode. *N*-CBZ-*L*-Asp undergoes ligand exchange with the enantiomeric coordination complexes of $[\text{Cu}(\text{II})(\text{D-Asp})_2]$ or $[\text{Cu}(\text{II})(\text{L-Asp})_2]$ to form a diastereomeric complex $[\text{D-Asp})\text{Cu}(\text{II})(\text{N-CBZ-L-Asp})]$ or $[(\text{L-Asp})\text{Cu}(\text{II})(\text{N-CBZ-L-Asp})]$ on the electrode surface. The copper complexes with each enantiomer co-exist in the analyte solution. Potentiometric enantioselectivity coefficients $K_{\text{D,L}}^{\text{pot}}$ were 4.0×10^{-5} and 5.0×10^{-5} for the D-Asp and L-Asp respectively, corresponding to an exceptional enantioselectivity.

The differentiation of mandelic acid (MA) enantiomers was successfully realized by using an ISE potentiometric sensor. The sensor was fabricated by immobilizing an ionophore chiral salen Co(II) complex on an ITO electrode surface modified with a SAM of 3-aminopropyl-triethoxysilane (APTES). The ITO surface was first subjected to a hydroxylation procedure to create $-\text{OH}$ anchoring sites for the APTES that in turn provided an ordered layer of amino groups for the Co(II) chiral selector to bound (Fig. 1a). The modified electrode surface was exposed to different concentrations of mandelic acid enantiomers (L-MA and D-MA) and the relevant calibration curves are reported in Fig. 1b. Enantiomeric differential detection is apparent in a quite wide concentration range with the Co(II) complex forming a more stable diastereomer with D-MA [54]. Similarly, a chiral salen Mn(III) complex was also capable of MA differential detection with the L-MA being the preferred enantiomer in this case [55]. A PVC membrane with different plasticizers and different amounts of salen were prepared. The effects of several parameters such as nature of plasticizer, concentration of ionophore, and pH were investigated in order to evaluate and optimize the performance of the sensor fully. Good figures of merit in both studies are provided with the detection limit, being in the micromolar range, and the enantioselectivity coefficient ($\log K^{\text{pot}}$) being -3.21 and -4.02 .

Moreover, high enantioselectivity coefficients values and low detection limit ($\sim 10^{-1}$ μM) for amino acid enantiomers, namely tryptophan (Try) and histidine (His), were obtained with a potentiometric sensor. An electroactive ion-pair complex composed by a metallocarbonate anion ($[\text{Co}(\text{C}_2\text{B}_9\text{H}_{11}_2)]^-$) and the protonated target enantiomer was implemented on a plasticized PVC membrane. As previously shown, this anion receptor can be used for sensing protonated nitrogen-containing molecules. Best enantioselectivity coefficients ($\log K^{\text{pot}}$) were achieved for D-Try (-3.79) and D-His (-5.79) [56].

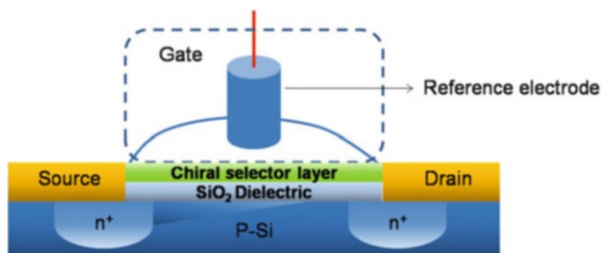
As already mentioned, electrochemical sensors can act as appropriate platforms for biosensing. Several electrochemical biosensors have been commercialized. The use of biological recognition elements (e.g., proteins, antibodies) for selective binding and thus enhanced sensitivity and selectivity can be realized for chiral discrimination as well. The enantioselective behavior of human serum albumin (HSA) has been reported. Selective potential response of HSA-modified ITO electrode was observed for tryptophan (Try). HSA was immobilized on ITO electrode surface modified with disuccinimidyl suberate (DSS). It was shown that the potential of the ITO electrode shifted in the negative direction after injecting the Try solution and this response was found different at all concentrations for each enantiomer. Furthermore, negative response was observed even if the ITO electrode was just DSS-modified without the addition of the protein but the response was the same for the two enantiomers. According to the authors, the presence of the protein prevents the L-Try to interact with DSS. The stronger binding affinity between L-Try and HSA results in the smaller negative potential shift as compared to D-Try [57].

Another approach for discriminating amino acids was adopted by Yin et al. [58]. Conducting de-doped polyaniline was used as the ion selective membrane of the electrochemical sensors. Optical active PANI nanofibers were synthesized by electropolymerization of aniline in aqueous solution containing (1S)-(+)- or (1R)-(-)-camphor sulfonic acid (CSA) and was uniformly coated on glassy carbon electrodes. The potentiometric enantioselective coefficient for the L-Phe was 0.2. The response of the sensor to each enantiomer revealed that (-)-PANI had a higher affinity for entrapping L-Phe and the (+)-PANI for the D-enantiomer.

2.1.2 Ion Sensitive Field Effect Transistors

A field effect transistor (FET) is a transducer in which the flow of current between two (source and drain) of its terminals is controlled by an applied voltage at a third terminal (gate). An ISFET is basically a metal oxide semiconductor field effect transistor (MOSFET) where the gate is an ion-sensitive electrode. From an analytical chemistry point of view, in the case of an ISFET the metal gate is replaced by a chemically sensitive membrane. The electric path is closed by a reference electrode and both are immersed in a conductive solution. Change of the gate charge by a chemical modification or chemical recognition event on the membrane alters the gating metal electrochemical potential and this directly impacts on the the transistor

Fig. 2 Schematic presentation of ISFET device bearing a chiral selector



threshold voltage, eventually affecting the drain current. A schematic illustration of the ISFET is shown in Fig. 2. ISFET-based sensors are rather popular among the transducers utilized for chiral and biosensing applications and generally sensing in liquid media.

A representative example of enantiomeric differentiation using ISFET-based sensors is the work of Lahav et al. [59]. ISFET-based sensors were employed for enantiomeric differentiation of three chiral organic acids (i.e., (*R/S*)-methylferrocene carboxylic acid, (*R/S*)-2-phenylbutanoic acid, and (*R/S*)-2-phenylpropanoic acid). Each enantiomer was used as template molecule and was imprinted in thin TiO₂ films on the gate surface of the ISFET device. More specifically, titanium(IV) butoxide-carboxylate complex is polymerized on the gate surface by hydration. The carboxylate units are removed with ammonia solution, leaving stereoselective sites for the respective enantiomer. Moreover, the hydrolysis of the carboxylate generates Ti-OH groups on the surface that control the gate potential. Upon interaction with the carboxylic acid, an amount of -OH groups is replaced by ester groups, thus altering the gate potential. Apart from high enantioselectivity of each imprinted gate for the corresponding enantiomer, the sensors exhibited high specificity among the (*R*)-enantiomers of 2-phenylbutanoic acid and 2-phenylpropanoic acid. The stereochemical specificity was attributed to the different structural configuration of each imprinted film that required appropriate orientation and size of the analyte to bind the Ti-OH.

More recently, Mastunaga et al. [60] reported the differentiation of alanine (Ala) enantiomers in solution by employing homocysteine (Hcy) SAM on the surface of the gate sensitive electrode of an ISFET-based transducer. An n-type FET was employed and, in order to minimize the current leakage (I_G) between the gold gate film and SiO₂, SAM of (3-mercaptopropyl)trimethoxysilane (MPTMS) was formed on the SiO₂ as an adhesive and insulating layer. The functionalization of the gate electrode is illustrated in Fig. 3a. Enantioselective formation of diastereomeric Cu complexes on both *L*- and *D*-Hcy SAM modified gate surface with the respective Ala enantiomer was observed. In each case the complex formation on the modified surface leads to charge accumulation on the gate and thus change of the FET threshold voltage. Moreover, the sensor was able to detect the excess of the one enantiomer in the mixture (Fig. 3b-d). In an additional study, the dependence of the ISFET response on the analyte amino acids, the central metal ions involved in complex formation, and the solution pH was further investigated [61].

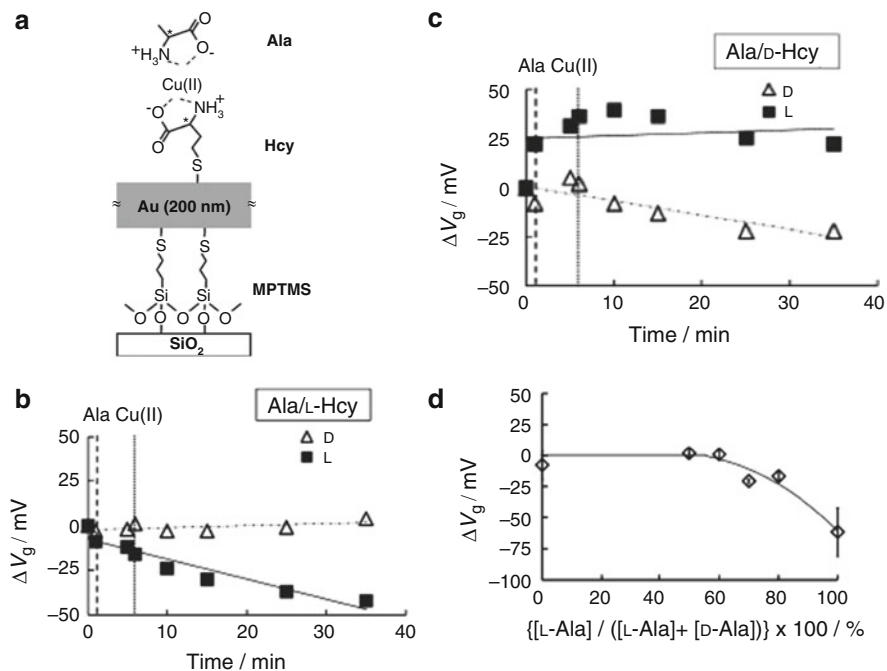


Fig. 3 (a) Illustration of Hcy/Au/MPTMS/SiO₂ and Cu complex formation on Hcy. Change of the gate potential with time after addition of Ala and Cu(II) for (b) L-Hcy gate and (c) D-Hcy gate. (d) Change of gate potential of L-Hcy sensor in different percentage composition ratio of L-Ala in the enantiomeric mixture. The total concentration was kept constant and the values depicted are taken 35 min after the beginning of measurement. Reprinted with permission from [60], © 2010 Elsevier

2.2 Voltammetric Sensors

The current–potential (I – V) relationship of an electrochemical cell provides the basis for voltammetric sensors. The most popular electroanalytical technique used at solid electrolytes is cyclic voltammetry. In this technique the applied potential is linearly cycled between two potentials. In one half of the cycle the oxidized form is reduced and in the other it is reoxidized to its original form. Differential pulse voltammetry (DPV) and electrochemical impedance spectroscopy (EIS) are utilized as well.

Cyclic voltammetry (CV) and electrochemical impedance spectroscopy (EIS) were used to investigate the enantioselective interaction between L-methotrexate (L-Mtx) and penicillamine (Pen). L-Mtx was chosen as a chiral selector to recognize Pen enantiomers using Zn(II) as central metal ion based on chiral ligand exchange through formation of complexes. The chiral selector was immobilized by the self-assembly technique. The L-Mtx modified electrode was able to recognize selectively the D-Pen enantiomer due to preferable formation of the [(L-Mtx)Zn(II) (D-Pen)] complex. The change of peak current had a linear relation with

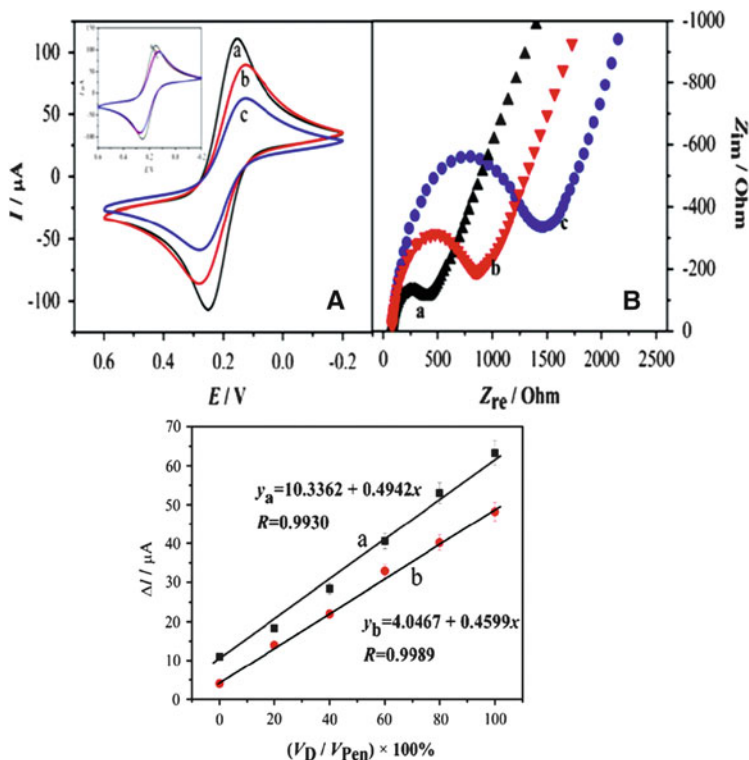


Fig. 4 *Top* (A) Cyclic voltammogram, (B) EIS of L-Mtx-Au (a) bare and after interaction with (b) L-Pen + Zn(II) and (c) D-Pen + Zn(II). *Bottom* Change of the peak currents of L-Mtx-Au in different enantiomeric mixtures expressed as D-Pen percentage composition ratio in the presence of Zn(II) at different concentrations: (a) 5 mM and (b) 2 mM. Reprinted from [62], © Springer-Verlag 2012, with kind permission from Springer Science and Business Media

concentration of L-Pen and D-Pen allowing the differentiation of the two enantiomers in a mixture (Fig. 4) [62]. The same principle was used for the differentiation of MA enantiomers in the presence of Zn(II) ions on an L-cysteine (L-Cys) self-assembled gold electrode. In this case, the sensor showed higher response in the presence of the (R)-enantiomer [63].

The use of γ -globulin protein as enantioselective surface for MA discrimination has been reported as well. The protein was integrated on a glassy carbon electrode (GCE). The immobilization of γ -globulin on the GCE was realized in two steps. First, gold nanoparticles were electrodeposited on the surface of the electrode so as to provide a suitable large and rough surface for the adsorption of the biomolecules. The electrode was immersed and left overnight in γ -globulin solution. The surface of the modified electrode was characterized by EIS. Moreover, DPV and AFM and QCM sensing measurements were carried out to investigate the enantioselective behavior of the protein. UV-vis spectroscopy was used to monitor and interpret the

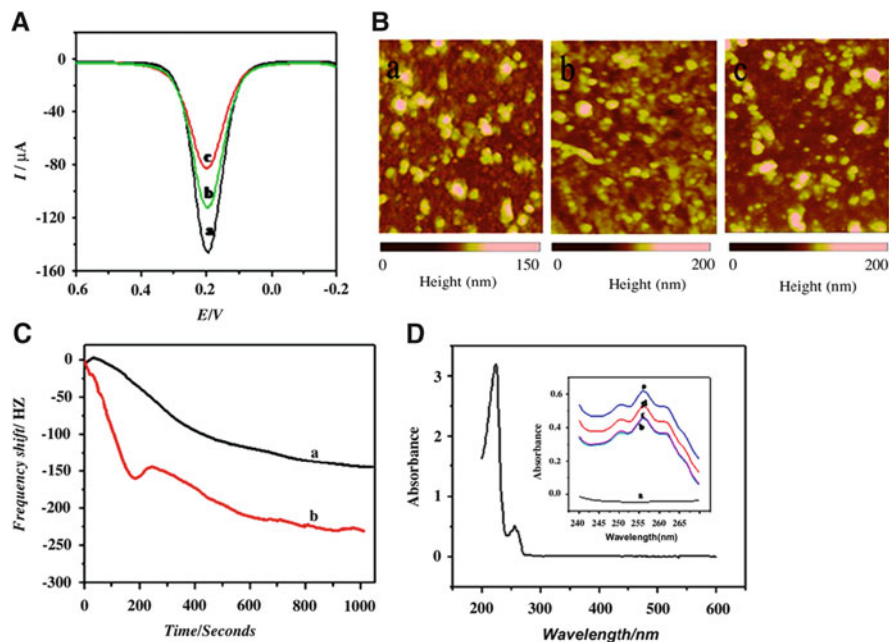


Fig. 5 (A) I - V curve of the electrochemical sensor using DPV of (a) bare γ -globulin/Au/GCE, and after exposure to (b) (*S*)-MA, and (c) (*R*)-MA. (B) AFM images of the electrode surface for (a) γ -globulin/Au/GCE, (b) (*R*)-MA/ γ -globulin/Au/GCE, and (c) (*S*)-MA/ γ -globulin/Au/GCE. (C) Response of the γ -globulin-gold coated QCM sensor vs time upon exposure to 1.25 mM (a) (*S*)-MA and (b) (*R*)-MA. (D) UV-vis spectra of MA; *insert*: the UV spectra of (a) γ -globulin, (b) (*S*)-MA, (c) (*R*)-MA, (d) (*S*)-MA + γ -globulin, and (e) (*R*)-MA + γ -globulin. Reprinted with permission from [64], © 2012 Elsevier

recognition mechanism of MA and γ -globulin. All results revealed that that the protein has higher affinity towards (*R*)-MA. This behavior was attributed to stronger interactions (e.g., hydrogen bonding, π - π interactions) of the (*R*)-MA enantiomer with γ -globulin due to more suitable molecular configuration than the (*S*)-enantiomer (Fig. 5) [64].

The enantioselective binding ability of HSA has been explored using cyclic voltammetry. Gold electrodes were modified with both the enantiomers of *N*-isobutyryl-cysteine (NIBC). The L-NIBC modified surface exhibited stronger affinity when exposed to HSA molecules than the D-NIBC modified surface, suggesting that the molecular configuration of L-NIBC leads to preferential adsorption of HSA on the electrode as compared to D-NIBC [65].

Enantioselective tailor made nucleic aptamers are an attractive alternative for discriminating and quantifying chiral compounds. Due to their natural chirality and structure flexibility, they exhibit high enantioselectivity. A new method was proposed by Challier et al. [15], based on the difference of diffusion rates between the target enantiomer and the aptamer/enantiomer complex. Enantioselective detection of trace amounts of L- and D-tyrosinamide (Tym) by D- and L-deoxyribooligonucleotide

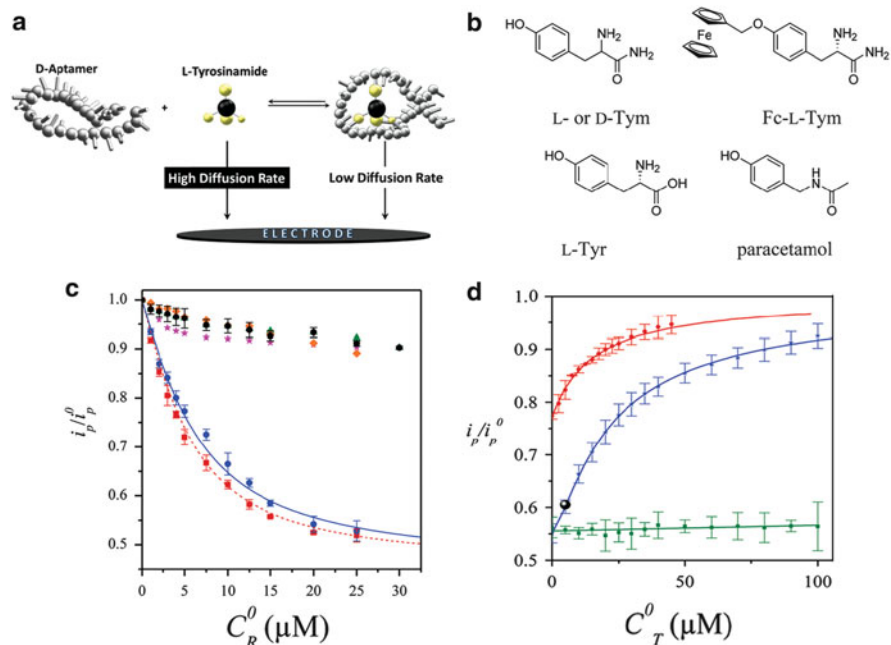


Fig. 6 (a) Principle of operation of the electrochemical assay. (b) Molecular structures of L and D-Tym, Ferrocene-labeled L-Tym, L-Tyrosine (L-Tyr) and Paracetamol. (c) Normalized catalytic peak current vs aptamer concentration for all aptamer couples: (blue) L-Tym/(D)-Apt49, (red) D-Tym/L-Apt49, (black) D-Tym/D-Apt49, (pink) L-Tyr /D-Apt49, (gold) paracetamol/D-Apt49, and (green) L-Tym/49-mer scramble oligonucleotide. (d) Competitive binding curves as the relative peak change in different concentrations of Tym (blue and red L-Tym, green D-Tym). The Fc-L-Tym concentration was 5 μM , whereas the D-Apt49 concentrations were $C_R = 10 \mu\text{M}$ for blue, green, and black and 3 μM for red points. (Black point): assay of 5 μM L-Tym in the presence of 5 mM D-Tym. Reprinted with permission from [15], © 2012 American Chemical Society

aptamer, respectively, was reported using CV. The general principle of the method is shown in Fig. 6a. Screen printed carbon paste electrodes placed on a polyethyleneterephthalate (PET) film, in order to reduce the solution volume for the analysis, were used. The electrodes were coated with BSA and electron transfer mediator couple ([OsIII/II(bpy)₃]^{3+/2+}) was used to avoid the passivation of the electrode. From the values of the catalytic peak current the diffusion coefficients in each case were evaluated. Each non-bound “free” enantiomer exhibited faster diffusion compared to the one bound to the aptamer receptor. Diffusion coefficients for free and bound L-Tym were determined and were in agreement with values in the literature. To examine the specificity as well as the enantioselectivity of the assay, binding experiments with the D-Tym enantiomer and two structurally related ligands (i.e., the L-tyrosine and paracetamol) were performed. In all cases, no current response changes were observed (Fig. 6b). The aptamer exhibited high enantioselectivity. Moreover, ferrocene labeled (Fc) L-Tym was synthesized and used in a competitive

assay experiment. The labeled compound L-Tym exhibited the same kinetic behavior with the respective non-labeled one. The enantioselectivity of the assay was examined using ferrocene labeled L-Tym and adding solutions containing the D-Tym enantiomer. No displacement of Fc-L-Tym from D-Apt by D-Tym could be observed over the 0–100 μM concentration range (Fig. 6d). Detection as low as 0.1% of the minor enantiomer in a non-racemic mixture was achieved [15].

PANI doped with either (*IR*)- or (*IS*)-camphorsulfonic enantiomers were also examined as sensors for dinoseb pesticide enantiomeric differentiation. The membrane was electropolymerized on a glassy carbon electrode (GCE). To prevent the degradation of the electrode, after each reductive scan and prior to the next redoping step the sensor was immersed in a stirred 0.1 M NaOH solution for 1 min. After fabrication optimization of the electrode, the sensors exhibited detection limit in the micromolar range for each selective electrode prepared [66].

Nanowires as enantioselective electrodes are also used in the construction of electrochemical sensors. Due to the high surface area of nanowires, more active binding sites are obtained compared to bulk films. In this way the sensitivity of the sensors could be enhanced. Molecularly imprinted size-monodispersed nanowires have been reported for enantioselective detection of phenylalanine. (*IR*)- and (*IS*)-camphorsulfonic acid doped PPy nanowires were fabricated by electrochemical polymerization on a Pt electrode. The CSA had a dual role: it was used both as a dopant for PPy and as template molecule. Faradaic impedance spectroscopy (FIS) was employed as technique for the enantioselective sensing. The conductivity of the nanowires increased due to doping caused from the selective binding of each enantiomer on the surface of the de-doped PPy. Each chiral MIP nanowire was able to differentiate the respective enantiomer. The L-CSA doped PPy exhibited stronger recognition ability for L-Phe compared to that of D-CSA for D-Phe. These results were confirmed by optical circular dichroism (OCD) measurements. The authors attributed this difference to the higher concentrations of anions in the L-Phe aqueous solution (higher pH) [67].

Monolithic polymer–carbon fibers were recently presented as electrochemical sensors for chiral recognition of Try enantiomers. In this case, a composite of carbon and nonconductive polymer was used for the formation of the MIP-fiber. The fiber becomes conductive due to the addition of carbon nanoparticles. In the scheme of Fig. 7, the protocol of the formation of MIP-carbon composite and the enantioselective binding of each enantiomer in the cavities of their respective MIPs are illustrated. Differential pulse anodic stripping voltammetry was used for the evaluation of the performance of the sensor. The sensor for L-Try was able to differentiate successfully the target molecule in the presence of other amino acids and in racemic mixtures in aqueous, biological, and pharmaceutical samples. The detection limit of L-Try was found to be 0.24 ng/mL [68]. As an expansion of this study, a detection limit down to 0.026 ng/mL of D- and L-Try was reported by the same research group [69]. This time the fiber served as micro-solid phase extraction media for the pre-concentration of the target enantiomer and as the sensitive electrode as well.

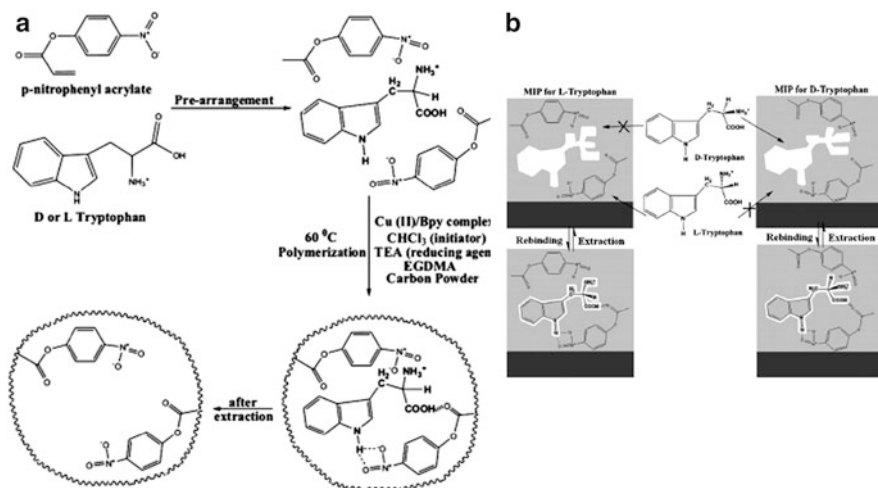


Fig. 7 (a) Schematic representation of the preparation of MIP-carbon composite. (b) Enantioselective binding of two enantiomers of Try in molecular cavities of their respective MIPs. Reprinted with permission from [68], © 2010 Elsevier

2.2.1 Amperometric Sensors

Another type of electrochemical sensors is represented by amperometric sensors. Specifically, in amperometric sensors a fixed potential is applied to the electrochemical cell, and a corresponding current, due to a reduction or oxidation reaction, is measured. This current can be used to quantify the species involved in the reaction.

Several biosensors in which enzymes are immobilized on the surface of the electrode have been reported for enantiomeric analysis. The enantioselectivity of oxidoreductases for organic acids, amino acids, and their derivatives is well known. The main disadvantages of enzyme receptors are the lack of regeneration of the electrode and the short life time. To overcome these drawbacks, electron transfer mediators are used to achieve recovery and addition of specific proteins is suggested for obtaining stability. The use of enzyme-based electrochemical sensors was reviewed recently by Trojanowicz et al. [6, 28] and Budnikov et al. [29]. Some representative examples are given below.

Amperometric enzyme-based sensors have been reported by Stefan et al. [70] for enantiomeric differentiation of (*R*)- and (*S*)-captopril using *L*- and *D*-amino acid oxidase (*L*-AAOD, *D*-AAOD), respectively. Each enantioselective electrode was fabricated by mixing each enzymatic solution with carbon paste. Chronoamperometric measurements were realized at +650 mV potential. The response of the *L*-AAOD sensor was found to be linear with concentration of the (*S*)-enantiomer in the range from 0.4 to 1.6 $\mu\text{mol/L}$ and with a detection limit at 0.2 $\mu\text{mol/L}$. The respective range of concentration of the (*R*)-enantiomer was from 0.12 to 0.95 $\mu\text{mol/L}$ with a detection limit at 15 nmol/L. The enantioselectivity coefficients pK_{amp} were 2.37 (*R/S*) and 2.5 (*S/R*). Similarly, mono- and bienzyme-based amperometric biosensors were developed to differentiate the two enantiomers (*D*, *L*) of

pipecolic acid (PA) [71]. The same enzymes were combined with horseradish peroxidase (HRP). Measurements in different potentials were carried out. The best enantioselectivity coefficient was obtained for the L-PA $pK_{amp} = 3.82$ at +400 mV from the L-AAOD + HRP sensor. The D-AAOD exhibited higher enantioselectivity coefficient for D-PA $pK_{amp} = 2.96$ at +130 mV. Moreover, enantioselective electrodes for detection of Mtx enantiomers (D,L) were developed using just the amino acid oxidases or different combinations of D- and L-AAOD with HRP and/or glucose oxidase. (Glox). Higher enantioselectivity was achieved using electrode fabricated with L-AAOD + HRP + Glox enzymes exhibiting $pK_{amp} = 3.09$ for the L-Mtx at +240 mV and with D-AAOD + HRP for the (D)-Mtx ($pK_{amp} = 2.91$ at +650 mV) [72]. In more recent published work of the same group, L-lysine oxidase was immobilized in diamond paste electrode [73]. The resulting electrode was investigated for enantioselective detection of the respective enantiomer of lysine. The measurements were held at +650 mV potential and exhibited linear response with the concentration in the range from 1 to 100 nmol/L and a 4 pmol/L limit of detection. The enantioselectivity coefficient pK_{amp} was 2.55. The proposed amperometric biosensors were successfully used for detecting each enantiomer in serum samples as well as in pharmaceutical compounds. In all the above cases the values of the enantioselectivity coefficients were determined using the mixed solution method. The ratio between the concentration of the main enantiomer and the other enantiomer (interfering compound) was 1:10.

Additionally, a competitive electrochemical assay for the discrimination/detection of saccharides using an imprinted electropolymerized matrix was recently developed by Granot et al. [74]. The polymer matrix was composed of phenol and 3-hydroxyphenylboronic acid. Boronic acid has the ability to form complexes with monosaccharides. Binding of boronic acid ligands with *cis*-diols leads to the formation of boronic complexes. The presence of these anchor ligands in the polymer matrix allows specific orientation of the respective saccharide and, along with the imprinted sites of each enantiomer in the polymer, enantioselectivity is possible. In each case, the target enantiomer competes with its analogous ferrocene modified saccharide which was utilized as a redox label (Fig. 8). The sensor was able to discriminate the two enantiomers (D, L) of glucose as well as different saccharides (i.e., D-glucose, D-mannose, and D-galactose).

3 Gravimetric-Mass Sensors-Resonators

Gravimetric/mass sensors are considered to be the leading platform among electronic sensors since they are capable of measuring sub-nanogram level changes, they exhibit long time stability, and have the ability to make real-time condensed-phase measurements. Quartz-crystal microbalances (QCMs), often called thickness shear mode resonators (TSMRs), and bulk acoustic wave (BAW) sensors have been thoroughly investigated for enantiomeric differentiation and detection.

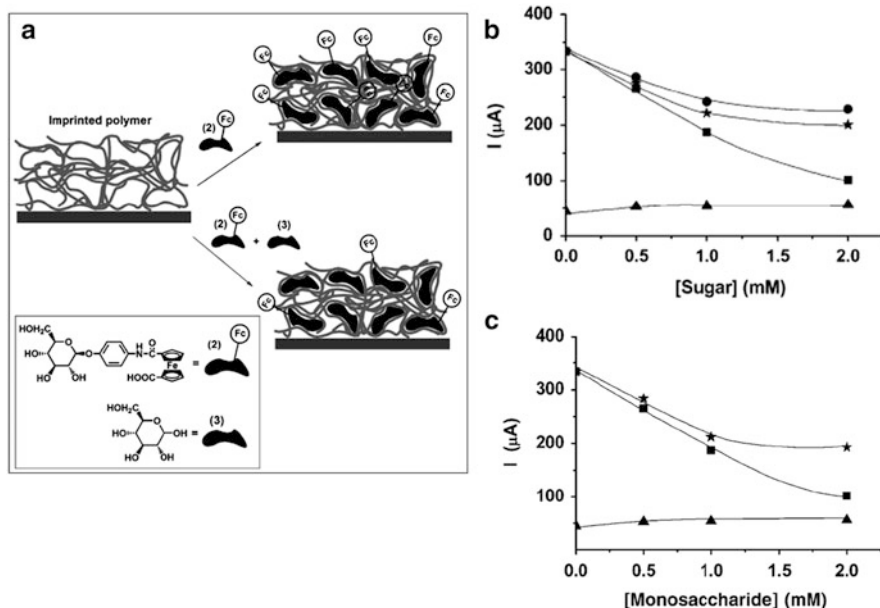


Fig. 8 (a) Illustration of the competitive assay for the detection of D-glucose using D-glucose-imprinted polymer. (b) Current change of D-glucose imprinted polymer (*squares*), non imprinted polymer (*triangles*) upon exposure to D-glucose, current change of D-glucose imprinted polymer exposed to D-mannose (*stars*), and D-galactose (*circles*), respectively. (c) Current change of D-glucose imprinted polymer upon exposure to L-glucose (*stars*), D-glucose (*squares*), and the change of current of non-imprinted polymer exposed at L-glucose (*triangles*). Reprinted from [74], © 2008 WILEY-VCH Verlag GmbH & Co. KGaA, Weinheim, with permission from John Wiley and Sons

QCM sensors are coated with enantioselective receptors films and the output signal of the coated sensor changes upon exposure to enantiomers. A quartz resonator consists of a resonator/piezoelectric quartz crystal and a sensing film coated on its surface. In Fig. 9 the structure of a QCM sensor is illustrated. Based on the piezoelectric phenomenon, the shift of the resonance frequency of QCM is proportional to the variations in mass of the sensing layer deposited on the electrode due to adsorption of analyte molecules onto the surface and/or absorption into the bulk of the material.

Herein, the latest achievements using gravimetric, mainly QCM, sensors, in the field of enantiomeric differentiation will be reviewed. The following section is divided based on the material utilized as chiral selector.

3.1 QCM Devices Based on Cyclodextrins

Cyclodextrins are considered to be efficient selectors for chiral sensing at interfaces. The molecule acts as host to various enantiomers. Parameters such as

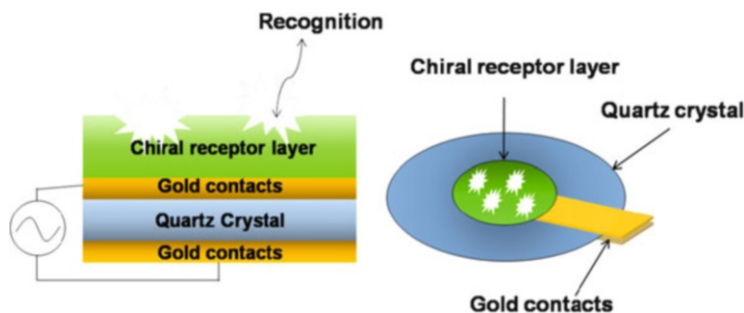


Fig. 9 Top and side views of a QCM device used as sensors for enantiomeric detection

shape, size, chemical nature of the cavity, and cavity entrance play an important role in the interaction with the enantiomers and the stability of the complex [13].

It is nearly 20 years since Ide et al. [75] reported the use of a QCM gas sensors for enantiomeric differentiation of both rose oxide and citronellol with modified per-alkylated cyclodextrins (α -, β -, γ -CDs). A more analytical and comprehensive study upon discrimination of enantiomers in gas phase was made 2 years later by Bodenhöfer et al. [76]. They successfully differentiated the enantiomers of methyl lactate, methyl-2-chloropropionate, and the inhalation anesthetics (i.e., enflurane, isoflurane, and desflurane) in the gas phase using octakis(3-O-butanoyl-2,6-di-n-O-pentyl)- γ -cyclodextrin. In an additional work, the possibility of estimating theoretically the sensors performance when exposed to the chiral analytes and their mixture was investigated. To this day the use of cyclodextrins was adapted by several groups working on chiral differentiation with QCM sensors [77, 78].

In order to enhance the sensitivity and improve the adhesion of the recognition sites on the surface of the transducer, the generation of imprinted recognition sites in monolayer or thin film assemblies is suggested. Ng and coworkers were the first to develop a chiral QCM sensor using a self-assembled monolayer (SAM) of perfunctionalized β -CDs [79–81]. As shown in Fig. 10a, mercaptyl-functionalized β -CDs with varying alkyl group and two different lengths of thiol linker (S-short and L-long) were synthesized and immobilized on the gold electrode surface of the sensor. Different pairs of enantiomers were tested in the gas phase: ethyl lactate, methyl lactate, 2-octanol. The adsorption capacity of the SAM and the ability to differentiate successfully the enantiomers was correlated to size cavity of the different alkylated CDs and fitting space occurring from the monolayer packing on the gold surface. Based on surface characterization and calculations of the surface coverage of the SAMs, it was suggested that the L-type CDs were immobilized in a more condensed way than those with small lengths of thiols and the surface density was inversely proportional to the bulkiness of the alkyl group. From the gas sensing measurements it was shown that functionalized β -CDs with long sulfide pendants exhibit better enantiomeric differentiation than those with short ones and that both L- and S-types of MP- β -CDs exhibited significantly enhanced enantioselectivities as compared to the rest due to interactions that allowed orientation and better matching of

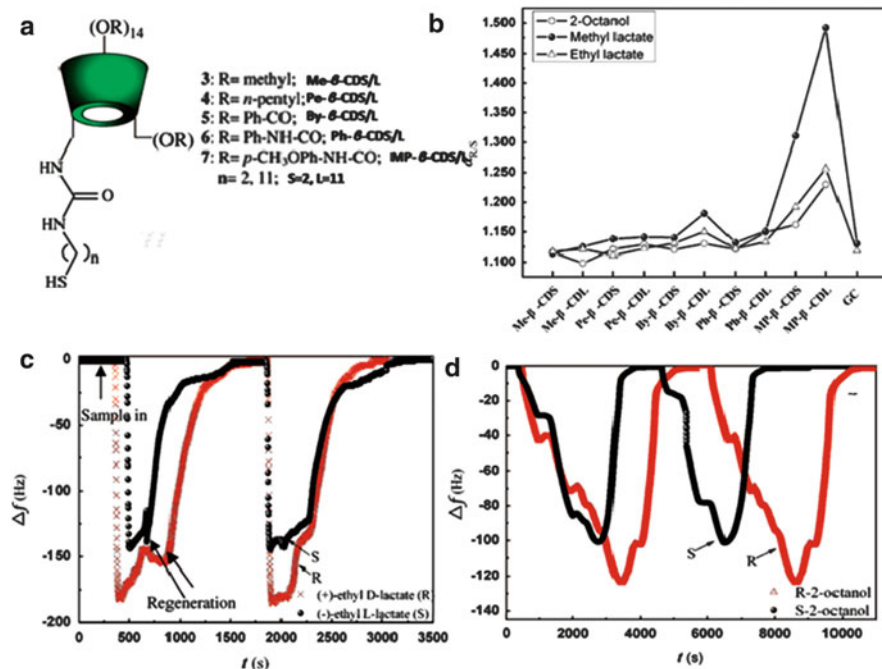


Fig. 10 (a) Schematic illustration of mercaptyl-functionalized β -cyclodextrins. (b) Chiral discrimination factors ($\alpha_{R/S}$) of the different alkylated CDs chiral sensors for the three enantiomers; 2-octanol, methyl lactate, and ethyl lactate. Frequency response of MP- β -CDL sensor toward (c) ethyl lactate and (d) 2-octanol enantiomers. Reprinted with permission from [81], © 2008 American Chemical Society

the cavity size with the analytes tested. Furthermore, the (*R*)-enantiomer caused larger shifts in the frequency, resulting in a higher enantioselectivity compared to reported values using GC. An example of the response of QCM with an electrode modified with a monolayer of functionalized β -CD is shown in Fig. 10c, d. In general, the enhanced enantioselectivity was attributed to the ordered surface morphology of the monolayers. The ordered packing on the surface resulted in increasing the number of binding sites and the monolayer structure enabled the analyte molecules to enter into the cavities [81].

The self-assembled monolayer of a modified β -cyclodextrin, Ph- β -CD-S, on a QCM sensor was also investigated as chiral selector for enantiomeric differentiation of (*R*)- and (*S*)-(3-methoxyphenyl)ethylamine [MPEA] by Luo et al. [82]. The interaction mechanism and complex formation were interpreted based on UV spectra analysis. The sensor was tested upon one concentration of the analytes in the gas phase and the enantioselectivity was found to be $\alpha_{R/S} = 1.33$. Based on UV analysis, both enantiomers were able to form complexes with the CD. The analyte molecules enter into the cavities because of hydrophobic and π - π interactions. Nevertheless, only the (*R*)-enantiomer was able to form a more stable complex through the hydrogen bonding of its amine group and of the carbonyl group of the modified β -CD.

3.2 QCM Devices Based on Molecular Imprinted Polymers

MIPs have been employed as biomimetic recognition sensing layers with the selectivity and binding affinity of MIP being comparable to antibody–antigen interactions. MIPs have mainly been investigated for enantiomeric differentiation in the liquid phase.

The use of MIPs as chiral selectors for enantiomeric differentiation was reviewed by Maier and Lindner et al. [16]. Nevertheless, it is noteworthy to refer briefly to the most interesting advances up to 2006. Haupt et al. [83] reported a novel study on the differentiation of the enantiomers of propanolol, acquiring an enantioseparation factor of nearly $\alpha_{S/R} = 5$. A few years later, an interesting approach to control the growth of the MIP and improve the sensitivity of the sensor was achieved by Piancham et al. [84]. Hayes and his group [85, 86] had also studied thoroughly the performance of QCM sensors coated with MIPs for the differentiation of menthol and serine enantiomers. In addition, an enantioselective MIP-coated QCM sensor for dansyl phenylalanine enantiomers was reported by Cao et al. [87]. The enantioseparation factor was $\alpha_{L,D} = 6.7$ and the detection limit of the sensor calculated from the calibration curve was 5 $\mu\text{g/mL}$ for the L-enantiomer.

A QCM sensor able to differentiate L- and D-tryptophan enantiomers in the liquid phase was developed by Liu et al. [88]. Non-covalent MIPs were synthesized on the gold electrodes of the quartz crystal, using acrylamide (AM) and trimethyl-propane trimethylacrylate (TRIM) as functional monomer and cross linking agent, respectively. The influence of the cross linking agent concentration, during the fabrication of molecular imprinted polymeric film in terms of enantioselectivity and sensitivity was investigated. According to the authors, the results indicated that, with increasing TRIM, the shift of resonant frequency upon exposure to the analyte increased. They suggested that there is an optimum cross linking density that reduces the chain flexibility and provides stabilization of the structure of the selective cavity, thus leading to an enhancement of the specific binding of the analyte. On the other hand, it might lead to a reduction of the number of sites for the analyte to be adsorbed/or entrapped in the cavity. From the films prepared and tested the highest value of enantioseparation factor was $\alpha_{L,D} = 6.4$, with the detection limit at 8.8 μM .

Electropolymerized L-aspartic acid (L-Asp) imprinted polypyrrole (PPy) films were exploited by Syritski et al. [89]. Electropolymerization offers the ability of having controllable thickness, morphology, and spatial localization of the polymeric films. Overoxidized polypyrrole (oPPy) matrix templated with either L- or D-aspartic acid (Asp) was evaluated as a potential enantioselective recognition element. In order to control the capability of the MIP to recognize enantioselectively the respective template (L-Asp), they used an electrochemical quartz crystal microbalance (EQCM) sensor. The set up apparatus is depicted in Fig. 11a. With EQCM the mass changes can be monitored during the electrochemical modulation of the film. It was found that synthesis parameters and pH value of the solution strongly influence the film quality of the resulting MIP. The electropolymerization of pyrrole in the presence of L-Asp in alkaline media and overoxidation of PPy enabled the formation of adherent, smooth, and uniform PPy/L-Asp films. The experiments also showed

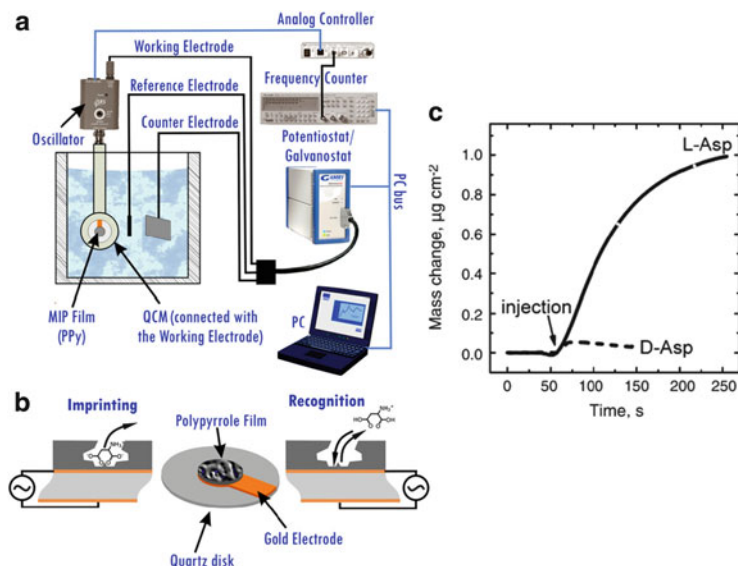


Fig. 11 (a) Schematic illustration of electrochemical quartz microbalance set up (apparatus). (b) Imprinting and recognition mechanism. (c) Mass change of PPY/L-Asp after the injection of L-Asp and D-Asp. Reprinted with permission from [89], © 2008 Elsevier

that a higher doping level of the template molecule in the film enhanced the enantioselectivity. The difference in mass uptake of the PPY/L-Asp sensor to the two enantiomers is depicted in Fig. 11c.

The same concept was also adopted by Kong et al. [90]. They reported the electrosynthesis of oPPy with L-tryptophan (L-Try) as a template to prepare an MIP used for the enantioselective detection of tryptophan. The sensing performance of the film was studied by the EQCM technique.

Imprinting of chiral counter-ions into polymeric matrices is also an appealing strategy for chiral sensing. As was reported by Huang et al. [91], if polyaniline is doped with chiral counter-ions, the backbone of the polymer can acquire a helical conformation and thus can be utilized for enantiomeric differentiation. According to the authors, a “memory effect” was observed. More specifically, they investigated the ability of the doped polyaniline to differentiate the two enantiomers of phenylalanine using different techniques (CV, UV, and a QCM sensor). From the results obtained it was shown that polyaniline can be used as a general polymer matrix to host various chiral dopants for enantiomeric differentiation. In addition, the imprinted chiral dopants can be fully recovered by simple acid/base chemistry. Another appealing concept of using conjugated polymers for enantiomeric differentiation was reported by Tanese et al. [92]. The poly(phenyleneethynylene) (PPE) substituted with D-glucose units was proposed as active layer in a QCM chiral sensor able to differentiate the two menthol enantiomers. This synthesized chiral-polymer had a higher affinity for natural (–)-menthol. Such polymers are promising candidates to be utilized as enantioselective materials in resistors and/or transistors.

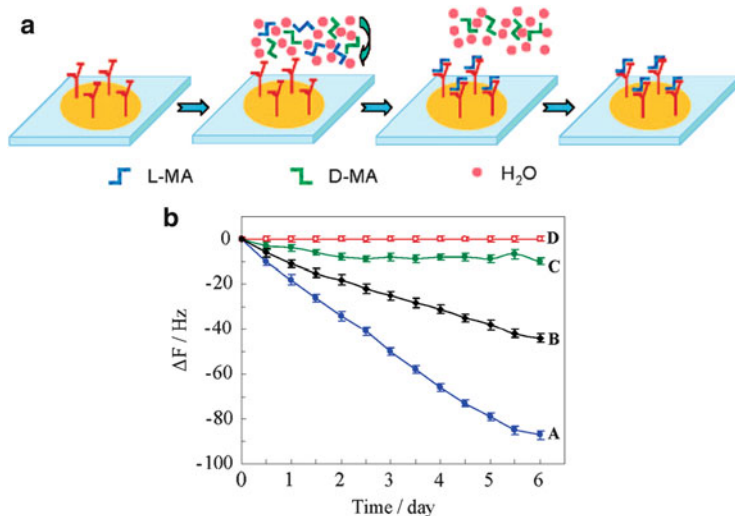


Fig. 12 (a) Schematic illustration of the vapor-diffused molecular assembly reaction of chiral mandelic acid on the L-Phe-modified QCM sensor surface. (b) Response of the 4-NH₂-L-Phe-modified QCM sensor upon exposure to (A) 1 mL of 0.05 mol/L L-MA, (B) 0.5 mL of 0.05 mol/L L-MA + 0.5 mL of 0.05 mol/L D-MA, (C) 1 mL of 0.05 mol/L D-MA, and (D) 1 mL of deionized H₂O vs time at 25 °C. Reprinted with permission from [94], © 2009 American Chemical Society

3.3 QCM Devices Based on Biological Recognition Elements

A chiral QCM sensor for differentiating the enantiomers of mandelic acid (MA) was reported by Guo et al. [93, 94]. As chiral selector, L-4-amino-phenylalanine (4NH₂-L-Phe) was immobilized on the gold surface of the electrode using the layer by layer (LbL) assembly procedure. In order to avoid the difficulties occurring during liquid biosensing, in terms of signal stability, sensitivity, and selectivity, a different protocol was adopted of producing vapors of the analyte and realizing the sensing measurements. Vapor-diffused molecular assembly (VDMA) was used (Fig. 12a).

According to this technique, the enantiomers are transferred and turned into vapors via solvent evaporation. The pure solvent is used as a blank measurement. The authors verified the adsorption/diffusion and selective binding of the analyte by AFM surface characterization and contact angle measurements. The enantioselectivity factor between L- and D-MA was found to be $\alpha_{L/D} \sim 9$ and the sensor was also tested upon exposure to the racemic mixture. However, the VDMA method proved to be rather time consuming since more than 5 days were needed for realizing a measurement (Fig. 12b).

Recently the same research group demonstrated a chiral recognition system for MA enantiomers for fast on-line monitoring. In this case the sensing was realized in the liquid phase and an amide-type (S)-MA derivative with a stereogenic carbon

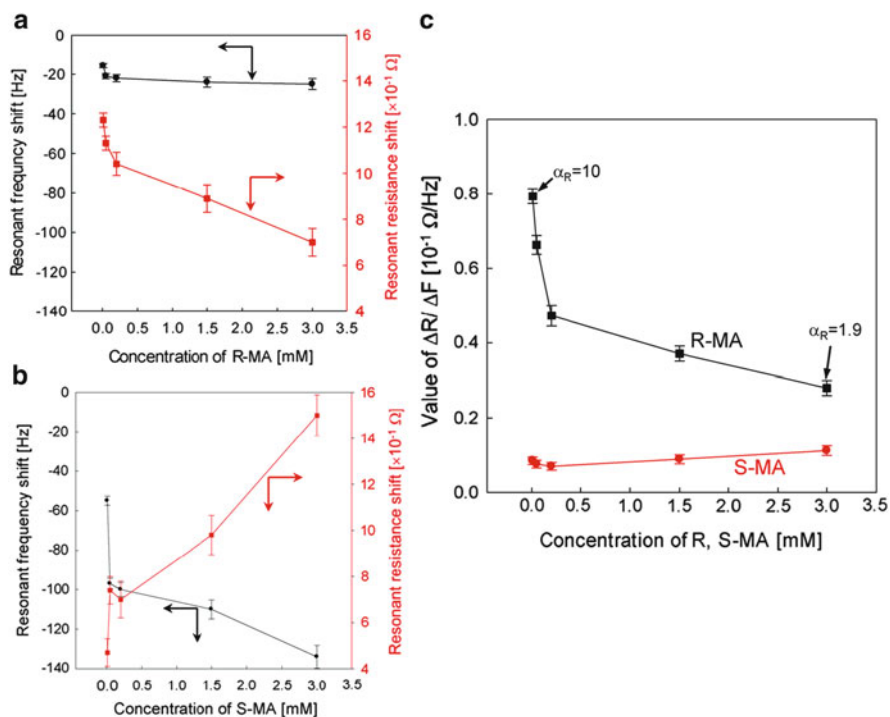


Fig. 13 Resonant frequency and resistance changes vs the concentration of (a) (*R*)-MA and (b) (*S*)-MA. (c) Combined R/F value change vs the concentration of the two MA enantiomers. Reprinted with permission from [95], © 2012 Elsevier

atom was used as a recognition chiral element and deposited on the QCM surface. Moreover, both the changes in resonant frequency (F) and the resonant resistance (R) changes upon exposing the sensor device to different concentrations of the enantiomers were monitored. As illustrated in Fig. 13, by combining the data from both measurements ($\Delta R/\Delta F$) the value of the enantioselectivity factor was enhanced from ~ 5 to 10 [95].

In addition, the integration of antibodies as recognition elements in sensing devices is a promising approach for highly sensitive and enantioselective sensors. In 1928, Landsteiner and van der Scheer had shown that antibodies can differentiate enantiomers [96]. In 2003, Dutta et al. [97] reported a nanomechanical immunosensor for the enantiomeric differentiation of α -amino acids (tryptophan and phenylalanine) in the liquid phase. An anti-L-AA monoclonal antibody was covalently attached on the micro-cantilever nanostructure.

In another study conducted by Su et al., bovine serum albumin (BSA) and human serum albumin (HSA) were immobilized onto a gold surface using the SAM technique [98]. The differentiation ability of BSA and HSA upon exposure to vapors of five pairs of enantiomers (*(R,S)*-1,2,3,4-tetrahydro-1-naphthylamine, *(R,S)*-1-(3-methoxyphenyl) ethylamine, *(R,S)*-1-(4-methoxyphenyl)ethylamine, *(R,S)*-2-octanol, and *(R,S)*-methyl lactate) was studied. The binding affinity of BSA and HSA was found to be

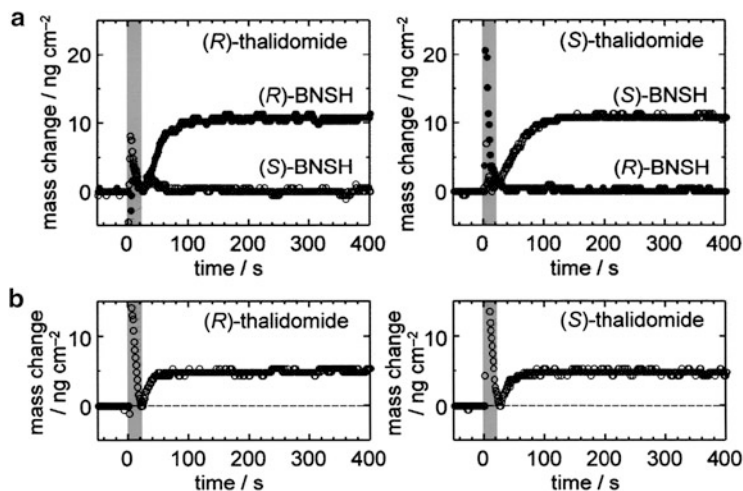


Fig. 14 (a) Responses of BNSH-modified QCM after addition of (*R*)- and (*S*)-thalidomide. (b) Responses of QCM with racemic SAM of BNSH after injection of (*R*)- and (*S*)-thalidomide. Reprinted from [100], © 2004 Wiley-Liss, Inc., A Wiley Company, with permission from John Wiley and Sons

enantioselective. BSA was able to differentiate preferentially (*R,S*)-4-MPEA and (*R,S*)-3-MPEA while the rest of the analytes were differentiated by HSA. UV and fluorescence spectra were also realized to investigate the interactions between the two proteins and the enantiomers. The results obtained were in agreement with the sensing measurements. More recently, for differentiation of the same pairs of enantiomers, goat serum albumin (GSA) and rabbit serum albumin (RbSA) were also investigated as chiral selectors by the same group [99].

3.4 Other Approaches Used for QCM Sensors Development

An interesting study for the enantiomeric differentiation of thalidomide was reported by Nakanishi et al. [100]. A QCM sensor able to differentiate thalidomide enantiomers by using a self-assembled monolayer of atropisomeric 1,1'-binaphthalene-2,2'-dithiol (BNSH) was fabricated. The QCM sensor exhibited high enantioselectivity. Only one enantiomer was adsorbed on each of the enantiomers of BNSH-SAM (Fig. 14a). Based on previous investigations and on calculations of the amount of molecules adsorbed on the modified surface of the QCM sensor with the BNSH-SAM, it was reported that chiral supermolecular assemblies of C_3 symmetric screw like units act as the adsorption sites for each molecule of the enantiomer. Moreover, the response of the racemic SAM of BNSH was found to be half of that caused by pure enantiomeric SAM (Fig. 14b).

Guo et al. [101] reported the use of calixarenes linked to cyclopeptides (bicyclodipeptide bearing calix[4]arenes) for enantiomer sensing of methyl lactate. Three different calixarenes were synthesized and studied as chiral selectors in QCM sensors. All three materials showed higher sensitivity towards the (*R*)-enantiomer. From the calibration curve of the two enantiomers, the linear shape of the isotherm reveals the non-specific bonding of the (*S*)-enantiomer (Henry isotherm) whereas for the (*R*)-enantiomer the Langmuir type shows the adsorption of the analyte in specific sites. (*R*) to (*S*) enantioseparation factors $\alpha_{R/S} = \Delta f(R)/\Delta f(S)$ were evaluated for all synthesized calixarenes ranging from 4 to 7. In accordance with other studies [76], the $\alpha_{R/S}$ values increased with decreasing analyte concentration, resulting from the domination of the specific absorption of the (*R*)-enantiomer, especially in the low concentration range.

4 Electrical Sensors

By definition an electrical sensor relies on changes of the electric properties of the sensitive material upon interaction with an analyte, whereby no electrochemical phenomena take place. The distinguishing features of these devices are the simplicity of their fabrication and set-up instrumentation. Typically, they involve placing a material between conducting electrodes, to which a voltage is applied and the electrical conductivity or capacitance is subsequently measured.

4.1 Chemiresistors

Conductometric (or resistive) sensors are among the most commonly employed devices in sensing applications and especially in the detection of gases and volatile organic compounds. The transduction principle of chemiresistors is based on chemical modulation of the surface or bulk conductivity of the sensitive layer. As the chemically sensitive layer, inorganic materials and organic conductive/semiconductive materials can be used. In addition, insulating polymers mixed with conductive particles such as graphite or metal powder are utilized. In this case the changes of bulk conductivity are due to swelling. These materials are considered “poor conductors.” Despite the fact that chemiresistors dominate the market as gas sensors, very little work has been reported on enantiomeric sensing.

Resistors based on carbon black (CB)-chiral polymer composites for the discrimination of enantiomeric volatile compounds were developed by Severin et al. in 1998 [102]. The composite films consisted of carbon-black and poly((*R*)-3-hydroxy-butyrate-*co*-(*R*)-3-hydroxyvalerate). Vapors of both enantiomers of 2-butanol, α -pinene, epichlorohydrin, and methyl 2-chloropropionate were tested. It was shown that the sensor was able to have differential responses to each pair of enantiomers, whereas the response was the same when each pair of analytes was

tested with an achiral composite material. The average value of the enantiomer separation factor for all pairs was $\alpha_{(+/-)} \sim 1.09$.

An attempt for chiral gas sensing with resistor-based sensors was reported by Benjamin et al. in 2003 [103]. In this work, the authors investigated the use of conducting polymers properly substituted with chiral moieties. For this purpose, 3-substituted pyrrole monomers with different chiral side groups (i.e., menthol (Men), phenylethanol (PE), boc-alaninol (Ala), boc-valinol (Val), and boc-prolinol (Pro)) were synthesized. The compounds were polymerized using ferric salts and the resulting polymers were deposited as conductive/sensitive materials onto the sensors. The three terpenes carvone, limonene, and menthol, as well as 2-butanol, were selected for vapor sensing. The pure enantiomers of 2-butanol, limonene, and carvone were tested in concentrations from 5,000 to 20,000 ppm in all pairs of chiral polymer sensors. In most cases, an increase in resistance was observed for all chiral polymer pairs under exposure to each vapor analyte. Only the PE-polymer sensors exhibited the opposite behavior (decrease). From the results reported it was shown that Ala-polymer could differentiate better the two enantiomers of 2-butanol with the (*R*)-Ala-polymer being more sensitive to (*S*)-2-butanol and the (*S*)-Ala-polymer to (*R*)-2-butanol. (*R*)-Men-polymer showed higher response to (*R*)-limonene and the (*S*)-Men-polymer to (*S*)-limonene. The enantiomers of carvone were better differentiated by the Val-polymer (*R*)-Val-polymer for (*S*)-carvone, (*S*)-Val-polymer for (*R*)-carvone). Menthol was only tested with the Men-polymer where the (*R*)-Men polymer showed higher affinity to the (*R*)-enantiomer and the (*S*)-Men-polymer to the (*S*)-enantiomer.

4.2 Organic Field Effect Transistors

Different from a chemiresistor, organic field effect transistors (OFETs) are three-terminal transducers consisting of an organic semiconductive layer, an insulating (dielectric) layer, and three conductive terminals, the source, drain, and gate (Fig. 15). The current (I_{DS}) that flows between the contact electrodes (source and drain) through the semiconductor, upon application of a source and drain bias (V_{DS}), is modulated by a perpendicular electric field. The electric field is generated by a voltage applied on the gate electrode (V_{GS}). OFETs are usually operated by grounding the source and biasing the gate and the drain contacts against it. When no voltage is applied to the gate electrode (*off*-state), bulk conduction occurs and the transistor behaves as a chemiresistor. In contrast, when a gate voltage (beyond threshold) is applied (*on*-state), charge carriers are induced in the organic semiconductor at the interface with the gate dielectric. The higher the gate bias applied the higher the density of charges in the channel. The *on* and *off* measured currents are, hence, based on different charge transport regimes. For this reason they are able to carry out two distinct sets of responses, one in the *off*-state, the other in the *on*-state. Recently it was reported that the OFET response is affected by the contact resistance variation only when operated in the *off*-regime, while the channel conductance is affected in the *on*-regime [104]. This unique way of operation makes these

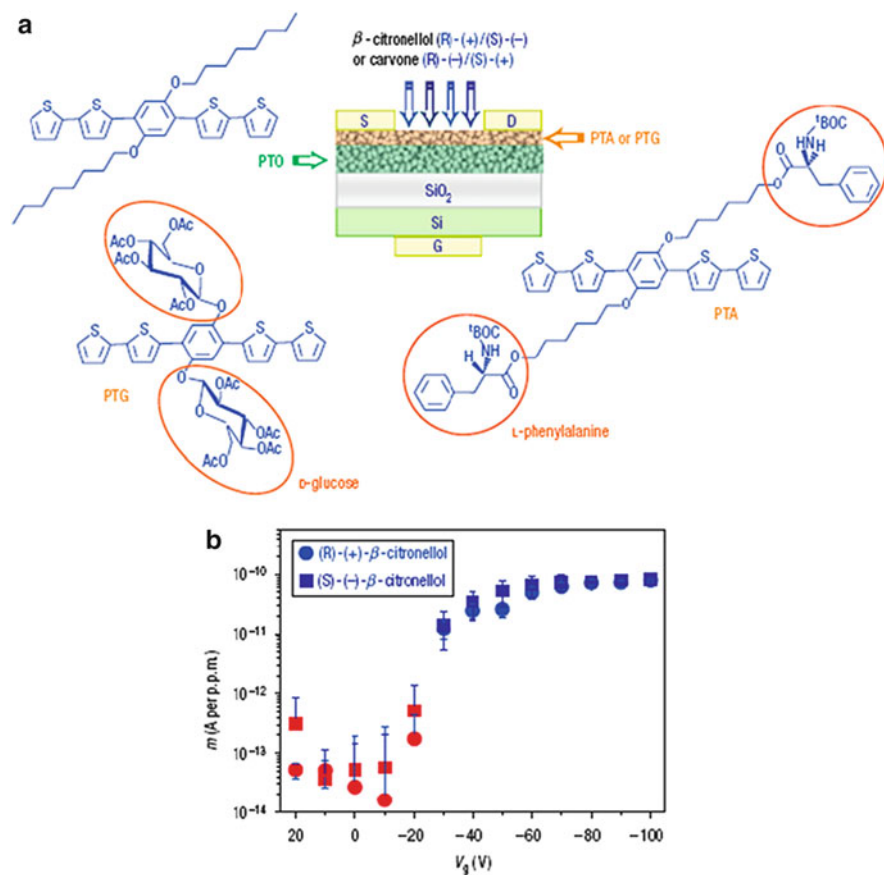


Fig. 15 (a) Illustration of the structure of the bilayer OFET. The chemical structure of the bare PTO organic semiconductor and of the two PTA and PTG organic semiconductors used for citronellol and carvon chiral differentiation respectively, is also reported. (b) The slopes of the calibration curves obtained for a PTO OFET exposed to the (R)-(+)- β -citronellol and (S)-(–)- β -citronellol at different gate biases are compared in the graph. Reprinted with permission from [113], © 2008 Macmillan Publishers Ltd

devices attractive in sensing applications. The sensing measurements can be realized by measuring either the $I_{\text{DS}}-V_{\text{DS}}$ output or the $I_{\text{DS}}-V_{\text{G}}$ transfer characteristics curves in the absence and in the presence of the analyte. OFET sensors can also be used for on-line monitoring. In this case, sensing measurements are performed by operating the device under a given set of V_{DS} and V_{G} .

OFET-based sensors have attracted great attention in the last decade [105]. This is mainly due to the possibility of being implemented in high performance portable sensing systems. They behave as multi-parameter sensors, exhibit high repeatability, fast and reversible responses [106], operate at room temperature, and offer good selectivity towards a broad range of analytes [107]. Moreover, the ability of OFETs to operate in the sub-voltage regime allows the realization of low power

consumption electronic sensing devices [108, 109]. In addition, OFETs have been employed for the development of label-free biosensors, having a field-effect transport directly coupled to a bio-recognition process [110–112].

OFET-based sensors rely on the effect of the interaction of the analyte with the organic semiconductor active channel. The sensing mechanism involves weak interactions between the functionalized organic molecules and the analyte. The adsorption of the analyte on the sensitive layer depends on the chemical affinity between the analyte and the semiconductive layer. Proper modification of the semiconductive layer with functional groups can improve the selectivity of the sensor. Such an approach can be successfully employed for enantiomeric differentiation.

An archetypal example is the recently proposed bilayer OFET structure for high performance chiral analysis by Torsi et al. [113]. The bilayer was engineered to combine field-effect and chiral recognition properties. The introduction of L-phenylalanine and β -D-glucosidic to alkoxyphenylene-thiophene oligomers affords two ad hoc designed organic semiconductors endowed with chiral side groups (Fig. 15a) named PTA and PTG respectively. Deposition of these two materials (PTA and PTG) on the top of an unfunctionalized organic layer (PTO) allowed the differentiation of the two enantiomers (*R,S*) of the chiral alcohol β -citronellol and of the chiral ketone carvone. The PTO-PTA OFET exhibited enantioselectivity towards β -citronellol and the PTO-PTG towards the enantiomers of carvone. In both cases the response of each sensor was higher in the presence of the (*R*)-enantiomer. The enantioselectivity factors $\alpha_{R,S}$ for β -citronellol and carvone were 2 and 1.31, respectively (the values are derived from the reported slope values of the calibration curves in the concentration range 2.5–30.6 ppm for β -citronellol and 10.8–64.7 ppm for carvone). These results provide convincing proofs that introduction of receptor groups in field-effect semiconductors is an efficient way to modulate the device functionality. Besides, one of the main interests of the transistor sensor relies in its capability of amplifying the source-drain current through the capacitance-coupled gate electrode. Even though this effect has been widely assessed, the first direct evidence for a gate field-induced sensitivity enhancement was only given with the elicited OFET chiral sensor. Figure 15b shows the sensitivity of an OFET sensor exposed to two β -citronellol enantiomers for various gate biases. There was an enhancement of several orders of magnitude when the device switches from the *off* (gate biases below threshold) to the *on* (gate biases above threshold) state. Similar gate-bias dependent sensitivity has been indirectly observed for Organic Electrochemical Transistors (OECT) glucose sensors [114]. All these pieces of evidence open interesting outcomes for the use of microscopic OFETs as ultra-sensitive electronic transducers.

4.3 Chemocapacitors

In the case of the capacitors, between the electrodes is a dielectric material. The electrical field that arises between the electrodes strongly depends on the materials dielectric properties. The response of a capacitor depends on the change of

permittivity of the dielectric sensitive layer (polymer) and also on the degree of swelling of the polymeric layer.

A capacitive sensor for enantioselective recognition of glutamic acid (Glu) in the liquid phase was proposed by Ouyang et al. [115]. A new MIP material was electrosynthesized on a gold electrode by copolymerization of *o*-phenylenediamine (*o*-PD) and dopamine (DOPA) in the presence of the respective template molecule. The resulting L-Glu and D-Glu MIP films were characterized with various techniques such as PFS, CV, X-PS, AFM. It was found that structure and enantioselectivity of the film towards the template molecule depended on its composition. The response of the sensor was found to be linear with the concentration of the two enantiomers in the range 16.7–250 μM . The detection limit of each MIP to its template molecule L-Glu and D-Glu was 4.7 μM and 5.9 μM , respectively. The enantioselectivity factor α for L-Glu MIP was 24 and for D-Glu was 15. In order to evaluate the cross-selectivity of the sensor, the L-Glu MIP sensor was exposed to a series of other L-amino acids. The sensor exhibited high enantioselectivity, good reversibility, and stability. In Fig. 16 the calibration curves of the sensors responses to each enantiomer and the relative response of L-Glu MIP towards different L-amino acids are shown.

The development of an enantioselective electrochemical-capacitive immunosensor for the detection of α -amino acids was reported by Zang et al. [116]. The sensor was prepared by first binding mercaptoacetic acid to the surface of a gold electrode, followed by modification with tyramine utilizing carbodiimide activation. The hapten 4-amino-D-phenylalanine was then covalently attached to the electrode by diazotization. Stereoselective binding of an anti-D-amino acid antibody to the hapten-modified sensor surface resulted in capacitance changes that were measured by using a potentiostatic step method. Detection limits of 5 pg of antibody/mL were achieved. In order to determine the concentration of the analyte D-phenylalanine in non-racemic samples of both enantiomers, a competitive assay was utilized. Trace impurities of D-phenylalanine as low as 0.001% were detected.

As far as chiral sensing in the gas phase is concerned, an analytical evaluation of capacitive sensors for enantiomeric differentiation was reported by Kurzawski et al. [117]. The capacitor was prepared by coating chiral selector/sensitive film on top of interdigitated electrodes. A schematic presentation of the capacitors is shown in Fig. 17. More specifically, the sensitive material consisted of chiral octakis(3-*O*-butanoyl-2,6-di-*n*-*O*-pentyl)- γ -cyclodextrin dissolved (50 wt%) in poly(dimethylsiloxane) (PDMS).

The sensor was exposed to the two enantiomers of (*S*)- and (*R*)-methyl-2-chloropropionate at different concentrations (from 20 to 1,600 ppm). The capacitor was able to detect and discriminate the two enantiomers providing an opposite signal upon exposure to the two enantiomers in low concentrations (up to 80 ppm). In higher concentrations the response was positive for both enantiomers but was always lower for the (*S*)-enantiomer (Fig. 18). This behavior allowed easy identification of the enantiomers.

At this point it is worth mentioning that if the film thickness of the insulating layer fully covers the electric field, swelling effects can be neglected and any

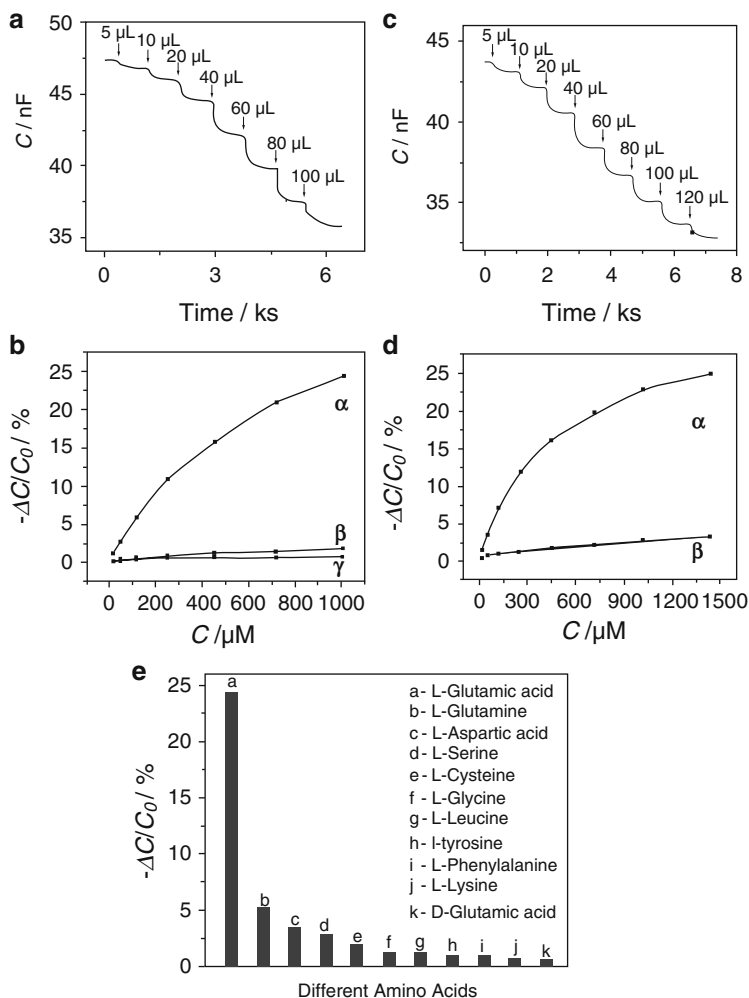


Fig. 16 Capacitance change of (a) L-Glu-imprinted and (b) L-Glu-imprinted copolymer upon injection of different concentrations of the respective enantiomers. (c) Relative capacitance changes at different concentrations of L-Glu at (α) L-Glu-MIP and (β) non-imprinted polymer films and (γ) D-Glu at the L-Glu-imprinted copolymer film. (d) Relative capacitance changes at different concentrations of (α) D-Glu and (β) L-Glu at the same D-Glu-MIP film. (e) Relative capacitance changes of the L-Glu-MIP capacitive sensor at 1.0 mM L-Glu and other L-amino acids and D-Glu. Reprinted from [115], © 2007 WILEY-VCH Verlag GmbH & Co. KGaA, Weinheim, with permission from John Wiley and Sons

change in the capacitance is only due to changes in permittivity of the sensitive material. Consequently, when the dielectric constant of the analyte is larger than that of the sensitive layer as in this case, an increase in capacitance is observed. This was true for the (*R*)-enantiomer but was not valid for the other enantiomer. The authors attributed this behavior to the higher affinity of the (*S*)-enantiomer

Fig. 17 Side view of schematic presentation of the interdigitated capacitor. Reprinted from [117], © 2008 WILEY-VCH Verlag GmbH & Co. KGaA, Weinheim, with permission from John Wiley and Sons

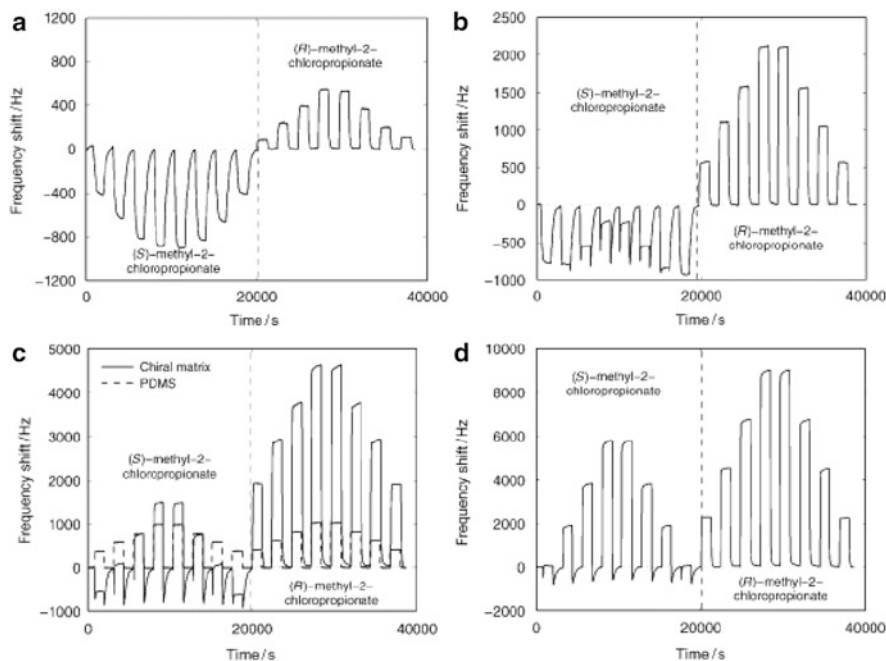
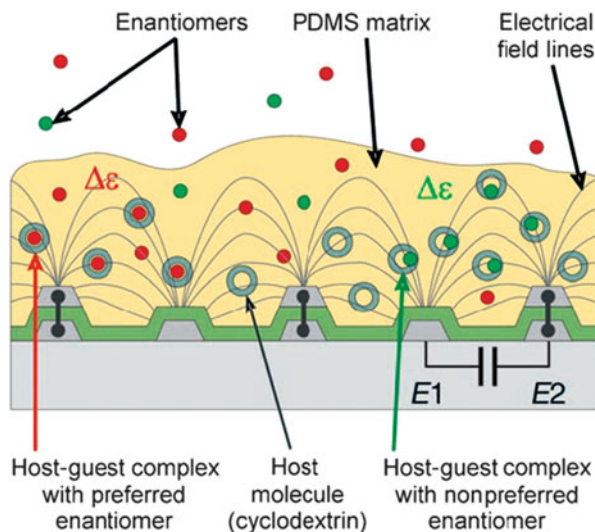


Fig. 18 Frequency change of capacitive sensors upon exposure to the enantiomers of methyl-2-chloropropionate at different concentrations (1 Hz corresponds to a capacitance change of 5.25 attoFarad). Analyte concentrations in ppm: (a) 20, 40, 60, 80, (b) 80, 160, 240, 320, (c) 320, 480, 640, 800, (d) 400, 800, 1,200, 1,600. Dashed line: response of an achiral reference sensor (coated with PDMS). Reprinted from [117], © 2008 WILEY-VCH Verlag GmbH & Co. KGaA, Weinheim, with permission from John Wiley and Sons

with the cyclodextrin selector. They suggested that the negative capacitance was due to the presence of orientation effects between the host and the guest molecule, which resulted in decreasing the dielectric coefficient of the enantiomer. With increasing analyte concentration, the cavity sites for specific binding of the analyte were filled. From this point, non-specific absorption occurred and the signal was reversed. These results were confirmed by exposing the sensor to vapors of methyl lactate as well. The behavior of the capacitor was further investigated in the presence of mixtures of the two enantiomers. The sorption kinetics was also analyzed [118]. In an extension of this work, a three-transducer microsystem (calorimetric, a gravimetric and a capacitor) was reported as a sensing platform for enantiomeric differentiation. Chiral and achiral analytes were tested. The sensor's response curves for all types of transducers were explained and fitted by applying models based on Langmuir and Henry sorption isotherms [119].

5 Optical Sensors

Optical sensors convert a physicochemical interaction into an optical signal. They utilize the interaction between light and matter, generally in the visible, infrared, and ultraviolet regions. These interactions cause the properties of the light waves to change, e.g., intensity, phase, polarization, wavelength, and spectral distribution. Various types of optical sensors exist and have been employed as sensing platforms for enantiomeric detection. In this chapter, the latest accomplishments regarding enantiomeric differentiation/detection using optical label free sensors will be presented.

5.1 Surface Plasmon Resonance (SPR) Sensors

SPR sensors have been widely applied in the development of sensors and mainly biosensors. In general, surface plasmon waves are generated by irradiating the surface of a thin metal film with a light. It is a high sensitive and versatile method that is used to measure changes in the refractive index caused on metal surfaces by interactions of the analyte and the sensing layer. The set up and signal change of an SPR is depicted in Fig. 19. In the case of enantiomeric discrimination, SPR sensors have been utilized mainly for sensing in the liquid phase.

Pioneering effort in the field of enantiomeric differentiation by combining an immunosensor with SPR detection was made by Hofstetter et al. [120]. Streptavidin was covalently linked to carboxymethylated dextran on the gold surface. Biotinylated D- and L-enantiomers of an α -amino acid were immobilized into separate channels of the sensor and a polyclonal rabbit antibody was injected. In the presence of D-enantiomer the antibodies were attached to the sensor which increased the signal, while the L-enantiomer did not cause the binding. A competitive assay format was used for the differentiation of the chiral analyte in solution and for determination of enantiomeric impurities (Fig. 20a). The sensor was able

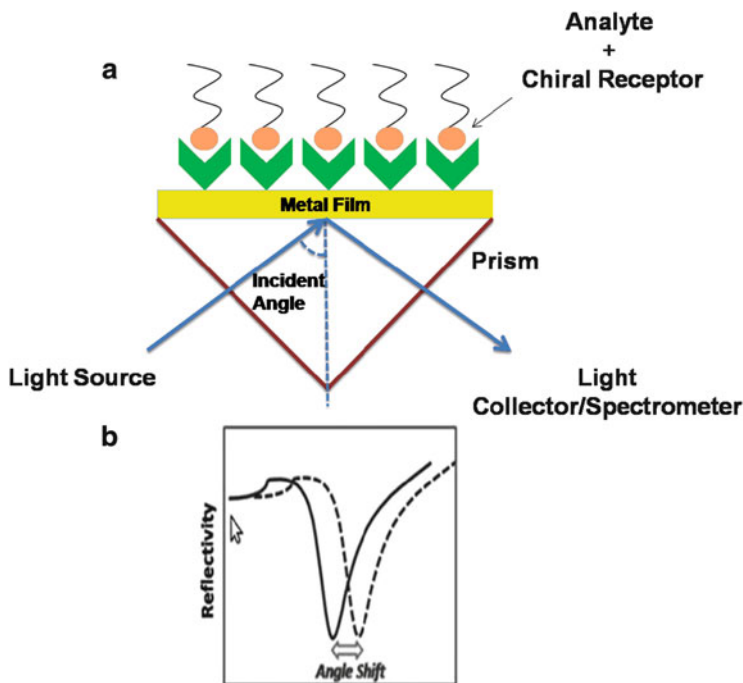


Fig. 19 (a) Schematic illustration of SPR structure and set up measurement. (b) Reflectivity vs incident angle

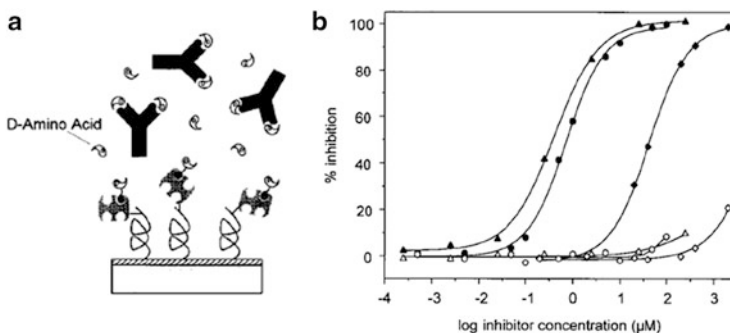


Fig. 20 (a) Competitive assay schematic illustration. (b) Inhibition curves of different α -amino acids: D-tyrosine (filled triangles), L-tyrosine (open triangles), D-DOPA (filled circles), L-DOPA (open circles), D-norleucine (filled diamonds), and L-norleucine (open diamonds) at different concentrations. Reprinted with permission from [120], © 1999 Macmillan Publishers Ltd

not only to differentiate the enantiomers of α -amino acids but also to determine quantitatively trace amount of impurities of one enantiomer in a large excess of the opposite enantiomer (e.g., D-Try at a concentration of $0.1 \mu\text{M}$ in the presence of $250 \mu\text{M}$ of L-Try). The sensor was also tested upon the enantiomers of tyrosine, DOPA, norleucine. The inhibition curves obtained after converting the SPR signal are shown in Fig. 20b.

Cyclodextrins have also been used as a sensitive layer in SPR-based sensors. Enantioselective sensing of thyroxine by SPR using modified β -CD was proposed by Shahgaldian et al. [121]. More specifically, a SAM of synthesized heptakis (6-deoxy-6-[12-(thiododecyl)undecanamido])- β -cyclodextrin was used as chiral selector. The chiral SAMs exhibited a greater affinity for the D-enantiomer of thyroxine compared to the L-enantiomer. The ability of modified CD to differentiate the two enantiomers of thyroxine was evaluated by measuring the apparent affinity constant with varying proportions of each enantiomer.

Moreover, aptamers have been utilized as chiral receptors in SPR platforms. The binding affinity and enantioselectivity of screened modified DNA aptamers from an arginine-modified DNA library with the dicarboxylic acid moiety of the D-enantiomer of glutamic acid was successfully evaluated by SPR measurements [14].

Amplified SPR sensing has been achieved by using metallic nanoparticles (NPs) [122]. Metallic nanoparticles provide high surface area films and exhibit localized plasmon excitons. Moreover, NPs can be used for functionalization of bio-recognition/chiral elements. This approach has inspired a lot of research groups working in the field of chiral sensing. Ha et al. [123, 124] synthesized gold nanoparticles modified with chiral receptor, and more specifically chiral substituted calix[4]arene ligands, that exhibited optical circular dichroism (OCD) and an active SPR absorption band. Two characteristic Cotton effects were observed in the OCD spectrum when the gold NPs were capped with (*R,S*) amino calixarene enantiomeric ligands. The first peak corresponds to the asymmetric π - π^* transition of the calixarene ligands at 270–300 nm and the second to the SPR band at 460–600 nm. The ellipticity peaks (cotton effects) of the (*R*)-enantiomeric ligand were positive and mirror images of the negative peaks of the (*S*)-enantiomeric ligand. Zero ellipticity was found for the bare gold NPs and the NPs capped with racemic mixture of the two enantiomers [123].

Impressive enantioselectivity towards mono- and disaccharides using molecularly imprinted boronic acid–gold NP composites has been achieved with SPR sensors by Ben-Amram et al. [125]. Gold NPs were functionalized with a capping monolayer consisting of 4-mercaptoaniline, mercaptoethane sulfonic acid, and mercaptophenyl boronic acid. The modified gold NPs were electropolymerized on gold-coated glass surfaces in the presence of the respective saccharide template molecule. Apart from the cavities originated by the addition/removal of the template, the resulting composites consisted of ligands for binding mono- or disaccharides (Fig. 21a). The mercaptophenyl boronic acid provided the anchoring ligands for the saccharide molecules to attach covalently. A boronate complex between the respective saccharide and the boronic acid is formed. Based on several control experiments, it was shown that the selectivity and sensitivity of the proposed MIP layer as sensing layer for the saccharides studied was strongly associated with the presence of both boronic ligands and NPs. Each different saccharide-imprinted film showed high selectivity toward its respective molecule and impressive enantioselectivity between the two enantiomers of the same saccharide as well (Fig. 21b, c). From the calibration curves obtained, the detection limits were determined for each analyte–MIP composite tested.

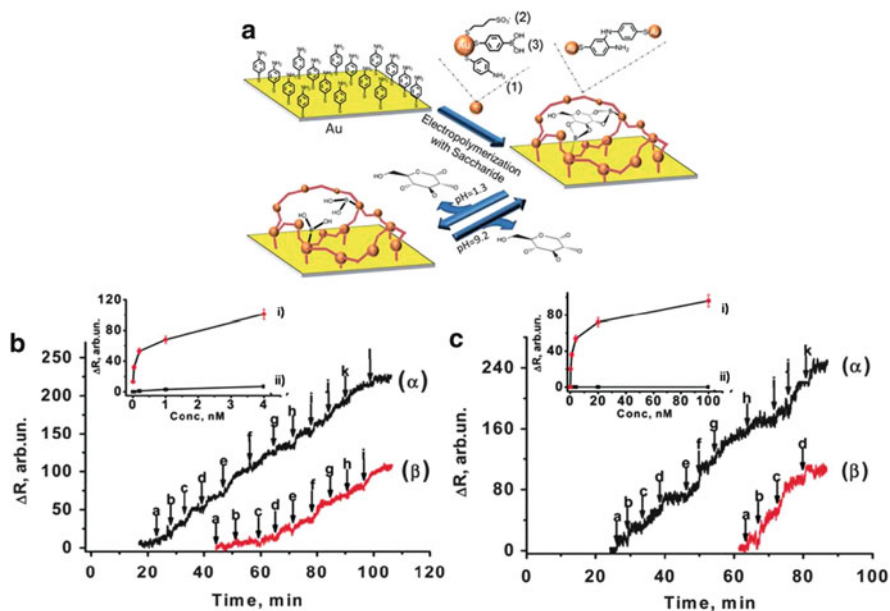


Fig. 21 (a) Schematic presentation of imprinting D-glucose by electropolymerization of a bis-aniline-crosslinked/gold NPs composite on a gold surface. (b) Sensograms showing the reflectance changes of the D-glucose-imprinted gold NPs composite upon exposure to different concentrations of (α) D-glucose and (β) L-glucose. (c) Sensograms showing the reflectance changes of the L-glucose-imprinted gold NPs composite upon exposure to different concentrations of (α) L-glucose and (β) D-glucose. In the *insets* of (b) and (c) the respective calibration curves are shown. Reproduced from [125], © 2010, with permission of The Royal Society of Chemistry. <http://dx.doi.org/10.1039/C0AN00268B>

5.2 Reflectometric Interference Spectroscopy-Based Sensors

RiFS is an optical technique which enables the detection of changes in the thickness of a sensitive layer upon sorption/adsorption of analyte. At each wavelength interference takes place due to the light traveling through the transparent layers, and the final reflectance spectrum is monitored. Upon interaction of the analyte molecules with the sensing layer, the film swells and the interference pattern is changed.

Chiral discrimination in the gas phase using RiFS technique and a TSMR sensor was reported by Bodenhöfer et al. [126, 127]. Herein, only the results of the optical RiFS sensor are presented. An array of optical transducers spin-coated with Chirasil-Val derivatives (Fig. 22) was used for the detection of an α -amino acid and lactates. Chirasil-Val is a diamide-based material used as stationary phase in GC. An array of sensors fabricated with (R,S) -receptors and non-chiral polymer (PDMS-SE-30) were simultaneously exposed to vapors of the analytes. Both

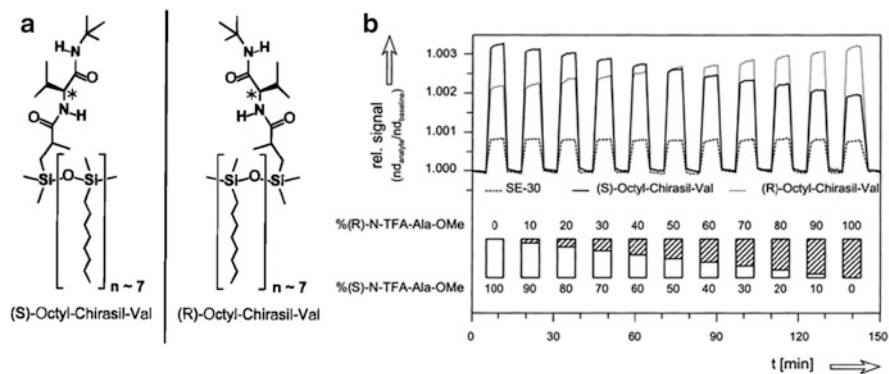


Fig. 22 (a) Molecular structure of the chiral polymer receptors. (b) Normalized sensor signal of (S)- and (R)-octyl-Chirasil-Val and of SE-30 upon exposure to different concentrations of enantiomeric mixtures. Reprinted with permission from [126], © 1997 American Chemical Society

enantiomers of ethyl lactate, methyl lactate, and *N*-trifluoroacetyl-alanine methyl ester (*N*-TFA-Ala-OMe) were tested. In Fig. 22 the relative responses of (R)- and (S)-octyl-Chirasil-Val-coated sensors and achiral sensors upon exposure to enantiomeric mixtures of (*N*-TFA-Ala-OMe) are presented. As is shown, a stronger affinity is observed for each receptor with its relative enantiomer and the signal of both chiral sensors is the same when exposed to the racemic mixture. The ability to differentiate the enantiomeric composition of various mixtures of both lactates quantitatively with Chirasil-Val derivatives was also demonstrated. Moreover, the data were evaluated by chemometric tools (multiple linear regression, partial component analysis, and principal component regression).

Optical (SPR, RIfS) and resonating (TSMR) sensors have also been employed for the enantioselective detection of chiral inhalation anesthetics [78]. Modified γ -cyclodextrin (Lipodex E) dissolved in polysiloxane matrix (SE-4) was used as chiral receptor for the differentiation of halogenated diether (1,1,1,3,3-pentafluoro-2-(fluoromethoxy)-3-methoxypropane) (halodiether B). Both enantiomers were tested in different concentrations and enantiomeric mixtures. The response of the sensor was higher in the presence of (*S*)-enantiomer revealing a stronger affinity between Lipodex E and the (*S*)-halodiether.

In addition, RIfS chiral sensors using MIPs as enantioselective layer has been reported [128]. The discrimination of 2,3-di-*O*-benzoyltartaric acid enantiomers using the respective enantiomers as template molecules was studied. In this case the polymer matrix was fabricated by *N,N'*-diethyl-4-vinyl-benzamidine and ethylene dimethacrylate as co-polymer and cross-linker. The MIP layers were exposed to different concentrations of the two enantiomers in water. The interaction of the target analytes with the MIP layers was observed directly by RIfS. For the (*S,S*)-MIP an enantioseparation factor $\alpha = 1.19$ was found, while for the (*R,R*)-MIP it was $\alpha = 1.23$.

6 Summary, Conclusions, and Outlook

Some of the most popular transduction platforms utilized in the field of enantiomer differentiation in both liquid and gas phases were described. Along with these descriptions, a large number of examples discussing the latest achievements of each type of transducer in the field of enantiomeric differentiation were presented. In addition, different chiral selectors and their immobilization strategies that have been used for the development of sensing devices exhibiting high enantioselectivity, repeatability, and stability were discussed.

Chiral sensors have the potential to replace conventional off-line analytical techniques in industrial process flow control and high throughput enantiomer screening procedures. Above all, the application itself always determines the type of transducer utilized. Selecting the materials suitable for each of the transducer's components and setting up the appropriate geometry for all these components in order to optimize the sensing performance is still a challenge for the future.

References

1. Hembury GA, Borovkov VV, Inoue Y (2008) Chirality-sensing supramolecular systems. *Chem Rev* 108(1):1–73
2. Hutt AJ (2005) Drug chirality and its pharmacological consequences. In: Smith J (ed) *Introduction to the principles of drug design and action*. Harwood Academic, Amsterdam, pp 117–183
3. Ward TJ, Baker BA (2008) Chiral separations. *Anal Chem* 80:4363–4372
4. Garrison AW, Schmitt-Kopplin P, Avants JK (2008) Analysis of the enantiomers of chiral pesticides and other pollutants in environmental samples by capillary electrophoresis. In: *Capillary electrophoresis*, vol 384. *Methods in molecular biology*TM. Humana, Totowa, pp 157–170
5. Zawirska-Wojtasiak R (2006) Chirality and the nature of food: authenticity of aroma. *Acta Sci Pol Technol Aliment* 5(1):21–36
6. Trojanowicz M, Kaniewska M (2008) Electrochemical chiral sensors and biosensors. *Electroanalysis* 21(3–5):229–238
7. Berthod A (2006) Chiral recognition mechanisms. *Anal Chem* 78(7):2093–2099
8. Cramer F (1994) *The lock and key principle*. Wiley, Chichester
9. Izake EL (2007) Chiral discrimination and enantioselective analysis of drugs: an overview. *J Pharm Sci* 96(7):1659–1676
10. Zhang J, Albelda MT, Liu Y, Canary JW (2005) Chiral nanotechnology. *Chirality* 17(7):404–420
11. Ali I, Saleem K, Hussain I, Gaitonde VD, Aboul-Enein HY (2009) Polysaccharides chiral stationary phases in liquid chromatography. *Sep Purif Rev* 38(2):97–147
12. Stefan-van Staden R-I, van Staden JF, Aboul-Enein HY, Mirica MC, Iorga M, Balcu I (2009) Maltodextrins as chiral selectors in biomedical enantioanalysis: a mini review. *Open Chem Biomed Meth J* 2:107–110
13. Shahgaldian P, Pieleas U (2006) Cyclodextrin derivatives as chiral supramolecular receptors for enantioselective sensing. *Sensors* 6(6):593–615

14. Ohsawa K, Kasamatsu T, Nagashima J, Hanawa K, Kuwahara M, Ozaki H, Sawai H (2008) Arginine-modified DNA aptamers that show enantioselective recognition of the dicarboxylic acid moiety of glutamic acid. *Anal Sci* 24(1):167–172
15. Challier L, Mavre F, Moreau J, Fave C, Schollhorn B, Marchal D, Peyrin E, Noel V, Limoges B (2012) Simple and highly enantioselective electrochemical aptamer-based binding assay for trace detection of chiral compounds. *Anal Chem* 84(12):5415–5420
16. Maier NM, Lindner W (2007) Chiral recognition applications of molecularly imprinted polymers: a critical review. *Anal Bioanal Chem* 389(2):377–397
17. Yashima E, Maeda K, Nishimura T (2003) Detection and amplification of chirality by helical polymers. *Chem-Eur J* 11(1):42–51
18. Yashima E, Maeda K (2008) Chirality-responsive helical polymers. *Macromolecules* 41(1):3–12
19. Kane-Maguire LAP, Wallace GG (2010) Chiral conducting polymers. *Chem Soc Rev* 39(7):2545–2576
20. Badis M, Tomaszekiewicz I, Joly JP, Rogalska E (2004) Enantiomeric recognition of amino acids by amphiphilic crown ethers in Langmuir monolayers. *Langmuir* 20(15):6259–6267
21. Diamond D, Nolan K (2001) Peer reviewed: calixarenes: designer ligands for chemical sensors. *Anal Chem* 73(1):22–29
22. Guangyan Q, Shunying L, Yongbing H (2008) Chiral recognition based on calix[4]arene. *Prog Chem* 20(12):1933–1944
23. Pietraszkiewicz M, Prus P, Bilewicz R (1999) pH dependent enantioselection of amino acids by phosphorous-containing calix[4]resorcinarene in Langmuir monolayers. *Polish J Chem* 73:2035–2042
24. Wen W, Jingli H, Youzun C, Xiaojia H (2007) Progress in chiral sensors. *Prog Chem* 19(11):1820–1825
25. Maier NM, Franco P, Lindner W (2001) Separation of enantiomers: needs, challenges, perspectives. *J Chromatogr A* 906(1):3–33
26. Inagaki S, Min JZ, Toyooka T (2008) Prediction for the separation efficiency of a pair of enantiomers during chiral high-performance liquid chromatography using a quartz crystal microbalance. *Anal Chem* 80(5):1824–1828
27. Hierlemann A, Baltes H, Schurig V (2001) Search for extraterrestrial enantioenrichment by using chemical microsensors. *Enantiomer* 6(2–3):129
28. Trojanowicz M, Wcislo M (2005) Electrochemical and piezoelectric enantioselective sensors and biosensors. *Anal Lett* 38(4):523–547
29. Budnikov G, Evtugin G, Budnikova YG, Al'fonsov V (2008) Chemically modified electrodes with amperometric response in enantioselective analysis. *J Anal Chem* 63(1):2–12
30. Stefan R-I, van Staden JF, Aboul-Enein HY (2004) Enantioselective, potentiometric membrane electrodes for the determination of L-pipecolic acid in serum. *Electroanalysis* 16(20):1730–1733
31. Stefan-van Staden R-I, Mashile TR (2006) Enantioselective assay of S(+)-ibuprofen using enantioselective, potentiometric membrane electrodes based on maltodextrins. *Sens Actuators B* 120(1):295–297
32. Stefan-van Staden R-I, Bokretson RG, Ozoemena KI (2006) Utilization of maltodextrin-based enantioselective, potentiometric membrane electrodes for the enantioselective assay of S-flurbiprofen. *Anal Lett* 39(6):1065–1073
33. Ozoemena KI, Stefan R-I (2004) Enantioselective, potentiometric membrane electrodes based on maltodextrins: their applications for the determination of L-proline. *Sens Actuators B* 98(1):97–100
34. Stefan R-I, van Staden JKF, Aboul-Enein HY (2000) Simultaneous detection of S and R-captopril using sequential injection analysis. *Talanta* 51(5):969–975
35. Ozoemena KI, Stefan R-I, Staden JF, Aboul-Enein HY (2004) Utilization of maltodextrin based enantioselective, potentiometric membrane electrodes for the enantioselective assay of S-perindopril. *Talanta* 62(4):681–685

36. Stefan-van Staden R-I, Bokretision RG, Ozoemena KI, van Staden JF, Aboul-Enein HY (2006) Enantioselective, potentiometric membrane electrodes based on different cyclodextrins as chiral selectors for the assay of *S*-flurbiprofen. *Electroanalysis* 18(17):1718–1721
37. Stefan R-I, van Staden JKF, Aboul-Enein HY (1999) Analysis of chiral drugs with enantioselective biosensors. An overview. *Electroanalysis* 11(16):1233–1235
38. Stefan R-I, van Staden JKF, Aboul-Enein HY (1999) A new construction for a potentiometric, enantioselective membrane electrode-its utilization to the *S*-captopril assay. *Talanta* 48(5):1139–1143
39. Aboul-Enein HY, Stefan R-I, van Staden JF (1999) Analysis of several angiotensin-converting enzyme inhibitors using potentiometric, enantioselective membrane electrodes. *Anal Lett* 32(4):623–632
40. Ratko AA, Stefan R-I, van Staden JKF, Aboul-Enein HY (2004) Enantioselective, potentiometric membrane electrode based on vancomycin: its application for the determination of *D*-pipecolic acid. *Sens Actuators B* 99(2):539–543
41. Ratko AA, Stefan R-I, van Staden JKF, Aboul-Enein HY (2004) Determination of *L*-carnitine using enantioselective, potentiometric membrane electrodes based on macrocyclic antibiotics. *Talanta* 63(3):515–519
42. Ratko AA, Stefan R-I, van Staden JKF, Aboul-Enein HY (2004) Macrocyclic antibiotics as chiral selectors in the design of enantioselective, potentiometric membrane electrodes for the determination of *L*- and *D*-enantiomers of methotrexate. *Talanta* 64(1):145–150
43. Stefan-van Staden R-I, Moldoveanu I, Sava D-F, Kapnissi-Christodoulou C, van Staden JF (2013) Enantioanalysis of pipecolic acid with stochastic and potentiometric microsensors. *Chirality* 25(2):114–118
44. Kaniewska M, Sikora T, Katakya R, Trojanowicz M (2008) Enantioselectivity of potentiometric sensors with application of different mechanisms of chiral discrimination. *J Biochem Biophys Methods* 70(6):1261–1267
45. Wulff G (1995) Molecular imprinting in cross-linked materials with the aid of molecular templates – a way towards artificial antibodies. *Angew Chem Int Ed Engl* 34(17):1812–1832
46. Andersson L, Sellergren BR, Mosbach K (1984) Imprinting of amino acid derivatives in macroporous polymers. *Tetrahedron Lett* 25(45):5211–5214
47. Chen Y, Chen L, Bi R, Xu L, Liu Y (2012) A potentiometric chiral sensor for *L*-phenylalanine based on crosslinked polymethylacrylic acid-polycarbazole hybrid molecularly imprinted polymer. *Anal Chim Acta* 754:83–90
48. Matsunaga M, Nakanishi T, Asahi T, Osaka T (2007) Highly enantioselective discrimination of amino acids using copper deposition on a gold electrode modified with homocysteine monolayer. *Electrochem Commun* 9(4):725–728
49. Zhou Y, Yu B, Levon K, Nagaoka T (2004) Enantioselective recognition of aspartic acids by chiral ligand exchange potentiometry. *Electroanalysis* 16(11):955–960
50. Davankov VA, Semechkin AV (1977) Ligand-exchange chromatography. *J Chromatogr A* 141(3):313–353
51. Galaverna G, Corradini R, Dallavalle F, Folesani G, Dossena A, Marchelli R (2001) Chiral separation of amino acids by copper(II) complexes of tetradentate diaminodiamido-type ligands added to the eluent in reversed-phase high-performance liquid chromatography: a ligand exchange mechanism. *J Chromatogr A* 922(1):151–163
52. Chen Z, Uchiyama K, Hobo T (2004) Chiral resolution of dansyl amino acids by ligand exchange-capillary electrophoresis using Cu(II)-*L*-prolinamides as chiral selector. *Anal Chim Acta* 523(1):1–7
53. Zhou Y, Nagaoka T, Yu B, Levon K (2009) Chiral ligand exchange potentiometric aspartic acid sensors with polysiloxane films containing a chiral ligand *N*-carbobenzyloxy-aspartic acid. *Anal Chem* 81(5):1888–1892
54. Yang Y, Hou J, Li B, Xu L (2010) Enantioselective ITO electrode modified with chiral salen Co(II) complex. *Chem Lett* 39(7):690–691

55. Xu L, Yang Y, Wang Y, Gao J (2009) Chiral salen Mn (III) complex-based enantioselective potentiometric sensor for L-mandelic acid. *Anal Chim Acta* 653(2):217–221
56. Stoica AI, Vinas C, Teixidor F (2009) Cobaltabisdicarbollide anion receptor for enantiomer-selective membrane electrodes. *Chem Commun* 33:4988–4990
57. Matsunaga M, Ueno T, Nakanishi T, Osaka T (2008) Enantioselective potential response of a human serum albumin-modified ITO electrode for tryptophan. *Electrochem Commun* 10(12):1844–1846
58. Yin X, Ding J, Zhang S, Kong J (2006) Enantioselective sensing of chiral amino acids by potentiometric sensors based on optical active polyaniline films. *Biosens Bioelectron* 21(11):2184–2187
59. Lahav M, Kharitonov AB, Willner I (2001) Imprinting of chiral molecular recognition sites in thin TiO₂ films associated with field-effect transistors: novel functionalized devices for chiroselective and chiro-specific analyses. *Chemistry* 7(18):3992–3997
60. Matsunaga M, Yamamoto D, Nakanishi T, Osaka T (2010) Chiral discrimination between alanine enantiomers by field effect transistor with a homocysteine monolayer-modified gate. *Electrochim Acta* 55(15):4501–4505
61. Yamamoto D, Nakanishi T, Osaka T (2011) Chiral sensing system based on the formation of diastereomeric metal complex on a homocysteine monolayer using field effect transistor. *Electrochim Acta* 56(26):9652–9655
62. Chen Q, Zhou J, Han Q, Wang Y, Fu Y (2012) A new chiral electrochemical sensor for the enantioselective recognition of penicillamine enantiomers. *J Solid State Electrochem* 16:2481–2485
63. Fu Y, Wang L, Chen Q, Zhou J (2011) Enantioselective recognition of chiral mandelic acid in the presence of Zn (II) ions by L-cysteine-modified electrode. *Sens Actuators B* 155(1):140–144
64. Fu Y, Chen Q, Zhou J, Han Q, Wang Y (2012) Enantioselective recognition of mandelic acid based on γ -globulin modified glassy carbon electrode. *Anal Biochem* 421:103–107
65. Chen Q, Zhou J, Han Q, Wang Y, Fu Y (2012) The selective adsorption of human serum albumin on N-isobutyryl-cysteine enantiomers modified chiral surfaces. *Biochem Eng J* 69:155–158
66. Basozabal I, Gomez-Caballero A, Unceta N, Goicolea MA, Barrio RJ (2011) Voltammetric sensors with chiral recognition capability: the use of a chiral inducing agent in polyaniline electrochemical synthesis for the specific recognition of the enantiomers of the pesticide dinoseb. *Electrochim Acta* 58:729–735
67. Huang J, Wei Z, Chen J (2008) Molecular imprinted polypyrrole nanowires for chiral amino acid recognition. *Sens Actuators B* 134(2):573–578
68. Prasad BB, Madhuri R, Tiwari MP, Sharma PS (2010) Enantioselective recognition of D- and L-tryptophan by imprinted polymer-carbon composite fiber sensor. *Talanta* 81(1):187–196
69. Prasad BB, Tiwari MP, Madhuri R, Sharma PS (2011) Enantioselective separation and electrochemical sensing of D- and L-tryptophan at ultratrace level using molecularly imprinted micro-solid phase extraction fiber coupled with complementary molecularly imprinted polymer-fiber sensor. *J Chromatogr B* 879(5):364–370
70. Stefan R-I, van Staden JKF, Aboul-Enein HY (2000) Amperometric biosensors/sequential injection analysis system for simultaneous determination of S- and R-captopril. *Biosens Bioelectron* 15(1):1–5
71. Stefan R-I, van Staden JF, Aboul-Enein HY (2003) Biosensors for the enantioselective analysis of pipercolic acid. *Sens Actuators B* 94(3):271–275
72. Stefan R-I, Bokretson RG, van Staden JF, Aboul-Enein HY (2003) Determination of L- and D-enantiomers of methotrexate using amperometric biosensors. *Talanta* 60(5):983–990
73. Stefan-van Staden R-I, van Staden JF, Aboul-Enein HY (2012) Amperometric biosensor based on diamond paste for the enantioanalysis of L-lysine. *Biosens Bioelectron* 35:439–442

74. Granot E, Tel-Vered R, Lioubashevski O, Willner I (2008) Stereoselective and enantioselective electrochemical sensing of monosaccharides using imprinted boronic acid-functionalized polyphenol films. *Adv Funct Mater* 18(3):478–484
75. Ide J, Nakamoto T, Moriizumi T (1995) Discrimination of aromatic optical isomers using quartz-resonator sensors. *Sens Actuators A* 49(1):73–78
76. Bodenhöfer K, Hierlemann A, Juza M, Schurig V, Göpel W (1997) Chiral discrimination of inhalation anesthetics and methyl propionates by thickness shear mode resonators: new insights into the mechanisms of enantioselectivity by cyclodextrins. *Anal Chem* 69(19):4017–4031
77. Fietzek C, Hermle T, Rosenstiel W, Schurig V (2001) Chiral discrimination of limonene by use of β -cyclodextrin-coated quartz-crystal-microbalances (QCMs) and data evaluation by artificial neuronal networks. *Fresenius J Anal Chem* 371(1):58–63
78. Kieser B, Fietzek C, Schmidt R, Belge G, Weimar U, Schurig V, Gauglitz G (2002) Use of a modified cyclodextrin host for the enantioselective detection of a halogenated diether as chiral guest via optical and electrical transducers. *Anal Chem* 74(13):3005–3012
79. Ng SC, Sun T, Chan HSO (2003) Durable chiral sensor based on quartz crystal microbalance using self-assembled monolayer of permethylated β -cyclodextrin. *Macromol Symp* 192:171–182
80. Ng SC, Sun T, Chan HSO (2002) Chiral discrimination of enantiomers with a self-assembled monolayer of functionalized β -cyclodextrins on Au surfaces. *Tetrahedron Lett* 43(15):2863–2866
81. Xu C, Ng SC, Chan HSO (2008) Self-assembly of perfunctionalized β -cyclodextrins on a quartz crystal microbalance for real-time chiral recognition. *Langmuir* 24(16):9118–9124
82. Luo ML, Zhang WG, Zhang S, Fan J, Su WC, Yin X (2010) Self-assembly and chiral recognition of quartz crystal microbalance chiral sensor. *Chirality* 22(4):411–415
83. Haupt K, Noworyta K, Kutner W (1999) Imprinted polymer-based enantioselective acoustic sensor using a quartz crystal microbalance. *Anal Commun* 36(11–12):391–393
84. Piacham T, Josell A, Arwin H, Prachayasittikul V, Ye L (2005) Molecularly imprinted polymer thin films on quartz crystal microbalance using a surface bound photo-radical initiator. *Anal Chim Acta* 536(1):191–196
85. Percival C, Stanley S, Galle M, Braithwaite A, Newton M, McHale G, Hayes W (2001) Molecular-imprinted, polymer-coated quartz crystal microbalances for the detection of terpenes. *Anal Chem* 73(17):4225–4228
86. Stanley S, Percival C, Morel T, Braithwaite A, Newton M, McHale G, Hayes W (2003) Enantioselective detection of L-serine. *Sens Actuators B* 89(1):103–106
87. Cao L, Zhou XC, Li SFY (2001) Enantioselective sensor based on microgravimetric quartz crystal microbalance with molecularly imprinted polymer film. *Analyst* 126(2):184–188
88. Liu F, Liu X, Ng SC, Chan HSO (2006) Enantioselective molecular imprinting polymer coated QCM for the recognition of L-tryptophan. *Sens Actuators B* 113(1):234–240
89. Syritski V, Reut J, Menaker A, Gyurcsanyi RE, Opik A (2008) Electrosynthesized molecularly imprinted polypyrrole films for enantioselective recognition of L-aspartic acid. *Electrochim Acta* 53(6):2729–2736
90. Kong Y, Zhao W, Yao S, Xu J, Wang W, Chen Z (2010) Molecularly imprinted polypyrrole prepared by electrodeposition for the selective recognition of tryptophan enantiomers. *J Appl Polym Sci* 115(4):1952–1957
91. Huang J, Egan VM, Guo H, Yoon JY, Briseno AL, Rauda IE, Garrell RL, Knobler C, Zhou F, Kaner RB (2003) Enantioselective discrimination of D- and L-phenylalanine by chiral polyaniline thin films. *Adv Mater* 15(14):1158–1161
92. Tanese M, Torsi L, Cioffi N, Zotti L, Colangiuli D, Farinola G, Babudri F, Naso F, Giangregorio M, Sabbatini L (2004) Poly(phenyleneethynylene) polymers bearing glucose substituents as promising active layers in enantioselective chemiresistors. *Sens Actuators B* 100(1):17–21

93. Guo HS, Kim JM, Chang SM, Kim WS (2009) Chiral recognition of mandelic acid by L-phenylalanine-modified sensor using quartz crystal microbalance. *Biosens Bioelectron* 24(9):2931–2934
94. Guo HS, Kim JM, Kim SJ, Chang SM, Kim WS (2009) Versatile method for chiral recognition by the quartz crystal microbalance: chiral mandelic acid as the detection model. *Langmuir* 25(2):648–652
95. Kim JM, Chang SM, He XK, Kim WS (2012) Development of real-time sensitive chiral analysis technique using quartz crystal analyzer. *Sens Actuators B* 171–172:478–485
96. Landsteiner K, Van der Scheer J (1928) Serological differentiation of steric isomers. *J Exp Med* 48(3):315–320
97. Dutta P, Tipple C, Lavrik N, Datskos P, Hofstetter H, Hofstetter O, Sepaniak M (2003) Enantioselective sensors based on antibody-mediated nanomechanics. *Anal Chem* 75(10):2342–2348
98. Su WC, Zhang WG, Zhang S, Fan J, Yin X, Luo ML, Ng SC (2009) A novel strategy for rapid real-time chiral discrimination of enantiomers using serum albumin functionalized QCM biosensor. *Biosens Bioelectron* 25(2):488–492
99. Chen WJ, Zhang S, Zhang WG, Fan J, Yin X, Zheng SR, Su WC, Zhang Z, Hong T (2012) A new biosensor for chiral recognition using goat and rabbit serum albumin self-assembled quartz crystal microbalance. *Chirality* 24:804–809
100. Nakanishi T, Yamakawa N, Asahi T, Shibata N, Ohtani B, Osaka T (2004) Chiral discrimination between thalidomide enantiomers using a solid surface with two-dimensional chirality. *Chirality* 16(S1):S36–S39
101. Guo W, Wang J, Wang C, He J-Q, X-W H, Cheng J-P (2002) Design, synthesis, and enantiomeric recognition of dicyclodipeptide-bearing calix[4]arenes: a promising family for chiral gas sensor coatings. *Tetrahedron Lett* 43(32):5665–5667
102. Severin EJ, Sanner RD, Doleman BJ, Lewis NS (1998) Differential detection of enantiomeric gaseous analytes using carbon black-chiral polymer composite, chemically sensitive resistors. *Anal Chem* 70(7):1440–1443
103. Costello BPJ, Ratcliffe NM, Sivanand PS (2003) The synthesis of novel 3-substituted pyrrole monomers possessing chiral side groups: a study of their chemical polymerisation and the assessment of their chiral discrimination properties. *Synth Met* 139(1):43–55
104. Torsi L, Marinelli F, Angione MD, Dell'Aquila A, Cioffi N, Giglio ED, Sabbatini L (2009) Contact effects in organic thin-film transistor sensors. *Org Electron* 10(2):233–239
105. Torsi L, Dodabalapur A (2005) Organic thin-film transistors as plastic analytical sensors. *Anal Chem* 77(19):380–387
106. Torsi L, Dodabalapur A, Sabbatini L, Zambonin PG (2000) Multi-parameter gas sensors based on organic thin-film-transistors. *Sens Actuators B* 67(3):312–316
107. Torsi L, Tafuri A, Cioffi N, Gallazzi M, Sassella A, Sabbatini L, Zambonin P (2003) Regioregular polythiophene field-effect transistors employed as chemical sensors. *Sens Actuators B* 93(1):257–262
108. Majewski LA, Schroeder R, Grell M (2005) One volt organic transistor. *Adv Mater* 17(2):192–196
109. Dost R, Das A, Grell M (2007) A novel characterization scheme for organic field-effect transistors. *J Phys D Appl Phys* 40(12):3563
110. Roberts ME, Mannsfeld SCB, Queralto N, Reese C, Locklin J, Knoll W, Bao Z (2008) Water-stable organic transistors and their application in chemical and biological sensors. *Proc Natl Acad Sci* 105(34):12134–12139
111. Sokolov AN, Roberts ME, Bao Z (2009) Fabrication of low-cost electronic biosensors. *Mater Today* 12(9):12–20
112. Angione MD, Cotrone S, Magliulo M, Mallardi A, Altamura D, Giannini C, Cioffi N, Sabbatini L, Fratini E, Baglioni P (2012) Interfacial electronic effects in functional bilayers integrated into organic field-effect transistors. *Proc Natl Acad Sci* 109(17):6429–6434

113. Torsi L, Farinola GM, Marinelli F, Tanese MC, Omar OH, Valli L, Babudri F, Palmisano F, Zambonin PG, Naso F (2008) A sensitivity-enhanced field-effect chiral sensor. *Nat Mater* 7(5):412–417
114. Bernards DA, Macaya DJ, Nikolou M, DeFranco JA, Takamatsu S, Malliaras GG (2007) Enzymatic sensing with organic electrochemical transistors. *J Mater Chem* 18(1):116–120
115. Ouyang R, Lei J, Ju H, Xue Y (2007) A molecularly imprinted copolymer designed for enantioselective recognition of glutamic acid. *Adv Funct Mater* 17(16):3223–3230
116. Zhang S, Ding J, Liu Y, Kong J, Hofstetter O (2006) Development of a highly enantioselective capacitive immunosensor for the detection of α -amino acids. *Anal Chem* 78(21):7592–7596
117. Kurzawski P, Bogdanski A, Schurig V, Wimmer R, Hierlemann A (2007) Opposite signs of capacitive microsensor signals upon exposure to the enantiomers of methyl propionate compounds. *Angew Chem Int Ed* 47(5):913–916
118. Kurzawski P, Bogdanski A, Schurig V, Wimmer R, Hierlemann A (2009) Direct determination of the enantiomeric purity or enantiomeric composition of methylpropionates using a single capacitive microsensor. *Anal Chem* 81(5):1969–1975
119. Kurzawski P, Schurig V, Hierlemann A (2009) Chiral sensing using a complementary metal-oxide semiconductor-integrated three-transducer microsensor system. *Anal Chem* 81(22):9353–9364
120. Hofstetter O, Hofstetter H, Wilchek M, Schurig V, Green BS (1999) Chiral discrimination using an immunosensor. *Nat Biotechnol* 17(4):371–374
121. Shahgaldian P, Hegner M, Piele U (2005) A cyclodextrin self-assembled monolayer (SAM) based surface plasmon resonance (SPR) sensor for enantioselective analysis of thyroxine. *J Incl Phenom Macrocycl Chem* 53(1):35–39
122. Lieberman I, Shemer G, Fried T, Kosower EM, Markovich G (2008) Plasmon-resonance-enhanced absorption and circular dichroism. *Angew Chem Int Ed* 47(26):4855–4857
123. Ha JM, Solovyov A, Katz A (2008) Postsynthetic modification of gold nanoparticles with calix[4]arene enantiomers: origin of chiral surface plasmon resonance. *Langmuir* 25(1):153–158
124. Ha JM, Solovyov A, Katz A (2009) Synthesis and characterization of accessible metal surfaces in calixarene-bound gold nanoparticles. *Langmuir* 25(18):10548–10553
125. Ben-Amram Y, Riskin M, Willner I (2010) Selective and enantioselective analysis of mono- and disaccharides using surface plasmon resonance spectroscopy and imprinted boronic acid-functionalized Au nanoparticle composites. *Analyst* 135(11):2952–2959
126. Bodenhöfer K, Hierlemann A, Seemann J, Gauglitz G, Christian B, Koppenhoefer B, Göpel W (1997) Chiral discrimination in the gas phase using different transducers: thickness shear mode resonators and reflectometric interference spectroscopy. *Anal Chem* 69(15):3058–3068
127. Bodenhöfer K, Hierlemann A, Seemann J, Gauglitz G, Koppenhoefer B, Göpel W (1997) Chiral discrimination using piezoelectric and optical gas sensors. *Nature* 387:577–579
128. Nopper D, Lammershop O, Wulff G, Gauglitz G (2003) Amidine-based molecularly imprinted polymers—new sensitive elements for chiral chemosensors. *Anal Bioanal Chem* 377(4):608–613

Enantiopure Supramolecular Cages: Synthesis and Chiral Recognition Properties

Thierry Brotin, Laure Guy, Alexandre Martinez, and Jean-Pierre Dutasta

Abstract Enantiopure compounds are ubiquitous in the chemical sciences and present a particular interest in the field of molecular recognition and host-guest systems. Indeed, chiral molecular receptors are at the basis of numerous biological recognition processes and have important implications in biochemistry or pharmacology. Chemists have been investigating this field for several decades, which has led to the development of the synthesis of chiral hosts, their enantiomeric differentiation, and the studies of their recognition properties towards important and bio-relevant chiral guest substrates. The design of molecular cages is a rather difficult task that is even more demanding when enantiopure molecules are required. In this review we chose to present the main families of synthetic organic supramolecular cages that have been developed, whose structures contain stereogenic centers or present an inherent chirality, giving rise to chiral supramolecular cages. Particular attention is given to obtaining enantiopure compounds. Their recognition properties are also underlined. A last important aspect of the review is to present how chiroptical spectroscopies can be used to characterize the recognition phenomena displayed by supramolecular cages.

Keywords Chiral cages · Chiral recognition · Chiroptical properties · Host-guest systems · Supramolecular chemistry

Contents

1	Introduction	179
1.1	General	179
1.2	Scope	179

2	From Vase Like Cavitands to Close-Shell Molecular Containers	181
2.1	Cyclodextrins	181
2.2	Calixarenes	182
2.3	Resorcin[4]arene-Based Host Molecules	185
2.4	And Others	188
3	Synthesis and Enantiomeric Separation of Supramolecular Cages	190
3.1	Carcerands and Carceplexes	191
3.2	Synthesis from C ₃ -Symmetrical Aromatic Platforms	191
3.3	Synthesis from C ₃ Cyclotribenzylene Platforms: Cryptophanes and Congeners ...	195
3.4	Synthesis from C ₃ Cyclotribenzylene Platforms: Hemicryptophanes	202
3.5	Cholic Acid-Based Scaffolds	207
3.6	Assignment of the Absolute Configuration	207
4	Chiral Recognition and Enantiomeric Differentiation	211
4.1	Use of Chiroptical Techniques for the Monitoring of Complexation Phenomena: ECD and VCD of Enantiopure Water-Soluble Cryptophane Cages	211
4.2	Recognition of Monovalent Cations by Enantiopure Water-Soluble Cryptophanes	215
4.3	Complexation of Chiral Guests	216
4.4	Biosensing: Xenon–Cryptophane Complexes	222
5	Conclusion	224
	References	225

Abbreviations

CD	Cyclodextrin
CTB	Cyclotribenzylene
CTV	Cyclotriveratrylene
DACH	Diaminocyclohexane
<i>de</i>	Diastereomeric excess
DFT	Density functional theory
DMF	Dimethylformamide
DMSO	Dimethyl sulfoxide
dppp	1,3-Bis(diphenylphosphino)propane
<i>dr</i>	Diastereomeric ratio
ECD	Electronic circular dichroism
<i>ee</i>	Enantiomeric excess
equiv.	Equivalent(s)
HPLC	High performance liquid chromatography
ITC	Isothermal titration calorimetry
Me	Methyl
min	Minute(s)
MOF	Metal organic framework
mol	Mole(s)
NMR	Nuclear magnetic resonance
Ns	2-Nitrobenzenesulfonyl
NTA	Nitrilotriacetic acid
Ph	Phenyl
rt	Room temperature

s	Second(s)
TBAF	Tetrabutylammonium fluoride
TBTQ	Tribenzotriquinacene
TEA	Triethylamine
Tf	Trifluoromethanesulfonyl (triflyl)
TFA	Trifluoroacetic acid
THF	Tetrahydrofuran
tren	Tris(2-aminoethyl)amine
VCD	Vibrational circular dichroism

1 Introduction

1.1 General

Supramolecular chemistry is closely related to molecular associations and to recognition phenomena, present in most of the chemical and biochemical processes of living systems. The “lock and key” model coined by Emil Fisher at the end of the nineteenth century brought a brilliant and realistic illustration of the stereoselective functioning of the enzyme proteins, and later became the emblematic concept of supramolecular chemistry [1]. These last 50 years have seen a huge development of this field of research, which seems unlimited according to its extraordinary application in many aspects of fundamental and applied domains of chemical sciences. The host–guest interactions and the formation of complexes are examples of these domains, which are strongly connected to molecular recognition in biological processes. Thereby, chiral recognition appears as one of the most important challenges in this field, when considering the main concerns in biology, pharmacology, or catalysis to name just a few. This is probably one of the factors that encouraged the development of artificial receptors that can generate host–guest complexes. Molecular containers with intramolecular cavities that intrinsically present a chiral environment are thus of prime importance. For instance, we can mention the cyclodextrins, where the chirality arises from the glucosidic walls, or the cavitands and calixarenes, which can also deliver a chiral environment if suitable substitutions and/or structures are adequately designed. Two main approaches can make the synthetic receptors chiral: the introduction of chiral moieties or the inherent chirality of the host arising from the bowl shape of the molecular scaffold. Thus, the chiral recognition with artificial receptors requires the preparation of enantiopure molecules or self-assembled systems, which present efficient recognition abilities toward chiral substrates.

1.2 Scope

The purpose of this review is to provide an overview of studies of the synthesis and functional properties of chiral entities that have three-dimensional molecular

cavities, namely supramolecular cages. By supramolecular we mean that the molecular hosts have the potential to form host–guest complexes, a terminology that is more accepted today. We will focus on synthetic systems mainly issued from organic chemistry and that have been enantiomerically resolved, so that their chiral properties have been successfully exploited. This appears to be a real challenge as the field has been increasing more and more over the last decades [2]. Thus, we have limited this review to the last 10–15 years, citing, when appropriate, previous seminal contributions. Furthermore, we tried to have a rational approach in terms of structure and receptor family. Although supramolecular receptors can be covalent or non-covalent entities, we will focus on the covalent structures, and will not refer to capsular self-assembled systems that can also lead to chiral entities such as coordination cages and MOFs [3, 4]. Similarly, we will not describe the chiral nanoribbons and nanotubes developed by Huc et al. [5–7]. These self-assembling systems constitute an original family of helical molecular capsules mainly based on oligo-amide sequences [8]. Generally, single or double helical strands self-assemble in a folded conformation delineating an inner chiral space capable of binding appropriate guests [9, 10]. It is outside the scope of this review to deal with biological systems, although they are the main source of inspiration in the field of chiral recognition.

Chiral molecular cages have been designed in most of the main families of organic receptors: calixarenes, cavitands, cryptophanes, cyclodextrins, cyclophanes, cholic acid-based scaffolds, etc. They can be the source of important investigations in pharmacology, materials technology (NLO materials, chromatographic phases), or asymmetric catalysis. It is thus of great interest to try to have a compendium of the supramolecular cages that were developed recently, for which synthesis, enantiomeric separation, and diastereoselective and enantioselective recognition properties have been reported. On the other hand, chirality can be used as a tool for characterizing encaged species and recognition processes, using modern spectroscopic techniques, e.g., NMR, ECD and VCD, or mass spectrometry.

First, we will briefly introduce chiral open-shell structures delineating a molecular cavity. This concerns cyclodextrins, calix[*n*]arenes, cavitands, and other chiral concave molecules, which often constitute starting entities for the design of chiral supramolecular cages. A second part is devoted to the design of enantiopure supramolecular cages. These chiral receptors are presented according to their constitutive scaffolds based on well-known concave moieties. Finally, the last part deals with the recognition of chiral or achiral guests and the consequences of encapsulation on the diastereoselectivity and enantioselectivity of the recognition in the confined space of the chiral cages. Furthermore, particular attention is given to recent progresses in chiroptical methods for investigating structural changes and characterization of guest recognition. Emphasis will be placed on the results from our own laboratory.

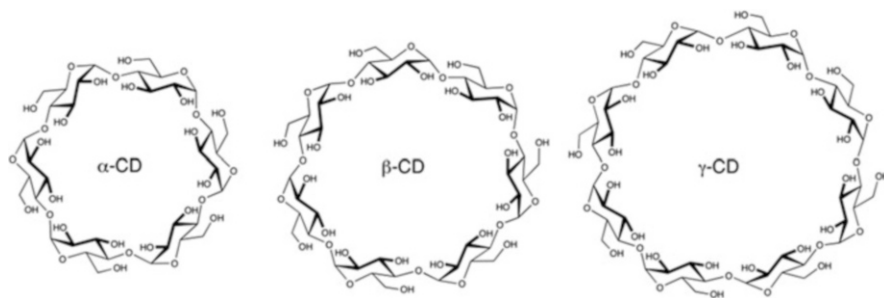


Fig. 1 Cyclodextrin (CD) hosts

2 From Vase Like Cavitands to Close-Shell Molecular Containers

In this chapter we will first refer briefly to families of molecules that present a chiral cavity and can constitute in some cases the starting material for the design of close-shell molecular cages. Then we will present more complex structures, obtained by sophisticated chemical design often based on elementary bowl-shape structures that lead to efficient enantiopure molecular containers.

2.1 Cyclodextrins

Cyclodextrins (CD) are water-soluble hosts made of glucopyranose units, which adopt a conical shape forming a funnel shaped receptor. According to the number of sugar units, six, seven, or eight in most of the usual derivatives, they are labeled as α , β , or γ -cyclodextrins (Fig. 1). Due to the chirality of the sugar moieties, they are by nature chiral hosts and numerous studies have been reported concerning their binding abilities thanks to their intrinsically chiral inner space. For instance, CDs are widely used as chiral selectors for the preparation of stationary phases for the enantiomeric differentiation of chiral guests [11]. Enantioseparation of racemic guests by crystallization of the inclusion complexes with cyclodextrins has been reported [12]. Recent developments in the functionalization of the cyclodextrins opened the route to very interesting compounds with stereogenic centers [13]. These new approaches allow the formation of original compounds on a large scale. The enantioselective recognition of chiral guests by CDs is well documented with particular attention on the recognition of L/D amino acids. For instance, this has been well illustrated by the host properties of suitably side-substituted β -cyclodextrins [14].

CDs are not closed shell molecules, but there exist capped cyclodextrins where an enforced molecular cavity is formed, and they now constitute an important family of chiral hosts [15]. Generally, they are synthesized from suitably

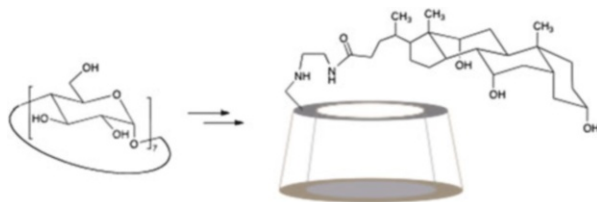


Fig. 2 Structure of cholic acid-modified β -CD

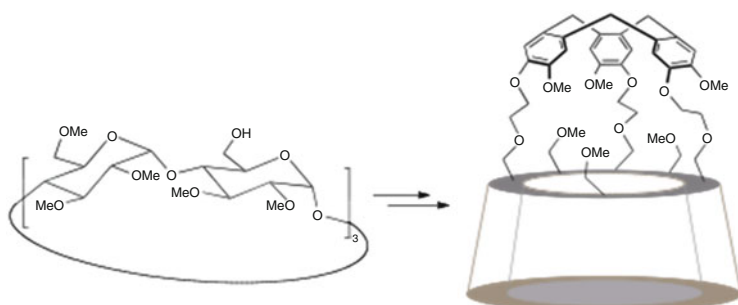


Fig. 3 Structure of the cyclotrimerarylene-capped α -CD

functionalized CDs, which can react with various capping units. For instance, recently, cholic and deoxycholic acids were bound to the rim of a β -CD to form a molecular container able to complex anionic species such as sulfonate-naphthalene derivatives (Fig. 2) [16]. The cyclotribenzylene (CTB) cap linked to a permethylated α -cyclodextrin forms the cavitant structure depicted in Fig. 3. Interestingly, the chirality of the pyranosyl units controls the chirality of the CTB unit formed during the reaction, leading to a diastereoselectivity with a diastereomeric ratio *dr* of 6:1 [17].

2.2 Calixarenes

Calix[*n*]arenes constitute a well known class of cone-shaped molecules useful in the design of molecular receptors (Fig. 4). It is outside the scope of this chapter to review this class of hosts, known since the mid-1950s, since many original structures were created on the basis of the calix structure. However, it is a fitting tribute to mention the pioneering works of Gutsche at the end of the 1970s [18], followed by the impressive works of the groups of Böhmer, Shinkai, Ungaro, and many others [19]. Herein, we will focus on some examples of closed molecular cavities built from calix structures presenting chiral properties.

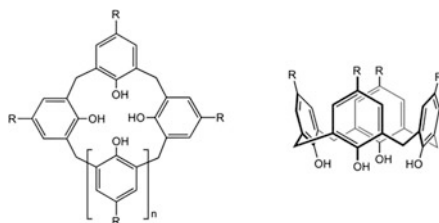
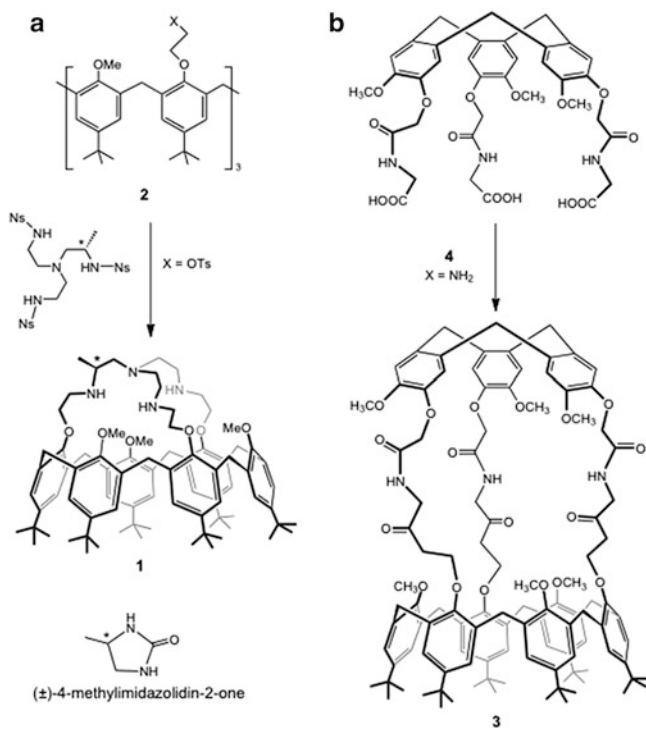


Fig. 4 Calix[*n*]arene and the cone shape structure of the calix[4]arene

Calix[4]arenes in their cone conformation are able to present enantiomerism by adding at least one chiral unit by substitution on either the wide or the narrow rim. In their partial cone, 1,2-alternate and 1,3-alternate conformations, the calix[4]arenes can give rise to chiral compounds [20]. This stereochemical behavior has also been observed with larger calix[*n*]arenes ($n > 4$) providing that conformational exchanges are avoided [21]. This can be achieved for instance with calix[6]arenes by bridging or capping the molecules or by metal binding. This is nicely illustrated by the work of Jabin et al., who synthesized several interesting closed-shell molecules based on the calix[6]arene scaffold and containing stereogenic centers. The enantiopure calix[6]aza-cryptand **1** was obtained by reaction of a chiral *tren* unit of known configuration with the 1,3,5-tris-tosylated calix[6]arene **2** (Scheme 1a). The tetra-ammonium salt of **1** exhibited remarkable host–guest properties toward (\pm)-4-methylimidazolidin-2-one and can differentiate between the two guest enantiomers [22]. The hemicryptophane cage **3** consists of a calix[6]arene moiety bound to the intrinsically chiral cyclotribenzylene **4** by means of amide linkers (Scheme 1b). In this example, only the racemic compound was reported, which presents a heteroditopic cavity suitable for the cooperative binding of ammonium chloride salts and neutral guest molecules. In the presence of (\pm)-4-methylimidazolidin-2-one two diastereomeric complexes are obtained with a diastereomeric excess of 44% [23].

The peculiar cone structure of the calixarene can also define an inherent chirality, which arises from the presence of a curvature created from a hypothetical planar structure which does not contain any mirror plane (Fig. 5) [24]. In Fig. 5 the presence of the Y substituent creates inherent chirality. The racemization is only possible by the cone inversion, a highly energetic process in the case of the calix[4]arenes. Examples of inherent chirality in calixarenes, as well as in the cavitands briefly described in the next paragraph, have been reported by Böhmer in 2000 [25], and different strategies for their syntheses were recently reviewed [26–28]. The enantiomeric separation of such molecules is possible, for instance, by means of the formation of diastereomers, which can be separated by chromatography [29]. However, we will not explore further these derivatives, as well as the numerous related homocalixarene hosts, which generally cannot be classified as true closed-shell host molecules and are beyond the scope of this review.



Scheme 1 Access to calix[6]aza-cryptand **3** (a), and to the CTB-capped calix[6]arene **1** (b) (Ns=2-nitrobenzenesulfonyl)

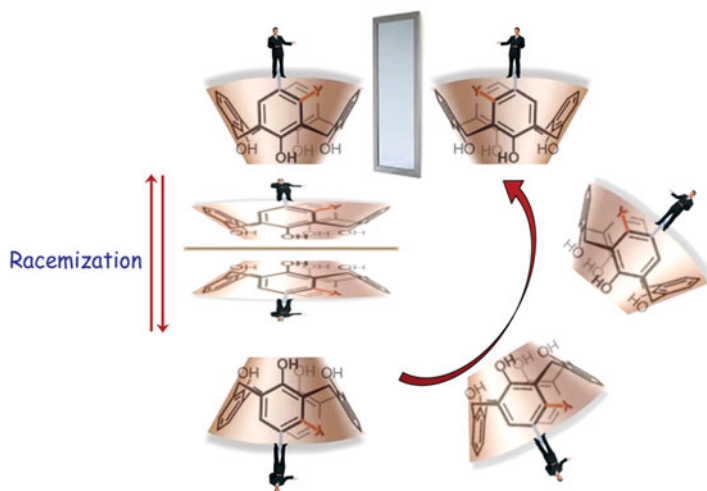


Fig. 5 Inherent chirality of the calixarene structure

2.3 Resorcin[4]arene-Based Host Molecules

These molecules are obtained from the cyclocondensation of resorcinol with aliphatic or aromatic aldehydes $R-C(O)H$ (Fig. 6a) [30]. They are able to complex suitable guest molecules through H-bonding with the phenolic OH groups and $\pi-\pi$, $CH-\pi$, or cation- π interactions. Most importantly, resorcin[4]arenes are starting compounds for the synthesis of molecular containers containing an enforced rigid molecular cavity obtained by rigidifying the structure by introducing bridging moieties on the hydroxyl functions (Fig. 6b) [31]. In the early 1980s, Cram introduced the term *cavitand* to name the bridged resorcin[4]arenes [32].

As for calixarenes, the introduction of stereogenic groups to the cavitand structure affords chiral molecules. On the other hand, inherently chiral cavitands were obtained by using different bridging units (Fig. 7a) [25] or by introducing one nonsymmetrical linker, as, for example, to form the enantiopure chiral cavitand depicted in Fig. 7b [33].

After the first enantioselective syntheses of enantiomerically pure resorcin[4]arene derivatives (Fig. 8; $R=C_{11}H_{23}$; $R'=(R)\text{-}\alpha\text{-methylbenzyl}$) [34], Schalley and Rissanen reported the synthesis of chiral resorcin[4]arene based hosts and their recognition properties towards chiral ammonium guests [35]. The reaction of resorcin[4]arene with formaldehyde and enantiopure *R*- or *S*-1-cyclohexylethylamine led to compounds (*R*)-**5** and (*S*)-**5** (Fig. 8). The stereochemical problem arising from the orientation of the newly formed six-membered rings was largely overcome due to the H-bond network and only two diastereomers were formed. All oxazines are clockwise oriented or anticlockwise with respect to the resorcicarene scaffold. The same reaction run with *S*-benzyl-1-methylbenzyl amine afforded the quickly interconverting isomers leading to average NMR signals. The complexation of chiral ammonium guests was investigated by mass spectrometry, without evidence for enantiodifferentiation.

Chiral C_4 symmetrical hosts were also reported and obtained by introducing moieties that form clockwise or anticlockwise directionalities. Their ability to form intramolecular hydrogen bonds at their wide rim with directionality leads formally to chiral molecules, which enantiomerize rapidly by exchange of the right and left arrangements of the H-bonds pattern. Typically, the so-formed cycloenantiomers presented in Fig. 9, where *R* and *R'* are alkyl groups, are representative of this class of chiral cavitands [36].

Phosphonatocavitands are particularly efficient in the recognition of various species [37]. In particular they show remarkable binding properties towards alcohols [38, 39], metal ions [40], and ammonium cations in organic solution [41, 42], and have been used to design inherently chiral cavitands. The diphosphonatocavitand (\pm)-**6** bearing a quinoxaline bridge has been synthesized. The three different bridges define an inherently chiral structure. The two enantiomers were separated by semi-preparative chiral HPLC. This method afforded enantiopure (+)-**6** and (-)-**6** with *ee* > 99%. The absolute configuration of each enantiomer was determined from the comparison between experimental and calculated VCD spectra, and allowed one to

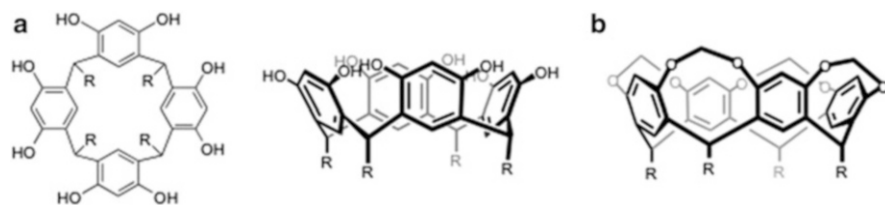


Fig. 6 Structures of resorcin[4]arene (a) and CH₂-bridged cavitant (b) molecules

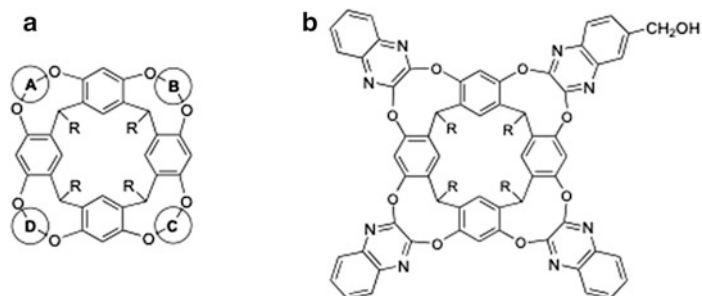


Fig. 7 Inherently chiral cavitants: (a) with different bridging moieties; (b) example of chiral cavitant ($R=C_6H_{13}$)

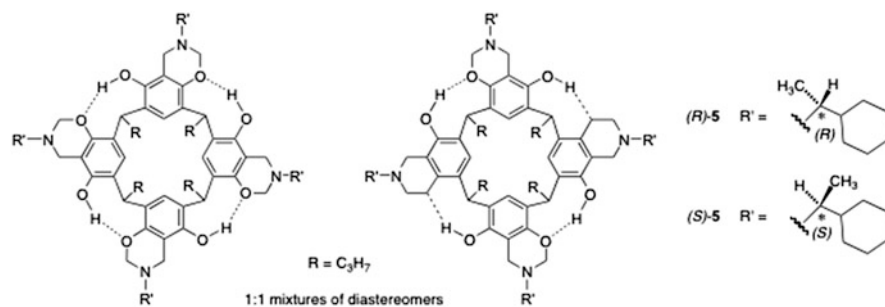


Fig. 8 Chiral resorcin[4]arene-based hosts (R)-5 and (S)-5

assign the *cR* configuration to (–)-6 (Fig. 10). The addition of L-adrenaline to a solution of (±)-6 showed the complexation of the neurotransmitter in the cavity of the host. NMR spectra showed the formation of the two diastereomeric complexes L-adrenaline@(+)-6 and L-adrenaline@(-)-6. Starting from the enantiopure cavitants, it was possible to assign each complex and to demonstrate that (+)-6 better accommodates L-adrenaline than (–)-6 with binding constants of 435 M⁻¹ and 140 M⁻¹, respectively (Table 1) [43].

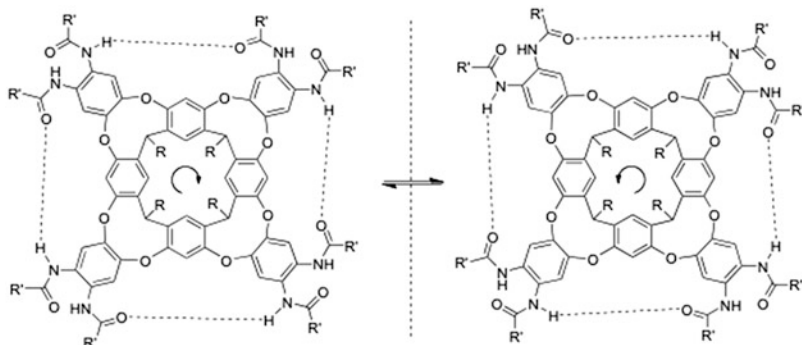


Fig. 9 Cycloenantiomeric cavitands with clockwise and counterclockwise directionality

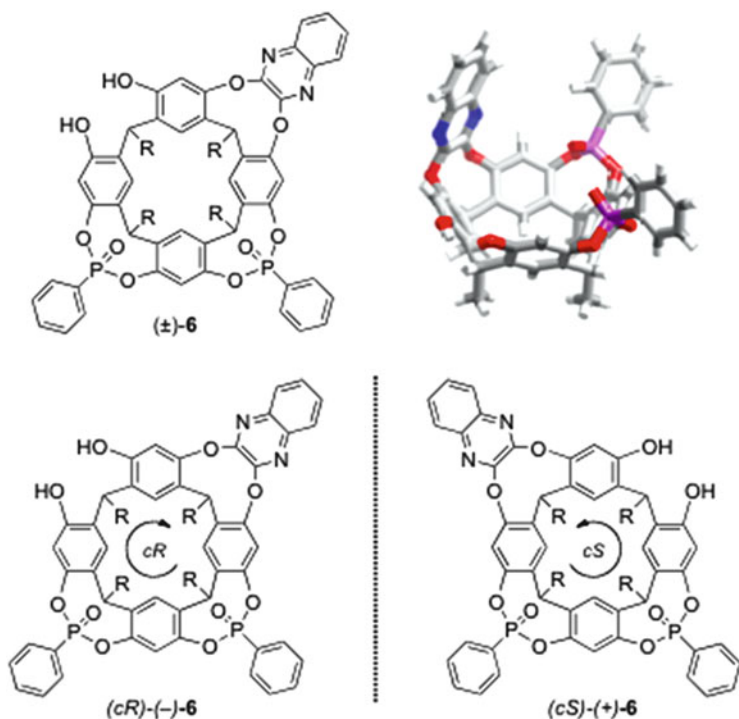
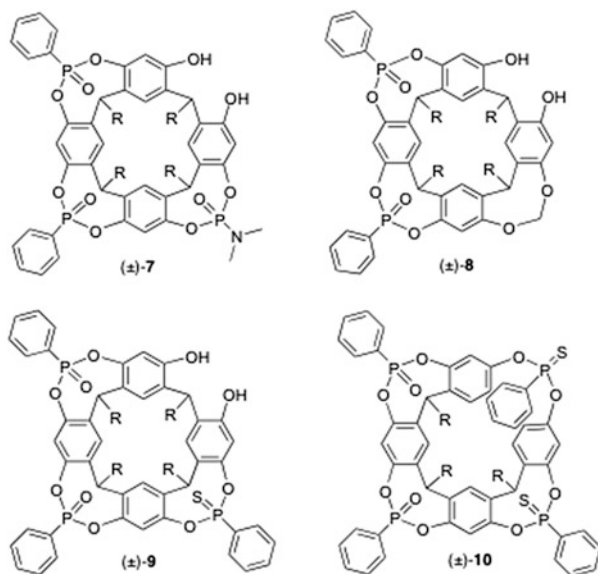


Fig. 10 Enantiomerically resolved diphosphonato-cavitands (+)-6 and (-)-6 ($R=C_{11}H_{23}$) and the calculated structure with $R=CH_3$

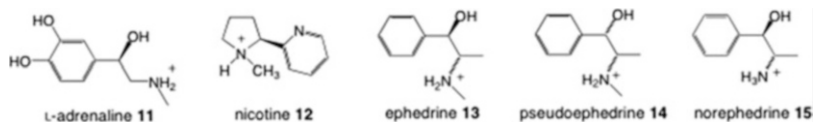
This strategy was extended to other phosphonatecavitands 7–10 bearing different bridging units. Examples are given in Fig. 11, of which only (\pm)-8 was resolved by chiral HPLC. Enantioselective complexation of ammonium guests was investigated by NMR experiments. Chiral ammonium of biological importance

Table 1 Diastereomeric ratios (*dr*) guest@(+)-host/guest@(-)-host, for the complexes of the racemic cavitands **6** and **8** with enantiopure ammonium guests **11–15**

Host					
Guest	11	12	13	14	15
(±)- 6	2:1	1:1	1:1	2.2:1	1:2.5
(±)- 8	1:1	1:1	1:1.3	2.5:1	–

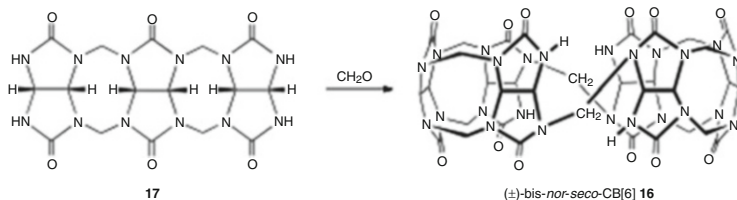
**Fig. 11** Inherently chiral phosphonatocavitands

11–15 were used and led to the formation of diastereomeric complexes observed by ^1H and ^{31}P NMR spectroscopy. Typical diastereomeric ratios obtained with the ammonium picrate salts are reported in Table 1 [44].



2.4 And Others...

The cucurbit[*n*]urils (CB[*n*]) constitute a particular class of molecular containers which are rapidly developing [45]. They present a hydrophobic molecular cavity in



Scheme 2 Formation of (±)-bis-nor-seco-CB[6] **16**

a large range of size (82–870 Å³ from CB[5] to CB[11]), capable of interacting with various guest substrates. They have been widely used for their recognition properties and to form supramolecular associations with non-polar molecules or ions. The modularity in their synthesis and purification is tedious and this is probably one reason why their chemical modifications are rare. Nevertheless, the synthesis and the recognition properties of the chiral bis-*nor-seco*-cucurbit[6]uril (±)-**16** has been reported. This particular form of cucurbituril is obtained by condensation of two glycoluril trimers **17** with formaldehyde, with complete stereochemical control (Scheme 2) [46]. Complexation of chiral amines led to moderate diastereoselectivity. In the present case the host was not enantiomerically resolved.

Finally we will mention the fullerene family, which represents the perfect cage, as it is impossible to observe the reversible encapsulation of a usual guest in their aromatic cavity. They are more like carcerands where the imprisoned guest is essentially obtained during the synthesis to form endohedral fullerene complexes. Chiral fullerenes were reviewed some years ago and can be classified depending on the origin of their chirality, which arises from its derivatization by chiral or achiral addends and their inherent or non-inherent chirality [47, 48]. The separation of non-substituted fullerene enantiomers is not trivial, but can be performed using, for instance, chiral hosts that strongly interact with the fullerene guest as recently reported in the case of (±)-C₇₆ [49]. On the other hand, enantioenriched substituted fullerenes could be obtained by grafting chiral addends. For instance, chiral C₆₀ pyrrolidinofullerene derivatives have been synthesized by Martin et al. by 1,3-dipolar cycloadditions of *N*-metalated azomethine ylides, with *ee* > 90% [50]. A similar approach afforded enantiopure endohedral metallofullerenes [51]. Enantiomerically pure C₆₀ fullerene bis-adducts (+)-**18** and (–)-**19** were recently obtained and separated by column chromatography (Fig. 12) [52], and enantiomerically pure C₃-symmetric tris-adducts of C₆₀ fullerene were isolated from the Bingel addition of a tris-malonate (*P*)- or (*M*)-CTB derivative to C₆₀ (Fig. 13) [53]. Fullerenes are outside the scope of this review, but it was important to mention this family of carbon cages, potentially chiral, that has seen considerable development since the 1990s. With the variety of fullerenes synthesized, their promising involvement in many aspects of chemistry physics and biology mainly rely on their stereochemistry and their structural richness.

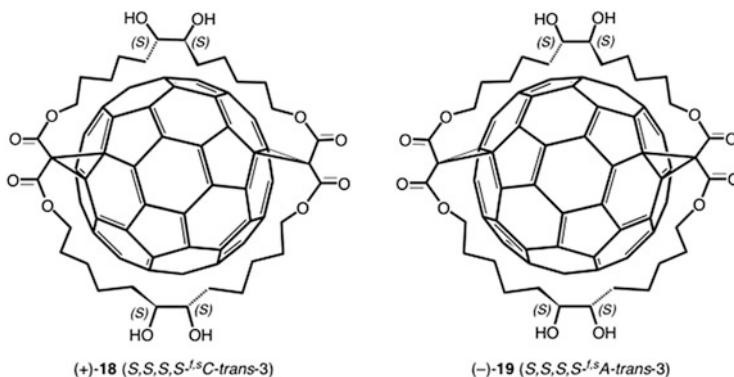


Fig. 12 The two enantiomerically pure C_{60} bis-adducts (+)-**18** and (-)-**19**

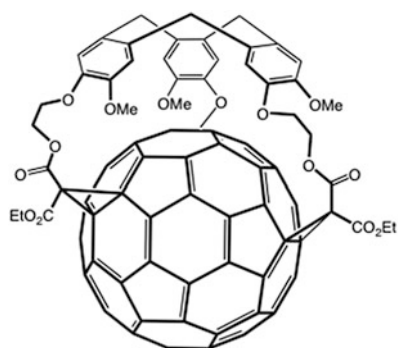


Fig. 13 Structure of one of the CTB- C_{60} conjugate obtained by the regioselective Bingel addition of a CTB scaffold to C_{60}

3 Synthesis and Enantiomeric Separation of Supramolecular Cages

This chapter deals with the synthesis of chiral molecular cages, some of which have led to enantiopure molecules. As for any chiral compounds, there are several methods to prepare chiral cages, mainly based on (1) the chirality pool, (2) the chiral catalysts (chemical or biological), (3) the chiral auxiliaries, and (4) the resolution of racemates. A common feature of all molecular containers reported in the literature is the low, even very low, overall yields of their syntheses. First, this is due to the high number of steps usually involved in their preparation. Second, because of their structure, a cyclization step is necessary in which several isomers and polymers can form. Thus, in order to optimize the global yield, very robust reactions are often chosen. Therefore, few attempts have been reported for the

access to enantiopure cages, including elaborated asymmetric syntheses. In recent literature we find mainly two types of chiral cages: the most frequently found concerns molecules built from chiral synthons, the other corresponds to inherently chiral compounds. In both cases, the molecular receptors may be obtained as racemic mixtures that have to be resolved in a last step.

An easy way to introduce chirality is to take advantage of the chirality pool. This strategy is the most represented in the literature. Molecular cages are often built from a C_n symmetry platform (mainly C_3), which is connected either to the same unit by three linkers or to a different C_n symmetry unit. Chirality arises from chiral linkers and/or from the platforms that can possess chiral substituents or are themselves inherently chiral.

In an attempt to make this report as clear as possible, we chose to classify the different syntheses of chiral molecular cages according to their constitutive platform, specifying in each example the different approaches which have been developed to connect the chiral blocks: the imine formation between chiral amines and aldehydes or ketones, S_N2 reactions, etc. Other important synthetic approaches involve the formation of diastereomeric precursors or the resolution of racemates.

3.1 *Carcerands and Carceplexes*

In the 1980s Cram designed a new family of molecular containers based on the resorcin[4]arene scaffold, covalently binding two cavitands to form carcerands and hemicarcerands. Carcerands are globe-shaped molecules which can accommodate a guest substrate to form a carceplex, whereas hemicarcerand contains a portal to offer access to a guest molecule to enter and leave the inner cavity to form a hemicarceplex [54]. This pioneering work led to the synthesis of many carcerands and hemicarcerands that revealed an ability to encapsulate various substrates efficiently [55, 56]. Their chemistry has been widely developed in the fields of molecular recognition, catalysis, or drug delivery. Among these molecular containers, chiral compounds have been obtained by the head to head covalent association of two cavitands by means of chiral linkers such as binaphthyl or 2,3-*O*-isopropylidene-*L*-threitol moieties (Fig. 14). Diastereomeric complexes are formed with chiral guests such as sulfoxides or alcohols, which are easily distinguished by NMR spectroscopy [57, 58].

3.2 *Synthesis from C_3 -Symmetrical Aromatic Platforms*

3.2.1 *Imination Reactions*

Imination reactions are now widely used in the dynamic covalent syntheses of molecular containers and capsules. They are of special interest for the formation of

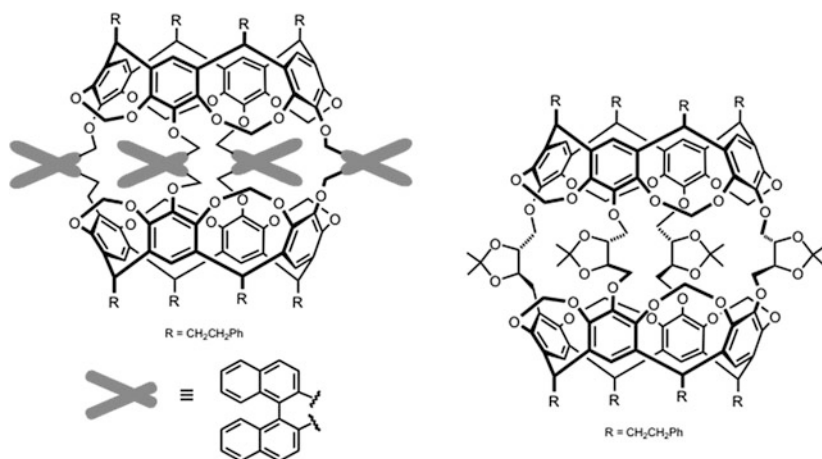


Fig. 14 Examples of structure of chiral carcerands

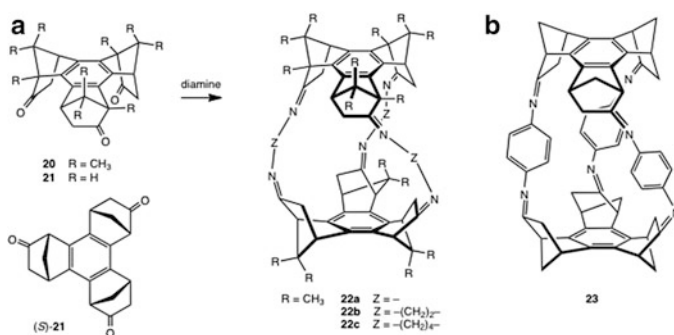
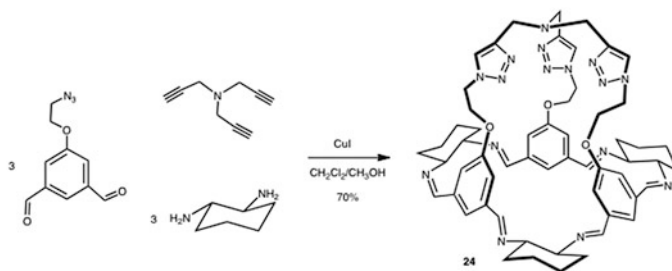


Fig. 15 Structures of the C_3 symmetric cage molecules **22** and **23**

multicomponent systems due to the reversibility of the self-assembling process. Furthermore, a reduction step often allows isolating new stable compounds with new functionalities [59].

The chiral *syn*-benzotricamphor **20** and *syn*-tris(norborneno)benzene **21** platforms were condensed with various diamines to synthesize C_3 symmetric host compounds. When (+)-*syn*-benzotricamphor **20** was condensed with hydrazine, 1,2-ethanediamine, or 1,4-butanediamine, the expected chiral cages **22a–c** were obtained (Fig. 15a) [60]. The yields varied from 91% (**22a**) to 25% (**22c**) depending on the length of the diamine. Condensation of *p*-phenylenediamine with (*R*)- or (*S*)-*syn*-tris(norborneno)benzene (*R*)-**21** or (*S*)-**21**, afforded the chiral phenylazomethine cages (*R*)-**23** and (*S*)-**23** in 50% and 56% yields, respectively (Fig. 15b) [61]. In all cases, among the possible four diastereomers due to the *E* or *Z* geometry of the double bonds



Scheme 3 One-pot synthesis of the hexa-imino chiral cage **24**

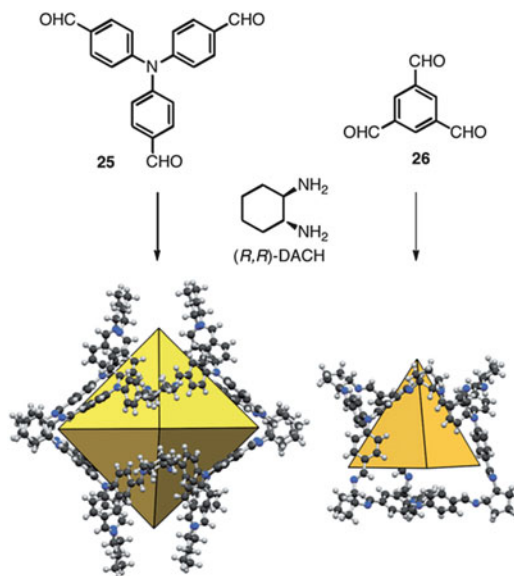
((*E,E,E*), (*E,E,Z*), (*E,Z,Z*), and (*Z,Z,Z*)), the (*E,E,E*) is calculated as being the most stable and is the only one observed in the solid state or by NOESY experiments, rendering this pathway highly diastereoselective. The host–guest properties of **22b** were investigated by NMR in CDCl₃ and revealed the formation of complexes with neutral gaseous molecules such as CH₄, C₂H₂, C₂H₄, and C₂H₆, the highest binding constant being observed with C₂H₂ ($K_a = 221 \text{ M}^{-1}$ at 228 K) [60].

Another type of C₃ symmetry molecular cage was synthesized in a one-pot procedure from a substituted *tren* analog and chiral 1,2-diaminocyclohexane (DACH) to form the hexa-imino hemispherical chiral cage **24** [62]. This cage was first synthesized step by step starting with the formation of a tripodal moiety bearing six aldehyde groups and followed by the imination reaction in the presence of 3 equiv. diamine. The access to this chiral cage has been dramatically improved by the successful one-pot synthesis to give **24** in 70% yield (Scheme 3). Complexation of metal ions was performed and experimental observations confirmed the location of the metal in the *tren*-triazole core.

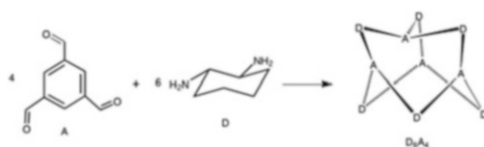
Chiral DACH and 1,2-diaminocyclo-4-hexene were also used for the formation of other examples of chiral cages. Using the same 4 to 6 ratio of an achiral C₃-symmetry trialdehyde and the diamine, different sizes of assemblies were observed depending on the nature of the aldehyde used. If the condensation is conducted with the tris-4-(formylphenyl)amine **25**, a large [8+12]-assembly is obtained (Scheme 4) [63]. If the more rigid 1,3,5-triformylbenzene **26** is used, only a [4+6] assembly is formed (Scheme 5) [64]. Crystals grown from this cage by Cooper [65] showed that it has a significantly smaller size and confirmed the tetrahedral shape cavity proposed by Gawronski. These modular assemblies based on the imination reactions from di- and tri-functionalized partners afforded chiral building blocks, which led to the construction of novel porous organic molecular crystals [66].

3.2.2 Boronic Esters Formation on Chiral Alcohols

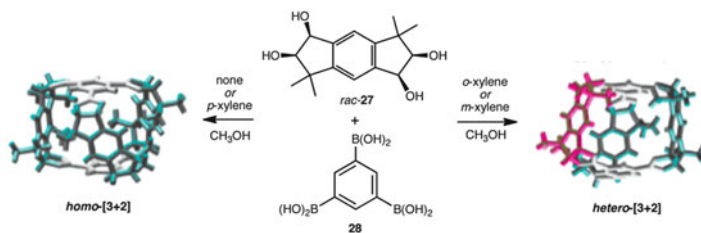
Another reaction that has been exploited for the synthesis of chiral cages is the formation of boronate esters. This reversible reaction has already been largely used



Scheme 4 Formation of the [8+12] and [4+6] assemblies from tris-aldehydes **25** or **26** and (*R,R*)-DACH

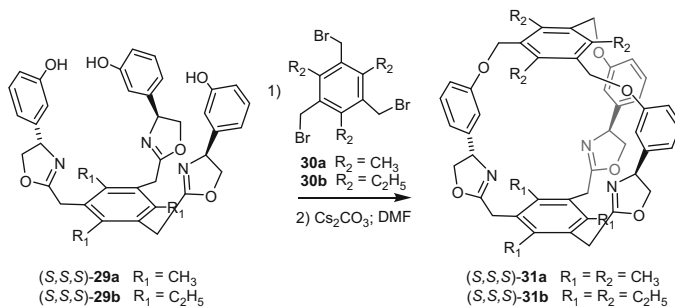


Scheme 5 Schematic representation of the formation of the tetrahedral structure of the D_6A_4 chiral cage (D=DACH; A=1,3,5-triformylbenzene **26**)



Scheme 6 Synthesis of the chiral *homo*- and *hetero*-[3+2] boronic-ester cages

for the formation of macrocycles, cages, and capsules [67]. Iwasawa described the [3+2]-assembly of the chiral tetrol **27** and 1,3,5-tri(boronic acid)benzene **28** (Scheme 6) [68]. In this work, *rac*-**27** was used in the synthesis. A templated-induced



Scheme 7 Synthesis of the enantiopure molecular cages (S,S,S)-**31a** and (S,S,S)-**31b**

selective formation of *homo*-[3+2] and *hetero*-[3+2] diastereomers was observed depending on the nature of the additive solvent used. However, although the authors have observed that the *homo*-[3+2] diastereomer gives enantiopure crystals, the solid is globally racemic because the synthesis has not been conducted on enantiopure **27**.

3.2.3 S_N2 Substitution

Kim and Ahn have also synthesized chiral cages by nucleophilic substitution of a chiral tripodal C₃-symmetry tris-phenol moiety on a tri-halide benzene derivative [69]. First, the chiral enantiopure oxazolines were obtained from the corresponding tricarboxylic acid by treatment with a chiral amino alcohol to give the pre-organized tris-phenol precursors **29a** and **29b**. Then coupling with the tri-bromide capping moiety **30a** or **30b** afforded the corresponding cages **31a** and **31b** with good yields (Scheme 7).

3.3 Synthesis from C₃ Cyclotribenzylene Platforms: Cryptophanes and Congeners

Cryptophanes are some of the most studied organic chiral cages [70]. Their synthesis involves various reactions leading to the assembly of two chiral cyclotribenzylene (CTB) moieties with three adequately functionalized linkers (Fig. 16). *Anti* and *syn* structures can be formed and the chirality of the CTB units makes the *anti* cryptophane chiral (D₃ or C₃ symmetry). In the case where X ≠ Y and/or W ≠ Z the *syn* and *anti* isomers are chiral. The chiral *anti* isomers are usually obtained as racemic mixtures and need improved strategies to get the enantiopure compounds. The different strategies that are more commonly used to synthesize chiral cryptophane derivatives are presented. Their properties will be discussed in the following sections.

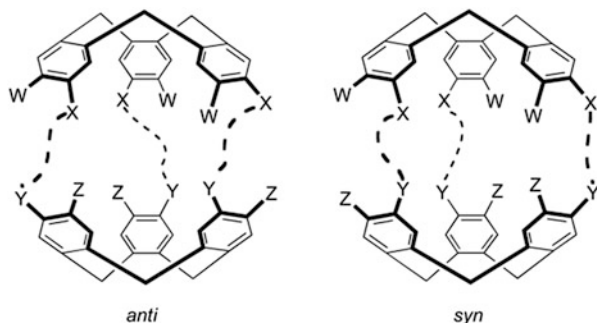


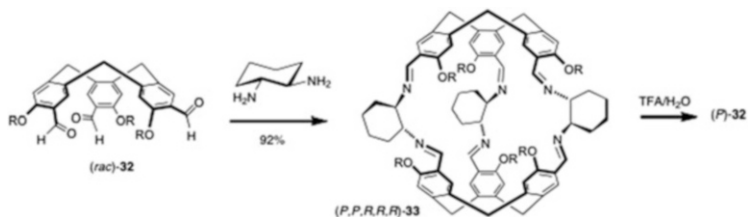
Fig. 16 Cryptophane structure: *anti* and *syn* isomers

3.3.1 Chiral Cryptophanes and Nanocubes Obtained by Imination Reactions

Warmuth achieved the synthesis of several enantiopure cryptophane derivatives by a dynamic covalent synthetic approach [71]. The reaction of (*rac*)-CTB **32** bearing three aldehyde moieties with (1*R*,2*R*)-diaminocyclohexane produced the enantiomerically pure cryptophane (*P,P,R,R,R*)-**33** in 92% yield (Scheme 8). In this reaction, the low inter-conversion barrier of the CTB unit is exploited to build the chiral cryptophane **33**. Indeed, the authors have observed that the CTB racemate leads almost quantitatively to the most stable diastereomer (*P,P,R,R,R*)-**33**. Interestingly, the enantiopure CTB (*P*)-**32** derivative was recovered after hydrolysis of **33**, under mild conditions, in 92% yield and with *ee* > 99%. The chiral cryptophane **33** finally serves as an intermediate in the resolution of *rac*-**32**.

From enantiopure CTB (*P*)-**32** the authors have elaborated larger chiral structures to form CTB-based homochiral nanocubes with C_3 symmetry in high yields. Using not racemizing conditions for the condensation of resolved (*P*)-**32** with 1,4-phenylenediamine allows the formation of an [8+12]-assembly, the (*P*)-CTB being located at the edges of a chiral nanocube (Fig. 17). Compared to Cooper's [8+12]-assembly described in Sect. 3.2.1, the shape of this cavity is no more octahedral but cubic [63].

Very recently, Kuck has proposed a very elegant and similar strategy to obtain enantiopure tribenzotriquinacene (TBTQ) derivatives [72]. Addition of (1*S*,2*S*)-diaminocyclohexane to the tribenzotriquinacene (*rac*)-**34** afforded a mixture of the three expected diastereomeric cryptophanes: the two *anti* (+)-(*P,P,S,S,S*)-**35** and (–)-(*M,M,S,S,S*)-**35** and the *syn* (+)-(*P,M,S,S,S*)-**35** isomers. Hydrolysis in aqueous trifluoroacetic acid gave the corresponding trialdehydes (+)-(*P*)-**34**, (–)-(*M*)-**34**, and (±)-**34** in high yields (Scheme 9). As for the previous example, this procedure allows the production of enantiopure trifunctionalized CTB and TBTQ derivatives that can be engaged in the construction of interesting supramolecular structures.



Scheme 8 Synthesis of cryptophane (*P,P,R,R,R*)-**33** from CTB *rac*-**32** and enantiopure DACH (R=hexadecyl)

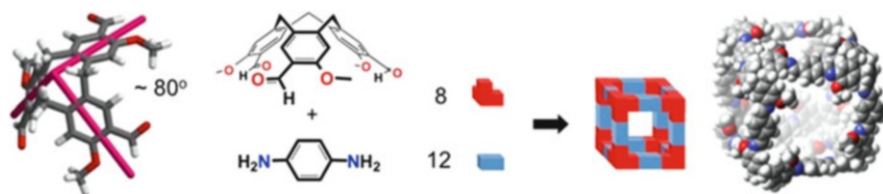
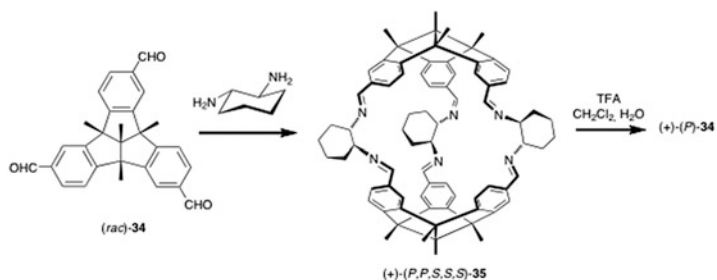


Fig. 17 Warmuth's synthesis of self-assembled chiral nanocubes



Scheme 9 Synthesis of enantiopure TBTQ **34** from (*rac*)-**34** via the enantiopure cryptophane **35**

3.3.2 Chiral Cryptophanes from Enantiomerically Resolved CTB

The first method used to prepare enantiopure cryptophanes consisted in the preliminary preparation of resolved CTB derivatives [73]. The main drawback of this method is the possible racemization of the CTB when temperatures above room temperature were needed. Nevertheless, following this strategy, Crassous et al. synthesized the enantioenriched thiomethylated analogs of cryptophane-E (*M,M*)-(+)-**36** and (*P,P*)-(-)-**36** with *ees* of 81.6 and 65.6, respectively (Fig. 18) [74].

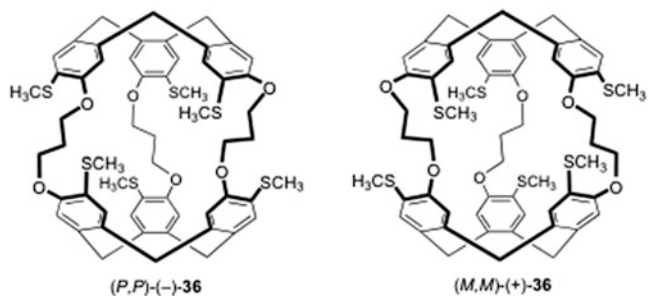


Fig. 18 Enantiomers of the thiomethylated cryptophane-E **36**

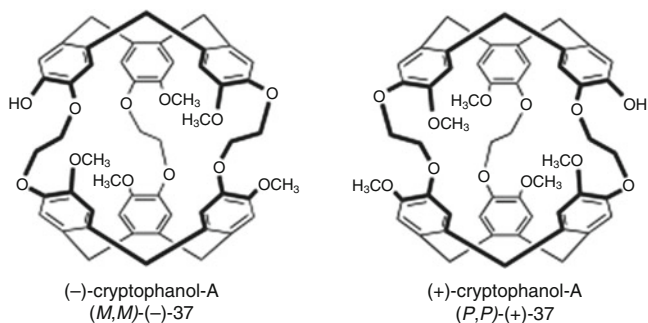


Fig. 19 Cryptophanol-A enantiomers (P,P) -(+)-**37** and (M,M) -(-)-**37**

3.3.3 Diastereomeric Derivatization Preceding Separation

Another approach has been proposed in 2003 for the enantiomeric resolution of the cryptophanol-A **37** (Fig. 19).

The strategy requires the formation of cryptophane diastereomers obtained from racemic cryptophanol-A and enantiomerically pure (*S*)-(-)-camphanic acid chloride. The reaction provides a mixture of two diastereomers (P,M) -(-)-**38** and (M,P) -(+)-**38** obtained in similar amounts, which are easily separated by crystallization in toluene. The separation is very efficient and leads to the two compounds with excellent diastereomeric excess $de > 99\%$ (Fig. 20). Then saponification in a KOH/H₂O/THF mixture affords the enantiomers of cryptophanol-A (P,P) -(+)-**37** and (M,M) -(-)-**37** with excellent enantiomeric excesses $ee > 99\%$ [75].

The interest of this approach is twofold. First, it gives rise to fair quantities of enantiopure cryptophanol-A and the amount of isolated enantiomers is only limited by the amount of racemic cryptophanol-A available. Second, the two enantiomers of cryptophanol-A can be used for subsequent reactions to give new compounds without any loss of enantiopurity. For instance, enantiopure cryptophane-A and cryptophane-ester were easily obtained by reaction of (P,P) -(+)-**37** or (M,M) -(-)-**37** with methyl iodide or bromomethyl acetate, respectively [75]. Similarly, an

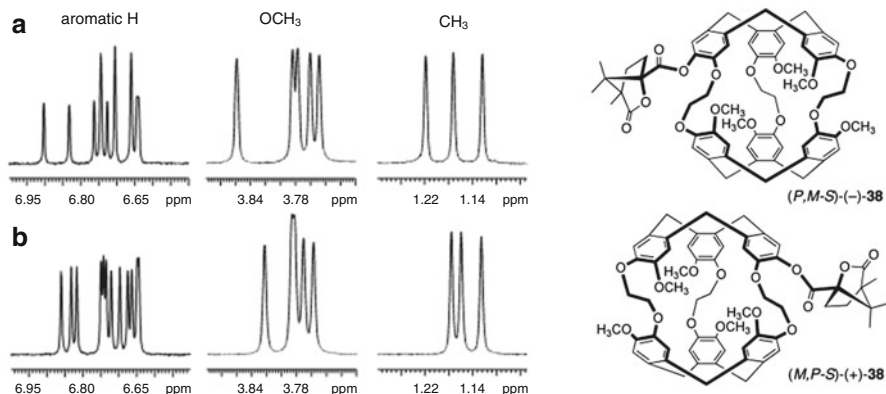
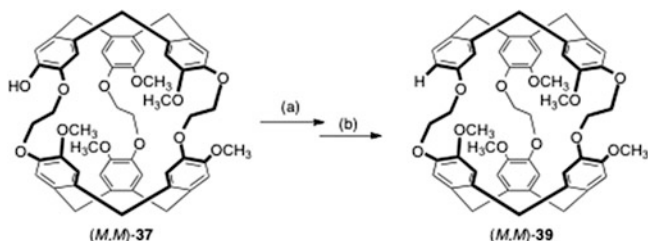


Fig. 20 ^1H NMR spectra of diastereomers (*P,M,S*)-(-)-**38** (a) and (*M,P,S*)-(+)-**38** (b) recorded in CHCl_3 at 298 K. Only the aromatic, the methoxy and the aliphatic regions are shown

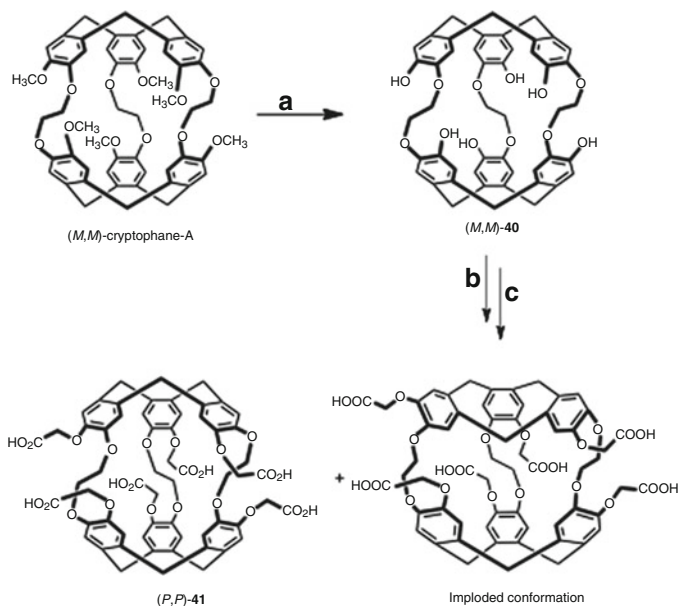


Scheme 10 Synthesis of enantiopure cryptophane-monoH **39** from cryptophanol-A **37** (experimental conditions: (a) pyridine/ CH_2Cl_2 /anhydride triflic; 0–20°C. (b) NBu_3 , $\text{PdCl}_2(\text{PPh}_3)_2$, dppp, HCOOH , DMF; 110°C)

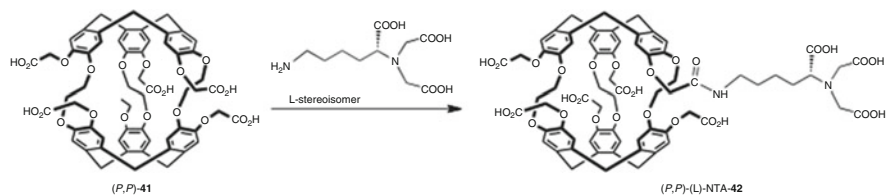
enantiopure cryptophane-biosensor bearing a DNA strain has been reported (see Sect. 4.4) [76].

The hydroxyl function of cryptophanol-A **37** has been used to introduce a triflate moiety, which in turn can be reduced in the presence of a palladium catalyst to give the cryptophane-monoH **39** (Scheme 10). Thus, this strategy affords new compounds with C_1 -symmetry; an enantiopure cryptophane dimer has also been synthesized by connecting two enantiopure cryptophanol-A molecules with a di-iododecane alkyl chain [77].

This approach has been exploited for the synthesis of enantiopure water-soluble cryptophanes. For instance, the selective demethylation of (*M,M*)- and (*P,P*)-cryptophane-A with lithium diphenylphosphide (PPh_2Li) gives the two enantiomers of compound **40** bearing six hydroxyl functions. In turn, the hexaphenol **40** can be used to prepare the two enantiomers of the hexa-carboxylic acid derivatives (*M,M*)-**41** and (*P,P*)-**41** [78]. The ^1H NMR spectra recorded in aqueous basic solution reveal two main conformations in solution: a bowl-shape conformation and an imploded conformation (Scheme 11). The proportion of the two conformers in



Scheme 11 Synthesis of cryptophane hexa-carboxylic acid (*PP*)-40 from (*MM*)-cryptophane-A (experimental conditions: (a) PPh_2Li (1M), THF, 60°C then $\text{HCl}/\text{H}_2\text{O}$; $0-20^\circ\text{C}$. (b) Bromomethylacetate, Cs_2CO_3 , DMF; 60°C . (c) $\text{KOH}/\text{H}_2\text{O}$ (1M), THF; 60°C then $\text{HCl}/\text{H}_2\text{O}$; $0-20^\circ\text{C}$)



Scheme 12 Synthesis of enantiopure molecular biosensor (*P,P*)-(L)-NTA-42 from the cryptophane (*PP*)-41 for the detection of Zn^{2+} cations in aqueous solution

solution strongly depends on the experimental conditions and in particular on the presence or absence of a substrate inside the cavity of the cryptophane.

The design of the molecular biosensor (L)-NTA-42 for the detection of Zn^{2+} cations in aqueous solution, was based on the two enantiomers (*M,M*)-41 and (*P,P*)-41 (see Sect. 4.4). This compound was prepared by coupling a single L-nitriilotriacetic acid (L-NTA) group to one of the six carboxylic acid functions of 41 as depicted in Scheme 12. Purification of the two diastereomers was achieved by HPLC [79].

Similarly, the two enantiomers of the penta-methoxylated derivative 39 were treated with lithium diphenylphosphide to furnish the penta-hydroxylated cryptophanes (*M,M*)-43 and (*P,P*)-43 (Fig. 21). In aqueous basic solution these

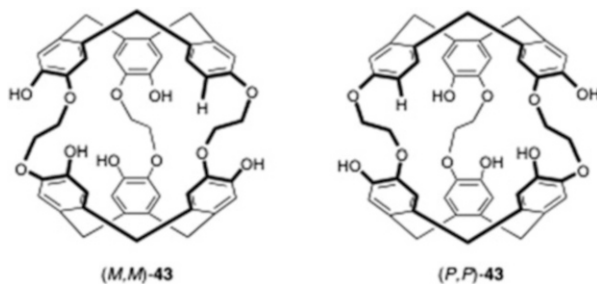
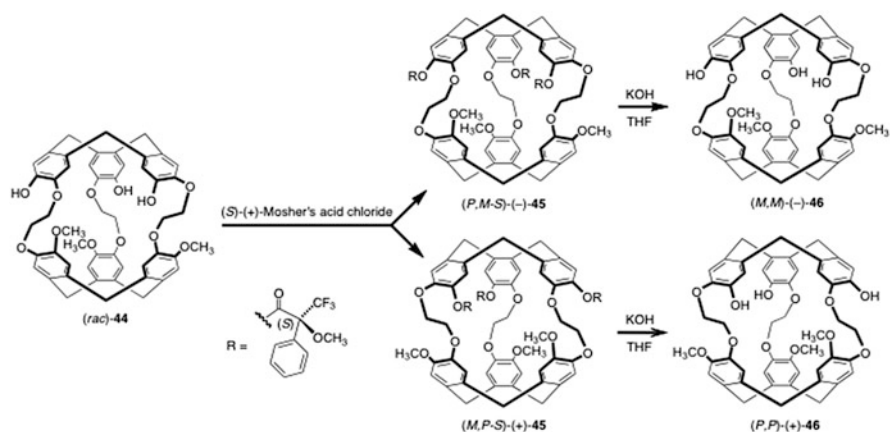


Fig. 21 Structure of the two enantiomers (M,M) -43 and (P,P) -43



Scheme 13 Synthesis of the (S) -Mosher acid cryptophane diastereomers $(P,M-S)$ -(-)-45 and $(M,P-S)$ -(+)-45 and trihydroxy congeners (M,M) -(-)-46 and (P,P) -(+)-46

compounds show interesting molecular recognition properties towards small chiral guests [80] and cesium or thallium cations even in the presence of large amounts of competitors (see Sect. 4.3.2) [81].

Using a similar strategy, Dmochowsky et al. prepared the two diastereomers of a tri-substituted cryptophane-A derivative bearing three (S) -Mosher acid moieties by starting from the trihydroxy cryptophane precursor (rac) -44 [82]. The two diastereomers $(P,M-S)$ -(-)-45 and $(M,P-S)$ -(+)-45 were efficiently separated by column chromatography. The removal of the Mosher moieties of the isolated diastereomers yielded the enantiopure trihydroxy cryptophanes (M,M) -(-)-46 and (P,P) -(+)-46, respectively (Scheme 13). The presence of the three OH groups allowed the preparation of new cryptophane derivatives [83].

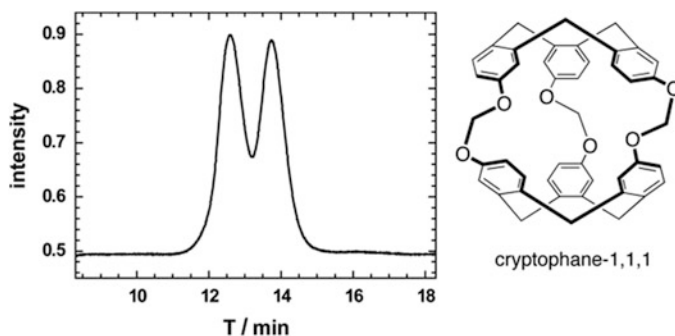


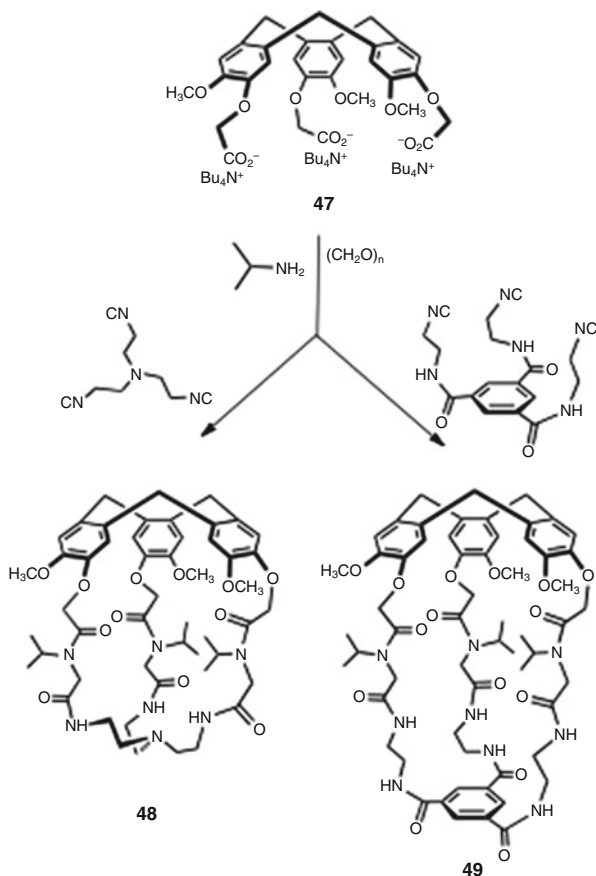
Fig. 22 Chiral HPLC chromatogram of (*rac*)-cryptophane-1,1,1 ((*S,S*)-Whelk-O1 column; THF/*n*-hexane 40/60; 1 mL/min; $T = 298$ K)

3.3.4 Enantioseparation by Chiral HPLC

Cryptophanes have been successfully enantioseparated by HPLC using chiral stationary phases [84]. The chiral stationary phase Chiralpak-OT(+) has been used to resolve a series of cyclotrimeratrylene and cryptophane derivatives. For instance, the two enantiomers of the cryptophane-A have been successfully separated using methanol as eluent (1.0 mL/min; $T = 288$ K) with retention times of 22.1 and 30.0 min for the (*P,P*)-(+ and the (*M,M*)-(–) enantiomers, respectively. Similarly, the two enantiomers of the cryptophane-E, which has three propylenedioxy linkers, were also easily separated on the Chiralpak-OT(+) chiral phase with retention times of 27.4 and 37.6 min for the (*P,P*)-(+ and the (*M,M*)-(–) enantiomers, respectively. However, this chiral stationary phase suffers from low stability and rapidly degrades over time. More recently, Crassous and co-workers successfully used (*S,S*)-Whelk-O1 column (eluent THF/*n*-pentane: 60/40; 1 mL/min) to differentiate the two enantiomers of the enantioenriched sulfur-containing cryptophane **36** [74]. The same column was also employed to distinguish, with low separation efficiency, the two enantiomers of cryptophane-1,1,1 (Fig. 22) [85].

3.4 Synthesis from C_3 Cyclotribenzylene Platforms: Hemicryptophanes

Hemicryptophanes are hollow molecules with a lipophilic cavity formed of a CTV unit and a second C_3 -symmetrical core. In comparison with the cryptophane structure, the hemicryptophanes possess a ditopic cavity that can introduce inner functionalities. As for the cryptophanes, the chiral environment is due to the *P* or *M* configuration of the cyclotrimeratrylene unit. Enantiopure hemicryptophanes have been obtained by different strategies, such as the resolution of racemic

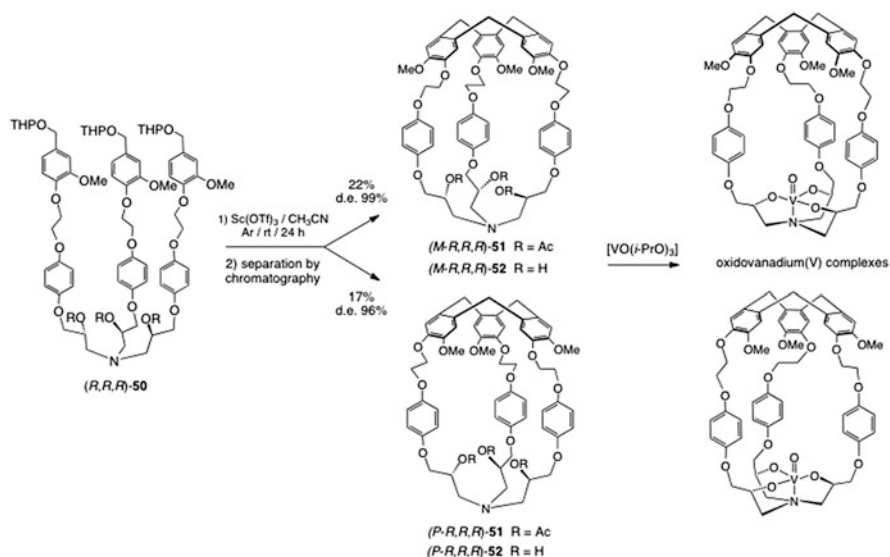


Scheme 14 Synthesis of the peptoid-based hemicryptophanes **48** and **49**

mixtures using chiral semi-preparative HPLC, or by introducing stereogenic centers to form diastereomers.

3.4.1 Combinatorial Strategies

The one-pot assembly of multicomponent mixtures of trifunctionalized building blocks and isocyanide derivatives, described as a Ugi-type macrocyclization [86, 87], has been applied to form cryptands and cage-like compounds [88]. By incorporating peptoid backbones in the reaction mixture, macrocyclic hosts were obtained. The procedure is quite simple and relies on a combinatorial strategy, which gave rise to complex synthetic molecular receptors. The modularity of this approach can lead to a variety of cryptand and cryptophane structures with possibilities to form inclusion complexes. Two examples are reported in Scheme 14,



Scheme 15 Synthesis of chiral hemicryptophanes and their oxidovanadium complexes

where the cyclotribenzylene **47** self-assemble in a threefold multicomponent macrocyclization to produce hemicryptophanes **48** and **49** [89].

3.4.2 Hemicryptophanes from $\text{S}_{\text{N}}2$ Reactions

The intramolecular cyclization reaction of the enantiopure C_3 -symmetric platform **50**, by using stoichiometric quantities of Lewis acid $\text{Sc}(\text{OTf})_3$, afforded the enantio- and diastereomerically pure hemicryptophane pairs (M,R,R,R) -**51**/ (P,S,S,S) -**51** and $(M-S,S,S)$ -**51**/ $(P-R,R,R)$ -**51**. The chiral precursor **50** was obtained following a multistep procedure starting from (R) - or (S) -glycidyl nosylate as the chiral pool reactant (Scheme 15). The diastereomers were separated by chromatography. The four diastereomers of the trihydroxy hemicryptophanes **52** were obtained quantitatively by removal the acetyl groups in **51** by hydrolysis with methanolic NaOH. Interestingly, the enantiopure oxidovanadium-hemicryptophane complexes were obtained by treatment of hosts **52** with oxidovanadium(V) triisopropoxide leading to the first transition-metal@hemicryptophane derivatives [90–92].

3.4.3 Enantioseparation by Chiral HPLC

A similar approach was used to prepare C_3 -symmetric triamide- and *tren*-hemicryptophane molecules. A nitrilotriacetic acid derivative was bound to a benzyl alcohol moiety to give a tripodal precursor of the hemicryptophane. As for compound **51**, a last cyclization step using $\text{Sc}(\text{OTf})_3$ as Lewis acid to build the CTV

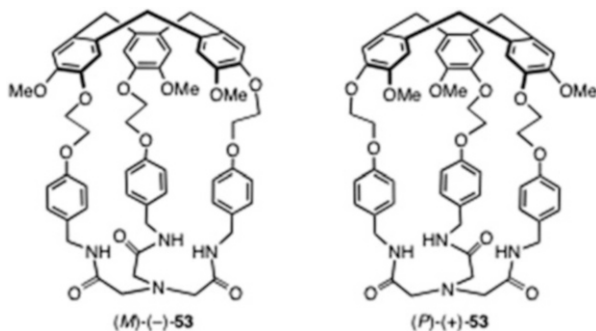


Fig. 23 Enantiomers of hemicryptophane **53** resolved by chiral HPLC



Scheme 16 Preparation of the enantiomers of the hemicryptophane-phosphatrane cages (*P*)-(+)-**55** and (*M*)-(-)-**55**

unit afforded the hemicryptophane triamide **53** as a racemic mixture (Fig. 23) [93]. The racemic hemicryptophane (\pm)-**53** was then resolved by semi-preparative HPLC on Whelk-O1 column, using a THF:*n*-hexane mixture as mobile phase. The absolute configuration of enantiomers (*P*)-(+)-**53** and (*M*)-(-)-**53** was extrapolated from the ECD spectra analysis [94]. The first eluted enantiomer, isolated with an enantiomeric excess $ee > 99\%$, corresponds to the (*P*)-(+)-**53** enantiomer, and the second with an $ee = 96\%$ corresponds to (*M*)-(-)-**53**.

The three amide functions of the supramolecular cage **53** can be reduced using BH_3/THF to afford the related *tren*-hemicryptophane **54**. The engaged triamine moiety has been used by Martinez et al. to prepare the hemicryptophane-phosphatrane **55** [95]. Following the method of Verkade [96], the addition of bis(*N*-dimethyl)-chlorophosphine $[(\text{CH}_3)_2\text{N}]_2\text{PCl}$ to **54**, gives the hemicryptophane **55** in 35% yield (Scheme 16). The phosphatranes are the conjugate acids of the proazaphosphatrane superbases, also named Verkade's superbases, which present interesting catalytic activities toward a large variety of reactions [97]. It was thus important to benefit from the chiral environment of the hemicryptophane structure to access chiral superbases. Later, the same authors performed the enantiomeric

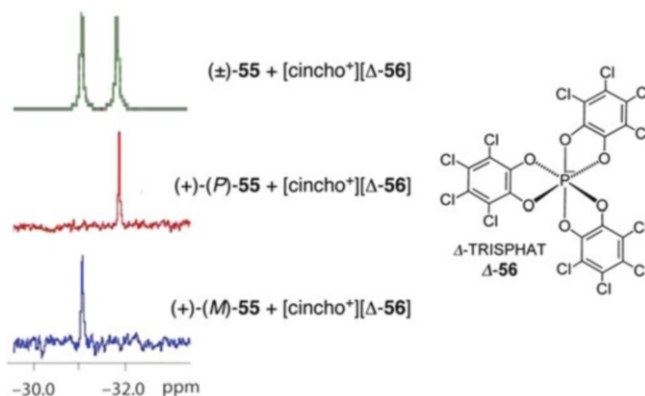
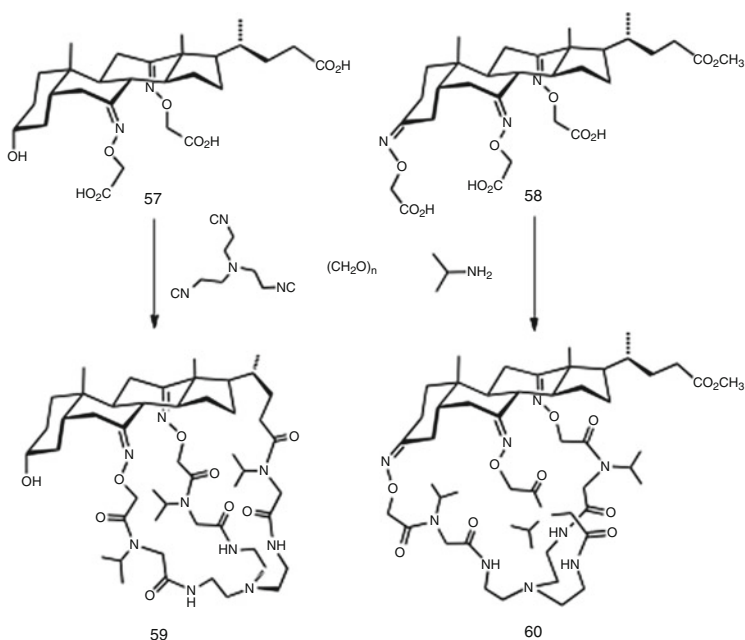


Fig. 24 ^{31}P NMR spectra (204.4 MHz, CDCl_3) of hemicryptophane (\pm)-**55** and of the isolated enantiomers (*P*)-(+)-**55** and (*M*)-(-)-**55** in the presence of the $[\text{cincho}^+][\Delta\text{-56}]$ cinchonidinium salt



Scheme 17 Synthesis of chiral cages **59** and **60**

resolution of the hemicryptophane-phosphatrane (\pm)-**55** by semi-preparative chiral HPLC on Chiralpak IC column, using EtOH/MeOH/TEA/TFA as the mobile phase. Due to a selectivity factor of 1.5 the first enantiomer was isolated with an

enantiomeric excess $ee > 99\%$ and the second with an $ee = 97\%$. The absolute configuration of each enantiomer was determined from analysis of their ECD spectra and allowed the assigning of the (*P*)-(+)-**55** and (*M*)-(–)-**55** enantiomers [98].

Furthermore, TRISPHAT anion Δ -**56** was found to act as a chiral solvating agent [99]. Addition of Δ -**56** to (*P*)-(+)-**55** and (*M*)-(–)-**55** led to non-equivalence of the ^1H and ^{31}P NMR signals for each enantiomer. The chiral environment induced by the inherently chiral CTB unit can be detected through the enantioseparation of the ^{31}P NMR signals of the azaphosphatrane unit (Fig. 24). Studies have been performed to scale up the enantioseparation using crystallization or ion-pair chromatography methods, although they have proved to be unsuccessful to date [98].

3.5 Cholic Acid-Based Scaffolds

Cholic acid constitutes an interesting chiral platform from which to build macrocyclic and cage molecules. The stereochemistry of this peculiar unit does fall into the category of facial amphiphiles combining a lipophilic outer face and a hydrophilic interior. This structure is therefore of great interest for the design of chiral molecular hosts. Such macrocycles have been designed by Davis et al. for the recognition and transport of anion guests [100, 101]. Using the combinatorial strategy described above (Sect. 3.4.1), cholic acid derivatives **57** and **58** are the basis of the molecular cages **59** and **60** (Scheme 17) [89].

3.6 Assignment of the Absolute Configuration

3.6.1 Hemicryptophanes

The determination of the absolute configuration of enantiopure hemicryptophanes host is usually achieved by ECD spectroscopy. ECD spectra of hemicryptophanes recorded between 230 and 400 nm in CHCl_3 show several ECD bands that can mainly be interpreted as the result of a strong excitonic coupling between the three aromatic rings of the CTB skeleton. This interaction gives a specific signature that can be used to assign the absolute configuration of hemicryptophanes. For instance, the ECD spectrum of hemicryptophane **53** presents ECD bands of weak intensities located between 270 and 300 nm that correspond to the $^1\text{L}_b$ spectral region. These bands are very sensitive to substituent and/or solvent effects. In consequence, this spectral region cannot be used with confidence to determine the absolute configuration. In contrast, the spectral region comprised between 230 and 270 nm ($^1\text{L}_a$ spectral region) appears to be less sensitive to substituent effects, and the bands in that spectral region usually show a bisignate, which is a characteristic signature of the chiral CTB skeleton. In the example of Fig. 25, the positive-negative bisignate (from low to high energies; blue spectrum) allows assignment of the *P* configuration to the (+)-**53**

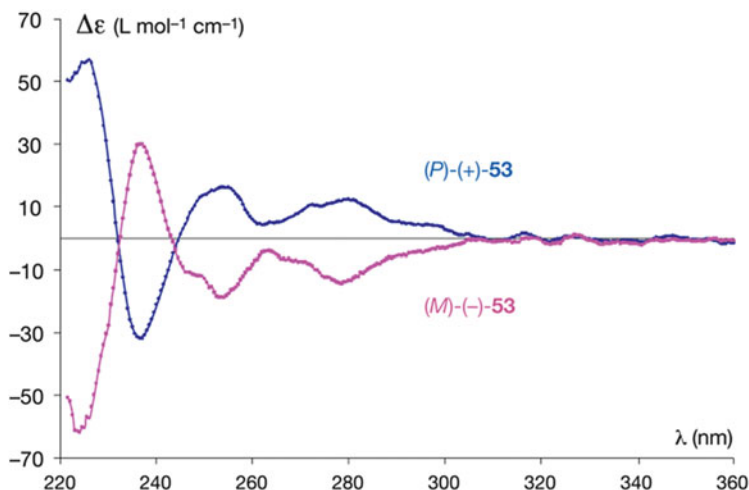


Fig. 25 ECD spectra (CHCl_3 ; 298 K) of the isolated enantiomers of hemicryptophane triamides (*P*)-(+)-**53** and (*M*)-(-)-**53**

derivative. In turn, the *M* configuration can be attributed to (-)-**53**, which exhibits a negative-positive bisignate (red spectrum) [94].

3.6.2 ECD and VCD of Enantiopure Cryptophane Hosts in Organic Solution

Collet and Gotarelli were the first to investigate the chiroptical properties of enantiopure cryptophane hosts and to study their ECD spectra. They prepared in small quantities a series of enantioenriched D_3 -symmetry cryptophanes ($ee > 90\%$) according to the method mentioned in Sect. 3.3.2. In this study assignment of the absolute configuration of the cryptophane derivatives was obtained indirectly from the known absolute configuration of the CTB skeleton used to prepare the enantioenriched cryptophanes [102]. The ECD spectra of these molecules were interpreted using the Kuhn–Kirkwood excitonic model. This model was found appropriate and simple enough to explain qualitatively the main characteristics of the ECD spectra of D_3 -symmetry cryptophanes for the two forbidden 1L_a and 1L_b bands. These two transitions were found to be sensitive to the nature of the substituents attached on the CTB skeleton and give rise to very different ECD spectra in shape. Nevertheless, as previously mentioned for the hemicryptophane derivatives, the ECD bands located in the 230–260 nm region (1L_a spectral region) allow assignment of the absolute configuration of cryptophane with D_3 -symmetry.

The ECD spectra of a series of (-)-cryptophane derivatives show characteristic bisignates in the 230–260 nm region that can be used to assign easily the absolute configuration of these compounds. Thus, the knowledge of the absolute

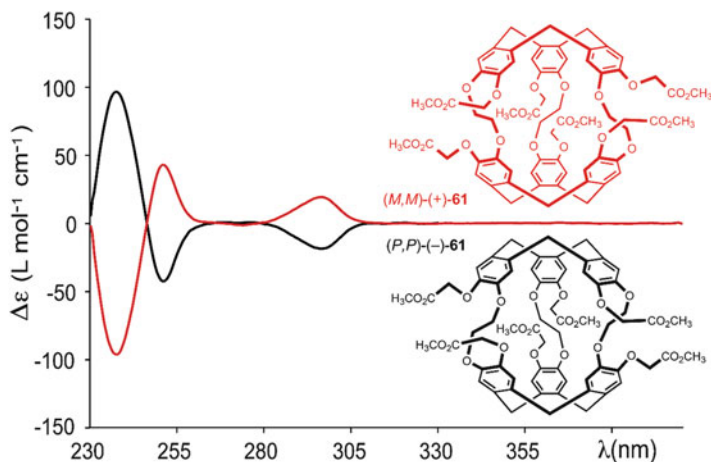


Fig. 26 ECD spectra (CH_2Cl_2 ; 293 K) of CH_2Cl_2 @cryptophanes (P,P)-(-)-**61** and (M,M)-(+)-**61**

configuration of the (M,M)-(-)-cryptophane-A allows by analogy the easy determination of the absolute configuration of its congeners. For instance, the (P,P) absolute configuration was attributed to the (-)-hexaacetate-cryptophane **61** (Fig. 26) and the (M,M) absolute configuration was attributed to the (-)-hexahydroxy-cryptophane **40** [78]. Since then, cryptophanes with different symmetry have been prepared by a multi-step synthesis and their chiroptical properties have been thoroughly studied. For example, the ECD spectrum of the C_1 -symmetry cryptophane-monoH **39** shows an ECD bisignate in the 230–260 nm region, allowing assignment of the absolute configuration (M,M)-(-)-**39** [77].

Buffeteau and co-workers showed that the absolute configuration of the two enantiomers of cryptophane-A could be unambiguously determined by using VCD spectroscopy in combination with *ab initio* calculations at the DFT level [103]. The VCD spectra recorded in CD_2Cl_2 , a solvent that can enter into the cavity of the host, or $\text{C}_2\text{D}_2\text{Cl}_4$, a solvent molecule too large to fit inside the cryptophane cavity, did not show significant modifications. DFT calculations performed for the empty cryptophane-A and for the CHCl_3 @cryptophane-A complex suggested that in all cases the anti-conformation of the linkers was the dominant conformation. This conclusion is in accord with the X-ray crystallographic structures of cryptophane-A complexes previously reported in the literature [104].

Similarly, several enantiopure cryptophane derivatives, such as compounds **39**, having C_1 -symmetry have been synthesized and thoroughly studied by VCD spectroscopy (Fig. 27). The VCD spectra of these derivatives reveal a lower intensity of the VCD bands observed in the $1,700$ – $1,000\text{ cm}^{-1}$ domain, which have been perfectly reproduced by means of DFT calculations (B3PW91/6-31G*) [77]. In a following paper, compound **39** was the object of further investigation by ECD and VCD spectroscopy [105]. This compound represents an interesting case where an encapsulated chloroform molecule can have two possible orientations since the molecular host present two different CTB caps.

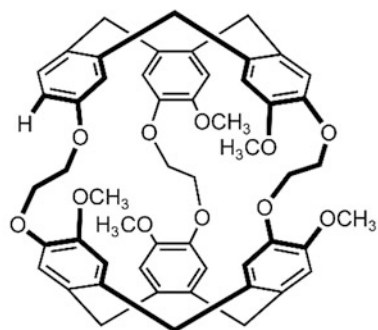
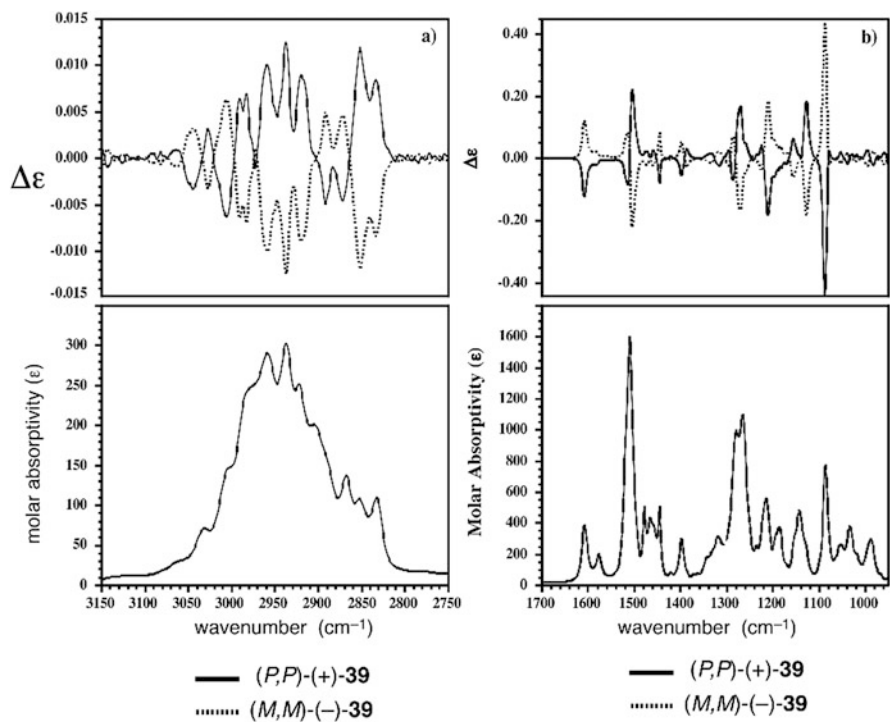


Fig. 27 Structure of cryptophane (*M,M*)-(-)-39 (only one enantiomer is shown), and experimental IR (lower frame) and VCD (upper frame) spectra of both enantiomers in CDCl₃ in (a) the 3,150–2,750 cm⁻¹ and (b) the 1,700–950 cm⁻¹ regions

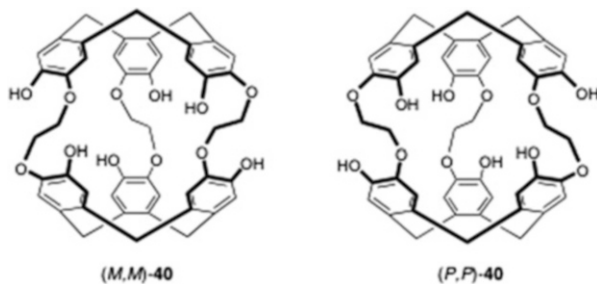


Fig. 28 Water-soluble cryptophanes (*M,M*)-40 and (*P,P*)-40

4 Chiral Recognition and Enantiomeric Differentiation

4.1 Use of Chiroptical Techniques for the Monitoring of Complexation Phenomena: ECD and VCD of Enantiopure Water-Soluble Cryptophane Cages

4.1.1 Water-Soluble Hydroxylated Cages

A restricted number of water-soluble cryptophanes have been described in the literature and only very few examples of chiral compounds have been reported. Brotin and Buffeteau reported the synthesis and the chiroptical properties of the hexahydroxy-cryptophane-A **40** (Fig. 28) [106]. This compound is only soluble in water under basic condition and can form inclusion complexes with neutral guests such as halogenomethanes, methane, or xenon. The authors investigated the complexation processes by polarimetry, ECD, and VCD spectroscopies. Their results have shown a very strong dependence of the chiroptical properties of the host molecule on the experimental conditions, such as the nature and the concentration of the counter-ion (Li^+ , Na^+ , K^+ , Cs^+) of the base used to dissolve the cryptophane in water. In addition, the polarimetry experiments performed with or without a guest inside the molecular cavity of the host also revealed large discrepancies. For instance, and in contrast to what was observed with enantiopure cryptophanes soluble in organic solution, the sign of the rotatory power at a given wavelength could change. In 0.1 M NaOH/H₂O solution, the $[\alpha]_{589}$ values for the enantiomers (*M,M*)-**40** and (*P,P*)-**40** are +0.8 and -1.4, respectively, while the $\text{CHCl}_3@(\textit{M,M})\text{-40}$ and $\text{CHCl}_3@(\textit{P,P})\text{-40}$ complexes have $[\alpha]_{589}$ values of -44.4 and +42.3, respectively. On the other hand, no encapsulation effect was noticed when the LiOH/H₂O or the NaOH/H₂O solutions were replaced by a CsOH/H₂O solution. These peculiar observations are the result of the specific trapping of the cationic species in the molecular cavity (see Sect. 4.2).

The impact of the experimental conditions on the ECD spectra has been evidenced with cryptophane **40** dissolved in a 0.1 M NaOH/H₂O solution in the presence of different neutral guest molecules (Fig. 29a). The ECD spectra are strongly modified

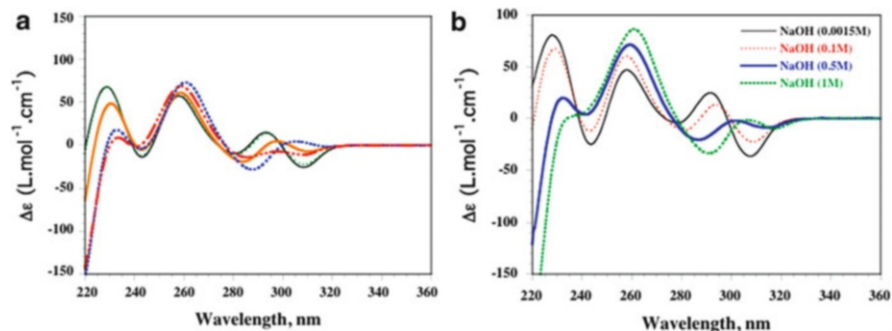


Fig. 29 (a) ECD spectra of guest-free (*M,M*)-**40** in NaOH/H₂O (*black*), and in presence of guests CH₄ (*green*), CH₃Cl (*orange*), CH₂Cl₂ (*blue*), and CHCl₃ (*red*). (b) ECD spectra of (*M,M*)-**40** in NaOH/H₂O at different concentrations (*T* = 298 K)

in the 220–320 nm region when substrates of increasing molecular volume (CH₄, CH₃Cl, CH₂Cl₂, CHCl₃) interact with the host cavity. This effect is especially important for the ECD bands of the ¹L_b and the ¹B_b transitions. A size effect of the guest molecule on the ECD spectrum was clearly observed since the larger the molecular volume of the guest the stronger the modification of the ECD spectrum. For instance, a direct correlation between the spectral modifications and the guest size can easily be made by looking at the intensity of the ECD band located at 220 nm. In turn, these spectral modifications provide direct information on the conformational distribution of the three linkers connecting the two CTB caps.

In water the free cryptophane tends to reduce the size of its cavity (hydrophobic effect) and the three linkers mainly adopt an *all-gauche* conformation. Upon complexation of a small guest such as CH₄ or CH₃Cl, the structure is not strongly modified and the three linkers still adopt the *gauche* conformation. This situation is no longer observed when a larger guest (CHCl₃) is present inside the cavity, which requires an enlarged cavity where the three linkers mainly adopt an *all-trans* conformation. A similar effect was also observed depending on the concentration of the basic solution used to dissolve the host molecule (Fig. 29b). In a diluted NaOH/H₂O solution (1.5 · 10⁻³ M) the hydrophobic effect dominates and the three linkers adopt preferentially the *all-gauche* conformation. By increasing the concentration the conformational distribution is strongly modified and in a 1.0 M NaOH/H₂O solution the three linkers prefer the *all-trans* conformation as this was observed with large guest molecules.

In CsOH/H₂O solution the situation was dramatically different. The ECD spectrum of **40** remains unchanged whatever the nature of the guest added to the solution, suggesting that the guest molecule cannot gain access to the cavity of the host. This has been clearly demonstrated by ¹³³Cs NMR, ECD and isothermal titration calorimetry (ITC) experiments. It has been shown that the cesium cations have a very high affinity for the electron-rich molecular cavity of the cryptophane, which prevents the neutral CH₂Cl₂ or CHCl₃ guest entering the cavity of the host [107]. This peculiar behavior is discussed in detail in Sect. 4.2.

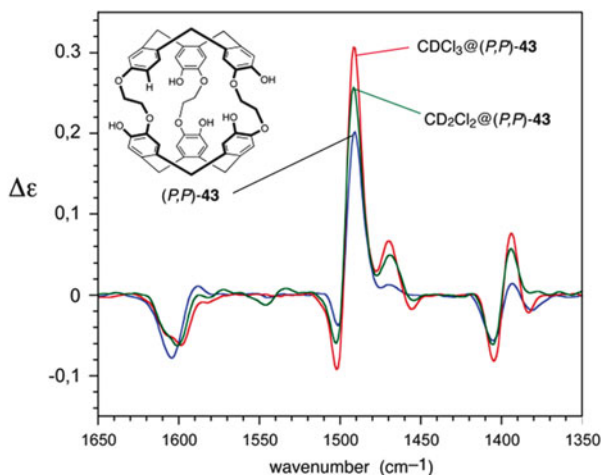


Fig. 30 VCD spectra of guest-free (*P,P*)-**43**, and its CD_2Cl_2 and CDCl_3 complexes in $\text{NaOD}/\text{D}_2\text{O}$ solution

The C_1 symmetrical cryptophane **43**, which contains five hydroxyl groups, has an enlarged portal, making the encapsulation of larger guest molecules easier. Upon encapsulation of neutral achiral guests in $\text{LiOH}/\text{H}_2\text{O}$ or $\text{NaOH}/\text{H}_2\text{O}$ solution, important modifications of its ECD spectrum have been observed [108]. In contrast, in $\text{CsOH}/\text{H}_2\text{O}$ solution the ECD spectrum remains unchanged whatever the nature of the guest added. In $\text{KOH}/\text{H}_2\text{O}$ solution an intermediate situation was observed since slight modifications of the ECD spectrum were observed upon addition of CH_2Cl_2 or CHCl_3 . In this case, the two guests compete with the K^+ cation to enter the cavity of the host. This effect is also characterized by an increase of the intensities of the VCD bands in the $1,700\text{--}1,200\text{ cm}^{-1}$ region (Fig. 30). For instance, the intensity of the band at $1,500\text{ cm}^{-1}$ ($\nu(\text{C}=\text{C})$ stretching) significantly increases upon encapsulation of a chloroform molecule, when compared to the empty host molecule. Both the ECD and VCD spectral modifications can be interpreted in terms of conformational rearrangement. These conclusions are fully supported by the DFT calculations performed on the empty and the complexed cryptophanes **40** and **43**.

4.1.2 Carboxylate Derivatives

Compound **41** possesses six carboxylic acid functions (D_3 -symmetry) and is soluble in water over a large range of pH. Surprisingly, this compound exhibits different chiroptical properties when compared to the hydroxylated derivatives **40** and **43**. The ECD and VCD spectra remain unaffected upon encapsulation of neutral guests (Fig. 31), in contrast to the ^1H NMR spectrum, which is very sensitive to the nature of the guest present inside the molecular cavity. Unlike what is observed with hosts **40** and **43**, guest encapsulation also occurs in $\text{KOH}/\text{D}_2\text{O}$ and $\text{CsOH}/\text{D}_2\text{O}$ solutions, suggesting that this host does not bind alkali cations [78].

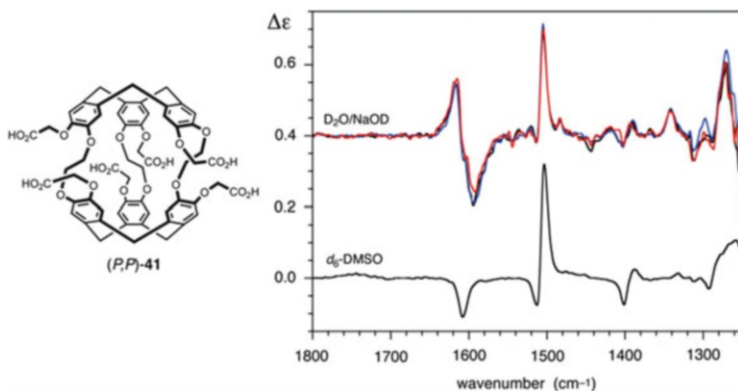


Fig. 31 VCD spectra of *(P,P)*-**41** in DMSO- d_6 and in NaOD/D $_2$ O (0.21M) solution (*top, black*). VCD spectra of *(P,P)*-**41** in the presence of CD $_2$ Cl $_2$ (*top, blue*) and CDCl $_3$ (*top, red*) are also reported

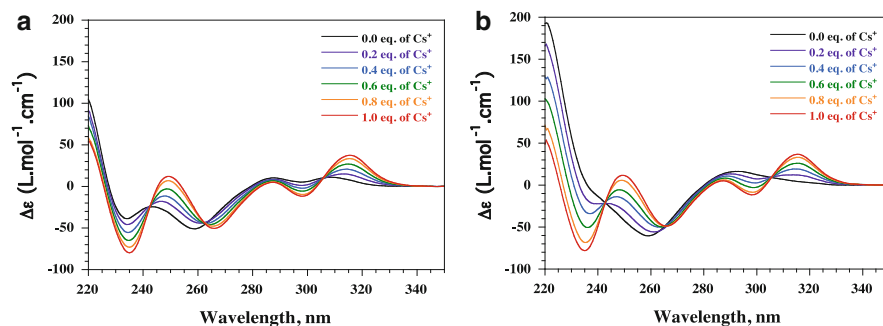


Fig. 32 ECD spectra recorded at 293 K of *(P,P)*-**43**: (a) in 0.1 M LiOH/H $_2$ O solution in the presence of different amounts of a CsOH/H $_2$ O solution; (b) in a saturated solution of CHCl $_3$ in LiOH/H $_2$ O in presence of different amounts of a CsOH/H $_2$ O solution. ECD spectra for higher concentration in Cs $^+$ are identical to that recorded for 1.0 equiv. of Cs $^+$

The structural differences observed between the three hosts **40**, **41**, and **43** shed light on the importance of the substituents of the CTB units on the overall chiroptical properties of the cryptophane molecules. For instance the remoteness of the negative charges in compound **41** when compared to **40** prevents cationic species from interacting with the phenolate moieties through coulombic interaction. The lack of phenolate moieties in compound **41** also alters less significantly the angle of polarization for the two forbidden 1L_b and 1L_a transition and the allowed 1B_b transition, making this system less ECD sensitive to conformational changes upon encapsulation of neutral guests.

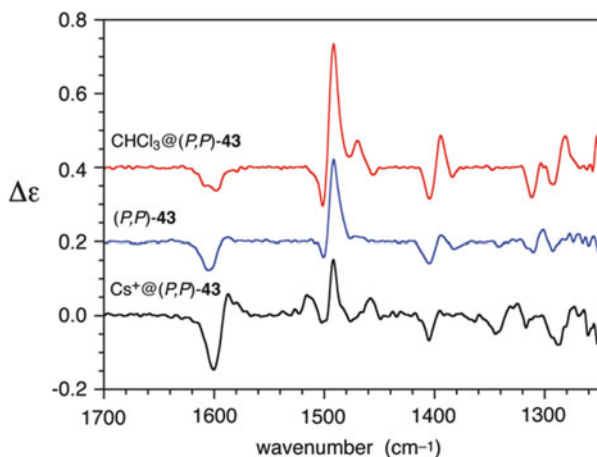


Fig. 33 VCD spectra of empty (P,P) -**43**, $\text{CHCl}_3@(\text{P,P})\text{-43}$ and $\text{Cs}^+@(\text{P,P})\text{-43}$ complexes

4.2 Recognition of Monovalent Cations by Enantiopure Water-Soluble Cryptophanes

Until recently, the complexation of charged species by cryptophane hosts mainly concerned ammonium guests. Akabori and Weber are probably the first to have reported the complexation of metal ions, in organic solvent, by cryptophane derivatives possessing specific functionalities capable of strong interactions with these guests, such as ether linkages [109] or carboxylic acid moieties [110]. None of these studies involved enantiopure cryptophanes. Recently, Brotin and co-workers demonstrated that cesium and thallium cations could interact strongly with hosts **40** and **43** in water. By using the enantiopure cages **40** and **43**, the complexation of the cationic guests could be followed by ECD, ^{133}Cs , or ^{205}Tl NMR spectroscopy, and the thermodynamic parameters of the complexation were obtained from titration experiments (ITC). The K^+ , Rb^+ , and Cs^+ cations are well recognized by cryptophane **43** in $\text{LiOH}/\text{H}_2\text{O}$ or $\text{NaOH}/\text{H}_2\text{O}$ solutions. The complexation is characterized by important modifications of the ECD spectra of **43** in the 220–320 nm region (Fig. 32a). The spectral changes are even more important when CHCl_3 , a competing guest, is used. Starting from the $\text{CHCl}_3@(\text{P,P})\text{-43}$ complex in $\text{LiOH}/\text{H}_2\text{O}$ solution, the addition of $\text{CsOH}/\text{H}_2\text{O}$ solution modifies the ECD band of the $^1\text{L}_b$ transition and to a larger extent the ECD bands of the allowed $^1\text{B}_b$ transition (Fig. 32b). These spectral modifications have been correlated to the conformational changes of the three ethylenedioxy linkers of the cage, when the encapsulated CHCl_3 molecule ($V_{\text{vdw}} = 72 \text{ \AA}^3$) is replaced by the smaller cationic guest ($V_{\text{ion}} = 20 \text{ \AA}^3$). The ^{133}Cs NMR spectra of the $^{133}\text{Cs}^+@43$ complex show two signals corresponding to the free Cs^+ ion in solution at 0 ppm, and the Cs^+ encapsulated in the cavity of **43** at -255 ppm. The $\text{Cs}^+@40$ complex displays an

even larger ^{133}Cs chemical shift at -270 ppm. Titration experiments performed at 278 K in $\text{LiOH}/\text{H}_2\text{O}$ shows that the binding process to host **40** and **43** is enthalpy driven ($\Delta H^\circ = -12.0$ kcal/mol) and that the entropic contribution can be neglected. These two host molecules also recognize K^+ and Rb^+ cations with lower binding constants [107].

In contrast to what is observed at low or moderate LiOH or NaOH concentrations, under severe experimental conditions (1M $\text{LiOH}/\text{H}_2\text{O}$ or $\text{NaOH}/\text{H}_2\text{O}$ solutions) cryptophane **43** binds to cesium as well as to thallium(I) cations, resulting in dramatic changes in the ECD spectra [81]. Upon encapsulation of Cs^+ or Tl^+ cations, the ECD spectra clearly reveal a strong reduction of the ECD band located at 220 nm, which was interpreted by a conformational change of the three linkers and a reduction of the cavity size to maximize host–guest interactions. It was noted that the spectral changes are more marked with the Tl^+ guest that interacts more strongly with the cavity of **43** as confirmed by titration experiments.

In $\text{NaOD}/\text{D}_2\text{O}$, the VCD spectrum of the $\text{Cs}^+@(\text{P},\text{P})\text{-43}$ complex is different in shape and intensity from the VCD spectra of the empty host **43** and the $\text{CHCl}_3@(\text{P},\text{P})\text{-43}$ complex. The strong reduction of the band at $1,490\text{ cm}^{-1}$ indicates the preferential *all-gauche* conformation of the linkers, characteristic of Cs^+ encapsulation, in contrast to the $\text{CHCl}_3@(\text{P},\text{P})\text{-43}$ complex, which exhibits a strong enhancement of this band, indicative of the preferential *all-trans* conformation of the three linkers to accommodate the CHCl_3 guest (Fig. 33).

These results show that cryptophanes **40** and **43** are among the most efficient host molecules reported in the literature for encapsulating Cs^+ and Tl^+ cations in aqueous solvents. The complexation of these toxic cations can be investigated under a large range of experimental conditions (concentration, temperature, etc.). Both ECD and VCD spectroscopy provide valuable information about how host molecules behave in solution with or without a guest inside their cavity.

4.3 Complexation of Chiral Guests

4.3.1 CHFClBr and Cryptophane-C: The First Example of Chiral Differentiation Using an Enantioenriched Cryptophane

Collet and co-workers studied the encapsulation of bromochlorofluoromethane, one of the smallest chiral molecules, by the chiral C_3 -symmetrical cryptophane-C. They demonstrated that cryptophane-C in CHCl_3 recognized differently the two enantiomers of CHFClBr. This was confirmed by the difference in intensity of the two sets of doublets in the ^1H NMR spectrum characterizing the two diastereomers $(-)\text{CHFClBr}@(\text{P},\text{P})\text{-}(+)\text{-cryptophane-C}$ and $(+)\text{CHFClBr}@(\text{P},\text{P})\text{-}(+)\text{-cryptophane-C}$ (Fig. 34). In this example, the enantiomeric differentiation was moderate ($ee = 4\%$) and in favor of $(+)\text{CHFClBr}@(+)\text{-cryptophane-C}$ diastereomer [111]. Later, the enantioselective complexation of CHFClBr by cryptophane-C was re-investigated in more detail using molecular dynamics simulation [112]. The finding that the $(R)\text{-CHFClBr}@(-)\text{-cryptophane-C}$ complex was

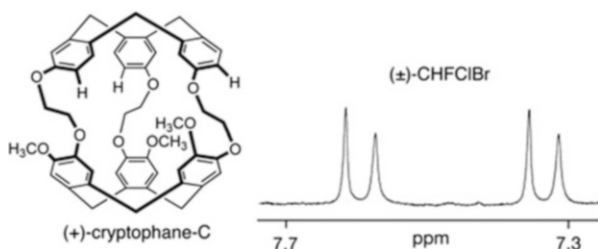


Fig. 34 Enantioselective complexation of CHFCIBr by (+)-cryptophane-C

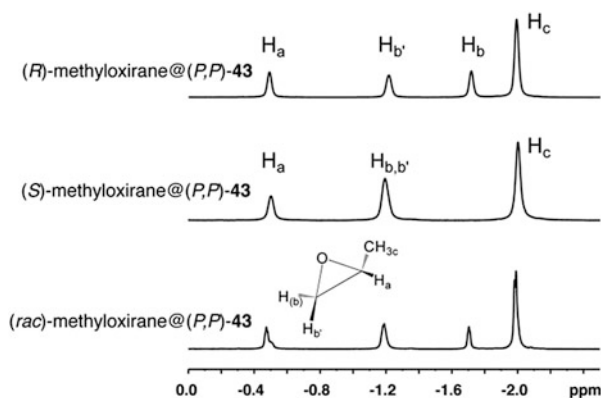


Fig. 35 Highfield part of the ^1H NMR spectra (500 MHz, 0.13 M NaOD/D₂O, 275 K) of (*P,P*)-**43** in the presence of (*R*)-methyloxirane, (*S*)-methyloxirane, and (*rac*)-methyloxirane

the most stable diastereomeric complex allowed the determination of the two enantiomers of CHFCIBr. Thus, from this work it was concluded that the absolute configuration of CHFCIBr must be (*R*)-(–) and (*S*)-(+). Interestingly, the same absolute configuration (*R*)-(–) and (*S*)-(+)) was assigned to the enantiomers of CHFCII [113].

4.3.2 Complexation of Chiral Epoxides by Enantiopure Water-Soluble Cryptophanes

The complexation of the (*R*) and (*S*) enantiomers of methyloxirane, under basic condition, was thoroughly studied by ^1H NMR spectroscopy and ECD spectroscopy [80]. In NaOD/D₂O at 278 K, (*R*)-methyloxirane is recognized by the (*M,M*)-**43** host with a binding constant K of 95 M^{-1} , whereas its (*S*)-methyloxirane enantiomer exhibits a higher affinity with $K = 194\text{ M}^{-1}$. This efficient enantioselective complexation was easily monitored by ^1H NMR spectroscopy: the protons of the methyloxirane molecule inside the cavity of the cryptophane undergo a strong shielding from the aromatic cavity and exhibit high field shifted signals (Fig. 35).

The ECD spectra obtained at 293 K under similar experimental conditions (0.1 M NaOH/H₂O) differentiate the two diastereomeric complexes (*R*)-methyloxirane@(*M*, *M*)-**43** and (*S*)-methyloxirane@(*M*, *M*)-**43**, and exhibit small but distinct bands corresponding to the ¹L_b transition in the 280–330 nm spectral range. In addition, a comparison with the ECD spectrum of the (*rac*)-methyloxirane@(*M*, *M*)-**43** reveals a clear preference of the (*S*)-methyloxirane enantiomer for (*M*, *M*)-**43**, in agreement with the ¹H NMR experiments. The experimental conditions have a strong impact on the ability of the methyloxirane to enter the cavity of **43**. For instance, in KOH/H₂O solution the association constant is strongly reduced due to the competitive binding of the potassium cations, and in CsOH/H₂O solution no binding was observed as a consequence of the strong affinity of the cesium cations for the cavity of the host (see Sect. 4.2). The free energy of the two diastereomeric forms determined from molecular dynamics and DFT calculations differs by 0.5–4.3 kJ/mol in accord with the experimental data.

This study was then extended to the enantioselective complexation of a series of small oxirane derivatives by the two enantiomers of cryptophane **41**. The enantiodifferentiation of the guests methyloxirane ($V_{\text{vdw}} = 57 \text{ \AA}^3$), epichlorohydrin ($V_{\text{vdw}} = 72 \text{ \AA}^3$), and ethyloxirane ($V_{\text{vdw}} = 78 \text{ \AA}^3$) was investigated by ¹H NMR spectroscopy. The signals of the guests' protons are strongly high-field shifted (Fig. 36) [78]. With the two enantiomers (*R*)-methyloxirane and (*S*)-methyloxirane, a decrease of the binding constants is observed when compared to cryptophane **43**, as a result of the steric hindrance due to the six carboxylate moieties. In an NaOH/H₂O solution binding constants of 128 M⁻¹ and 99 M⁻¹ were determined for the (*R*)-methyloxirane@(*P*, *P*)-**41** and (*R*)-methyloxirane@(*M*, *M*)-**41**, respectively, reflecting a lower enantioselectivity when compared to **43**. Surprisingly, increasing the size of the guest resulted in even lower binding constants but in better enantioselectivities. For instance, (*S*)-ethyloxirane is recognized by host (*M*, *M*)-**41** in NaOD/D₂O solution with a binding constant $K = 11 \text{ M}^{-1}$, whereas the complexation of (*R*)-ethyloxirane was not observed.

4.3.3 Enantioselective Recognition of Carbohydrates by Enantiopure Hemicryptophanes

The molecular recognition of carbohydrates by proteins is involved in several important biological processes such as protein folding, cell–cell recognition, and tumor metastasis. In spite of numerous biomimetic receptors synthesized for carbohydrate complexation, few deal with their enantioselective recognition. The inner space of the cavity of hemicryptophanes **52** and **53** displays both polar functionalities and apolar surfaces, which should induce selective sugar complexation. Enantioselective recognition of carbohydrates by the chiral enantiopure hemicryptophane supramolecular cages (*M*-*R*,*R*,*R*)-**52**, (*P*-*R*,*R*,*R*)-**52**, (*M*-*S*,*S*,*S*)-**52**, (*P*-*S*,*S*,*S*)-**52**, (*M*)-**53**, and (*P*)-**53** has been investigated [114]. Octyl-β-D-glucopyranoside (OctβGlc) and octyl-α-D-glucopyranoside (OctαGlc) were used as soluble glycosidic guests and the related binding constants, obtained by ¹H NMR

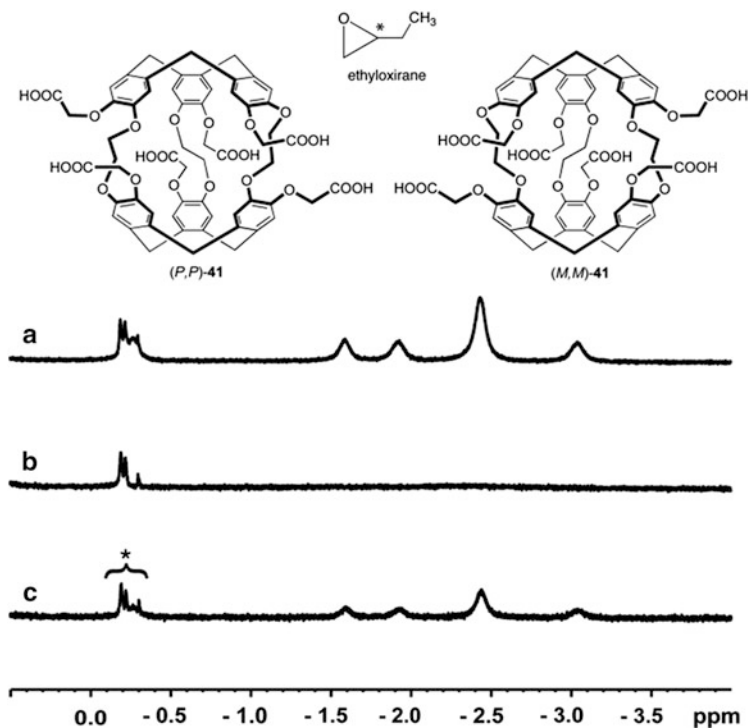


Fig. 36 ¹H NMR spectra (275 K) of (M,M)-41 in the presence of (a) (S)-ethyloxirane, (b) (R)-ethyloxirane, (c) (rac)-ethyloxirane (NaOD/D₂O; pD = 13.2) (* belongs to the imploded conformer)

Table 2 Binding constants K_a of enantiopure hemicryptophane **52** and **53** with octyl-glucosides in CDCl₃ ($T = 298$ K)

Entry	Receptor	<i>octaGlc</i> K_a (M ⁻¹)	<i>octβGlc</i> K_a (M ⁻¹)
1	(M)-53	216	64
2	(P)-53	30	–
3	(M-R,R,R)-52	123	226
4	(P-S,S,S)-52	–	115
5	(M-S,S,S)-52	155	184
6	(P-R,R,R)-52	–	–

titration experiments, are shown in Table 2. Modest to high diastereoselectivities were observed. Most strikingly, enantioselectivity was found to be profoundly dependent on the inherent chirality of the CTB moiety. Indeed, in most cases, exclusive binding of the (M)-enantiomer is observed, demonstrating the crucial role of the inherent chirality of the CTB part in this enantioselective complexation. In contrast, the three stereogenic carbon centers in hosts **52** only smoothly affect the

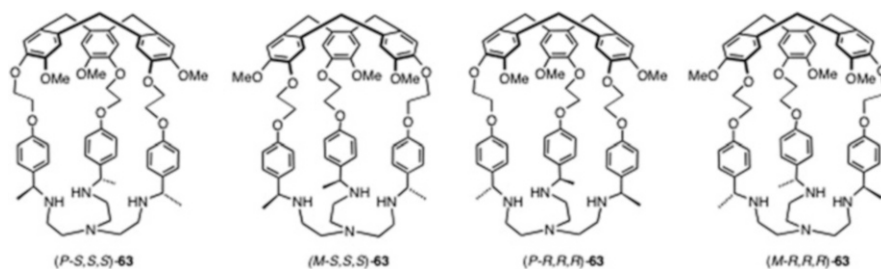


Fig. 37 Structure of the four diastereomers of hemicryptophane hosts **63**

stereoselective recognition process. For instance, the (*M-R,R,R*)-**52** and (*M-S,S,S*)-**52** stereoisomers display similar binding constants for the recognition of Oct β Glc (respectively 123 and 155 M⁻¹), whereas no complexation can be detected for the (*P-R,R,R*)-**52** and (*P-S,S,S*)-**52** host molecules.

4.3.4 Enantioselective Recognition of Chiral Ammonium by Enantiopure Supramolecular Cages

The organic ammonium salts have long been the guests of choice for testing the properties of molecular recognition of cationic species. Regarding the results for the supramolecular cages that bind chiral ammonium, one can refer to the recent work of Ahn et al. who reported the enantioselective binding of organoammonium ion by the cage-like chiral receptors based on tripodal oxazolines **31a** and **31b** (see Sect. 3.2.3) [69]. The addition of α -phenylethylammonium or alanine methyl ester to a solution of **31a** or **31b** was followed by ¹H NMR at different temperatures, and compared to a model open receptor. Due to the change in size and space shape available for guest complexation, the chiral differentiation observed with the cage compounds was found to differ from that observed with model open receptors. For instance, the cage-like receptor differentiates the enantiomers of alanine methyl ester with high enantioselectivity, whereas the chiral differentiation is poor with α -phenylethylammonium. In all cases, the chiral differentiation is in favor of the (*R*)-guest with cages (*S,S,S*)-**31a** and (*S,S,S*)-**31b**.

Another important family of chiral guests investigated are the ammonium neurotransmitters. The ability of the C₃ symmetrical enantiopure hemicryptophanes **63** to differentiate the neurotransmitters ephedrine (**13**) and norephedrine (**15**), as well as their diastereoisomers and enantioselective recognition properties, has also been studied (Fig. 37) [115].

The binding constants were obtained by ¹H NMR titration (Table 3). Moderate to high diastereoselectivities were observed for both the recognition of ephedrine and norephedrine, the highest ones being found for norephedrine. For instance, the stereoisomers (*P-R,R,R*)-**63** and (*M-S,S,S*)-**63** display β_1 binding constants (1:1 host-

Table 3 Binding constants β_1 (1:1 host:guest) and β_2 (1:2 host:guest) of enantiopure receptors **63** with ephedrine and norephedrine (CDCl₃/CD₃OD 95:5, 298 K)

	Norephedrine			Ephedrine		
	(<i>M-R,R,R</i>)	(<i>M-S,S,S</i>)	(<i>P-S,S,S</i>)	(<i>P-R,R,R,R</i>)	(<i>M-S,S,S</i>)	(<i>P-S,S,S</i>)
β_1 (M ⁻¹)	–	1.52 10 ⁵	3.99 10 ³	2.50 10 ⁵	4.71 10 ⁴	8.06 10 ³
β_2 (M ⁻²)	1.39 10 ⁷	2.64 10 ⁹	2.18 10 ⁷	1.95 10 ⁹	2.18 10 ⁸	2.52 10 ⁷

(P-*R,R,R,R*)(P-*S,S,S*)(M-*S,S,S*)(M-*R,R,R,R*)(P-*R,R,R,R*)(P-*S,S,S*)(M-*S,S,S*)(M-*R,R,R,R*)(P-*R,R,R,R*)

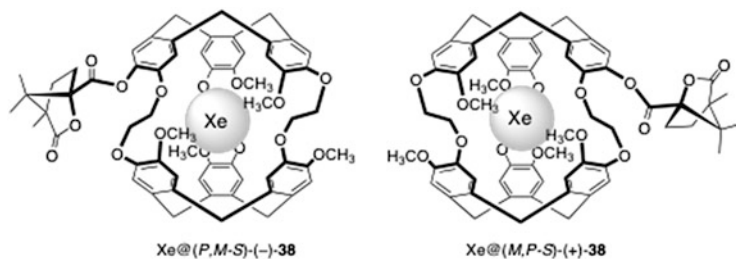
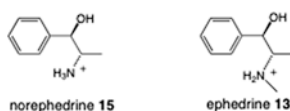


Fig. 38 Structure of the xenon complexes of cryptophane diastereomers (*P,M-S*)-(-)-**38** and (*M,P-S*)-(+)-**38**

guest complex) for norephedrine, 60 and 40 times higher than that of (*P-S,S,S*)-**63**, respectively. The β_2 constants (1:2 host-guest complex) with the (*P-R,R,R*)-**63** and (*M-S,S,S*)-**63** isomers were found to be much more efficient than the (*P-S,S,S*)-**63** and (*M-R,R,R*)-**63** ones with association constants two order of magnitude higher. This emphasizes the crucial role played by the stereogenic carbon centers and the configuration of the CTB unit in the stereoselectivity of the recognition process. Furthermore, a modest enantioselectivity was observed in the recognition of chiral ammonium neurotransmitters. For example, the (*M-S,S,S*)-**63** enantiomer showed higher β_1 and β_2 binding constants with ephedrine than the (*P-R,R,R*)-**63** one. Moreover, good enantioselectivity in favor of the (*M-R,R,R*)-**63** enantiomer over the (*P-S,S,S*)-**63** one was achieved for the recognition of norephedrine.



4.4 Biosensing: Xenon–Cryptophane Complexes

Xenon encapsulation by cryptophane hosts has been thoroughly investigated by several groups, who have demonstrated that small cryptophane derivatives can accommodate rare gases such as xenon [70] or radon [116]. Xenon–cryptophane complexes are still widely investigated as new potential contrast agents for MRI applications. Thanks to laser-polarization techniques of xenon gas, it is possible to detect the xenon–cryptophane complexes at low concentration in organic or aqueous solution using ^{129}Xe NMR. The particular behavior of xenon encapsulated in chiral cryptophane derivatives has been reported in some cases. The two diastereomeric cryptophanes (*P,M-S*)-**38** and (*M,P-S*)-**38** bearing a camphanic residue form complexes with xenon in tetrachloroethane- d_2 (Fig. 38), which display two different ^{129}Xe NMR signals [117]. The NMR spectrum exhibits the signal of the free xenon in solution at 228 ppm associated with two other resonances shifted towards

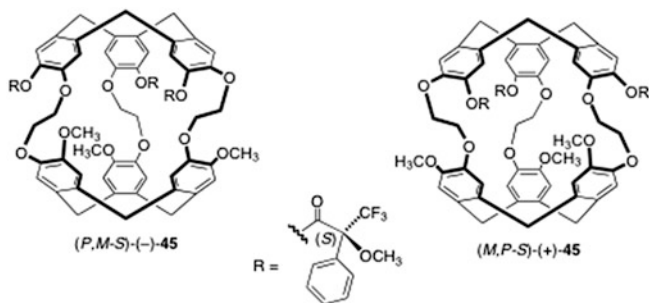


Fig. 39 Structure of cryptophane diastereomers (*P,M-S*)-(-)-45 and (*M,P-S*)-(+)-45

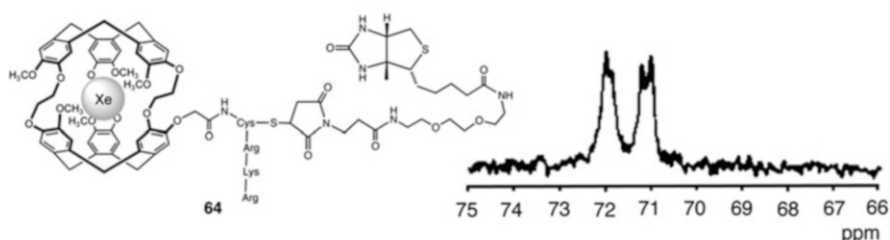


Fig. 40 Structure of biosensor **64** and the laser-polarized ^{129}Xe NMR spectrum

low frequencies by 160 ppm. These two signals are separated by 7 ppm and stand for the two diastereomeric complexes $\text{Xe}@(\textit{P,M-S})\text{-38}$ and $\text{Xe}@(\textit{M,P-S})\text{-38}$, which exhibit binding constants K_a $2,000\text{ M}^{-1}$ and $3,200\text{ M}^{-1}$, respectively.

Dmochowski and co-workers found similar results with the two diastereomers of a tris-substituted cryptophane-A derivative made of an enantiopure cryptophane-A derivative bearing three (*S*)-Mosher acid moieties (Fig. 39) [83]. Using ^{129}Xe NMR spectroscopy the authors showed that the diastereomeric xenon complexes exhibit different xenon chemical shifts at 67.3 and 77.4 ppm for the (*P,M-S*)-(-)-45 and the (*M,P-S*)-(+)-45 diastereomers, respectively.

The synthesis of enantiopure cryptophanes can find application in the elaboration of molecular biosensors, used in combination with hyperpolarized xenon, for the detection of *in vitro* or *in vivo* biological events. Pines et al. noticed that complex biosensors involving cryptophane derivatives in their racemic form could lead to ^{129}Xe NMR spectra difficult to interpret due to the formation of several diastereomeric xenon complexes. This arises when one or several stereogenic groups are bound to a racemic cryptophane core. For instance, in the presence of xenon gas dissolved in the solution, the ^{129}Xe NMR spectrum of the biosensor **64** aimed at binding the avidin protein displays four distinct signals (Fig. 40). Each of them stands for a diastereomeric species showing a specific affinity for the xenon atom encapsulated in the cavity of the cryptophane. Thus, the presence of several diastereomers in solution may significantly complicate the interpretation of the ^{129}Xe spectrum of the biosensor with or without the biological

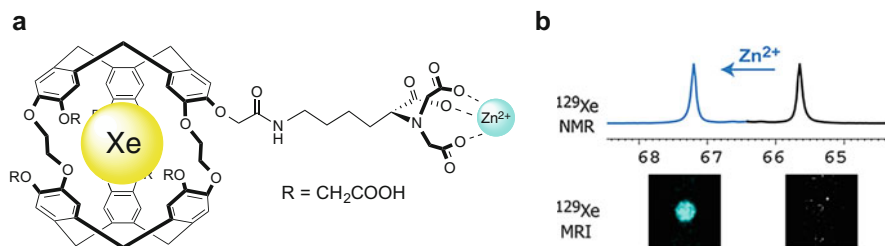


Fig. 41 (a) Structure of biosensor (L)-NTA-42 designed for the detection of Zn^{2+} ions. (b) ^{129}Xe NMR spectra of the biosensor (black) and the biosensor binding Zn^{2+} cations (blue)

target. To overcome this problem, Roy et al. synthesized a chiral cryptophane-biosensor able to recognize specifically a DNA strand. At low concentration the biosensor binds specifically the complementary strand, and the recognition process is characterized by a shift of the ^{129}Xe NMR signal. In contrast, in the presence of a non-complementary DNA strand, the ^{129}Xe NMR signal remains unchanged [76].

The following experiment illustrates the consequences of using enantiopure host molecules instead of the racemic form. The biosensor (L)-NTA-42 made of a water-soluble cryptophane in its racemic form and bearing a chiral L-nitriilotriacetic acid group, used for chelating Zn^{2+} ions, was synthesized (see Sect. 3.3.3). The complexation of Zn^{2+} cations is detected indirectly via a hyperpolarization technique of the xenon gas trapped in the cavity of the cryptophane and exchanging quickly with xenon present in the bulk. In the absence of Zn^{2+} the xenon NMR spectrum of the two (*M,M*)-(L)-NTA-42 and (*P,P*)-(L)-NTA-42 diastereomers show a single signal. However, upon Zn^{2+} binding by the L-NTA probe, two ^{129}Xe NMR signals are observed at $\delta = 65.75$ and 67.2 ppm, with respect to the free biosensor in solution ($\delta = 65.6$ ppm). These two signals correspond to the two diastereomeric biosensors that respond differently in the presence of Zn^{2+} . In order to assign the two ^{129}Xe NMR signals, the two diastereomerically pure cryptophane-biosensors (*M,M*)-(L)-NTA-42 and (*P,P*)-(L)-NTA-42 have been synthesized independently. Their ^{129}Xe NMR spectra recorded separately in the presence of Zn^{2+} allowed the unambiguous assignment of the two ^{129}Xe NMR signals. Thanks to the technique of laser-polarized xenon, the authors demonstrated that Zn^{2+} could be detected at a concentration as low as 100 nM in short time. In addition, they showed that the significant chemical shift difference observed between the free biosensor and the diastereomer (*M,M*)-(L)-NTA-42, which presents the largest chemical shift difference when chelating the Zn^{2+} ion, was sufficient to perform MRI experiments (Fig. 41) [79].

5 Conclusion

The aim of this review was to present selected examples of chiral supramolecular cages, with a short introduction to the well-known cavitand-type structures that are often at the basis of these closed-shell supramolecular containers. We chose to

present essentially covalent organic structures, and we hope we have demonstrated the diversity and the modularity of the different synthetic approaches to these chiral hosts. The access to enantiopure compounds often needs peculiar strategies, some being presented in this review. These cages are “supramolecular” in the sense that they can host very different substrates (neutral guests, chiral guests, ionic species). We show that the supramolecular complexes can now be studied by modern spectroscopic techniques such as NMR spectroscopy or by means of chiroptical techniques such as ECD or VCD spectroscopy. The ability of these host molecules to encapsulate a guest, that can be chiral or achiral, may strongly affect the chiroptical properties of the host molecules. Some examples studied in our laboratory have been used to illustrate the effect of the binding process on the overall chiroptical properties of supramolecular cages. Despite the synthetic difficulties in preparing enantiopure supramolecular cages, we hope to have shown throughout this review that enantiomeric vessels are of great interest in today’s chemistry and may find numerous applications in chiral differentiation, and further applications in catalytic reactions in the confined space of the cages or in bio-medical sciences are promising. The example of using chiral cages for the design of biosensors is indeed extremely thrilling.

References

1. Fischer E (1894) Einfluss der Configuration auf die Wirkung der Enzyme. *Ber Dt Chem Ges* 27:2985–2993
2. Kubik S (2012) Molecular cages and capsules with functionalized inner surfaces. *Top Curr Chem* 319:1–34
3. Saalfrank RW, Scheurer A (2012) Coronates, spherical containers, bowl-shaped surfaces, porous 1D-, 2D-, 3D-metallo-coordination polymers, and metallo-dendrimers. *Top Curr Chem* 319:125–170
4. Ousaka N, Grunder S, Castilla AM, Whalley AC, Stoddart JF, Nitschke JR (2012) Efficient long-range stereochemical communication and cooperative effects in self-assembled Fe_4L_6 cages. *J Am Chem Soc* 134:15528–15537
5. Brizard A, Oda R, Huc I (2005) Chirality effects in self-assembled fibrillar networks. *Top Curr Chem* 256:167–218
6. Huc I (2004) Aromatic oligoamide foldamers. *Eur J Org Chem* 17–29
7. Oda R, Artzner F, Laguerre M, Huc I (2008) Molecular structure of self-assembled chiral nanoribbons and nanotubes revealed in the hydrated state. *J Am Chem Soc* 130:14705–14712
8. Berni E, Garric J, Lamit C, Kauffmann B, Léger JM, Huc I (2008) Interpenetrating single helical capsules. *Chem Commun* 1968–1970
9. Ferrand Y, Kendhale AM, Kauffmann B, Grélard A, Marie C, Blot V, Pipelier M, Dubreuil D, Huc I (2010) Diastereoselective encapsulation of tartaric acid by helical aromatic oligoamide. *J Am Chem Soc* 132:7858–7859
10. Ferrand Y, Chandramouli N, Kendhale AM, Aube C, Kauffmann B, Grélard A, Laguerre M, Dubreuil D, Huc I (2012) Long range effects on the capture and release of a chiral guest by a helical molecular capsule. *J Am Chem Soc* 134:11282–11288
11. Kieser B, Fietzek C, Schmidt R, Belge G, Weimar U, Schurig V, Gauglitz G (2002) Use of a modified cyclodextrin host for the enantioselective detection of a halogenated diether as chiral guest via optical and electrical transducers. *Anal Chem* 74:3005–3012

12. Grandeury A, Petit S, Gouhier G, Agasse V, Coquerel G (2003) Enantioseparation of 1-(p-bromophenyl)ethanol by crystallization of host-guest complexes with permethylated β -cyclodextrin: crystal structures and mechanisms of chiral recognition. *Tet Asymm* 14:2143–2152
13. Zaborova E, Guitet M, Prencipe G, Blériot Y, Ménand M, Sollogoub M (2013) An against the rules double bank shot with diisobutylaluminium hydride to allow triple functionalization of α -cyclodextrin. *Angew Chem Int Ed* 52:639–644
14. Liu Y, You CC, Zhang HY, Zhao YL (2003) Enantioselective recognition of aliphatic amino acids by β -cyclodextrin derivatives bearing aromatic organoselenium moieties on the primary or secondary side. *Eur J Org Chem* 1415–1422
15. Engeldinger E, Armspach D, Matt D (2003) Capped cyclodextrins. *Chem Rev* 103:4147–4173
16. Zhao YL, Zhang HY, Wang M, Yu HM, Yang H, Liu Y (2006) Organic anion recognition of naphthalenesulfonates by steroid-modified cyclodextrins: enhanced molecular binding ability and molecular selectivity. *J Org Chem* 71:6010–6019
17. Bregier F, Karuppanan S, Chambron JC (2012) A hybrid cavitand made by capping permethylated α -cyclodextrin with cyclotrimeratrylene. *Eur J Org Chem* 1920–1925
18. Gutsche CD, Muthukrishnan R (1978) Calixarenes 1. Analysis of the product mixtures produced by the base-catalyzed condensation of formaldehyde with para-substituted phenols. *J Org Chem* 43:4905–4906
19. Gutsche CD (2008) Calixarenes: an introduction. RSC Publishing, Cambridge
20. Iwamoto K, Shimizu H, Shinkai S (1993) Synthesis and optical resolution of calix[4]arenes with molecular asymmetry. Systematic classification of all possible chiral isomers derivable from calix[4]arene. *J Am Chem Soc* 115:3997–4006
21. Otsuka H, Shinkai S (1996) Stereochemical control of calixarenes useful as rigid and conformationally diversiform platforms for molecular design. *Supramol Sci* 3:189–205
22. Garrier E, Le Gac S, Jabin I (2005) First enantiopure calix[6]aza-cryptand: synthesis and chiral recognition properties towards neutral molecules. *Tet Asymm* 16:3767–3771
23. Le Gac S, Jabin I (2008) Synthesis and study of calix[6]cryptamides: a new class of heteroditopic receptors that display versatile host-guest properties toward neutral and organic associated ion-pair salts. *Chem Eur J* 14:548–557
24. Dalla Cort A, Mandolini L, Pasquini C, Schiaffino L (2004) Inherent chirality and curvature. *New J Chem* 28:1198–1199
25. Vysotsky M, Schmidt C, Böhmer V (2000) Chirality in calixarenes and calixarene assemblies. *Adv Supramol Chem* 7:139–233
26. Szumna A (2010) Inherently chiral concave molecules – from synthesis to applications. *Chem Soc Rev* 39:4274–4285
27. Zheng Y-S, Luo J (2011) Inherently chiral calixarenes: a decade's review. *J Incl Phenom Macrocycl Chem* 71:35–36
28. Cherenok S, Dutasta JP, Kalchenko V (2006) Phosphorus-containing chiral macrocycles. *Curr Org Chem* 10:2307–2331
29. Luo J, Zheng QY, Chen CF, Huang ZT (2005) Synthesis and optical resolution of a series of inherently chiral calix[4]crowns with cone and partial cone conformations. *Chem Eur J* 11:5917–5928
30. Timmerman P, Verboom W, Reinhoudt DN (1996) Resorcinarenes. *Tetrahedron* 52:2663–2704
31. Cram DJ, Karbach S, Kim HE, Knobler CB, Maverick EF, Ericson JL, Helgeson RC (1988) Host guest complexation 46. Cavitands as open molecular vessels form solvates. *J Am Chem Soc* 110:229–2237
32. Moran JR, Karbach S, Cram DJ (1982) Cavitands: synthetic molecular vessels. *J Am Chem Soc* 104:5826–5828
33. Soncini P, Bonsignore S, Dalcanale E, Ugozzoli F (1992) Cavitands as versatile molecular receptors. *J Org Chem* 57:4608–4612

34. Bulman Page PC, Heaney H, Sampler EP (1999) The first enantioselective syntheses of axially chiral enantiomerically pure calix[4]resorcinarene derivatives. *J Am Chem Soc* 121:6751–6752
35. Beyeh NK, Fehér D, Luostarinen M, Schalley CA, Rissanen K (2006) Synthesis of chiral resorcinarene-based hosts and a mass spectrometric study of their chemistry in solution and the gas phase. *J Inclusion Phenom Macrocyclic Chem* 56:381–394
36. Shivanyuk A, Rissanen K, Körner SK, Rudkevich DM, Rebek J Jr (2000) Structural studies of self-folding cavitands. *Helv Chim Acta* 83:1778–1790
37. Dutasta JP (2004) New phosphorylated hosts for the design of new supramolecular assemblies. *Top Curr Chem* 232:55–91
38. Melegari M, Suman M, Pirondini L, Moiani D, Massera C, Ugozzoli F, Kalenius E, Vainiotalo P, Mulatier JC, Dutasta JP, Dalcanale E (2008) Supramolecular sensing with phosphonate cavitands. *Chem Eur J* 14:5772–5779
39. Melegari M, Massera C, Pinalli R, Yebeutchou RM, Dalcanale E (2013) Supramolecular sensing of short chain alcohols with mixed-bridged thio-phosphonate cavitands. *Sens Actuators B* 179:74–80
40. Bibal B, Tinant B, Declercq JP, Dutasta JP (2003) Preparation and structure of [iiii] tetraphosphonatocavitands bearing long chain functionality at the lower rim: metal picrates extraction studies. *Supramol Chem* 15:25–32
41. Delange P, Mulatier JC, Tinant B, Declercq JP, Dutasta JP (2001) Synthesis and binding properties of iiii (4i) stereoisomers of phosphonatocavitands – cooperative effects in cation complexation in organic solvents. *Eur J Org Chem* 3695–3704
42. Dionisio M, Oliviero G, Menozzi D, Federici S, Yebeutchou RM, Schmidtchen FP, Dalcanale E, Bergese P (2012) Nanomechanical recognition of *N*-methylammonium salts. *J Am Chem Soc* 134:2392–2398
43. Vachon J, Harthong S, Dubessy B, Dutasta JP, Vanthuynne N, Roussel C, Naubron JV (2010) Absolute configuration of an inherently chiral phosphonatocavitand and its use towards enantioselective recognition of adrenaline. *Tet Asymm* 21:1534–1541
44. Vachon J, Harthong S, Jeanneau E, Aronica C, Vanthuynne N, Roussel C, Dutasta JP (2011) Inherently chiral phosphonatocavitands as artificial chemio- and enantio-selective receptors of natural ammoniums. *Org Biomol Chem* 9:5086–5091
45. Kim K, Selvapalam N, Ko YH, Park KM, Kim D, Kim J (2007) Functionalized cucurbiturils and their applications. *Chem Soc Rev* 36:267–279
46. Huang WH, Zavalij PY, Isaacs L (2007) Chiral recognition inside a chiral cucurbituril. *Angew Chem Int Ed* 46:7425–7427
47. Thilgen C, Gosse I, Diederich F (2003) Chirality in fullerene chemistry. *Top Stereochem* 23:1–124
48. Thilgen C, Diederich F (2006) Structural aspects of fullerene chemistry—a journey through fullerene chirality. *Chem Rev* 106:5049–5135
49. Shoji Y, Tashiro K, Aida T (2010) One-pot enantioselective extraction of chiral fullerene C₇₆ using a cyclic host carrying an asymmetrically distorted, highly π -basic porphyrin module. *J Am Chem Soc* 132:5928–5929
50. Filippone S, Maroto EE, Martin-Domenech A, Suarez M, Martin N (2009) An efficient approach to chiral fullerene derivatives by catalytic enantioselective 1,3-dipolar cycloadditions. *Nat Chem* 1:578–582
51. Sawai K, Takano Y, Izquierdo M, Filippone S, Martin N, Slanina Z, Mizorogi N, Waelchli M, Tsuchiya T, Akasaka T, Nagase S (2011) Enantioselective synthesis of endohedral metallofullerenes. *J Am Chem Soc* 133:17746–17752
52. Riala M, Chronakis N (2011) A facile access to enantiomerically pure [60]fullerene bisadducts with the inherently chiral trans-3 addition pattern. *Org Lett* 13:2844–2847
53. Kraszewska A, Riviera-Fuentes P, Rapenne G, Crassous J, Petrovic AG, Alonso-Gomez JL, Huerta E, Diederich F, Thilgen C (2010) Regioselectivity in tether-directed remote functionalization – the addition of a cyclotrimeratrylene-based trimalonate to C₆₀ revisited. *Eur J Org Chem* 4402–4411

54. Cram DJ, Cram JM (1994) Container molecules and their guests. Monographs in supramolecular chemistry. The Royal Society of Chemistry, Cambridge
55. Jasat A, Sherman JC (1999) Carceplexes and hemicarceplexes. *Chem Rev* 99:931–967
56. Warmuth R, Yoon J (2001) Recent highlights in hemicarcerands chemistry. *Acc Chem Res* 34:95–105
57. Yoon J, Cram DJ (1997) Chiral recognition properties in complexation of two asymmetric hemicarcerands. *J Am Chem Soc* 119:11796–11806
58. Park BS, Knobler CB, Eid CN, Warmuth R, Cram DJ (1998) Chiral and somewhat hydrophilic hemicarceplexes. *Chem Commun* 55–56
59. Rue NM, Warmuth R (2011) Polyimine container molecules and nanocapsules. *Isr J Chem* 51:743–768
60. Tartaggia S, Scarso A, Padovan P, De Lucchi O, Fabris F (2009) Gases as guests in benzocyclootrimer cage hosts. *Org Lett* 11:3926–3929
61. Shomura R, Higashibayashi S, Sakurai H, Matsushita Y, Sato A, Higuchi M (2012) Chiral phenylazomethine cage. *Tet Lett* 53:783–785
62. Steinmetz V, Couty F, David ORP (2009) One step synthesis of chiral cages. *Chem Commun* 343–345
63. Jelfs KE, Wu X, Schmidtman M, Jones JTA, Warren JE, Adams DJ, Cooper AI (2011) Large self-assembled chiral organic cages: synthesis, structure, and shape persistence. *Angew Chem Int Ed* 50:10653–10656
64. Skowronek P, Gawronski J (2008) Chiral iminospherand of a tetrahedral symmetry spontaneously assembled in a [6+4] cyclocondensation. *Org Lett* 10:4755–4758
65. Tozawa T, Jones JTA, Swamy SI, Jiang S, Adams DJ, Shakespeare S, Clowes R, Bradshaw D, Hasell T, Chong SY, Tang C, Thompson S, Parker J, Trewin T, Bacsá J, Slawin AMZ, Steiner A, Cooper AI (2009) Porous organic cages. *Nat Mater* 8:973–978
66. Jones JTA, Hasell T, Wu X, Bacsá J, Jelfs KE, Schmidtman M, Chong SY, Adams DJ, Trewin A, Schiffman F, Cora F, Slater B, Steiner A, Day GM, Cooper AI (2011) Modular and predictable assembly of porous organic molecular crystals. *Nature* 474:367–371
67. Nishiyabu R, Kubo Y, James TD, Fossey JS (2011) Boronic acid building blocks: tools for self-assembly. *Chem Commun* 47:1124–1150
68. Takahagi H, Fujibe S, Iwasawa N (2009) Guest induced dynamic self-assembly of two diastereomeric cage-like boronic esters. *Chem Eur J* 15:13327–13330
69. Sambasivan S, Kim SG, Choi SM, Rhee YM, Ahn KH (2010) C_3 -Symmetric cage-like receptors: chiral discrimination of α -chiral amines in a confined space. *Org Lett* 12:4228–4231
70. Brotin T, Dutasta JP (2009) Cryptophanes and their complexes – present and future. *Chem Rev* 109:88–130
71. Xu D, Warmuth R (2008) Edge-directed dynamic covalent synthesis of a chiral nanocube. *J Am Chem Soc* 130:7520–7521
72. Wang T, Zhang YF, Hou QQ, Xu WR, Cao XP, Chow HF, Kuck D (2013) C_3 -Symmetrical tribenzotriquinacene derivatives: optical resolution through cryptophane synthesis and supramolecular self-assembly into nanotubes. *J Org Chem* 78:1062–1069
73. Garcia C, Andraud C, Collet A (1992) New key compounds in cyclotriveratrylene chemistry. Synthesis, optical resolution, absolute configuration and circular dichroism of C_3 -cyclotriveratrylenes with sulfur substituents. *Supramol Chem* 1:31–45
74. Soulard P, Asselin P, Cuisset A, Aviles Moreno JR, Huet TR, Petitprez D, Demaison J, Freedman TB, Cao X, Nafie LA, Crassous J (2006) Chlorofluoroiodomethane as a potential candidate for parity violation measurements. *Phys Chem Chem Phys* 8:79–92
75. Brotin T, Barbe R, Darzac M, Dutasta JP (2003) Novel synthetic approach for optical resolution of cryptophanol-A: a direct access to chiral cryptophanes and their chiroptical properties. *Chem Eur J* 9:5784–5792
76. Roy V, Brotin T, Dutasta JP, Charles MH, Delair T, Mallet F, Huber G, Desvaux H, Boulard Y, Berthault P (2007) A cryptophane biosensor for the detection of specific nucleotide targets through xenon NMR spectroscopy. *ChemPhysChem* 8:2082–2085

77. Cavagnat D, Buffeteau T, Brotin T (2008) Synthesis and chiroptical properties of cryptophanes having C_1 -symmetry. *J Org Chem* 73:66–75
78. Bouchet A, Brotin T, Linares M, Cavagnat D, Buffeteau T (2011) Influence of the chemical structure of water-soluble cryptophanes on their overall chiroptical and binding properties. *J Org Chem* 76:7816–7825
79. Kotera N, Tassali N, Léonce E, Boutin C, Berthault P, Brotin T, Dutasta JP, Delacour L, Traoré T, Buisson DA, Taran F, Couderc S, Rousseau B (2012) A sensitive zinc-activated ^{129}Xe MRI probe. *Angew Chem Int Ed* 51:4100–4103
80. Bouchet A, Brotin T, Linares M, Ågren H, Cavagnat D, Buffeteau T (2011) Enantioselective complexation of chiral propylene oxide by an enantiopure water-soluble cryptophane. *J Org Chem* 76:4178–4181
81. Brotin T, Cavagnat D, Berthault P, Montserret R, Buffeteau T (2012) Water-soluble molecular capsule for the complexation of cesium and thallium cations. *J Phys Chem B* 116:10905–10914
82. Taratula O, Hill PA, Bai Y, Khan NS, Dmochowski IJ (2011) Shorter synthesis of trifunctionalized cryptophane-A derivatives. *Org Lett* 13:1414–1417
83. Taratula O, Kim MP, Bai Y, Philbin JP, Riggle BA, Haase DN, Dmochowski IJ (2012) Synthesis of enantiopure, trisubstituted cryptophane-A derivatives. *Org Lett* 14:3580–3583
84. Tambuté A, Canceill J, Collet A (1989) Optical resolution of C_3 cyclotrivertatrylenes and D_3 cryptophanes by liquid chromatography on chiral stationary phase chirapak-OT(+). *Bull Chem Soc Jpn* 62:1390–1392
85. Fogarty HA, Berthault P, Brotin T, Huber G, Desvaux H, Dutasta JP (2007) A cryptophane core optimized for xenon encapsulation. *J Am Chem Soc* 129:10332–10333
86. Dömling A (2004) Recent developments in isocyanide based multicomponent reactions in applied chemistry. *Chem Rev* 106:17–89
87. Dömling A, Ugi I (2000) Multicomponent reactions with isocyanides. *Angew Chem Int Ed* 39:3168–3210
88. Wessjohann LA, Rivera DG, Vercillo OE (2009) Multiple multicomponent macrocyclizations (MiBs): a strategic development toward macrocycle diversity. *Chem Rev* 109:796–814
89. Rivera DG, Wessjohann LA (2006) Supramolecular compounds from multiple Ugi multicomponent macrocyclizations: peptoid-based cryptands, cages and cryptophanes. *J Am Chem Soc* 128:7122–7123
90. Gautier A, Mulatier JC, Crassous J, Dutasta JP (2005) Chiral trialkanolamine-based hemicyptophanes: synthesis and oxovanadium complex. *Org Lett* 7:1207–1210
91. Martinez A, Robert V, Gornitzka H, Dutasta JP (2010) Controlling helical chirality in atrane structures: solvent-dependent chirality sense in hemicyptophane-oxidovanadium(V) complexes. *Chem Eur J* 16:520–527
92. Martinez A, Guy L, Dutasta JP (2010) Reversible solvent-induced chirality switch in atrane structure: control of the unidirectional motion of the molecular propeller. *J Am Chem Soc* 132:16733–16734
93. Dimitrov Raytchev P, Perraud O, Aronica C, Martinez A, Dutasta JP (2010) A new class of C_3 -symmetrical hemicyptophane hosts: triamide- and tren-hemicyptophanes. *J Org Chem* 75:2099–2102
94. Perraud O, Dimitrov Raytchev P, Martinez A, Dutasta JP (2010) Resolution and absolute configuration assignment of a chiral hemicyptophane molecular cage. *Chirality* 22:885–888
95. Dimitrov Raytchev P, Martinez A, Gornitzka H, Dutasta JP (2011) Encaging the Verkade's superbases: thermodynamic and kinetic consequences. *J Am Chem Soc* 133:2157–2159
96. Liu X, Ilankumaran P, Guzei IA, Verkade JG (2000) P[S, S, S]-PhHMe CNCH₂CH₂]₃N: a new chiral 31P and ¹H NMR spectroscopic reagent for the direct determination of ee values of chiral azides. *J Org Chem* 65:701–706
97. Verkade JG, Kisanga PB (2003) Proazaphosphatranes: a synthesis methodology trip from their discovery to vitamin A. *Tetrahedron* 59:7819–7858

98. Payet E, Dimitrov Raytchev P, Chatelet B, Guy L, Grass S, Lacour J, Dutasta JP, Martinez A (2012) Absolute configuration and enantiodifferentiation of a hemicyptophane incorporating an azaphosphatrane moiety. *Chirality* 24:1077–1081
99. Lacour J, Ginglinger C, Grivet C, Bernardinelli G (1997) Synthesis and resolution of the configurationally stable tris(tetra-chlorobenzenediolato)phosphate(V) ion. *Angew Chem Int Ed* 36:608–609
100. Whitmarsh SD, Redmond AP, Sgarlata V, Davis AP (2008) Cationic cyclocholamides; toroidal facial amphiphiles with potential for anion transport. *Chem Commun* 3669–3671.
101. Brotherhood PR, Davis AP (2010) Steroid-based anion receptors and transporters. *Chem Soc Rev* 39:3633–3647
102. Canceill J, Collet A, Gottarelli G, Palmieri P (1987) Synthesis and exciton optical activity of D₃-cryptophanes. *J Am Chem Soc* 109:6454–6464
103. Brotin T, Cavagnat D, Dutasta JP, Buffeteau T (2006) Vibrational circular dichroism study of optically pure cryptophane-A. *J Am Chem Soc* 128:5533–5540
104. Cavagnat D, Brotin T, Bruneel JL, Dutasta JP, Thozet A, Perrin M, Guillaume F (2004) Raman microspectrometry as a new approach to the investigation of molecular recognition in solids: chloroform–cryptophane complexes. *J Phys Chem B* 108:5572–5581
105. Brotin T, Cavagnat D, Buffeteau T (2008) Conformational changes in cryptophane having C₁-symmetry studied by vibrational circular dichroism. *J Phys Chem A* 112:8464–8470
106. Bouchet A, Brotin T, Cavagnat D, Buffeteau T (2010) Induced chiroptical changes of a water-soluble cryptophane by encapsulation of guest molecules and counterion effects. *Chem Eur J* 16:4507–4518
107. Brotin T, Montserret R, Bouchet A, Cavagnat D, Linares M, Buffeteau T (2011) High affinity of water-soluble cryptophanes for cesium cations. *J Org Chem* 77:1198–1201
108. Bouchet A, Brotin T, Linares M, Ågren H, Cavagnat D, Buffeteau T (2011) Conformational effects induced by guest encapsulation in an enantiopure water-soluble cryptophane. *J Org Chem* 76:1372–1383
109. Akabori S, Miura M, Takeda M, Yuzawa S, Habata Y, Ishii T (1996) Synthesis of diethyleneoxy bridged cryptophanes and their complexing abilities with alkali metal and alkylammonium cations. *Supramol Chem* 7:187–193
110. Roesky CEO, Weber E, Rambusch T, Stephan H, Gloe K, Czugler M (2003) A new cryptophane receptor featuring three endo-carboxylic acid groups: synthesis, host behavior and structural study. *Chem Eur J* 9:1104–1112
111. Canceill J, Lacombe L, Collet A (1985) Analytical optical resolution of bromochlorofluoromethane by enantioselective inclusion into a tailor-made cryptophane and determination of its maximum rotation. *J Am Chem Soc* 107:6993–6996
112. Costante-Crassous J, Marrone TJ, Briggs JM, McCammon JA, Collet A (1997) Absolute configuration of bromochlorofluoromethane from molecular dynamics simulation of its enantioselective complexation by cryptophane-C. *J Am Chem Soc* 119:3818–3823
113. Crassous J, Jiang Z, Schurig V, Polavarapu PL (2004) Preparation of (+)-chlorofluoroiodomethane, determination of its enantiomeric excess and of its absolute configuration. *Tet Asymm* 15:1995–2001
114. Perraud O, Martinez A, Dutasta JP (2011) Exclusive enantioselective recognition of glucopyranosides by inherently chiral hemicyptophanes. *Chem Commun* 47:5861–5863
115. Schmitt A, Chatelet B, Collin S, Dutasta JP, Martinez A (2013) Chiral Discrimination of Ammonium Neurotransmitters by C₃-Symmetric Enantiopure Hemicyptophane Hosts. *Chirality* 25:475–479
116. Jacobson DR, Khan NS, Collé R, Fitzgerald R, Lauréano-Perez L, Bai Y, Dmochowski JJ (2011) Measurement of radon and xenon binding to a cryptophane molecular host. *PNAS* 108:10969–10973
117. Huber JG, Dubois L, Desvaux H, Dutasta JP, Brotin T, Berthault P (2004) NMR study of optically active monosubstituted cryptophanes and their interaction with xenon. *J Phys Chem A* 108:9608–9615

Interconversion of Stereochemically Labile Enantiomers (Enantiomerization)

Oliver Trapp

Abstract The investigation of the molecular dynamics of stereoisomers is of fundamental interest in chemistry, biochemistry, medicine, and related areas. In recent years enantioselective dynamic chromatography and enantioselective dynamic capillary electrophoresis (DCE) have been established as versatile tools to investigate the kinetics of interconversions of stereoisomers. The term dynamic chromatography and dynamic electrophoresis, following the term dynamic NMR (DNMR) (Grathwohl and Wüthrich, *Biopolymers* 20:2623–2633, 1981; Wüthrich, *Angew Chem Int Ed* 42:3340–3363, 2003; Binsch et al., *Angew Chem Int Ed* 10:570–572, 1971), stresses the dynamic (Herschbach, *Angew Chem Int Ed* 26:1221–1243, 1987) behavior of analytes to interconvert between two stereoisomeric forms during the separation process. If the interconversion process is slow compared to the separation of the enantiomers, which can be achieved by accelerating the separation process or lowering the temperature, partial separation with characteristic plateau formation or peak broadening is observed.

This chapter gives an overview of recent advances in the study of stereodynamics of molecules by dynamic chromatography (Trapp et al., *Chirality* 13:403–414, 2001; D'Acquarica et al., *J Sep Sci* 29:1508–1516, 2006; Wolf, *Chem Soc Rev* 34:595–608, 2005; Wolf, *Dynamic stereochemistry of chiral compounds – principles and applications*. RSC Publishing, Cambridge, 2008) and capillary electrophoresis. Models and algorithms to evaluate interconversion profiles obtained by separation techniques are discussed with respect to the challenging demands of high separation efficiencies typical of modern separation techniques. Models used for evaluation are based on iterative computer simulation algorithms using the theoretical plate model (TPM) or stochastic model of chromatography, empirical calculation methods, derived from equations used in chemical engineering, namely Damköhler analysis, and direct access using the approximation function, and more recently the unified

O. Trapp (✉)
Ruprecht-Karls-Universität Heidelberg, Organisch-Chemisches Institut, Im Neuenheimer
Feld 270, 69120 Heidelberg, Germany
e-mail: trapp@oci.uni-heidelberg.de

equation of chromatography, which can be applied to all kinds of first-order reactions taking place during a chromatographic or electrophoretic separation. Furthermore, areas of applications to investigate stereodynamic processes are presented and discussed to give a practical guide for using dynamic chromatography and capillary electrophoresis.

Keywords Activation parameters · Chirality · Computer simulation · Drugs · Dynamic capillary electrophoresis · Dynamic gas chromatography · Dynamic high performance liquid chromatography · Dynamic super-critical chromatography · Enantiomerization · Enantioselective chromatography · Interconversion · Kinetics · Stopped-flow techniques · Theoretical plate model · Unified equation

Contents

1	Introduction	233
2	Experimental and Theoretical Aspects	235
2.1	Definition of Enantiomerization and Racemization	235
2.2	Experimental Setups	236
2.3	Determination of Rate Constants of Enantiomerization by Enantioselective Dynamic Chromatography	240
2.4	Determination of Activation Parameters by Temperature-Dependent Measurements	251
3	Applications	252
3.1	Dynamic GC	252
3.2	Stopped-Flow Gas Chromatography	253
3.3	Stopped-Flow MDGC	254
3.4	Dynamic HPLC	257
3.5	Dynamic SFC	261
3.6	Electrophoretic Methods	261
4	Outlook	263
	References	263

Abbreviations

CE	Capillary electrophoresis
CSP	Chiral stationary phase
DCE	Dynamic capillary electrophoresis
DGC	Dynamic gas chromatography
DHPLC	Dynamic high performance liquid chromatography
DNMR	Dynamic nuclear magnetic resonance
DSFC	Dynamic supercritical fluid chromatography
ee	Enantiomeric excess
GC	Gas chromatography
HPLC	High performance liquid chromatography
SFC	Supercritical fluid chromatography
sfGC	Stopped-flow gas chromatography
sfMDGC	Stopped-flow multidimensional gas chromatography

TLC Thin layer chromatography

1 Introduction

The stereodynamics of molecules is of great importance in chemistry, physics, biochemistry, and medicine [1–3]. There are currently several techniques available for the study of these conformational or configurational changes. Among the most commonly used techniques are dynamic NMR (DNMR) spectroscopy, the measurement of H/D exchange by high resolution mass spectrometry [4] especially applicable to biomolecules, stopped-flow chromatography, and dynamic chromatography (Fig. 1).

DNMR spectroscopy [5, 6] is well established and widely used to investigate interconversions in the lower kJ-range [7] and therefore commonly used to investigate conformational changes in molecules. Its applicability is limited by the experimental temperature range and the time-scale. DNMR spectroscopy is best suited to determine rate constants at the coalescence point, the temperature at which the signals of the individual interconvertomers collapse to a single signal. Under other experimental conditions a line shape analysis has to be performed. Still, DNMR spectroscopy has made and continues to make indispensable contributions to the understanding of protein folding on molecular and functional levels. For the investigation of stereochemical changes, e.g., in compounds containing stereogenic nitrogen, DNMR spectroscopy has enabled one to understand factors influencing the interconversion barrier and consequently to apply this knowledge in the synthesis of compounds characterized by improved stereointegrity [8, 9].

In stopped-flow chromatography and electrophoresis [10–15] the reaction time is extended by stopping the chromatographic or electrophoretic flow after a separation of the stereoisomers is achieved. Column switching techniques, if appropriate, are often used to trap one interconvertomer and transfer it to a second column. Then the particular column is heated to initiate the interconversion process and then, after cooling down to the separation temperature, the stereoisomers are separated to determine the de novo stereoisomeric ratio. This method is very well suited to the determination of high interconversion barriers; however, a baseline separation is required. Furthermore, peak broadening caused by diffusion during the trapping process requires high separation factors, α . This effect can be avoided in GC by using cryo-focusing techniques.

Dynamic and stopped-flow chromatographic and electrophoretic techniques have been used for the determination of kinetic parameters of stereolabile compounds, i.e., compounds with stereogenic chirotopic nitrogen [16–25], atropisomers [11, 26–36], pheromones [37], drugs [38–43], inherently chiral compounds [44], natural products [45, 46], and even organic radicals [47]. The low configurational stability of certain chiral drug substances is an issue of pharmaceutical and pharmacological relevance, as most biochemical processes are stereochemically controlled and enantiomeric drug substances can interact

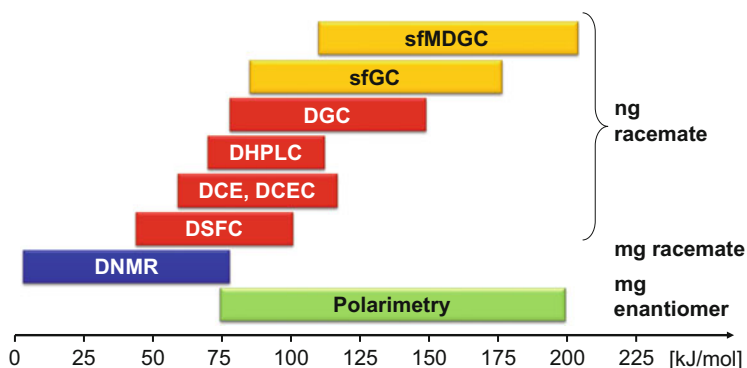


Fig. 1 Overview of methods available for the determination of enantiomerization barriers in dependency of the targeted enantiomerization barrier (*D* dynamic, *sf* stopped flow, *MD* multidimensional)

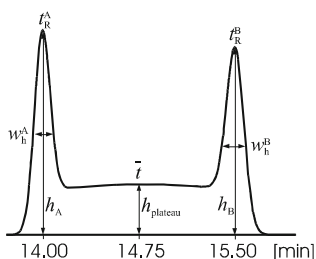


Fig. 2 Example of an elution profile obtained by dynamic chromatography of interconverting enantiomers with the experimental parameters: stochastic model, $t_M = 1.0$ min, $t_R^A = 14.0$ min, $t_R^B = 15.5$ min, $N = 50,000$, and $k_1^{app} = 1 \times 10^{-3}$ s $^{-1}$. Parameters calculated from the chromatogram: widths at half height $w_A = 9.42$ s, $w_B = 10.72$ s, and $h_{plateau} = 24.81\%$

differently in terms of pharmacodynamics, pharmacokinetics, and toxicological activity. Consequently, the pharmaceutical industry, as well as regulatory authorities such as the US Food and Drug Administration (FDA), are interested in methods able to determine quantitatively the stereochemical stability of chiral drug substances. The FDA not only restricts the sale of racemic drugs but also demands unambiguous data on the configurational stability of the pure enantiomers. Consequently drug manufacturers are bound to consider the stereochemical integrity of enantiomers and “assess the potential for interconversion...of the individual isomers” [48, 49].

In dynamic chromatography, typical peak profiles are characterized by peak broadening, plateau formation, and eventually peak coalescence (Fig. 2) [50].

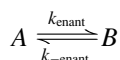
Whereas in conventional chromatographic separations the occurrence of such elution profiles is considered as a complication, in dynamic chromatography such peak profiles are the prerequisite for the determination of interconversion barriers. Depending on the physical properties of the analyte molecule and the expected

interconversion barrier, different dynamic chromatographic or electrophoretic techniques (e.g., DGC, DSFC, DHPLC, DCE, DCEC, DMEKC) can be chosen for the quantification of the interconversion process (Fig. 1). The major advantages of enantioselective dynamic chromatographic and electrophoretic techniques is that only minute amounts of analytes are necessary, which even do not need to be isolated from a product mixture or purified from a natural product extract, and that the enrichment or isolation of single isomers, which can be quite complex for isomers with low stereochemical integrity, is not necessary.

2 Experimental and Theoretical Aspects

2.1 Definition of Enantiomerization and Racemization

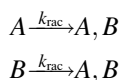
Enantiomerization defines the microscopic interconversion from one enantiomer (A) into the other (B), can be described by a reversible first-order reaction, and is independent of the mechanism of interconversion:



The integrated rate law of an enantiomerization is given by

$$\ln \frac{[A]_0}{[A]_0 - 2[B]_t} = 2k_{\text{enant}}t \quad (1)$$

If a molecule has more than one stereogenic element, this definition also takes the simultaneous interconversion of all n stereogenic elements into consideration. In contrast to enantiomerization, racemization is defined as an irreversible macroscopic process, which forms the racemate from a nonracemic starting material [51]:



The integrated rate law of racemization is given by

$$\ln \frac{[A]_0}{[A]_0 - [A, B]_t} = k_{\text{rac}}t \quad (2)$$

Equations (1) and (2) can be summarized, giving the relationship of the rate constants of enantiomerization and racemization:

$$k_{\text{rac}} = 2k_{\text{enant}} \quad (3)$$

The half-life τ can be then calculated according to

$$\tau = \frac{\ln 2}{2k_{\text{enant}}} = \frac{\ln 2}{k_{\text{rac}}} \quad (4)$$

The factor of 2 can be also experimentally proven by coupling three HPLC columns in-line (see below), where each column is independently set to a defined temperature. The first and last column are chiral columns, where the stereodynamic phenomenon is observed; the center column is packed with an achiral stationary phase, where racemization takes places. By this setup racemization and enantiomerization can be experimentally observed under exactly the same reaction conditions and can therefore be directly compared [35]. It is important to note that enantiomerization describes an interconversion process on the molecular level whereas racemization describes the conversion of the bulk material.

2.2 Experimental Setups

2.2.1 Enantioselective Dynamic Chromatography

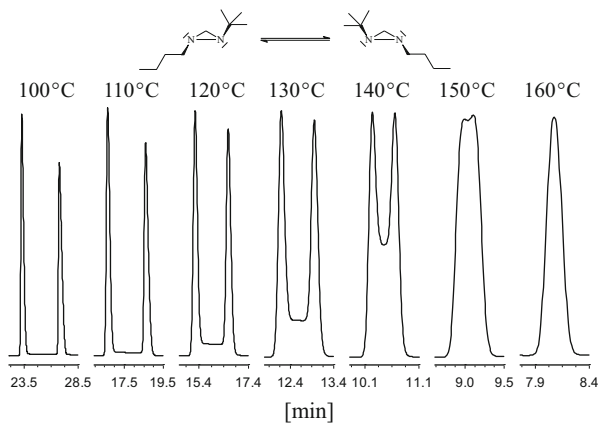
Enantioselective chromatography and electrophoresis can be easily performed. The only prerequisite is a successful enantioseparation of the interconverting stereoisomers. Depending on the molecular properties, enantioselective GC, HPLC, SFC, or electrophoretic techniques can be chosen. In a next step typically a suitable chiral stationary phase (CSP) has to be found and separation conditions have to be optimized. In contrast to conventional separations the separation conditions should be applicable for a broader temperature range to determine temperature-dependent kinetic data, which allows calculation activation parameters. Experience shows that shorter separation columns are suitable to investigate lower enantiomerization barriers, whereas longer separation columns extend the reaction time at the cost of peak broadening, which lowers the resolution.

Minute amounts of racemic mixtures can be injected on the column and the elution profiles characterized by pronounced plateau formations recorded for evaluation (Fig. 3).

2.2.2 Enantioselective Stopped-Flow Chromatography

Single-column stopped-flow gas chromatography, which does not require computer simulation, is typically performed as follows. After quantitative separation of the enantiomers on the CSP in the first part of the column, the flow is stopped and enantiomerization of the separated fractions is effected at increased temperature by

Fig. 3 Selected experimental enantiomerization profiles of 1-*n*-butyl-2-*tert*-butyldiaziridine between 100°C and 160°C. Chromatographic conditions: 25 m Chirasil- β -Dex (0.25 mm i.d., film thickness 0.5 μ m). Carrier gas: He

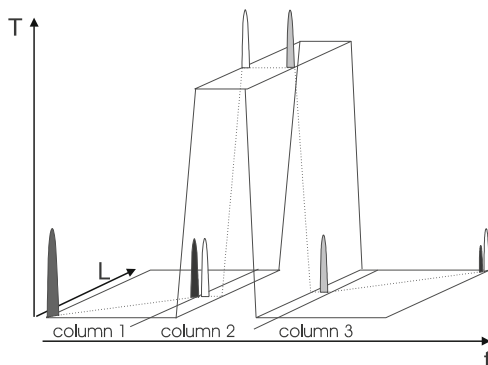


heating the entire column. After a given enantiomerization time, the former enantiomerization temperature is restored and the enantiomerized fractions are separated in the second part of the column. The enantiomerization barriers of each of the two enantiomers are calculated from the four peak areas a_i , the enantiomerization time t , and the enantiomerization temperature T . By single-column stopped-flow GC [11], enantiomerization barriers of 70–180 kJ mol^{-1} can be determined. Similar experiments can be performed in capillary electrophoresis [10].

2.2.3 Enantioselective Multidimensional Gas Chromatography

As in dynamic methods, single column stopped-flow experiments require that the enantiomerization process takes place in the presence of the CSP. However, the presence of the CSP can affect the enantiomerization barrier. The barrier can be increased or lowered, e.g., by catalytic effects [52]. Efforts have therefore been devoted to combine the advantages of the stopped-flow approach with the option to perform enantiomerization in an achiral and inert environment. Stopped-flow multidimensional GC (sfMDGC) enhances the experimental range of enantiomerization barriers (Fig. 1) [12, 14, 53]. This fast and simple technique allows the determination of enantiomerization barriers in the range of $\Delta G^\ddagger(T) = 70\text{--}200 \text{ kJ mol}^{-1}$. After complete gas chromatographic separation of the enantiomers in the first column, gas phase enantiomerization of the heart-cut fraction of one single enantiomer is performed in the second (reactor) column at increased temperature in reaction time t . Afterwards this fraction is separated into the enantiomers in the third column and the enantiomeric ratio, er , is determined (Fig. 4). From the de novo enantiomeric ratio er , the enantiomerization time t , and the enantiomerization temperature T , the enantiomerization (inversion) barrier $\Delta G^\ddagger(T)$ is determined (5) and the activation enthalpy ΔH^\ddagger and the activation entropy ΔS^\ddagger are obtained by temperature-dependent experiments:

Fig. 4 Schematic representation of the sfMDGC technique (variables are enantiomerization time t , enantiomerization temperature T , and three columns lengths L)



$$k = \frac{1}{2t} \ln \frac{er + 1}{er - 1} \quad (5)$$

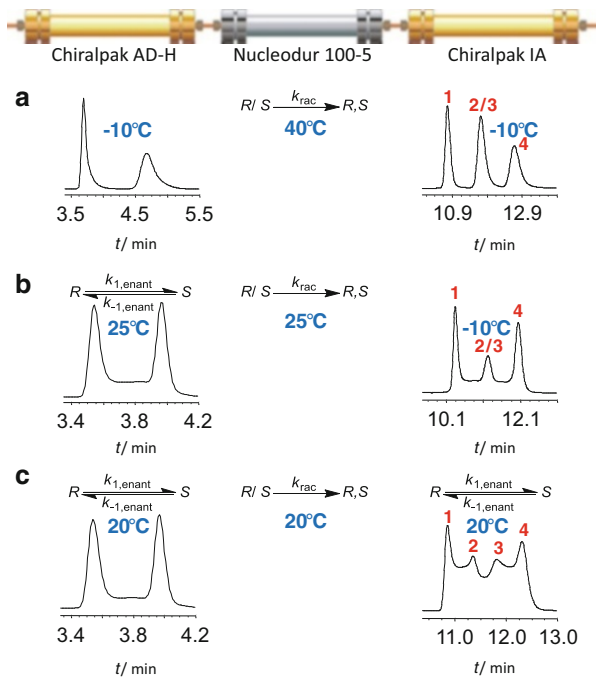
2.2.4 Stereodynamics and Kinetics in a Single Setup: Three-Column HPLC Technique

Solvent effects and stationary phase effects are often discussed and it has to be pointed out that the quantification of such effects is a challenging task. The three-column HPLC technique (Fig. 5) allows the investigation of such effects in great detail [35].

The analyte passes through the first column which affords separation of the enantiomers, then through a second column containing an achiral support, that permits partial re-racemization, and finally through a third chiral column that allows the degree of re-racemization to be analyzed accurately. Such an arrangement has become feasible by the development of high-pressure resistant chiral packing materials in HPLC, overcoming limitations in the solvent back-pressure range. With this setup one can simultaneously investigate dynamic and kinetic processes, i.e., enantiomerization and racemization, under identical conditions.

Depending on the applied temperatures in the respective column sections, elution profiles of varying complexity can be obtained. Consider Fig. 5a where the first and third column is at a lower temperature and the intermediate achiral column at an elevated temperature. The elution profile on exiting the second column will not change from the exit to the first column, but all analyte molecules will be subject to racemization depending on the reaction time Δt , temperature T , and stationary phase. Passage through the third column separates the de novo enantiomeric mixture, leading to a third peak 2/3 (coincidence of peaks 2 and 3) that is distinct from peaks 1 and 4. The racemization rate constant, k_{rac} , can be directly calculated from the integrated peak areas and the reaction time.

Fig. 5 Experimental setup of the three-column arrangement to study enantiomerization and racemization processes and to quantify stationary phase effects



Elevation of the temperature of the first column leads to dynamic interconversion profiles in the first column, followed by racemization in the second. The interconversion of the de novo enantiomeric mixture can be “frozen” by lowering the temperature in the third column (Fig. 5b), which allows one to determine independently the dynamics (enantiomerization) and kinetics (racemization) in a single experimental setup.

In the case of elevated temperatures in all three columns (Fig. 5c), racemization of the separated enantiomers also takes place in the second column, accompanied by simultaneous doubled dynamic interconversion of peaks 1 and 2 ($1 \rightleftharpoons 2$), 3, and 4 ($3 \rightleftharpoons 4$) (both in the third column), as well as 1 and 4 ($1 \rightleftharpoons 4$) (in the first and third column). Enantiomers of peaks 2 and 3 do not interconvert because of opposite elution order leading to separation, which reveals the height of the overall plateau and allows the simultaneous determination of enantiomerization and racemization rate constants.

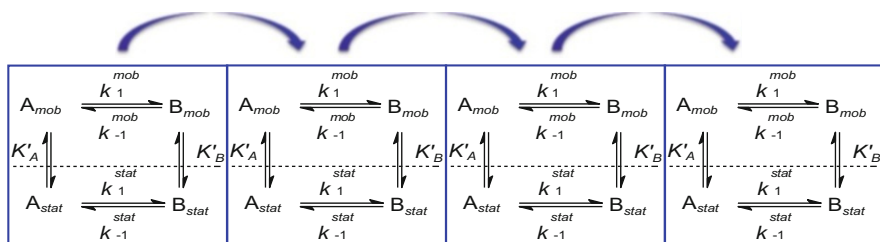


Fig. 6 Application of the theoretical plate model of chromatography to evaluate on-column reactions in a chromatographic setup. Every theoretical plate is considered as a chemical reactor

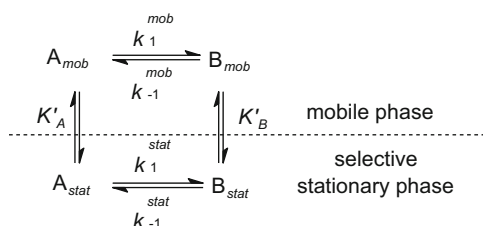


Fig. 7 Equilibria and reaction kinetics of interconverting enantiomers in a single theoretical plate. *A* is the first eluted stereoisomer, *B* is the second eluted stereoisomer, *k* represents the rate constant, and *K* the phase distribution constant

2.3 Determination of Rate Constants of Enantiomerization by Enantioselective Dynamic Chromatography

2.3.1 Theoretical Plate Model of Chromatography

The theoretical plate model (TPM), which was originally developed to describe a separation process based on partitioning, is the most illustrative model. Here the separation is described by a discontinuous process, assuming that all steps proceed repeatedly in separate uniform sections of a multi-compartmentalized column consisting of *N* theoretical plates [54–56].

To integrate a reaction in this model, every theoretical plate is considered as a distinct chemical reactor (Fig. 5) [57] and three steps are performed in each plate: (1) distribution of the stereoisomers or reactant and product *A* and *B* between the mobile and the selective stationary phase, (2) (inter-) conversion of the species in the mobile and selective stationary phase if applicable, and, finally, (3) shifting of the mobile phase to the next theoretical plate (Figs. 6 and 7).

The distribution of the stereoisomers *A* and *B* between the mobile phase (mob) and the selective stationary phase (stat) is determined according to (6) and (7), respectively:

$$\begin{aligned}
 A_{\text{mob}} &= \frac{1}{1 + k'_A} (A^{\circ}_{\text{mob}} + A^{\circ}_{\text{stat}}) \\
 B_{\text{mob}} &= \frac{1}{1 + k'_B} (B^{\circ}_{\text{mob}} + B^{\circ}_{\text{stat}})
 \end{aligned}
 \tag{6}$$

$$\begin{aligned}
 A_{\text{stat}} &= \frac{k'_A}{1 + k'_A} (A^{\circ}_{\text{mob}} + A^{\circ}_{\text{stat}}) \\
 B_{\text{stat}} &= \frac{k'_B}{1 + k'_B} (B^{\circ}_{\text{mob}} + B^{\circ}_{\text{stat}})
 \end{aligned}
 \tag{7}$$

where A_{mob} , B_{mob} , A_{stat} , and B_{stat} are the amounts of the stereoisomers A and B at the equilibrium, A°_{mob} , B°_{mob} , A°_{stat} , and B°_{stat} are the amounts of A and B before the equilibrium, and k'_A and k'_B are the retention factors of A and B , calculated from the retention time t_R and the hold-up time t_0 , determined by methane or regression of the retention times of n -alkanes, according to $k' = (t_R - t_0)/t_0$.

The interconverted part of the stereoisomers or reactant during the residence time $\Delta t = t_0/N$ in the CSP and in the achiral mobile phase in a theoretical plate is determined by the respective rate constants. In the case of enantiomers or any other degenerated interconversion process the forward and backward rate constants k_1^{mob} and k_{-1}^{mob} in the mobile phase are equal and the equilibrium constant K^{mob} is unity, whereas the equilibrium constant in the CSP depends on the two-phase distribution constants (i.e., partition coefficients) K_A and K_B according to the principle of microscopic reversibility [18, 58]:

$$K^{\text{stat}} = \frac{k_1^{\text{stat}}}{k_{-1}^{\text{stat}}} = \frac{K_B}{K_A} = \frac{k'_B}{k'_A}
 \tag{8}$$

This equation implies that the backward rate constant k_{-1}^{stat} is already determined for given values of k_1^{stat} , k'_A and k'_B , and that k_1^{stat} differs from k_{-1}^{stat} when $K_B \neq K_A$, i.e., when the enantiomers are discriminated and hence separated in the presence of the CSP ($\Delta\Delta G \neq 0$). For the interconversion of enantiomers in an achiral environment the principle of microscopic reversibility has to be neglected because the individual enantiomers show inherently different retentions. This means that the rate constants depend only on the equilibrium constant (8). Typically only apparent rate constants k_1^{app} and k_{-1}^{app} , which represent a weighted mean of the reaction rate constants in the mobile and stationary phase, are experimentally accessible (9). By performing complementary experiments these reaction rate constants can be accessed [59]:

$$\begin{aligned}
 k_1^{\text{app}} &= \frac{1}{1 + k'_A} k^{\text{mob}} + \frac{k'_A}{1 + k'_A} k_1^{\text{stat}} \\
 k_{-1}^{\text{app}} &= \frac{1}{1 + k'_B} k^{\text{mob}} + \frac{k'_B}{1 + k'_B} k_{-1}^{\text{stat}}
 \end{aligned}
 \tag{9}$$

The reversible first-order kinetics is described by

$$\frac{dx}{dt} = k_1^{\text{app}}([A_0] - [X]) - k_{-1}^{\text{app}}([B_0] + [X]) \quad (10)$$

where the amount $[X]$ is the change of A and B . Equation (10) is solved by integration, using the initial conditions:

$$[A] = \frac{k_{-1}^{\text{app}}}{k_1^{\text{app}} + k_{-1}^{\text{app}}} ([A_0] + [B_0]) + \frac{k_1^{\text{app}}[A_0] - k_{-1}^{\text{app}}[B_0]}{k_1^{\text{app}} + k_{-1}^{\text{app}}} e^{-(k_1^{\text{app}} + k_{-1}^{\text{app}})\Delta t} \quad (11)$$

The amount of $[B]$ is calculated from the mass balance due to $[A_0] + [B_0] = [A] + [B]$. After these two steps (partitioning of the present species between mobile phase and stationary phase and undergoing interconversion) the content of the mobile phase is shifted to the subsequent theoretical plate, whereas the stationary phase is retained. While the given amount of the enantiomers is initially introduced in the first theoretical plate, the content of the mobile phase of the last theoretical plate is finally recorded as a chromatogram featuring an interconversion profile over time t . The first simulation program, developed by Bürkle et al. was published in 1984 [18] and was based on the TPM. It was later extended by Jung and Schurig in 1992 to simulations of up to 120,000 effective plates (SIMUL) [19]. The TPM and especially algorithms based on Jung and Schurig have been applied by many authors, especially for HPLC [60, 61].

Trapp and Schurig presented in 2000 the Windows-based program ChromWin running on a PC [15, 62], which allows simulation with the TPM, the stochastic, and a modified stochastic model without any restriction regarding theoretical plate numbers N .

2.3.2 Stochastic Model

The stochastic model (SM) [46, 63–65], which was originally developed by Giddings et al. for interconversion processes taking place in TLC, describes the chromatographic separation using time-dependent distribution functions $\Phi_i(t)$ with the input parameters hold-up time t_M , retention times t_R^A and t_R^B and plate numbers N_A and N_B . The concept of this model is that probability distributions are calculated for the relative times spent as molecules A and B . This means that the probabilities have to be calculated that a molecule starts as enantiomer A and ends as enantiomer B , and A ends after “two interconversion cycles” again as enantiomer A . The same has to be applied to isomer B . The elution profile $P(t)$ (12) for an interconversion process in the time-scale of separation is given by the sum of the distribution functions $\Phi_{A'}(t)$ and $\Phi_{B'}(t)$ of the non-interconverted stereoisomers A' and B' and the probability density functions $\Psi_{A''}(t, t')$ and $\Psi_{B''}(t, t')$ of the interconverted stereoisomers A'' and B'' :

$$P(t) = \Phi_{A'}(t) + \Phi_{B'}(t) + \Psi_{A''}(t, t') + \Psi_{B''}(t, t') \quad (12)$$

For the entire process the mass balance $[A] + [B] = [A'] + [B'] + [A''] + [B'']$ must be fulfilled. Taking into account that an interconversion process takes place in the (achiral) mobile as well as in the enantioselective stationary phase, only apparent rate constants for the forward and backward reaction (k_1^{app} and k_{-1}^{app}) are obtained applying the principle of microscopic reversibility. In the first step the concentration of the non-interconverted enantiomers A' and B' are calculated according to an irreversible first-order reaction. An irreversible first-order reaction is considered, because all stereoisomers which undergo conversion are separated from the peak of non-interconverted stereoisomers. The reaction time is defined by the migration times t_R^A and t_R^B [cf. (13) and (14)]:

$$c_{A'}(t_R^A) = c_A^0 e^{-k_1^{\text{app}} t_R^A} \quad (13)$$

$$c_{B'}(t_R^B) = c_B^0 e^{-k_{-1}^{\text{app}} t_R^B} \quad (14)$$

The concentration profiles of the edging peaks are described by Gaussian distributions. The standard deviation σ of the Gaussian distribution function is calculated from the peak width at half-height ω_h according to

$$\sigma^2 = \frac{t_R^2}{N} \quad \text{and} \quad \sigma = \frac{\omega_h}{\sqrt{8 \ln 2}} \quad (15)$$

It seems to be a contradiction to use plate numbers in a stochastic distribution model, but the plate number characterizes the sequence of partition steps during which the equilibrium is not completely reached. The partitioning illustrated by the TPM can be statistically described by the Poisson distribution. Transformation of the Poisson distribution by Stirling's equation gives a stochastic distribution (Gaussian functions) [66]. The envelope of the non-interconverted stereoisomers A' and B' is calculated by the time-dependent Gaussian distribution function $\Phi(t)$:

$$\Phi(t, t_R^i, \sigma_i, c_i t) = \sum_i \frac{c_i t}{\sigma_i \sqrt{2\pi}} e^{-\frac{(t-t_R^i)^2}{2\sigma_i^2}} \quad \text{with } i = A \text{ and } B \quad (16)$$

The concentration profile of the interconverted enantiomers A'' and B'' is calculated using a probability density function which is proportional to the concentration profile \bar{c}_i (17). The retention times of the stereoisomers t_R^A and t_R^B , the apparent rate constants k_1^{app} and k_{-1}^{app} , and the initial concentrations of the stereoisomers are required for the calculation:

$$\bar{c}_i(t) = (S_1 + S_2) \cdot e^{(-k_1^{\text{app}} - k_{-1}^{\text{app}})t} \quad (17)$$

$$S_1 = (c_A k_1^{\text{app}} + c_B k_{-1}^{\text{app}}) \sum_{j=0}^{\infty} \frac{(k_1^{\text{app}} \cdot k_{-1}^{\text{app}} t^2)^j}{j! j!} \quad (18)$$

$$S_2 = k_1^{\text{app}} \cdot k_{-1}^{\text{app}} \left(c_A \frac{t_R^A \cdot (t_R^B - t)}{t_R^B - t_R^A} + c_B \frac{t_R^B - t_R^A \cdot t_R^B}{t_R^B - t_R^A} \right) \sum_{j=0}^{\infty} \frac{(k_1^{\text{app}} \cdot k_{-1}^{\text{app}} t^2)^j}{(j+1)! j!} \quad (19)$$

The terminating condition for the variable j in expressions S_1 and S_2 is achieved, when the contribution approaches zero. Effects like tailing can be considered by multiplication of (17) with an exponential function [44, 67–69]. For practical reasons the concentration profile \bar{c}_i is fragmented in arbitrary intervals, which are then replaced by distribution curves using the migration times t_R^A and t_R^B and the mean theoretical plate number N_{AB} ($N_{AB} = (N_A + N_B)/2$). The variable t' in (20) represents the running time and t the integration variable. By integration over all distribution curves a concentration profile $\Psi(t, t')$ is obtained, which complies with an elution profile in non-ideal linear chromatography:

$$\Psi(t, t') = \sqrt{\frac{N_{AB}}{2\pi}} \int_{t_R^A}^{t_R^B} \bar{c}_i e^{-\frac{N_{AB}}{2} \left(\frac{t-t'}{t'}\right)^2} \frac{1}{t'} dt \quad (20)$$

The advantage of the SM over the TPM is the calculation speed, which is about 400 times faster for the SM.

Occasionally large differences in plate numbers N_A and N_B are experimentally observed. This complicates the evaluation of elution profiles because the peak with the higher plate number becomes broader while the peak with the lower plate number will be narrower than observed in the experiment. The modified stochastic model (SM+) [61] overcomes these limitations by applying a linear gradient of the plate numbers N_A and N_B , and the corresponding migration times t_R^A and t_R^B to obtain the plate number $N(t')$ which is dependent on the running time t' :

$$N(t') = \frac{\Delta_{A,B} N}{\Delta_{A,B} t_R} (t' - t_R^A) + N_A \quad (21)$$

Comparing the TPM with the stochastic model (SM) it has to be noted that the TPM requires considerably longer calculation times (e.g., for an average calculation with 50,000 theoretical plates the calculation time is 2 h with the TPM compared to 30 s with the SM). The results of the two independent models are generally in very good accordance with each other (Figs. 8 and 9).

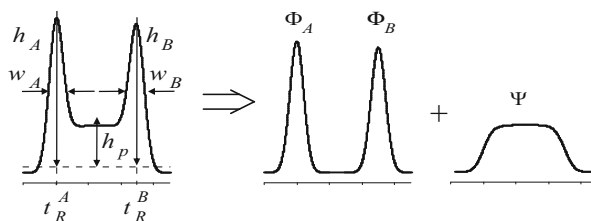


Fig. 8 Mathematical separation of an elution profile of enantiomerization into non-interconverted peaks, represented by time-dependent Gaussian distribution functions $\Phi_A(t)$ and $\Phi_B(t)$, and the interconverted part, represented by the stochastic distribution functions $\Psi(t)$

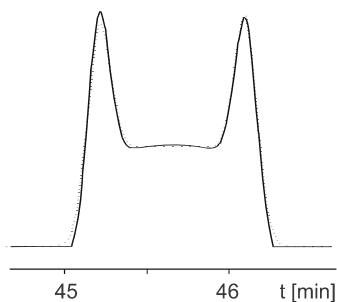


Fig. 9 Comparison of simulations obtained by the modified stochastic model (*dotted line*) and the theoretical plate model (*plain line*)

2.3.3 Empirical Computer-Assisted Peak Deconvolution Methods

Peak deconvolution methods to determine conversions from chromatographic data have been used in dynamic gas chromatography (DGC) [70]. Krupcik et al. [71, 72] have developed computer assisted strategies to deconvolute such elution profiles based on the concept, that the non-interconverted enantiomers and the converted part can be fitted by Gaussian/Lorentzian as well as exponentially modified Gaussian functions to approximate the peak shapes in the deconvolution procedure. An advantage of this method is that essentially no knowledge about the separation mechanism is necessary. However, Krupcik et al. [73] pointed out that it is problematic to determine initial peak parameters for a deconvolution procedure. In particular overlapping peak clusters are difficult to deconvolute because the number of peaks to the number of functions necessary to represent the non-Gaussian shaped interconversion profile is unknown. Krupcik et al. assume in their approach irreversible or pseudo-irreversible first-order kinetics. Peak areas determined by peak deconvolution and the retention times are used as parameters to calculate the reaction rate constant.

2.3.4 Dynamic Model Based on Continuity Equations

Gaš et al. [74] proposed a dynamic model of DCE based on solving a set of continuity equations [75] for all constituents of the separation system together with complexation and acid–base equilibria. The model is also based on the general scheme depicted in Fig. 7.

Gaš et al. defined, very similar to the model of distributing enantiomers between a mobile and a pseudo-stationary phase, a non-complexed and a complexed state, here denoted by dissolved (dis) and complexed (com). This means the total concentration of the individual enantiomers R and S is given by $c = c^{\text{dis}} + c^{\text{com}}$. The total concentration of the chiral selector CS is given by $c_{\text{CS}} = c_R^{\text{com}} + c_S^{\text{com}} + c_S^{\text{dis}}$.

The complexation equilibria with the complexation constant K are defined by

$$K_R = \frac{c_R^{\text{com}}}{c_R^{\text{dis}} c_{\text{CS}}^{\text{dis}}} \quad \text{and} \quad K_S = \frac{c_S^{\text{com}}}{c_S^{\text{dis}} c_{\text{CS}}^{\text{dis}}} \quad (22)$$

The complete electromigration process is described by the following set of continuity equations in a one-dimensional separation column (D denotes the overall diffusion coefficient of the enantiomers, k the reaction rate constants, and x is the axial coordinate of the column):

$$\frac{\partial c_R}{\partial \tau} = D_R \frac{\partial^2 c_R}{\partial x^2} - \frac{\partial}{\partial x} (v_R c_R) - k_R^{\text{dis}} c_R^{\text{dis}} + k_S^{\text{dis}} c_S^{\text{dis}} - k_R^{\text{com}} c_R^{\text{com}} + k_S^{\text{com}} c_S^{\text{com}} \quad (23)$$

$$\frac{\partial c_S}{\partial \tau} = D_S \frac{\partial^2 c_S}{\partial x^2} - \frac{\partial}{\partial x} (v_S c_S) - k_S^{\text{dis}} c_S^{\text{dis}} + k_R^{\text{dis}} c_R^{\text{dis}} - k_S^{\text{com}} c_S^{\text{com}} + k_R^{\text{com}} c_R^{\text{com}} \quad (24)$$

Assuming that the concentration of the enantiomers is lower than the concentration of the BGE, the electrophoretic velocities can be regarded as constant and the whole process is in a linear range.

Gaš et al. define a global reaction rate constant k^{glob} with the following relationships, especially the relation to the apparent rate constant k^{app} :

$$k^{\text{glob}} = k_R^{\text{dis}} + k_R^{\text{com}} K_R c_{\text{CS}}^{\text{dis}} = k_S^{\text{dis}} + k_S^{\text{com}} K_S c_{\text{CS}}^{\text{dis}} \quad (25)$$

$$k_R^{\text{app}} = \frac{k^{\text{glob}}}{1 + K_R c_{\text{CS}}^{\text{dis}}} \quad k_S^{\text{app}} = \frac{k^{\text{glob}}}{1 + K_S c_{\text{CS}}^{\text{dis}}} \quad (26)$$

Considering these equations and the principle of microscopic reversibility, the following general continuity equations can be derived:

$$\frac{\partial c_R}{\partial \tau} = D_R \frac{\partial^2 c_R}{\partial x^2} - \frac{\partial}{\partial x} (v_R c_R) - \frac{k^{\text{glob}}}{1 + K_R c_{\text{CS}}^{\text{dis}}} c_R + \frac{k^{\text{glob}}}{1 + K_S c_{\text{CS}}^{\text{dis}}} c_S \quad (27)$$

$$\frac{\partial c_S}{\partial \tau} = D_S \frac{\partial^2 c_S}{\partial x^2} - \frac{\partial}{\partial x} (v_S c_S) - \frac{k^{\text{glob}}}{1 + K_S c_{\text{CS}}^{\text{dis}}} c_S + \frac{k^{\text{glob}}}{1 + K_R c_{\text{CS}}^{\text{dis}}} c_R \quad (28)$$

Based on these equations, Gaš et al. developed a computer program SimulChir to evaluate reaction rate constants from dynamic experiments. These equations are numerically solved providing simulated electropherograms.

2.3.5 Direct Calculation Methods: Approximation Function and Unified Equation

In 2001 Trapp and Schurig [76] introduced the approximation function for the direct calculation of reaction rate constants from elution profiles of interconverting enantiomers. The elution profile $P(t')$ for interconverting enantiomers with running time t' is given by the sum of the two Gaussian distribution functions $\Phi_A(t')$ and $\Phi_B(t')$ of the non-interconverted enantiomers, and the probability density functions $\Psi_A(t')$ and $\Psi_B(t')$ of the interconverted enantiomers:

$$P(t') = \Phi_A(t') + \Phi_B(t') + \Psi_A(t') + \Psi_B(t') \quad (29)$$

Since the time-dependent concentration profile $\bar{c}(t')$ of the interconverting enantiomers has to be Gaussian modulated and the integral cannot be solved analytically, the probability density functions $\Psi_A(t')$ and $\Psi_B(t')$ have to be calculated numerically. Therefore the strategy was first to calculate distribution functions $\Phi_A(t')$ and $\Phi_B(t')$ of the non-interconverted enantiomers, and second to replace the time-dependent profile $\bar{c}(t')$ by a function for which the concentration is time-independent and the integral of the Gaussian modulation can be approximated (Fig. 7). Here, a box-car function $\bar{c}_{\text{boxcar}}(t')$ (30) is introduced, which is then modulated by Gaussian functions (31):

$$\bar{c}_{\text{boxcar}}(t_{\text{R}}^A \leq t' \leq t_{\text{R}}^B) = \frac{c_{\text{plateau}}}{t_{\text{R}}^B - t_{\text{R}}^A} = \frac{c_A^0 - c_A' + c_B^0 - c_B'}{t_{\text{R}}^B - t_{\text{R}}^A} \quad (30)$$

$$\Psi(t) = \frac{\bar{c}_{\text{boxcar}}(t)}{\sqrt{\pi}} \int_{t_1}^{t_2} \sqrt{\frac{N}{2}} e^{-\frac{N}{2} \left(\frac{t-t'}{\tau}\right)^2} \frac{1}{t} dt \quad (31)$$

The necessary data points at the migration times t_{R}^A , t_{R}^B and \bar{t} can be easily approximated. Equation (32) represent the solution of the concentration profile at the times t_{R}^A , t_{R}^B , and \bar{t} :

$$\begin{aligned}\Psi(t_R^A) &\approx \left(0.5 + \frac{1}{\sqrt{2\pi N}}\right) \bar{c}_{\text{boxcar}}(t_R^A) \\ \Psi(t_R^B) &\approx \left(0.5 - \frac{1}{\sqrt{2\pi N}}\right) \bar{c}_{\text{boxcar}}(t_R^B) \\ \Psi(\bar{t}) &\approx 1.0 \bar{c}_{\text{boxcar}}(\bar{t})\end{aligned}\quad (32)$$

With these functions the concentration at the peak migration times t_R^A and t_R^B and the concentration at the plateau in the time-middle \bar{t} ($\bar{t} = (t_R^A + t_R^B)/2$) can be calculated, which allows correlation of the relative plateau height h_p with the enantiomerization rate constant.

The relative plateau height h_p is defined as the ratio of the concentration at the time-middle \bar{t} and the concentration of the higher peak at the migration times t_R^A and t_R^B of the enantiomers *A* or *B*. It has to be noted that in the case of tailing, the plateau height is raised. In such cases it is recommended to take a point closer to the later eluted peak if appropriate.

A detailed mathematical derivation of the approximation function is given in [28].

Two cases (1) and (2) have to be differentiated, where (1) peak *A* is higher ($c(t_R^A)$) than peak *B* ($c(t_R^B)$) and (2) vice versa. For the first case (1) h_p is defined by

$$h_p = 100 \frac{c(\bar{t})}{c(t_R^A)} \quad (33)$$

and the approximation function to calculate the reaction rate constant k_1^{approx} is given by

$$k_1^{\text{approx}} = -\frac{1}{t_R^A} \left[\begin{aligned} &\ln \left[\frac{2}{t_R^B - t_R^A} \left(1 - \frac{h_p}{100} \left(0.5 + \frac{1}{\sqrt{2\pi N}} \right) \right) \right] \\ &- \ln \left[\frac{2}{t_R^B - t_R^A} \left(1 - \frac{h_p}{100} \left(0.5 + \frac{1}{\sqrt{2\pi N}} \right) \right) \right] + \frac{0.01 h_p e^{-\frac{(t_R^B - t_R^A)^2}{8\sigma_A^2}}}{\sigma_A \sqrt{2\pi}} + \frac{0.01 h_p e^{-\frac{(t_R^A - t_R^B)^2}{2\sigma_B^2}} - e^{-\frac{(t_R^A - t_R^B)^2}{8\sigma_B^2}}}{\sigma_B \sqrt{2\pi}} \end{aligned} \right] \quad (34)$$

For the second case (2) the following equations have to be considered:

$$h_p = 100 \frac{c(\bar{t})}{c(t_R^B)} \quad (35)$$

and

$$k_1^{\text{approx}} = -\frac{1}{t_R^A} \left[\ln \left[\frac{2}{t_R^B - t_R^A} \left(1 - \frac{h_p}{100} \left(0.5 - \frac{1}{\sqrt{2\pi N}} \right) \right) \right] - \ln \left[\frac{2}{t_R^B - t_R^A} \left(1 - \frac{h_p}{100} \left(0.5 - \frac{1}{\sqrt{2\pi N}} \right) \right) + \frac{0.01 h_p e^{-\frac{(\frac{B}{R} - \frac{A}{R})^2}{2\sigma_A^2}} - e^{-\frac{(\frac{B}{R} - \frac{A}{R})^2}{8\sigma_A^2}}}{\sigma_A \sqrt{2\pi}} + \frac{0.01 h_p e^{-\frac{(\frac{A}{R} - \frac{B}{R})^2}{8\sigma_B^2}}}{\sigma_B \sqrt{2\pi}} \right] \right] \quad (36)$$

The approximated backward reaction rate constant of enantiomerization k_{-1}^{approx} can be calculated from the forward reaction rate. The approximation function can only be applied to investigate enantiomerizations of racemic mixtures or any degenerated first-order reaction where the ratio of the reactant and product concentration equals 1. The unified equation of dynamic and reaction chromatography overcomes this limitation [77, 78] and opened a completely new field to study reactions beyond stereodynamic processes, and it unifies synthesis and analytics in the field of high-throughput screening of catalytic reactions [79–82]. Here the elution profiles are separated into non-converted peaks, represented by two Gaussian distribution functions $\Phi_A(t)$ and $\Phi_B(t)$ and a probability density functions $\Psi(t)$ for the converted part. As the time-dependent Gaussian distribution functions $\Phi_A(t)$ and $\Phi_B(t)$ and the approximated distribution function $\Psi_{\text{ue}}(t)$ depend on the forward and backward reaction rate constants k_1 and k_{-1} of the first-order reaction, the forward reaction rate constant k_1^{ue} of the unified equation equals a function of the time-dependent Gaussian distribution functions $\Phi_A(t)$ and $\Phi_B(t)$ and the approximated distribution function $\Psi_{\text{ue}}(t)$:

$$k_1^{\text{ue}} = f(\Phi_A(t), \Phi_B(t), \Psi_{\text{ue}}(t)) \quad (37)$$

The following extended equations can be derived:

$$k_1^{\text{app}} = \frac{1}{1 + kI_A} k_1^{\text{mob}} + \frac{kI_A}{1 + kI_A} k_1^{\text{stat}}$$

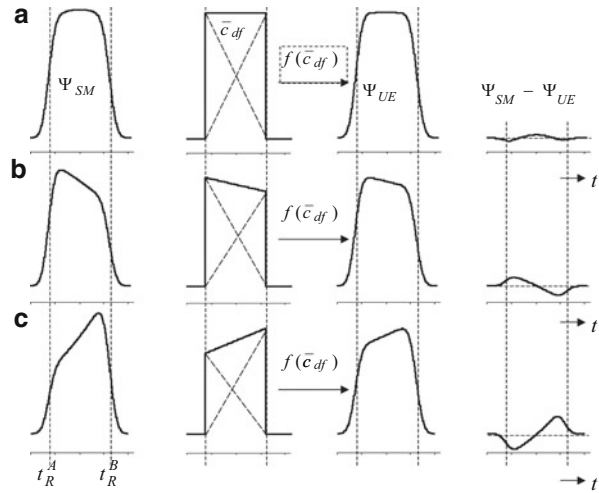
$$k_{-1}^{\text{app}} = \frac{1}{1 + kI_B} k_{-1}^{\text{mob}} + \frac{kI_B}{1 + kI_B} k_{-1}^{\text{stat}} = \frac{A_\infty}{B_\infty} \left(\frac{1}{1 + kI_B} k_{-1}^{\text{mob}} + \frac{kI_B}{1 + kI_B} \frac{kI_A}{kI_B} k_{-1}^{\text{stat}} \right) \quad (38)$$

The different reaction rates and times complicate the derivation of a function covering rate constants from dynamic or on-column reaction chromatographic experiments and therefore the following relationships are introduced:

$$k_1^{\text{ue}} t_R^A = k_1^{\text{app}} t_R^A \quad (39)$$

$$k_{-1}^{\text{ue}} t_R^B = \frac{A_\infty}{B_\infty} k_1^{\text{app}} t_R^A = \frac{A_\infty}{B_\infty} k_1^{\text{ue}} t_R^A \quad (40)$$

Fig. 10 Distribution function $\Psi_{SM}(t)$ of the stochastic model (*left*), distribution function $\Psi_{UE}(t)$ of the unified equation (*center*), and the time-dependent difference between $\Psi_{SM}(t)$ and $\Psi_{UE}(t)$ (*right*). **(a)** Degenerated reversible (pseudo-) first-order reaction with an equilibrium constant $K_{A/B} = 1$; **(b)** reversible (pseudo-) first-order reaction with $K_{A/B} > 1$; **(c)** reversible (pseudo-) first-order reaction with $K_{A/B} < 1$



The distribution of B , converted from A , is proportional to a linear function where the starting amount ($A_0 - A(t)$) decreases to 0 and vice versa for the distribution of A , converted from B (Figs. 8 and 10).

The following conversion density function $\bar{c}(t)$ approximates the probability density function between the migration times t_R^A and t_R^B :

$$\begin{aligned} \bar{c}_{df}(t_R^A \leq t \leq t_R^B) &= -\frac{2(A_0 - A(t_R^A))}{(t_R^B - t_R^A)^2} (t - t_R^A) + \frac{2(A_0 - A(t_R^A))}{t_R^B - t_R^A} + \frac{2(B_0 - B(t_R^B))}{(t_R^B - t_R^A)^2} \\ &\quad \times (t - t_R^A) \end{aligned} \quad (41)$$

With (41) it is possible to calculate the amount with the conversion density function $\bar{c}_{df}(t)$ at the most interesting migration times, namely t_R^A , t_R^B , and the mean time \bar{t} (Fig. 8):

$$\bar{c}_{df}(t_R^A) = \frac{2(A_0 - A(t_R^A))}{t_R^B - t_R^A} \quad (42)$$

$$\bar{c}_{df}(t_R^B) = \frac{2(B_0 - B(t_R^B))}{t_R^B - t_R^A} \quad (43)$$

$$\bar{c}_{df}(\bar{t}) = \frac{A_0 - A(t_R^A) + B_0 - B(t_R^B)}{t_R^B - t_R^A} \quad (44)$$

A detailed mathematical derivation of the unified equation is given in [76]. Similar to the approximation function, two different cases have to be considered: (45) is used in the case where the first eluted peak is higher than the second peak and (46) is used in all other cases:

$$k_1^{\text{ue}} = -\frac{1}{t_{\text{R}}^{\text{A}}} \left(\ln \left(B_0 e^{-\frac{A_{\infty}}{B_{\infty}} k_1^{\text{ue}} t_{\text{R}}^{\text{A}}} \left(\frac{100 e^{-\frac{\left(\frac{B_{\text{R}}-A_{\text{R}}}{8\sigma_{\text{B}}^2}\right)^2}}{\sigma_{\text{B}}\sqrt{2\pi}} - h_{\text{P}} e^{-\frac{\left(\frac{B_{\text{R}}-A_{\text{R}}}{2\sigma_{\text{B}}^2}\right)^2}}}{t_{\text{R}}^{\text{B}}-t_{\text{R}}^{\text{A}}} - \frac{100}{t_{\text{R}}^{\text{B}}-t_{\text{R}}^{\text{A}}} \right) + \frac{100B_0 + A_0 \left(100 - h_{\text{P}} \left(1 + \sqrt{\frac{2}{\pi N}}\right)\right)}{t_{\text{R}}^{\text{B}} - t_{\text{R}}^{\text{A}}} \right) \right) - \ln \left(A_0 \left(\frac{h_{\text{P}} - 100 e^{-\frac{\left(\frac{A_{\text{R}}-B_{\text{R}}}{8\sigma_{\text{A}}^2}\right)^2}}{\sigma_{\text{A}}\sqrt{2\pi}} + 100 - h_{\text{P}} \left(1 + \sqrt{\frac{2}{\pi N}}\right)}{t_{\text{R}}^{\text{B}} - t_{\text{R}}^{\text{A}}} \right) \right) \right) \quad (45)$$

$$k_1^{\text{ue}} = -\frac{1}{t_{\text{R}}^{\text{A}}} \left(\ln \left(B_0 e^{-\frac{A_{\infty}}{B_{\infty}} k_1^{\text{ue}} t_{\text{R}}^{\text{A}}} \left(\frac{100 e^{-\frac{\left(\frac{A_{\text{R}}-B_{\text{R}}}{8\sigma_{\text{B}}^2}\right)^2}}{\sigma_{\text{B}}\sqrt{2\pi}} - h_{\text{P}} + h_{\text{P}} \left(1 - \sqrt{\frac{2}{\pi N}}\right) - 100}{t_{\text{R}}^{\text{B}} - t_{\text{R}}^{\text{A}}} - \frac{100A_0 + B_0 \left(100 - h_{\text{P}} \left(1 + \sqrt{\frac{2}{\pi N}}\right)\right)}{t_{\text{R}}^{\text{B}} - t_{\text{R}}^{\text{A}}} \right) \right) - \ln \left(A_0 \left(\frac{h_{\text{P}} e^{-\frac{\left(\frac{t_{\text{R}}^{\text{B}}-t_{\text{R}}^{\text{A}}}{2\sigma_{\text{A}}^2}\right)^2}}{\sigma_{\text{A}}\sqrt{2\pi}} - 100 e^{-\frac{\left(\frac{t_{\text{R}}^{\text{B}}-t_{\text{R}}^{\text{A}}}{8\sigma_{\text{A}}^2}\right)^2}}}{t_{\text{R}}^{\text{B}} - t_{\text{R}}^{\text{A}}} + \frac{100}{t_{\text{R}}^{\text{B}} - t_{\text{R}}^{\text{A}}} \right) \right) \right) \quad (46)$$

For the determination of forward reaction rate constants with the unified equation an iterative step is necessary, because an analytical solution can only be obtained when the ratio A_{∞}/B_{∞} equals 1. Therefore k_1^{ue} has to be varied until $f(k_1^{\text{ue}})$ coincides with k_1^{ue} . The whole evaluation process is reduced to a minimum because all other parts of these equations are constant and are directly calculated from the experimental parameters. Equations (45) and (46) can be reduced to the following simplified expression where a , b , c , d , and e represent constants:

$$k_1^{\text{ue}} = a (\ln(b e^c k_1^{\text{ue}} + d) - e) = f(k_1^{\text{ue}}) \quad (47)$$

These equations and extended equations to reflect different absorption coefficients [83] of the interconverting analytes have been implemented in the DCXplorer software [84].

2.4 Determination of Activation Parameters by Temperature-Dependent Measurements

The Gibbs free activation energy $\Delta G^{\ddagger}(T)$ can be calculated according to the Eyring equation (48) with k_{B} as the Boltzmann constant ($k_{\text{B}} = 1.380662 \times 10^{-23} \text{ J K}^{-1}$), T as the reaction temperature [K], h as Planck's constant ($h = 6.62617 \times 10^{-34} \text{ J s}$),

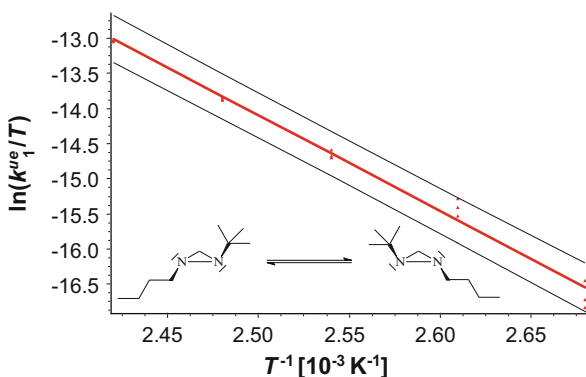


Fig. 11 Eyring plot for the determination of the activation parameters ΔH^\ddagger and ΔS^\ddagger of the enantiomerization of 1-*n*-butyl-2-*tert*-butyldiaziridine from the DGC experiment. The *upper* and *lower curves* represent the error bands of the linear regression with a level of confidence of 95%. For the linear regression 15 data points were considered

and R as the gas constant ($R = 8.31441 \text{ J K}^{-1} \text{ mol}^{-1}$). The statistical factor κ is set to 0.5 for a reversible and degenerated interconversion process, as it is the case for enantiomerizations:

$$\Delta G^\ddagger(T) = -RT \ln\left(\frac{k_1 h}{\kappa k_B T}\right) \quad (48)$$

By temperature-dependent measurements, reaction rate constants as a function of the temperature are obtained. The activation enthalpy ΔH^\ddagger is then obtained from the slope and the activation entropy ΔS^\ddagger from the intercept of the Eyring plot ($\ln(k_1/T)$ as a function of T^{-1}) (Fig. 11).

3 Applications

3.1 Dynamic GC

In 1979 Schurig et al. predicted that complexation GC is a useful tool to detect stereolabile compounds during the separation process [16]. In 1982 Bürkle and Schurig reported about the plateau formation in an elution profile of 1-chloro-2,2-dimethylaziridine **1** and 1,6-dioxaspiro[4.4]nonane **2**. Subsequently Lai et al. reported on the determination of the rotation barrier of 9,10-bis(2,3-dimethylphenyl)phenanthrenes **3–5** by means of gas chromatography [26, 85]. Marriott et al. described isomerization processes of chromium compounds **6** and **7** [86]. In 1992 Jung et al. described the computer program SIMUL, which allowed simulations with up to 120,000 theoretical plates. The enantiomerization barrier of 1,2,3,3-tetramethyldiaziridine **8** and 1-isopropyl-3,3-dimethylaziridine **9** was determined

by inclusion gas chromatography with the CSP permethylated β -cyclodextrin, dissolved in OV 1701 [19]. The investigations of compounds with stereogenic nitrogen were extended to 3,3-unsubstituted 1,2-disubstituted diaziridines **10**, **11**, and **12**, which show very high enantiomerization barriers of up to 128 kJ mol^{-1} [23, 87]. The enantiomerization barrier of homofuran **13** using Chirasil-Nickel(II) (polysiloxane-anchored nickel(II)-bis[3-(heptafluorobutanoyl)-(1*R*)-camphorate]) at 95–130°C was determined by simulation of the experimental elution profiles with SIMUL [51]. An excellent agreement of the reaction rate obtained in this experiment was found with the polarimetric data. Another application for SIMUL is described by Roth et al. [88] for the separation of trimethylenemethane-derivatives and 2,6-dimethylenebicyclo[3.1.0]-hexane **14**.

Wolf et al. investigated the influence of substituents on the rotational energy barrier of atropisomeric biphenyls, e.g., **15**, **16**, by DGC and polarimetry [28, 29]. They found that electron-donating groups decrease the rotational energy barrier of 2,2'-bis(trifluoromethyl)biphenyl **15** derivatives but increase the barrier of 2,2'-diisopropylbiphenyl **15** derivatives. Electron-accepting groups were found to exhibit the opposite behaviour. Jung et al. evaluated elution profiles of 2,2'-disopropylbiphenyl **15** by SIMUL and compared the data with the polarimetric measurements of Wolf et al. [89]. The determined barrier was in good agreement with the values obtained by polarimetry. Hochmuth et al. determined the rotational energy barrier of substituted planar-chiral dioxa[*n*]cyclophanes, e.g., **17**. The influence of the substituents due to electronic or secondary steric effects was negligible [31]. In continuation of their studies, carbocyclic[11]paracyclophanes **18** were synthesized and the rotational energy barrier determined. As expected, the barriers were about 10 kJ mol^{-1} lower than found for the dioxa[11]cyclophanes **17**. Trapp et al. determined the enantiomerization barrier of Tröger's base **19** on the CSP Chirasil- β -Dex by dynamic chromatography in combination with the stopped-flow multidimensional gas chromatographic technique [15]. Schurig et al. determined the enantiomerization barrier of 1-chloro-2,2-dimethylaziridine **1** by temperature-dependent studies and could calculate the activation parameters by computer simulation with ChromWin [14] (Fig. 12).

DGC combined with computer simulation has been extended to epimerizations. This has been exemplified by the determination of the individual epimerization processes of chalcogran **20** in presence of the CSP Chirasil- β -Dex [37] (Fig. 13).

3.2 Stopped-Flow Gas Chromatography

Schurig et al. determined the rotational energy barrier of the atropisomeric PCB 132 (**23**) by this method [11]. After semipreparative HPLC separation a single enantiomer was subjected to enantiomerization on Chirasil- β -Dex. The very high

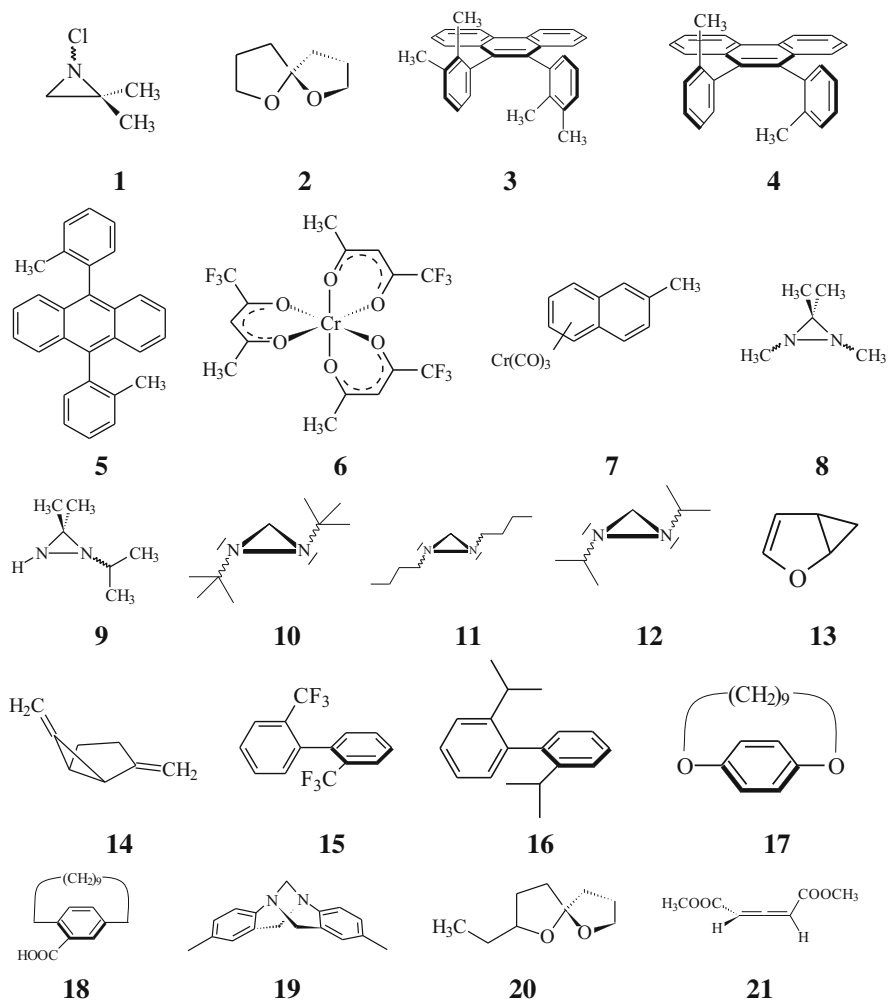


Fig. 12 Chemical structures of compounds investigated by enantioselective DGC

barrier of PCB 132 ($\sim 182 \text{ kJ mol}^{-1}$) demonstrated the extended range for the determination of high enantiomerization barriers.

3.3 Stopped-Flow MDGC

The stopped-flow multidimensional gas chromatographic technique was applied for the first time by Schurig et al. [12, 52] for the determination of the enantiomerization barrier of atropisomeric polychlorinated biphenyls (PCB). Out of 209 PCB congeners, 78 show axial chirality in non-planar conformation. Due to

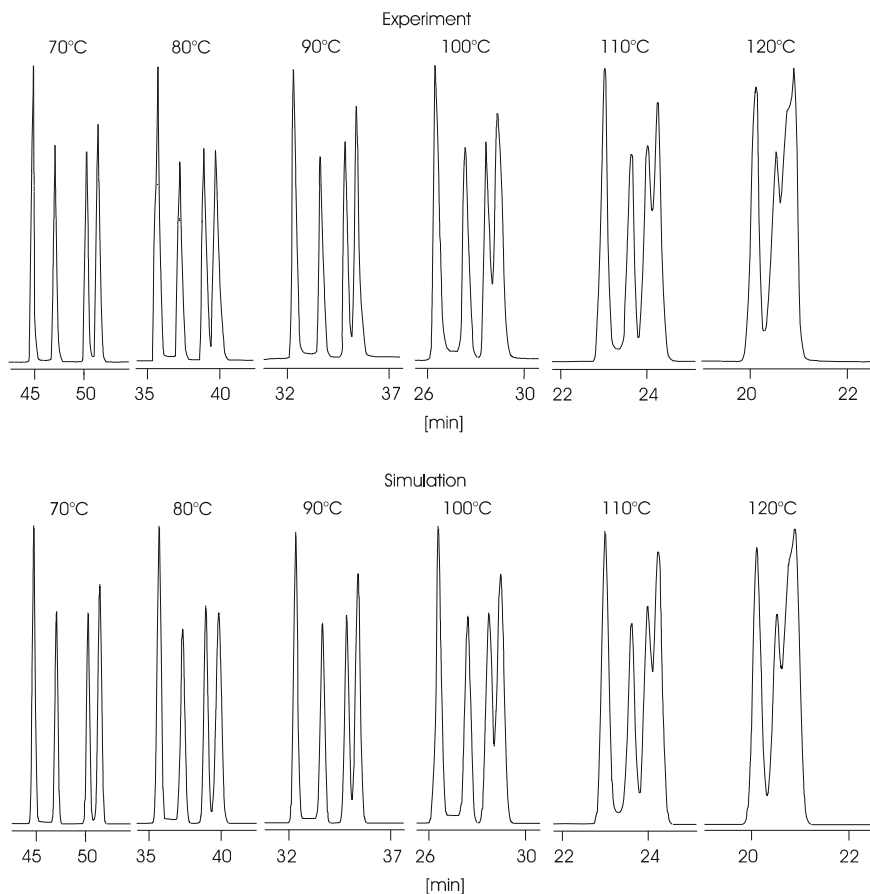


Fig. 13 Epimerization of **20** at different temperatures: experimental chromatograms (*top*) versus simulated chromatograms (*bottom*)

their wide distribution in the environment and their persistence, there is an interest in the examination of enantiomeric enrichment and enantioselective degradation of PCB in biological samples and their toxicological impact. The very high enantiomerization barriers (about 180 kJ mol^{-1}) of PCB 95 (**22**), PCB 132 (**23**), PCB 136 (**24**), and PCB 149 (**25**) could be determined and the accuracy and precision of the applied method was proven. The data provided a means to evaluate results from molecular modelling studies which varied over 100 kJ mol^{-1} [90] (Fig. 14).

Schurig et al. determined the enantiomerization barrier of the axially chiral allene dimethyl-2,3-pentadienedioate **21** in presence of the CSPs Chirasil-Ni(II) and Chirasil- β -Dex. By comparison with the values from the stopped-flow

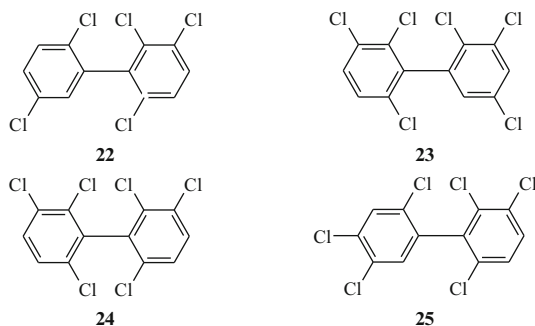


Fig. 14 Chemical structures of PCBs investigated by stopped-flow multidimensional gas chromatography

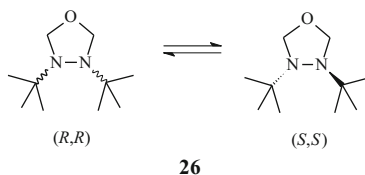


Fig. 15 Structures of the enantiomers of 3,4-di-*tert*-butyl-1,3,4-oxadiazolidine

multidimensional gas chromatographic experiment, catalytic effects of the CSPs could be determined. It could be shown that in presence of chiral metal(II) bis [3-(heptafluorobutanoyl)-(1*R*)-camphorate] complexes one of the enantiomers is enriched with an ee of up to 82% [75, 91–93]. Using the method described here the enantiomerization barrier could be determined in the absence of a CSP and the results showed that the enantiomerization barrier increased remarkably.

The enantiomerization of 1-chloro-2,2-dimethylaziridine **1** was studied by sfMDGC and compared with values obtained from classical racemization kinetics, DGC, and DNMR studies. With the data from the sfMDGC experiment it was possible to distinguish the rate constants of the dynamic chromatographic experiment toward the contribution of the CSP and mobile gas phase. This enabled the quantification of the influence of the CSP on the enantiomerization barrier.

The inherent chirality of Tröger's Base **19** was recognized in 1944 by Prelog and Wieland and was proved by resolution into optically active fractions ($op = 0.99$) by liquid chromatography on a 0.9-m column containing lactose hydrate and subsequent fractional crystallization [94]. Ever since, Tröger's Base **19** has represented a lucid target for resolution trials by novel innovative chromatographic techniques. As already recognized by Prelog and Wieland, interconversion occurs under acidic conditions. The enantioselective gas chromatographic separation of Tröger's base **19** on Chirasil- β -Dex shows plateau formation with increasing temperature. Trapp and Schurig could confirm the thermal interconversion by sfMDGC and in a complementary dynamic experiment quantify the stabilizing

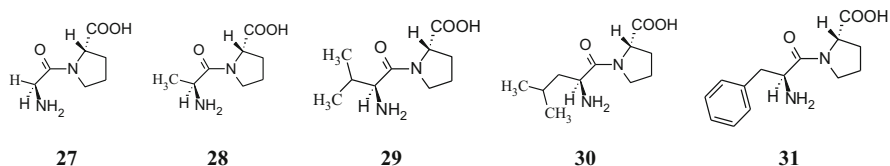


Fig. 16 Chemical structures of dipeptides investigated by HPLC

effect of the chiral selector [15]. Kostyanovsky et al. and Schurig et al. reported on the highest barrier of chiral pyramidal nitrogen in a five-membered heterocycle determined in 3,4-di-*tert*-butyl-1,3,4-oxadiazolidine **26** by sfMDGC [20]. At 126.2°C the barrier has been determined to be $136.7 \pm 0.8 \text{ kJ mol}^{-1}$ (Fig. 15).

3.4 Dynamic HPLC

Dynamic HPLC (DHPLC) can be used for the determination of interconversion barriers between 70 and 120 kJ mol^{-1} . An earlier review of DHPLC compared with DNMR is given by Gasparini et al. [95]. Advantages of DHPLC experiments compared to DGC or DCE studies are the relatively low plate numbers that allow calculations and computer simulations even with older programs (e.g., SIMUL), combined with the good resolution factors that permit the fast separation of the enantiomers.

The first advances to exploit the information given by the occurrence of plateau formation in a chromatogram obtained from an HPLC separation is due to Horváth et al. for the investigation of *cis*–*trans* isomerizations of several proline-containing dipeptides **27**–**31**. Since the publication of “effect of molecular structure and conformational change of proline-containing dipeptides in reversed phase chromatography” in 1982, many papers dealing with interconversion profiles obtained by DHPLC of peptidyl-proline dipeptides have been published, but not in all cases were the rate constants of *cis*–*trans* isomerization determined. In 1984 the group of Horváth published a theoretical paper about the determination of rate constants in dynamic reversed phase chromatography with the help of the Damköhler number [96–104] (Fig. 16).

In 1983 Lebl et al. presented a method to calculate rate constants from the areas of an interconversion profile of anomers of a muramyldipeptide **32** in HPLC [105]. This method has also been applied by Moriyasu for the evaluation of elution profiles of *cis*–*trans* isomers of *o*-substituted acetanilides **33** [106].

The first use of DHPLC for enantiomerization studies followed the results obtained by GC. Thus, Stephan et al. [107] determined the energy barrier for the thermally reversible ring opening of 2,2′-spirobichromenes **34** by dynamic HPLC on tribenzoyl-cellulose. They obtained plateau formation in their chromatograms with both photometric and polarimetric detection. As one of the very first theoretical applications of DHPLC combined with computer simulation, Veciana and Crespo [46] described the

determination of the enantiomerization barrier of tris(2,4,6-trichlorophenyl)methane **35** on a (+)-poly(triphenylmethylmethacrylate) column and the epimerization barrier of the *meso*-biradical of perchloro-1,3-bisdiphenylmethylbenzene **36** on a C₁₈ reversed phase column. Another example of the determination of enantiomerization barriers by DHPLC is given by Cabrera et al. [38, 108] who described the determination of the interconversion barrier of the enantiomers of phenylthiohydantoin-phenylalanine **37**, chlorthalidone **38**, oxazepam **39**, and prominal **40** on a chemically bonded β -cyclodextrin (ChiraDex) stationary phase. Computer simulation of the typical elution profiles exhibiting plateau formation was performed with SIMUL to determine the rate constants and the corresponding enantiomerization barriers. The calculated data were compatible with independently determined values, but a rather strong solvent dependency was observed. The enantiomerization of the atropisomeric drug 10-(3-chlorophenyl)-6,8,9,10-tetrahydrobenzo[*b*][1,8]naphthyridin-5(*7H*)-one (Telenzepine) **41** in DHPLC was described by Friary et al. [109]. The dynamic elution profiles obtained on an ovomucoid CSP exhibited plateau formation between 0°C and 30°C and were simulated with the computer program SIMUL. From the calculated rate constants a linear Arrhenius plot was obtained.

With a modified version of the SIMUL program, Gasparriani et al. determined the enantiomerization barriers and the stationary phase effects of four atropisomeric naphthamides **42–45** on the brush-type (3*R*,4*S*)-Whelk-O1 CSP [110]. They found only a very small deviation of the activation energies obtained by computer simulation from those obtained by off-column thermal racemization. By comparison of these two sets of data, the CSP was found to increase the isomerization barrier by 2.0–4.0 kJ mol⁻¹. The same group also investigated the atropisomerism in sterically hindered sulfones **46** and **47** by DNMR and DHPLC [27].

Another example of the application of the SIMUL simulation program was given by Oxelbark et al. [61]. They determined the free activation energies for the enantiomerization at sulfur of a series of racemic *N*-aryl-1,3,2-benzodithiazole-1-oxides **48**, **49** by DHPLC on a (3*R*,4*S*)-Whelk-O1 CSP. Pirkle et al. [111] also observed hindered inversion at sulfinyl and sulfonyl naphthalene derivatives, but did not evaluate the interconversion barrier.

Lorenz et al. [13] used DHPLC for enantiomeric enrichment of stereolabile spiro-compounds. Separation of the spirochromenes **34** and **50** was performed on a Chiracel OD column. After an initial enantiomer separation, one enantiomer was transferred to a second column. During an equilibration reaction at an elevated temperature, the other enantiomer was formed through racemization of the enantiomer. By repeated removal of one enantiomer the almost total conversion of a racemic mixture into the pure enantiomers was observed.

Gasparriani et al. [112] presented an application of the SIMUL program to the DHPLC investigation of interconverting *syn/anti* stereoisomers of *tert*-butyl-1-(2-methyl-1-naphthyl)phosphine oxide **51**. They found that the interconversion barrier measured by DNMR yields essentially the same value as that measured by DHPLC (Fig. 17).

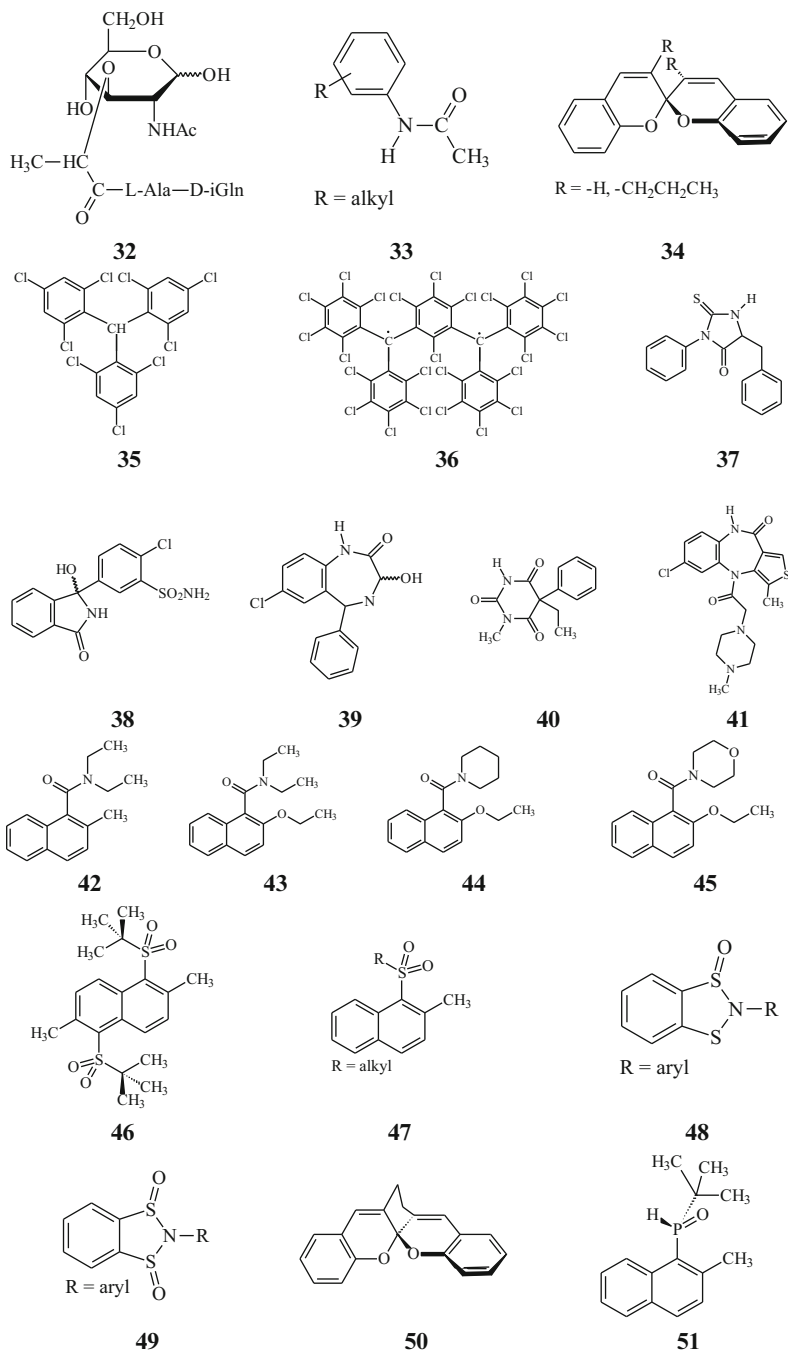


Fig. 17 Chemical structures of interconverting compounds investigated by HPLC

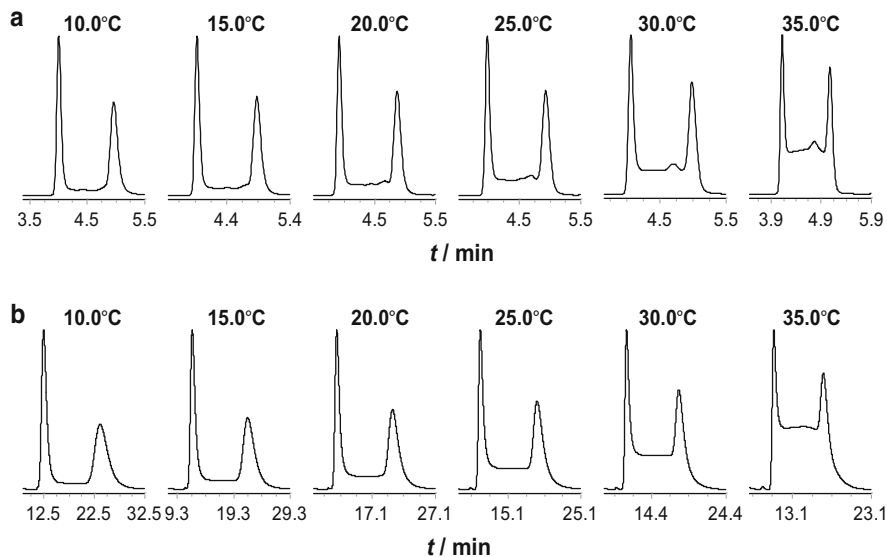


Fig. 18 Selected experimental interconversion profiles of (a) BIPHEP and (b) oxidized BIPHEPO obtained by enantioselective DHPLC between 10°C and 35°C

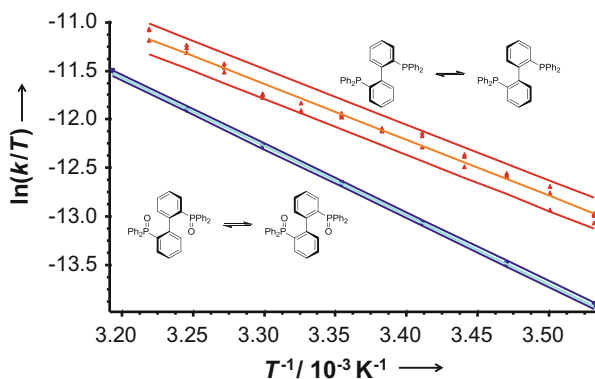


Fig. 19 Eyring plot of BIPHEP and oxidized BIPHEPO

More recently Trapp et al. reported the investigation of atropis BIPHEP ligands by enantioselective DHPLC in the presence of Chiralpak AD-H. BIPHEP ligands are of great interest in the design and synthesis of stereodynamic ligand systems in catalysis. In these studies stationary phase effects could also be quantified [35, 113] (Figs. 18 and 19).

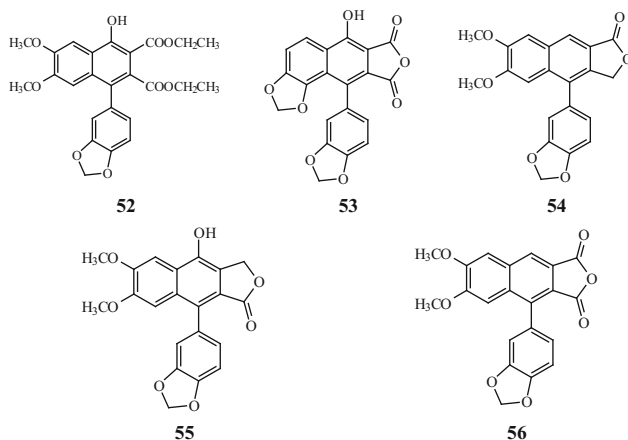


Fig. 20 Chemical structures of interconverting compounds investigated by SFC

3.5 Dynamic SFC

Enantioselective supercritical fluid chromatography enhances the measurement range to very low temperatures for the determination of enantiomerization barriers. Hence low enantiomerization barriers can also be measured. Wolf et al. [30] applied this chromatographic technique to the separation of aryl-naphthalenes **52–56** on the brush-type CSP Whelk-O1 between -25°C and 50°C . The rate constants and Gibbs free activation energies ΔG^{\ddagger} for the internal rotation of these atropisomers have been determined by computer simulation with the program Mimesis [114] which is based on the TPM (Fig. 20).

3.6 Electrophoretic Methods

Temperature-dependent stopped flow and dynamic capillary electrophoretic (DCE) techniques represent a useful tool for the determination of enantiomerization barriers between 70 and 120 kJ mol^{-1} , where DNMR experiments can no longer be employed and GC experiments are not applicable because of poor volatility of the analyte. Even though measurement of interconverting species in capillary electrophoresis covers approximately the same range of interconversion barriers as conventional HPLC, this method constitutes a valuable tool because of the large variety of chiral additives, surfactants, and columns available. Dual recognition systems have been shown to solve separation problems that could hardly be solved by HPLC before.

It has to be pointed out that the evaluation of elution profiles obtained by DCE experiments was highly challenging in the past due to the very high separation efficiencies. This problem was solved by the introduction of ChromWin and later the unified equation of chromatography [77]. Another explanation for the negligence of CE methods could be the difficulties of effective capillary thermostating which are slowly overcome by the development of new, improved instruments. In addition, the large separation factors necessary for the determination of interconversion barriers by stopped flow capillary electrophoresis and the requirement to perform the separation at a temperature below measurable interconversion occurs limit the described technique to only a few applications.

The first publications which report the measurement of interconversion barriers in capillary electrophoresis by Weseloh et al. [10, 115] describe the determination of rotational energies of axially chiral biphenyls. 4,4'-Diammonio-2,2'-bis(trifluoromethyl)biphenyl **57** and 4,4'-diamino-2,2'-diisopropylbiphenyl **58** were separated and enantiomerized using permethylated β -cyclodextrin as chiral selector. The energy barrier in this study was determined by stopped flow capillary electrophoresis, a method so far only used in gas chromatography. The determination of the rotational energy with this method did not require the single enantiomers and needed no computer simulation.

Rathore and Horváth [101] estimated the rate constants of interconverting *cis-trans* conformers of peptidyl-proline dipeptides **27-31** in dynamic capillary electrophoresis (DCE) with the Damköhler number which is given by the ratio of the migrants' residence time to the characteristic time of reaction in the capillary. The kinetic data obtained between 1°C and 40°C showed good agreement with those measured by NMR.

Other publications by Schoetz et al. [39-42, 116] describe dynamic MEKC experiments followed by computer simulation with ChromWin. The enantiomerization barriers of the three benzodiazepines oxazepam **39**, lorazepam **59**, and temazepam **60** were determined temperature-dependently by dynamic micellar electrokinetic chromatography using sodium cholate as the chiral surfactant. Comparison of the calculated rate constants of enantiomerization with those of independent studies shows a very good correlation. As well as the stopped flow experiment, this method also requires the quantitative separation of the enantiomers but the interconversion process is allowed to take place during the separation as an ongoing reaction in a chiral environment. For this reason, and also the smaller technical expense compared to the stopped flow experiment, this method has a broader application spectrum. The same group also reported the determination of the enantiomerization barriers of thalidomide **61** [42] by DMEKC and DEKC, and chlorthalidone **38** by DEKC. Even the determination of the *cis-trans* isomerization barrier of the three dipeptides L-alanyl-L-proline **28**, L-leucyl-L-proline **30**, and L-phenylalanyl-L-proline **31** [43] were determined by DCE experiments and computer simulation with ChromWin. More recently, DEKC and DCE were applied to

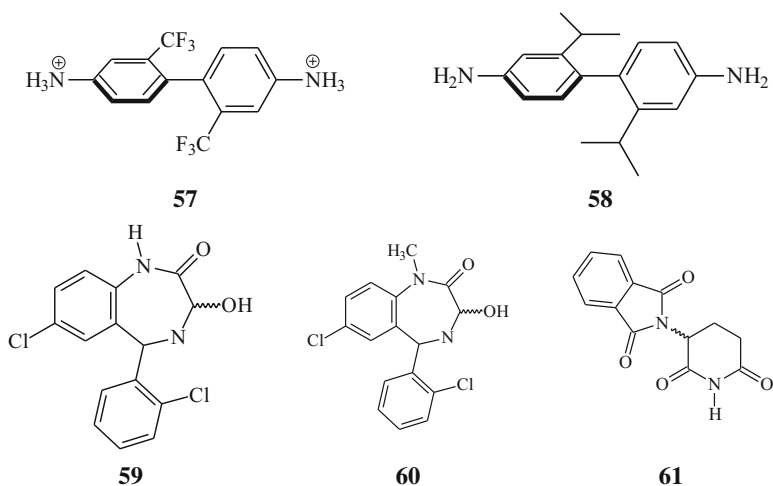


Fig. 21 Chemical structures of interconverting compounds investigated by capillary electrophoresis

determine rotational *cis-trans* isomerization barriers of proline-containing drugs, i.e., enalapril and captopril [117–120] (Fig. 21).

4 Outlook

The methods presented here constitute a valuable tool for the determination of enantiomerization barriers over a wide range of energy barriers by chromatography. Advantages of these methods are the small sample consumption in the nanogram range and the use of racemic mixtures, which make these methods very convenient in application. With the simulation tools available today the determination of enantiomerization barriers from experimental chromatographic elution profiles in dynamic chromatography is dramatically simplified and automation of the dynamic chromatographic methods can be envisaged.

It can be assumed that these techniques will revolutionize many areas of chemistry and analytical chemistry, because reaction and separation are integrated in a single step, which makes rapid high-throughput screening of potential catalysts and development of novel analytical devices feasible.

References

1. Lambert JB, Takeuchi Y (1992) Cyclic organonitrogen stereodynamics. VCH Publisher Inc., New York

- Berl V, Huc I, Khoury RG, Krische MJ, Lehn J-M (2000) Interconversion of single and double helices formed from synthetic molecular strands. *Nature* 407:720–723
- Dugave C, Demange L (2003) *Cis-trans* isomerization of organic molecules and biomolecules: implications and applications. *Chem Rev* 103:2475–2532
- Busenlehner LS, Armstrong RN (2005) Insights into enzyme structure and dynamics elucidated by amide H/D exchange mass spectrometry. *Arch Biochem Biophys* 433:34–46
- Kessler H (1968) Use of nuclear magnetic resonance to detect intramolecular rotations. *Angew Chem Int Ed* 7:898
- Kalinowski H-O, Kessler H (1973) Fast isomerizations about double bonds. *Top Stereochem* 7:295–383
- Binsch G, Kessler H (1980) The kinetic and mechanistic evaluation of NMR spectra. *Angew Chem Int Ed* 19:411–494
- Lehn JM (1970) Nitrogen inversion – experiment and theory. *Top Curr Chem* 15:311–377
- Lambert JB (1971) Pyramidal atomic inversion. *Topics Stereochem* 6:19–105
- Weseloh G, Wolf C, König WA (1995) A new application of capillary zone electrophoresis: determination of energy barriers of configurationally labile chiral compounds. *Angew Chem Int Ed* 34:1635–1636
- Schurig V, Glausch A, Fluck M (1995) On the enantiomerization barrier of atropisomeric 2,2',3,3',4,6'-hexachlorobiphenyl (pcb 132). *Tetrahedron Asymmetry* 6:2161–2164
- Reich S, Schurig V (1999) Stopped-flow multidimensional GC – a new method for the determination of enantiomerization barriers. *J Microcolumn Sep* 11:475–479
- Lorenz K, Yashima E, Okamoto Y (1998) Enantiomeric enrichment of stereolabile chiral spiro compounds by dynamic hplc on chiral stationary phases. *Angew Chem Int Ed* 37:1922–1925
- Reich S, Trapp O, Schurig V (2000) Enantioselective stopped-flow multidimensional gas chromatography – determination of the inversion barrier of 1-chloro-2,2-dimethylaziridine. *J Chromatogr A* 892:487–498
- Trapp O, Schurig V (2000) Stereointegrity of Tröger's base: gas-chromatographic determination of the enantiomerization barrier. *J Am Chem Soc* 122:1424–1430
- Schurig V, Bürkle W, Zlatkis A, Poole CF (1979) Quantitative resolution of pyramidal nitrogen invertomers by complexation chromatography. *Naturwissenschaften* 66:423–424
- Schurig V, Bürkle W (1982) Extending the scope of enantiomer resolution by complexation gas chromatography. *J Am Chem Soc* 104:7573–7580
- Bürkle W, Karfunkel H, Schurig V (1984) Dynamic phenomena during enantiomer resolution by complexation gas chromatography. *J Chromatogr* 288:1–14
- Jung M, Schurig V (1992) Determination of enantiomerization barriers by computer simulation of interconversion profiles: enantiomerization of diaziridines during chiral inclusion gas chromatography. *J Am Chem Soc* 114:529–534
- Kostyanovsky RG, Kadorkina GK, Kostyanovsky VR, Schurig V, Trapp O (2000) Pronounced steric hindrance for nitrogen inversion in 1,3,4-oxadiazolidines. *Angew Chem Int Ed* 39:2938–2940
- Kostyanovsky RG, Schurig V, Trapp O, Lyssenko KA, Averkiev BA, Prosyaniy AV, Kadorkina GK, Kostyanovsky VR (2002) Chiral 1-alkoxyaziridines: resolution, nitrogen inversion, structure, and diastereomeric transformations. *Mendeleev Commun* 12:137–140
- Trapp O, Trapp G, Kong J, Hahn U, Vögtle F, Schurig V (2002) Probing the stereointegrity of Tröger's base – a dynamic electrokinetic chromatographic study. *Chem Eur J* 8:3629–3634
- Trapp O, Sahraoui L, Hofstadt W, Könen W (2010) The stereodynamics of 1,2-dipropyldiaziridines. *Chirality* 22:284–291
- Trapp O (2010) Chromatographic peak deconvolution of constitutional isomers by multiple reaction monitoring mass spectrometry. *J Chromatogr A* 1217:1010–1016
- Kamuf M, Trapp O (2011) Stereodynamics of tetramezine. *Chirality* 23:113–117

26. Lai Y-H, Marriott PJ, Tan B-C (1985) The barrier to rotation in 9,10-bis(2,3-dimethylphenyl)phenanthrene: conformational interconversion observed at high temperatures by means of gas chromatography. *Aust J Chem* 38:307–314
27. Gasparrini F, Lunazzi L, Alcaro S, Villani C (1995) Atropisomerism in hindered naphthyl sulfones investigated by dynamic NMR and dynamic HPLC techniques. *J Org Chem* 60:5515–5519
28. Wolf C, König WA, Roussel C (1995) Influence of substituents on the rotational energy barrier of atropisomeric biphenyls – studies by polarimetry and dynamic gas chromatography. *Liebigs Ann* 1995:781–786
29. Wolf C, König WA, Roussel C (1995) Conversion of a racemate into a single enantiomer in one step by chiral liquid chromatography: studies with rac-2,2'-diiodobiphenyl. *Chirality* 7:610–611
30. Wolf C, Pirkle WH, Welch CJ, Hochmuth DH, König WA, Chee G-L, Charlton JL (1997) Determination of the enantiomerization barrier of aryl-naphthalene ligands by cryogenic subcritical fluid chromatography and computer simulation. *J Org Chem* 62:5208–5210
31. Hochmuth DH, König WA (1999) Synthesis, resolution and determination of energy barriers to rotation of atropisomeric, planar-chiral [n]paracyclophanes by dynamic enantioselective gas chromatography and computer simulation. *Tetrahedron Asymmetry* 10:1089–1097
32. Scharwächter KP, Hochmuth DH, Dittmann H, König WA (2001) Synthesis, resolution, and investigation of the rotational interconversion process of atropisomeric 1, n-diaza[n]paracyclophanes using cyclodextrin-mediated capillary zone electrophoresis. *Chirality* 13:679–690
33. Spivey AC, Charbonneau P, Fekner T, Hochmuth DH, Maddaford A, Malardier-Jugroot C, Redgrave AJ, Whitehead MA (2001) Energy barriers to rotation in axially chiral analogues of 4-(dimethylamino)pyridine. *J Org Chem* 66:7394–7401
34. Tobler E, Lämmerhofer M, Mancini G, Lindner W (2001) On-column deracemization of an atropisomeric biphenyl by quinine-based stationary phase and determination of rotational energy barrier by enantioselective stopped-flow HPLC and CEC. *Chirality* 13:641–647
35. Maier F, Trapp O (2012) Stationary phase and solvent effects on the stereodynamics of tropos biphenyl ligands revealed by a novel HPLC technique. *Angew Chem Int Ed* 51:2985–2988
36. Rotzler J, Gsellinger H, Neuburger M, Vonlanthen D, Häussinger D, Mayor M (2011) Racemisation dynamics of torsion angle restricted biphenyl push-pull cyclophanes. *Org Biomol Chem* 9:86–91
37. Trapp O, Schurig V (2001) Determination of interconversion barriers by dynamic gas chromatography: epimerization of chalcogran. *Chem Eur J* 7:1495–1502
38. Cabrera K, Jung M, Fluck M, Schurig V (1996) Determination of enantiomerization barriers by computer simulation of experimental elution profiles obtained by high-performance liquid chromatography on a chiral stationary phase. *J Chromatogr A* 731:315–321
39. Schoetz G, Trapp O, Schurig V (1999) Determination of the enantiomerization barrier of chlorthalidone by dynamic electrokinetic chromatography and computer simulation. *J Capill Electrophor Microchip Technol* 6:169–175
40. Schoetz G, Trapp O, Schurig V (2000) Determination of the enantiomerization barrier of oxazepam by dynamic micellar electrokinetic chromatography – comparison of experiment and simulation with ChromWin 99. *Enantiomer* 5:391–396
41. Schoetz G, Trapp O, Schurig V (2000) Dynamic micellar electrokinetic chromatography – determination of the enantiomerization barrier of oxazepam, temazepam and lorazepam. *Anal Chem* 72:2758–2764
42. Schoetz G, Trapp O, Schurig V (2001) Determination of the enantiomerization barrier of thalidomide by dynamic electrokinetic chromatography. *Electrophoresis* 22:3185–3190
43. Schoetz G, Trapp O, Schurig V (2001) Determination of the *cis-trans* isomerization barrier of several l-peptidyl-l-proline dipeptides by dynamic capillary electrophoresis and computer simulation. *Electrophoresis* 22:2409–2415

44. Trapp O, Caccamese S, Schmidt C, Böhmer V, Schurig V (2001) Enantiomerization of an inherently chiral resorcarene derivative: determination of the interconversion barrier by computer simulation of the dynamic HPLC experiment. *Tetrahedron Asymmetry* 12:1395–1398
45. Wistuba D, Trapp O, Gel-Moreto N, Galensa R, Schurig V (2006) Stereoisomeric separation of flavanones and flavanone-7-*o*-glycosides by capillary electrophoresis and determination of interconversion barriers. *Anal Chem* 78:3424–3433
46. Hinterwirth H, Lämmerhofer M, Preinerstorfer B, Gargano A, Reischl R, Bicker W, Trapp O, Brecker L, Lindner W (2010) Selectivity issues in targeted metabolomics: separation of phosphorylated carbohydrate isomers by mixed-mode hydrophilic interaction/weak anion exchange chromatography. *J Sep Sci* 33:3273–3282
47. Veciana J, Crespo MI (1991) Dynamic HPLC, a method for the determination of rate constants, energy barriers and equilibrium constants of dynamic molecular processes. *Angew Chem Int Ed* 30:74–77
48. FDA (1992) FDA's policy statement for the development of new stereoisomeric drugs. *Chirality* 4:338–340
49. de Camp WH (1989) The FDA perspective on the development of stereoisomers. *Chirality* 1:2–6
50. Schurig V (1998) Peak coalescence phenomena in enantioselective chromatography. *Chirality* 10:140–146
51. Reist M, Testa B, Carrupt P-A, Jung M, Schurig V (1995) Racemization, enantiomerization, diastereomerization, and epimerization: their meaning and pharmacological significance. *Chirality* 7:396–400
52. Schurig V, Jung M, Schleimer M, Klärner F-G (1992) Investigation of the enantiomerization barrier of homofuran by computer simulation of interconversion profiles obtained by complexation gas chromatography. *Chem Ber* 125:1301–1303
53. Schurig V, Reich S (1998) Determination of the rotational barriers of atropisomeric polychlorinated biphenyls (PCBs) by a novel stopped-flow multidimensional gas chromatographic technique. *Chirality* 10:316–320
54. Martin AJP, Syngé RLM (1941) A new form of chromatogram employing two liquid phases. *Biochem J* 35:1358–1368
55. Craig LC (1944) Identification of small amounts of organic compounds by distribution studies. *J Biol Chem* 155:519–534
56. Bassett DW, Habgood HW (1960) A gas chromatographic study of the catalytic isomerization of cyclopropane. *J Phys Chem* 64:769–773
57. Kallen J, Heilbronner E (1960) Das Gas-Chromatogramm einer labilen Verbindung (System a -> b). *Helv Chim Acta* 43:489–500
58. Felinger A (2008) Molecular dynamic theories in chromatography. *J Chromatogr A* 1184:20–41
59. Lange J, Below E, Thede R (2004) Separate determination of mobile-phase rate constants for reversible reactions. *J Liq Chromatogr Relat Technol* 27:715–725
60. D'Acquarica I, Gasparri F, Pierini M, Villani C, Zappia G (2006) Dynamic HPLC on chiral stationary phases: a powerful tool for the investigation of stereomutation processes. *J Sep Sci* 29:1508–1516
61. Oxelbark J, Allenmark S (1999) Barriers to stereoinversion of *n*-aryl-1,3,2-benzodithiazole 1-oxides studied by dynamic enantioselective liquid chromatography. *J Org Chem* 64:1483–1486
62. Trapp O, Schurig V (2001) Chromwin – a computer program for the determination of enantiomerization barriers in dynamic chromatography. *Comput Chem* 25:187–195
63. Keller RA, Giddings JC (1960) Multiple zones and spots in chromatography. *J Chromatogr* 3:205–220
64. Kramer R (1975) Simultan-Reaktionschromatographie mit reversibler Reaktion erster Ordnung. *J Chromatogr* 107:241–252

65. Cremer E, Kramer R (1975) Simultan-Reaktionschromatographie mit reversibler Reaktion erster Ordnung. ii. *J Chromatogr* 107:253–263
66. Dondi F, Cavazzini A, Pasti L (2006) Chromatography as Levy stochastic process. *J Chromatogr A* 1126:257–267
67. Yau WW (1977) Characterizing skewed chromatographic band broadening. *Anal Chem* 49:395–398
68. Barber WE, Carr PW (1981) Graphical method for obtaining retention time and number of theoretical plates from tailed chromatographic peaks. *Anal Chem* 53:1939–1942
69. Foley JP, Dorsey JG (1984) A review of the exponentially modified Gaussian (EMG) function: evaluation and subsequent calculation of universal data. *J Chromatogr Sci* 22:40–46
70. Lee HK, Li SFY, Marriott PJ (1990) A study on the gas chromatographic column as a chemical reactor. *Bull Sing N I Chem* 18:109–114
71. Krupcik J, Oswald P, Spánik I, Májek P, Bajdichová M, Sandra P, Armstrong DW (2000) On the use of a peak deconvolution procedure for the determination of energy barrier to enantiomerization in dynamic chromatography. *Analisis* 28:859–863
72. Krupcik J, Mydlova J, Majek P, Simon P, Armstrong DW (2008) Methods for studying reaction kinetics in gas chromatography, exemplified by using the 1-chloro-2,2-dimethylaziridine interconversion reaction. *J Chromatogr A* 1186:144–160
73. Krupcik J, Oswald P, Majek P, Sandra P, Armstrong DW (2003) Determination of the interconversion energy barrier of enantiomers by separation methods. *J Chromatogr A* 1000:779–800
74. Dubsy P, Tesarová E, Gas B (2004) Dynamics of interconversion of enantiomers in chiral separation systems: a novel approach for determination of all rate constants involved in the interconversion. *Electrophoresis* 25:733–743
75. Thede R, Below E, Haberland D, Langer SH (1997) Theoretical treatment of first-order reversible reactions occurring in a chromatographic reactor, on the basis of consecutive reactions. *Chromatographia* 45:149–154
76. Trapp O, Schurig V (2001) Approximation function for the direct calculation of rate constants and Gibbs activation energies of enantiomerization of racemic mixtures from chromatographic parameters in dynamic chromatography. *J Chromatogr A* 911:167–175
77. Trapp O (2006) Unified equation for access to rate constants of first-order reactions in dynamic and on-column reaction chromatography. *Anal Chem* 78:189–198
78. Trapp O (2006) Fast and precise access to enantiomerization rate constants in dynamic chromatography. *Chirality* 18:489–497
79. Trapp O (2008) Gas chromatographic high-throughput screening techniques in catalysis. *J Chromatogr A* 1184:160–190
80. Trapp O, Weber SK, Bauch S, Bäcker T, Hofstadt W, Spliethoff B (2008) High throughput kinetic study of hydrogenations over palladium nanoparticles – combination of reaction and analysis. *Chem Eur J* 14:4657–4666
81. Trapp O, Weber SK, Bauch S, Hofstadt W (2007) High-throughput screening of catalysts by combining reaction and analysis. *Angew Chem Int Ed* 46:7307–7310
82. Weber SK, Bremer S, Trapp O (2010) Integration of reaction and separation in a micro capillary column reactor – palladium nanoparticle catalyzed C–C bond forming reactions. *J Chem Eng Sci* 65:2410–2416
83. Trapp O, Bremer S, Weber SK (2009) Accessing reaction rate constants in on-column reaction chromatography: an extended unified equation for reaction educts and products with different response factors. *Anal Bioanal Chem* 395:1673–1679
84. Trapp O (2008) A novel software tool for high throughput measurements of interconversion barriers: DCXplorer. *J Chromatogr B* 875:42–47
85. Marriott PJ, Lai Y-H (1988) Capillary column gas chromatographic method for the study of dynamic intramolecular interconversion behaviour. *J Chromatogr* 447:29–41
86. Marriott PJ, Lai Y-H (1986) Isomerization process observed for chromium compounds by using the gas chromatographic reactor. *Inorg Chem* 25:3680–3683

87. Trapp O, Schurig V, Kostyanovsky RG (2004) The control of the nitrogen inversion in alkylsubstituted diaziridines. *Chem Eur J* 10:951–957
88. Roth WR, Winzer M, Korell M, Wildt H (1995) Konjugativ stabilisierte Trimethylenmethan-Derivate. Geometrieabhängigkeit der Singulett-Triplett-Aufspaltung. *Liebigs Ann* 897–919
89. Jung M, Fluck M, Schurig V (1994) Enantiomerization of 2,2'-diisopropylbiphenyl during chiral inclusion gas chromatography: determination of the rotational energy barrier by computer simulation of dynamic elution profiles. *Chirality* 6:510–512
90. Biedermann PU, Schurig V, Agratn I (1997) Enantiomerization of environmentally significant overcrowded polychlorinated biphenyls (PCBs). *Chirality* 9:350–353
91. Naruse Y, Watanabe H, Inagaki S (1992) A facile access to chiral allenedicarboxylates by deracemization process. *Tetrahedron Asymmetry* 3:603–606
92. Naruse Y, Watanabe H, Ishiyama Y, Yoshida T (1997) Enantiomeric enrichment of allenedicarboxylates by a chiral organoeuropium reagent. *J Org Chem* 62:3862–3866
93. Schurig V, Keller F, Reich S, Fluck M (1997) Dynamic phenomena involving chiral dimethyl-2,3-pentadienedioate in enantioselective gas chromatography and NMR spectroscopy. *Tetrahedron Asymmetry* 8:3475–3480
94. Prelog V, Wieland P (1944) Über die Spaltung der Tröger'schen Base in optische Antipoden, ein Beitrag zur Stereochemie des dreiwertigen Stickstoffs. *Helv Chim Acta* 27:1127–1134
95. Gasparrini F, Lunazzi L, Misiti D, Villani C (1995) Organic stereochemistry and conformational analysis from enantioselective chromatography and dynamic nuclear magnetic resonance measurements. *Acc Chem Res* 28:163–170
96. Melander WR, Lin H-J, Jacobson J, Horváth C (1984) Dynamic effect of secondary equilibria in reversed phase chromatography. *J Phys Chem* 88:4527–4536
97. Jacobson J, Melander W, Vaisnys G, Horváth C (1984) Kinetic study on *cis-trans* proline isomerization by high-performance liquid chromatography. *J Phys Chem* 88:4536–4542
98. Henderson DE, Horváth C (1986) Low temperature high-performance liquid chromatography of *cis-trans* proline dipeptides. *J Chromatogr A* 368:203–213
99. Ma S, Kálmán F, Kálmán A, Thuncke F, Horváth C (1995) Capillary zone electrophoresis at subzero temperatures. separation of the *cis* and *trans* conformers of small peptides. *J Chromatogr A* 716:167–182
100. Thuncke F, Kálmán A, Kálmán F, Ma S, Rathore AS, Horváth C (1996) Kinetic study on the *cis-trans* isomerization of peptidyl-proline dipeptides. *J Chromatogr A* 744:259–272
101. Rathore AS, Horváth C (1997) Capillary zone electrophoresis of interconverting *cis-trans* conformers of peptidyl-proline dipeptides: estimation of the kinetic parameters. *Electrophoresis* 18:2935–2943
102. Friebe S, Krauss GJ (1992) High-performance liquid chromatographic separation of *cis-trans* isomers of proline-containing peptides – separation on cyclodextrin bonded silica. *J Chromatogr A* 598:139–142
103. Gebauer S, Friebe S, Scherer G, Gübitz G, Krauss GJ (1998) High-performance liquid chromatography on calixarene-bonded silica gels – separations of *cis/trans* isomers of proline-containing peptides. *J Chromatogr Sci* 36:388–394
104. Krauss GJ, Friebe S, Gebauer S (1998) Cavity supported hplc of *cis/trans* isomers of proline-containing peptides using cyclodextrins and calixarenes. *J Protein Chem* 17:515–516
105. Lebl M, Gut V (1983) Calculation of the rate constant of a constant of a reversible reaction from the chromatographic peaks for muramyl dipeptide anomers. *J Chromatogr* 260:478–482
106. Moriyasu M, Kawanishi K, Kato A, Hashimoto Y, Sugiura M, Sai T (1985) Kinetic studies of fast equilibrium by means of high-performance liquid chromatography. xii. Rate constants and energy barriers of intramolecular carbonyl–nitrogen bond rotation of o-substituted acetanilides. *Bull Chem Soc Jpn* 58:3351–3355
107. Stephan B, Zinner H, Kastner F, Mannschreck A (1990) Enantiomers of 2,2'-spirobichromenes: energy barrier for thermal racemization during hplc on tribenzoyl-cellulose. *Chimia* 10:336–338

108. Cabrera K, Lubda D (1994) Influence of temperature on chiral high-performance liquid chromatographic separations of oxazepam and prominal on chemically bonded β -cyclodextrin as stationary phase. *J Chromatogr A* 666:433–438
109. Friary RJ, Spangler M, Osterman R, Schulman L, Schwerdt JH (1996) Enantiomerization of an atropisomeric drug. *Chirality* 8:364–371
110. Gasparrini F, Misiti D, Pierini M, Villani C (1997) Enantiomerization barriers by dynamic HPLC. Stationary phase effects. *Tetrahedron Asymmetry* 8:2069–2073
111. Villani C, Pirkle WH (1995) Chromatographic resolution of the interconverting stereoisomers of hindered sulfinyl and sulfonyl naphthalene derivatives. *Tetrahedron Asymmetry* 6:27–30
112. Gasparrini F, Lunazzi L, Mazzanti A, Pierini M, Pietrusiwickz KM, Villani C (2000) Comparison of dynamic HPLC and dynamic NMR in the study of conformational stereodynamics: case of the enantiomers of a hindered secondary phosphine oxide. *J Am Chem Soc* 122:4776–4780
113. Maier F, Trapp O (2013) The stereodynamics of 5,5'-disubstituted BIPHEPs. *Chirality* 25:126–132
114. Hochmuth DH (1995) Program package Mimesis 1.1, University of Hamburg
115. Weseloh G, Wolf C, König WA (1996) New technique for the determination of interconversion processes based on capillary zone electrophoresis: studies with axially chiral biphenyls. *Chirality* 8:441–445
116. Trapp O, Schoetz G, Schurig V (2001) Determination of enantiomerization barriers by dynamic and stopped flow chromatographic methods. *Chirality* 13:403–414
117. Bouabdallah S, Trabelsi H, Ben-Dhia T, Sabbah S, Bouzouita K, Khaddar R (2003) RP-HPLC and NMR study of *cis-trans* isomerization of enalaprilat. *J Pharm Biomed Anal* 31:731–741
118. Trapp O, Trapp G, Schurig V (2004) Determination of the *cis-trans* isomerization barrier of enalaprilat by dynamic capillary electrophoresis and computer simulation. *Electrophoresis* 25:318–323
119. Ledger R, Stellwagen E (2005) The sensitivity of the *cis/trans*-isomerization of enalapril and enalaprilat to solvent conditions. *J Pharm Pharmacol* 57:845–850
120. Trapp O (2005) Direct calculation of interconversion barriers in dynamic chromatography and electrophoresis: isomerization of captopril. *Electrophoresis* 26:487–493

Anisotropy Spectra for Enantiomeric Differentiation of Biomolecular Building Blocks

A.C. Evans, C. Meinert, J.H. Bredehöft, C. Giri, N.C. Jones, S.V. Hoffmann, and U.J. Meierhenrich

Abstract All biopolymers are composed of homochiral building blocks, and both D-sugars and L-amino acids uniquely constitute life on Earth. These monomers were originally enantiomerically differentiated under prebiotic conditions. Particular progress has recently been made in support of the *photochemical* model for this differentiation: the interaction of circularly polarized light with racemic molecules is currently thought to have been the original source for life's biological homochirality. The differential asymmetric photoreactivity of particular small molecules can be characterized by both circular dichroism and anisotropy spectroscopy. Anisotropy spectroscopy, a novel derivative of circular dichroism spectroscopy, records the anisotropy factor $g = \Delta\epsilon/\epsilon$ as a function of the wavelength.

A.C. Evans

Institut de Chimie de Nice, University of Nice-Sophia Antipolis, UMR 7272 CNRS,
28 Avenue Valrose, 06108 Nice Cedex 2, France

Murray Edwards College, University of Cambridge, Cambridge CB3 0DF, UK

C. Meinert and U.J. Meierhenrich (✉)

Institut de Chimie de Nice, University of Nice-Sophia Antipolis, UMR 7272 CNRS,
28 Avenue Valrose, 06108 Nice Cedex 2, France

e-mail: Uwe.Meierhenrich@unice.fr

J.H. Bredehöft

Institute for Applied and Physical Chemistry (IAPC), University of Bremen, Leobener Str.,
NW2, 28359 Bremen, Germany

C. Giri

Institut de Chimie de Nice, University of Nice-Sophia Antipolis, UMR 7272 CNRS,
28 Avenue Valrose, 06108 Nice Cedex 2, France

Max Planck Institute for Solar System Research, Max-Planck-Str. 2, 37191 Katlenburg-Lindau,
Germany

N.C. Jones and S.V. Hoffmann

Department of Physics and Astronomy, Aarhus University, Ny Munkegade, 8000 Aarhus,
Denmark

Anisotropy spectroscopy promisingly affords the wavelength-dependent determination of the enantiomeric excess (ee) inducible into chiral organic molecules by photochemical irradiation with circularly polarized light. Anisotropy spectra of small molecules therefore provide unique means for characterizing the different photochemical behaviors between enantiomers upon exposure to various wavelengths of circularly polarized light. This chapter will: (1) present the theory and configuration of anisotropy spectroscopy; (2) explain experimentally recorded anisotropy spectra of selected chiral biomolecules such as amino acids; and (3) discuss the relevance of these spectra for the investigation of the origin of the molecular homochirality observed in living organisms. This review describes a new chiroptical technique that is of significance for advances in asymmetric photochemistry and that is also highly relevant for the European Space Agency Rosetta Mission, which will determine enantiomeric excesses (ees) in chiral organic molecules in cometary ices when it lands on Comet 67P/Churyumov–Gerasimenko in November 2014.

Keywords Amino acids · Anisotropy spectroscopy · Chirality · Circular dichroism · Circularly polarized radiation · COSAC · ROSETTA

Contents

1	Introduction to Photochemical Enantiomeric Differentiation of Biological Building Blocks	273
1.1	CD Spectroscopy	274
1.2	SRCD Spectroscopy	274
1.3	Anisotropy Spectroscopy	275
2	CD and Anisotropy Spectroscopy: Theory and Configuration	276
2.1	UV/VUV SRCD Spectroscopy of Small Molecules: Theory	277
2.2	Anisotropy Spectroscopy of Small Molecules: Theory	277
2.3	Configuration and Measurement of SRCD and Anisotropy Spectra	279
3	CD and Anisotropy Spectroscopy of Amino Acids: Applications	281
3.1	UV/VUV CD Spectroscopy of Amino Acids	282
3.2	UV/VUV Anisotropy Spectroscopy of Amino Acids	283
3.3	Application of Anisotropy Spectra Towards Enantioselective Photochemistry	285
4	The ROSETTA Mission and the COSAC Experiment	288
4.1	The Cometary Mission ROSETTA	289
4.2	The COSAC Experiment	289
5	Future Outlook: Anisotropy Spectroscopy as a Means for Chiral Differentiation	293
	References	295

Abbreviations

CD	Circular dichroism
COSAC	Cometary Sampling and Composition Experiment
cpl	Circularly polarized light
cpsr	Circularly polarized synchrotron radiation
d	Day(s)

DMF-DMA	Dimethylformamide dimethylacetal
DMSO	Dimethyl sulfoxide
ee	Enantiomeric excess
ESA	European Space Agency
GC	Gas chromatography
HFiP	1,1,1,3,3,3-Hexafluoro-2-propanol
HV	High voltage
l-	Left
Me	Methyl
MgF ₂	Magnesium fluoride
min	Minute(s)
PEM	Photoelastic modulator
PMT	Photomultiplier tube
r-	Right
SRCD	Synchrotron radiation circular dichroism
TFA	Trifluoroacetic acid
TFAA	Trifluoroacetic anhydride
TOFMS	Time-of-flight mass spectrometer
UV	Ultraviolet
VUV	Vacuum ultraviolet

1 Introduction to Photochemical Enantiomeric Differentiation of Biological Building Blocks

Biopolymers such as carbohydrates, proteins, and nucleic acids are all composed of homochiral building blocks: life on Earth is uniquely handed [1, 2]. However, the source of the homochirality of these building blocks remains unknown, in spite of decades of research into both planetary and extraterrestrial origins. Of many possible hypotheses, that homochirality originated from random asymmetric crystallization effects [3, 4] or parity violation of the universal weak nuclear interaction [5, 6], one highly plausible source of this original enantiomeric differentiation between small chiral molecules is thought to be inter- and circumstellar circularly polarized light (cpl) [7–13]. The interaction of key biological building blocks in interstellar environments [14–18] with circularly polarized electromagnetic radiation [8, 19] is thought to have afforded a differentiating absorption of circularly polarized photons, yielding a photosynthetic or photolytic preference for the preservation of one enantiomeric form over its counterpart [20–22]. Currently, the main evidence for these prebiotic photochemical reactions occurring in interstellar and circumstellar environments are interstellar ice simulation experiments [23–28] and carbonaceous chondritic meteorite analyses [29–34]. It is hoped that further evidence for interstellar photodifferentiation of enantiomers [35] will be provided by such ambitious missions as the European Space Agency's Rosetta Mission [36], which will actually land on a comet and analyze its surface for enantiomeric

excesses (ees) [37–39]. The photochemical behavior that results upon exposure of small molecules to cpl likely originally served as a fascinating means for enantiomeric differentiation and remains a novel way to characterize photochemical differences between enantiomers.

1.1 CD Spectroscopy

CD spectroscopy provides a well-precedented means for characterizing the behavior of molecules in the presence of cpl. It reflects the differential absorption of chiral photons of both left- (l-) and right- (r-) handedness in the UV, visible, and IR wavelengths by chiral molecules. For small molecules, the differential absorption of cpl can be directly characterized using CD spectroscopy. The differential extinction coefficient $\Delta\epsilon$ measured in CD spectra is defined by $\Delta A = (\Delta\epsilon)c/l$ where ΔA is the difference in absorption of left- and right-handed cpl (the CD signal), c is the sample concentration, and l is the sample pathlength. For any given molecule, $\Delta\epsilon$ is determined for a range of wavelengths and can be used as a means for predicting how that molecule will behave upon exposure to cpl. Both the rate and the degree of asymmetric photochemical induction that the molecule will experience are thus predictable from CD spectroscopic characterization. However, traditional CD spectroscopy presents limitations when considering small molecules. Conventional CD instruments use xenon arc lamps that provide light fluxes too low for measurements conducted at vacuum UV (VUV) wavelengths below 200 nm. Low light flux results in low signal-to-noise data and limits the amount of structural information obtainable from a series of CD spectroscopic measurements. In order to obtain a clearer understanding of the photochemical behavior of small molecules upon exposure to cpl, given that many small molecules tend to absorb in the VUV, it is necessary to extend CD spectroscopic measurements down into the lower VUV wavelength range and increase the signal-to-noise ratios.

1.2 SRCD Spectroscopy

Synchrotron radiation circular dichroism (SRCD) bypasses the limitations encountered in characterizing chiral small molecules using standard CD spectroscopy. In conventional circular dichroism spectrometers the light source is often a xenon arc lamp. Although omnidirectional, these sources are intense in the visible and UV spectral range, but the intensity decreases significantly below about 200 nm. In contrast, bright and highly collimated synchrotron radiation is not only an excellent UV source, but remains intense deep into the VUV spectral range [40]. This results in much higher signal-to-noise ratios and more rapid throughput for obtaining spectra. Most importantly, SRCD affords much more accurate data at lower wavelengths that can be used to characterize electronic transitions within the

molecule. In order to accomplish measurements at wavelengths lower than 190 nm, the solid phase of the analytes must be produced, as the presence of both hydrophobic and hydrophilic solvents can mask the electronic behavior of the small molecules being characterized. The CD spectra of amino acids at UV and VUV wavelengths have now been recorded by a number of groups internationally using SRCD [41, 42] and progress in the characterization of other families of small biologically-relevant enantiomeric pairs continues [43].

1.3 Anisotropy Spectroscopy

In 1895, while at the Ecole Normale Supérieure in Paris, Aimé Cotton studied the interactions of cpl with optically active molecules. He found that right-handed cpl is absorbed differently to left-handed cpl (circular dichroism). He also discovered the Cotton effect describing that in wavelength regions of high absorption the absolute magnitude of optical rotation (optical rotary dispersion) of a chiral molecule will vary greatly, passing through a maximum/minimum, then through zero at the wavelength of maximum absorption and then through a further minimum/maximum of equal magnitude but opposite sign [44]. However, Cotton did not attempt to induce chiral bias into racemates using cpl irradiation. Results on actual chirality transfer from chiral photons to racemic organic molecules were first reported by Kuhn and Braun in 1929 [45]. At the University of Heidelberg Kuhn and Braun subjected racemic solutions of the ethyl ester of α -bromopropanoic acid in ethanol to either r-cpl or to l-cpl in separate experiments. The cpl wavelength was fixed to 280 nm and optical activity of opposite sign was photochemically induced into the ester. Follow-up experiments afforded the induction of enantiomeric excess in *n*-hexane solutions of α -cyanopropanoic acid dimethylamide at 300 nm after exposure to cpl irradiation [46].

The photochemical induction of molecular asymmetry is the result of faster reaction kinetics and increased rate constants for the photolysis of the more absorbing enantiomer, resulting in an increased abundance of the less absorbing enantiomer. Thus chirality can be successfully – but not quantitatively – transferred from chiral photons to chiral organic molecules by a process described today as asymmetric photolysis, a process requiring different cpl absorption of the enantiomers. The maximum ee-value inducible by asymmetric photolysis does not exclusively depend on the differential extinction coefficient $\Delta\epsilon$ obtained by CD spectroscopy between two enantiomers. The degree of chiral bias induced also depends upon the extinction coefficient, ϵ , of the chiral molecule. The ratio of these two values is called the anisotropy factor, g , and it is defined as $g = \Delta\epsilon/\epsilon$ [7, 9, 47, 48]. The anisotropy factor (or dissymmetry factor) has become of key importance in understanding enantioselective photolysis as first discovered by Kuhn and Braun. The anisotropy factor is a dimensionless quantity.

The anisotropy factor has been found to be pH-dependent, as reported by the ERATO research team of Inoue at the University of Osaka in Japan [11]. Aqueous

solutions of the amino acid leucine were subjected to cpl and ees were determined after irradiation. Inoue et al. found that the induced ee-values were dependent on the degree of protonation of leucine's carboxylic group, such that pH values close to 1 generated higher anisotropies. The highest ee value obtained was reported to be close to 0.2% [11, 41, 49].

The anisotropy factor, g , is highly characteristic for the chiral molecule under investigation. The team of Bonner at Stanford University selected leucine for the study of enantioselective photolysis [10]. They found that up to 2.50% ee could be induced into a racemate of leucine by irradiating with wavelengths of 212.8 nm. Leucine has often been chosen for such experiments due to its large anisotropy factor ($g = 0.0244$) measured at 211 nm in 1 N HCl [10]. Nordén at the Gothenburg University selected the amino acid alanine ($g = 0.007$) for photochemical ee generation at 203 nm and observed an induction of up to 0.06% ee [50]. In addition, Cohen and coworkers at Harvard University have recently reported on the excitation of chiral molecules with circularly polarized electromagnetic radiation described as "superchiral" light. The use of superchiral light provided anisotropy factors increased by a factor of 11 compared to cpl [51], but standing waves were used for these enantioselective studies on biperylene enantiomers which cannot be considered relevant to the origin of biomolecular asymmetry and the prebiotic differentiation between chiral organic precursor molecules of life.

The anisotropy factor of a molecule is also dependent on the wavelength, λ , of the cpl carrying the chiral information to which the molecule is exposed. Therefore systematic understanding of enantioselective photolysis reactions cannot exclusively rely on CD data and requires the recording of the anisotropy factor as a function of wavelength, or $g(\lambda)$. These measurements are now known as anisotropy spectroscopy [52].

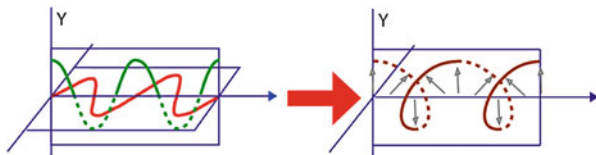
2 CD and Anisotropy Spectroscopy: Theory and Configuration

A chiral molecule will experience r-cpl and l-cpl differently, and the CD spectrum for that molecule will display maxima/minima at the optimal differential absorption wavelengths for the molecule's electronic transitions. This difference in light absorption, corrected for sample concentration and pathlength, is known as the differential extinction coefficient, $\Delta\epsilon$, and is defined as

$$\Delta\epsilon = \epsilon_{\text{r-cpl}} - \epsilon_{\text{l-cpl}}. \quad (1)$$

CD spectroscopy of small molecules can provide great insight into the optimal wavelengths for asymmetric excitation, and subsequent photoreactive chiral differentiation, of these molecules.

Fig. 1 Two linear polarized and perpendicular waves (left) are added to produce circular polarized light (right)



2.1 UV/VUV SRCD Spectroscopy of Small Molecules: Theory

Circularly polarized light is a polarization state of light where the polarization vector (the electric field vector) of the electromagnetic radiation rotates and traces out a circle when polarized to the right or to the left (Fig. 1).

Circularly polarized light is in itself chiral, and interacts differentially with chiral molecules, leading to a difference in absorption when exposed to r-cpl or l-cpl. In quantum mechanical terms this differential absorption is determined by the rotational strength operator [53, 54]

$$R = \text{Im}(\boldsymbol{\mu} \cdot \mathbf{m}), \quad (2)$$

where Im denotes the imaginary component, $\boldsymbol{\mu}$ is the electric dipole moment operator (also used to calculate normal absorption), and \mathbf{m} is the magnetic dipole moment operator. For a molecule to be optically active (i.e., have a CD signal), the excitation of the molecule upon photon absorption must result in both a displacement (dipole moment) and a rotation (magnetic moment) of the electrons.

CD spectroscopy is commonly used to determine the secondary structure of proteins, amongst other applications [55]. These polymers have CD signals starting below ~ 240 nm and the extended wavelength range offered by synchrotron radiation sources allows for more types of secondary structures to be determined with higher accuracy [40]. The extended wavelength range of synchrotron radiation is not only beneficial for protein structure determination. Many small biologically relevant molecules demonstrate significant extinction coefficients below 200 nm. For example, the lowest energy transition ($n \rightarrow \pi^*$) in amino acids lies close to 200 nm [56, 57] and carbohydrates are transparent to wavelengths above 200 nm. SRCD is therefore an important tool for the study of small chiral molecules.

2.2 Anisotropy Spectroscopy of Small Molecules: Theory

UV and VUV CD spectra of small molecules such as amino acids have recently been recorded in the solid phase due to the limitations experienced when measuring CD spectra in solution, such as solvent-induced polarizations and solvent absorption effects in the VUV [12, 42, 58]. DFT calculations of Nakagawa et al. match experimentally obtained amino acid CD data for the UV and VUV spectral region quite well. These calculations were performed considering the solid state and allow

the assignment of electronic transitions to individual CD signals [59]. Conveniently, these experimental and theoretical solid-phase CD data provide the most accurate models for the interstellar and circumstellar solid state environments that prebiotic precursors are likely to have evolved in. However, CD spectra alone do not offer a direct understanding of the asymmetric photochemical influences that cpl can have on a given molecule. As outlined above, these influences are more directly provided by the anisotropy factor, g . This is given by the equation $g = \Delta\epsilon/\epsilon$, which utilizes the differential extinction coefficient recorded during CD measurements as well as the extinction coefficient recorded during absorption measurements. For a given wavelength of cpl, g can be determined from CD and absorption spectra: for a known extent of reaction ξ for the asymmetric photochemical process, the maximum ee inducible by the process can be predicted using [52]

$$ee \geq \left(1 - (1 - \xi)^{\frac{g}{2}}\right) \times 100\%. \quad (3)$$

During asymmetric photolysis of a racemate, the R - and S -enantiomers will photodegrade at different rates. These two separate reactions can be considered to be pseudo-first-order and their rate constants (defined as k_R and k_S respectively) will necessarily not be equal. The difference between these rate constants dictates the efficiency of the photolysis reaction. As these rate constants are directly proportional to the molar absorption coefficients (defined as ϵ_R and ϵ_S respectively), the efficiency of photolysis is dependent upon the anisotropy factor, g [45, 46]. This relationship between g and reaction rate has also been shown to exist for non-first-order kinetics [60]:

$$g = 2 \frac{\epsilon_R - \epsilon_S}{\epsilon_R + \epsilon_S} = 2 \frac{k_R - k_S}{k_R + k_S}. \quad (4)$$

By determining g for every wavelength of cpl measured during CD spectroscopy, it becomes possible to generate plots of anisotropy spectra that afford full and direct characterization of the photochemical interactions of cpl with a given small molecule [52]. Anisotropy spectra therefore provide a means for directly predicting photochemical differentiation between enantiomers at given wavelengths of light and provide a unique methodology for tuning photochemical behavior to produce enantiomeric excesses that can be amplified using alternative chemical means [61–64]. Once a pair of enantiomers has been characterized by anisotropy spectra, the optimal wavelengths for inducing ee can be selected and utilized in photochemical experiments such as interstellar ice photolytic simulations. A number of groups have reported both solid and solution phase asymmetric photochemical induction by using cpl [10, 11, 50], and it has already been demonstrated that by using the data anisotropy spectroscopy provides, it is possible to induce ees of $>5\%$ [13]. Given that such experiments have frequently been conducted within the context of interstellar ice simulations, it is reasonable to postulate that this sort of anisotropic chiral irradiation bias occurred in the molecular cloud that later collapsed to form

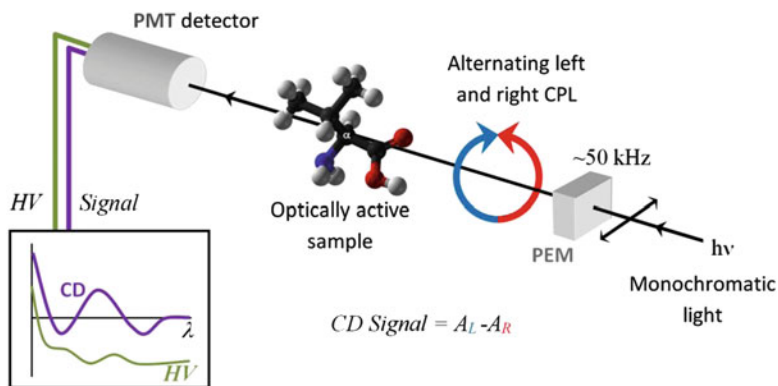


Fig. 2 Experimental configuration for measuring SRCD and anisotropy spectra. The PEM converts monochromatic light into alternating left and right handed cpl. Optically active organic molecules have differential absorptions of chiral photons in the form of cpl. In SRCD spectroscopy this differential absorption is recorded by the PMT detector

our Solar System and afforded the creation of homochirality in biomolecular prebiotic precursor molecules. This hypothesis will be tested in 2014, when the European Space Agency (ESA) Rosetta Mission lands on Comet 67P/Churyumov–Gerasimenko and will demonstrate the relevance of anisotropy spectroscopy for photochemical asymmetry generation.

2.3 Configuration and Measurement of SRCD and Anisotropy Spectra

CD spectroscopy is most commonly measured as illustrated in Fig. 2 [65]. A monochromatic source of light is linearly polarized, and a photoelastic modulator (PEM) converts the polarization into alternating left- and right-handed cpl. This alternating cpl is then passed through the sample and detected with a photomultiplier tube (PMT). If there is a difference in absorption between left- and right-handed polarization, the signal from the PMT oscillates with the same frequency as the alternating polarization (typically 50 kHz). The amplitude of the small oscillation (a CD signal is typically only 10^{-4} to 10^{-3} of the total absorption) is picked up using a lock-in amplifier, with both frequency and phase locked to the PEM oscillation. The signal from the PMT is dependent on the light intensity and also on the high voltage (HV) applied to the detector. If the PMT is operated in a varying HV mode, where the long period signal (i.e., for periods much longer than the PEM oscillation period) is kept constant, the measured amplitude is directly proportional to the CD signal. The magnitude of the HV depends on the intensity of the light source and, most importantly, on the amount of sample absorption.

The detector HV is therefore directly related to the sample absorbance. The light hitting the PMT's cathode produces a current of photoelectrons which is amplified (denoted as Gain) via the HV and is to a good approximation given by

$$\text{Gain(HV)} = b(\text{HV})^a. \quad (5)$$

If the sample absorption is A_{sample} , the signal from the detector is proportional to

$$\text{Signal} \sim \text{Gain(HV)} \cdot 10^{-A_{\text{sample}}} \cdot I_{\text{beam}}, \quad (6)$$

where I_{beam} is the light source intensity (or beam current in the case of SRCD). The HV and the beam current are recorded simultaneously with the CD signal and are thus a function of wavelength: $\text{HV}(\lambda)$ and $I_{\text{beam}}(\lambda)$. Since the signal from the detector is kept constant by varying the HV, (6) is also valid for the reference measurement, which is essential for absorption spectroscopy, hence:

$$\text{Gain(HV}_{\text{sample}}) \cdot 10^{-A_{\text{sample}}} \cdot I_{\text{beam, sample}} = \text{Gain(HV}_{\text{ref}}) \cdot 10^{-A_{\text{ref}}} \cdot I_{\text{beam, ref}}. \quad (7)$$

From (7), and using (5), the absorbance can be calculated:

$$A = A_{\text{sample}} - A_{\text{ref}} = a \log\left(\frac{\text{HV}_{\text{sample}}}{\text{HV}_{\text{ref}}}\right) + \log\left(\frac{I_{\text{beam, sample}}}{I_{\text{beam, ref}}}\right). \quad (8)$$

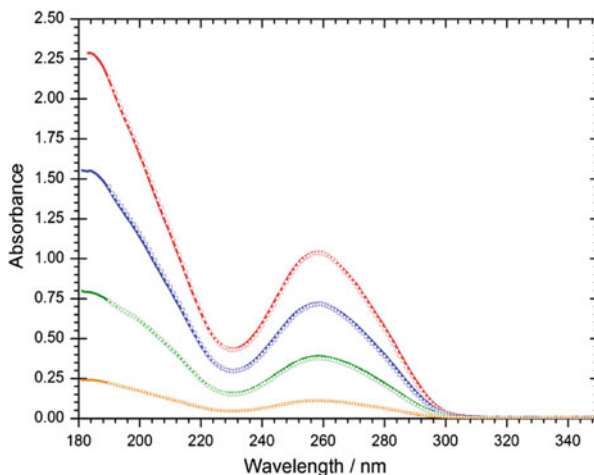
Only the detector-dependent constant a needs to be calibrated for the absorbance, $A(\lambda)$, in (8) to be evaluated from the spectroscopic measurement.

The calibration of the detector constant a can be made against a sample of known absorbance¹ (see Fig. 3). The same samples were measured both on a calibrated Thermo EVO300 spectrometer and on the CD1 beam line [66, 67] at the ASTRID synchrotron radiation source at Aarhus University in Denmark. This method is very robust as it determines the single parameter a from four spectra (each containing 160 data points) in a full range of absorbances from 0 to about 2. We have found that this method produces absorbance spectra of typical accuracies of a few thousands of an absorption unit, which is suitable for anisotropy spectroscopy.

An important aspect of the simultaneous measurement of the CD spectrum and the absorbance spectrum is that they are recorded with exactly the same conditions of concentration and light spot profile and position. The anisotropy spectra can thus be readily calculated as $g(\lambda) = \Delta\epsilon/\epsilon = \Delta A/A$, independent of any determination of sample concentration and optical pathlength (for liquid samples) or film thickness and density (for solid samples).

¹For example, solutions of deoxyribonucleic acid from calf thymus (CT DNA Sigma Aldrich D4522) at 1, 0.66, and 0.33 mM base pair concentrations, have been measured in both 0.1 and 1 mm pathlength quartz cells (type 121.000 Hellma, Germany) over a wavelength range from 190 to 350 nm.

Fig. 3 Absorbance spectra of CT DNA recorded on a Thermo EVO300 spectrometer (*markers*) and calculated absorbance spectra from detector high voltage (HV) data recorded at the CD1 beam line (*lines*) using a single detector constant of $a = 7.85$



As anisotropy spectra are formed by dividing two spectra, any noise in either the CD or the absorption spectra will be amplified. In order to obtain high quality anisotropy spectra, a large data set is required. Typical measurements on solid amino acid films (and the reference substrate) are made in a wavelength range of 330–130 nm in 1-nm increments, with a dwell time of 2 s for each step. All spectra are repeated at least twice and the solid sample is rotated around the surface normal in steps of 90° , a CD spectrum being measured for each rotation. This rotation process ensures that the sample is essentially free from linear dichroism effects originating from possible crystal alignment within the sample. This total data set is then used to calculate the anisotropy spectra.

Measurements of samples in solution are made with the same 1 nm step size and 2 s dwell time as for solids, but the lowest wavelength recorded is 170 nm for aqueous solutions and 160 nm for more VUV transparent solvents such as 1,1,1,3,3,3-hexafluoro-2-propanol (HFiP). At least three repeat measurements of both the sample (and reference) over a range of sample concentrations are used to form an anisotropy spectrum which spans wavelength ranges where the sample extinction coefficient varies by more than an order of magnitude.

3 CD and Anisotropy Spectroscopy of Amino Acids: Applications

Both UV and VUV SRCD measurements have been conducted on a wide range of molecular substrates, but the family of small molecules most thoroughly studied by UV/VUV SRCD spectroscopy has historically been amino acids. Because these molecules serve as the basic building blocks for proteins [1], their unique VUV CD spectra are of great interest to both prebiotic and synthetic chemists [12]. The CD

spectra for amino acids all indicate that cpl is differentially absorbed by D- and L-enantiomers. Additionally, the anisotropy spectra of amino acids measured to date all indicate that >1% ee can be induced by photochemical exposure to cpl [52]. Asymmetric photochemistry could therefore have induced a non-racemic bias under prebiotic conditions. This chiral bias could then have triggered an autocatalytic enhancement of asymmetry [61] that resulted in today's biomolecular homochirality. A comparative study on the amino acid content of organisms from all three domains of life (bacteria, archaea, and eukaryote) allowed for the determination of the recruitment order of amino acids in proteins [68]. Alanine, valine, leucine, proline, and serine are all among the amino acids first recruited for the early evolution of proteins. Indeed, both photolytic and photosynthetic cometary ice simulation experiments have demonstrated that cpl can induce enantiomeric bias in amino acids such as alanine [27] and leucine [12, 13].

3.1 UV/VUV CD Spectroscopy of Amino Acids

Amino acids have highly characteristic UV and VUV CD spectra. The theoretical calculation for the $n_{\text{O}} \rightarrow \pi_{\text{CO}}^*$ electronic transition for amino acids in aqueous solution has been predicted to produce a CD signal at around 200 nm [56, 57]. Experimentally the maximum peaks observed in the CD spectra of most amino acids, and even diamino acids, in aqueous solution at around 205 nm have been assigned to this transition [69]. One of the main limitations for measuring CD spectra in aqueous solution is that water – one of the most popular solvents for CD spectroscopy – starts to absorb photons at 190 nm [70]. Thus, even though there are some unique CD signals present at or above 200 nm, most of the characteristic electronic transitions for amino acids are not observable.

Hence researchers interested in measuring CD of small chiral molecules into the VUV spectral region are now choosing to prepare amorphous solid state samples that are commonly prepared on windows made of MgF_2 . It is convenient that the amino acids are measured in the solid state, as this is the likely physical state in which they would exist in interstellar contexts.

The $n_{\text{O}} \rightarrow \pi_{\text{CO}}^*$ electronic transition CD signal for amino acids in amorphous samples is experimentally observable at around 200 nm; however, this CD signal is likely a combination of the $n_{\text{O}} \rightarrow \pi_{\text{CO}}^*$ electronic transition and the $n_{\text{O}} \rightarrow \sigma_{\text{O}}^*$ electronic transition [71] (Fig. 4). Additionally, the major peak observable in the CD spectra of most amino acids is postulated to be the $\pi_{\text{O}} \rightarrow \pi_{\text{CO}}^*$ transition [59] between 165 and 180 nm. Branched chain amino acids (valine, leucine, isoleucine) have been observed to show additional strong minima between 170 and 175 nm that straight-chain amino acids do not demonstrate [59].

It is interesting to note that α -methylated amino acids such as isovaline and α -methyl valine display CD signals of the opposite sign to the family of α -H amino acids. This change in sign can be attributed to the steric bulk located around the

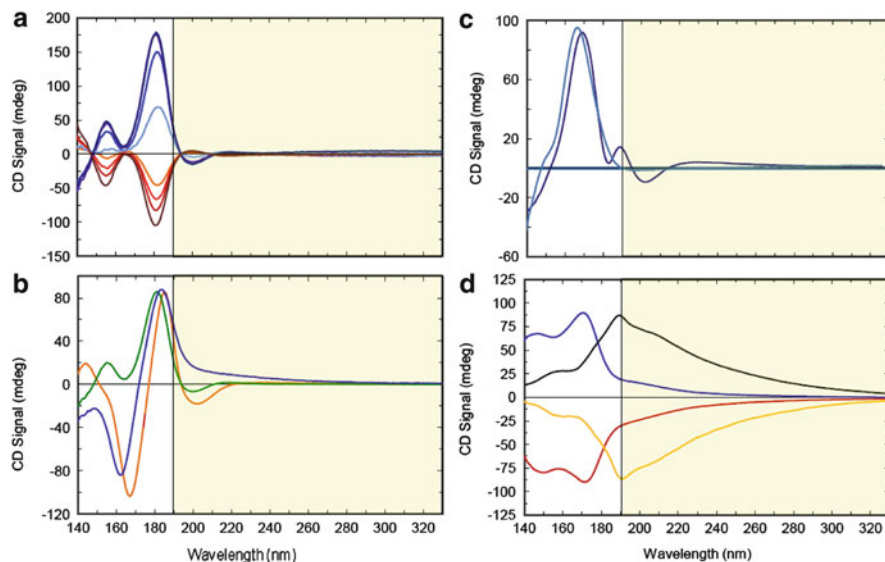


Fig. 4 VUV CD spectra of amorphous solid-state amino acid enantiomers immobilized on MgF_2 windows [42]. (a) D-Ala (red) and L-Ala (blue); (b) L-Ala (green), L-Val (orange) and L-Leu (blue); (c) L-Aba (dark blue) and L-Ser (light blue); (d) D-Iva (blue), L-Iva (red), D-Me-Val (black), and L-Me-Val (yellow). Water starts to absorb below 190 nm and makes the spectral region between 140 and ~ 175 nm inaccessible if amino acid CD spectra are recorded in aqueous solution

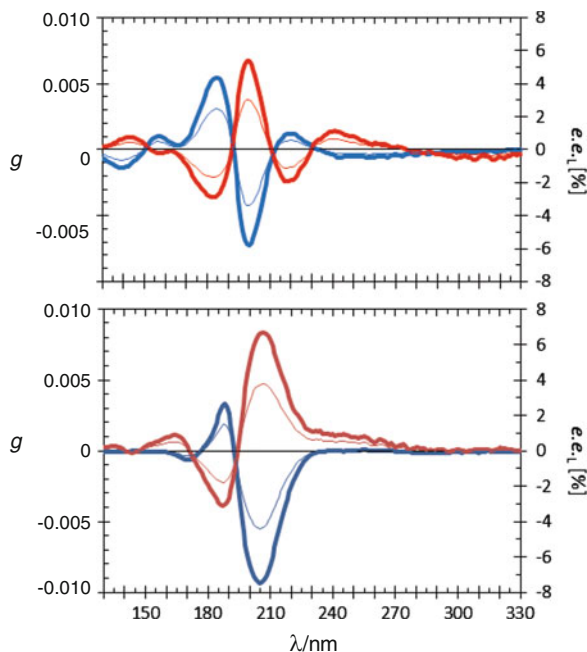
α -carbon – such crowding likely interferes with the molecular orbitals involved in the $n_{\text{O}} \rightarrow \pi_{\text{CO}}^*$ transition and results in the inversion of the expected CD signal [42].

3.2 UV/VUV Anisotropy Spectroscopy of Amino Acids

An anisotropy spectrum plots the anisotropy factor g as a function of the cpl wavelength used to measure CD and absorption data for a given compound [52]. Using anisotropy spectra and (1), the optimum percentage ee inducible (assuming photolytic reaction completion) for a range of wavelengths of cpl can also be included within an anisotropy plot. Figure 5 depicts anisotropy spectra of the amino acids D-alanine and L-alanine (top); and D-valine and L-valine (bottom).

Anisotropy spectra have now successfully been recorded between 130 and 330 nm in the VUV and UV spectral region using synchrotron radiation for a number of both α -H and α -methyl amino acids [52]. L-Alanine and L-valine demonstrate characteristic maxima in the range 180–185 nm and minima in the range 200–210 nm, and their enantiomers display equal and opposite anisotropy spectra. These wavelength regions are thus considered important for the induction of enantiomeric bias in amino acids, as the energy of the cpl photons at these

Fig. 5 Thick lines show anisotropy spectra of selected α -amino acids in the vacuum UV and UV spectral region; thin lines represent the corresponding ee_L inducible by either l- or r-cpl at the extent of reaction $\xi = 0.9999$. *Top*: Anisotropy spectra of D-alanine (red) and L-Ala (blue). *Bottom*: Anisotropy spectra of D-Val (brown) and L-Val (blue) [52]. Amino acids were sublimated using a temperature-controlled UHV chamber and condensed in form of isotropic amorphous films on an MgF_2 window as described in [13]



wavelengths is sufficient to provoke enantioselective photolysis. The IR wavelength regions are not considered to be important to include in the recording of anisotropy spectra, even if Vibrational Circular Dichroism (VCD) spectroscopy continues to attract much attention with respect to the determination of the configuration, as these wavelengths of cpl cannot provide enough energy to the molecule to result in chiral photolysis.

The current experimental set-up, which uses a PEM composed of CaF_2 and employs MgF_2 windows as sample holders, restricts the ability to record anisotropy spectra below 130 nm. This is due to the fact that both CaF_2 and MgF_2 absorb cpl photons below this wavelength. Experiments on PEM-free recording of anisotropy spectra using tunable cpl generation via synchrotron based undulator insertion devices [72] might circumvent this problem in the future.

The secondary axis of the anisotropy spectra of alanine and valine enantiomers represented in Fig. 5 depicts the theoretically inducible ee possible upon exposure to cpl for racemic alanine and racemic valine respectively. At 200 nm, an ee of greater than 5% can potentially be photochemically induced into *rac*-alanine and *rac*-valine via a photolytic irradiation process, assuming the extent of reaction $\xi = 0.9999$ is reached. It can be seen that any cpl irradiation at 300 nm, where the anisotropy signal is zero, will not result in asymmetric induction. Anisotropy spectroscopy therefore serves as a highly useful tool for both characterizing and predicting the photochemical behavior of amino acids. The application of anisotropy spectroscopy towards enantioselective (asymmetric) photochemical synthesis

is currently under investigation and may prove to serve as a unique predictive tool for understanding how key chiral synthetic building blocks can be differentiated solely by chiral light.

3.3 *Application of Anisotropy Spectra Towards Enantioselective Photochemistry*

Amino acids constitute the key building blocks of proteins, which provide both biological structure and biochemical function for all life on Earth. It remains undetermined whether amino acids originated terrestrially or extraterrestrially, and many hypotheses currently exist. Another issue is how amino acids were rendered homochiral, and at what point throughout the evolution of life this homochirality became predominant. The *photochemical* model for the origin of amino acids supports an extraterrestrial origin and favours the asymmetric influence of interstellar chiral light as the original source for life's homochirality.

The earliest evidence of extraterrestrial amino acids came from the meteorite that fell at Murchison, Australia in 1969. Physico-chemical and enantioselective analyses of Murchison meteorite samples have detected of almost 90 mono- [73, 74] and diamino acids [32] with a slight excess of L-enantiomers relative to D-enantiomers. These findings were the first indication that life's enantiomeric bias may have come from an extraterrestrial source. It must be noted that amino acids (apart from glycine, detected in strewn comet Wild two dust particles by the Stardust space probe [75]) have not been detected in interstellar space using conventional analytical methods, although key precursor molecules such as formic acid and acetic acid have been detected in abundance.

Further understanding of the origin of amino acids has been facilitated by laboratory experiments committed to the spontaneous photosynthesis and/or photolysis of amino acids under simulated interstellar conditions. The first two landmark experiments in this area were independently conducted by Bernstein et al. and Muñoz Caro et al., both in 2002, and published side on side in Nature. The Bernstein group prepared an ice mixture of molar composition $\text{H}_2\text{O}:\text{NH}_3:\text{CH}_3\text{OH}:\text{CH}_3\text{CN}=20:2:1:1$ that was subsequently irradiated, warmed to room temperature, and analyzed for its composition using HPLC. The amino acids alanine, glycine, and serine were detected [24].

The Muñoz Caro group prepared an ice mixture of molar composition $\text{H}_2\text{O}:\text{}^{13}\text{CH}_3\text{OH}:\text{NH}_3:\text{}^{13}\text{CO}:\text{}^{13}\text{CO}_2=2:1:1:1:1$. The ice mixture of the Muñoz Caro group included the most abundant interstellar molecules – CO and CO_2 – and specifically avoided using CH_3CN , which is less abundant in interstellar environments. The authors isotopically labeled carbon-containing molecules to exclude any terrestrial contamination. The mixture was irradiated, warmed to room temperature, acid hydrolyzed, derivatized with ECEE, and analyzed for composition by enantioselective GC-qMS. The irradiated mixture yielded six

proteinogenic amino acids and ten non-proteinogenic amino acids [23]. The Muñoz Caro experiment reported the presence of numerous amino acids relative to the Bernstein experiment. One common factor in both experiments was the observation of high quantities of glycine, indicating that glycine could possibly be present in greater abundances in interstellar space than originally detected. These groundbreaking interstellar ice simulation experiments demonstrated that amino acids could have been among the first chiral molecules produced in the universe. However, neither of these experiments addressed the origin of the homochirality of amino acids.

In 1929, Kuhn and Braun subjected racemic solutions of ethyl 2-bromopropanoate to cpl [45] to probe whether chiral photons could be used to induce chiral asymmetry into racemic organic molecules [76]. The current focus for experiments investigating cpl asymmetric photochemistry has instead been directed to amino acids due to their fundamental role in biological structure and function [1]. There are two kinds of asymmetric photochemistry that are currently being investigated using synchrotron-sourced cpl: asymmetric photolysis and asymmetric photosynthesis.

Asymmetric photolysis experiments are carried out by subjecting a thin film of racemic amino acid to circularly polarized synchrotron radiation (cpsr) of either right- or left-handedness. Recently, the exposure of racemic leucine to cpsr resulted in a photolytic asymmetric induction of 2.6% ee [12]. This sample of leucine was specifically irradiated at a wavelength of 182 nm in the VUV region of its anisotropy spectrum where highest anisotropy values were found. Given that the sample was in solid form upon exposure to cpsr and was contained in an environment of very low temperatures and pressures, these experiments can be considered to simulate the conditions the racemic amino acid would encounter in interstellar space. Such an enantiomeric enhancement would not have been possible if an aqueous solution of racemic leucine had been irradiated due to the general light absorption of water below 190 nm. Follow-up experiments irradiating racemic leucine films that had been sublimated and condensed in order to provide an amorphous film lacking long-range order and of a defined film thickness resulted in an even greater photolytic asymmetric induction of 5.2% ee [13].

Asymmetric photosynthetic experiments have also been successfully carried out in order to investigate and simulate the postulated light-induced origin of biomolecular asymmetry. Anisotropy spectroscopy of amino acids, fully characterizing their behavior as chiral species over a span of wavelengths, has proven invaluable in conducting these experiments.

Asymmetric photosynthetic cometary ice simulations mimic the cometary formation process, which is now well-understood [77]. Comets form via an agglomeration of interstellar dust particles that are surrounded by layers of interstellar ices. Within these ices lie the key synthetic ingredients for the formation of life's building blocks, and the cometary body serves as a very cold and unstable reaction vessel for these species. Today the physico-chemical processes that result in cometary formation can be simulated in the laboratory under cryogenic temperatures and it is possible to form small amounts of artificial comets in the laboratory. Surprisingly, such artificial comets have been shown to contain more

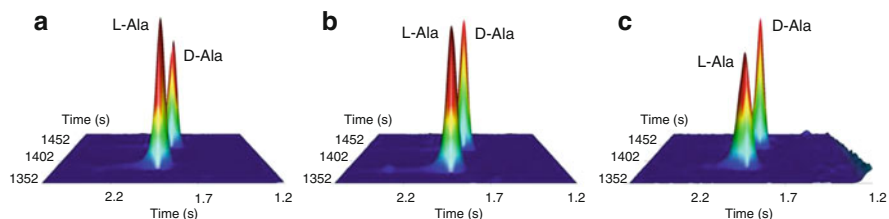


Fig. 6 At cryogenic temperatures H_2O , $^{13}\text{CH}_3\text{OH}$, and NH_3 were subjected to left-cpl (a), linearly polarized light (b), and right-cpl (c) of $h\nu = 6.64$ eV. The amino acid ^{13}C -alanine was subsequently observed to form in an asymmetric manner. The multidimensional gas chromatograms show an ee of L-alanine in the sample irradiated with l-cpl and an ee of D-alanine was observed in the sample irradiated with r-cpl. As expected, the sample irradiated with linearly polarized light showed racemic alanine

than 26 amino acids that have photochemically formed out of small interstellar starting molecules such as water, carbon monoxide, carbon dioxide, ammoniac, and methanol [23, 28]. Thus it can be assumed that the photosynthetic formation of the first chiral molecules in the universe can be reproduced under well-defined conditions in the laboratory today.

In 2011, a microscale quantity of an artificial comet was photochemically synthesized in the laboratory using irradiation from cpsr photons. Former such studies had all used unpolarized light for simulating photochemical interstellar processes, but the discovery of cpl in the Orion star formation region [8] enabled de Marcellus et al. to replace the source of unpolarized light for their simulations with cpsr. Numerous amino acids were detected by enantioselective multidimensional gas chromatography [78] in the analytes from the artificial comet. However, more interestingly, an ee of 1.34% was detected for the amino acid alanine as the result of asymmetrical photochemical exposure to cpsr [27]. By changing the helicity of the cpl photons the sample was exposed to, the detected ee of alanine was found to invert (Fig. 6).

In 2007, the team of Kobayashi at the Yokohama National University in Japan simulated the formation of interstellar amino acid precursor molecules in a similar manner by irradiating carbon monoxide, ammonia, and water with 3.0 MeV protons. The resulting intermediates were then individually subjected to right- and left-handed cpsr. Enantioselective liquid chromatographic analyses of the irradiated products detected asymmetric photochemical induction of up to 0.65% ee in the alanine that had been produced under these simulated cometary conditions [79].

In interstellar space, chiral molecules including amino acids are known to undergo racemization [80]. In particular, radioracemization is assumed favored to be induced by ionizing α -, β -, γ -, x-, and/or synchrotron radiation in an interstellar context. Racemization phenomena should thus be systematically taken into account for the interpretation of data on enantiomeric enhancements of chiral molecules in interstellar space including comets [80].

Within photosynthetic contexts, it currently remains difficult to determine whether the photochemical asymmetrical induction process is purely the result of photochemical synthesis or is the result of a combination of both photosynthetic and photolytic reactions occurring within the cometary ice simulation. However, further investigation should afford greater understanding of the mechanism of asymmetric photoreactivity of amino acids. What is highly encouraging is that novel techniques such as anisotropy spectroscopy afford innovative ways of understanding exactly how cpl can interact with chiral molecules to produce enantiomeric differentiation and selectivity.

These experiments simulating cometary environments, in which cpl has been shown to have an asymmetrical influence on the enantioselectivity of photochemical reactions, provide an indirect means for furthering understanding of the origin of the homochirality of life's key molecular building blocks. These studies are supported by the meteorite evidence [73]. However, such indirect evidence is less than satisfactory and ultimately the *photochemical* model for life's homochiral origins must be evaluated in situ. Further knowledge about the prebiotic ability of chiral light to differentiate between enantiomers can only come from interstellar environments. This knowledge will potentially be provided by the pioneering space mission ROSETTA, which will land on a cometary nucleus in November 2014. The COSAC experiment that is carried onboard ROSETTA's landing component Philae is equipped to analyze organic molecules in the cometary ices and has been custom-designed to carry out a series of separation, identification, and quantification analyses on any enantiomers found on the cometary body.

4 The ROSETTA Mission and the COSAC Experiment

The European Space Agency (ESA) has been the first space organization to launch missions specifically targeted to study comets in close proximity, although other space agencies have since established their own independent programs [81]. In 1986 the ESA launched its first cometary mission GIOTTO that made a close fly-by of Halley's Comet (1P/Halley) during its 1986 perihelion. This mission also managed to fly in close proximity to another comet, 26P/Grigg-Skjellerup, in 1992. GIOTTO was the first mission to begin successful analysis of the shape and size of both of these cometary nuclei. Apart from the precise dimensional analysis, GIOTTO also provided data on the composition and velocities of dust particles and gases emitted by cometary nuclei [82]. The initial success of GIOTTO therefore inspired the development of a cometary landing mission aiming to touch down directly upon a cometary nucleus. This would provide enhanced understanding of the composition of cometary nuclei. This next generation cometary landing mission, known as ROSETTA, has become a cornerstone mission for the ESA.

4.1 *The Cometary Mission ROSETTA*

ROSETTA was first designed to land on its target comet 46P/Wirtanen [83] but a technical delay with the Ariane 5 launch vehicle postponed the schedule by 1 year and resulted in a change in the target comet. On March 2, 2004, ROSETTA was successfully launched and its new target was chosen to be comet 67P/Churyumov–Gerasimenko [84].

ROSETTA consists of two major mission components – the Rosetta orbiter and the Philae lander. The ROSETTA spacecraft will encounter comet 67P in November 2014 and throughout this same period it will orbit the comet. Once an appropriate landing position has been selected during the orbital reconnaissance, the Philae lander component will be released from the orbiter to descend to the cometary nucleus surface. This descent will take place at a solar distance of 3 astronomical units (AU) under near zero-gravity conditions [85].

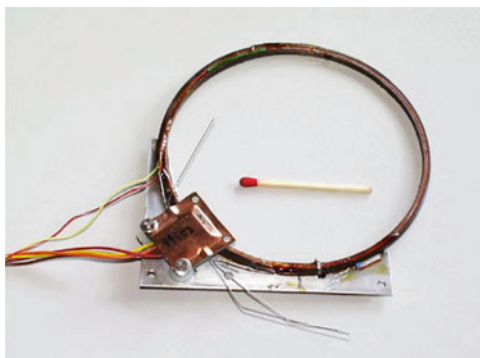
The Philae lander is a unique and highly innovative probe: it will be the first probe ever to land on a cometary nucleus and it will be the first to analyze pristine cometary material *in situ*. One of the main analytical objectives of Philae is to look for any chiral organic compounds [86] extant on the cometary surface. Amino acids are of primary interest due to the fundamental role they play as the building blocks of life's essential proteins. Given that chiral amino acids have been found in meteorites and in cometary ice simulations, it is postulated that enantioenriched amino acids will also be found on 67P. Such a discovery would implicate chiral light as a fundamental differentiating influence between enantiomers in interstellar contexts. Biological homochirality could subsequently have been delivered to Earth by cometary impact events.

In order to determine the organic and chiral composition of comet 67P, gas chromatography-mass spectrometry (GC-TOFMS) instrumentation known as the Cometary Sampling and Composition (COSAC experiment) has been developed and installed on the Philae lander. The COSAC instrument, designed to enable enantiomeric detection and separation in interstellar environments, was constructed at the Max Planck Institute for Solar System Research in Germany [87].

4.2 *The COSAC Experiment*

The COSAC experiment is an enantioselective GC-TOFMS instrumental suite custom-designed to determine the organic composition of the cometary nucleus by separating, identifying, and quantifying individual molecular components from a volatilized sample mixture. Due to the payload requirements of the Philae lander, the COSAC experiment has been miniaturized. It consists of eight independent chromatographic columns of varying lengths and diameters. Each of these columns is capable of separating different classes of organic molecules, such as amino acids, carboxylic acids, alcohols, and hydrocarbons. Three of these eight columns are

Fig. 7 Capillary column including heating device and thermo conductivity detector as manufactured and installed on the chirality module of the COSAC instrument onboard ROSETTA's lander Philae



enantioselective gas-chromatographic columns (Fig. 7) and, in combination with the TOFMS, these columns constitute the chirality module of the COSAC experiment (Fig. 8). Further technical descriptions of the COSAC experiment can be found in Goesmann et al. [88].

After landing on the surface of comet 67P, the Philae instrument Sample Drill and Distribution System (SD2) will extract cometary ice samples from the nucleus and will transfer them into one of two oven types (High Temperature Oven – heats up to 600°C; Medium Temperature Oven – heats up to 180°C) of the COSAC unit to convert the sample into the gaseous phase. The cometary sample will be heated in a step-wise manner and the pressure generated will be monitored throughout the heating process. Complex organic material with low volatility will require two pre-processing techniques: evaporation and pyrolysis in COSAC ovens; and methylation derivatization of the cometary samples with a suitable reagent (DMF-DMA) to a more volatile ester form that can then be injected into the COSAC chromatographic columns.

The enantioselective columns of COSAC have been chosen in order to afford resolution of a wide variety of chiral organic molecules that are anticipated to be found on the nucleus surface of 67P (Table 1).

There are three different chiral stationary phases that have been chosen in order to encompass the potential diversity of compounds to be detected. The Chirasil-Val stationary phase is well-known and belongs to the first generation of enantioselective phases used in enantioselective GC. This stationary phase is thermally stable due to low volatility and high viscosity of its organic siloxane polymer [89]. The chiral side-chain of Chirasil-Val consists of covalently bonded valine-diamide selectors that distinguish between enantiomers on the basis of dipole–dipole and Van der Waal's forces, and mainly hydrogen bonding interactions. The diamide moieties in the stationary phase can be integrated with the amino acid valine in both its L- and its D-configuration (Chirasil-L-Val and Chirasil-D-Val, respectively). The chiral side-chain of the stationary phase has the ability to resolve both amino acid and carboxylic acid enantiomers using two specific hydrogen bonding interactions. A Chirasil-L-Val stationary phase column has therefore been systematically tested under space conditions with respect to

chromatography today [91]. Cyclodextrin stationary phases are composed of glycosidically bonded cyclic oligosaccharides consisting of six, seven, or eight D-glucose units, known as α -, β -, and γ -cyclodextrin respectively. Each of these kinds of cyclodextrin can accommodate varying sizes of analyte molecules and can be successfully applied towards resolving enantiomers. The inclusion interaction between a “guest” analyte and “host” cyclodextrin is not observed in Chirasil-Val phases and is thus useful as an orthogonal characterization tool. The enantioselectivity of a cyclodextrin can furthermore be manipulated by varying the chemical function of the side chain [1].

The Cyclodextrin G-TA stationary phase consists of a 2,6-di-*O*-pentyl-3-trifluoroacetyl derivative of γ -cyclodextrin. It is important for resolution of a wide range of analytes (such as amines, alcohols and diols) with great accuracy [86]. Cyclodextrin G-TA is particularly useful for resolving specific enantiomers with single functional groups: this is not possible using a Chirasil-L-Val stationary phase. γ -Cyclodextrins like Cyclodextrin G-TA can accommodate guest molecules as large as phenanthrene and anthracene. However, Cyclodextrin G-TA is not bonded chemically to the stationary polymer and is hence considered less stable as a stationary phase relative to Chirasil-L-Val against the thermal and radiation damage it will encounter during the 10-year voyage to the comet.

The third enantioselective chromatographic column to be used in the COSAC experiment is the Chirasil-Dex CB phase [38]. Chirasil-Dex CB is composed of permethylated β -cyclodextrin chemically bonded to a polysiloxane phase [92, 93]. It affords excellent resolution of chiral hydrocarbon analytes [94, 95], has been tested under space conditions [88], and has been selected as an enantioselective column on the COSAC experiment to explore possible chiral hydrocarbons present on the cometary surface [39].

One of the most important goals of the chirality module of the COSAC experiment is to identify and resolve chiral amino acids on the surface of comet 67P (see Fig. 9). These amino acids are likely to be present in zwitterionic form. Because they are highly polar, most of the amino acid zwitterions have low volatility. This will make their detection and resolution with gas chromatographic techniques difficult. In order to increase the detectability of these important low volatile molecules, derivatization techniques will be deployed in situ. Methylation derivatization is a commonly used technique for allowing the chromatographic resolution of zwitterionic amino acids. Esters are more volatile and less polar than the original amino acids and they are easily resolved by GC. In order to prevent the use of any solvent on the surface of the cometary nucleus under nearly zero gravity conditions, an alternate “dry” technique of methylation is required. The chosen methylation derivatization technique chosen for the COSAC experiment thus involves the use of dimethylformamide dimethylacetal (DMF-DMA) as a gas-phase derivatization agent which is activated by pyrolysis. Adequate alloy capsules containing DMF-DMA, which melt at 100°C, have been constructed and placed in selected COSAC pyrolysis ovens. Once the pyrolysis oven temperature reaches 100 °C, the alloy will melt and release DMF-DMA, and amino acid analytes from the cometary sample will be converted into their corresponding dimethylamino methyl esters.



Fig. 9 This artist's impression shows the ROSETTA lander Philae anchored to the comet's surface, where it will work for a minimum mission target of 65 h, although its operations may continue for many months. The lander structure contains the COSAC experiment, a multicolumn GC-TOFMS. Chiral stationary phases will afford the separation of enantiomers detected in the cometary ice. The lander also carries a drilling system to collect samples of subsurface material for analysis. Reproduction with permission of ESA/AOES Medialab

These derivatized amino acids will readily be detected by the enantioselective columns present on the COSAC experiment. The DMF-DMA methylation derivatization technique will also be used to convert D,L -carboxylic acids and D,L -hydroxycarboxylic acids into their less polar, more volatile, and chromatographically resolvable D,L -alkyl ester and D,L -methyl ester counterparts respectively [96].

The COSAC experiment has already provided a unique opportunity for technological development. The miniaturization and column design of this novel GC-TOFMS instrumentation have been highly innovative in order to address the requirements of the ROSETTA Mission, and inventive approaches have been taken in the development of methodologies such as the DMF-DMA pyrolytic methylation derivatization procedure. More importantly, the COSAC experiment currently provides the potential to address fundamental questions about the origins of biological homochirality: it will provide a direct means for evaluating the extent to which interstellar cpl can photochemically differentiate between enantiomers of prebiotic small molecules.

5 Future Outlook: Anisotropy Spectroscopy as a Means for Chiral Differentiation

Today, the basic biological coding underpinning proteomes and genomes of various species is well understood [97] and the mechanisms of gene expression are even being artificially modified in order to design and engineer novel proteins with innovative functions [98]. However, the fundamental question of how these

fascinating biological codes evolved in the first place remains unknown. In this pioneering era of genomics and proteomics such continued historical ignorance is rather astonishing.

The *photochemical* model for the origin of life's chirality remains an intriguing hypothesis. There exist many indirect sources of evidence to substantiate the claim that interstellar chiral photons provided the primary source of biological chiral bias and enantiomeric differentiation, including both meteorite analysis data and cometary ice simulation experiments. SRCD spectra of chiral amino acids show maxima and minima in the spectral VUV range from 160 to 220 nm, indicating that cpl irradiation can best induce enantiomeric excesses at these wavelengths. The technique of anisotropy spectroscopy presented here facilitates a direct measurement of the anisotropy factor g over a range of wavelengths and provides a prediction tool for the extent to which cpl can differentiate between small molecule enantiomers and induce ee during enantioselective photolysis. Anisotropy spectroscopy has already revealed that amino acids show anisotropy extrema in the UV range from 185 to 220 nm. This range of wavelengths of chiral light could thus be considered likely to have been an interstellar photochemical source for inducing and triggering biomolecular asymmetry in these basic biological building blocks.

Kuhn pointed out that the optical rotation of a given enantiomer and its susceptibility to differential photochemical change with circular radiation sum to zero over the entire electromagnetic spectrum [99]. Condon supported this assumption by reporting that the CD band areas sum to zero over the spectrum [100]. This effect is known as the Kuhn–Condon zero sum rule [101]. The intensity of cpl capable of inducing enantioselective photolysis in defined interstellar environments is assumed to differ in various wavelength domains due to different radiation sources, interstellar filters, and scattering processes. In agreement with the Kuhn–Condon zero sum rule, this assumption necessitates an $ee \neq 0$ upon irradiation. Thus, after enantioselective photolysis in interstellar space and delivery to the early Earth, enantioenriched small molecules such as amino acids might have provided a non-racemic environment triggering the molecular evolution of primitive cellular life [102]. Anisotropy spectroscopy provides a direct means for quantifying how large an enantioselective differentiating effect the various wavelengths of cpl might have on prebiotic molecules in interstellar space.

Excitingly, there will soon be direct evidence for the extent to which chiral light can photochemically differentiate between enantiomers of small molecules. In 2014 the ROSETTA Philae lander will detach from its orbiter and soft-land on the surface of the nucleus of comet 67P/Churyumov–Gerasimenko, and the COSAC experiment will analyze its chemical composition in situ. The COSAC instrumentation will facilitate the identification of any organic molecules embedded in the cometary ice, focusing specifically on the asymmetry present in the cometary organic molecules it detects. This identification and quantification of enantiomers of chiral organic molecules, including amino acids, in cometary ices by ROSETTA's COSAC experiment will be unprecedented and will significantly contribute to our understanding of the role of chiral light in the origin of life's homochirality.

Acknowledgements We thank the Agence Nationale de la Recherche for grants ANR-07-BLAN-0293 and ANR-12-IS07-0006, the Centre National d'Etudes Spatiales (CNES) for a post-doc scholarship (CM), and the International Max-Planck-Research School (IMPRS) for a PhD scholarship (CG). This work was furthermore supported by the European Community's Integrated Infrastructure Initiative Activity on Synchrotron and Free Electron Laser Science (contract number RII3-CT-2004-506008) and the European Community's Seventh Framework Program (FP7/2007–2013; grant no. 226716).

References

1. Meierhenrich UJ (2008) Amino acids and the asymmetry of life. Springer, Heidelberg
2. Evans AC, Meinert C, Giri C, Goesmann F, Meierhenrich UJ (2012) Chirality, photochemistry and the detection of amino acids in interstellar ice analogues and comets. *Chem Soc Rev* 41:5447–5458
3. Thiemann W (1974) Disproportionation of enantiomers by precipitation. *J Mol Evol* 4:85–97
4. Kondepudi DK, Kaufmann RJ, Singh N (1990) Chiral symmetry breaking in sodium chlorate crystallization. *Science* 250:975–976
5. Yamagata Y (1966) A hypothesis for the asymmetric appearance of biomolecules on Earth. *J Theor Biol* 11:495–498
6. Quack M (2002) How important is parity violation for molecular and biomolecular chirality? *Angew Chem Int Ed Engl* 41:4618–4630
7. Balavoine G, Moradpour A, Kagan HB (1974) Preparation of chiral compounds with high optical purity by irradiation with circularly polarized light, a model reaction for the prebiotic generation of optical activity. *J Am Chem Soc* 96:5152–5158
8. Bailey J, Chrysostomou A, Hough JH, Gledhill TM, McCall A, Clark S, Ménard F, Tamura M (1998) Circular polarization in star-formation region: implications for biomolecular homochirality. *Science* 28:672–674
9. Rau H (2004) Direct asymmetric photochemistry with circularly polarized light. In: Inoue Y, Ramamurthy V (eds) *Chiral photochemistry*. Marcel Dekker, New York
10. Flores JJ, Bonner WA, Massey GA (1977) Asymmetric photolysis of (RS) leucine with circularly polarized ultraviolet light. *J Am Chem Soc* 99:3622–3625
11. Nishino H, Kosaka A, Hembury GA, Aoki F, Kiyouchi K, Shitomi H, Onuki H, Inoue Y (2002) Absolute asymmetric photoreactions of aliphatic amino acids by circularly polarized synchrotron radiation: critically pH-dependent photobehavior. *J Am Chem Soc* 124:11618–11627
12. Meierhenrich UJ, Nahon L, Alcaraz C, Bredehöft JH, Hoffmann SV, Barbier B, Brack A (2005) Asymmetric vacuum UV photolysis of the amino acid leucine in the solid state. *Angew Chem Int Ed Engl* 44:5630–5634
13. Meierhenrich UJ, Filippi J-J, Meinert C, Hoffmann SV, Bredehöft JH, Nahon L (2010) Photolysis of *rac*-Leucine with circularly polarized synchrotron radiation. *Chem Biodivers* 7:1651–1659
14. Oró J (1961) Comets and the formation of biochemical compounds on the primitive Earth. *Nature* 190:389–390
15. Huebner WF, Boice DC (1992) Comets as a possible source of prebiotic molecules. *Origins Life Evol Biosph* 21:299–315
16. Chyba CF, Sagan C (1992) Endogenous production, exogenous delivery and impact-shock synthesis of organic molecules: an inventory for the origins of life. *Nature* 355:125–132
17. Ehrenfreund P (1999) Molecules on a space odyssey. *Science* 283:1123–1124
18. Muñoz Caro GM, Dartois E (2013) Prebiotic chemistry in icy grain mantles in space. An experimental and observational approach. *Chem Soc Rev* 42:2173–2185

19. Buschermöhle M, Whittet DCB, Chrysostomou A, Hough JH, Lucas PW, Adamson AJ, Whitney BA, Wolff MJ (2005) An extended search for circularly polarized infrared radiation from the OMC-1 region of Orion. *Astrophys J* 624:821–826
20. Meinert C, Filippi J-J, Nahon L, Hoffmann SV, d'Hendecourt L, de Marcellus P, Bredehöft JH, Thiemann WH-P, Meierhenrich UJ (2010) Photochirogenesis: photochemical models on the origin of biomolecular homochirality. *Symmetry* 2:1055–1080
21. Meinert C, de Marcellus P, d'Hendecourt LS, Nahon L, Jones NC, Hoffmann SV, Bredehöft JH, Meierhenrich UJ (2011) Photochirogenesis: photochemical models on the absolute asymmetric formation of amino acids in interstellar space. *Phys Life Rev* 8:307–330
22. Meierhenrich U (2013) Amino acids and the asymmetry of life. *Eur Rev* 21:190–199
23. Muñoz Caro GM, Meierhenrich UJ, Schutte WA, Barbier B, Arcones Segovia A, Rosenbauer H, Thiemann WH-P, Brack A, Greenberg JM (2002) Amino acids from ultraviolet irradiation of interstellar ice analogues. *Nature* 416:403–406
24. Bernstein MP, Dworkin JP, Sandford SA, Cooper GW, Allamandola LJ (2002) Racemic amino acids from the ultraviolet photolysis of interstellar ice analogues. *Nature* 416:401–403
25. Meierhenrich UJ, Muñoz Caro GM, Schutte WA, Thiemann WH-P, Barbier B, Brack A (2005) Precursors of biological cofactors from ultraviolet irradiation of circumstellar/interstellar ice analogues. *Chem Eur J* 11:4895–4900
26. Nuevo M, Bredehöft JH, Meierhenrich UJ, d'Hendecourt L, Thiemann WH-P (2010) Urea, glycolic acid, and glycerol in an organic residue produced by ultraviolet irradiation of interstellar/precometary ice analogues. *Astrobiology* 10:245–256
27. De Marcellus P, Meinert C, Nuevo M, Filippi J-J, Danger G, Deboffe D, Nahon L, d'Hendecourt LS, Meierhenrich UJ (2011) Non-racemic amino acid production by ultraviolet irradiation of achiral interstellar ice analogues with circularly polarized light. *Astrophys J Lett* 727:L27
28. Meinert C, Filippi J-J, de Marcellus P, d'Hendecourt LS, Meierhenrich UJ (2012) *N*-(2-Aminoethyl)glycine and amino acids in interstellar ice analogues. *ChemPlusChem* 77:186–191
29. Engel MA, Macko SH (1997) Isotopic evidence for extraterrestrial non-racemic amino acids in the Murchison meteorite. *Nature* 389:265–268
30. Cronin JR, Pizzarello S (1997) Enantiomeric excesses in meteoritic amino acids. *Science* 275:951–955
31. Pizzarello S, Cronin JR (2000) Non-racemic amino acids in the Murray and Murchison meteorites. *Geochim Cosmochim Acta* 64:329–338
32. Meierhenrich UJ, Muñoz Caro GM, Bredehöft JH, Jessberger EK, Thiemann WH-P (2004) Identification of diamino acids in the Murchison meteorite. *Proc Natl Acad Sci U S A* 101:9182–9186
33. Glavin DP, Dworkin JP (2009) Enrichment of the amino acids L-isovaline by aqueous alteration on CI and CM meteorite parent bodies. *Proc Natl Acad Sci U S A* 106:5487–5492
34. Burton AS, Stern JC, Elsila JE, Glavin DP, Dworkin JP (2012) Understanding prebiotic chemistry through the analysis of extraterrestrial amino acids and nucleobases in meteorites. *Chem Soc Rev* 41:5459–5472
35. Giri C, Goesmann F, Meinert C, Evans AC, Meierhenrich UJ (2013) Synthesis and chirality of amino acids under interstellar conditions. *Top Curr Chem* 333:41–82
36. Schulz R, Alexander C, Boehnhardt H, Glassmeier KH (2009) ROSETTA – ESA's mission to the origin of the solar system. Springer, New York
37. Thiemann WH-P, Rosenbauer H, Meierhenrich UJ (2001) Conception of the “Chirality-experiment” on ESA's mission ROSETTA to comet 46P/Wirtanen. *Adv Space Res* 27:323–328
38. Meierhenrich UJ, Thiemann WH-P, Goesmann F, Roll R, Rosenbauer H (2001) Enantiomer separation of hydrocarbons in preparation of Rosetta's “Chirality-experiment. *Chirality* 13:454–457

39. Meierhenrich UJ, Nguyen M-J, Barbier B, Brack A, Thiemann WH-P (2003) Gas chromatographic separation of saturated aliphatic hydrocarbon enantiomers on permethylated β -cyclodextrin. *Chirality* 15:S13–S16
40. Wallace BA (2009) Protein characterization by synchrotron radiation circular dichroism spectroscopy. *Q Rev Biophys* 42:317–370
41. Nishino H, Kosaka A, Hembury GA, Matsushima K, Inoue YJ (2002) The pH dependence of the anisotropy factors of essential amino acids. *J Chem Soc Perkin Trans 2*:582–590
42. Meierhenrich UJ, Filippi J-J, Meinert C, Bredehöft JH, Takahashi J-I, Nahon L, Jones NC, Hoffmann SV (2010) Circular dichroism of amino acids in the vacuum-ultraviolet region. *Angew Chem Int Ed Engl* 49:7799–7802
43. Berova N, Polavarapu PL, Nakanishi K, Woody RW (2012) *Comprehensive chiroptical spectroscopy, applications in stereochemical analysis of synthetic compounds, natural products, and biomolecules*. Wiley, New York
44. Cotton A (1895) Anomalous rotatory dispersion in absorbing bodies. *Compt Rend* 120:1044–1046
45. Kuhn W, Braun E (1929) Photochemische erzeugung optisch aktiver stoffe. *Die Naturwissenschaften* 17:227–228
46. Kuhn W, Knopf E (1930) Photochemische erzeugung optisch aktiver stoffe. *Die Naturwissenschaften* 18:183
47. Burchardt O (1974) Photochemistry with circularly polarized light. *Angew Chem Int Ed Engl* 13:179–185
48. Barron L (2004) *Molecular light scattering and optical activity*, 2nd edn. Cambridge University Press, Cambridge
49. Nishino H, Kosaka A, Hembury GA, Shitomi H, Onuki H, Inoue Y (2001) Mechanims of pH-dependent photolysis of aliphatic amino acids and enantiomeric enrichment of racemic leucine by circularly polarized light. *Org Lett* 3:921–924
50. Norden B (1977) Was photoresolution of amino acids the origin of optical activity in life? *Nature* 266:567–568
51. Tang Y, Cohen AE (2011) Enhanced enantioselectivity in excitation of chiral molecules by superchiral light. *Science* 332:333–336
52. Meinert C, Bredehöft JH, Filippi J-J, Baraud Y, Nahon L, Wien F, Jones NC, Hoffmann SV, Meierhenrich UJ (2012) Anisotropy spectra of amino acids. *Angew Chem Int Ed Engl* 51:4484–4487
53. Cantor CR, Shimmel PR (1980) *Biophysical chemistry part II*. Freeman, New York
54. Rosenfeld L (1929) Quantenmechanische theorie der natürlichen optischen aktivität von flüssigkeiten und gasen. *Z Physik* 52:161–174
55. Miller AJ, Wallace BA (2006) Synchrotron radiation circular dichroism spectroscopy of proteins and applications in structural and functional genomics. *Chem Soc Rev* 35:39–51
56. Osted A, Kongsted J, Mikkelsen KV, Christiansen O (2006) The electronic spectrum of the micro-solvated alanine zwitterion calculated using the combined coupled cluster/molecular mechanics method. *Chem Phys Lett* 429:430–435
57. Fukuyama T, Matsuo K, Gekko KJ (2005) Vacuum-ultraviolet electronic circular dichroism of L-alanine in aqueous solution investigated by time-dependent density functional theory. *Phys Chem A* 109:6928–6933
58. Takahashi J, Shinojima H, Seyama M, Ueno Y, Kaneko T, Kobayashi K, Mita H, Adachi M, Hosaka M, Katoh M (2009) Chirality emergence in thin solid films of amino acids by polarized light from synchrotron radiation and free electron laser. *Int J Mol Sci* 10:3044–3064
59. Tanaka M, Yagi-Watanabe K, Kaneko F, Nakagawa K (2010) Chiroptical study of α -aliphatic amino acid films in the vacuum ultraviolet region. *J Phys Chem* 114:11928–11932
60. Nakamura A, Nishino H, Inoue Y (2001) Synchronous enantiomeric enrichment of both reactant and product by absolute asymmetric synthesis using circularly polarized light. Part 2. Verification of the validity of assuming first-order kinetics upon deriving the equation for the

- relationship between conversion and enantiomeric excess. *J Chem Soc Perkin Trans* 2:1701–1705
61. Soai K, Shibata T, Morioka H, Choji K (1995) Asymmetric autocatalysis and amplification of enantiomeric excess of a chiral molecule. *Nature* 378:767–768
 62. Islas JR, Lavabre D, Grevy J-M, Lamonedá RH, Cabrera HR, Micheau J-C, Buhse T (2005) Mirror-symmetry breaking in the Soai reaction: a kinetic understanding. *Proc Natl Acad Sci U S A* 102:13743–13748
 63. Breslow R, Levine M (2006) Amplification of enantiomeric concentrations under credible prebiotic conditions. *Proc Natl Acad Sci U S A* 103:12979–12980
 64. Klussmann M, Iamura H, Mathew S, Wells D, Pandya U, Armstrong A, Blackmond D (2006) Thermodynamic control of asymmetric amplification of amino acid catalysis. *Nature* 441:621–623
 65. Nordén B, Rodger A, Daffron T (2010) Linear dichroism and circular dichroism. A text-book on polarized-light spectroscopy. RCS Publishing, Cambridge
 66. Miles AJ, Hoffmann SV, Tao Y, Janes RW, Wallace BA (2007) Synchrotron radiation circular dichroism (SRCD) spectroscopy: new beamlines and new applications in biology. *Spectroscopy* 21:245–255
 67. Miles AJ, Janes RW, Brown A, Clarke DT, Sutherland JC, Tao Y, Wallace BA, Hoffmann SV (2008) Light flux density threshold at which protein denaturation is induced by synchrotron radiation circular dichroism beamlines. *J Synchrotron Radiat* 15:420–422
 68. Jordan IK, Kondrashov FA, Adzhubei IA, Wolf YI, Koonin EV, Kondrashov AS, Sunyaev S (2005) A universal trend of amino acid gain and loss in protein evolution. *Nature* 433:633–638
 69. Bredehöft JH, Breme K, Meierhenrich UJ, Hoffmann SV, Thiemann WH-P (2007) Chiroptical properties of diamino carboxylic acids. *Chirality* 19:570–573
 70. Berova N, Nakanishi K, Woody RW (2000) Circular dichroisms. Principles and applications. Wiley-VCH, New York
 71. Kaneko F, Yagi-Watanabe K, Tanaka M, Nakagawa K (2009) Natural circular dichroism spectra of alanine and valine films in vacuum ultraviolet region. *J Phys Soc Jpn* 78(1):013001
 72. Tanaka M, Yagi-Watanabe K, Kaneko F, Nakagawa K (2009) First observation of natural circular dichroism spectra in the extreme ultraviolet region using a polarizing undulator-based optical system and its polarization characteristics. *J Synchrotron Rad* 16:455–462
 73. Oro J, Gibert J, Lichtenstein H, Wikstrom S, Flory DA (1971) Amino-acids, aliphatic and aromatic hydrocarbons in the Murchison meteorite. *Nature* 230:105–106
 74. Bredehöft JH, Meierhenrich UJ (2008) Amino acid structures from UV irradiation in space. In: Takenaka N (ed) Recent developments of chemistry and photochemistry in ice. Transworld Research Network, Kerala
 75. Sandford SA et al (2006) Organics captured from comet 81P/Wild 2 by the stardust spacecraft. *Science* 314:1720–1724
 76. Pracejus H (1967) Asymmetrische synthesen. *Fortschr Chem Forsch* 8:493–553
 77. Greenberg JM (1994) Interstellar dust, chirality, comets and the origins of life: life from dead stars? *J Biol Phys* 20:61–70
 78. Meinert C, Meierhenrich UJ (2012) A new dimension in separation science – comprehensive two-dimensional gas chromatography. *Angew Chem Int Ed Engl* 51:10460–10470
 79. Takano Y, Takahashi J, Kaneko T, Marumo K, Kobayashi K (2007) Asymmetric synthesis of amino acid precursors in interstellar complex organics by circularly polarized light. *Earth Planet Sci Lett* 254:106–114
 80. Trapp O, Schurig V (2001) Interconversion of chiral molecules in interstellar space. *Enantiomer* 6:193–194
 81. Bonnet RM (1985) The new mandatory scientific programme for ESA. *ESA Bull* 43:8–13
 82. Huber MCE, Schwehm G (1991) Comet nucleus sample return: plans and capabilities. *Space Sci Rev* 56:109–115
 83. Schwehm G, Schulz R (1999) ROSETTA goes to Comet Wirtanen. *Space Sci Rev* 90:313–319

84. Glassmeier K-H, Boehnhardt H, Koschny D, Kührt E, Richter I (2008) The ROSETTA mission: flying towards the origin of the solar system. In: Schulz R, Alexander C, Boehnhardt H, Glassmeier K-H (eds) ROSETTA ESA's mission to the origin of the solar system. Springer, New York
85. Bibring J-P, Rosenbauer H, Boehnhardt H, Ulamec S, Biele J, Espinasse S, Feuerbacher B, Gaudon P, Hemmerich P, Klestzki P, Moura D, Mugnuolo R, Nietner G, Pätz B, Roll R, Scheuerle H, Szegö K, Wittmann K, Philae Project Office and the Entire Philae Team (2007) The ROSETTA lander "PHILAE" investigations. *Space Sci Rev* 128:205–220
86. Szopa C, Sternberg R, Raulin F, Rosenbauer H (2003) What can we expect from the in situ chemical investigation of a cometary nucleus by gas chromatography: first results from laboratory studies. *Planetary Space Res* 51:863–877
87. Goesmann F, Rosenbauer H, Roll R, Boehnhardt H (2005) COSAC onboard Rosetta: a bioastronomy experiment for the short-period comet 67P/Churyumov–Gerasimenko. *Astrobiology* 5:622–631
88. Goesmann F, Rosenbauer H, Roll R, Szopa C, Raulin F, Sternberg R, Israel G, Meierhenrich UJ, Thiemann W, Muñoz Caro GM (2007) COSAC, the cometary sampling and composition experiment on PHILAE. *Space Sci Rev* 128:257–280
89. Schurig V (1986) Current methods for determination of enantiomeric compositions (part 3): gas chromatography on chiral stationary phases. *Kontakte* 1:3–22
90. Szopa C, Meierhenrich UJ, Coscia D, Janin L, Goesmann F, Sternberg R, Brun J-F, Israel G, Cabane M, Roll R, Raulin F, Thiemann W, Vidal-Madjar C, Rosenbauer H (2002) Gas chromatography for in situ analysis of a cometary nucleus IV. Study of capillary column robustness for space application. *J Chrom A* 982:303–312
91. Schurig V, Nowotny H-P (1990) Gas chromatographic separation of enantiomers on cyclodextrin derivatives. *Angew Chem Int Ed Engl* 29:939–957
92. Schurig V, Nowotny H-P (1988) Separation of enantiomers on diluted permethylated β -cyclodextrin by high-resolution gas chromatography. *J Chromatogr* 441:155–163
93. Schurig V, Schmalzing D, Mühleck U, Jung M, Schleimer M, Mussche P, Duvekot C, Buyten JC (1990) Gas chromatographic enantiomer separation on polysiloxane-anchored permethyl- β -cyclodextrin (Chirasil-Dex). *J High Res Chromatogr* 13:713
94. Sicoli G, Kreidler D, Czesla H, Hopf H, Schurig V (2009) Gas chromatographic enantioseparation of unfunctionalized chiral alkanes: a challenge in separation science. *Chirality* 21:183–198
95. Schurig V, Kreidler D (2013) Gas-chromatographic enantioseparation of unfunctionalized chiral hydrocarbons: an overview. In: Scriba GKE (ed) *Chiral separations, methods and protocols*, 2nd edn. Humana, Totowa, pp 45–67
96. Meierhenrich U, Thiemann WH-P, Rosenbauer H (2001) Pyrolytic methylation assisted enantioseparation of chiral hydroxycarboxylic acids. *J Anal App Pyrol* 60:13–26
97. Lander ES and the International Human Genome Sequencing Consortium (2001) Initial sequencing and analysis of the human genome. *Nature* 409:860–921
98. Budisa N (2004) Prolegomena to future experimental efforts on genetic code engineering by expanding its amino acid repertoire. *Angew Chem Int Ed Engl* 43:6426–6463
99. Kuhn W (1930) The physical significance of optical rotatory power. *Trans Faraday Soc* 26:293–310
100. Condon EU (1937) Theories of optical rotatory power. *Rev Mod Phys* 9:432–457
101. Mason SF (1997) Extraterrestrial handedness. *Nature* 389:804
102. Meierhenrich UJ, Filippi J-J, Meinert C, Vierling P, Dworkin JP (2010) On the origin of primitive cells – from nutrient intake to elongation of encapsulated nucleotides. *Angew Chem Int Ed Engl* 49:3738–3750

Self-disproportionation of Enantiomers of Enantiomerically Enriched Compounds

Alexander E. Sorochinsky and Vadim A. Soloshonok

Abstract This review describes self-disproportionation of enantiomers (SDE) of non-racemic mixtures, subjected to distillation, sublimation, or chromatography on achiral stationary phase using achiral eluent, which leads to the substantial enantiomeric enrichment and corresponding depletion in different fractions, as compared to the enantiomeric composition of the starting material. This phenomenon is of a very general nature as SDE has been reported for different classes of chiral organic compounds bearing various functional groups and possessing diverse elements of chirality. The literature data discussed in this review clearly suggests that SDE is typical for enantiomerically enriched chiral organic compounds and special care should always be taken in evaluation of the stereochemical outcome of enantioselective reactions as well as determination of enantiomeric ratios of non-racemic mixtures of natural products after any purification process. The role of molecular association of enantiomers on the magnitude and preparative efficiency of SDE, as a new, nonconventional method for enantiomeric purifications, is emphasized and discussed.

Keywords Achiral chromatography · Chiral recognition · Distillation · Physicochemical phase transitions · Sublimation

Contents

1	Introduction	302
2	Examples of SDE via Distillation; Liquid–Vapor Phase Transition	303
2.1	α-Hydroxy Acids	304
2.2	α-Amino Acids	304

A.E. Sorochinsky
Faculty of Chemistry, Department of Organic Chemistry I, University of Basque Country
UPV/EHU, 20018 San Sebastian, Spain

V.A. Soloshonok (✉)
IKERBASQUE, Basque Foundation for Science, 48011 Bilbao, Spain
e-mail: vadym.soloshonok@ehu.es

3	Examples of SDE via Sublimation; Solid–Vapor Phase Transition	305
3.1	Carboxylic Acids	305
3.2	α -Hydroxy Acids and Their Derivatives	306
3.3	α -Amino Acids	309
3.4	Sulfides	314
3.5	Aromatics	314
3.6	Rational Application of SDE via Sublimation: A Novel Methodological Dimension for Enantiomeric Purifications	315
4	Examples of SDE via Achiral Chromatography	316
4.1	Amides	316
4.2	Alcohols and Phenols	320
4.3	Ketones	325
4.4	Carboxylic Acids and Esters	326
4.5	Sulfoxides	327
4.6	α -Amino Acids and Dipeptides Derivatives	329
4.7	Heterocycles	331
5	Conclusions and Outlook	335
	References	335

Abbreviations

MOM	Methoxymethyl
PMB	4-Methoxyphenyl
SEC	Size-exclusion chromatography
Tol	4-methylphenyl

1 Introduction

Self-disproportionation of enantiomers (SDE) is a new and still evolving concept that has been invoked to provide for most accurate and generalized descriptions of nonlinear behavior of non-racemic (enantiomerically enriched, scalemic) compounds. One of the basic principles of SDE is that non-racemic compounds should be viewed as a mixture of racemate with the excess enantiomer in line with the definition of the enantiomeric excess (ee), that is in contrast to the more prevailing definition of a non-racemic compound as a mixture of unevenly proportioned enantiomers. The fundamental difference between these viewpoints is that a mixture of enantiomers should show linear behavior with the original ratio of enantiomers being unchanged. In sharp contrast, a mixture of racemate with the excess enantiomer is expected to undergo disproportionation, producing enantiomerically enriched and correspondingly depleted fractions, relative to the original enantiomeric composition, in purification processes. The ultimate outcome

of this process is a complete separation of racemic and enantiomerically pure components of the original mixture. That is the second principle of SDE, suggesting that enantiomerically enriched compound, under spontaneous or carefully designed conditions, will eventually produce fractions of racemic and enantiomerically pure forms. The third principle of SDE is its ultimately general nature, suggesting that absolutely any type of chiral non-racemic compound will undergo SDE regardless of its structure and functionalization. The structural features of a given compound will only influence a magnitude of SDE – the efficiency and ease of a separation of racemate from the excess enantiomer.

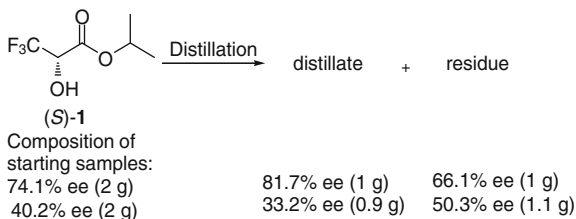
There are three major areas of SDE manifestation: gravitational field, physico-chemical phase transitions, and achiral chromatography. SDE in gravitational fields is based on the different densities of racemic and enantiomerically pure crystals resulting in different rates of precipitation or behavior in a centrifuge. In the case of phase transitions, the mechanism of SDE is not uniform and depends on the type of transition. Basically, racemic and enantiomerically pure forms have different physicochemical properties and will therefore behave differently (rates) under the conditions of phase transition, leading to their separation. Mechanistically, the case of achiral chromatography is the most difficult as, besides homo-/heterochiral intermolecular interactions, there are also interactions of a chiral compound with solvent and stationary phase. However, basically the origin of SDE in this case is the formation of homo-/heterochiral high-order species behaving differently as compared with the corresponding monomers.

In this chapter we provide the most detailed and up-to-date account of all examples reported in the literature of SDE via phase transition and achiral chromatography. The major goal of this chapter is to bring the promising and multidisciplinary potential of SDE to the attention of the chemical community and to highlight its generality and the various forms of its manifestation. We also hope that this chapter will stimulate greater awareness, intellectual interest, new ideas, and further research into this fascinating and important, though challenging, field of scientific endeavor.

2 Examples of SDE via Distillation; Liquid–Vapor Phase Transition

As a high-energy process, distillation generally does not favor formation of homo-/heterochiral dimers/oligomers and early examples of insignificant enantiomeric enrichment via distillation mentioned in some articles [1–4] have been received quite sceptically [5, 6]. However, more recently reported new results confirmed that the enantiomeric composition of enriched mixtures can be changed under a distillation process.

Scheme 1 SDE of isopropyl (3,3,3-trifluoro)lactate (*S*)-**1** via distillation



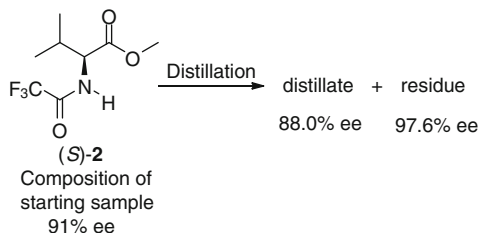
2.1 α -Hydroxy Acids

One of the most thoroughly studied examples is a distillation of isopropyl (3,3,3-trifluoro)lactate. It was shown that distillation of isopropyl (3,3,3-trifluoro)lactate (*S*)-**1** of 74.1% ee resulted in noticeably optically enriched distillate (81.7% ee) and more racemic residue (66.1% ee) (Scheme 1) [7]. It should be emphasized that the observed magnitude of SDE ($\Delta ee = 15.6\%$) renders this distillation procedure as a potential enantiomeric purification method comparable with crystallization. In contrast, the distillation of (*S*)-**1** of 40.2% ee resulted in enantiomerically depleted distillate (33.2% ee) and enantiomerically enriched residue (50.3% ee). Moreover, boiling points of the (3,3,3-trifluoro)lactate varied by 43°C depending on its enantiomeric excess. This change of boiling point, depending on the initial enantiomeric excess of isopropyl (3,3,3-trifluoro)lactate, indicated a very complex mechanism of SDE via distillation. Low-angle X-ray diffraction measurement has shown that isopropyl (3,3,3-trifluoro)lactate was highly associated by hydrogen bonding in the liquid state [8–10]. The IR spectra of the compound having different enantiomeric excesses also suggested contribution of hydrogen bonding in the liquid state. Therefore the phenomena could be caused by homo-chiral and hetero-chiral hydrogen bonding association in the system. The energetic difference between the homo-chiral and hetero-chiral hydrogen bonding association caused by the electrostatic repulsion of negatively charged trifluoromethyl groups may explain the observed, quite unusual difference of the boiling points depending on enantiomeric excess of isopropyl (3,3,3-trifluoro)lactate.

2.2 α -Amino Acids

The distillation of *N*-trifluoroacetyl valine methyl ester (*S*)-**2** of 91% ee affording distillate of 88.0% ee and residue of 97.6% ee has been reported by Koppenhoefer and Trettin (Scheme 2) [11]. The authors did not observe a large change in boiling point between the racemate and highly enriched enantiomer of *N*-trifluoroacetyl valine methyl ester. The trifluoroacetyl group in this case increases both the volatility of compound **2**, allowing its distillation at lower temperatures, and the hydrogen-donor ability of the trifluoroacetamide moiety for hydrogen bonding with the carbonyl group, thus providing a basis for strong intermolecular interactions.

Scheme 2 SDE of *N*-(trifluoroacetyl)-Val-OMe (*S*)-**2** via distillation



The gas chromatographic ee determination on Chirasil-L-Val and Chirasil-D-Val [11] can be considered as very reliable.

3 Examples of SDE via Sublimation; Solid–Vapor Phase Transition

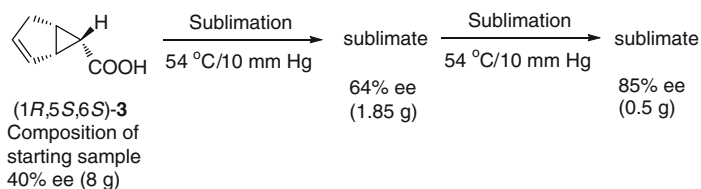
The separation of racemate from the excess enantiomer by sublimation is generally a complex phenomenon which can be used as a new enantiomeric purification method for chiral organic compounds possessing different crystallographic structures of racemic and enantiomeric pure crystals. The crystallographic lattice energy and overall stability of crystals may play the most important role in distribution of the enantiomers between the solid and vapor phases.

3.1 Carboxylic Acids

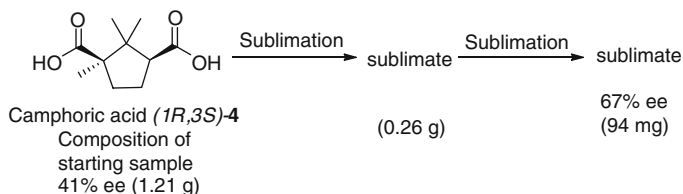
The systematic study dealing with sublimation of enantiomerically enriched samples of carboxylic acids has shown that partial sublimation of bicyclo[3.1.0]hex-2-ene-6-carboxylic acid (1*R*,5*S*,6*S*)-**3** of 40% ee in sublimation apparatus under vacuum gave the first sublimed fraction of markedly increased enantiomeric excess (Scheme 3) [12]. Resubmission of this fraction to a sublimation procedure under the same conditions allowed for a further increase of enantiomeric excess to 85% ee. Additional experiments have demonstrated that neither rearrangement nor new product formation has occurred during the sublimation procedure. The authors also emphasized the lower melting point (72–73°C) of enantiomerically pure crystals of acid **4** compared to that of the racemic form (89–90.5°C), suggesting that “the modification with the lower melting point should exhibit the greater volatility and should sublime preferentially.”

Attempts to extend this approach to other carboxylic acids also worked well. Two sublimations starting with 1.2 g of camphoric acid (1*R*,3*S*)-**4** of 41% ee afforded 9.4 mg of material of 67% ee (Scheme 4).

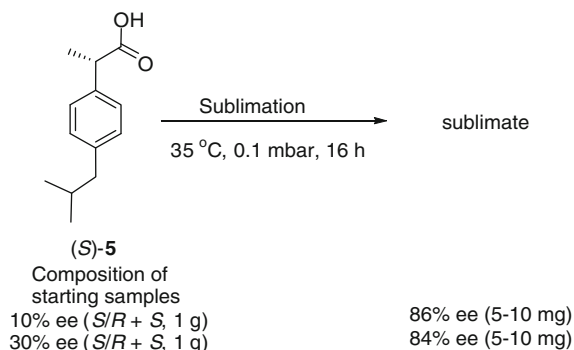
The partial sublimation of carboxylic acid (*S*)-**5** with various enantiomeric excess was performed at 35°C in vacuo of 0.1 mbar for 16 h, allowing about 1%



Scheme 3 SDE of bicyclo[3.1.0]hex-2-ene-6-carboxylic acid (1*R*,5*S*,6*S*)-**3** via sublimation



Scheme 4 SDE of *d*-camphoric acid **4** via sublimation

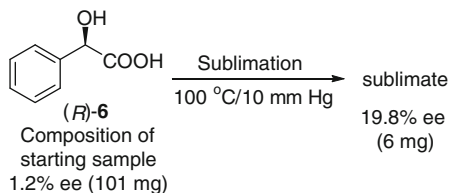


Scheme 5 SDE of (*S*)-**5** via sublimation

(5–10 mg) of the starting mixture to sublime (Scheme 5) [13]. As emphasized by the authors, the sublimation method could be a very efficient and simple approach to obtain on a preparative level samples of compound (*S*)-**5** of about 85% ee starting from mixtures of relatively low (10–30% ee) enantiomeric excess. The eutectic composition for the solid **5** has been determined at 90% ee and observed results have been explained by the preferential sublimation of a vapor eutectic.

3.2 α -Hydroxy Acids and Their Derivatives

Enantiomeric purification via sublimation of mandelic acid (*R*)-**6** demonstrated that a sample of 60.2% ee resulted in fractions of 52.5% ee, 60.0% ee, 64.1% ee, and 74.3% ee. On the other hand, sublimation of a sample of 20.7% ee gave fractions of

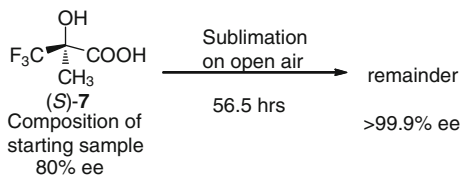
Scheme 6 SDE of mandelic acid (*R*)-**6** via sublimation

37.2% ee, 31.5% ee, 25.2% ee, 16.0% ee, and 4.7% ee [12]. Thus, for the first time it was observed that increase or decrease of the ee of the sublimate depended on the enantiomeric excess of the starting mixture. In order to explain these unexpected results the authors proposed that the sublimation is controlled by the eutectic ee of the chiral compound. Another important demonstration the authors did in this work was showing how efficient a sublimation method can be when there is a need to obtain material of high enantiomeric excess starting from material of low enantiomeric excess. Sublimation of acid (*R*)-**6** of only 1.2% ee allowed for quick and convenient preparation of a sample of 19.8% ee containing practically all of the excess enantiomer initially present in the starting material (Scheme 6). Attempts to use fractional crystallization were very inefficient in this case, thus highlighting the advantage of sublimation over crystallization as an enantiomeric purification method. Reinvestigation of the partial sublimation of mandelic acid (*S*)-**6** with various enantiomeric excesses allowed the authors to suggest that the ees of sublimes were controlled by the formation of a gas phase with a eutectic composition independent of the enantiomeric excess of the starting mixture [13].

The first example of complete enantiomeric purification via sublimation was demonstrated using α -(trifluoromethyl)lactic acid **7** [14]. Due to the high volatility of compound **7**, the sublimation took place at ambient temperature and atmospheric pressure. It was shown in a series of experiments that racemic crystals of α -(trifluoromethyl)lactic acid **7** sublimed about 1.5 times faster than the enantiomerically pure crystals under the conditions of zero-order kinetics. This unusual order of sublimation led to complete (>99.9% ee) purification of the sample of α -(trifluoromethyl)lactic acid (*S*)-**7** with enantiomeric excess of 80% ee without any special condition apart from being exposed to the open atmosphere (Scheme 7).

It is interesting to note that enantiomerically pure crystals of compound **7** have a higher melting point than that of the racemic form (110°C and 88°C, respectively). The difference in melting points may suggest that the racemic crystals are less stable, although calculations of the crystallographic lattice energy gave inconclusive results [15]. Since spectroscopic study of homo- and heterochiral dimers of acid **7** in the gaseous phase confirmed noticeably higher volatility of the racemic form [16], it is reasonable to suppose that the α -(trifluoromethyl)lactic acid sublimed as dimers. Finally, the molecular arrangement and packing in crystals of the racemate and enantiomer might be a physico-chemical reason for the observed differences in the sublimation rates as well as the melting points of the racemic and

Scheme 7 SDE of α -(trifluoromethyl)lactic acid (*S*)-**7** via sublimation



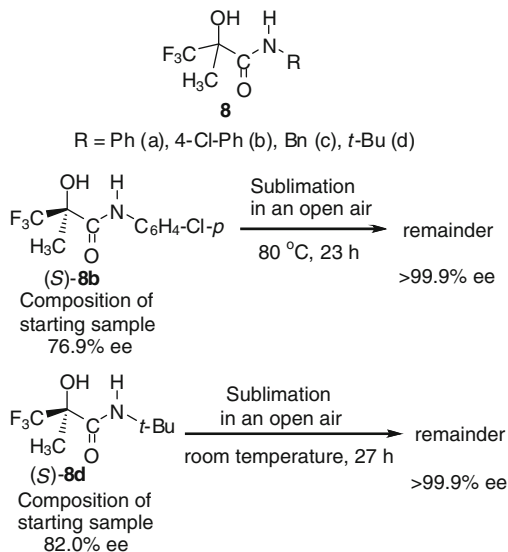
optically pure compounds. While the crystal lattice of the racemate is composed of heterochiral dimers with two hydrogen bonds between (*R*) and (*S*) enantiomers, the molecules in the crystal of the (*S*) enantiomer form four hydrogen bonds with another four adjacent molecules. Moreover, the F...F contact of the CF₃ groups in the racemate is closer than that in the enantiomerically pure crystal, for which no appreciable interactions are observed.

According to the previous example, amide derivatives of α -(trifluoromethyl)lactic acid **8a–d** possessed relatively high volatility, allowing one to study their SDE via sublimation from room temperature to 80°C and atmospheric pressure (Scheme 8). Compounds **8a–d** are easily available in racemic and enantiomerically enriched forms, highly crystalline, and chemically and configurationally stable. Study of their SDE via sublimation is not complicated by any problems with chemical decomposition, which is a very important factor in collecting reliable and reproducible results. Similar to α -(trifluoromethyl)lactic acid **7**, racemic crystals of **8a–c** sublimed faster than enantiomerically pure crystals of (*S*)-**8a–c** and the difference in rates of sublimation markedly depended on the amide substituent [17]. For example, racemic **8a** and **8b** sublime about 1.4 and 1.6 times faster than the corresponding enantiomerically pure counterparts. These differences in the rates of sublimation suggest that the sublimed material undergoes optical depletion while the remainder is expected to be more enantiomerically enriched. Thus a sample of *p*-(chloro)phenyl amide derivative (*S*)-**8b** of 76.9% ee was easily transformed to the enantiomerically pure form after 23 h via sublimation conducted at 80°C. The *t*-Bu amide derivative (*S*)-**8d** could sublime efficiently at room temperature under normal pressure. The sublimation starting from a sample of 82.0% ee resulted in an increase of the enantiomeric excess of the remainder up to >99% ee after 27 h.

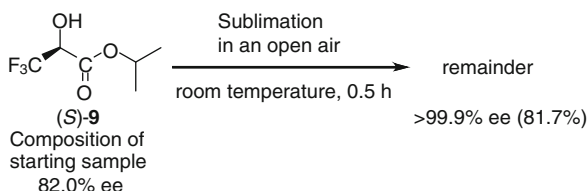
In a similar manner, the racemic form of isopropyl (3,3,3-trifluoro)lactate **9** sublimed at a substantially higher rate compared to the optically pure form, at temperature 23–25°C and normal atmospheric pressure [18]. Thus, regardless of the starting enantiomeric excess of the enriched mixtures ranging from 20.8% ee to 79.4% ee, more racemic fractions sublimed faster, leaving behind an enantiomerically pure remainder. In a typical experiment, sublimation of compound (*S*)-**9** of 79.4% ee allowed the preparation of an enantiomerically pure sample in 81.7% yield in 30 min (Scheme 9). Sublimation of the samples of lower ee was less efficient in terms of the yield of enantiomerically pure compound (*S*)-**9**.

In contrast to the results reported for isopropyl 3,3,3-(trifluoro)lactate **9**, the opposite order of sublimation between racemic and enantiomerically pure crystals

Scheme 8 SDE of α -(trifluoromethyl)lactic acid amide derivatives (*S*)-**8a–d** via sublimation



Scheme 9 SDE of 3,3,3-(trifluoro)lactate (*S*)-**9** via sublimation

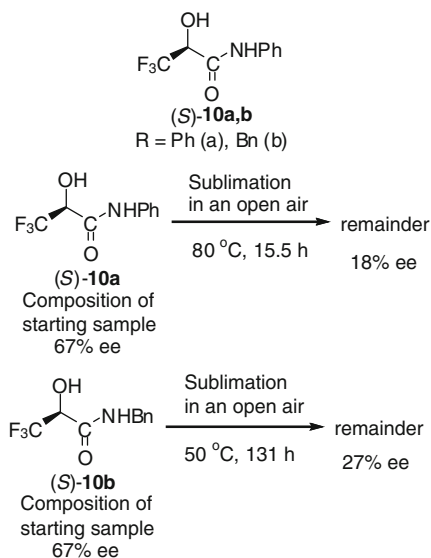


was observed for amide derivatives of 3,3,3-trifluorolactic acid **10a** and **10b** (Scheme 10) [19]. Thus, racemic crystals of **10a** sublimed substantially slower than the enantiomerically pure crystals of (*S*)-**10a**; the ratio of rates was 1.6/1. When a sample of (*S*)-**10a** of 67% ee was subjected to sublimation at 80°C and atmospheric pressure, the enantiomeric excess of the remainder gradually decreased to 18% ee after 15.5 h. Similarly, when a sample of benzyl amide (*S*)-**10b** of 67% ee was subjected to sublimation at 50°C, the enantiomeric excess optical purity of the remainder gradually decreased to 27% ee after 131 h. In these cases the sublimed material was enantiomerically enriched, leaving behind eventually racemic remainder. Therefore enantiomeric purification in such cases would require repeated collection of the sublimate.

3.3 α -Amino Acids

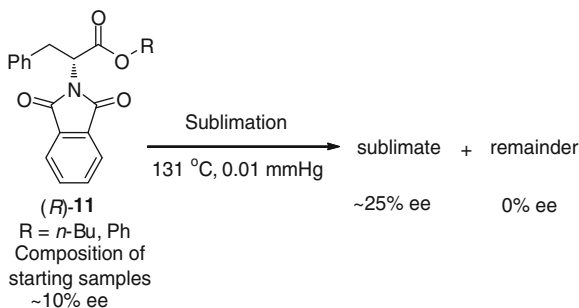
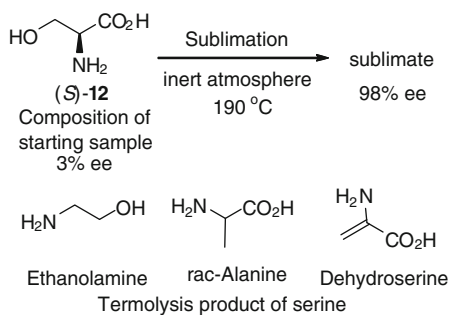
Enantiomeric purification of α -amino acids via sublimation is a very attractive and inspiring subject. This process can take place in the universe (cosmos) provided some heat from a nearby star, and this can be the most probable mechanism

Scheme 10 SDE of 3,3,3-trifluorolactic acid amide derivatives (*S*)-**10a** and **b** via sublimation



explaining the relatively high enantiomeric enrichment discovered in meteorites [20]. The first example of SDE of α -amino acids via sublimation described the purification of enantioenriched phenylalanine derivatives (*R*)-**11** (Scheme 11) [21]. It was observed that sublimation of (*R*)-**11** of about 10% ee gave a completely racemic remainder. Careful investigation of the sublimation procedure revealed that the initial sublimed fraction was of noticeably higher (~25% ee) enantiomeric excess. No other details were reported in this work, but it should be emphasized that racemic crystals have a higher melting point than that of the optically pure form.

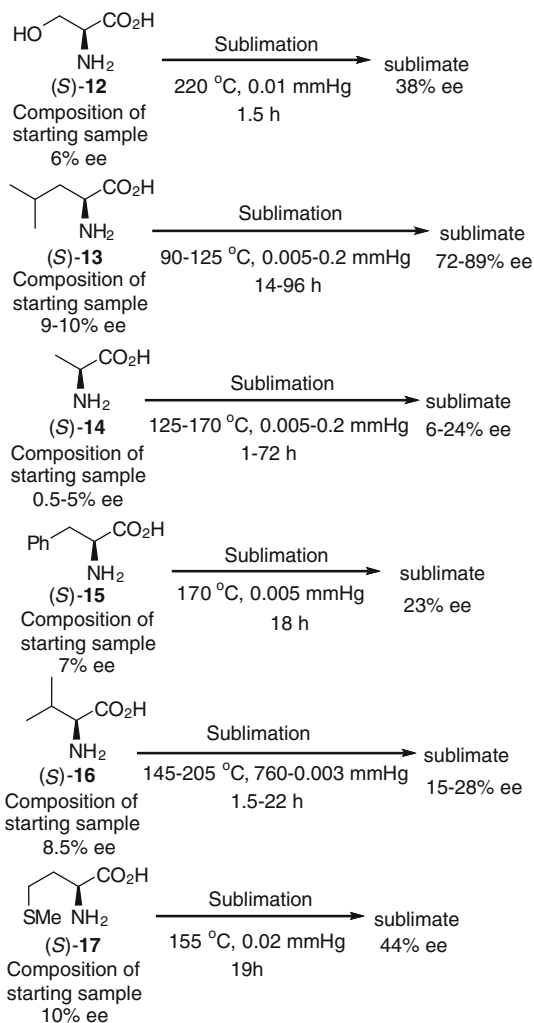
Another example in this area concerns SDE via sublimation of enantiomerically enriched samples of serine [22]. Heating serine (*S*)-**12** with starting enantiomeric excess of 3–75% ee to temperature 175–230°C gave sublimed material highly enriched in the major enantiomer. For example, when amino acid (*S*)-**12** of 3% ee was heated at 190°C in a flow of nitrogen for 2 h, the collected sublimed material showed enantiomeric purity up to 98% ee (Scheme 12). The total amount of collected sublimate ranged from 1 to 3 mg and was contaminated by substantial amounts of thermolysis (decomposition) products which increased with temperature. It should be noted that the samples under study were prepared by mixing (*S*)-**12** and (*R*)-**12** in required proportions, representing the case of conglomerates sublimation. On the other hand, a noticeably different stereochemical outcome was observed using the samples prepared by crystallization from water. For example, the sample of (*S*)-**12** of 3% ee at 205°C gave sublimed material of 61% ee while (*R*)-**12** of 3% ee yielded a sublimate of 47% ee. Interestingly, very insignificant SDE via sublimation was observed for other amino acids, such as alanine (starting 8% ee; sublimed 4% ee) and threonine (starting 7% ee; sublimed 1.2% ee). It was hypothesized that formation of serine specific homochiral clusters in the gas phase [23, 24] was responsible for the enrichments of the ee of the sublimate.

Scheme 11 SDE of α -amino ester (*R*)-**11** via sublimation**Scheme 12** Self-disproportionation of enantiomers of serine (*S*)-**12** via sublimation

In a subsequent publication, studying SDE via sublimation of a wider range of amino acids with a very low initial ee value afforded quite different results [25]. For example, sublimation of leucine (*S*)-**13** of 9–10% ee gave the sublimate of 72–89% ee depending on the temperature and pressure used (Scheme 13). These samples were prepared by mixing the racemic compound with excess pure *S*-enantiomer. Importantly, enantiomerically enriched alanine **14**, phenylalanine **15**, serine **12**, valine **16**, and methionine **17** gave sublimed material of higher enantiomeric purity than that of the starting mixtures when heating in sublimation apparatus under vacuum. As in the previous study [23, 24], only a small fraction of the sample underwent sublimation and the stereochemical outcome markedly depended on the sublimation temperatures. The authors concluded that the enantioenrichment of amino acids by sublimation is likely caused by intermolecular interactions.

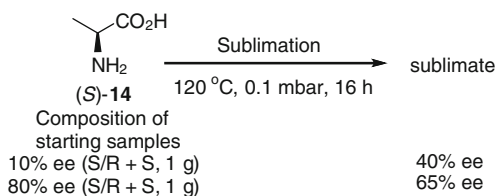
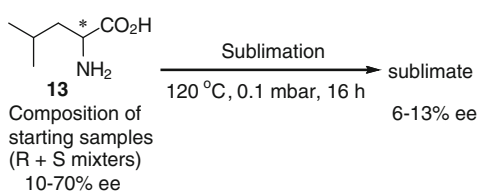
The reproducibility of the experiments on SDE via sublimation of amino acids was addressed in separate work [26]. In order to generate comparable results, the authors defined standard conditions in terms of the amount of a sublimating mixture (1 g), pressure (0.1 mbar), temperature (120°C), and time of sublimation (16 h). These experimental conditions gave only very small amounts (5–10 mg) of sublimate (0.5–1%) for analysis. Amino acids leucine, alanine, and proline were chosen for the study based on their stability under the standard conditions. The mixtures of various ee percentages were prepared by mixing racemic crystals with the corresponding enantiomerically pure form. The major conclusion of this work was as follows: when the enantiomeric purity of the starting mixture is $\leq 50\%$ ee,

Scheme 13 SDE of various α -amino acids via sublimation



the sublimate obtained is also of less than 50% ee, although its ee value is greater than that of the starting compound. When the enantiomeric purity of the starting mixture is $\geq 50\%$ ee, the percentage ee of the obtained sublimate is also higher than 50% ee, although its ee value is lower than that of the starting compound. For example, sublimation of alanine (S)-14 of 10% ee gave sublimate of 40% ee, while the sublimation of mixture of 80% ee gave the sublimed alanine (S)-14 of 65% ee (Scheme 14). These experiments were reproduced several times with a deviation from the average of about $\pm 5\%$.

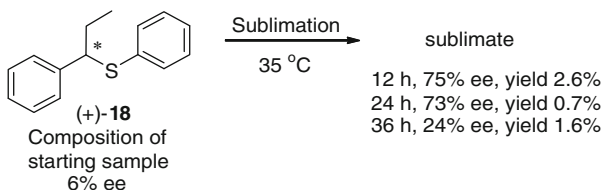
Using other experimental conditions, and particularly starting from the mixtures of (R)- and (S)-enantiomers, led to a strong decrease of the ee of the sublimate. For example, independent of the starting ee (20–70%) of enantioenriched leucine 13,

Scheme 14 SDE of alanine
(*S*)-**14** via sublimation**Scheme 15** SDE of leucine
13 via sublimation

the first sublimate was obtained with 8–13% enantiomeric excess (Scheme 15). The sublimation in these cases appears to be controlled only by the saturated vapor pressures at the temperature of sublimation of the (*R*)- and (*S*)-leucine, which are equal.

Very recently an unusual procedure for the conversion of valine **16** – which crystallizes as a racemic compound – by sublimation into a racemic conglomerate that, upon further sublimation, is enriched in the major enantiomer has been described [27]. The experiments were carried out in tightly closed vessels. The crystals of valine **16** at the bottom of the vessels were heated at 430°C. When almost all solid material had sublimed and condensed on the walls of the vessel, the initially formed sublimation ring moved to higher parts of the vessel. Initially it was shown by powder X-ray diffraction spectra that the racemic crystals of valine are transformed into a racemic conglomerate during the sublimation–condensation process. After initial sublimation of valine **16** of 40% ee prepared by mixing the racemic (*S/R*) compound with excess pure (*S*)-enantiomer, chiral HPLC analysis did not reveal any enantioenrichment. However, when the subsequent sublimation occurred to the higher parts of the vessel, the sublimate was found to be enriched up to 56% ee. Furthermore, similar enrichment was observed from starting material prepared by mixing the appropriate amounts of pure (*S*)- and pure (*R*)-enantiomers. Examination of the enantioenrichment at different positions of the sublimate revealed an even greater increase of the ee up to 80% at the bottom of the sublimate. The total amount of recovered sublimated material was almost 100%, suggesting overall enantioenrichment of the starting sample. Similar amplification with slightly lower ees was observed when the experiment was repeated in an open system. Thus the sublimation of enantioenriched valine involves recrystallization from a racemic compound into a racemic conglomerate followed by substantial enrichment in the enantiomeric excess under prolonged heating.

Scheme 16 SDE of α -ethylbenzylphenyl sulfide **18**



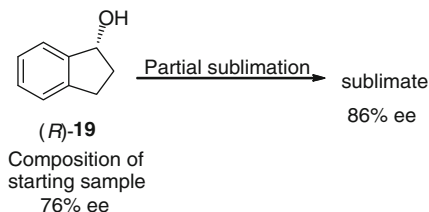
3.4 Sulfides

Observation of SDE via sublimation was also reported during work on isolation of enantioenriched α -ethylbenzylphenyl sulfide **18** [28]. The authors noticed that enantiomeric purity of the samples of compound **18** obtained depended on the time for which the samples were subjected to routine drying in vacuum. Detailed analysis of the sublimation procedure revealed that the fractions of sulfide **18** subliming faster had substantially higher enantiomeric excess compared to the original sample, and enantiomeric purity of successive fractions of sublimed material gradually decreased (Scheme 16). Starting from a sample of 12% ee, complete optical depletion of the remainder was observed after 85 h of sublimation at 35°C. In this case the faster subliming enantiomerically pure crystals of compound **14** have a lower melting point (32–35°C) compared to the racemate (39–42°C). An important observation was made by conducting a sublimation experiment at 48°C. At this temperature the sample subjected to sublimation was completely molten and the sublimate as well as the remainder had the same enantiomeric purity as the original sample. This experiment demonstrated the importance of maintaining the crystalline state of a compound during sublimation. The authors also conducted a series of experiments comparing sublimation and fractional crystallization for the most efficient separation of the racemic form from the excess enantiomer. The sublimation method was more efficient when taking into consideration the yield and enantiomeric excess of material obtained.

3.5 Aromatics

During work on catalytic asymmetric hydroboration/oxidation of vinylarenes, low reproducibility in ee percentage of (*R*)-2,3-dihydro-1*H*-inden-1-ol **19** was observed (Scheme 17) [29]. Careful analysis of the experimental procedure has shown that the original ee of 76% can be increased to 86% by partial sublimation of the volatile secondary alcohol during the removal of the solvent in a rotary evaporator. Since the dihydroindanol **19** crystallizes as a conglomerate the authors suggested that the vapor phase should be racemic, thus allowing enantiomeric purification of the remainder.

This and previous examples should provide significant warning to chemistry practitioners that simple and quite routine procedures, such as drying a sample in

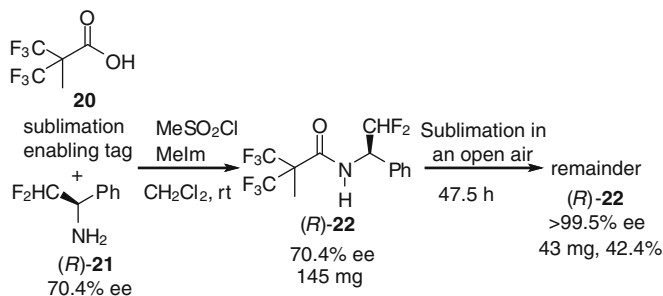
Scheme 17 SDE of
(*R*)-dihydroindenol **19**

vacuum, can result in altered enantiomeric purity. All chemists must be aware of the vagaries of SDE via sublimation to avoid unfortunate errors in reporting the stereochemical outcome of asymmetric catalytic reactions.

3.6 Rational Application of SDE via Sublimation: A Novel Methodological Dimension for Enantiomeric Purifications

SDE via sublimation as an enantiomeric purification procedure can be used only for crystalline and relatively volatile compounds. In a recent study hexafluoropivalic acid **20** was proposed as sublimation-enabling tag which could impart the required physicochemical properties to organic compounds [30]. Racemic and enantiomerically pure amide derivative **22** showing high crystallinity and reasonable volatility due to the presence of two trifluoromethyl groups was prepared from acid **20** and liquid α -(phenyl)ethylamine (*R/S*)-**21** or (*R*)-**21** under the standard conditions usually used for the formation of amide bonds. When compound (*R*)-**22** of 70.4% ee was evenly spread over a Petri dish and left on a bench in open air for 47.5 h the remaining sample was collected in 42.4% yield and its enantiomeric purity was found to be >99.5% ee (Scheme 18).

Attempts to interpret or predict the stereochemical outcome of sublimation of enantiomerically enriched organic compounds can be summarized as follows: (1) “the eutectic composition is predicted to sublime preferentially regardless of the initial composition” [12, 31, 32]; (2) “the modification with the lowest melting point should exhibit the greater volatility and should sublime preferentially” [12, 31, 32]; (3) the nature of the intermolecular interactions may be a reason for the observed differences in the sublimation rates as well as the melting points of the racemic and enantiomerically pure compounds [14, 25]; (4) in the sublimation of “kinetic conglomerates” a mixture of enantiopure *R* and *S* crystals behaves rather as a conglomerate before solid–solid equilibration is attained [33, 34]. However, recent observations have shown that none of them can be taken as general rules and interpretations largely depend on sample preparation. Undoubtedly SDE via sublimation still holds a lot of exciting possibilities in terms of both fundamental knowledge and practical applications.



Scheme 18 Synthesis and sublimation of amide (*R*)-22

4 Examples of SDE via Achiral Chromatography

In general, the interactions, which may lead to molecular associations of different properties in solution, are usually very weak, and therefore their detection and evaluation is not an easy task. However, these associations are believed to be responsible for several remarkable phenomena observed for nonracemic compounds, such as nonlinear behavior of optical rotation [35–38] and UV absorbance [39], as well as nonlinear effects in asymmetric catalysis [40–43] and NMR spectroscopy. The first physical observation of the macromolecular associations of enantiomers was observed when studying ^1H NMR spectra of non-racemic dihydroquinines [44]. Two sets of peaks for some protons were detected with peak areas proportional to the relative ratio of the enantiomers. Further ^1H NMR examples of this type of association were reported for the nonracemic samples of certain chiral compounds such as 1,2-diols [45], carboxamides [46, 47], dicarboxamides [48], phosphinamides [49], and phosphinothioic acids [50], all of which can easily form relatively strong intermolecular hydrogen bonds. Since then many publications on the separation of an excess enantiomer from the racemate of various structural types of organic compounds under HPLC, MPLC, flash and regular chromatography have appeared. However, there is clearly unexplored potential of SDE via achiral chromatography as a new enantiomeric purification technique.

4.1 Amides

Theoretical considerations [51–55] clearly indicate that SDE under the conditions of achiral chromatography should be expected for organic amides bearing hydrogen-bond donor (NH) and acceptor (C=O) sites. Consequently, formation of homo-/heterochiral associations, necessary for the manifestation of SDE, would be facilitated by strong hydrogen bonding between N–H...O atoms. Based on these considerations, SDE of *N*-acetyl derivatives of chiral amines **23a–d** under achiral

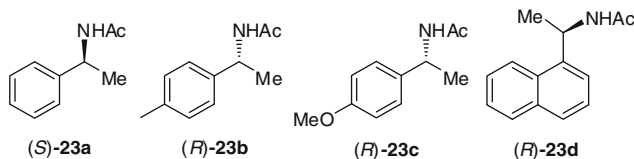


Fig. 1 Structures of amides **23a–d**

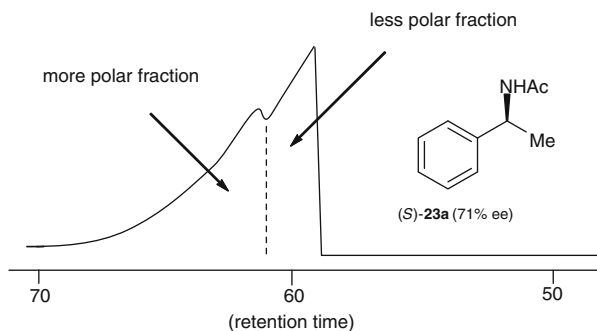


Fig. 2 SDE of (*S*)-**23a** (71% ee) via MPLC using achiral column (packed 10 μm of silica gel, 20 mm \times 250 mm, eluent: *n*-hexane/AcOEt 5:4)

MPLC was systematically studied (Fig. 1) [56]. Amides **23** are very simple structurally and can serve as very representative examples, suggesting that many other amides might manifest SDE via achiral chromatography.

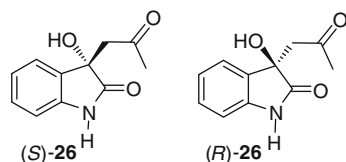
MPLC of non-racemic acetamide (*S*)-**23a** (71% ee) using an achiral silica gel column and achiral eluent (*n*-hexane/AcOEt) gave a chromatogram showing two distinct peaks as would be observed for a mixture of two chemically different compounds (Fig. 2).

The eluted product was collected into two fractions at the boundary point. Analysis of enantiomeric excess of these fractions revealed that the less polar fraction contained enantiomerically pure (*S*)-**23a** (>99% ee) while the second fraction was significantly enantiomerically depleted (28% ee) (Table 1). The initial enantiomeric purity of the compound (*S*)-**23a** has little effect on the efficiency of purification procedure and enantiomerically pure (*S*)-**23a** was prepared starting from samples of 60% ee, 49% ee, and 30% ee. On the other hand, the choice of eluent is important for the magnitude of SDE. When *n*-hexane and 2-propanol instead of *n*-hexane and ethyl acetate were used as eluents in MPLC of (*S*)-**23a**, no noticeable SDE was observed.

Even more impressive results were obtained for amides (*R*)-**23b–d** containing Tol, PMB, as well as naphthyl groups. Thus, chromatography of amides **23b** of 70% ee, **23c** of 71% ee and **23d** of 67% ee under the same achiral conditions allowed separation of first, less polar fractions containing enantiomerically pure (>99% ee) (*R*)-**23b–d** (Table 2). The yields of the pure enantiomers in these cases were

Table 5 SDE of compounds (*S*)-**25b** and **c** via gravity-driven achiral chromatography

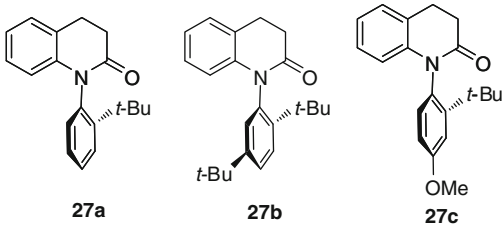
Entry	Amide	Starting ee (%)	Eluent	Minimum ee (%)	Maximum ee (%)
1	25b	95.0	<i>n</i> -Hexane/EtOAc, 5:1	91.0	99.6
2	25c	95.0	<i>n</i> -Hexane/EtOAc, 5:1	90.8	97.6
3	25b	31.1	<i>n</i> -Hexane/EtOAc, 5:1	28.9	39.1
4	25c	31.1	<i>n</i> -Hexane/EtOAc, 5:1	27.1	53.4
5	25b	61.1	<i>n</i> -Hexane/EtOAc, 5:1	55.1	70.3
6	25c	61.1	<i>n</i> -Hexane/EtOAc, 5:1	49.9	92.3
7	25b	66.6	<i>n</i> -Hexane/EtOAc, 5:1	59.9	78.8
8	25c	66.6	<i>n</i> -Hexane/EtOAc, 5:1	58.4	99.9
9	25b	66.6	<i>n</i> -Hexane/Et ₂ O, 1:1	64.8	72.1
10	25c	66.6	<i>n</i> -Hexane/Et ₂ O, 1:1	55.7	95.2
11	25b	66.6	CHCl ₃	66.6	66.6
12	25c	66.6	CHCl ₃	65.8	68.6

Fig. 4 Structure of 3-hydroxyindolin-2-ones **26**

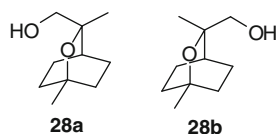
polar fraction was found to be enantiomerically pure (*S*)-**27a** while the second was enantiomerically depleted. It should be emphasized again that in this experiment 41% of the excess (*S*)-enantiomer (>99% ee) was easily separated from the starting material of 73% ee, rendering this method of obvious preparative value. The separation by MPLC was also observed for other lactam substrates **27b** and **27c** which, similar to **27a**, were isolated in almost enantiomerically pure form (Table 6). On the other hand separation depended strongly on the eluent and when the mixture *n*-hexane/*i*-PrOH 50:1 was used as eluent the separation of an excess enantiomer was not observed at all.

4.2 Alcohols and Phenols

An example of SDE on an achiral column dealing with enantiomerically enriched samples of natural products was observed for cineole metabolites **28a** and **28b** (Fig. 5). It was shown that preparative HPLC of mixture of alcohols **28a** and **28b** in ratio 72:28 on silica gel using ethyl acetate/*n*-hexane 1:1 as eluent provided four consecutive fractions having enantiomeric purity 84% ee, 74% ee, 26% ee, and 22% ee [62]. The authors suggested that enrichment and depletion of enantiomeric excess in different fractions occurred due to the conversion of an initially achiral column into a chiral stationary phase by the adhesion of chiral moving phase because chromatography of a more dilute enriched mixture afforded less effective

Table 6 SDE of antipisomeric lactam derivatives **27a–c** via MPLC using achiral silica gel column, eluent *n*-hexane/AcOEt 10:1


Entry	Lactam	Less polar fraction	More polar fraction
1	27a , 73% ee	99.5% ee, 41.0%	59.5% ee, 73.0%
2	27b , 73% ee	99.7% ee, 31.8%	62.9% ee, 67.0%
3	27c , 80% ee	99.4% ee, 56.2%	51.5% ee, 43.8%

Fig. 5 Structures of cineole metabolites **28a** and **28b** showing SDE via achiral HPLC

separation. As pointed out in this work, SDE can cause problems associated with enantiomeric analysis of complex mixtures of natural products.

The chromatographic behavior in HPLC of 1-anthryl-2,2,2-trifluoroethanol **29** was studied on aminopropyl silica using *n*-hexane/dichloromethane as eluent (Fig. 6) [63]. In this case, the stationary phase possesses good H-donor properties and a long, flexible propyl chain to bind with associates without influence the existing interactions. On the other hand, the eluent, selected for a polar non-racemic mixture, is apolar enough to allow homochiral and heterochiral self-associations in solution. The chromatography chart of 1-anthryl-2,2,2-trifluoroethanol **29** gave two distinct peaks: the excess enantiomer (first) and the racemate (second). The importance of the aminopropylsilica gel as stationary phase choice has also been proved. Application of other stationary phases such as silica gel, diol phase, and RP18 for the HPLC of 1-anthryl-2,2,2-trifluoroethanol **29** did not produce clear separation of the excess enantiomer and racemic peaks.

α -Trifluoromethyl-containing secondary alcohols (*S*)-**30a–f** also showed a significant level of SDE via achiral chromatography on silica gel (Fig. 7).

Flash chromatography of amino alcohol (*S*)-**30a** of ~75% ee using cyclohexane, benzene, and di-*tert*-butyl ether in a ratio of 1/1/0.1 as eluent, which could not significantly interfere with H-bonded interactions between molecules of compound **30a**, produced enantiomerically depleted first fractions and last fractions containing pure (*S*)-**30a** enantiomer (Table 7) [64]. The magnitude of SDE under these conditions was about 50% Δ ee and the overall amount of collected enantiomerically pure (*S*)-**30a** was 55 mg out of 157.5 mg of the (*S*)-enantiomer contained in the initial mixture, which corresponded to 35% chemical yield.

Fig. 6 Structure 1-(anthracen-9-yl)-2,2,2-trifluoroethanol **29** showing strong magnitude of SDE via achiral HPLC

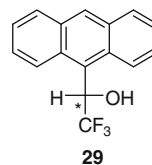


Fig. 7 Structures of secondary α -CF₃ alcohols (*S*)-**30a-f**

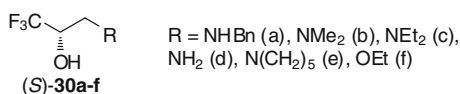


Table 7 SDE of compound (*S*)-**30a** via flash chromatography on achiral silica gel using cyclohexane/benzene/*di-tert*-butyl ether 1/1/0.1 as eluent

Fraction	Mass (mg)	(<i>S</i>)/(<i>R</i>) (mg)	ee (%)
Starting sample	180	157.5/22.5	75
1	16	12.1/3.9	51
2	23	17.8/5.2	55
3	27	21.5/5.5	59
4	30	24.4/5.6	63
5	25	22.5/2.5	80
6	26	26/0	>99
7	17	17/0	>99
8	10	10/0	>99
9	2	2/0	>99

Compound **30b** bearing *N,N*-dimethyl moiety showed a chromatographic profile similar to that of **30a**, allowing isolation of enantiomerically pure **30b** in the last eluted fractions. In this case, the magnitude of SDE was a bit greater ($\Delta ee = 68\%$) and the isolated yield of enantiomerically pure (*S*)-**30b** was higher (Table 8). Compound **30c**, containing the diethylamino group, showed results very similar to those obtained for the *N,N*-dimethyl-derivative **30b**, suggesting that the presence of the N–H moiety in **30a** does not play any critical role in the mechanism of SDE in this series. The enantiomerically pure (*S*)-**30c** was collected with 41% chemical yield. On the other hand, derivative **30d** containing an unsubstituted amino group, gave better results showing 71% Δee and allowing isolation of the enantiomerically pure (*S*)-**30d** in 44% yield. Compound **30e** bearing the piperidyl moiety gave lower values of SDE (69% Δee) but still the enantiomerically pure (*S*)-**30e** was isolated in quite reasonable 40% yield. Finally, the ethoxy-containing derivative **30f**, structurally different from the rest of compounds used in this study, gave the most notable results. In this case the first fraction was noticeably enantiomerically depleted, providing for the highest Δee in this study of 78% ee. The isolated yield of enantiomerically pure (*S*)-**30f** was 53%.

It should be emphasized that several compounds in this study were liquids, in particular **30f**, and therefore the only available methods for preparation of their enantiomerically pure samples is provided by chromatography on a chiral stationary phase. As shown in this work, SDE via achiral chromatography represents a remarkable inexpensive alternative easily reproducible in any chemistry laboratory.

Table 8 SDE of compounds (*S*)-**30b–f** (75% ee) via flash chromatography on achiral silica gel using cyclohexane/benzene/*di-tert*-butyl ether 1:1:0.1 as eluent

Entry	(<i>S</i>)- 1	Highest ee (%)	Lowest ee (%)	Δ ee (%)	Yield of pure enantiomer (%)
1	30b	99	31	68	39
2	30c	99	33	66	41
3	30d	99	28	71	44
4	30e	99	30	69	40
5	30f	99	21	78	53

Recently the chromatographic behavior of enantiomerically enriched compounds **31–33** having a tertiary trifluoromethyl alcohol center on an achiral silica-gel stationary phase has been carefully investigated (Table 9) [65]. An enantiomeric enrichment in the faster eluted fractions was observed for samples of **31a** with enantiomeric excess of 10–54% ee subjected to flash silica gel chromatography and eluted with *n*-hexane/EtOAc 1:2 or ether (Table 9). The difference between the maximum and minimum ee for the most enantiomerically enriched/depleted fractions was found to be 66.9% ee when ether was used as the eluent (Table 9, entry 3). The difference between enriched/depleted fractions was slightly improved to 71.6% ee at medium-pressure chromatographic conditions (Table 9, entry 4) and lowered with a decrease in the enantiomeric purity of the loading samples (Table 9, entries 5 and 6). In these experiments enantiomerically pure **31a** with 99.9% ee was obtained from the starting sample of 40% ee. Interestingly, the very structurally similar derivative **31b** showed less pronounced ability for separation of excess enantiomer under the same conditions. Starting with compound **31b** of 37.5% ee, the earlier-eluted fraction gave **31b** of 82.3% ee (Table 9, entry 7). SDE was practically not observed for the other derivatives **32** and **33** independent of their enantiomeric purity (Table 9, entries 8–11).

One of the classic examples of SDE via achiral chromatography is BINOL **34** (Fig. 8). Its chromatographic behavior was initially studied on aminopropyl silica using *n*-hexane/2-PrOH 6:4 as eluent [63]. For example, HPLC of BINOL of 33% ee gave first peak of excess enantiomer and second peak of racemate with a difference in the retention times of 2.9 min. On loading a mixture with 86% ee the difference in the retention times between excess enantiomer and racemate increases to 10.7 min. The authors also showed that, at dilution, intermolecular associations become unfeasible, leading to a complete quenching of SDE. Application of other stationary phases such as silica gel, diol phase, and RP18 for the HPLC experiments with BINOL was not effective for separation of the excess enantiomer and racemic peaks.

Chromatographic behavior of enantiomerically enriched BINOL **34** has been studied on LichroCART[®] (NH₂) derived stationary phase [66]. Using CHCl₃, CH₂Cl₂ or mixtures of *n*-hexane/2-PrOH as eluent afforded a first peak of enantiomerically pure form (>99% ee) and a second peak of racemic mixture (0% ee). The theoretical treatment of the phenomenon assumed that enantiomers of BINOL can associate in solution to form homochiral (*RR* and *SS*) and

Table 9 SDE of **31**–**33** on achiral silica-gel flash chromatography

Entry	Substrate	Starting ee (%)	Eluent	Minimum ee (%)	Maximum ee (%)
1 ^a	31a	47.3	<i>n</i> -Hexane/EtOAc, 1:2	25.0	80.2
2 ^a	31a	47.3	Et ₂ O	29.2	96.9
3 ^a	31a	52.1	Et ₂ O	33.0	99.9
4 ^b	31a	52.0	Et ₂ O	28.3	99.9
5 ^b	31a	30.3	Et ₂ O	17.0	79.7
6 ^b	31a	9.9	Et ₂ O	4.2	44.6
7 ^b	31b	37.5	Et ₂ O	26.1	82.3
8 ^a	32a	52.7	<i>n</i> -Hexane/Et ₂ O, 4:1	52.2	52.4
9 ^a	32b	52.5	<i>n</i> -Hexane/Et ₂ O, 4:1	53.7	54.0
10 ^a	33a	96.5	<i>n</i> -Hexane/Et ₂ O, 1:1	96.0	97.0
11 ^a	33b	92.0	<i>n</i> -Hexane/EtOAc, 9:1	91.3	93.3

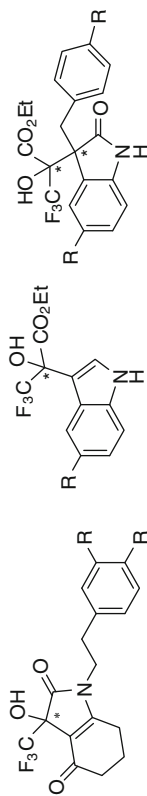
^aFlash silica-gel in glass column was used under atmospheric pressure^bFlash silica-gel in polypropylene column was used under medium pressure

Fig. 8 1,1'-Bi-2-naphthol **34** (BINOL) possessing axial chirality

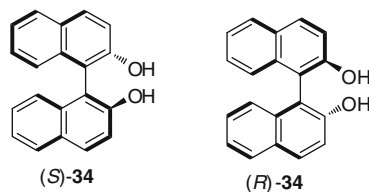
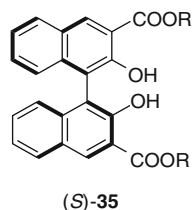


Fig. 9 BINOL derivatives (S)-**35**



R = Me (a), Et (b), Bn (c), *t*-Bu (d)

heterochiral (*RS*) dimers both in the stationary phase and in the mobile phase. This model was called a “hybrid” model as opposed to other models in which homo- and heteroassociations occur on the stationary phase or in the mobile phase. Finally, the chromatographic behavior of an enantiomerically enriched BINOL was reinvestigated on LiChrospher[®] (100 NH₂) stationary phase using CHCl₃ as eluent and more accurate dual on-line detection (polarimetric and UV) [67, 68]. According to previous study [63, 66], for a sample of BINOL (*S*)-**34** of 60% ee the first peak was optically pure BINOL (*S*)-**34** and the second was racemate with a difference in retention time of 3 min. The racemate peak is reproducibly retarded by slightly more than 1 min with respect to the single enantiomer peak of the same overall concentration. This is probably a very simple test estimating a magnitude of SDE for a particular chiral compound and given set of chromatography conditions. Several BINOL derivatives (*S*)-**35a–c** also showed a strong magnitude of SDE on silica gel under the simple conditions of gravity driven chromatography (Fig. 9) [69, 70].

4.3 Ketones

Despite a lack of hydrogen bonding, unsaturated diketone **36** demonstrates high magnitude of SDE via achiral chromatography (Fig. 10). Chromatography of unsaturated diketone (*S*)-**36** of 65% ee on silica gel using *n*-hexane/EtOAc 4:1 afforded collected fractions with enantiomeric composition ranging from 84% ee to 51% ee [71]. In contrast, chromatography under the same conditions of the pure (*S*)-enantiomer or racemic sample resulted in enantiomerically pure or racemic fractions. The mechanistic rationale of SDE could assume strong dipole–dipole interactions of the carbonyl groups in this case. While the preparation of

Fig. 10 Structure of unsaturated diketone **36**

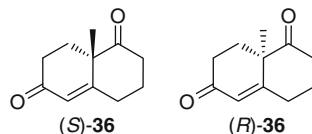
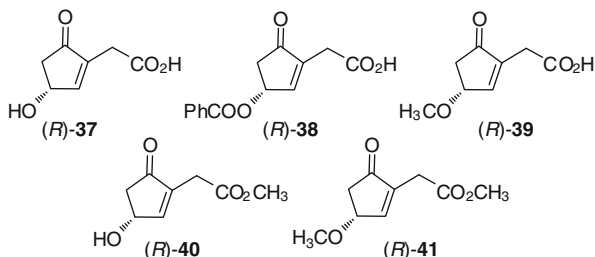


Fig. 11 Structure of cyclopentanones **37–41**



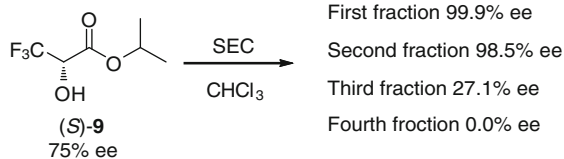
enantiomerically pure samples was not achieved in this study, the difference in ee percentage between the most enantiomerically enriched/depleted fractions was rather notable (33%), underscoring the generality of SDE for various types/classes of non-H-bonding compounds.

4.4 Carboxylic Acids and Esters

The phenomenon of SDE by achiral phase chromatography has been observed in the case of such carboxylic acids as 4-hydroxy-2-carboxymethyl-2-cyclopentenone **37** and its derivatives **38–41** (Fig. 11) [72]. All compounds showed enantiomeric enrichment in the first part of the chromatographic peak and gradual depletion in the following part of the peak under achiral HPLC on silica gel using a mixture of *n*-hexane/EtOAc as eluent. In addition, samples obtained from divided chromatographic peaks by preparative HPLC of the corresponding cyclopentenone derivatives were chromatographically and spectroscopically non-distinctive and total optical activity of the fractionated samples were equal to those before chromatography. SDE remained after changing the HPLC column to the usual chromatography column, although the magnitude of the separation was not so expressive. Optical rotation data combined with purity control by analytical HPLC provided a reasonable basis to consider that the results obtained reflected the change in enantiomeric composition during chromatography of the investigated compounds. Moreover, carboxylic acids **37–39** should be able to form more strong H-bonding associates than in the cases of alcohol **40** and cyclopentenone **41**. However, substantial SDE was not observed among the compounds of this group.

Earlier in this chapter it was said that isopropyl 3,3,3-(trifluoro)lactate (*S*)-**9** represents an extreme example of SDE via distillation and sublimation and crystallographic analysis of enantiomerically pure crystals of (*S*)-**9** has provided important

Fig. 12 SDE of (*S*)-**9** via size-exclusion chromatography



information about the nature of the corresponding homochiral interactions. Quite unexpectedly, the crystallographic analysis of racemic isopropyl 3,3,3-(trifluoro) lactate **9** has revealed that H-bonded heterochiral (*R*)/(*S*)-dimer is not present in the unit cell [73]. Instead, it consists of two (*R*)- and two (*S*)-enantiomers not involved in any H-bonding interactions between them. Moreover, the infinite homochiral H-bonded chains of (*S*)- and (*R*)-molecules, observed in the racemic crystals, were absolutely identical to the corresponding (*S*)-homochiral chains found in the enantiomerically pure crystals of (*S*)-**9**. These data strongly suggested that **9** has the ultimate preference for homochiral intermolecular interactions which can explain unusual phase-transition behavior of compound **9**. The determined preference of **9** for homochiral oligomers formation was used to perform partial separation of racemic and enantiomerically pure forms of **9** using SDE via size-exclusion chromatography (SEC). The SEC chart for a sample of (*S*)-**9** of 75% ee presented peaks of the racemate with the excess enantiomer having rather a clear boundary. The first collected fraction contained enantiomerically pure ester (*S*)-**9** (Fig. 12). Consequently, the final fraction was fraction virtually racemic.

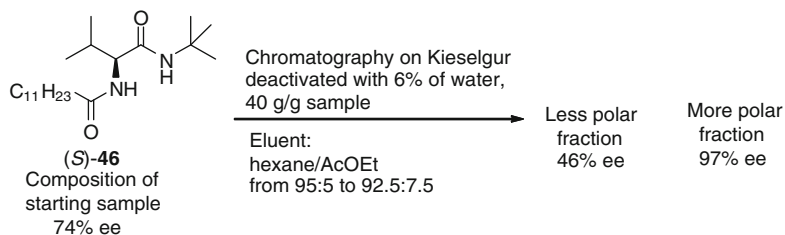
4.5 Sulfoxides

Kagan et al. observed remarkable SDE of enantiomerically enriched sulfoxides on achiral stationary phases [74]. For example, flash chromatography of methyl *p*-tolyl sulfoxide (*R*)-**42** with 86% ee on silica gel using AcOEt as eluent gave (*R*)-**42** of 99.5% ee in the first fraction and (*R*)-**42** of 73.5% ee in the last fraction according to determination of their enantiomeric excess by HPLC analysis on a chiral stationary phase (Table 10, entry 1). Similar results were obtained with a sample of 20% ee under the same conditions: highest enantiomeric excess at the beginning (37% ee) and lowest value at the end (18% ee) (Table 10, entry 1). It should be emphasized that increasing the amount of silica gel did not improve the efficiency of the enantiomeric enrichment. Thus this simple laboratory purification procedure allowed isolation of the sample with ee > 99% for methyl *p*-tolyl sulfoxide (*R*)-**42** prepared by asymmetric catalytic synthesis with only moderate enantioselectivity 80–90% ee. Flash chromatography of methyl *p*-tolyl sulfoxide (*R*)-**42** on reverse-phase silica and alumina also demonstrated enantiomeric enrichment in the first fractions while depletion occurred in the last fractions (Table 10, entries 3 and 4). These experiments demonstrated the general character of SDE on achiral phases. Kagan's group also observed a similar increase in ee at the beginning of the

Table 10 SDE of chiral sulfoxides **42–45** during achiral flash chromatography

Entry	Sulfoxide % ee	Eluent	First fraction % ee	Last fraction % ee
1 ^a	(<i>R</i>)- 42 , 86.0	AcOEt	(<i>R</i>)- 42 , 99.5	(<i>R</i>)- 42 , 73.5
2 ^a	(<i>R</i>)- 42 , 20.0	AcOEt	(<i>R</i>)- 42 , 37.0	(<i>R</i>)- 42 , 18.0
3 ^b	(<i>R</i>)- 42 , 91.0	AcOEt	(<i>R</i>)- 42 , 99.5	(<i>R</i>)- 42 , 73.0
4 ^c	(<i>R</i>)- 42 , 86.0	–	(<i>R</i>)- 42 , 91.0	(<i>R</i>)- 42 , 80.5
5 ^a	(<i>S</i>)- 42 , 82.0	AcOEt	(<i>S</i>)- 42 , 89.0	(<i>S</i>)- 42 , 70.0
6 ^a	(<i>S</i>)- 43 , 44.5	AcOEt	(<i>S</i>)- 43 , 53.0	(<i>S</i>)- 43 , 42.0
7 ^a	(<i>R</i>)- 44 , 90.5	AcOEt/Et ₂ O 1:1	(<i>R</i>)- 44 , 99.5	(<i>R</i>)- 44 , 82.0
8 ^a	(<i>R</i>)- 45 , 65.0	AcOEt/cyclohexane 1:1	(<i>S</i>)- 45 , 79.0	(<i>R</i>)- 45 , 94.0

^aFlash chromatography on silica gel^bFlash chromatography on reverse-phase silica^cFlash chromatography on Al₂O₃



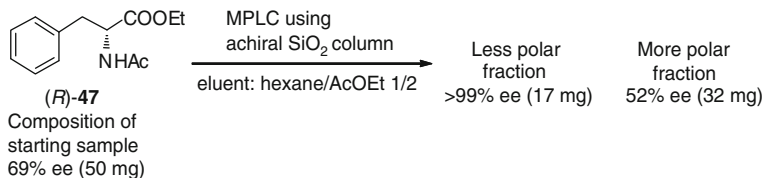
Scheme 19 SDE of *N*-acyl valine *tert*-butylamide (S)-**46** during achiral phase chromatography on Kieselgur deactivated with 6% of water

elution on silica gel for methyl *p*-tolyl sulfoxide (S)-**42** (Table 10, entry 5), benzyl *tert*-butyl sulfoxide (S)-**43** (Table 10, entry 6), and methyl ferrocenyl sulfoxide (R)-**44** (Table 10, entry 7). Unexpectedly, when a sample of phenyl ferrocenyl sulfoxide (R)-**45** of 65% ee was subjected to flash chromatography on silica gel, elution with AcOEt/cyclohexane 1:1 provided in the first fraction minor enantiomer (S)-**45** of 79% ee and in the last fraction sulfoxide (R)-**45** of 94% ee (Table 10, entry 8). It was supposed in this report that the physicochemical basis of SDE of chiral sulfoxides was formation of macromolecular associations of enantiomers in the mobile phase, giving rise to diastereomeric species of different chromatographic mobilities.

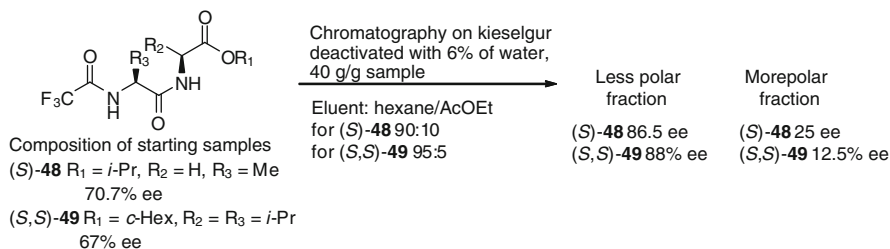
4.6 α -Amino Acids and Dipeptides Derivatives

Amplification of optical activity of enantiomerically enriched α -amino acid and dipeptide derivatives during achiral phase chromatography is one of the most interesting examples of SDE. The first time this phenomenon was observed in the case of valine derivatives. It was shown that chromatography of *N*-acyl valine *tert*-butylamide (S)-**46** of 74% ee on Kieselgur deactivated with 6% of water using *n*-hexane/AcOEt from 95:5 to 92.5:7.5 as eluent led to the first fraction containing 30% of sample with only of 46% ee while the latter fractions furnished *N*-acylvaline *tert*-butylester (S)-**46** with an average 90% ee running up to 97% ee in the last fraction (Scheme 19) [75]. Later the similar chromatographic behavior of a mixture of ^{14}C -labeled racemic *N*-acetyl valine *tert*-butylester and the unlabeled (S)-enantiomer on silica gel has been observed [76].

The MPLC of *N*-acetyl phenylalanine ethyl ester (R)-**47** was subsequently investigated on achiral silica gel column and the opposite order of elution between more racemic and enantiomerically enriched samples was observed. Enantiomerically enriched phenylalanine derivative (R)-**47** of 69% ee was separated using mixtures of *n*-hexane/AcOEt as eluents into less polar fractions containing optically pure form and more polar fractions with lower ee of the substrate (Scheme 20) [56]. Although the boundary for the separation was slightly unclear, the enantiomerically pure *N*-acetyl phenylalanine ethyl ester (R)-**47** was



Scheme 20 MPLC separation of enantiomerically enriched *N*-acetyl phenylalanine ethyl ester (*R*)-**47**



Scheme 21 SDE of dipeptides (*S*)-**48** and (*S,S*)-**49** during achiral phase chromatography on Kieselgur deactivated with 6% of water

obtained in relatively good chemical yield. HPLC separation of the excess enantiomer (first fraction) and racemate (second fraction) of *N*-benzoyl alanine methyl ester on aminopropylsilica gel as achiral stationary phase using *n*-hexane/2-PrOH mixture was also briefly described in the literature [63].

Enantiomeric enrichment in the first fractions and depletion in the last fractions was also demonstrated during the chromatography of *N*-trifluoroacetyl dipeptides (*S*)-**48** and (*S,S*)-**49** on water-deactivated Kieselgur (Scheme 21) stationary phase [75]. When a sample of dipeptide (*S*)-**48** of 70.7% ee was loaded on a silica gel column using *n*-hexane/AcOEt 9:1 as eluent the highest 86.5% ee and the lowest 25% ee were observed during the chromatographic experiments. A similar result was obtained with the dipeptide (*S,S*)-**49** of 67% ee giving fractions of highest 88% ee and lowest 12.5% ee optical purity. In both cases more enantiomerically enriched samples were eluted first and more racemic product collected in latter fractions. The authors assumed that high order association of the enantiomers occurs efficiently only on the stationary phase, while in the mobile phase association is insignificant due to hydrogen bonding of the solute with the polar component.

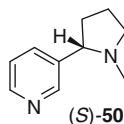


Fig. 13 Structure of natural (*S*)-nicotine

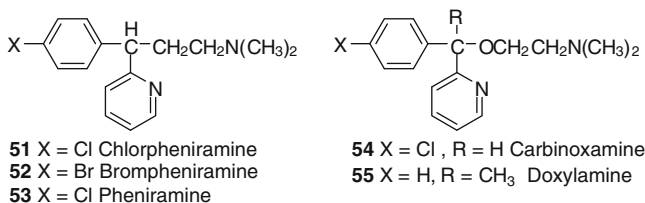
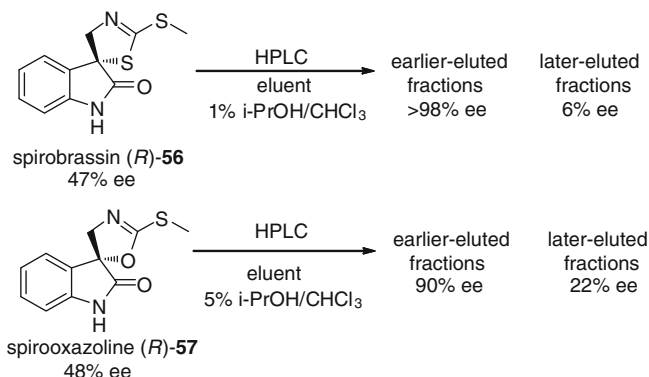


Fig. 14 Structure of antihistamines **51–55**

4.7 Heterocycles

The first example of SDE via chromatography was reported in 1983 during a study of the metabolism of ¹⁴C-labelled nicotine by HPLC on reversed phase columns [77]. Cundy and Crooks observed splitting of the radioactivity into two distinct peaks for racemic radiolabeled compounds co-injected with unlabeled (*S*)- or (*R*)-nicotine **50** as standard – herewith the enantiomer in excess was eluted first (Fig. 13). On the other hand, radiolabeled compound alone eluted as a single radioactive peak and using unlabeled racemic nicotine as standard also showed one ¹⁴C peak. They also were the first to show the advantage of SDE via chromatography over other purification methods for preparation of enantiomerically pure samples of ¹⁴C-labelled (*S*)- or (*R*)-nicotine **50**.

Several antihistamines **51–55** underwent enantiomeric enrichment and depletion in different fractions under achiral chromatography on an aminopropyl silica gel column with an *n*-hexane-2-propanol mobile phase (Fig. 14) [78]. For example, racemic chlorpheniramine **51** and enantiomerically pure (*S*)-**51** eluted as a single peak, while enriched (*S*)-**51** of 48% ee and 34% ee exhibited two overlapping peaks. Other antihistamines **52–54** gave similar results. It was also demonstrated that SDE of antihistamines **52–54** is concentration-dependent and diluted samples were not separated. The composition of the mobile phase was also important in achieving separation of racemic mixtures from pure enantiomers. Mobile phases consisting of ethanol (1%), 2-propanol (1%, 5%, or 20%), or *tert*-butanol (20%) with *n*-hexane, effected the separation, whereas higher concentrations of alcohol or using chloroform and tetrahydrofuran as well as the presence of acid or base in the mobile phase resulted in a loss of separation. These data supported the idea that SDE was the result of homo-/heterochiral associations between the (*R*)- and



Scheme 22 SDE of spirobrassinin (*R*)-**56** and spirooxazoline (*R*)-**57** during achiral HPLC using *i*-PrOH/CHCl₃ as eluent

(*S*)-enantiomers. The benzylic hydrogen on the chiral carbon appears to play a crucial role in SDE process because doxylamine **55**, which has a methyl group in place of the benzylic hydrogen, did not exhibit any enrichment/depletion of enantiomeric purity. Additional experiments have shown that racemic chlorpheniramine **51** was retained longer on the aminopropyl silica column than the pure enantiomers. Hence, the first fractions were enriched in the excess enantiomer.

A more significant change of enantiomeric excesses under conditions of achiral HPLC chromatography was observed for natural (*R*)-spirobrassinin **56** (Scheme 22). Chromatographic purification of compound (*R*)-**56** (47% ee) using achiral eluent 1% *i*-PrOH/CHCl₃ gave less polar, earlier-eluted fractions containing enantiomerically pure (*R*)-**56** (>98% ee), while the later-eluted fraction was significantly enantiomerically depleted (only 6% ee) [79, 80]. Interestingly, under the same conditions related derivative spirooxazoline (*R*)-**57** showed much less pronounced separation of racemic fraction from the (*R*)-enantiomer. Starting with compound (*R*)-**57** of 48% ee, earlier-eluted fractions contained significantly enantiomerically enriched (90% ee) but not pure (*R*)-**57**, while more polar fractions were expectedly enantiomerically depleted (22% ee).

Another example of SDE via achiral chromatography was observed during the isolation of *C*₂-symmetric pyrrolidine and morpholine derivatives **58–61** of moderate enantiomeric excess (53–88% ee) [81]. MPLC on silica gel using a mixture of *n*-hexane/AcOEt as eluent gave enhancement of enantiomeric excess in the first fractions while enantiomeric purity of following fractions were gradually decreased (Table 11). In practice, this procedure allowed isolation of pyrrolidine derivatives (2*R*,5*R*)-**58**, (2*S*,5*S*)-**58**, (2*R*,5*R*)-**59**, and (2*S*,5*S*)-**59** in almost enantiomerically pure form (>98% ee). The authors assumed that *C*₂-symmetry azacycloalkanes **58–61** may be associated in the mobile phase, giving rise to homochiral or heterochiral dimers/oligomers with different chromatographic mobilities.

The example of SDE of helical molecules on an achiral phase was demonstrated during the work on enzymatic resolution of racemic helicenediol with lipases in

Table 11 SDE of C_2 -symmetric O-protected pyrrolidine and morpholine derivatives **58–61** during medium-pressure achiral chromatography

Entry	Substrate % ee	Eluent	First fraction % ee	Last fraction % ee
1	(2 <i>R</i> ,5 <i>R</i>)- 58 , 82	<i>n</i> -Hexane/AcOEt 50:1	99	33
2	(2 <i>S</i> ,5 <i>S</i>)- 58 , 88	<i>n</i> -Hexane/AcOEt 50:1	99	67
3	(2 <i>R</i> ,5 <i>R</i>)- 59 , 81	<i>n</i> -Hexane/AcOEt 50:1	98	15
4	(2 <i>S</i> ,5 <i>S</i>)- 59 , 87	<i>n</i> -Hexane/AcOEt 50:1	99	53
5	(2 <i>R</i> ,5 <i>R</i>)- 60 , 79	<i>n</i> -Hexane/AcOEt 15:1	84	73
6	(2 <i>S</i> ,5 <i>S</i>)- 60 , 84	<i>n</i> -Hexane/AcOEt 15:1	89	80
7	(2 <i>R</i> ,6 <i>R</i>)- 61 , 53	<i>n</i> -Hexane/AcOEt 60:1	70	42

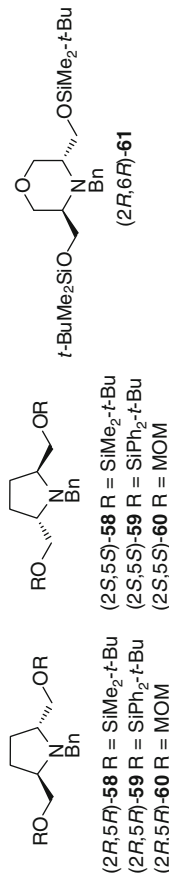
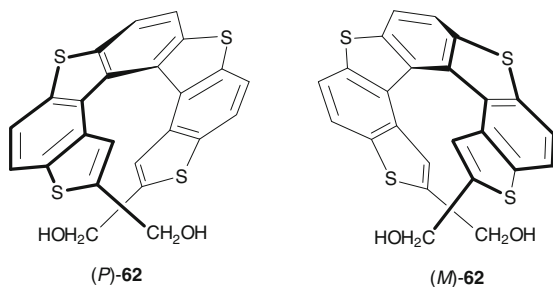


Table 12 SDE of helicenediols (*M*)- and (*P*)-**62** during achiral chromatography on silica gel with *n*-hexane/ethyl acetate 3:1 as eluent

Entry	Helicenediol % ee	First fraction % ee	Last fraction % ee
1	(<i>M</i>)- 27 , 82	69	89
2	(<i>M</i>)- 27 , 66	55	77
3	(<i>P</i>)- 27 , 92	90	95
4	(<i>P</i>)- 27 , 67	64	72
5	(<i>P</i>)- 27 , 50	50	50
6	(<i>P</i>)- 27 , 42	42	42
7	(<i>P</i>)- 27 , 20	20	20

organic solvents. It was observed that isolation of both (*M*)- and (*P*)-enantiomers of helicenediol **62** with 66–92% ee by column chromatography on silica gel with *n*-hexane/AcOEt 3:1 as eluent gave depletion of enantiomeric excess in the first fractions and enantiomeric enhancement in the last fractions (Table 12, entries 1–4) [82]. The highest enantiomeric purity of 95% ee was obtained in the last fraction starting from the (*P*)-enantiomer **62** with 92% ee (Table 12, entry 3). Further analysis of the separation procedure revealed that no appreciable SDE was observed during the chromatography of helicenediols (*M*)- and (*P*)-**62** with $\leq 50\%$ ee (Table 12, entries 5–7). The authors suggested that heterochiral association between two enantiomers (*PM*- and *MP*-dimers) by intermolecular hydrogen bonding is more favorable than homochiral association (*PP*- and *MM*-dimers). As a result, the more chromatographically mobile heterochiral dimers would elute faster than the less mobile enantiomers with increase of ee being observed in the last fractions. The hypothesis was confirmed by recrystallization of helicenediol (*P*)-**62** of 69% ee from *n*-hexane/AcOEt 3:1 giving rise to racemic crystals of **62** while the ee of the filtrate increased to 97%.

Examples of SDE of chloromezanone **63** [63], camazepam **64** [63], chloropyridin derivative **65** [83], tetrahydropyridazine derivative **66** [84], and hydroxycoumarin derivatives **67** [85] under the conditions of achiral chromatography have been mentioned in the literature (Fig. 15).

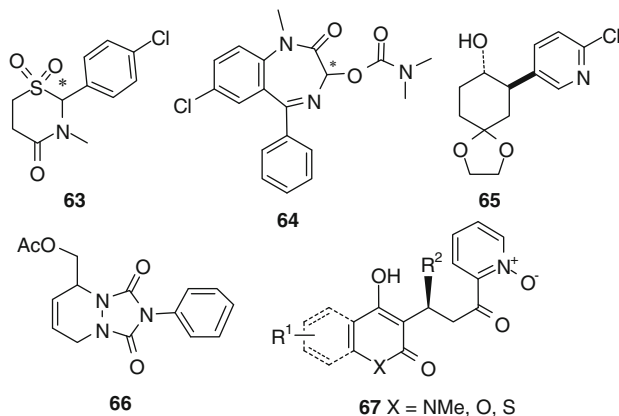


Fig. 15 Structures of heterocyclic compounds **63–67** showing SDE during achiral chromatography

5 Conclusions and Outlook

After consulting this account, one may draw three general conclusions. First, the phenomenon of SDE is indeed of very general nature as the reported literature cases deal with compounds of wide structural and functional variety. Furthermore, if under certain conditions the magnitude of SDE is not pronounced, the conditions can be adjusted to achieve the desired separation of racemate from the excess enantiomer. Second, SDE via phase transitions and achiral chromatography holds true practical potential for the development of unconventional enantiomeric purifications. Thus, on numerous examples, it has been demonstrated that sublimation or achiral chromatography provided a similar or better yield of the recovered excess enantiomer as compared to traditional crystallization. Third, the understanding of physicochemical background and mechanistic rationale for various manifestation of SDE is rather confusing and full of discrepancies. It would not be an understatement to say that this area of research is in its infancy and still awaits comprehensive systematic study.

References

1. Groh J (1912) Untersuchungen über die Existenz von Racemkörpern in flüssigem Zustande. *Chem Ber* 45:1441–4447
2. Mauser H (1957) Zur Thermodynamik optischer Antipoden, I. *Chem Ber* 90:299–306
3. McGinn CJ (1961) Diastereoazeotropes as a means of resolution. *J Phys Chem* 65:1896–1897
4. Nerdel F, Diepers W (1962) Zum Destillationsverhalten flüssiger Gemische optischer Antipoden. *Tetrahedron Lett* 4:783–786

5. Guetté JP, Boucherot D, Horeau A (1973) Interactions diastereoisomeres d'énantiomeres en phase liquide – II' Peut-on separer les antipodes d'un compose chiral distillation? *Tetrahedron Lett* 15:465–468
6. Horeau A, Guetté JP (1974) Interactions diastereoisomeres d'antipodes en phase liquide. *Tetrahedron* 30:1923–1931
7. Katagiri T, Yoda C, Furuhashi K, Ueki K, Kubota T (1996) Separation of an enantiomorph and its racemate by distillation: strong chiral recognizing ability of trifluorolactates. *Chem Lett* 115–116
8. Katagiri T, Uneyama K (2001) Chiral recognition by multicenter single proton hydrogen bonding of trifluorolactates. *Chem Lett* 1330–1331
9. Katagiri T, Duan M, Mukae M, Uneyama K (2003) A crystal engineering utilization of hexafurcated hydrogen bonding to construction of subnano fluorinated tunnels. *J Fluorine Chem* 120:165–172
10. Katagiri T, Takahashi S, Tsuboi A, Suzaki M, Uneyama K (2010) Discrimination of enantiomeric excess of optically active trifluorolactate by distillation: evidence for a multi-center hydrogen bonding network in the liquid state. *J Fluorine Chem* 131:517–520
11. Koppenhoefer B, Trettin U (1989) Is it possible to affect the enantiomeric composition by a simple distillation process? *Fresenius Z Anal Chem* 333:750
12. Garin DL, Grieco DJC, Kelly L (1977) Enhancement of optical activity by fractional sublimation. An alternative to fractional crystallization and a warning. *J Org Chem* 42:1249–1251
13. Bellec A, Guillemin JC (2010) Attempts to explain the self-disproportionation observed in the partial sublimation of enantiomerically enriched carboxylic acids. *J Fluorine Chem* 131:545–548
14. Soloshonok VA, Ueki H, Yasumoto M, Mekala S, Hirschi JS, Singleton DA (2007) Phenomenon of optical self-purification of chiral non-racemic compounds. *J Am Chem Soc* 129:12112–12113
15. Tsuzuki S, Orita H, Ueki H, Soloshonok VA (2010) First principle lattice energy calculations for enantiopure and racemic crystals of α -(trifluoromethyl)lactic acid: is self-disproportionation of enantiomers controlled by thermodynamic stability of crystals? *J Fluorine Chem* 131:461–466
16. Albrecht M, Soloshonok VA, Schrader L, Yasumoto M, Suhm MA (2010) Chirality-dependent sublimation of α -(trifluoromethyl)-lactic acid: relative vapor pressures of racemic, eutectic, and enantiomerically pure forms, and vibrational spectroscopy of isolated (*S,S*) and (*S,R*) dimers. *J Fluorine Chem* 131:495–504
17. Yasumoto M, Ueki H, Soloshonok VA (2010) Self-disproportionation of enantiomers of α -trifluoromethyl lactic acid amides via sublimation. *J Fluorine Chem* 131:540–544
18. Yasumoto M, Ueki H, Ono T, Katagiri T, Soloshonok VA (2010) Self-disproportionation of enantiomers via sublimation: isopropyl 3,3,3-(trifluoro)lactate. *J Fluorine Chem* 131:535–539
19. Yasumoto M, Ueki H, Soloshonok VA (2010) Self-disproportionation of enantiomers of 3,3,3-trifluorolactic acid amides via sublimation. *J Fluorine Chem* 131:266–269
20. Cronin JR, Pizzarello S (1997) Enantiomeric excesses in meteoritic amino acids. *Science* 275:951–955
21. Pracejus G (1959) Optische Aktivierung von *N*-phthalyl- α -aminosäure-derivaten durch tert.-Basen-Katalyse. *Liebigs Ann Chem* 622:10–22
22. Perry RH, Wu C, Neffliu M, Cooks G (2007) Serine sublimates with spontaneous chiral amplification. *Chem Commun* 1071–1073
23. Nanita SC, Cooks RG (2006) Serine octamers: cluster formation, reactions, and implications for biomolecule homochirality. *Angew Chem Int Ed* 45:554–569
24. Yang P, Xu R, Nanita SC, Cooks RG (2006) Thermal formation of homochiral serine clusters and implications for the origin of homochirality. *J Am Chem Soc* 128:17074–17086
25. Fletcher SP, Jagt RBC, Feringa BL (2007) An astrophysically-relevant mechanism for amino acid enantiomer enrichment. *Chem Commun* 2587–2580

26. Bellec A, Guillemin JC (2010) A simple explanation of the enhancement or depletion of the enantiomeric excess in the partial sublimation of enantiomerically enriched amino acids. *Chem Commun* 46:1482–1484
27. Viedma C, Noorduyn WL, Ortiz JE, de Torres T, Cintas P (2011) Asymmetric amplification in amino acid sublimation involving racemic compound to conglomerate conversion. *Chem Commun* 47:671–673
28. Kwart H, Hoster DP (1967) Separation of an enantiomorph and its racemate by sublimation. *J Org Chem* 32:1867–1870
29. Doucet H, Fernandez E, Layzell TP, Brown JM (1999) The scope of catalytic asymmetric hydroboration/oxidation with rhodium complexes of 1,1'-(2-diarylphosphino-1-naphthyl) isoquinolines. *Chem Eur J* 5:1320–1330
30. Ueki H, Yasumoto M, Soloshonok VA (2010) Rational application of self-disproportionation of enantiomers via sublimation: a novel methodological dimension for optical purifications. *Tetrahedron Asymmetry* 21:1396–1400
31. Jacques J, Collet A, Wilen S, Krieger H (1981) *Enantiomers, racemates, and resolutions*. Wiley, New York
32. Cintas P (2008) Sublime arguments: rethinking the generation of homochirality under prebiotic conditions. *Angew Chem Int Ed* 47:2918–2920
33. Blackmond DG, Klussmann LM (2007) Spoilt for choice: assessing phase behavior models for the evolution of homochirality. *Chem Commun* 3990–3996
34. Klussmann M, Mathew SP, Iwamura H, Wells DH Jr, Armstrong A, Blackmond DG (2006) Kinetic rationalization of nonlinear effects in asymmetric catalysis based on phase behavior. *Angew Chem Int Ed* 45:7989–7992
35. Horeau A (1969) Interactions d'enantiomeres en solution; influence sur le pouvoir rotatoire: pureté optique et pureté énantiomérique. *Tetrahedron Lett* 10:3121–3124
36. Schurig V (1996) Terms for the quantitation of a mixture of stereoisomers. *Enantiomer* 1:139–143
37. Baciocchi R, Zenoni G, Valentini M, Mazzotti M, Morbidelli M (2002) Measurement of the dimerization equilibrium constants of enantiomers. *J Phys Chem A* 106:10461–10469
38. Baciocchi R, Juza M, Classen J, Mazzotti M, Morbidelli M (2004) Determination of the dimerization equilibrium constants of Omeprazole and Pirkle's alcohol through optical-rotation measurements. *Helv Chim Acta* 87:1917–1926
39. Georges J (1995) Deviations from Beer's law due to dimerization equilibria: theoretical comparison of absorbance, fluorescence and thermal lens measurements. *Spectrochim Acta A* 51:985–994
40. Girard C, Kagan HB (2000) On diastereomeric perturbations. *Can J Chem* 78:816–828
41. Kitamura M, Suga S, Oka H, Noyori R (1998) Quantitative analysis of the chiral amplification in the amino alcohol-promoted asymmetric alkylation of aldehydes with dialkylzincs. *J Am Chem Soc* 120:9800–9809
42. Shibata T, Yamamoto J, Matsumoto N, Yonekubo S, Osanai S, Soai KJ (1998) Amplification of a slight enantiomeric imbalance in molecules based on asymmetric autocatalysis: the first correlation between high enantiomeric enrichment in a chiral molecule and circularly polarized light. *J Am Chem Soc* 120:12157–12158
43. Soai K, Kawasaki T (2006) Discovery of asymmetric autocatalysis with amplification of chirality and its implication in chiral homogeneity of biomolecules. *Chirality* 18:469–478
44. Williams T, Pitcher RG, Bommer P, Gutzwiller J, Uskokovic M (1969) Diastereomeric solute-solute interactions of enantiomers in achiral solvents. Nonequivalence of the nuclear magnetic resonance spectra of racemic and optically active dihydroquinine. *J Am Chem Soc* 91:1871–1872
45. Luchinat C, Roelens S (1986) Enantiomeric purity determination of 1,2-diols through NMR spectroscopy without chiral auxiliaries. *J Am Chem Soc* 108:4873–4878
46. Dobashi A, Saito N, Motoyama Y, Hara S (1986) Self-induced nonequivalence in the association of D- and L-amino acid derivatives. *J Am Chem Soc* 108:307–308

47. Jursic BS, Goldberg SI (1992) Enantiomer discrimination arising from solute-solute interactions in partially resolved chloroform solutions of chiral carboxamides. *J Org Chem* 57:7172–7174
48. Cung MT, Marraud M, Neel J, Aubry A (1978) Experimental study on aggregation of model dipeptide molecules. V. Stereoselective association of leucine dipeptides. *Biopolymers* 17:1149–1173
49. Harger MJP (1977) Proton magnetic resonance non-equivalence of the enantiomers of alkylphenylphosphinic amides. *J Chem Soc Perkin Trans 2* 1882–1887
50. Harger MJP (1978) Chemical shift non-equivalence of enantiomers in the proton magnetic resonance spectra of partly resolved phosphinothioic acids. *J Chem Soc Perkin Trans 2* 326–331
51. Schurig V (2009) Elaborate treatment of retention in chemoselective chromatography – the retention increment approach and non-linear effects. *J Chromatogr A* 1216:1723–1736
52. Trapp O, Schurig V (2010) Nonlinear effects in enantioselective chromatography: prediction of unusual elution profiles of enantiomers in non-racemic mixtures on an achiral stationary phase doped with small amounts of a chiral selector. *Tetrahedron Asymmetry* 21:1334–1340
53. Jung M, Schurig V (1992) Computer simulation of three scenarios for the separation of non-racemic mixtures by chromatography on achiral stationary phases. *J Chromatogr A* 605:161–166
54. Gil-Av E, Schurig V (1994) Resolution of non-racemic mixtures in achiral chromatographic systems: a model for the enantioselective effects observed. *J Chromatogr A* 666:519–525
55. Kurganov A (1996) Effect of solute association on the apparent adsorption isotherm. A model of the separation of non-racemic mixtures of enantiomers in achiral chromatographic systems. *Chromatographia* 43:17–24
56. Nakamura T, Tateishi K, Tsukagoshi S, Hashimoto S, Watanabe S, Soloshonok VA, Aceña JL, Kitagawa O (2012) Self-disproportionation of enantiomers of non-racemic chiral amine derivatives through achiral chromatography. *Tetrahedron* 68:4013–4017
57. Soloshonok VA, Berbasov DO (2006) Self-disproportionation of enantiomers on achiral phase chromatography. One more example of fluorine's magic powers. *Chim Oggi/Chem Today* 24:44–47
58. Soloshonok VA (2006) Remarkable amplification of the self-disproportionation of enantiomers on achiral-phase chromatography columns. *Angew Chem Int Ed* 45:766–769
59. Soloshonok VA, Berbasov DO (2006) Self-disproportionation of enantiomers of (*R*)-ethyl 3-(3,5-dinitrobenzamido)-4,4,4-trifluorobutanoate on achiral silica gel stationary phase. *J Fluorine Chem* 127:597–603
60. Luppi G, Cozzi PG, Monari M, Kaptein B, Broxterman QB, Tomasini C (2005) Dipeptide-catalyzed asymmetric aldol condensation of acetone with (*N*-alkylated) isatins. *J Org Chem* 70:7418–7421
61. Takahashi H, Tanabe T, Nakamura D, Kuribara T, Yamazaki O, Kitagawa O (2010) Atropisomeric lactam chemistry: catalytic enantioselective synthesis, application to asymmetric enolate chemistry and synthesis of key intermediates for NET inhibitors. *Tetrahedron* 66:288–296
62. Carman RM, Klika KD (1991) The optical fractionation of a partially racemic natural product by chromatography over an achiral substrate. *Aust J Chem* 44:895–896
63. Matusch R, Coors C (1989) Chromatographic separation of the excess enantiomer under achiral conditions. *Angew Chem Int Ed* 28:626–627
64. Sorochinsky AE, Katagiri T, Ono T, Wzorek A, Aceña JL, Soloshonok VA (2013) Optical purifications via self-disproportionation of enantiomers by achiral chromatography; case study of a series of α -CF₃-containing secondary alcohols. *Chirality* (accepted)
65. Ogawa S, Nishimine T, Tokunaga E, Nakamura S, Shibata N (2010) Self-disproportionation of enantiomers of heterocyclic compounds having a tertiary trifluoromethyl alcohol center on chromatography with a non-chiral system. *J Fluorine Chem* 131:521–524
66. Nicoud R-M, Jaubert J-N, Rupprecht I, Kinkel J (1996) Enantiomeric enrichment of non-racemic mixtures of binaphthol with non-chiral packings. *Chirality* 8:234–243

67. Baciocchi R, Zenoni G, Mazzotti M, Morbidelli M (2002) Separation of binaphthol enantiomers through achiral chromatography. *J Chromatogr A* 944:225–240
68. Baciocchi R, Mazzotti M, Morbidelli M (2004) General model for the achiral chromatography of enantiomers forming dimers: application to binaphthol. *J Chromatogr A* 1024:15–20
69. Nakajima M, Kanayama K, Miyoshi I, Hashimoto S (1995) Catalytic asymmetric synthesis of binaphthol derivatives by aerobic oxidative coupling of 3-hydroxy-2-naphthoates with chiral diamine–copper complex. *Tetrahedron Lett* 36:9519–9520
70. Nakajima M, Miyoshi I, Kanayama K, Hashimoto S (1999) Enantioselective synthesis of binaphthol derivatives by oxidative coupling of naphthol derivatives catalyzed by chiral diamine-copper complexes. *J Org Chem* 64:2264–2271
71. Tsai W-L, Hermann K, Hug E, Rohde B, Dreiding AS (1985) Enantiomer-differentiation induced by an enantiomeric excess during chromatography with achiral phases. *Helv Chim Acta* 68:2238–2243
72. Loža E, Lola D, Kemme A, Freimanis J (1995) Enantiomeric enrichment of partially resolved 4-hydroxy-2-carboxymethylcyclopentanone derivatives by achiral phase chromatography. *J Chromatogr A* 708:231–243
73. Aceña JL, Sorochinsky AE, Katagiri T, Soloshonok VA (2013) Unconventional preparation of racemic crystals of isopropyl 3,3,3-trifluoro-2-hydroxypropanoate and their unusual crystallographic structure: the ultimate preference for homochiral intermolecular interactions. *Chem Commun* 49:373–375
74. Diter P, Taudien S, Samuel O, Kagan HB (1994) Enantiomeric enrichment of sulfoxides by preparative flash chromatography on an achiral phase. *J Org Chem* 59:370–373
75. Charles R, Gil-Av E (1984) Self-amplification of optical activity by chromatography on an achiral adsorbent. *J Chromatogr A* 298:516–520
76. Dobashi A, Motoyama Y, Kinoshita K, Hara S, Fukasaku N (1987) Self-induced chiral recognition in the association of enantiomeric mixtures on silica gel chromatography. *Anal Chem* 59:2209–2211
77. Cundy KC, Crooks PA (1983) Unexpected phenomenon in the highperformance liquid chromatographic analysis of racemic ¹³C-labeled nicotine: separation of enantiomers in a totally achiral system. *J Chromatogr* 281:17–33
78. Stephani R, Cesare V (1998) Enantiomeric enrichment of non-racemic antihistamines by achiral high-performance liquid chromatography. *J Chromatogr A* 813:79–84
79. Monde K, Harada N, Takasugi M, Kutschy P, Suchy M, Dzurilla M (2000) Enantiomeric excess of a cruciferous phytoalexin, spirobrassinin, and its enantiomeric enrichment in an achiral HPLC system. *J Nat Prod* 63:1312–1314
80. Suchy M, Kutschy P, Monde K, Goto H, Harada N, Takasugi M, Dzurilla M, Balentova E (2001) Synthesis, absolute configuration, and enantiomeric enrichment of a cruciferous oxindole phytoalexin, (S)-(–)-spirobrassinin, and its oxazoline analog. *J Org Chem* 66:3940–3947
81. Takahata H, Takahashi S, Kouno S, Momose T (1998) Symmetry-assisted synthesis of c2-Symmetric trans- α , α' -bis(hydroxymethyl)pyrrolidine and -piperidine derivatives via double Sharpless asymmetric dihydroxylation of α , ω -terminal dienes. *J Org Chem* 63:2224–2231
82. Tanaka K, Osuga H, Suzuki, H, Shogase Y, Kitahara Y (1998) Synthesis, enzymic resolution and enantiomeric enhancement of bis(hydroxymethyl)[7]thiaheterohelicenes. *J Chem Soc Perkin Trans 1* 935–940
83. Kosugi H, Abe M, Hatsuda R, Uda H, Kato M (1997) A study of asymmetric protonation with chiral β -hydroxy sulfoxides. Asymmetric synthesis of (–)-epibatidine. *Chem Commun* 1857–1858
84. Ernholt BV, Thomsen IB, Lohse A, Plesner IW, Jensen KB, Hazell RG, Liang X, Jacobsen A, Bols M (2000) Enantiospecific synthesis of 1-azafagomine. *Chem Eur J* 6:278–287
85. Ray SK, Singh PK, Molleti N, Singh VK (2012) Enantioselective synthesis of Coumarin derivatives by PYBOX-DIPH-Zn(II) complex catalyzed Michael reaction. *J Org Chem* 77:8802–8808

Index

A

Absolute configuration, 1
(*S*)-*O*-Acetyl mandelic acid, 9
N-Acetyl phenylalanine ethyl esters, 329
Achiral chromatography, 301
Acrylamide (AM), 153
Activation parameters, 231, 252
N-Acyl valine *tert*-butylamide, 328
Adamantanones, 43
Adrenaline, 186
Alcohols, 15, 320
 boronic esters formation, 193
cis-2-Alkyl-3-oxy-tetrahydropyran, 106
Allene dimethyl-2,3-pentadienedioate, 254
Amides, 78, 316
Amines, 16
Amino acid esters, 17
Amino acid methyl esters, 101
 N-3,5-dinitrobenzoyl derivatives, 83
L/*D*-Amino acid oxidase, 148
Amino acids, 30, 111, 162, 271, 281, 304, 309
 extraterrestrial, 285
Amino alcohols, 12, 18, 20, 23, 29, 36, 78, 80,
 101, 111, 195, 321
cis-4-Amino-1-benzyl-3-phenylpiperidine, 19
L-4-Amino-phenylalanine, 155
Aminophosphonates, 3
3-Aminopropyltriethoxysilane (APTES), 140
Anhydrides, 15
Anisotropy spectroscopy, 271, 275
2-(Anthracene-2,3-dicarboximido)
 cyclohexane carboxylic acid, 13
2-(9-Anthryl)-2-*tert*-butoxyacetic acid, 10
1-(9-Anthryl)ethylamine, 16
 α -(9-Anthryl)- α -methoxyacetic acid
 (9-AMA), 5
1-Anthryl-2,2,2-trifluoroethanol, 321

Antihistamines, 331
 α -Arabinopyranosides, 15
Aromatics, 314
 α -Arylalkylamines, 79
N-Aryl-1,3,2-benzodithiazole-1-oxides, 258
3-Arylcarbonyl-2,2-dimethyloxazolidine-
 4-carboxylic acids, 13
Arylnaphthalenes, 260
3-Aryl-2-oxo-4-oxazolidinones, 43
Atropisomers, 40, 78, 89, 233
Azaphosphatrane-hemicryptophane cages, 82

B

Benzene-1,3-bis(carboxamide), 85
Benzimidazole, 93
Benzo[de]isoquinoline 1,3-dione amino
 acids, 79
Benzodiazepines, 262
syn-Benzotricamphor, 192
3-(Benzoyl)-(1*R*)-camphor, 39
trans-*N*-Benzylhydroxypiperidinemethanols, 12
(*S*)-1-Benzyl-6-methylpiperazine-2,5-dione, 79
1-*N*-Benzylxycarbonylaminoalkanephosphonic
 acid, 88
Bicyclodipeptide bearing calix[4]arenes, 158
Bicyclo[3.1.0]hex-2-ene-6-carboxylic acid, 305
Binaphthyl CSAs, 77
1,1'-Binaphthyl-2,2'-diol (BINOL), 77, 325
1,1'-Binaphthalene-2,2'-dithiol (BNSH), 157
BINOL, 77, 323
BINPHAT, 81
Biopolymers, 271
N,N'-Bis(6-acylamino-2-pyridinyl)
 isophthalamide, 101
Bis[(*R*)-1,1'-bi-2-naphtholato]borate, 82

- 9,10-Bis(2,3-dimethylphenyl)phenanthrenes, 252
- Bis-imidazole *N*-oxides, 78
- N,N'*-Bis(mesitylmethyl)-1,2-diphenyl-1,2-ethanediamine, 47
- Bis-*nor-seco*-cucurbit[6]uril, 189
- Bis[(*S*)- α -phenylethyl]cyclohexane-1,2-diamine, 21
- α,α' -(Bis-trifluoromethyl)-9,10-anthracenedimethanol, 84
- Borate CSAs, 83
- Boronate esters of (*R*)/(*S*)-2-(1-methoxyethyl)phenylboronic acid, 23
- Boron-containing reagents, 22
- Boronic acids, 23
- Bovine serum albumin (BSA), 156
- Bulk acoustic wave (BAW) sensors, 149
- 2-Butanol, 15, 39, 158, 159
- cis*-But-2-ene-1,4-diols, 77
- 2-*tert*-Butoxy-2-(2-naphthyl)acetic acid, 10
- 2-*tert*-Butoxy-2-phenylacetic acid, 10
- p-tert*-Butylcalix[4]arene, 97
- 18-(*tert*-Butyldimethylsilyloxy)-5-octadecayne-7-ol, 7
- 3-(*tert*-Butylhydroxymethylene)-(1*R*)-camphor, 37
- tert*-Butyl-1-(2-methyl-1-naphthyl)phosphine oxide, 258
- 2-Butylphenyl ethers, 42
- Butylphenylphosphinothioic acid, 78
- C**
- Cages, supramolecular, 177
- Calixarenes, 182
- calix[4]arenes, 97, 136, 183
- Calix[4]crown carboxylic acid, 97
- Calix[4]resorcinarenes, 3, 32, 98
- Camazepam, 334
- Camphor sulfonamide, 19
- Camphor sulfonyl chloride, 19
- Camphoric acid, 305
- (1*S*)-(+)-10-Camphorsulfonate, 111
- Camphorsulfonic acid (CSA), 78, 141, 147
- Capillary electrophoresis (CE), 133
- (*S*)-Captopril, 138, 148
- Carbamates, 20, 87, 98, 318
- Carboxamine, 25
- Carbocyclic[11]paracyclophanes, 253
- Carbon black (CB)-chiral polymer composites, 158
- 2-[4-(2-Carboxy-2-methylpropyl)phenyl]propionic acid, 116
- 1-[2-Carboxy-6-(trifluoromethyl)phenyl]pyrrole-2-carboxylic acid, 77
- Carboxylic acids, 4, 75, 305, 326
- Carceplexes, 191
- Carcerands, 191
- Carvone, 159
- Catechin, 89, 90
- Chemiresistors, 158
- Chemocapacitors, 161
- Chiral cages, 177
- Chiral derivatizing agents (CDA), 1, 70
- Chiral discrimination, 69
- Chiral ionic liquids (CILs), 110
- Chiral lanthanide shift reagents (CLSRs), 70
- Chiral ligand exchange potentiometry (CLEP), 139
- Chiral liquid crystals, 1
- Chiral recognition, 177, 301
- Chiral sensors, 133
- Chiral shift reagent (CSR), 83
- Chiral solvating agents (CSAs), 1, 69, 70
- Chiral stationary phases (CSPs), 83, 236
- Chirality, 231, 271
- Chirasil-nickel(II) (polysiloxane-anchored nickel(II)-bis [3-(heptafluorobutanoyl)-(1*R*)-camphorate]), 252
- Chiroptical properties, 177
- 2-Chloro-(4*R*,5*R*)-bis[(1*S*,2*S*,5*R*)-menthyl-yloxy-carbonyl]-1,3,2-dioxaphospholane, 21
- 1-Chloro-2,2-dimethylaziridine, 253, 255
- Chloromezanone, 334
- 10-(3-Chlorophenyl)-6,8,9,10-tetrahydrobenzo [b][1,8]naphthyridin-5(7*H*)-one (Telenzepine), 258
- 2-Chloropropionic acid, 80, 102
- Chloropyridin, 334
- Chlorpheniramine, 26, 331
- Chlorthalidone, 257, 262
- Cholic acid, 207
- Cineole, 321
- Circular dichroism, 147, 167, 271, 274
- Circularly polarized radiation, 271
- Citronellol, 160
- Colletotrichum acutatum*, 7
- Computer simulation, 231
- Conductometric (or resistive) sensors, 158
- COSAC, 271, 289
- Crown ethers, 28, 108
- Crown-6-tetracarboxylic acid, 108
- Cryptophanes, 42, 109, 111, 195
- Cryptophanol-A, 198

- Cucurbit[*n*]urils, 188
 α -Cyano- α -fluoro-*p*-tolylacetic acid (CFTA), 5
 Cyclic voltammetry (CV), 143
 Cyclodextrins, 24, 90, 116, 136, 181, 292
 hosts, 181
 QCM, 150
 Cyclohexane carboxamide, 318
trans-1,2-Cyclohexane dicarboxylic acid, 23
 (R,R)-1,2-Cyclohexanediamine, 103
 Cyclohexenols, *endo/exo*-monocyclic, 9
 Cyclopentanones, 326
 Cyclopeptides, 158
 Cyclotribenzylene (CTB), 182, 195, 202
 Cyclotrimeratrylene, 182
 Cycloveratrylenes, 42
- D**
- cis*-Decalin, 52
 Deoxyribooligonucleotides, 145
 Derivatizing agents, chiral, 4
 1,6-Dialkylpiperazine-2,5-diones, 79
 1,2-Diaminocyclohexane (DACH), 78, 87,
 102, 193
 4,4'-Diamino-2,2'-diisopropylbiphenyl, 261
 4,4'-Diammonio-2,2'-bis(trifluoromethyl)
 biphenyl, 261
 Dibenzoyltartaric acid, 77, 169
 Dicumylolmethane, 37
 (2,6-Dichloro-4-methoxyphenyl)
 (2,4-dichlorophenyl)methanol, 20
N,N'-Diethyl-4-vinyl-benzamidine, 169
 Differential pulse voltammetry (DPV), 143
 Diffusion-ordered NMR spectroscopy
 (DOSY-NMR), 109
 (*R*)-Dihydroindenol, 314
 Dihydroquinines, 316
 2,2'-Dihydroxybenzophenone, 19
 2,2'-Dihydroxy-1,1'-binaphthalene
 (BINOL), 18
 Di-(*R,R*)-1-[10-(1-hydroxy-2,2,2-
 trifluoroethyl)-9-anthryl]-2,2,2-
 trifluoroethyl phthalate, 85
 Diketones, 325
 Diketopiperazine, 14
 Dimethindene, 91
 2,6-Dimethylenebicyclo[3.1.0]-hexane, 252
 Dimethylformamide dimethylacetal
 (DMF-DMA), 292
N,N-Dimethyl-1-(1-naphthyl)ethylamine, 46
 Dimethyl-1-phenylethylamine, 44, 46
 3,5-Dinitrobenzamides, 319
 3,5-Dinitrobenzoyl amino acids, 89
 3,5-Dinitrobenzoyl-derived 1-naphthylethyl
 amide, 84
 Dioxo[11]cyclophanes, 253
 Dioxolanoadamantanes, 43
 Dipeptides, 329
 2,2-Diphenyl-[1, 3]-dioxolane-4,5-
 dicarboxylic acid, 14
 2-(Diphenylmethanesulfinyl)acetamide
 (modafinil, MDL), 115
 Diporphyrin receptor, 102
 Disaccharides, 167
 Distillation, 301
 Disuccinimidyl suberate (DSS), 141
 3,4-Di-*tert*-butyl-1,3,4-oxadiazolidine, 256
 Dithiolano adamantanes, 43
 DNA aptamers, 167
 Dopamine (DOPA), 162
 Doxylamine, 25, 332
 Drug formulations, chiral, 115
 Drugs, 231
 Dynamic capillary electrophoresis (DCE),
 231, 261
 Dynamic gas chromatography (DGC),
 231, 244, 252
 Dynamic high performance liquid
 chromatography, 231, 256
 Dynamic supercritical fluid chromatography,
 231, 258
 Dysprosium, 26
- E**
- Eburnamonine, 54
 Electrical sensors, 158
 Electrochemical impedance spectroscopy
 (EIS), 143
 Electrochemical quartz crystal microbalance
 (EQCM) sensor, 153
 Electrochemical sensors, 136
 Electropolymerization, 153
 α -Eleostearic acid, 51
 Enalapril, 262
 Enantiomeric differentiation, 1, 133
 Enantiomeric excess, 69, 271
 Enantiomerization, 231, 235
 Enantioselective chromatography, 231
 Encapsulation, 96
 Ephedrine, 111, 188
 Epichlorohydrin, 109, 158
 1,2-Epoxybutane, 109
 Ethyl-2-(9-anthryl)-2-hydroxyacetate, 15
 α -Ethylbenzylphenyl sulfide, 314
 Ethyl lactate, 169

4-Ethyl-4-methyloctane (C*MeEtPrBu), 8
Europium, 38

F

Faradaic impedance spectroscopy (FIS), 146
Fatty acids, 50
 α -Ferrocenylethylphosphine, 13
Field effect transistors (FET), 141
4-Fluoro-2-formylphenylboronic acid, 22
1-(*o*-Fluorophenyl)ethanol, 2
(*S*)-Flurbiprofen, 138
N-Fmoc-*N'*-Boc-L-tryptophan, 80
2-Formylphenylboronic acid, 22
Fullerenes, 114, 189

G

Gamma-globulin, 144
Gas chromatography (GC), 94, 133, 168, 289
Gibbs free activation energy, 252
GIOTTO, 288
Glassy carbon electrode (GCE), 144
Glucose, 15, 150, 168
sensors, 168
OEET, 161
Glucose oxidase, 149
Glutamic acid, 162, 167
Glycopeptides, 89
 β -Glycopyranosides, 15
Glycosides, 15
Goat serum albumin (GSA), 157
Gravimetric/mass sensors, 149

H

Helicenediol, 332
Hemicarceplexes, 191
Hemicarcerands, 191
Hemicryptophanes, 202, 207
3-Heptafluorobutyryl-(1*R*)-camphor, 37
Heptafluoro-2,2-dimethyl-3,5-octanedione, 40
Heptakis(3-*O*-acetyl-2,6-di-*O*-pentyl)- β -cyclodextrin
(Lipodex D), 94
Heptakis(6-deoxy-6-[12-(thiododecyl)
undecanamido])- β -cyclodextrin, 167
Heptakis(2,3-di-*O*-acetyl-6-*O*-*tert*-
butyldimethylsilyl)- β -cyclodextrin
(AcSiCD7), 95
Heterocycles, 331
Hexaazapyridinophanes, 107
Hexacarboxylic acid cryptophane-A, 109

High performance liquid chromatography
(HPLC), 83, 133, 238
Homocalixarene hosts, 183
Homochirality, life, 285
Homocysteine, 142
Host-guest systems, 177
Human serum albumin (HSA), 141, 156
Hydroxyacids, 23, 304
4-Hydroxy-2-carboxymethyl-2-
cyclopentenone, 326
Hydroxycoumarin derivatives, 334
(+)-*cis*-4-Hydroxy-6-deoxyscytalone, 7
3-Hydroxyindolin-2-ones, 319
 α -Hydroxyisovaleric acid, 80
3-Hydroxy-2-methylpropanoic acid, 44
 α -Hydroxyphosphinates, 7
2-Hydroxy-3-trimethylaminopropyl- β -CD, 138

I

(*S*)-Ibuprofen, 54, 77, 114, 116
Imination, 191
Indium tin oxide (ITO) glass, 139
Indoles, 33
Interconversion, 231
Ionic liquids (IL), 109
Ion-selective electrodes (ISE), 137
Ion-sensitive field effect transistors (ISFET),
141
Isobenzofuran-1,3-dione, 36
N-Isobutyryl-cysteine (NIBC), 145
Isocyanates, 17
Isophthalate, 85
Isopropyl(trifluoro)lactate, 304, 308, 326
2,3-*O*-Isopropylidene-L-threitol, 191
(1*S*,2*S*)-*N*-[(2-Isothiocyano)cyclohexyl]
trifluoromethanesulfonamide, 17
Isothiouronium, chiral, 41

K

Kemp's acid diamide, 78
Ketones, 325
Kinetics, 231

L

Lactams, atropisomeric, 319
bicyclic, 43
Lanthanide complexes, chiral, 3
Lanthanide tris β -diketonates, chiral, 37
Lanthanides, paramagnetic, 38
Leucine, 111, 275, 276, 282, 286, 311–313

- Limonene, 159
Linoleate, epoxidation, 51
Liquid crystals, chiral, 3, 47
Liquid-vapor phase transition, 303
Lithium bis(trifluoromethane)sulfonimide, 111
Lithium diphenylphosphide (PPh₂Li), 199
Lorazepam, 262
Ludartin, 53
Lupanine, 77
Lutetium, 38
- M**
- Macrocycles, 24
 synthetic, 96
Maltodextrins, 137
Mandelic acid, 22, 75, 140, 155
Mandelic acid-dimethylaminopyridine, 83
Memory effect, 154
Menthol, 154, 159
4-Mercapto-2-alkenones, 11
Metabolites, chiral, 115
Metal complexes, 36
Metal oxide semiconductor field effect transistor (MOSFET), 141
Metal(II) bis[3-(heptafluorobutanoyl)-(1*R*)-camphorate], 255
Metalloporphyrins, 87
Methionine, 45
L-Methotrexate, 143
α-Methoxy(1-naphthyl)acetic acid (1-NMA), 10
2'-Methoxy-1,1'-binaphthalene-8-carbaldehyde, 18
2-Methoxy-2-(1-naphthyl)propionic acid (MαNP), 5
(*S*)-2-Methoxy-2-phenylpent-3-ynoic acid, 9
(*R*)-/(*S*)-(3-Methoxyphenyl)ethylamine (MPEA), 152
α-Methoxyphenylacetic acid (MPA), 5, 115
α-Methoxy-α-trifluoromethylphenylacetic acid (MTPA), 4, 111, 115
Methyl-*N*-benzoylleucinate, 79
(*R*)/(*S*)-Methyl benzyl amine, 100
Methyl carbamate, 318
Methyl 2-chloropropionate, 94, 158, 162
Methyl-β-cyclodextrin, 93
3-Methylcyclohex-2-en-1-ol, 39
(*syn*)-Methyl-2,3-dihydroxy-3-phenylpropionate, 23
3-Methyl-1,3-dioxolan-2-one, 54
Methyl ferrocenyl sulfoxide, 328
(±)-4-Methylimidazolidin-2-one, 183
Methyl lactate, 102, 169
Methyl linoleate, 50
4-Methylsulfanylbutylglucosinolate, 40
Methyl *p*-tolyl sulfoxide, 327
Methyl vernoleate, 50
Molecular imprinted polymers (MIPs), 136, 139, 153
Molecular recognition, 133
Molecular tweezers, 84
Monosaccharides, 15, 167
Morpholine derivatives, 332
Mosher's acid, 110, 111, 201, 223
Mosher's salt, 111
Myrioneurinol, 9
- N**
- Nanocubes, 196
Nanowires, 146
Naphthalenedicarboxyl-*tert*-leucinate, 45
Naphtho[2,3-*c*]furan-1,3-dione, 36
(*S*)-(-)-1,1'-(2-Naphthol), 115
3-(2-Naphthoyl)-(1*R*)-camphor, 39
1-Naphthyl reagents, 6
1-(1-Naphthyl)ethylamine, 16, 84
(1-Naphthyl)(trifluoromethyl) *O*-carboxy anhydride, 15
(*S*)-Naproxen, 77
Natural products, 87
Nicotine, 188, 331
L-Nitritotriacetic acid (L-NTA), 200
N-(2-Nitrophenyl)proline, 13
1,4-Nitrophenylethylamines, 138
NMR, 69
 dynamic (DNMR), 231, 233
 shift reagents, 1
Nonadecanol, 6
Norephedrine, 111, 188
- O**
- Octakis(3-*O*-butanoyl-2,6-di-*n*-*O*-pentyl)-γ-cyclodextrin, 162
OFETs, sensors, 133, 159
Omeprazole, 77, 91
One-dimensional exchange spectroscopy by sideband alteration (ODESSA), 55
Optical circular dichroism (OCD), 146, 167
Optical sensors, 165
Organic electrochemical transistors (OECT) glucose sensors, 161
Organic field effect transistors (OFETs), 133, 159

Organoleptic, 135
 Oxazepam, 257, 262
 Oxazolidinones, 78, 102
 Oxazolones, 44
 Oxetanes, 77
 Oxiranes, 77
 2-Oxo-3-indolylacetic acids, 19

P

Palladium complexes, 45
 Pantoprazole, 91
 Paracetamol, 146
 Penicillamine, 143
 Pentafluoro-2-(fluoromethoxy)-3-methoxypropane (halodiether B), 95, 169
 10-(Pentafluorophenylcarbamoyloxy)-60-methoxy-11-norcinchonane-9-ol, 88
 9-*O*-(Pentafluorophenylcarbamoyl)quinine, 88
 Pentahydroxyl cryptophane-A, 109
 (*S*)-Pentorpril, 138
 Peptide mimetics, 86
 Peptidyl-proline dipeptides, 257, 262
 Permethylated β -cyclodextrin, 96
 Per-*O*-(*S*)-2-methyl butyrate, 15
 (*S,S*)-Petrocortyne, 6
 Phase transitions, physicochemical, 301
 Pheniramine, 25
 Phenols, 320
 (*R*)-2-Phenoxypropionic acid, 114
 (*S*)-3-Phenyl-2-(selenophenyl)propan-1-ol, 23
 2-Phenyl-2-oxazolidinone, 19
 Phenylalanine, 146
 Phenylalanine ethyl ester bis(trifluoromethane) sulfonimide, 111
 Phenylalanine methyl ester hydrochloride, 35
 Phenylazomethine cages, 192
 (*S*)-2-(Phenylcarbamoyloxy)propionic acid, 84
trans-2-Phenylcyclopropanes, 40
o-Phenylenediamine (*o*-PD), 162
 1-Phenylethylamine (PEA), 16, 71, 80
 Phenylpropionic acid, 2, 35
 (*R*)-2-Phenylselenopropanoic acid, 24
 Phenylthiohydantoinphenylalanine, 257
 Phosphazenes, 74
 Phosphine oxides, 80
 Phospholenes, 78
 Phosphonamidates, 80
 Phosphonates, 80
 Phosphonocarboxylate (PC), 91

Phosphorus-containing reagents, 20
 Photochemical model, 271, 285
 (*S*)-*N*-Phthaloyl-(*S*)-*tert*-leucine, 45
 Phthalyl alanine (PA), 100
 Pincer structure, 85
 Pincer-like CSAs, 85
 α -Pinene, 55, 158
 L-Pipecolic acid (PA), 138, 148
 L-Pipecolinic acid, 34
 Piperazines, 31
 Piperidines, 31
 Plasticized polyvinyl chloride (PVC), 137
 Platinum complexes, 46
 Polyaniline, conducting de-doped, 141
 Polychlorinated biphenyls (PCBs), 253
 Polymethacrylic acid (PMAA), 139
 Polypyrrole, overoxidized (oPPy), 153
 Polysodium *N*-undecanoyl-L-leucylvanilate (SULV), 138
 Polysodium *N*-undecanoyl-L-vanilate (SUV), 138
 Poly- γ -benzyl-D-glutamate (PBDG), 50
 Poly- γ -benzyl-L-glutamate (PBLG), 49
 Poly- γ -ethyl-L-glutamate (PELG), 49
 Poly- ϵ -carbobenzyloxy-L-lysine (PCBLL), 49
 Poly[2-(*N*-carbazolyl)ethyl methacrylate-*co*-methacrylic acid]s (PCEMMAs), 139
 Poly((*R*)-3-hydroxy-butylate-*co*-(*R*)-3-hydroxyvalerate), 158
 Poly(phenylenethynylene) (PPE), 154
 Potentiometric Sensors, 137
 Praseodymium, 38
 Prolines, 32–34, 79, 98, 138, 257, 282, 311
 Prominal, 257
 Propranolol, 25, 34
 Propylene oxide, 109
 Propylenediaminetetraacetic acid, 41
 Pseudoephedrine, 188
 Pseudoproline, 13
 PVC membranes, 138
 Pyridine-2,6-bis-carboxamide, 85
 Pyrrolidines, 332
 Pyrrolidinofullerene, 189

Q

Quartz-crystal microbalances (QCMs), 149
 Quinidine, 89
 Quinine, 7, 83, 87–89, 113
 Quinoxaline, 99
 Quinuclidine, 88

R

Rabbit serum albumin (RbSA), 157
Rabeprazole, 91
Racemization, 235
Real-time monitoring, 133
Reflectometric interference spectroscopy-based sensors, 168
Residual dipolar couplings (RDCs), 53
Resorcinarenes, 99, 135, 185
Resorcinol, 33, 185
Rhodium complexes, 42
ROSETTA, 271, 288

S

Saccharides, 167
Selenium-containing reagents, 23
(*S*)-2-(Selenophenyl)propan-1-ol, 24
Self-assembled monolayers (SAMs), 137
Self-disproportionation of enantiomers (SDE), 302
Sense of nonequivalence, 70
Sensing receptors, 115
Sensors, amperometric, 148
Serine, 13
Sibutramine, 93
Silver complexes, 47
Size-exclusion chromatography (SEC), 327
Solid–vapor phase transition, 305
Spirobichromenes, 257
Spirobrassinin, 77, 332
Spirochromenes, 258
Spirooxazoline, 332
Stochastic model (SM), 242, 244
Stopped-flow multidimensional GC (sfMDGC), 237, 253
Stopped-flow techniques, 231
Streptavidin, 165
Strychnine, 53
Sublimation, 301, 315
Succinoglycan, 89
Sucro-neolambertellin, 54
Sulfides, 314
Sulfoxides, chiral, 76, 327
Supercritical fluid chromatography, 258
Supramolecular cages, 190
Supramolecular chemistry, 177
Surface plasmon resonance (SPR) sensors, 165
Synchrotron radiation circular dichroism (SRCD), 274

T

Teicoplanin, 138
Temazepam, 262
Terephthalate, 85
Tetraalkylammonium carboxylates, 101
Tetraamidic cyclic CSAs, 103
meso-Tetra(*tert*-butyl)porphine, 114
Tetrahydro-1,4-epoxynaphthalene-1-carboxylic acid, 14
Tetrahydropyridazine derivatives, 334
Tetrakis(pyridylmethyl)propylene diamine, 41
Tetramethylammonium iodides, 101
Tetraphenylporphine, 114
Tetra(4-sulfophenyl)porphyrin (TSPP), 138
Thalidomide, 262
Theoretical plate model (TPM), 231, 239
Thiacalix[4]arene, 98
Thickness shear mode resonators (TSMRs), 149
Thioureas, C₂-symmetrical chiral, 81
CSAs, 81
Thyroxine, 167
1,3,5-Tri(boronic acid)benzene, 194
Tribenzotriquinacene (TBTQ), 196
Tridioxethylene triphenylene, 52
Trifluoroacetamide, 318
N-Trifluoroacetyl dipeptides, 330
N-Trifluoroacetyl valine methyl ester, 304
N-Trifluoroacetyl-alanine methyl ester (*N*-TFA-Ala-OMe), 169
3-Trifluoroacetyl-(1*R*)-camphor (tfc), 37
Trifluoro-1-(9-anthryl)ethanol (Pirkle's alcohol), 15, 74
 α -(Trifluoromethyl)lactic acid, 306
2,2,2-Trifluoro-1-phenylethanol, 71
Trifluoro-3-phenylpropan-2-amine, 319
Trifluoro-1-(1-pyrenyl)ethanol, 75
Triformylbenzene, 193
Trimethylcyclooctanol, 7
Trimethyl-propane trimethyl acrylate (TRIM), 153
Triphenyl(1-phenylethyl)phosphonium bromide, 83
Tris-4-(formylphenyl)amine, 193
syn-Tris(norborneno)benzene, 192
Tris(2,4,6-trichlorophenyl)methane, 257
TRISPHAT, 81, 207
Tryptophan, 106, 141, 154
Tyrosinamide, 145
Tyrosine, 166

U

- Unified equation, 231
- Uranyl–cavitand–salen CSA, 100
- UV/VUV anisotropy spectroscopy, 283
- UV/VUV CD spectroscopy, 282

V

- Vancomycin, 138
- Vapor-diffused molecular assembly (VDMA), 155
- Vernoleate, epoxidation, 51
- Voltammetric sensors, 143

X

- Xenon–cryptophane, 222

Y

- Ytterbium, 26

Z

- Zn-tetra(4-sulfophenyl)porphyrin (ZnTSPP), 138